Stable isotopes in small mammal dental carbonate: investigating their applications for reconstructing Quaternary climate variability

Elizabeth Peneycad

Royal Holloway, University of London

(Volume 1)

Submitted for the degree of Doctor of Philosophy

September 2018

Declaration of Authorship

I, Elizabeth Peneycad, hereby declare that this thesis and the work presented in it is entirely my own. Where I have consulted the work of others, this is always clearly stated.

Signed: 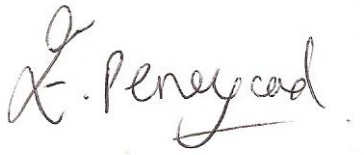

Date: 20th September 2018

Abstract

The stable oxygen ($\delta^{18}O$) and carbon ($\delta^{13}C$) isotope ratios of small mammal dental carbonate are potentially valuable proxies for past environmental conditions. However, the application of these proxies to reconstructing Quaternary climate variability has hitherto been limited, due to 1) uncertainties in the relationship between the $\delta^{18}O$ values of rodent teeth and meteoric water, and 2) a poor understanding regarding the influences of ecological and environmental factors on tooth isotopic compositions.

A modern study was therefore undertaken to investigate how the $\delta^{18}O$ and $\delta^{13}C$ compositions of rodent dental carbonate reflect environmental conditions in Britain. The results demonstrate that a robust relationship exists between the $\delta^{18}O$ values of rodent teeth and meteoric water in mid-latitude regions. Since the $\delta^{18}O$ of meteoric water correlates with temperature, the $\delta^{18}O$ values of rodent teeth reflect climate. The modern relationship was applied to three British Quaternary sites (West Runton, Cudmore Grove, and Marsworth) to reconstruct the $\delta^{18}O$ of past meteoric water. Reconstructed $\delta^{18}O$ values were coupled with the $\delta^{18}O$ compositions of fossil shells to quantify mean summer palaeotemperatures. These palaeotemperatures are comparable with existing palaeoclimate evidence from the three sites. Rodent remains from British cave deposits (Westbury Cave and Gully Cave) were also investigated to reconstruct millennial-scale palaeoclimatic fluctuations. Stratigraphic changes in average tooth $\delta^{18}O$ values are consistent with expected palaeoclimate changes at the sites. These results demonstrate that the $\delta^{18}O$ values of rodent teeth can generate reliable records of Quaternary climate variability.

The modern study also showed that the $\delta^{13}C$ values of rodent teeth from Britain record the $\delta^{13}C$ of C_3 vegetation. However, the $\delta^{13}C$ compositions of modern teeth are significantly depleted relative to pre-modern teeth. Isotopic analyses of recent rodent teeth indicate that this $\delta^{13}C$ change must have occurred within the past 2000 years, due to anthropogenic impacts on atmospheric CO_2 and vegetation.

Table of Contents

Volume 1:

List of abbreviations

$\delta^{18}O_{rt}$ – oxygen isotope ratio of rodent tooth bioapatite

$\delta^{18}O_{mw}$ – oxygen isotope ratio of surface meteoric water

$\delta^{18}O_{pt}$ – oxygen isotope ratio of precipitation

$\delta^{18}O_{bw}$ – oxygen isotope ratio of body water

$\delta^{18}O_{dw}$ – oxygen isotope ratio of drinking water

$\delta^{18}O_{ms}$ – oxygen isotope ratio of mollusc shell aragonite

δD – the deuterium (^{2}H) isotope ratio of water

$\delta^{13}C_{rt}$ – carbon isotope ratio of rodent teeth

$\delta^{13}C_{d}$ – carbon isotope ratio of rodent diet

$\delta^{13}C_{p}$ – carbon isotope ratio of a plant

$\delta^{13}C_{a}$ – carbon isotope ratio of atmospheric carbon dioxide

$\delta^{13}C_{ms}$ – carbon isotope ratio of mollusc shell aragonite

pCO_2 – the partial pressure of atmospheric CO_2 (in ppmv)

VPDB – Vienna Pee Dee Belemnite

VSMOW – Vienna Standard Mean of Ocean Water

DIC – Dissolved Inorganic Carbon

MIS – Marine Oxygen Isotope Stage

LGI – Lateglacial Interstadial

LLS – Loch Lomond Stadial

yr BP – years before AD 1950

List of Figures

List of Tables

Acknowledgements

Firstly, I would like to thank my supervisors Ian Candy and Danielle Schreve, for their support and guidance throughout the PhD. I am particularly grateful to Ian for his eternal optimism despite issues encountered during the project, and his willingness for a discussion of the data. I am also grateful to Danielle for her knowledgeable insight, for providing rodent teeth from Surrey and Gully Cave, and for kindly collecting water samples from Somerset.

I am also incredibly grateful to the London NERC DTP for providing me with the opportunity to undertake this PhD, and NERC for funding the project (NERC training grant 1492278). I am also extremely grateful to Historic England for funding the radiocarbon dating of the *Arvicola terrestris* mandibles from Longstone Edge, and to Peter Marshall at Historic England for arranging the radiocarbon dating of the specimens, and for providing the dating results.

I am grateful to following people for collecting and providing the owl pellets for the modern study: David Cottle from the Wells Natural History and Archaeology Society (Somerset), David Blanchard (East Yorkshire) and Barry Caudwell (Perthshire). I also thank Ash Abrook and Ian Matthews for collecting the modern water samples from Perthshire.

I would like to thank the following museum curators for their help and hospitality, and for providing fossil material for my project: Mike Palmer at the Buckinghamshire County Museum Resource Centre, for providing the material from Marsworth; Roula Pappa and Pip Brewer at the Natural History Museum, London, for accepting my application for the destructive sampling of the teeth from Westbury Cave; Polydora Baker and her team at Fort Cumberland, Historic England, for providing the material from Longstone Edge; David Allen at the Hampshire Cultural Trust, for providing the material from Danebury. I

also thank Polydora Baker, Peter Marshall and Jonathan Last at Historic England for sharing their knowledge on Longstone Edge, and for engaging in an interesting discussion of the results. I am additionally grateful to Peter Andrews for taking the time to review the specimens that I selected from Longstone Edge and correcting my taphonomic observations. I also thank Dr Tom White for identifying the mollusc shells from Marsworth.

I thank Claire Gallant, Iñaki Valcarcel and Marta Perez for their assistance with the laboratory preparation of the rodent teeth, and Pierre Schreve for help with the sieving of the sediments from Marsworth. I am also grateful to David Lowry for undertaking the analyses of the rodent teeth at Royal Holloway. I also thank Anne-Lise Jourdan for training me in the stable isotope analysis of carbonate samples, for undertaking the analyses on the rodent teeth at the Bloomsbury Environmental Isotope Facility, UCL, and for collaborating on the investigation of the material from Longstone Edge and Danebury. I thank Melanie Leng and her team at the BGS for analysing the modern water samples, and Jerry Morris at Royal Holloway University of London, for assisting with the XRD analyses.

Finally, I would like to thank my parents for their unwavering support and companionship throughout my PhD. I also thank my friends for their support, advice, and general willingness for a good chat. I could not have done this without them.

1. Introduction

1.1. Context of research

The Quaternary period, which spans from 2.6 million years ago to the present day, is characterised by long-term (hundreds of thousands of years) and short-term (thousands of years) climatic fluctuations (Dansgaard et al., 1993; McManus et al., 1999; Lisiecki & Raymo, 2005; Lang & Wolff, 2011). Proxy reconstructions of these climatic fluctuations are playing an increasingly important role in our understanding of recent and future environmental changes (Masson-Delmotte et al., 2006; Tzedakis et al., 2009; Candy et al., 2014; Yin & Berger, 2015). The interval in which we live, the Holocene epoch, is an interglacial (warm) stage that is experiencing rapid shifts in environmental and climatic conditions as a result of anthropogenic activities. By studying interglacial stages in the recent past, we can therefore investigate how Holocene-like climates evolved in the absence of anthropogenic forcing (Yin & Berger, 2015). Investigating the nature of abrupt palaeoclimate events can also aid in our understanding of how the Earth system may respond to current and future rapid changes. This is especially important for regions that play a key role in influencing the global climate system. Northwest Europe is one such region; past variations in the temperature, salinity and circulation of the North Atlantic Ocean, plus changes in the Northern Hemisphere ice sheets, have had strong impacts on local and hemispheric climates (Bond et al., 1993; Moros et al., 2004; Nesje et al., 2004; Marshall et al., 2007).

Despite the importance of studying past climates, our understanding of this topic is currently constrained by the limited range of palaeoclimate proxies and archives that is available for investigation. Whilst marine cores and ice cores can provide long and high-resolution palaeoclimate records, few detailed terrestrial archives exist (e.g. Lang & Wolff, 2011), and quantitative proxy reconstructions from these archives are generally lacking. This is problematic, because it is well-established that 1) patterns of climate change may be highly spatially variable, and 2) terrestrial environments may experience greater magnitude changes than marine settings.

Generating local proxy reconstructions for terrestrial areas is also crucial for understanding the responses of fauna, and especially hominins, to environmental changes (e.g. Lister & Stuart, 2008; Kahlke et al., 2011; Leroy et al., 2011). Cave archives provide some of our richest records of faunal and archaeological remains. However, the value of these archives is currently limited by the lack of quantitative climate records with which fossil assemblages can be directly compared. This is due to the fact that the palaeoecological proxies that are commonly used to generate quantitative climate data for terrestrial areas (e.g. pollen, beetles) are often not preserved within caves.

There is, therefore, a pressing need to develop and test quantitative approaches to reconstructing Quaternary environmental variability in terrestrial areas, in order to: 1) build on our existing palaeoenvironmental records, 2) generate robust reconstructions of the spatial and temporal variations in the patterns of environmental changes, and 3) provide new data for understanding the climatic contexts of faunal and archaeological records from cave sites.

1.2. Stable isotopes in small mammal bioapatite as palaeo-environmental proxies

1.2.1. Importance of small mammal bioapatite as a palaeo-environmental archive

The stable oxygen and carbon isotope analysis of fossil mammalian bones and teeth is a well-established quantitative tool in palaeoclimate research. This tool has been widely-utilized to infer past changes in temperature, humidity, climate seasonality, mammalian diets, and vegetation in terrestrial areas (Longinelli, 1984; Luz & Kolodny, 1985; Quade et al., 1992; Genoni et al., 1998; Grimes et al., 2003; Sharma et al., 2004; Higgins & MacFadden, 2009; Iacumin et al., 2010; Royer et al., 2014). The pioneering work of Longinelli (1984) demonstrated that the ratio of oxygen-18 to oxygen-16 isotopes in bioapatite ($\delta^{18}O$), the constituent mineral of bones and teeth, is strongly correlated with the $\delta^{18}O$ value of local meteoric water. In mid-latitude regions

such as Northwest Europe, air temperature has a major control on the $\delta^{18}O$ of meteoric water (Dansgaard, 1964; Rozanski et al., 1993). Oxygen isotopes in mammalian bioapatite can, therefore, potentially act as a powerful proxy for past temperatures in this region (e.g. Bernard et al., 2009; Fabre et al., 2011).

On the other hand, the ratio of carbon-13 to carbon-12 isotopes within mammalian bioapatite ($\delta^{13}C$) can provide a record of a mammal's diet (Lee-Thorp & Van der Merwe, 1987; Lee-Thorp, 1989; Cerling & Harris, 1999). In herbivorous mammals, the $\delta^{13}C$ value of the diet is influenced by 1) the types of plants that are available for consumption (C_3 or C_4), and 2) variations in the environmental factors that control the $\delta^{13}C$ values of these plants, which include the $\delta^{13}C$ value and concentration of atmospheric CO_2, and climate (Tieszen, 1991; Heaton, 1999). Carbon isotopes in fossil mammalian bioapatite therefore provide a potential means for reconstructing past variations in vegetation resulting from environmental and climatic changes (e.g. Quade et al., 1992; Arppe et al., 2015).

Hitherto, much of the research into stable isotopes in bioapatite has focussed on the bones and teeth of large herbivorous mammals (Ayliffe et al., 1992; Genoni et al., 1998; Arppe & Karhu, 2006; Bernard et al., 2009; Chritz et al., 2009; Pushkina et al., 2014). This is because sufficient sample material for isotopic analysis is much easier to obtain, and isotopically-modified metabolic water has a lesser influence on the $\delta^{18}O$ of bioapatite compared to smaller-bodied mammals (Bryant & Froelich, 1995). Nevertheless, over the past 20 years, there has been a growing interest in the potential value of using stable isotopes in small mammal teeth as palaeoenvironmental proxies (Lindars et al., 2001; Navarro et al., 2004; Grimes et al., 2008; Gehler et al., 2012; Royer et al., 2013a; Jeffrey et al., 2015). This is due to the fact that small mammals hold several advantages over large mammals as palaeoenvironmental archives. Firstly, the fossil remains of small mammals, and specifically rodents, are often abundantly preserved in Quaternary sediments. Due to the broad ecological preferences of rodent taxa, and the deposition of pellets and scats by the rodents' predators, abundant rodent remains can be found in a range of climatic zones and depositional environments, including caves (Andrews, 1990; Hernández Fernández et al., 2007; Sesé & Villa, 2008; López-García et al., 2015). Furthermore, most

rodent species have small home ranges and do not exhibit migratory behaviour, and as a result, the isotope values of their teeth closely parallel local environmental conditions (Lindars et al., 2001; Grimes et al., 2003, 2004; Gehler et al., 2012). In addition, due to the rapid mineralization and turnover of rodent teeth, combined with the seasonal activities of predators, the stable isotope values of rodent teeth are capable of recording variations in climate and diet at high temporal resolutions (Royer et al. 2013a; Calandra et al., 2015). Finally, recent advances in mass spectrometric techniques have facilitated the analysis of increasingly smaller sample sizes, enabling individual small mammal teeth, or components of small teeth (e.g. enamel), to be analysed separately (Lindars et al., 2001; Passey & Cerling, 2006; Gehler et al., 2012).

Fossil rodent teeth are consequently a valuable resource that can potentially be used to generate large isotopic datasets at high spatial and temporal resolutions from a range of terrestrial archives (Grimes et al., 2003; Navarro et al., 2004; Royer et al., 2013a; Royer et al., 2013b). These datasets can be utilized in producing quantitative reconstructions of short- and long-term environmental variations. Despite these advantages, the applications of stable isotopes in rodent teeth to reconstructing Quaternary climate variability have thus far been limited, due to three key reasons. Firstly, there are significant discrepancies between the published calibrations that relate the $\delta^{18}O$ of rodent bioapatite ($\delta^{18}O_{rt}$) to the $\delta^{18}O$ of meteoric water ($\delta^{18}O_{mw}$) in mid-latitude regions (Navarro et al., 2004; Royer et al., 2013a). This has led to uncertainties regarding which calibration is the most appropriate and reliable for reconstructing past $\delta^{18}O_{mw}$ values for subsequent use in quantifying past temperatures (e.g. Héran et al., 2010). Secondly, the significance of isotopic variability between rodent teeth within a sample, and the factors that contribute to this variability, are both poorly understood (Jeffrey et al., 2015). This has limited our ability to make meaningful interpretations of $\delta^{18}O$ and $\delta^{13}C$ data from fossil rodent teeth. Finally, the various applications of stable isotopes in rodent teeth for reconstructing palaeoenvironmental conditions have not been explored in a range of depositional and environmental contexts. Consequently, further testing is required in order to assess the reliability of the paleoenvironmental reconstructions generated from these applications.

1.2.2. Applications of stable isotopes in rodent teeth to reconstructing past environmental variability

Previous applications of stable isotopes in rodent teeth to palaeoenvironmental reconstructions include: 1) using a coupled isotope approach that involves combining the $\delta^{18}O$ values of rodent teeth with the $\delta^{18}O$ values of freshwater carbonates (e.g. mollusc shells) to estimate past seasonal temperatures (Grimes et al., 2003; Grimes et al., 2005), 2) using stratigraphic variations in the $\delta^{18}O$ values of rodent teeth from cave sequences to reconstruct short-term climatic fluctuations (Navarro et al., 2004; Royer et al., 2013b; Royer et al., 2014), and 3) using the $\delta^{13}C$ of carbonate in rodent bioapatite to investigate temporal shifts in vegetation and climate (Hynek et al., 2012; Arppe et al., 2015; Jeffrey, 2016). The first of these applications has been shown to generate reliable palaeotemperature estimates for pre-Quaternary contexts (Fricke & Wing, 2004; Grimes et al., 2005). Therefore, this approach also has the potential to provide quantitative temperature data for the Quaternary period (Grimes et al., 2004). Nevertheless, thus far, this approach has only been applied to Quaternary contexts in two (unpublished) studies (Ruddy, 2005; Peneycad, 2013). Hence, additional testing of this method on material from multiple Quaternary sites is required in order to determine the reliability and applicability of the approach.

Rodent teeth from cave sequences have also received relatively little attention as isotope archives. Hitherto, rodent teeth from caves have been largely used as a palaeoecological proxy, whereby stratigraphic changes in the representation of rodent taxa with different ecological preferences are interpreted in terms of changes in climate (e.g. Hernández Fernández et al., 2007; López-García et al., 2015; Fernández-García et al., 2016). However, recent studies have demonstrated the value of using the $\delta^{18}O$ compositions of rodent teeth from caves for generating quantitative reconstructions of changes in temperature, humidity, and the seasonality of the climate (Navarro et al., 2004; Royer et al., 2013b; Royer et al., 2014; Jeffrey, 2016). Unlike palaeoecological proxy methods, isotope-based climate reconstructions do not rely on the presence or absence of species, which are subject to preservational biases. Independent reconstructions of local

palaeoenvironmental conditions, generated from the stable isotope values of rodent teeth, can therefore potentially be used to validate existing palaeoecological records. Moreover, at many cave sites, rodent remains occur alongside archaeological material. Climate reconstructions generated from the isotope values of rodent teeth can therefore be used to address questions relating to the responses of early humans to environmental changes (Royer et al., 2014; Jeffrey, 2016). Despite this, previous studies have highlighted the difficulties associated with interpreting the $\delta^{18}O$ values of rodent teeth from cave sites in Northwest Europe (Royer et al., 2013b; Royer et al., 2014). Further research on this topic is therefore required in order to assess whether the $\delta^{18}O$ values of rodent teeth from caves can provide reliable records of local and regional palaeoclimatic changes.

Applications of the $\delta^{13}C$ values of rodent bioapatite to Quaternary palaeoenvironmental reconstructions have likewise been sparse. This is likely due to concerns regarding the preservation of isotopic signatures within bioapatite (e.g. Lee-Thorp, 1989; Lee-Thorp & Sponheimer, 2003), and the consequent preference for the analysis of carbon isotopes in bone or tooth collagen (e.g. Gąsiorowski et al., 2014; Reynard et al., 2015). Nevertheless, a small number of studies has shown that the $\delta^{13}C$ values of rodent teeth are capable of providing reliable and valuable records of changes in past vegetation and climate (Hynek et al., 2012; Arppe et al., 2015; Jeffrey, 2016). Additional research would aid in assessing whether the $\delta^{13}C$ values of Quaternary rodent bioapatite are affected by diagenesis, or whether useful palaeoenvironmental information can be obtained from this archive.

In order to utilize these three applications, however, an in-depth understanding of the relationships between the $\delta^{18}O$ and $\delta^{13}C$ values of rodent bioapatite and environmental variables is needed. In particular, the reconstruction of past temperatures by coupling the $\delta^{18}O$ values of rodent teeth and freshwater carbonates requires the use of a modern calibration relating the $\delta^{18}O$ of rodent bioapatite to the $\delta^{18}O$ of meteoric water (Grimes et al., 2008). As mentioned, existing calibrations for this relationship vary significantly. New calibrations are therefore needed in order to establish whether the existing calibrations can provide reliable reconstructions of past $\delta^{18}O_{mw}$ values.

The utilization of the $\delta^{18}O$ and $\delta^{13}C$ values of rodent teeth for palaeoenvironmental reconstructions also requires a knowledge of 1) the factors that contribute to variations in the isotope values of different teeth within a sample, and 2) the magnitudes of the effects that these factors have on the measured $\delta^{18}O$ and $\delta^{13}C$ values of rodent teeth. The key sources of variability in tooth isotopic values are: 1) inter-species differences in the ways in which environmental signals are recorded within rodent teeth, 2) differences in the periods during which rodent teeth, and specifically molars and incisors, mineralize, and 3) variations in the $\delta^{18}O$ of meteoric water and the $\delta^{13}C$ of the diet recorded in teeth from different individuals within a rodent population (Gehler et al., 2012; Royer et al., 2013a). Thus far, few studies have examined the magnitudes of these variations across multiple rodent populations. This issue consequently needs to be addressed in order to develop suitable strategies for sampling fossil rodent teeth for isotopic analysis, and to enable meaningful interpretations of data from the fossil teeth to be made.

This thesis addresses these gaps in our knowledge through two key components. Firstly, a modern analogue study is used to investigate the variability in the $\delta^{18}O$ and $\delta^{13}C$ values of rodent teeth within modern populations, and the relationships between these isotope values and environmental variables. Secondly, the understanding gained from the modern study is used to explore the applications of stable isotopes in rodent teeth for reconstructing Quaternary climate variability. This is achieved via three studies: 1) a study that uses the coupled $\delta^{18}O$ values of rodent teeth and mollusc shells to reconstruct past interglacial temperatures, 2) a study that applies the $\delta^{18}O$ values of rodent teeth from cave sequences to reconstruct short-term climatic fluctuations, and 3) a study that explores temporal variations in the $\delta^{13}C$ values of rodent bioapatite, in relation to potential diagenesis and environmental factors. The aims and objectives related to these studies are outlined in the following section.

1.3. Research aims and strategy

The overall goal of this research is to explore the applications of stable isotopes in rodent dental carbonate for reconstructing Quaternary climate variability. The research aims associated with this goal are:

1. To examine and quantify the relationship between the $\delta^{18}O$ of rodent dental carbonate and the $\delta^{18}O$ of meteoric water in mid-latitude regions.
2. To investigate the magnitudes and causes of variations in the $\delta^{18}O$ and $\delta^{13}C$ values of rodent teeth in modern populations.
3. To test whether coupling the $\delta^{18}O$ values of rodent dental carbonate and mollusc shell aragonite can be routinely used to reconstruct reliable interglacial palaeotemperatures.
4. To investigate whether the $\delta^{18}O$ values of rodent teeth from stratified cave sequences can provide reliable records of short-term palaeoclimatic fluctuations.
5. To assess the potential influences of diagenesis and environmental factors on temporal variations in the $\delta^{13}C$ values of rodent teeth during the Quaternary period.

To address the first and second aims, the $\delta^{18}O$ and $\delta^{13}C$ values of modern vole teeth are investigated at four sites in Britain (Somerset, Surrey, East Yorkshire and Perthshire) that follow a gradient in the $\delta^{18}O$ value of meteoric water. The data generated from this study will be used to develop a modern calibration for the relationship between the $\delta^{18}O$ of rodent dental carbonate and the $\delta^{18}O$ of meteoric water in mid-latitude regions. The reasons for developing this calibration are to: 1) assess the validity of existing calibrations for modern rodents in mid-latitude regions, and 2) provide a new calibration that can be applied to the reconstruction of palaeoclimatic conditions.

The $\delta^{18}O$ and $\delta^{13}C$ values of the modern teeth will additionally be used to investigate: 1) whether the stable isotope values of molars and incisors from modern voles are significantly different, and 2) the magnitudes of the variations in the $\delta^{18}O$ and $\delta^{13}C$ values of vole teeth within modern populations. These investigations are undertaken in order to determine the numbers and types of

teeth that are most suitable for use in the reconstruction of palaeoenvironmental conditions. The findings from the modern study will be applied to the collection and interpretation of the data for Aims 3-5.

To address the third aim, the $\delta^{18}O$ values of fossil vole teeth and mollusc shells from three interglacial sites in Britain (West Runton, Cudmore Grove and Marsworth) are analysed. The modern calibration developed in Aim 1 is used to calculate the $\delta^{18}O$ of past meteoric water at each site. These calculated $\delta^{18}O_{mw}$ values are then coupled with the $\delta^{18}O$ values of fossil shells to generate quantitative estimates of past summer temperatures. These palaeotemperature estimates will be compared and validated against existing palaeoclimate reconstructions for each site, in order assess the reliability of the coupled isotope approach for quantifying past interglacial temperatures.

The fourth aim is explored via the isotopic analysis of vole teeth from two British cave sites (Westbury Cave and Gully Cave). Stratigraphic patterns in the $\delta^{18}O$ values of the teeth will be examined in order to assess whether climatic shifts can be identified in the data. The $\delta^{18}O$ records from the vole teeth will then be compared with the existing palaeoecological records from the caves, plus regional climate records for the intervals during which the cave sequences accumulated. These comparisons will be used to examine whether the $\delta^{18}O$ values of rodent teeth from caves can provide reliable records for short-term climatic variations during the Quaternary period.

The final aim will be addressed by examining the carbon isotope data from all rodent teeth analysed in this thesis. Notable temporal patterns in the data will be identified and explored in relation to the possible contributions of environmental factors to these patterns. The $\delta^{13}C$ values of recent vole teeth from two archaeological sites in Britain (Longstone Edge and Danebury) will additionally be used in order to: 1) assess whether diagenesis may have contributed to differences between the $\delta^{13}C$ values of modern and fossil rodent teeth, and 2) examine recent changes in the $\delta^{13}C$ values of rodent teeth resulting from anthropogenic impacts on the environment.

All of the rodent teeth investigated in this thesis originate from sites in Britain. Britain was chosen as the focus region for this research for three main reasons. Firstly, fossil rodent teeth are abundant at many Quaternary sites in Britain, and thus suitable material is available for isotopic analysis. In addition,

the Quaternary record in Britain has been extensively studied and is well-understood. Consequently, detailed proxy records exist against which isotope-based palaeoenvironmental reconstructions can be compared and tested. Finally, isotope data for rodent teeth from Britain are currently very limited. As aforementioned, Northwest Europe is a key region for understanding global climatic changes, and the stable isotope values of rodent teeth from this region have the potential to provide new proxy records of palaeoclimatic change. There is, therefore, great scope for further research to be undertaken on stable isotopes in small mammal bioapatite from this important region of the world.

1.4. Thesis structure

This thesis is divided into ten chapters. This chapter explains the context and rationale of the research and introduces the research aims. Chapter 2 provides a review of the existing literature on: 1) the processes involved in influencing stable isotope ratios in the terrestrial environment, 2) the relationships between the $\delta^{18}O$ and $\delta^{13}C$ values of biogenic minerals and local environmental factors, and 3) the $\delta^{18}O$ and $\delta^{13}C$ values of modern and fossil rodent bioapatite and their specific uses as palaeoenvironmental proxies. This review provides the context for the interpretation of the data generated from the isotope analyses undertaken in this research, and outlines the current limitations with the existing research on the stable isotope values of rodent bioapatite in further detail. Chapter 3 introduces the modern and Quaternary environmental context of Britain, which is the focus region of this research. The sedimentological, environmental and geochronological contexts of the study sites are also introduced in this chapter in order to justify the selection of these sites for this research. Chapter 4 begins with an overview of the rationale behind the sampling strategies that were employed in the selection of the rodent teeth and mollusc shells for the research, by explaining how the ecological and taphonomic influences on the isotope values of teeth and shells make them suitable as palaeoenvironmental proxies. The chapter subsequently provides a review of the preservation of the biogenic carbonates,

before describing the chemical pre-treatment and analytical methods that were undertaken on the sampled teeth and shells.

Chapters 5-8 present and discuss the results of the research. Chapter 5 presents the results of the modern analogue study on the $\delta^{18}O$ and $\delta^{13}C$ values of modern rodent teeth from four sites across Britain. This chapter explores the significance of $\delta^{18}O$ and $\delta^{13}C$ variability between different teeth within a rodent individual, different individuals within a rodent population, and different populations across a geographical region. The modern relationship between the $\delta^{18}O$ of rodent dental carbonate and the $\delta^{18}O$ of local meteoric water is also investigated, in order to generate a modern calibration that can be applied to the reconstruction of past climatic conditions. The implications for sampling fossil rodent teeth for isotopic analyses, and for using the $\delta^{18}O$ and $\delta^{13}C$ values of rodent teeth as palaeoenvironmental proxies, are discussed.

Chapters 6-8 investigate the applications of stable isotopes in rodent teeth to the reconstruction of Quaternary climate variability. Chapter 6 assesses the reliability of coupling the $\delta^{18}O$ values of rodent teeth and mollusc shells for calculating mean summer palaeotemperatures, using examples from three interglacial sites in Britain. The oxygen isotope and temperature values are compared with existing palaeoclimate data to assess the accuracy and precision of this approach to palaeotemperature quantification. Chapter 7 examines whether the $\delta^{18}O$ values of rodent teeth from stratified cave sequences can provide records of abrupt climatic fluctuations over time, by investigating two cave sites in Britain. The faunal evidence from these sites indicates that the sequences span intervals in which the climate underwent considerable, short-term fluctuations. The $\delta^{18}O$ data from the rodent teeth are compared with this faunal evidence, in order to assess the potential of the proxy for generating new climate records for cave sites that contain important archaeological evidence. Chapter 8 examines the carbon isotope data obtained from all rodent teeth analysed in this research, to explore how Quaternary palaeoenvironmental changes and potential diagenetic alteration have influenced the $\delta^{13}C$ values of biogenic carbonates. Isotope data are also presented from rodent teeth from two British sites, dating to the Bronze Age and Iron Age. The $\delta^{13}C$ values of these teeth are used to assess how recent

anthropogenic impacts are expressed in the stable carbon isotope ratios of mammalian tissues.

Chapter 9 discusses the main findings of the thesis in order to highlight the advantages and limitations of the applications of stable isotopes in rodent teeth to Quaternary palaeoenvironmental research. The possibilities and requirements for further work on this topic are also suggested. Finally, in Chapter 10, the conclusions of the research are outlined in relation to the five key aims of the study.

2. Stable isotopes as palaeoenvironmental proxies

2.1. Introduction

The main focus of this research is in investigating the applications of stable isotopes in small mammal teeth for reconstructing palaeoenvironmental and palaeoclimatic conditions. This chapter therefore introduces the factors that influence oxygen and carbon isotope ratios in hydrological and biological environments. This chapter also explains the processes by which these isotopes are fractionated, from the food and water sources consumed by mammals, to the tissues that they build using these sources. A brief review of isotope fractionation in molluscan shells is also provided. These fractionation processes control the ways in which biogenic carbonates record local environmental conditions, and are therefore key to the understanding and interpretation of the isotope data from the modern and fossil material analysed in this research. Finally, this chapter will review previous research on the stable isotope ratios of modern and fossil small mammal tissues, and their uses in palaeoenvironmental reconstructions.

2.2. Stable isotopes in the terrestrial environment

2.2.1. Oxygen isotopes

Oxygen isotopes in ice cores, marine cores and terrestrial archives have been widely used for the reconstruction of past climatic conditions. This is because the $\delta^{18}O$ value of meteoric water reflects either temperature (in high- and mid-latitude regions) or the amount of precipitation (in low-latitude regions). Oxygen within mammalian tissues is primarily derived from meteoric water that is consumed 1) directly, by drinking surface water sources such as rivers and lakes, and 2) indirectly, from water contained within foods. As a result, environmental factors that fractionate oxygen isotopes in meteoric water,

namely temperature or precipitation, play a key role in influencing the $\delta^{18}O$ values of mammalian tissues. The following sections consequently review the rationale behind the relationship between the $\delta^{18}O$ of meteoric water and climate, in order to aid the interpretation of the $\delta^{18}O$ data from the modern and fossil rodent teeth.

2.2.1.1. $\delta^{18}O$ of precipitation

Meteoric water is derived from precipitation, and this, in turn, is derived from the evaporation of ocean surface water (Figure 2.1). Equilibrium and kinetic processes during evaporation lead to the fractionation of oxygen isotopes, whereby the lighter ^{16}O isotope is more readily evaporated compared to the heavier ^{18}O isotope (Dansgaard, 1964; Gat, 1996). As a result, atmospheric water vapour is depleted in the heavier isotope relative to ocean surface water. Rising water vapour condenses as it cools, leading to the formation of precipitation. Precipitation occurs under Rayleigh distillation conditions, whereby water vapour is continually lost from the air mass in a process known as "rainout" (Figure 2.1) (Dansgaard, 1964; Gat, 1996). Equilibrium fractionation during rainout causes the preferential condensation of ^{18}O (Dansgaard, 1964; Gat, 1996). This results in a depletion in the ratio of ^{18}O to ^{16}O in the air mass relative to precipitation. Continued rainout leads to a linear depletion in the oxygen ($\delta^{18}O$) and hydrogen (δD) isotope ratios of precipitation (Gat, 1996). This linear relationship between $\delta^{18}O$ and δD is described by the Global Meteoric Water Line (GMWL), which is approximated by the following equation (Craig, 1961):

$$\delta D = 8 \times \delta^{18}O + 10 \qquad (2.1).$$

Variability in the $\delta^{18}O$ of precipitation ($\delta^{18}O_{pt}$) along this line is correlated with the degree of rainout relative to the distance from the water vapour source (Rozanski et al., 1993; Gat, 1996). However, the processes that control the extent of rainout are also strongly temperature-dependent, and consequently, variations in $\delta^{18}O_{pt}$ are closely correlated with climate (Dansgaard, 1964; Gat, 1996; Fricke & O'Neil, 1999).

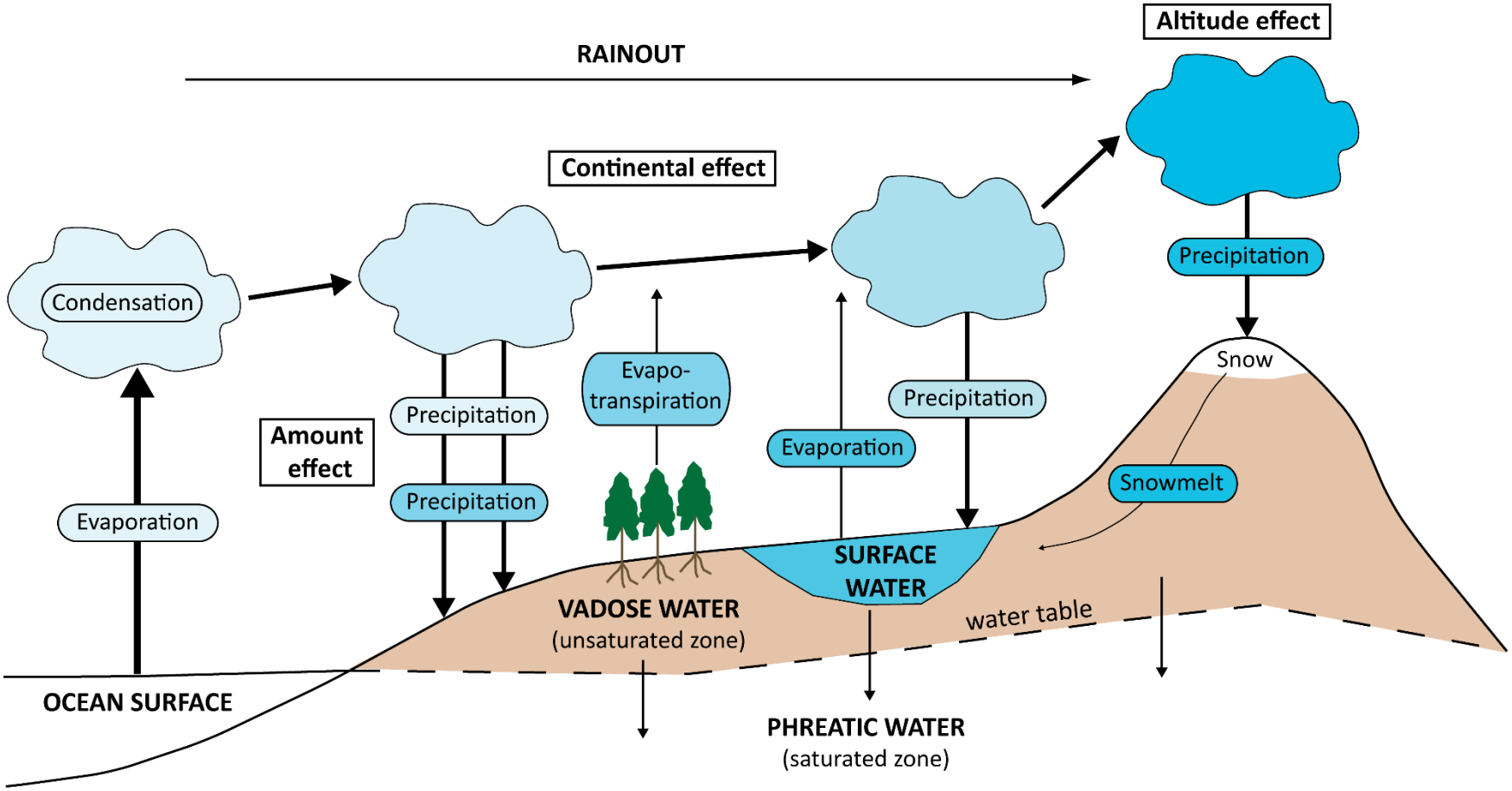

***Figure 2.1**: Diagram illustrating the rainout process. The blue shading indicates the degree of isotopic depletion during rainout; darker shading signifies a greater depletion in $\delta^{18}O$ values. Diagram adapted from Fig. 5 in Gat (1996).*

In his seminal paper, Dansgaard (1964) identified four key parameters that influence $\delta^{18}O_{pt}$: 1) latitude, 2) altitude, 3) amount of rainfall (the "amount effect"), and 4) distance from the moisture source (the "continental effect") (Figure 2.1).

Firstly, the proportion of ^{18}O in condensates from a cooling air mass decreases as its temperature falls and moisture is lost as rain or snow (Dansgaard, 1964). Consequently, mean annual $\delta^{18}O_{pt}$ decreases as the amount of cooling from the vapour source to the site of precipitation increases. This leads to a generally positive correlation between mean air temperature and mean annual $\delta^{18}O_{pt}$, and a general decrease in $\delta^{18}O_{pt}$ with increasing latitude and altitude (Dansgaard, 1964; Rozanski et al., 1993; Fricke & O'Neil, 1999). In mid- and high-latitude regions, mean air temperature and $\delta^{18}O_{pt}$ values correlate well, with an average rate of ~0.55-0.66‰/°C (Dansgaard, 1964; Rozanski et al., 1992; Rozanski et al., 1993; Fricke & O'Neil, 1999; Kohn & Welker, 2005). Consequently, $\delta^{18}O_{pt}$ values also vary seasonally, reaching a maximum during mid-July in areas poleward of 30°N (Dansgaard, 1964; Rozanski et al., 1993; Darling & Talbot, 2003; Feng et al., 2009).

However, the relationship between $\delta^{18}O_{pt}$ and temperature deviates from linearity towards low-latitude regions (Dansgaard, 1964; Rozanski et al., 1993; Fricke & O'Neil, 1999). This is due to the influence of the amount effect, whereby intense convectional precipitation leads to the progressive rainout of the ^{18}O isotope (Figure 2.1) (Dansgaard, 1964). As a consequence, $\delta^{18}O_{pt}$ is negatively correlated with rainfall amount (Rozanski et al., 1993). This effect is mainly predominant in tropical areas, though can also be observed in mid-latitude regions during summer (Dansgaard, 1964; Rozanski et al., 1982; Darling & Talbot, 2003).

For a given mean air temperature, $\delta^{18}O_{pt}$ values also decline with increasing distance from the moisture source (or continentality) (Dansgaard, 1964). This is caused by 1) the progressive rainout of ^{18}O, and 2) the evaporation of $H_2{}^{16}O$ from the surface as an air mass moves overland (Figure 2.1) (Dansgaard, 1964). In Europe, this continental effect is less pronounced during summer, because warm temperatures cause increased evapo-transpiration of the ^{18}O isotope (Rozanski et al., 1982; Jacob & Sonntag, 1991;

Koster et al., 1993). Isotopically-enriched moisture is consequently returned to the atmosphere, thereby reducing the isotopic gradient with continentality.

This effect demonstrates that, in addition to temperature, the recycling of continental moisture via evapo-transpiration has an important influence on seasonal changes in the $\delta^{18}O$ of precipitation (Koster et al., 1993; Field, 2010). Indeed, in mid-latitude regions, the intercept and strength of the $\delta^{18}O_{pt}$-temperature correlation is lower in summer compared to winter (Jacob & Sonntag, 1991; Koster et al., 1993; Fricke & O'Neil, 1999; Field, 2010). The $\delta^{18}O_{pt}$-temperature relationship is, therefore, likely to change according to the climate mode (i.e. interglacial or glacial conditions) (Fricke & O'Neil, 1999; Kohn & Welker, 2005). Moreover, as the primary control on $\delta^{18}O_{pt}$ is the degree of rainout, the location of the moisture source and the transportation history of an air mass will also play key roles in determining $\delta^{18}O_{pt}$ (Rozanski et al., 1982; Lawrence & White, 1991). These factors are closely linked to atmospheric circulation patterns, and thus temporal changes in these patterns can alter the $\delta^{18}O_{pt}$-temperature relationship (Fricke & O'Neil, 1999; Birks & Edwards, 2009; Field, 2010). These issues have led some researchers to question the validity of using modern $\delta^{18}O_{pt}$-temperature relationships to reconstruct palaeotemperature changes (Lawrence & White, 1991; Fricke & O'Neil, 1999). Therefore, additional, independent proxy data are needed in order to understand how the $\delta^{18}O$ values of environmental water and air temperatures have varied over geological timescales. Also, new approaches need to be developed for quantifying robust palaeotemperatures from the $\delta^{18}O$ values of environmental water, which do not rely on the $\delta^{18}O_{pt}$-temperature relationship.

2.2.1.2. $\delta^{18}O$ of meteoric water

Surface meteoric waters are primarily fed by rainfall, and thus their oxygen isotope values ($\delta^{18}O_{mw}$) are a reflection of the $\delta^{18}O$ of precipitation (Darling, 2004). However, the $\delta^{18}O$ values of surface water bodies are modified following precipitation, due to 1) evaporative fractionation, and 2) the mixing of different sources of meteoric water (e.g. precipitation, groundwater, and snowmelt) (Figure 2.1).

Kinetic fractionation during evaporation leads to the preferential loss of the lighter ^{16}O isotope, with a consequent enrichment in $\delta^{18}O_{mw}$ (Craig, 1961; Dansgaard, 1964). The extent of evaporation is dependent upon the duration in which the water is exposed to the atmosphere without addition or replacement (Darling, 2004). For example, a closed, stagnant lake will experience a much greater degree of evaporative enrichment than a fast-flowing stream (Darling et al., 2003; Darling, 2004). Evaporative potential also varies with temperature and atmospheric humidity, such that evaporation is greatest in arid regions and during summer (Clark & Fritz, 1997). The $\delta^{18}O$ values of water bodies that have experienced significant evaporation deviate from the GMWL (Equation 2.1), and instead follow an evaporation line (EL) with a slope of less than 8 (Dansgaard, 1964; Gat, 1996; Clark & Fritz, 1997; Darling et al., 2003). However, in humid regions such as Northwest Europe, the evaporative enrichment of meteoric waters is relatively minor, and isotope values usually fall close to the GMWL (e.g. Darling et al., 2003; Brown et al., 2011; Darling & Bowes, 2016).

The $\delta^{18}O$ values of meteoric water are also dependent on the residence time of the water body. Surface water $\delta^{18}O$ values can fluctuate seasonally, in accordance with temperature-dependent variations in $\delta^{18}O_{pt}$ (Soulsby et al., 2000; Speed et al., 2011). However, seasonal variations in $\delta^{18}O_{pt}$ are dampened in surface water bodies, due to 1) the storage and mixing of water from multiple precipitation events, and 2) inputs from groundwater discharge (Soulsby et al., 2000; Darling et al., 2003; Darling & Bowes, 2016). Infiltrating precipitation is generally well-mixed, and as a consequence, the $\delta^{18}O$ of groundwater typically reflects the long-term mean $\delta^{18}O$ of precipitation (Darling, 2004). Therefore, streams and rivers that are sustained by base flow have relatively constant $\delta^{18}O$ values, with only small inter-annual variations of ~2‰ (Darling et al., 2003). Conversely, water bodies with shorter residence times, or a lesser contribution from groundwater, are more sensitive to short-term fluctuations in $\delta^{18}O_{pt}$ (Darling et al., 2003).

The seasonality of water inputs can also have an important influence on $\delta^{18}O_{mw}$ values. For instance, in areas where aquifer recharge predominantly occurs during winter, the $\delta^{18}O$ of groundwater is weighted towards the lighter isotope values of winter precipitation (Darling & Bath, 1988;

Soulsby et al., 2000; Darling et al., 2003). Surface water sources that are fed by groundwater consequently inherit these depleted $\delta^{18}O$ values (e.g. Soulsby et al., 2000). In high-altitude and high-latitude regions, this depletion is seasonally enhanced due to the input of snowmelt during spring (Figure 2.1) (Soulsby et al., 2000; Darling, 2004). Snow can have highly depleted $\delta^{18}O$ values, because the freezing of water prevents isotopic exchange and equilibration with the atmosphere following its formation at low temperatures (Gat, 1996). Snowmelt events can therefore lead to short-term depletions in $\delta^{18}O_{mw}$ values (Laudon et al., 2002).

In summary, due to the varying influences of evaporation, groundwater discharge, and inputs from snowmelt, the $\delta^{18}O$ values of surface waters vary on both spatial and temporal scales. This variability is likely to be reflected in the $\delta^{18}O$ values of tissues from mammals that consume these meteoric water sources.

2.2.1.3. $\delta^{18}O$ of water in plants

The $\delta^{18}O$ values of tissues from small herbivorous mammals may also be influenced by the $\delta^{18}O$ values of water within their diet. Water in terrestrial plants is obtained through the uptake of soil water from the vadose zone via the plants' roots. No significant isotopic fractionation occurs during this uptake (Wershaw et al., 1966; Zimmerman et al., 1967; Dawson & Ehleringer, 1991), and thus variations in the $\delta^{18}O$ of soil water have a direct influence on the $\delta^{18}O$ composition of a plant (Barbour, 2007). The $\delta^{18}O$ of soil water is derived from precipitation, and is subsequently modified by surface processes (Barbour, 2007). For example, evaporation causes the isotopic enrichment of soil water in the shallow subsurface (< 20 cm depth), whereas the $\delta^{18}O$ values of deeper soil waters (> 50 cm) are relatively unmodified (Gazis & Feng, 2004).

Processes within a plant can also modify the $\delta^{18}O$ of plant water. Due to kinetic fractionation during evapo-transpiration, leaf water $\delta^{18}O$ values are usually significantly enriched relative to the mean $\delta^{18}O_{mw}$ (Dongmann et al., 1974; Epstein et al., 1977; Flanagan et al., 1991). Therefore, leaf-eating mammals will inherit these enriched $\delta^{18}O$ values. This may be especially

significant for herbivorous rodents that predominantly feed on the leaves of shallow-rooted plants (e.g. grasses). This is because the $\delta^{18}O$ of water in these plants will reflect the evaporatively-enriched $\delta^{18}O$ values of shallow soil waters, combined with further isotopic enrichment due to evapo-transpiration.

2.2.1.4. Summary

In mid-latitude regions, the $\delta^{18}O$ value of precipitation is primarily controlled by air temperature. The $\delta^{18}O$ of precipitation also varies spatially according to the relative distance from the moisture source. The $\delta^{18}O$ values of surface meteoric waters parallel variations in $\delta^{18}O_{pt}$, but are modified due to evaporation, groundwater discharge, and snowmelt in high-latitude or mountainous areas. The $\delta^{18}O$ of plant water reflects the $\delta^{18}O$ of meteoric water, but is often further enriched due to evapo-transpiration. Since mammals derive their oxygen from surface meteoric water and plant water sources, the $\delta^{18}O$ values of their tissues will reflect the $\delta^{18}O$ of precipitation, and in turn, air temperature.

2.2.2. Carbon isotopes

The carbon isotope ratios of fossil plant and mammalian tissues have been widely utilized in the reconstruction of past vegetation changes. Small mammals, such as rodents, are predominantly herbivorous, and thus the carbon isotope ratios ($\delta^{13}C$) of their tissues are a reflection of the carbon in the plants that they consume. The $\delta^{13}C$ values of plants are primarily controlled by the photosynthetic pathway that the plant uses (C_3, C_4 or Crassulacean Acid Metabolism), plus spatial and temporal variations in environmental factors (e.g. moisture and light availability, temperature, atmospheric carbon dioxide). In humid regions of northern Europe, the vegetation is dominated by C_3 plants that have been primarily influenced by temporal changes in atmospheric carbon dioxide. The following sections introduce the biological and environmental controls on plant $\delta^{13}C$ values, which determine how the $\delta^{13}C$ values of mammalian tissues relate to environmental factors.

2.2.2.1. $\delta^{13}C$ and plant photosynthesis

The primary control on the $\delta^{13}C$ value of a plant is the pathway by which carbon is fixed during photosynthesis. There are two main photosynthetic pathways: C_3 and C_4. The fixation of the ^{12}C isotope is favoured during photosynthesis, and consequently all plants have $\delta^{13}C$ values that are depleted relative to atmospheric CO_2 (Park & Epstein, 1960; Farquhar et al., 1982; O'Leary, 1988). However, carbon isotopes are fractionated differently through each photosynthetic pathway, and as a result, the $\delta^{13}C$ values of C_3 and C_4 plants fall within distinct and well-defined isotopic envelopes (Figure 2.2) (Bender, 1971; Smith & Epstein, 1971; O'Leary, 1988).

The majority of plants employ the C_3 pathway, which uses the enzyme ribulose bisphosphate carboxylase (RuBisCO) to produce a 3-carbon compound (3-phosphoglycerate) through a process known as the Calvin-Benson cycle (Ehleringer & Cerling, 2002). During this process, RuBisCO strongly discriminates against the heavy ^{13}C isotope, resulting in a large degree of isotopic fractionation between atmospheric CO_2 and the phosphoglycerate product (Park & Epstein, 1960; O'Leary, 1988). Farquhar et al. (1982) developed a model to explain this fractionation process in C_3 plants:

$$\delta^{13}C_p = \delta^{13}C_a - a - (b - a) \times C_i/C_a \qquad (2.2)$$

where $\delta^{13}C_p$ is the carbon isotope value of the plant, $\delta^{13}C_a$ is the carbon isotope value of atmospheric CO_2, a is the isotopic fractionation caused by the slower diffusion of $^{13}CO_2$ through air compared to $^{12}CO_2$, b is the overall isotopic fractionation during carbon fixation by RuBisCO, and C_i/C_a is the ratio of the partial pressure (in ppmv) of CO_2 (pCO_2) in the intercellular air spaces in the leaf (C_i) relative to atmospheric CO_2 (C_a). This model shows that isotopic fractionation occurs in 2 stages: 1) during the uptake of CO_2 from the atmosphere and subsequent diffusion through the leaf, and 2) during the carbon fixation process (Farquhar et al., 1982; O'Leary, 1988). Of these two processes, carbon fixation causes the greatest degree of isotopic fractionation (Wong et al., 1979; O'Leary, 1981; O'Leary, 1988). The result of this fractionation is that modern C_3 plants have global average $\delta^{13}C$ values of

around -28.5‰, with a range spanning -20 to -38‰ (Kohn, 2010). However, most C_3 plants have values between -23 and -32‰, with a mean of around -27‰ (Figure 2.2) (O'Leary, 1988; Kohn, 2010).

In contrast, C_4 plants use the enzyme phosphoenolpyruvate carboxylase (PEP) to capture additional carbon dioxide in the form of 4-carbon compounds, prior to carbon fixation via the Calvin-Benson cycle (O'Leary, 1988; Ehleringer & Cerling, 2002). Carbon fixation is consequently more efficient in C_4 plants, and results in a lesser degree of isotopic fractionation (Smith & Epstein, 1971). Therefore, C_4 plants have heavier $\delta^{13}C$ values, with a global average of around -13‰ and a range from -9 to -20‰ (Figure 2.2) (O'Leary, 1988).

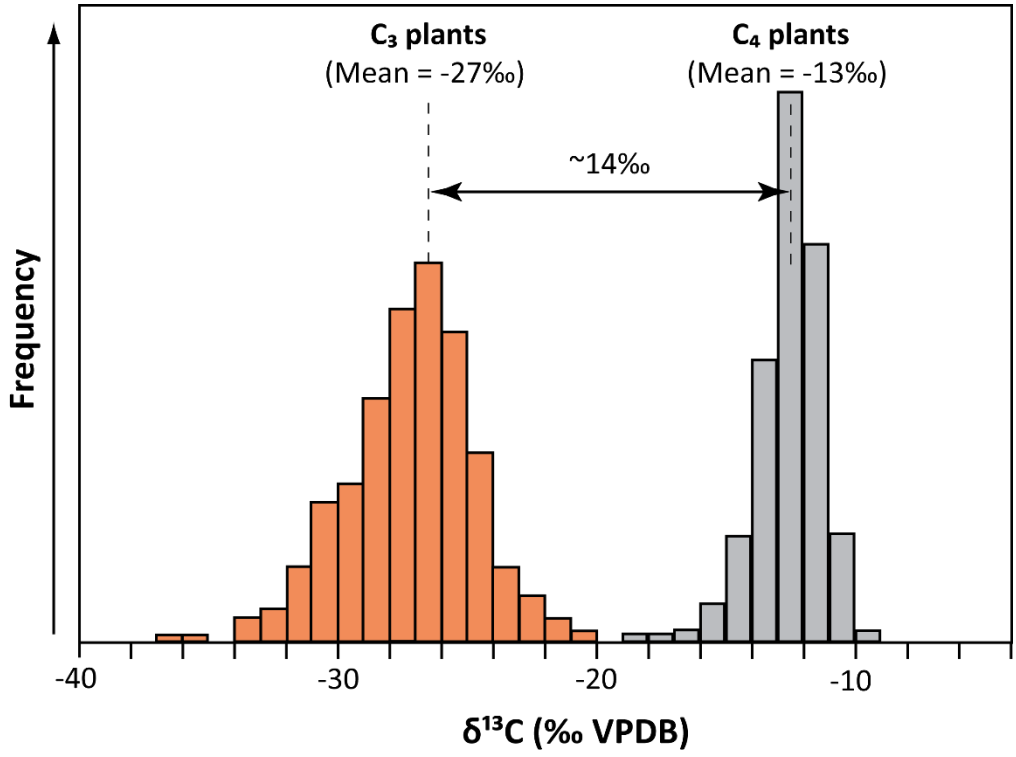

***Figure 2.2**: Carbon isotope values of C_3 and C_4 plants. Diagram adapted from Fig. 3 in Kohn & Cerling (2002) to include new data from Kohn (2010).*

In addition to isotopic differences relating to the photosynthetic pathway, $\delta^{13}C_p$ values vary depending on the taxonomic group and individual plant. For example, studies have found that the $\delta^{13}C$ values of plants of the same species differ by 0-3‰, while different plants within a single community vary by 2-7‰ (Troughton, 1972; O'Leary, 1981; Smedley et al., 1991; Brooks et al., 1997; Heaton, 1999; Diefendorf et al., 2010; Bonafini et al., 2013). This variability results from differences in the physiological responses of plants to the ambient environmental conditions.

Within a plant, the $\delta^{13}C$ values of seeds, roots, fruits and woody stems are consistently ~1-4‰ enriched compared to the leaves (Vogel, 1982; Hobbie & Werner, 2004; Badeck et al., 2005; Cernusak et al., 2009). Rodents, and in particular voles, predominantly feed on the leaves of grasses, though will also eat roots, fruits and seeds (MacDonald & Barrett, 1993). Thus, the average $\delta^{13}C$ composition of the voles' food source may be slightly enriched relative to the average $\delta^{13}C$ of the local vegetation. Moreover, it would be expected that inter-individual differences in the plant species and organs consumed by rodents will lead to variations in the $\delta^{13}C$ values of their teeth.

2.2.2.2. Biogeographical distribution of plants

C_3 plants are taxonomically diverse (comprising all trees, most shrubs and many grasses) and are capable of inhabiting various different environments across the world (Ehleringer & Cerling, 2002). Nevertheless, C_3 photosynthesis is most efficient under elevated atmospheric CO_2 levels and temperatures less than ~22°C (Ehleringer et al., 1997; Ehleringer & Cerling, 2002). As a consequence, C_3 plants are dominant in high- and mid-latitude biomes (Figure 2.3), and comprise nearly 100% of the vegetation across much of northern Europe (Sage & Monson, 1999; Still et al., 2003).

In contrast, the relative efficiency of C_4 photosynthesis enables C_4 plants to thrive in areas with low pCO_2 levels, low moisture availability, and high temperatures (Smith & Epstein, 1971; van der Merwe, 1982; Collins & Jones, 1986; Ehleringer et al., 1997). As a result, C_4 plants are generally restricted to tropical, subtropical and semi-arid regions, where they sometimes

replace C_3 plants as the dominant vegetation type (Figure 2.3) (Sage & Monson, 1999; Still et al., 2003).

Temporal changes in temperature, precipitation and pCO_2 levels have consequently influenced the productivity of C_3 and C_4 plants, leading to shifts in their biogeographical distributions (Teeri & Stowe, 1976; Collins & Jones, 1986; Ehleringer & Cerling, 2001; Rao et al., 2012). Nonetheless, throughout the Late Quaternary period, vegetation in northwest Europe has consisted almost entirely of C_3 plants, as temperatures in this region are generally too low to enable the growth of C_4 plants (Collins & Jones, 1986; Rao et al., 2012). Therefore, the following sections will only consider the influences of environmental factors on C_3 plants.

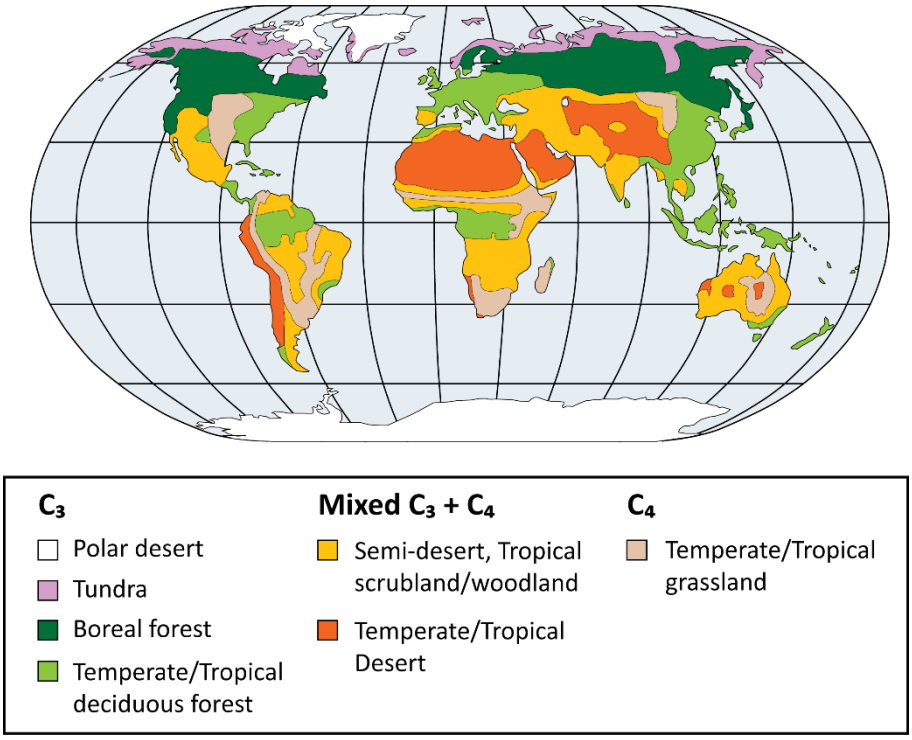

***Figure 2.3**: Biogeographical distribution of C_3 and C_4 plants, according to the major global biomes. Diagram adapted from Fig. 2 in Cerling & Quade (1993).*

2.2.2.3. Environmental influences on the $\delta^{13}C$ of C_3 plants

The broad range in $\delta^{13}C$ values of C_3 plants (Figure 2.2) is due to the sensitivity of these plants to variations in environmental factors. These factors include water and light availability, temperature, vegetation density or the "canopy effect", and the $\delta^{13}C$ value and partial pressure of atmospheric CO_2 (O'Leary, 1981; Tieszen, 1991; Heaton, 1999; Arens et al., 2000). Several of these factors are closely linked to the stomatal conductance of a leaf (Tieszen, 1991). This is because the stomata limit the uptake and loss of CO_2 for photosynthesis, and the loss of water via evapo-transpiration (O'Leary, 1981; Tieszen & Fagre, 1993). Changes in CO_2 concentration or water availability can consequently affect the extent to which the stomata remain open or closed, which in turn influences the partial pressure of CO_2 inside a leaf (C_i) (O'Leary, 1988; Tieszen, 1991; Arens et al., 2000). As demonstrated by Equation 2.2, a change in C_i will result in a corresponding change in $\delta^{13}C_p$. Indeed, studies have shown that a rise in the partial pressure of atmospheric CO_2 (C_a) leads to an increase in C_i and a decrease in plant $\delta^{13}C$ values (Park & Epstein, 1960; Polley et al., 1993; Schubert & Jahren, 2012).

In contrast, the closure of stomata during periods of water stress results in a decrease in C_i, and an increase in $\delta^{13}C_p$ (Farquhar & Richards, 1984; Hubick et al., 1986; Ehleringer & Cooper, 1988; Toft et al., 1989; Arens et al., 2000). As a consequence, the $\delta^{13}C$ values of C_3 plants have a significant negative correlation with precipitation amount (Stewart et al., 1995; Diefendorf et al., 2010; Kohn, 2010; Rao et al., 2017). Nevertheless, moisture availability is only an important factor in areas where the mean annual precipitation is less than ~500 mm/yr (Kohn, 2010). Conversely, in humid mid- and high-latitude regions, precipitation amount has no significant impact on the $\delta^{13}C$ values of C_3 plants (Bonafini et al., 2013).

Similarly, temperature only has a significant impact on $\delta^{13}C_p$ in high-latitude and high-altitude areas (Körner et al., 1991). This is because sub-optimum temperatures limit the rate of CO_2 diffusion into the leaf tissue, resulting in a decrease in C_i and an increase in $\delta^{13}C_p$ (Morecroft & Woodward, 1990; Körner et al., 1991). However, experimental studies indicate that $\delta^{13}C_p$ enrichment at low temperatures is generally small (<1‰) (Smith et al., 1973;

Troughton & Card, 1975; Morecroft & Woodward, 1990). Thus, the influence of temperature on $\delta^{13}C_p$ is minor, and may only be important during large magnitude climatic changes, such as between interglacial and glacial stages.

The $\delta^{13}C$ values of plants also vary with height within a forest canopy. The leaves of understorey plants have $\delta^{13}C$ values that are typically ~2-5‰ more depleted than the leaves in the upper canopy (Vogel, 1978; Medina & Minchin, 1980; Schleser & Jayasekera, 1985; van der Merwe & Medina, 1991). This vertical isotopic gradient is often suggested to result from the mixing of ^{13}C-depleted CO_2, produced during soil respiration processes (-23 to -36‰), with atmospheric CO_2 (~ -8‰) (Vogel, 1978; Medina & Minchin, 1980; Schleser & Jayasekera, 1985; Sternberg, 1989). Carbon dioxide proximal to the soil is consequently isotopically depleted compared to CO_2 at the canopy level. However, the recycling of soil-respired CO_2 is insufficient to explain the depletion in $\delta^{13}C_p$ values; variations in other factors, such as light availability, must also contribute to this effect (Schleser & Jayasekera, 1985; van der Merwe & Medina, 1991; Sternberg, 1989). Low light levels have been shown to cause a depletion in the $\delta^{13}C$ values of shaded plants (Smith et al., 1976; Ehleringer et al., 1986; Zimmerman & Ehleringer, 1990). The degree of isotopic depletion is therefore dependent on the density of vegetation (van der Merwe & Medina, 1991; Bonafini et al., 2013). As a consequence, $\delta^{13}C_p$ values are typically more enriched in open environments compared to the shaded understories of forests (Ehleringer et al., 1986; Bonafini et al., 2013).

The environmental factors discussed in this section are summarised in Table 2.1. It is clear from this table that spatial or temporal changes in these factors may cause significant shifts in the $\delta^{13}C$ values of C_3 plants. In mid-latitude regions, the factors that are likely to have the greatest influence on the $\delta^{13}C$ values of C_3 plants on decadal and centennial timescales are: 1) intra- and inter-species differences in the degree of isotopic fractionation during photosynthesis, 2) spatial variations in vegetation density, and 3) temporal changes in the partial pressure of atmospheric CO_2. On longer timescales, during the Quaternary period, changes in moisture availability and temperature between glacial and interglacial stages may also play a significant role in influencing the $\delta^{13}C$ values of C_3 plants. These variations in $\delta^{13}C_p$ may be inherited by mammalian consumers at higher trophic levels (Heaton, 1999).

Table 2.1: *Summary of the main environmental and ecological factors that can influence the $\delta^{13}C$ values of C_3 plants. References: 1) O'Leary (1981), 2) Smedley et al. (1991), 3) Brooks et al. (1997), 4) Bonafini et al. (2013), 5) Park & Epstein (1960), 6) Polley et al. (1993), 7) Schubert & Jahren (2012), 8) Kohn (2010), 9) Rao et al. (2017), 10) Troughton & Card (1975), 11) Morecroft & Woodward (1990), 12) Körner et al. (1991), 13) Schleser & Jayasekera (1985), 14) Sternberg (1989), 15) Ehleringer et al. (1986), 16) Zimmerman & Ehleringer (1990).*

Factor	**Effect on C_i/C_a**	**Effect on $\delta^{13}C_p$**		**Climatic/Ecological context**	**References**
		Magnitude	**Direction**		
Variation in plant species and growth forms	Increase or decrease	2-7 ‰	Positive or negative	Ecosystem with a variety of plant types (trees, forbs, grasses, deciduous, evergreen)	1-4
Increase in the partial pressure of atmospheric CO_2	Increase	1-3 ‰/100 ppm	Negative	Transition from glacial to interglacial stage	5-7
Reduced water availability/humidity	Decrease	0.2-0.4 ‰/100 mm	Positive	Open environments, semi-arid and arid conditions, glacial conditions	8-9
Low temperature (< 10°C)	Decrease	0-2 ‰	Positive	Polar and high altitude regions, glacial conditions	10-12
Recycling of soil-respired CO_2	Minimal	1-3 ‰	Negative	Dense, closed forest canopies	13-14
Reduced light availability	Increase	2-5 ‰	Negative	Understorey in dense woodlands and forests; shaded areas	13-16

2.2.2.4. $\delta^{13}C$ and atmospheric CO_2

Equation 2.2 demonstrates that both the $\delta^{13}C$ value and partial pressure of atmospheric CO_2 can have important influences on isotopic fractionation in C_3 plants. Temporal changes in these environmental variables may consequently be reflected in plant $\delta^{13}C$ values (Arens et al., 2000).

Atmospheric CO_2 concentrations have varied greatly over the Quaternary period, from ~180-200 ppm during glacials, to ~280-300 ppm during interglacials (Figure 2.4a) (e.g. Petit et al., 1999; Ahn et al., 2004). Records from fossil C_3 plants indicate that $\delta^{13}C_p$ values have fluctuated in response to these pCO_2 changes. For example, $\delta^{13}C_p$ values are ~1-5‰ more enriched during the last glacial stage relative to the current interglacial (Krishnamurthy & Epstein, 1990; Van de Water et al., 1994; Bump et al., 2007). This is due to a ~2‰ reduction in carbon isotope fractionation during photosynthesis under glacial pCO_2 conditions (Schubert & Jahren, 2015).

These changes in pCO_2 were likely accompanied by variations in the $\delta^{13}C$ value of atmospheric CO_2, although Quaternary proxy records for $\delta^{13}C_a$ are relatively scarce (Figure 2.4b). The limited records available suggest that $\delta^{13}C_a$ is ~0.3-1.0‰ lower during cold stages than during temperate stages (Leuenberger et al., 1992; Marino et al., 1992; Elsig et al., 2009; Lourantou et al., 2010; Eggleston et al., 2016). This depletion is thought to result from a reduction in the productivity and storage of organic carbon (^{12}C) in the biosphere and oceans during cold stages (Marino et al., 1992; Elsig et al., 2009). Experimental studies have shown that $\delta^{13}C_p$ values are strongly positively correlated with $\delta^{13}C_a$ (Marino & McElroy, 1991; Arens et al., 2000; Jahren et al., 2008). Consequently, $\delta^{13}C_p$ values are expected to have declined during glacial stages, in response to the depleted $\delta^{13}C$ values of atmospheric CO_2 (e.g. Marino et al., 1992).

However, there is a strong covariance between pCO_2 and $\delta^{13}C_a$ (Arens et al., 2000). This poses difficulties for differentiating the influences of these variables on temporal shifts in the $\delta^{13}C$ values of biogenic material. Nevertheless, Arens et al. (2000) suggest that when C_3 plants are grown under controlled conditions, > 90% of the variation in $\delta^{13}C_p$ is explained by variations

in $\delta^{13}C_a$. This relationship holds, regardless of variations in temperature and pCO_2 (Jahren et al., 2008).

Despite this, the majority of studies find that the $\delta^{13}C$ values of plant and mammal tissues are more enriched during the last glacial period than during the Holocene (Figure 2.4c) (Krishnamurthy & Epstein, 1990; Van de Water et al., 1994; Stevens & Hedges, 2004; Bump et al., 2007; Hare et al., 2018). This is the opposite of the effect expected from changes in $\delta^{13}C_a$. This is likely because glacial-interglacial variations in plant $\delta^{13}C$ values reflect the combined effects of multiple environmental factors, including pCO_2, $\delta^{13}C_a$, temperature and humidity. During glacial periods, depleted $\delta^{13}C_a$ values result in a decrease in $\delta^{13}C_p$. However, this effect is mediated by the declines in pCO_2, temperature and precipitation, which cause an increase in $\delta^{13}C_p$. Understanding the combined influences of these factors is therefore essential for interpreting past changes in the $\delta^{13}C$ values of C_3 plants and herbivorous mammals (Schubert & Jahren, 2015; Hare et al., 2018).

In addition to these glacial-interglacial variations, pCO_2 and $\delta^{13}C_a$ have undergone recent shifts as a result of anthropogenic activities since the Industrial Revolution. The $\delta^{13}C$ value of atmospheric CO_2 has declined by ~2‰ over the past 150-200 years, from pre-industrial values of -6.5‰, to modern values of around -8.5‰ (Figure 2.4b) (Friedli et al., 1986; Francey et al., 1999; Rubino et al., 2013; Graven et al., 2017). This decline results from the release of ^{12}C-enriched CO_2 into the atmosphere, produced from the anthropogenic burning of fossil fuels. Fossil fuel burning has also led to an increase in pCO_2 levels of ~120 ppm over the same period (Figure 2.4a) (Rubino et al., 2013). These atmospheric changes have correspondingly been recorded in the $\delta^{13}C$ values of plants and mammalian tissues, with declines of ~0.8-2.0‰ over the past ~150 years (Stuiver et al., 1984; Marino & McElroy, 1991; Cerling & Harris, 1999; Berninger et al., 2000; Saurer et al., 2004; Long et al., 2005; Bump et al., 2007).

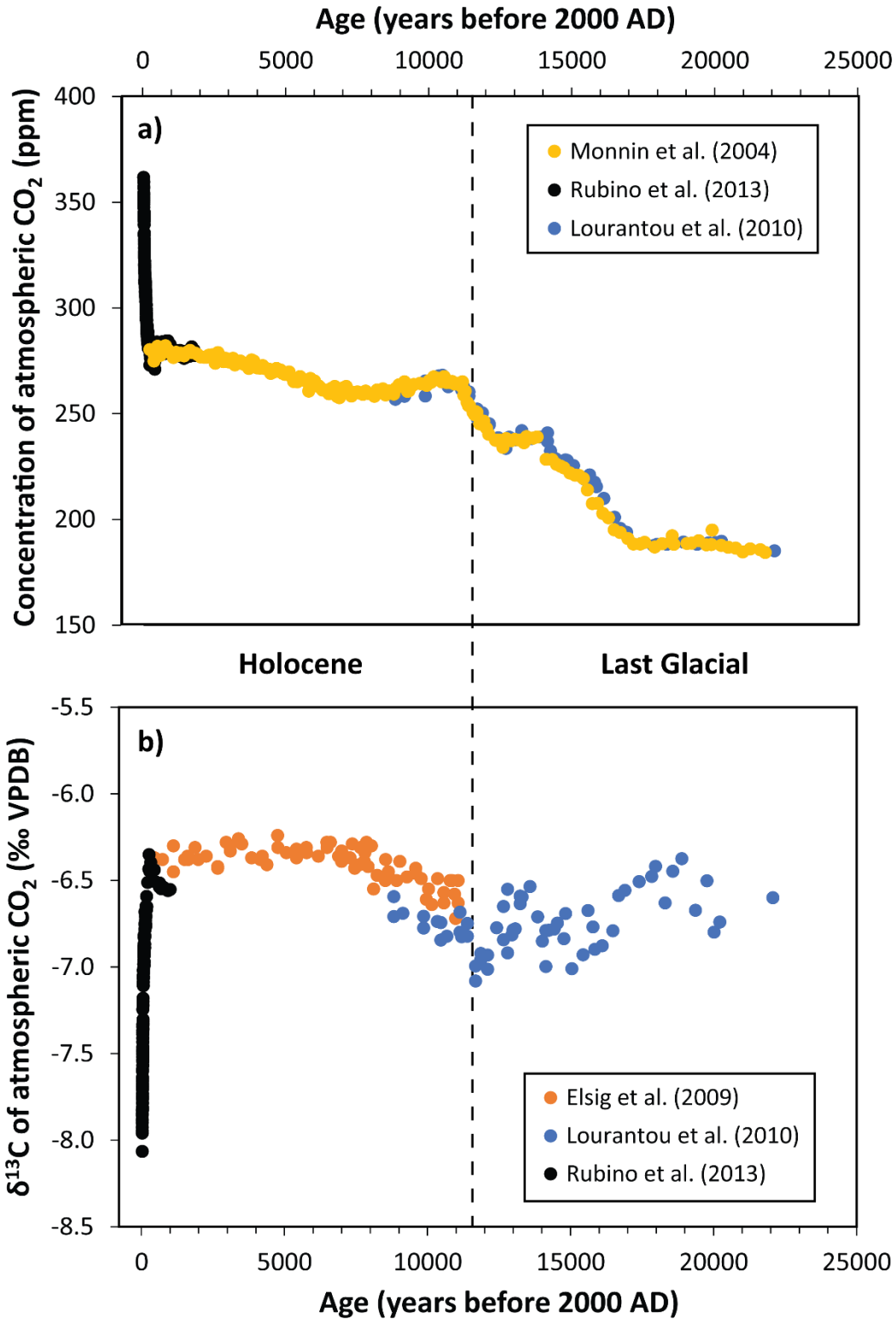

Figure 2.4. *(for caption see overleaf)*

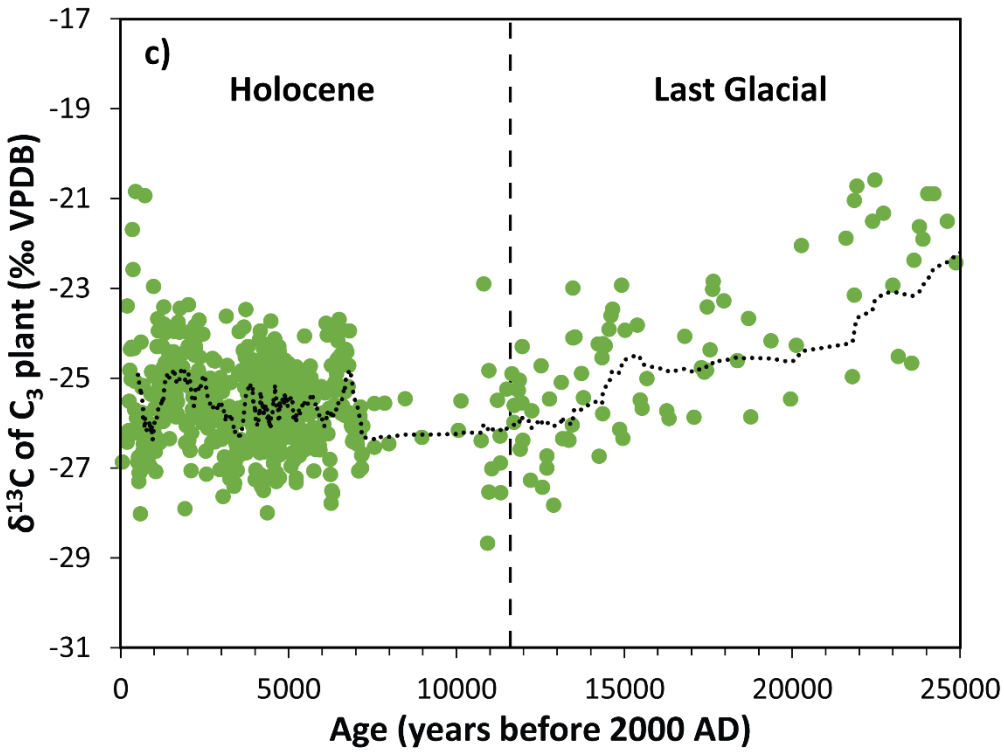

Figure 2.4: *Changes over the past 25,000 years in: a) the partial pressure (or concentration) of atmospheric CO_2, b) the $\delta^{13}C$ value of atmospheric CO_2, recorded in Antarctic ice cores, and c) the $\delta^{13}C$ values of C_3 plants. Graph c is based upon data presented in Hare et al. (2018), which was adapted from the following original sources: Yapp & Epstein (1977), Krishnamurthy & Epstein (1990), Vogel et al. (1993), Van de Water et al. (1994), McCormac et al. (1994), and Pearson et al. (2014). The black dotted line in graph c is a 20 year moving average through the data.*

Due to these shifts in atmospheric CO_2, several studies have recommended that $\delta^{13}C$ data from modern and fossil mammalian tissues should be corrected for temporal changes in the isotopic baseline (e.g. Long et al., 2005; Casey & Post, 2011). These corrections are essential for 1) comparing mammalian $\delta^{13}C$ data from different time intervals, and 2) identifying $\delta^{13}C$ changes that result from variations in climate. Therefore, in Chapter 8, the $\delta^{13}C$ values of the modern and fossil rodent teeth will be adjusted for temporal changes in $\delta^{13}C_a$ and pCO_2, after the methods of Hare et al. (2018). These corrections were made using $\delta^{13}C_a$ and pCO_2 datasets from Antarctic ice core records (Monnin et al., 2004a; Rubino et al., 2013;

Eggleston et al., 2016; Graven et al., 2017). Further details regarding these corrections are provided in Chapter 8.

2.2.2.5. $\delta^{13}C$ in meteoric water

While herbivorous land animals obtain their carbon directly from plants, the $\delta^{13}C$ values of freshwater carbonates are related to the isotopic value of Dissolved Inorganic Carbon (DIC) in meteoric waters (Andrews et al., 1993; Aucour et al., 2003; Leng & Marshall, 2004). In lowland areas of Europe, DIC is predominantly derived from the dissolution of CO_2 generated from the respiration of organic matter in local soils (Andrews et al., 1993; Andrews et al., 1997; Darling & Bowes, 2016). Decaying C_3 plant matter produces soil CO_2 with an average $\delta^{13}C$ value of around -25 to -27‰ (Schleser & Jayasekera, 1985; Cerling et al., 1991). DIC in meteoric water is in equilibrium with soil CO_2, but is isotopically discriminated by +8-10‰ at 25°C (Emrich et al., 1970; Romanek et al., 1992). As a result, the $\delta^{13}C$ of DIC is enriched compared to soil CO_2 (Andrews et al., 1993).

The $\delta^{13}C$ of DIC is typically further enriched due to the input of isotopically-heavy bicarbonate ions derived from the dissolution of marine limestone bedrock (Deines et al., 1974; Andrews et al., 1993). Marine limestones usually have $\delta^{13}C$ values of ~0‰ (Deines et al., 1974; Hudson, 1977). In lowland streams and rivers, the mixing of isotopically-depleted soil CO_2 with isotopically-enriched limestone results in $\delta^{13}C$ values of around -12 to -15‰ (Deines et al., 1974; Darling & Bowes, 2016).

In water bodies with longer residence times (e.g. closed-basin lakes), the equilibration of DIC (minimum $\delta^{13}C$ = -16‰) with atmospheric CO_2 ($\delta^{13}C$ = -8.5‰ at present) also leads to an enrichment in $\delta^{13}C$ values (Andrews et al., 1993). This process, known as degassing, favours the loss of $^{12}CO_2$ from the water body (Andrews, 2006), and can result in DIC $\delta^{13}C$ values of +0-3‰ (Andrews et al., 1993; Leng & Marshall, 2004).

Enriched $\delta^{13}C$ values of DIC can also be associated with a similar enrichment in the $\delta^{18}O$ value of the water (Fritz & Poplawski, 1974; Talbot, 1990). This co-variance between $\delta^{18}O$ and $\delta^{13}C$ has been suggested to relate

to the degree of hydrological “closure” of a lake basin (Talbot, 1990; Li & Ku, 1997). In lakes that have been hydrologically isolated for a long period of time (e.g. several thousand years), or in which the lake volume is declining due to net evaporation, evaporative fractionation will cause an enrichment in $\delta^{18}O_{mw}$ (Li & Ku, 1997). This evaporation will also cause the $\delta^{13}C$ of DIC to become enriched, as a reduction in lake volume leads to an increase in the concentration of dissolved CO_2 within the water, and this, in turn, results in CO_2 degassing (Li & Ku, 1997; Horton et al., 2016). Therefore, the correlation between the $\delta^{18}O$ and $\delta^{13}C$ values of fossil meteoric carbonates can potentially be used as an indicator of the hydrological closure and evaporation of a former water body.

2.2.2.6. Summary

Vegetation in northern Europe primarily consists of plants that use the C_3 photosynthetic pathway. The $\delta^{13}C$ values of these plants are, on average, around -27 to -28.5‰ at the present day. However, $\delta^{13}C_p$ values have varied during the Quaternary period, due to fluctuations in the $\delta^{13}C$ value and partial pressure of atmospheric CO_2. A particularly notable shift in atmospheric CO_2 has occurred over the past 200 years, due to the anthropogenic burning of fossil fuels. Corrections must consequently be applied to the $\delta^{13}C$ values of modern plants and mammals, to enable comparisons to be made with data from fossil material. Temporal fluctuations in moisture and temperature may have also influenced $\delta^{13}C_p$ values during the Quaternary period. On the other hand, inter-species differences in $\delta^{13}C$ fractionation and variations in vegetation density can result in spatial variability in the $\delta^{13}C$ values of C_3 plants. Due to the combined effects of these environmental factors, the average $\delta^{13}C$ values of plants generally increase during cold stages and decrease during warm stages, although there is a significant degree of scatter around these average values (Figure 2.4).

The $\delta^{13}C$ values of freshwater carbonates reflect the $\delta^{13}C$ of dissolved inorganic carbon in meteoric water. This, in turn, reflects the average isotopic value of carbon derived from soil-respired CO_2, isotopically-enriched marine carbonates, and atmospheric CO_2.

2.3. Stable isotopes in biogenic minerals

2.3.1. Mammalian dental tissues

Mammalian teeth are predominantly composed of crystals of a calcium phosphate mineral that has a structure analogous to hydroxyapatite [$Ca_5(PO_4)_3(OH)$], and which is known as bioapatite (Hillson, 2005). Teeth contain two main types of dental tissue: 1) a tough outer core of enamel, comprising ~96% bioapatite, ~3% water, and ~1% organic matter (by weight), and 2) an inner core of dentine, which consists of 70-75% bioapatite, 5-10% water, and ~20% organic matter (Williams & Elliott, 1989; Driessens & Verbeeck, 1990; Hillson, 2005). The bioapatite within each tissue is composed of crystallites, which are single, microscopic mineral crystals that form a regular structure. Enamel has a compact structure composed of long crystallites (>1000 nm), whereas dentine is more porous, comprising shorter crystallites (20-100 nm) and collagen, a fibrous protein (Hillson, 2005). Bone has a similar structure to dentine, consisting of collagen mineralized within hydroxyapatite.

Phosphate is a dominant component of hydroxyapatite, and is the mineral ion most often analysed in studies investigating the $\delta^{18}O$ values of mammalian bones and teeth. However, modern mammalian bioapatite also contains approximately 2-5% carbonate by weight (Rink et al., 1996; Koch et al., 1997; Sponheimer & Lee-Thorp, 1999; Zazzo et al., 2004a). Carbonate ions (CO_3^{2-}) substitute into two sites within the hydroxyapatite crystal structure: 1) the hydroxyl (OH^-) sites, in which ~10% of the carbonate ions are weakly bound (Type A carbonate), and 2) the phosphate (PO_4^{3-}) sites, in which the remaining ~90% of the carbonate ions reside to form 'structural carbonate' (Type B carbonate) (Elliott et al., 1985; Sonju Clasen & Ruyter, 1997). This carbonate originates from the exchange of bicarbonate ions (HCO_3^-), dissolved within the blood, with the hydroxyapatite mineral. Carbonate within bioapatite is consequently in isotopic equilibrium with both oxygen and carbon in the blood.

2.3.2. $\delta^{18}O$ in mammalian bioapatite

The oxygen isotope value of mammalian bioapatite is related to: 1) the $\delta^{18}O$ value of the mammal's body water ($\delta^{18}O_{bw}$), and 2) the body temperature during bioapatite mineralization (Figure 2.5) (Longinelli, 1984; Luz et al., 1984; Luz & Kolodny, 1985). Since mammals are endotherms, body temperature remains relatively constant at 37°C, although in the case of small mammals, this can vary by ± 2°C (Lovegrove, 2003). On the other hand, the $\delta^{18}O$ of the body water is controlled by the $\delta^{18}O$ values of the various inputs and outputs of oxygen to and from the body (Figure 2.5) (Luz et al., 1984; Luz & Kolodny, 1985; Bryant & Froelich, 1995; Kohn et al., 1996). However, the primary control on $\delta^{18}O_{bw}$ is thought to be the $\delta^{18}O$ value of the drinking water source ($\delta^{18}O_{dw}$) (Longinelli, 1984; Luz et al., 1984).

During the transport of oxygen from the external source to mammalian bioapatite, oxygen isotopes are fractionated via two stages: 1) during the formation of body water, and 2) during the mineralization of bioapatite (Figure 2.5) (Luz et al., 1984). The degree of isotope fractionation during stage 1 is dependent upon the rates of drinking and respiration of the mammal, which vary in accordance with body size and animal physiology (Luz et al., 1984; Bryant & Froelich, 1995; Kohn et al., 1996). In general, as body size increases, the importance of drinking water to the total oxygen flux also increases, such that $\delta^{18}O_{bw}$ approaches the average $\delta^{18}O$ of total ingested water (Bryant & Froelich, 1995).

However, food water can also constitute a significant proportion of the total oxygen intake from which $\delta^{18}O_{bw}$ is derived (Kohn et al., 1996; Podlesak et al., 2008). Plant water sources are usually enriched in $\delta^{18}O$ due to evapotranspiration (see Section 2.2.1.3). The consumption of these sources by non-obligate drinkers therefore results in $\delta^{18}O_{bw}$ values that are enriched compared to mammals that drink frequently. Small mammals are less dependent upon drinking compared to larger mammals, and thus food water may have an important influence on $\delta^{18}O_{bw}$ in these organisms (Bryant & Froelich, 1995). Nevertheless, Podlesak et al. (2008) report that in the woodrat [*Neotoma cinerea* (Ord, 1815)], a small rodent, 56% of the oxygen atoms in body water are derived from drinking water, whereas only 15% are derived from food

water. The remaining 30% originates from metabolic oxygen. Therefore, in small mammals, drinking water is likely to be the major contributor to $\delta^{18}O_{bw}$ (Figure 2.5).

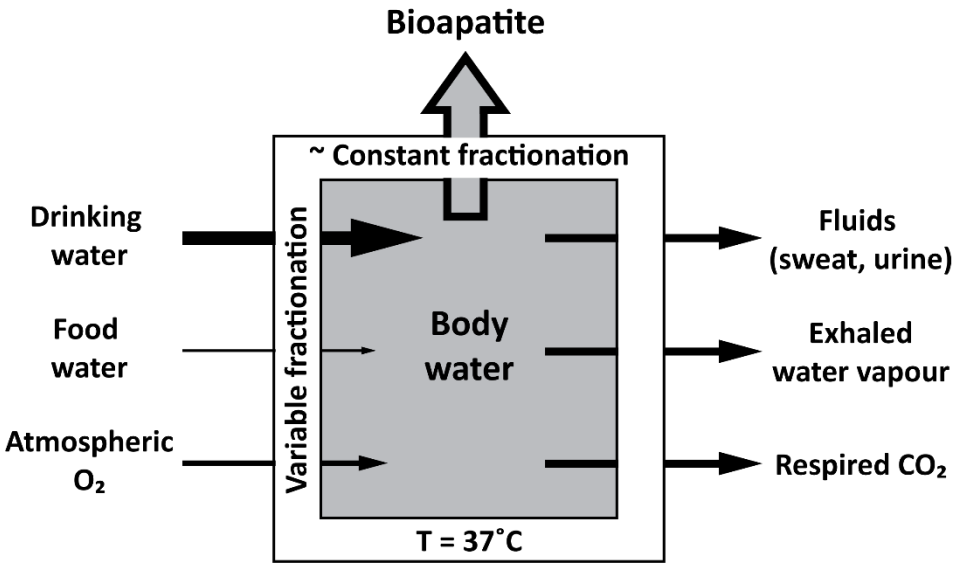

Figure 2.5: *Schematic diagram showing the oxygen fluxes with body water (adapted from Fig. 2 in Luz et al., 1984). The thickness of each arrow indicates the relative contribution of the oxygen source to the $\delta^{18}O$ of rodent body water (based on Podlesak et al., 2008).*

Podlesak et al. (2008) also found that oxygen in the body water of woodrats has a relatively rapid turnover rate; $\delta^{18}O_{bw}$ reaches a steady state within 1-2 weeks following a switch in the $\delta^{18}O$ of drinking water. Similar turnover rates have been measured in experimental studies on laboratory rats (Longinelli & Peretti Padalino, 1980; Luz et al., 1984). This indicates that $\delta^{18}O_{bw}$ in rodents is highly sensitive to variations in the $\delta^{18}O$ values of drinking water, and by extension, changes in climate. Furthermore, due to the constant turnover of oxygen within the body, the short delay in the response of $\delta^{18}O_{bw}$ to changes in $\delta^{18}O_{dw}$ (1-2 weeks), and the rapid maturation of rodent enamel (~2 weeks), there is a minimal time-averaging of the $\delta^{18}O_{mw}$ signal recorded in mineralizing rodent teeth (Kohn, 2004). Consequently, the $\delta^{18}O$ values of

rodent teeth can potentially be used to understand seasonal changes in the $\delta^{18}O$ of meteoric water (Royer et al., 2013a).

During the second stage of fractionation, bioapatite mineralizes in isotopic equilibrium with body water (Luz et al., 1984). As a result, the $\delta^{18}O$ value of bioapatite is offset from $\delta^{18}O_{bw}$ and $\delta^{18}O_{dw}$, but is linearly correlated with both of these variables (Longinelli, 1984; Luz et al., 1984; Luz & Kolodny, 1985). However, the relationship between the $\delta^{18}O$ of bioapatite and $\delta^{18}O$ of drinking water varies between mammalian taxa (e.g. D'Angela & Longinelli, 1990). Conversely, the fractionation factor between the $\delta^{18}O$ of bioapatite and the $\delta^{18}O$ of body water is relatively constant in both small and large mammals (Luz et al., 1984; D'Angela & Longinelli, 1990; Longinelli et al., 2003; Podlesak et al., 2008). Therefore, most of the variability in the $\delta^{18}O$ relationship between bioapatite and drinking water results from the influence of inter-taxon differences in biology (e.g. rates of drinking and respiration) on body water $\delta^{18}O$ (Figure 2.5).

The $\delta^{18}O$ of bioapatite also varies depending on the mineral ion (carbonate or phosphate) that is analysed. Data from modern bioapatite indicate a strong correlation between the $\delta^{18}O$ values of carbonate and phosphate (Figure 2.6) (Iacumin et al., 1996; Martin et al., 2008; Pellegrini et al., 2011). This suggests that both of these mineral ions form in isotopic equilibrium with body water (Iacumin et al., 1996). However, the $\delta^{18}O$ of carbonate is ~7-11‰ enriched compared to phosphate (Figure 2.6) (Iacumin et al., 1996; Martin et al., 2008; Lécuyer et al., 2010). This $\delta^{18}O$ offset between the two mineral ions results from differences in the magnitude of fractionation during mineral formation, due to differences in the molar masses of carbonate and phosphate (Martin et al., 2008).

The carbonate-phosphate offset also varies within and between species (Martin et al., 2008; Pellegrini et al., 2011). For example, in water vole bioapatite [*Arvicola terrestris* (L., 1758)] the offset is 10.9 ± 0.9‰ (Gehler et al., 2012), whereas in laboratory rats, the offset varies between 8.5 and 11.4‰ (Kirsanow & Tuross, 2011). Therefore, the $\delta^{18}O$ values of carbonate and phosphate in rodent bioapatite are expected to have comparable correlations with $\delta^{18}O_{dw}$, but with an offset of ~8-11‰. A study by Lécuyer et al. (2010) also demonstrated that the carbonate-water and phosphate-water oxygen isotope

relationships approximately parallel each other, but are offset by 7.5‰ at 37°C (body temperature). Nevertheless, this study used inorganically-precipitated hydroxyapatite, as opposed to biogenic carbonate, to determine the carbonate-water relationship. Consequently, the fractionation relationship between the $\delta^{18}O$ of carbonate in mammalian bioapatite and the $\delta^{18}O$ of environmental water has not hitherto been quantified for mid-latitude regions. Thus, the comparability of the carbonate-water and phosphate-water $\delta^{18}O$ relationships in mammals is currently untested.

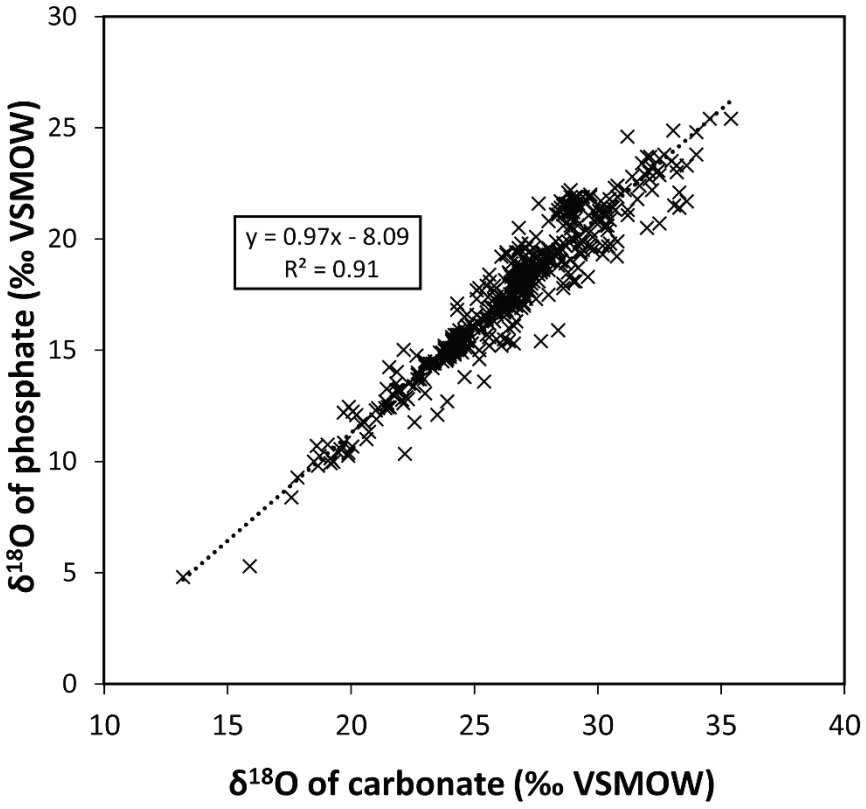

Figure 2.6: *Plot showing the correlation between the $\delta^{18}O$ of phosphate and $\delta^{18}O$ of carbonate in mammalian bioapatite. Data sourced from: Bryant et al. (1996), Iacumin et al. (1996), Shahack-Gross et al. (1999), Fox & Fisher (2001), Jones et al. (2001), Iacumin et al. (2004a, b), Sanchez et al. (2004), Zazzo et al. (2004a), Martin et al. (2008), Kirsanow & Tuross (2011) Pellegrini et al. (2011); Chenery et al. (2012), and Gehler et al. (2012).*

In summary, the $\delta^{18}O$ of mammalian bioapatite is primarily related to the $\delta^{18}O$ value of drinking water, but this relationship varies depending on 1) the taxon and 2) the mineral ion of bioapatite. Consequently, the $\delta^{18}O$ values of fossil mammalian teeth can potentially be used as a proxy for the past $\delta^{18}O$ of meteoric water, provided that a modern calibration is available that is specific to the taxon and mineral ion being investigated.

2.3.3. $\delta^{13}C$ in mammalian bioapatite and collagen

Isotopic relationships in food resources are inherited by organisms at higher trophic levels, and as a result, the $\delta^{13}C$ values of mammalian tissues can provide a proxy for the $\delta^{13}C$ composition of a mammal's diet (DeNiro & Epstein, 1978; van der Merwe, 1982; Tieszen et al., 1983; Jim et al., 2004). For herbivorous mammals such as rodents, the $\delta^{13}C$ value of a tissue will reflect the $\delta^{13}C$ values of the plants consumed during tissue formation. As discussed in Section 2.2.2., the $\delta^{13}C$ composition of a herbivore's diet will also be dependent on the dietary preferences of the animal (e.g. leaves vs. stems), the plant types (C_3 or C_4) and species available for consumption, and the ambient environmental conditions that influence $\delta^{13}C_p$ values (Ehleringer & Cerling, 2002). Consequently, the $\delta^{13}C$ values of mammalian tissues can potentially provide an indication of palaeoenvironmental changes (van der Merwe, 1982).

Carbon isotopes are fractionated within the body during tissue formation. As a result, the $\delta^{13}C$ values of bioapatite and collagen are enriched relative to the diet (DeNiro & Epstein, 1978; Krueger & Sullivan, 1984; Lee-Thorp et al., 1989; Jim et al., 2004). The $\delta^{13}C$ fractionation between the tissue and the diet is commonly expressed as an enrichment factor (ε), which can be calculated using the following equations (Passey et al., 2005):

$$\alpha_{tissue\text{-}diet} = \frac{1000 + \delta_{tissue}}{1000 + \delta_{diet}} \quad (2.3)$$

$$\varepsilon_{tissue\text{-}diet} = (\alpha_{tissue\text{-}diet} - 1) \times 1000 \quad (2.4)$$

where α is the fractionation factor, and ε is the enrichment factor. Nevertheless, the magnitude of the enrichment factor varies depending on the tissue type (DeNiro & Epstein, 1978; Tieszen et al., 1983; Jim et al., 2004). This is because each tissue is built from different types and proportions of macronutrients (carbohydrates, lipids and proteins) (Krueger & Sullivan, 1984; Ambrose & Norr, 1993; Tieszen & Fagre, 1993). These macronutrients have different isotopic compositions and follow different routes within the body (Figure 2.7).

Experimental and modelling studies have demonstrated that carbon within herbivore bioapatite is primarily derived from plant carbohydrates, with minor contributions from lipids and proteins (Krueger & Sullivan, 1984; Ambrose & Norr, 1993; Tieszen & Fagre, 1993). These dietary components are metabolized to form CO_2, which is then transported in the blood as dissolved inorganic carbon (DIC) (Krueger & Sullivan, 1984). Since blood DIC is used in the formation of structural carbonate within bioapatite, the $\delta^{13}C$ of bioapatite can provide a valuable indicator of the average $\delta^{13}C$ value of the whole diet (Krueger & Sullivan, 1984; Ambrose & Norr, 1993; Tieszen & Fagre, 1993; Jim et al., 2004).

Field and laboratory studies on large herbivorous mammals have reported enrichment factors between bioapatite carbonate and the diet ($\varepsilon_{apatite\text{-}diet}$) of 12-15‰ (Sullivan & Krueger, 1981; Krueger & Sullivan, 1984; Lee-Thorp et al., 1989; Cerling & Harris, 1999; Passey et al., 2005). In contrast, controlled feeding experiments indicate a smaller enrichment factor in rodents, with values between 9.5 ± 0.96‰ for mice and rat bones (see Appendix A), 11.0 ± 0.09‰ for woodrat teeth (Podlesak et al., 2008), and 11.5 ± 0.15‰ for vole teeth (Passey et al., 2005). This variability in the enrichment factor results from inter-taxon differences in digestive physiology, and differences in the period of mineralization between bones and teeth (Passey et al., 2005). Since the present research involved analyses of vole teeth, the enrichment factor determined by Passey et al. (2005) is considered the most appropriate for the calculation of dietary $\delta^{13}C$ values in this thesis.

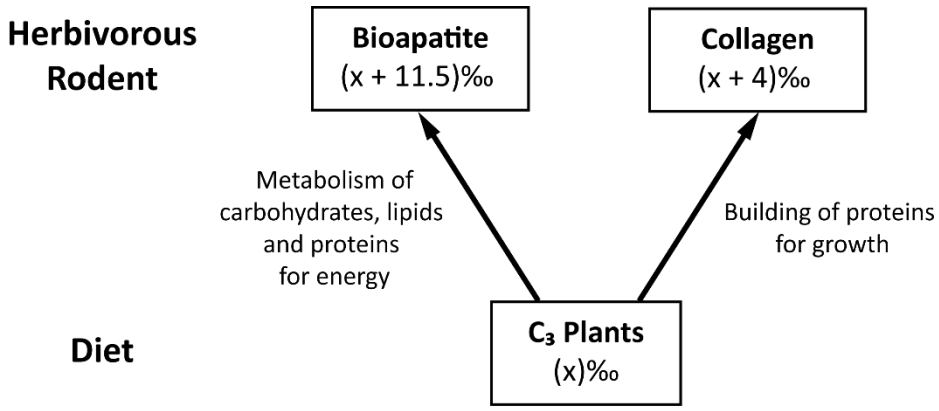

Figure 2.7: *Schematic illustrating the carbon isotope fractionation between a C_3 diet and rodent bioapatite and collagen (adapted from Fig. 2 in Krueger & Sullivan, 1984).*

While the $\delta^{13}C$ of bioapatite records the carbon isotope composition of the whole diet, the $\delta^{13}C$ of collagen reflects carbon derived from dietary protein (Figure 2.7) (Krueger & Sullivan, 1984; Ambrose & Norr, 1993; Jim et al., 2004). The $\delta^{13}C$ enrichment factor between bone collagen and the diet ($\varepsilon_{collagen\text{-}diet}$) is much less than $\varepsilon_{apatite\text{-}diet}$, with values of ~5‰ in large mammals (Krueger & Sullivan, 1984; Lee-Thorp et al., 1989), and 3.9 ± 0.60‰ for mice and rats fed on a pure C_3 diet (see Appendix A). The average $\delta^{13}C$ fractionation between bone collagen and bioapatite carbonate ($\Delta^{13}C_{apatite\text{-}collagen}$) is consequently around +7-9‰ in large herbivorous mammals (Sullivan & Krueger, 1981; Krueger & Sullivan, 1984; Lee-Thorp et al., 1989), and +6.0 ± 0.65‰ in mice and rats (see Appendix A). Similar $\Delta^{13}C_{apatite\text{-}collagen}$ offsets of +4-9‰ have also been reported in modern wild gerbils (Jeffrey, 2016).

In summary, the $\delta^{13}C$ value of mammalian bioapatite reflects the average $\delta^{13}C$ of the whole diet, while the $\delta^{13}C$ value of collagen reflects the $\delta^{13}C$ of dietary protein. The enrichment between rodent bioapatite carbonate and the diet is ~11.5‰, and the enrichment between rodent collagen and a C_3 diet is ~3.9‰. Since rodents, and specifically voles, are predominantly herbivorous, the $\delta^{13}C$ values of their tissues can be used to reconstruct changes in the $\delta^{13}C$ values of plants.

2.3.4. Stable isotopes in molluscan shell carbonate

2.3.4.1. Oxygen isotopes

Molluscan shell carbonates mineralize in isotopic equilibrium with the $\delta^{18}O$ and $\delta^{13}C$ values of the meteoric water source (Mook & Vogel, 1968; Stuiver, 1970; Fritz & Poplawski, 1974). As with mammalian bioapatite, the $\delta^{18}O$ values of mollusc shells ($\delta^{18}O_{ms}$) are dependent upon two environmental factors: 1) the $\delta^{18}O$ value of the water source within which the carbonate precipitated, and 2) the water temperature during carbonate precipitation (Stuiver, 1970; Fritz & Poplawski, 1974). The relationship between these variables has been investigated by several workers, yielding a number of similar fractionation equations (Craig, 1965; Anderson & Arthur, 1983; Hays & Grossman, 1991; Kim & O'Neil, 1997, in Leng & Marshall, 2004). However, the equation developed by White et al. (1999), shown below, is considered the most relevant for this research, because it was specifically generated using data from the aragonitic shells of the freshwater gastropod, *Radix peregra* (Müller, 1774):

$$T = 21.36 - 4.83 \times (\delta^{18}O_{ms} - \delta^{18}O_{mw}) \quad (2.5)$$

where T is the temperature in °C, $\delta^{18}O_{ms}$ is the oxygen isotope value of mollusc shell aragonite (relative to Vienna Pee Dee Belemnite, VPDB), and $\delta^{18}O_{mw}$ is the oxygen isotope value of the meteoric water source (in Vienna Standard Mean of Ocean Water, VSMOW). This isotopic relationship between shell aragonite and meteoric water is relatively consistent across different molluscan taxa (White et al., 1999; Bugler et al., 2009). As a result, average $\delta^{18}O_{ms}$ values of different species from the same site are usually very similar (Waghorne et al., 2012; Apolinarska & Pelechaty, 2017). Therefore, Equation 2.5 is likely an accurate reflection of the $\delta^{18}O$ relationship in most aragonitic freshwater gastropod species.

While mammalian bioapatite mineralizes at a constant body temperature, the water temperature at which molluscan aragonite precipitates can vary considerably. This means that a change in $\delta^{18}O_{ms}$ may reflect a change in: 1) the $\delta^{18}O$ of meteoric water, 2) the water temperature, or 3) a combination of both (Equation 2.5). Oxygen isotope fractionation during carbonate precipitation is temperature-dependent, at a rate of approximately +0.24‰/-1°C (Craig, 1965). Therefore, an increase in environmental temperature will result in a decrease in $\delta^{18}O_{ms}$. However, due to the positive relationship between temperature and the $\delta^{18}O$ of precipitation (Dansgaard, 1964), a rise in temperature may also cause an increase in $\delta^{18}O_{mw}$, with a corresponding increase in $\delta^{18}O_{ms}$ (White et al., 1999). In Northwest Europe, the influence of temperature on $\delta^{18}O_{mw}$ is overriding (~0.58‰/+1°C) (Rozanski et al., 1993), and thus the $\delta^{18}O$ of mollusc shell aragonite is usually positively correlated with $\delta^{18}O_{mw}$. However, as discussed in Section 2.2.1.2., surface processes modify $\delta^{18}O_{mw}$ values relative to precipitation. This means that $\delta^{18}O_{ms}$ values can only be used to calculate palaeotemperatures if the $\delta^{18}O$ of the meteoric water source is known or quantifiable (Fritz & Poplawski, 1974; White et al., 1999).

Despite this, there are certain situations in which $\delta^{18}O_{mw}$ can be estimated or calculated. For example, shells precipitating within large, groundwater-fed rivers will have relatively consistent $\delta^{18}O$ values, because $\delta^{18}O_{mw}$ values vary little intra-annually (e.g. Waghorne et al., 2012; Darling & Bowes, 2016). Therefore, provided that past climatic and hydrological conditions were similar to today, modern $\delta^{18}O_{mw}$ values can be combined with $\delta^{18}O$ values of fossil shells in order to calculate temperature (e.g. Rose et al., 2008). However, $\delta^{18}O_{mw}$ values likely varied during the Quaternary period, due to temporal changes in temperature and humidity. Therefore, alternative approaches are needed in order to quantify the past $\delta^{18}O$ of meteoric water. One such approach is to use the $\delta^{18}O$ values of mammalian bioapatite to calculate $\delta^{18}O_{mw}$ (Grimes et al., 2003). This approach will be discussed in further detail in Section 2.4.2.

2.3.4.2. Carbon isotopes

The $\delta^{13}C$ of mollusc shell carbonate ($\delta^{13}C_{ms}$) primarily records the $\delta^{13}C$ value of DIC (Fritz & Poplawski, 1974). Given that the $\delta^{13}C$ of DIC can be influenced by various factors (Section 2.2.2.5.), $\delta^{13}C_{ms}$ values are difficult to interpret in terms of palaeoenvironmental change. Moreover, several studies have shown that $\delta^{13}C_{ms}$ values are ~1-6‰ depleted relative to DIC (McConnaughey & Gillikin, 2008; Apolinarska & Pelechaty, 2017). This offset is thought to result from the incorporation of metabolic carbon, derived from $\delta^{13}C$-depleted food resources, during shell precipitation (McConnaughey & Gillikin, 2008). Differences in dietary preferences consequently result in inter-species differences in $\delta^{13}C_{ms}$ values (Apolinarska & Pelechaty, 2017). Therefore, while $\delta^{13}C_{ms}$ values predominantly reflect the $\delta^{13}C$ of DIC, temporal variations in $\delta^{13}C_{ms}$ may also result from changes in molluscan diet.

2.3.5. Summary

The oxygen isotope values of mammalian bioapatite and molluscan shell aragonite reflect the $\delta^{18}O$ of local meteoric water. However, oxygen isotopes are fractionated during bioapatite and shell mineralization. In mammals, this fractionation is dependent upon the taxon and the mineral ion that is analysed, whereas in molluscs, the fractionation depends on environmental temperature. Therefore, modern calibrations are required in order to calculate past $\delta^{18}O_{mw}$ values from the $\delta^{18}O$ values of fossil bioapatite and shells. Since $\delta^{18}O_{mw}$ is related to air temperature, bioapatite and shell $\delta^{18}O$ values can provide records of palaeoclimatic conditions.

The $\delta^{13}C$ values of mammalian bioapatite and collagen reflect the $\delta^{13}C$ of the diet. Therefore, the $\delta^{13}C$ values of tissues from herbivorous mammals can be used reconstruct past changes in the $\delta^{13}C$ of vegetation, and by association, changes in the environmental factors that influence $\delta^{13}C_p$ values (e.g. atmospheric CO_2, climate). The $\delta^{13}C$ of molluscan aragonite primarily reflects the $\delta^{13}C$ of dissolved inorganic carbon. However, due to the various influences on DIC, mollusc shell $\delta^{13}C$ values are difficult to interpret.

2.4. Stable isotopes in rodent bioapatite

2.4.1. Modern analogue studies

2.4.1.1. Relationship between the $\delta^{18}O$ of rodent bioapatite and $\delta^{18}O$ of meteoric water

Previous modern analogue studies have consistently demonstrated that a strong linear relationship exists between the $\delta^{18}O$ of rodent bioapatite and the $\delta^{18}O$ of local meteoric water (Luz et al., 1984; Luz & Kolodny, 1985; D'Angela & Longinelli, 1990; Longinelli et al., 2003; Navarro et al., 2004; Kirsanow & Tuross, 2011; Royer et al., 2013a). Nevertheless, these studies have also shown that regressions on this relationship have significantly different slope and intercept coefficients (Figure 2.8). As a result, $\delta^{18}O_{mw}$ values, reconstructed using the $\delta^{18}O$ values of rodent teeth ($\delta^{18}O_{rt}$), differ greatly depending on the regression equation that is used (Fabre et al., 2011; Héran et al., 2010).

Several factors have been suggested as possible causes of these discrepancies between published equations, including: 1) inter-species differences in $\delta^{18}O$ fractionation, 2) inaccuracies in the modelled $\delta^{18}O_{mw}$ values, 3) uncertainties regarding the $\delta^{18}O$ values of the water sources ingested by the sampled rodents (Longinelli et al., 2003; Navarro et al., 2004; Royer et al., 2013a), and 4) differences in the skeletal material chosen for analysis (bones or teeth) (Gehler et al., 2012).

Firstly, various taxa, including laboratory rats, wild mice (*Apodemus*), and wild voles (mainly *Microtus*, *Arvicola*, and *Myodes*), have been sampled to generate the modern regression equations. However, as discussed in Section 2.3.2., the oxygen isotope fractionation between drinking water and body water varies between species due to differences in their physiology (Royer et al., 2013a). Indeed, Velivetskaya et al. (2014) discovered that species identity has an important influence on the slope of the relationship between $\delta^{18}O_{rt}$ and air temperature. Therefore, the relationship between $\delta^{18}O_{rt}$ and $\delta^{18}O_{mw}$ in individual rodent species needs to be investigated in order to: 1) test the influence of species-specific factors on this relationship, and 2) validate existing equations that are based upon multiple species.

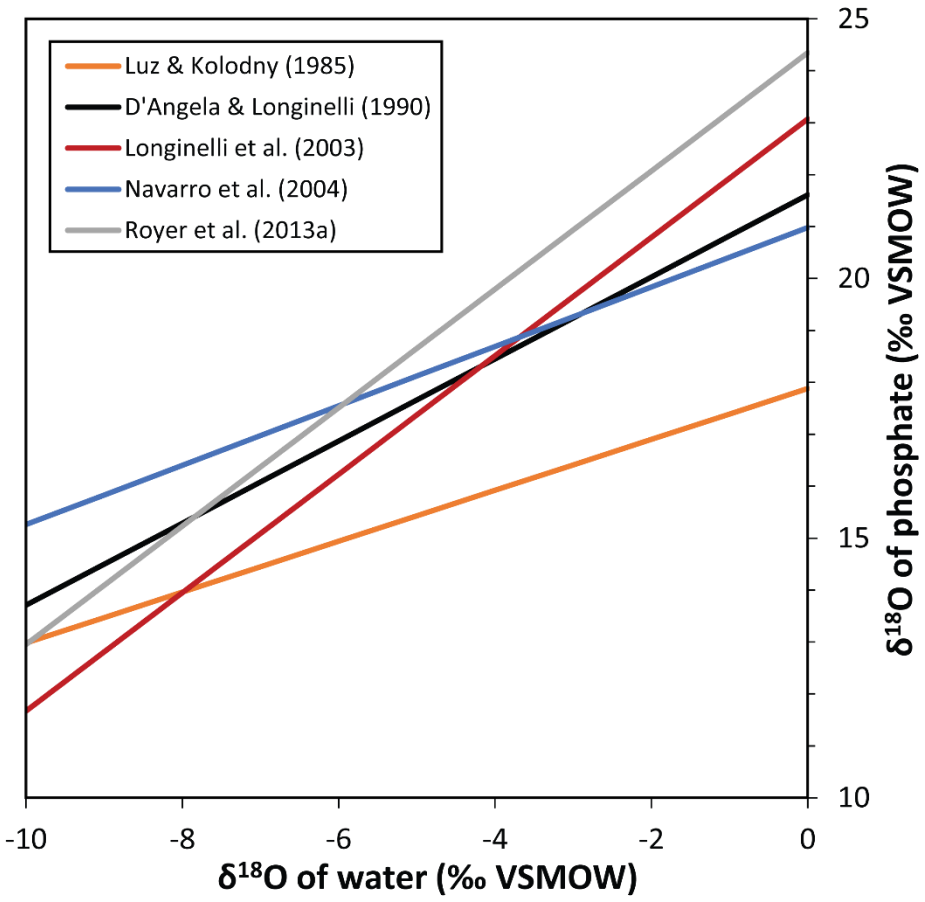

Figure 2.8: *Published regression lines for the relationship between the $\delta^{18}O$ of phosphate in rodent bioapatite and the $\delta^{18}O$ of environmental water.*

Despite this, the equations developed by Navarro et al. (2004) and Royer et al. (2013a) use $\delta^{18}O$ data from the same species of European voles. Nevertheless, the slopes of these regressions are different by a factor of 2. Consequently, other factors must be responsible for these discrepancies. One possible cause may be uncertainties or inaccuracies in the $\delta^{18}O$ values of the water source. Fractionation equations based on field studies are typically generated using $\delta^{18}O$ values of local precipitation, modelled using data collected via the Global Network for Isotopes in Precipitation (GNIP) (IAEA/WMO, 2018). Modelled $\delta^{18}O_{pt}$ values have improved in accuracy and precision over time, as the number of measurements in the GNIP database has increased. As a result, some of the equations in earlier publications may

be based on inaccurate or imprecise $\delta^{18}O_{pt}$ data. For example, Longinelli et al. (2003) recalculated an earlier equation (D'Angela & Longinelli, 1990) using new, more reliable $\delta^{18}O_{pt}$ estimates. The new regression equation was found to have a significantly different slope compared to the original relationship (Figure 2.8). This indicates that inaccurate data may be a key contributor to the differences between equations.

Furthermore, although most equations use $\delta^{18}O_{pt}$ values, mammals do not obtain their drinking water directly from precipitation. Instead, mammals consume plant water and surface water sources, which have $\delta^{18}O$ values that are typically enriched compared to $\delta^{18}O_{pt}$ (Flanagan et al., 1991; Darling et al., 2003; Speed et al., 2011; Darling & Bowes, 2016). Consequently, published equations may not reliably reflect the relationship between $\delta^{18}O_{rt}$ and the $\delta^{18}O$ values of the water sources consumed by rodents.

Finally, the $\delta^{18}O$ values of bones and teeth from the same individual are likely to differ due to differences in the duration of their mineralization. Bone bioapatite usually mineralizes over a period of several months to years, whereas rodent teeth mineralize within a few weeks or months (von Koenigswald & Golenishev, 1979; Klevezal et al., 1990). Therefore, bones and teeth reflect $\delta^{18}O_{mw}$ values averaged over different intervals of time. This may explain some of the differences between published calibrations (Gehler et al., 2012). Nevertheless, the equations by Longinelli et al. (2003) and Royer et al. (2013a), which are based on bone and tooth data, respectively, have comparable slope and intercept values (Figure 2.9).

Due to the uncertainties outlined above, the applicability of existing regression equations for reconstructing the $\delta^{18}O$ of past meteoric water is currently unclear. These issues will consequently be explored in Chapter 5, in the modern analogue study on vole teeth from Britain.

2.4.1.2. Isotope variability

In addition to the differences in the slope and intercept coefficients, the data are often fairly scattered around the published regression lines (Royer et al., 2013a). This scatter results from the variability in the $\delta^{18}O$ values of teeth from

a single locality, due to: 1) inter-species differences in metabolic processes and ecological preferences, 2) intra- and inter-individual variations in the season and duration of tooth mineralization (Royer et al., 2013a), and 3) variations in the $\delta^{18}O$ values of local drinking water sources. Likewise, inter-individual and seasonal variations in rodent diet, plus variations in the $\delta^{13}C$ values of local vegetation, may cause variability in tooth $\delta^{13}C$ values.

Fossil mammalian assemblages typically contain a variety of tooth types (upper and lower molars and incisors) from different individuals. In previous studies, the isotope values of continuously-growing molars and incisors from arvicoline rodents have been assumed to be comparable (e.g. Navarro et al., 2004). This is because molars and incisors from the same individual mineralize over similar periods of time (Navarro et al., 2004). Nonetheless, empirical evidence to support this assumption is currently limited.

Only three previous studies have investigated tooth isotopic variability in modern rodent populations from western Europe. Firstly, Gehler et al. (2012) analysed the $\delta^{18}O$ and $\delta^{13}C$ values of rodent teeth from a single site in northwest Germany. This study revealed that the isotope values of teeth from ten different individuals within a vole population can vary by several per mil. Gehler et al. (2012) also found that in *Arvicola terrestris*, the $\delta^{18}O$ values of the incisors are generally enriched compared to the molars, whereas the $\delta^{13}C$ values of the incisors are consistently depleted relative to the molars. Therefore, the assumption that the isotope values of different teeth are comparable may not be valid. This is potentially problematic, as some researchers have combined several molars or incisors to form a single bulk sample for analysis (Navarro et al., 2004; Royer et al., 2013a). The isotope results generated from these bulk analyses reflect averages of multiple teeth from different individuals, which when considered separately, could have significantly different isotopic values.

The second study, undertaken by Royer et al. (2013a), investigated the $\delta^{18}O$ values of rodent teeth from various localities across Europe. This study found that inter-species differences in $\delta^{18}O_{rt}$ values can reach up to 3‰. In contrast, variations in $\delta^{18}O_{rt}$ values within the same species are small (≤ ~1‰).

However, only 3-4 teeth were analysed per site. These limited sample sizes may not have captured the full variation in isotope values within each population, and thus the significance of inter-individual isotopic differences cannot be reliably tested.

Royer et al. (2013a) additionally normalized their data in order to compare the average $\delta^{18}O$ values of rodent molars and incisors across all sites. Their results showed that molars and incisors have similar distributions in $\delta^{18}O$ values. However, as aforementioned, the data in this study are based on bulk samples comprising teeth from multiple individuals. The isotopic averaging resulting from this method may consequently mask any true differences in the isotope values of the molars and incisors from each population.

The final study, by Calandra et al. (2015), examined how the $\delta^{13}C$ composition of collagen within rodent teeth varies in response to seasonal changes in the diet. In voles, the collagen $\delta^{13}C$ values of individuals trapped during spring were found to be ~1-3‰ higher compared to individuals trapped during autumn. Calandra et al. (2015) attribute these seasonal $\delta^{13}C$ differences to the increased consumption of isotopically-enriched graminoids during winter-spring, followed by the consumption of a more varied diet of isotopically-depleted herbaceous plants and mosses during summer-autumn. Seasonal dietary variations are also likely to be recorded in the $\delta^{13}C$ values of rodent tooth carbonate. However, at present, data that may support this suggestion are only available for a single site and species (Gehler et al., 2012).

Therefore, while these studies have advanced our understanding of population-level variability in the isotope values of rodent teeth, the consistency of this variability across different species and geographical locations has not yet been tested using large isotope datasets. Furthermore, intra-individual differences in tooth isotope values have only been investigated in one rodent species (*A. terrestris*). Thus, it is not currently known whether the patterns observed in *A. terrestris* are comparable in other European rodent taxa [e.g. *Microtus agrestis* (Linnaeus, 1761)]. Additional studies on inter-tooth isotopic differences are also critical for assessing whether bulk sampling strategies (Navarro et al., 2004; Royer et al., 2013a) can yield isotope values that accurately reflect the population mean. In summary, there is great scope

for further research to be undertaken on this topic. These issues are consequently addressed in the modern analogue study in Chapter 5.

2.4.1.3. Summary

The utilization of isotopes in rodent bioapatite for reconstructing palaeoenvironmental conditions has been hampered by a poor understanding regarding the isotope ecology of modern rodents in mid-latitude regions. Published equations that relate the $\delta^{18}O$ values of rodent bioapatite and meteoric water differ greatly, and there is no consensus on which equation(s) is the most reliable for reconstructing past $\delta^{18}O_{mw}$ values. This variability in the isotopic relationship may result from several factors, including: 1) inter-species differences in isotopic fractionation, 2) inaccuracies in the measured or modelled $\delta^{18}O$ values of local meteoric water sources, 3) isotopic variability between different skeletal elements, and in particular, molars and incisors, and 4) isotopic differences between individuals within a rodent population. At present, very few studies have investigated these potential sources of variability, and those studies that have been undertaken are based on data from a small number of samples from few study sites. Therefore, the consistency of the relationship between $\delta^{18}O_{rt}$ and $\delta^{18}O_{mw}$ in mid-latitude regions, and the significance of isotopic variability in influencing this relationship, require further testing.

2.4.2. Paleoenvironmental studies

Previous research on the $\delta^{18}O$ and $\delta^{13}C$ values of rodent bioapatite has largely focused on understanding palaeoenvironmental conditions in the Tertiary Period between 66 and 2.6 million years ago (Grimes et al., 2003; Grimes et al., 2005; Hopley et al., 2006; Tütken et al., 2006; Héran et al., 2010; García-Alix et al., 2013; Kimura et al., 2013; García-Alix, 2015; Arppe et al., 2015). Conversely, despite more than 30 years of research into stable isotopes in rodent bioapatite, the application of these proxies to Quaternary palaeoenvironmental reconstructions (2.6 million years ago to present) has

thus far been relatively limited (Rogers & Wang, 2002; Navarro et al., 2004; Royer et al., 2013b; Royer et al., 2014; Jeffrey et al., 2016). Grimes et al. (2004) argue that rodent teeth may be particularly valuable for reconstructing Quaternary palaeoenvironments, because 1) rodent skeletal remains are abundant in Quaternary deposits, 2) recent remains are less likely to have experienced diagenetic alteration compared to pre-Quaternary fossils, and 3) we have a good understanding of the ecology of modern rodent taxa and their recent evolutionary ancestors. This means that modern isotope fractionation equations are applicable to Quaternary rodent remains, and can potentially be used to generate accurate and abundant palaeoenvironmental information.

Studies that have analysed rodent bioapatite have utilized the $\delta^{18}O$ data in two key applications: 1) to quantify past seasonal temperatures, by coupling the $\delta^{18}O$ of rodent bioapatite with the $\delta^{18}O$ values of other freshwater carbonates (henceforth referred to as the "coupled isotope approach"), and 2) to reconstruct millennial-scale climatic changes, using rodent remains from stratified cave deposits. The $\delta^{13}C$ values of rodent bioapatite have been used to understand past atmospheric and climatic changes, although studies on this topic are currently very limited. The following sections provide an overview of these applications to Quaternary palaeoenvironmental studies.

2.4.2.1. Oxygen isotopes

One of the major benefits of using mammalian teeth to reconstruct past climates is that the $\delta^{18}O$ of bioapatite is dependent on only one variable: the $\delta^{18}O$ of the body water (Figure 2.9) (Longinelli, 1984; Luz et al., 1984; Luz & Kolodny, 1989; Bryant & Froelich, 1995). In contrast, the $\delta^{18}O$ values of freshwater carbonates are controlled by two environmental variables: the $\delta^{18}O$ of the water source, and environmental temperature (Figure 2.9) (Fritz & Poplawski, 1974; White et al., 1999). Consequently, in order to calculate palaeotemperatures from these archives, both the $\delta^{18}O$ of the freshwater carbonate and the $\delta^{18}O$ of the water in which the carbonate precipitated must be quantified (Equation 2.5). While the former can be easily measured through isotopic analyses of fossil carbonates, the latter variable is usually unknown.

However, Grimes et al. (2003) developed an approach that can address this problem. This approach involves coupling the $\delta^{18}O$ values of rodent teeth with other palaeoproxies (e.g. mollusc shells) in order to calculate past seasonal temperatures (Figure 2.9). Firstly, the $\delta^{18}O$ of rodent bioapatite is substituted into a modern regression equation in order to calculate the $\delta^{18}O$ value of the drinking water source. Since rodents have small home ranges, this $\delta^{18}O_{dw}$ value can provide an estimate for the average $\delta^{18}O$ value of local meteoric water. The $\delta^{18}O$ values of mollusc shells that have precipitated from the same water source will consequently also reflect this $\delta^{18}O_{mw}$ value (Figure 2.9). The calculated $\delta^{18}O_{mw}$ can therefore be coupled with measured $\delta^{18}O_{ms}$ values, to enable the temperature during shell mineralization to be quantified (e.g. using Equation 2.5). This approach to utilizing the $\delta^{18}O$ of rodent bioapatite consequently offers a potentially valuable means of generating quantitative palaeotemperature estimates.

The distinct advantage of this approach is that it does not rely on using the modern relationship between $\delta^{18}O_{pt}$ and air temperature to calculate past temperatures (Fricke & Wing, 2004; Grimes et al., 2008). This consequently eliminates the necessity of assuming that this modern relationship is applicable to the past, when this assumption may not be valid (Fricke & O'Neil, 1999). In addition, this method has the potential to provide reliable temperature reconstructions, regardless of whether $\delta^{18}O_{mw}$ is comparable to $\delta^{18}O_{pt}$ (Fricke & Wing, 2004; Grimes et al., 2008). This is because rodent bioapatite and mollusc shell carbonate reflect the same meteoric water source, and thus both archives will record the same modifications (e.g. evaporative fractionation) to the $\delta^{18}O$ of meteoric water (Grimes et al., 2008).

Despite these advantages, only two studies have applied this approach to reconstructing Quaternary palaeotemperatures (Ruddy, 2005; Peneycad, 2013). The first study, by Ruddy (2005), investigated water vole incisors [*Arvicola cantiana* (Hinton, 1910)] and gastropod shells [*Valvata piscinalis* (O.F. Müller, 1774)] from the British interglacial site of Cudmore Grove, Essex, which is correlated with Marine Oxygen Isotope Stage (MIS) 9 (~300-340 ka) (Roe et al., 2009). The mean summer palaeotemperature, calculated by coupling the $\delta^{18}O$ values of incisor phosphate and shell aragonite, is 22°C. This palaeotemperature is consistent with the mean temperature of the

warmest month (16-22°C), estimated using fossil beetle assemblages from the site (Roe et al., 2009). While uncertainties on the calculated palaeotemperature are large (range = 15-31°C), this study demonstrates the potential of the coupled isotope approach for generating accurate mean palaeotemperature estimates for Quaternary interglacial stages.

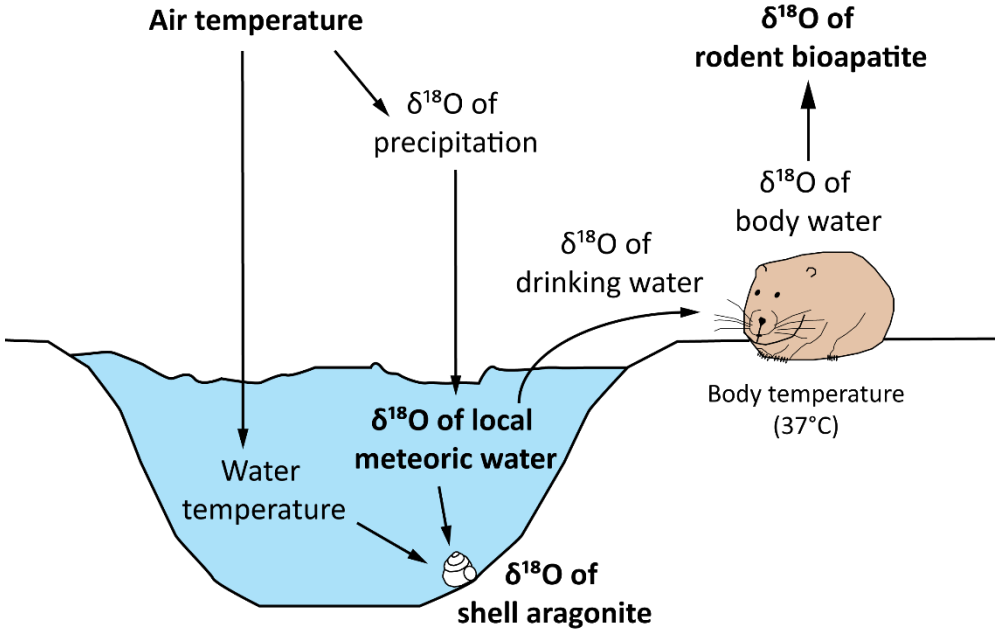

Figure 2.9: *Schematic illustrating how the $\delta^{18}O$ compositions of rodent bioapatite and mollusc shell aragonite can be coupled to reconstruct air temperature (adapted from Fig. 1 in Grimes et al., 2008).*

This approach was further tested by Peneycad (2013), using material from two British sites: 1) the West Runton Freshwater Bed, Norfolk, which dates to the Early Middle Pleistocene (~700 ka), and 2) the lower deposits of the Aveley Silts and Sands Member, Essex, which corresponds to the early part of MIS 7 (~235-245 ka) (Candy & Schreve, 2007). For West Runton, incisors from the extinct water vole, *Mimomys savini* (Hinton, 1911), were analysed to determine the $\delta^{18}O$ value of the tooth carbonate. The $\delta^{18}O_{rt}$ results

were converted to $\delta^{18}O_{bw}$ and $\delta^{18}O_{dw}$ values using modern calibration equations (Luz et al., 1984; White et al., 1999). The mean calculated $\delta^{18}O_{dw}$ value was then coupled with published $\delta^{18}O$ values of *V. piscinalis* shells (Davies et al., 2000; Rose et al., 2008) to generate mean temperature estimates of 16.6-20.3°C. These estimates are entirely consistent with the beetle- and ostracod-based mean warmest month temperatures for the site (16-19°C) (Coope, 2010a; T.S. White, pers. comm.). In contrast, for Aveley, the mean $\delta^{18}O_{mw}$ value, calculated using the $\delta^{18}O$ values of water vole (*A. cantiana*) incisors, was significantly lower than the mean $\delta^{18}O_{mw}$ calculated by combining the $\delta^{18}O$ values of *V. piscinalis* shells with an estimated mean summer temperature of 17°C. This mean summer temperature was based upon the presence of *Emys orbicularis* (European pond terrapin) remains within the Aveley deposits, a species which is presently restricted to regions with summer temperatures of > 17°C. These results suggest that the isotope values of the teeth and shells reflect different water sources. Therefore, while these studies demonstrate the potential of the coupled isotope approach for Quaternary palaeotemperature reconstruction, further testing of the reliability of this approach is required. To address this, additional analyses were undertaken on rodent material from the West Runton Freshwater Bed and Cudmore Grove, and the approach was additionally applied to the MIS 7 site of Marsworth in Buckinghamshire. The results of this investigation are presented in Chapter 6.

The $\delta^{18}O$ values of rodent bioapatite have additionally been applied to the reconstruction of millennial-scale climatic fluctuations using fossil material derived from cave sequences (Navarro et al., 2004; Peneycad, 2013; Royer et al., 2013b; Royer et al., 2014; Jeffrey et al., 2016). For example, Navarro et al. (2004) investigated variations in the $\delta^{18}O$ values of arvicoline rodents through the La Baume de Gigny cave sequence in France. The results of this study suggest that $\delta^{18}O_{rt}$ peaks and troughs can be correlated with warm (interstadial) and cold (stadial) intervals in the Greenland ice core records.

Royer et al. (2013b, 2014) also used stratigraphic shifts in the $\delta^{18}O$ values of rodent teeth from cave sites in France to infer changes in temperature, seasonality and aridity between interstadial and stadial episodes. However, Royer et al. (2013b) also highlight the difficulties in interpreting the $\delta^{18}O$ values of rodent teeth from caves. Rodent material accumulates in caves over a number of years, and as a result, skeletal remains within a single stratigraphic level represent a time-averaged record of environmental conditions. As a consequence, $\delta^{18}O_{rt}$ values are often highly variable within each stratigraphic level in a cave sequence. Royer et al. (2013b; 2014) therefore suggest that climatic interpretations of stratigraphic shifts in $\delta^{18}O_{rt}$ values should be made with caution, and with a detailed knowledge of the depositional and environmental context of the cave.

Peneycad (2013) used the $\delta^{18}O$ values of *A. terrestris* teeth from Gully Cave, in Ebbor Gorge, Somerset, to investigate climatic fluctuations from the Lateglacial period to the early Holocene. The results of this study showed an overall pattern of higher average values during the Lateglacial Interstadial and early Holocene, and a lower average value during the Loch Lomond Stadial. While these results suggest that the $\delta^{18}O_{rt}$ values paralleled climatic changes, the interpretation of the data was complicated by the small number of samples analysed, combined with the large variability in values within each stratigraphic level.

These studies illustrate that the $\delta^{18}O$ values of rodent teeth from cave sequences can potentially be used to reconstruct millennial-scale climatic variability during the Late Quaternary period. Nevertheless, further studies are needed on material from well-stratified and well-studied cave sequences, in order to assess the reliability of this proxy for generating high-resolution climate records. Therefore, new and additional isotope analyses were undertaken on vole teeth from two British cave sites: 1) Westbury Cave, Somerset, and 2) Gully Cave, Somerset. The results of these analyses are presented in Chapter 7.

2.4.2.2. Carbon isotopes

Hitherto, only two studies have used the $\delta^{13}C$ values of rodent bioapatite ($\delta^{13}C_{rt}$) to reconstruct Quaternary palaeoenvironmental changes. The first study, by Gąsiorowski et al. (2014), investigated the $\delta^{13}C$ values of vole and lemming teeth from a cave sequence in Poland, which accumulated during the last interglacial (MIS 5) and glacial (MIS 4-2) stages. The results indicate that average $\delta^{13}C_{rt}$ values declined during the warm stages (MIS 5 and Lateglacial Interstadial) and increased during the glacial stage. The low $\delta^{13}C$ values during the warm stages were attributed to an increase in the canopy effect due to forest growth. High $\delta^{13}C$ values under glacial conditions were related to low temperatures and high aridity. This study demonstrates that $\delta^{13}C$ records from rodent teeth can be used to reconstruct glacial-interglacial climatic fluctuations.

The second study, undertaken by Jeffrey (2016), analysed the isotope values of modern and fossil gerbil teeth from North Africa. The $\delta^{13}C$ values of teeth dating to the last glacial stage were found to be ~4-7‰ more enriched than modern teeth. Jeffrey (2016) suggests that this offset is predominantly due to the recent decline in the $\delta^{13}C$ of atmospheric CO_2 (Figure 2.4). However, the $\delta^{13}C$ offset between the modern and fossil teeth is larger than the recent change in $\delta^{13}C_a$ (~2‰). Therefore, further research is required in order to 1) determine whether these temporal $\delta^{13}C_{rt}$ shifts are consistent across different geographical regions, and 2) identify the potential causes of Quaternary changes in $\delta^{13}C_{rt}$ values. These issues are considered further in Chapter 8, which examines the $\delta^{13}C$ values of Quaternary rodent teeth from Britain.

2.4.2.3. Summary

Previous research on the $\delta^{18}O$ and $\delta^{13}C$ values of fossil rodent bioapatite has demonstrated the potential value of these proxies for reconstructing past environmental changes. Coupling the $\delta^{18}O$ values of rodent teeth and mollusc shells can potentially generate accurate summer palaeotemperature estimates. The $\delta^{18}O$ values of rodent teeth from stratified cave records can be

used to understand temporal variations in the $\delta^{18}O$ value of meteoric water. On the other hand, the $\delta^{13}C$ values of rodent teeth can provide information on past changes in vegetation, climate, and the $\delta^{13}C$ value of atmospheric CO_2. However, the utilization of $\delta^{18}O_{rt}$ and $\delta^{13}C_{rt}$ values in Quaternary palaeoenvironmental research has thus far been limited. The reliability and applicability of these proxies therefore require further investigation.

2.5. Summary

Rodent teeth are abundant but relatively untapped sources of palaeoenvironmental information. The oxygen and carbon isotope values of fossil rodent teeth can potentially be used to reconstruct the past $\delta^{18}O$ of meteoric water and the $\delta^{13}C$ of vegetation. Reconstructed $\delta^{18}O$ values of meteoric water can in turn be used to infer changes in climate. However, a better understanding of the modern relationships between the isotope values of rodent teeth and environmental conditions must first be acquired, to enable the accurate interpretation of isotope data from fossil rodent teeth. This issue is addressed in Chapter 5.

The modern isotopic relationships can then be applied to the reconstruction of past environmental conditions. In Chapter 6, the coupled isotope approach is applied to three British sites to reconstruct past summer temperatures, in Chapter 7, the $\delta^{18}O$ values of fossil rodent teeth are used to understand temporal palaeoclimatic changes recorded in two British cave records, and in Chapter 8, the $\delta^{13}C$ values of the rodent teeth from the modern, Holocene and Pleistocene sites are compared to assess changes in the $\delta^{13}C$ of vegetation during the Quaternary period in Britain. The next chapter introduces the British study sites from which the modern and fossil material were obtained for isotopic analysis.

3. The Quaternary environmental context of Britain

3.1. Introduction

In this research, rodent teeth were sampled from eleven sites across Britain, including: four modern sites (1. West Horrington, 2. Cobham, 3. Beeford, 4. Perth), five Pleistocene sites (5. West Runton, 6. Cudmore Grove, 7. Marsworth, 8. Westbury Cave, 9. Gully Cave), and two Late Holocene archaeological sites (10. Longstone Edge, 11. Danebury). The locations of these study sites are shown in Figure 3.1. The following chapter provides an overview of the Quaternary environmental context of these sites.

The first part of the chapter outlines the climate, isotope hydrology and vegetation of Britain at the present day. The modern environment of Britain forms the context for the modern analogue study on $\delta^{18}O$ and $\delta^{13}C$ variability in rodent teeth (Chapter 5), and also provides a reference point with which the palaeoenvironmental information from the Pleistocene and Late Holocene sites can be compared. The second part of the chapter provides a brief overview of the British Quaternary record and its relevance to this research. Finally, the Pleistocene and Late Holocene study sites are introduced. Reviews of the stratigraphic context, palaeoenvironmental and palaeoclimate evidence, and geochronology of each site are provided, in order to provide a basis for the interpretation of the isotope data in Chapters 6-8.

3.2. Modern environment of Britain

3.2.1. Climate

Britain has a temperate oceanic climate, characterised by warm wet summers and cool winters (Peel et al., 2007). The temperate climate is maintained by the transport of warm ocean currents from the Gulf of Mexico to northwest Europe, via the thermohaline circulation. Warm water evaporates from the

ocean surface, generating low-pressure systems over the North Atlantic. South-westerly winds transport moist air within these systems across Britain, resulting in a west to east gradient in precipitation. In the west of Britain, the average annual amount of precipitation is ~1000-3000 mm, whereas in the east, the annual precipitation is ~600-1000 mm (Met Office, 2018). The mean annual temperature is generally 9-11°C across much of lowland England, and 7-9°C in northern England and lowland Scotland (Met Office, 2018).

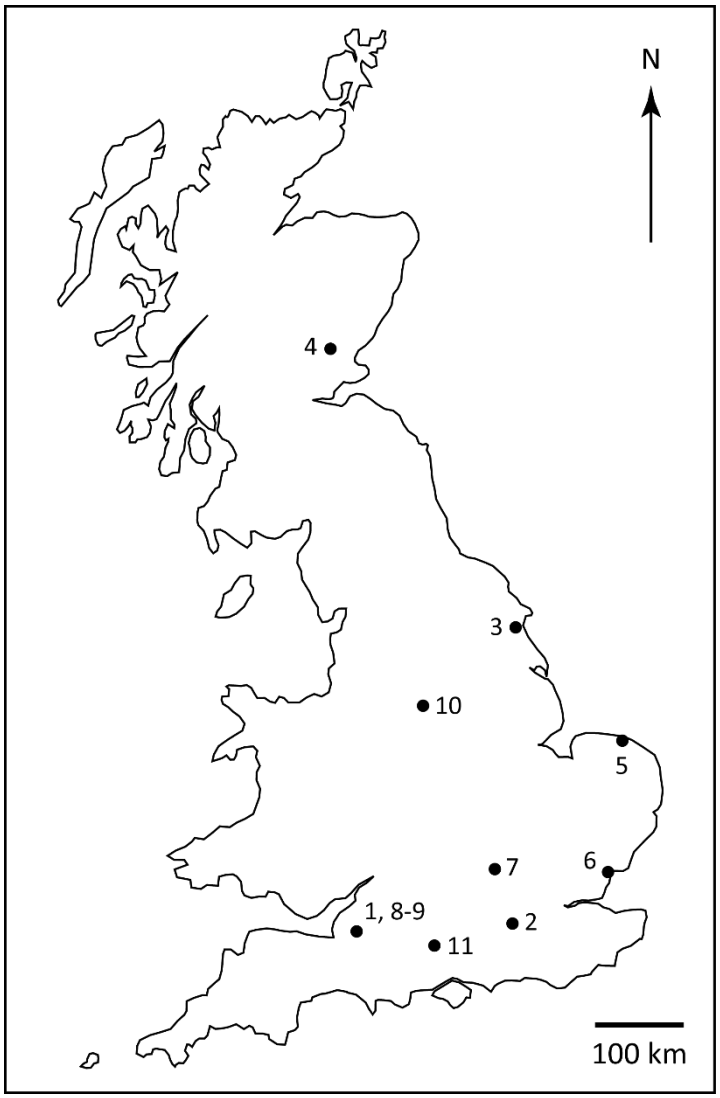

Figure 3.1: *Locations of the study sites investigated in this thesis: 1) West Horrington, Somerset, 2) Cobham, Surrey 3) Beeford, East Yorkshire, 4) Perth, Perthshire, 5) West Runton, Norfolk, 6) Cudmore Grove, Essex, 7) Marsworth, Buckinghamshire, 8) Westbury Cave, Somerset, 9) Gully Cave, Somerset, 10) Longstone Edge, Derbyshire, 11) Danebury, Hampshire.*

The modern climatic conditions at each study site are shown in Table 3.1. At most sites, the mean July temperature is ~16-18°C, and the mean January temperature is ~4-5°C. The mean annual rainfall is ~700-900 mm in western and central England and Scotland, and 500-700 mm in eastern England. These modern data provide a useful reference for comparison with the isotope data and climate proxies from the study sites.

3.2.2. $\delta^{18}O$ of precipitation

In accordance with the continental effect, the heavy ^{18}O isotope is progressively rained out during the passage of south-westerly air masses across western Europe (Rozanski et al., 1993; Darling, 2004). As a result, the $\delta^{18}O$ of precipitation in Britain decreases from the southwest to the northeast (Darling & Talbot, 2003). The amount effect has an important influence on $\delta^{18}O_{pt}$ values in Britain (Darling & Talbot, 2003), although this effect is generally only significant during April-August (Darling & Talbot, 2003; Darling & Bowes, 2016).

As is typical for mid-latitude regions, the $\delta^{18}O$ of precipitation is also strongly controlled by air temperature (Darling & Talbot, 2003). The relationship between average $\delta^{18}O_{pt}$ and temperature in Britain (~0.22-0.32‰/+1°C) is lower than for mid-latitude regions as a whole (~0.58‰/+1°C) (Rozanski et al., 1993), but is still significant on monthly and seasonal timescales (Darling & Talbot, 2003). Due to this relationship, the average $\delta^{18}O_{pt}$ varies seasonally, with values more enriched during summer than in winter (Darling & Talbot, 2003). However, the amplitude of seasonal $\delta^{18}O_{pt}$ variability varies with location. Seasonal ranges in $\delta^{18}O_{pt}$ are generally smaller (~3‰) in western coastal areas of Britain, moderate (~5-7‰) in inland areas due to an increased continental effect, and large (~8-15‰) in upland areas of Scotland due to depleted $\delta^{18}O$ values of snowfall during winter (Darling & Talbot, 2003; Soulsby et al., 2000; Speed et al., 2011).

Table 3.1: *Geographical information for the study sites, and modern climate data from the nearest weather stations to each of the study sites. The data are for the period between 1981 and 2010. Mean July and January temperatures are shown because the palaeoclimate reconstructions for the Pleistocene study sites are largely based upon estimates of the mean temperatures of the warmest (July) and coldest (January) months of the year. These palaeoclimate reconstructions (see section 3.4) can therefore be directly compared with the data in this table. The data were obtained from the Meteorological Office (2018).*

Location on Fig. 3.1	Study site				Weather station (distance from study site)	Mean July temperature (°C)	Mean January temperature (°C)	Mean annual rainfall (mm)
	Name	Latitude (°)	Longitude (°)	Altitude (m above sea level)				
1	West Horrington, Somerset	51.22	-2.61	159	Bath (24 km NE)	17.1	4.8	814
2	Cobham, Surrey	51.32	-0.41	22	Wisley (4.6 km W)	17.7	5.0	657
3	Beeford, East Yorkshire	53.98	-0.29	9	Bridlington MRSC (11 km NE)	15.8	4.5	621
4	Perth, Perthshire	56.43 56.47	-3.25 -3.20	33 103	Mylnefield (9.8 km E)	15.2	3.6	722
5	West Runton, Norfolk	52.94	1.25	1	Weybourne (7.4 km W)	16.8	4.8	627
6	Cudmore Grove, Essex	51.79	0.99	5	Walton-on-Naze (20 km NE)	17.9	4.4	549

7	Marsworth, Buckinghamshire	51.82	-0.65	120	Rothamsted (20 km E)	16.9	4.0	712
8	Westbury Cave, Somerset	51.25	-2.71	175	Weston-super-Mare (24 km NW)	17.5	5.5	900
9	Gully Cave, Somerset	51.23	-2.68	134				
10	Longstone Edge, Derbyshire	53.30	-1.69	349	Sheffield Cdl (16 km NE)	16.9	4.4	835
11	Danebury, Hampshire	51.14	-1.54	126	Middle Wallop (3.8 km W)	17.1	4.5	779

At the annual scale, weighted average $\delta^{18}O_{pt}$ values across Britain are relatively stable from one year to the next (Darling & Talbot, 2003; Darling & Bowes, 2016). The relationship between the $\delta^{18}O$ and δD of precipitation is also fairly invariable, with typical slope coefficients of around 6.9 (Darling & Talbot, 2003) to 7.5 (Darling & Bowes, 2016) that are slightly less than the GMWL (Equation 2.1). However, data for the isotope values of precipitation in Britain are sparse, and long-term records are only available for two sites in central England (IAEA/WMO, 2018). Therefore, the local variability in $\delta^{18}O_{pt}$ values is poorly understood.

3.2.3. $\delta^{18}O$ of meteoric water

The $\delta^{18}O$ values of groundwaters across Britain parallel the spatial trend in $\delta^{18}O_{pt}$ (Figure 3.2). Average groundwater $\delta^{18}O$ values vary by around 4‰, with enriched values of -5 to -7‰ in the west, and depleted values of -7.5 to -9‰ in the east and in the Scottish Highlands (Soulsby et al., 2000; Darling et al., 2003). Isotopic measurements on aquifers with longer residence times have also shown that during the last glacial stage (before 10 ka), groundwater $\delta^{18}O$ values were ~1.5‰ more depleted than the present day (Darling et al., 2003).

On the other hand, relatively little is known about the $\delta^{18}O$ values of surface meteoric waters in this region (Darling et al., 2003; Darling, 2004). Since surface water bodies are a product of precipitation and groundwater discharge, the $\delta^{18}O$ values of surface waters would be expected to follow a similar spatial pattern as precipitation and groundwater (Figure 3.2). The limited data that are currently available generally support this statement. However, the balance between precipitation and groundwater inputs, plus modifications due to evaporation, have key effects on $\delta^{18}O_{mw}$ values in Britain (Soulsby et al., 2000; Darling et al., 2003; Brown et al., 2011).

Rivers in lowland Britain have relatively constant $\delta^{18}O$ values, with annual ranges of only ~1-3‰, resulting from minor isotopic enrichments during late summer and autumn, and depletions during the winter months (Lawler, 1987; Darling et al., 2003; Waghorne et al., 2012; Darling & Bowes, 2016). The temporal variation in $\delta^{18}O_{mw}$ values is therefore dampened relative to the

$\delta^{18}O$ of precipitation. This is because major rivers in the region have catchment residence times spanning several years, and are largely sustained by the discharge of groundwater from aquifers (Lawler, 1987; Darling et al., 2003; Brown et al., 2011; Waghorne et al., 2012; Darling & Bowes, 2016). The $\delta^{18}O$ of groundwater varies little intra-annually, and is close to the mean annual $\delta^{18}O$ of precipitation (Darling et al., 2003; Darling & Bowes, 2016). Accordingly, the $\delta^{18}O_{mw}$ values of British streams reflect the near-constant $\delta^{18}O$ of local groundwater (Lawler, 1987; Darling et al., 2003).

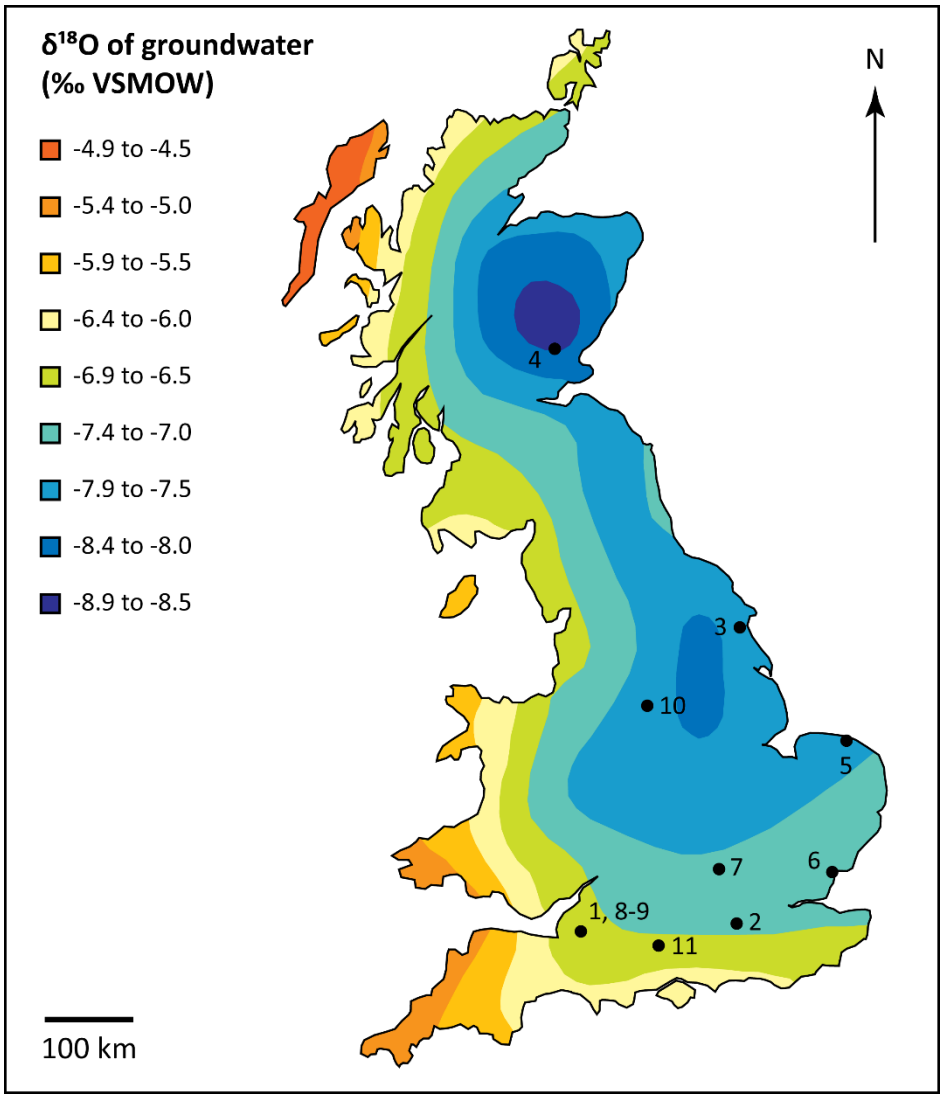

Figure 3.2: *Map showing the spatial distribution in the $\delta^{18}O$ of groundwater across Britain (modified from Darling et al., 2003 and Pellegrini et al., 2016). The locations of the study sites are also shown.*

Conversely, the $\delta^{18}O$ values of water sources that are not sustained by base flow, or that have short residence times (e.g. ditches and ponds), are more sensitive to variations in $\delta^{18}O_{pt}$ (e.g. Brown et al., 2011). Surface water sources in Britain are also affected by evaporative enrichment, particularly during summer (Darling et al., 2003; Darling & Bowes, 2016). Nevertheless, due to the high relative humidity of the climate in this region (75-85%) (Jenkins et al., 2009), average $\delta^{18}O_{mw}$ values are usually only ~0.5-1‰ more enriched than the mean annual $\delta^{18}O_{pt}$ (Darling et al., 2003; Darling & Bowes, 2016). This evaporative enrichment means that the $\delta^{18}O$ and δD values of surface waters fall along a shallower slope than the GMWL (Darling et al., 2003). The relationship between $\delta^{18}O$ and δD has been measured for the River Thames in southeast England, and is described by the following equation (Darling & Bowes, 2016):

$$\delta D = 5.33 \times \delta^{18}O - 8.92 \quad (3.1).$$

In highland areas, the $\delta^{18}O$ of meteoric water is also affected by inputs from isotopically-depleted winter precipitation and snowmelt. As a consequence, the $\delta^{18}O$ values of streams in mountain catchments in Scotland are generally -8 to -10‰, and are sometimes lower than the mean annual $\delta^{18}O_{pt}$ (Soulsby et al., 2000; Speed et al., 2011).

3.2.4. Vegetation

As discussed in Section 2.2.2.2., modern vegetation in Britain only comprises C_3 plants (Collins & Jones, 1986). Data on the $\delta^{13}C$ values of modern plants from Britain are limited, but isotopic analyses on oak trees from England indicate average values of between -26 and -28‰ (Robertson et al., 1997; Loader et al., 2003; Young et al., 2012). These values are consistent with the global average $\delta^{13}C$ value of C_3 plants (Kohn, 2010).

The $\delta^{13}C$ values of oak trees also record the recent decline in the $\delta^{13}C$ value of atmospheric CO_2. The average $\delta^{13}C$ values of tree rings formed during the late 1800s are around -23 to -25‰, indicating that average $\delta^{13}C_p$

values in Britain have decreased by ~2-3‰ over the past ~150 years (Robertson et al., 1997; Young et al., 2012).

3.2.5. Modern study sites

The first major aim of this thesis is to develop a modern calibration between the $\delta^{18}O$ values of rodent teeth and meteoric water, which can be later applied to the reconstruction of palaeoclimatic conditions. The second major aim is to investigate $\delta^{18}O$ and $\delta^{13}C$ variability in modern rodent populations. To address these aims, modern rodent teeth were sampled from four study sites across Britain that follow a gradient in the $\delta^{18}O$ of meteoric water: 1) West Horrington in southwest England, 2) Cobham in southeast England, 3) Beeford in northeast England, and 4) Perth in eastern Scotland (Sites 1-4 in Figure 3.2). The localities in England were also chosen due to their relative proximity to the Pleistocene and Late Holocene study sites (Figure 3.1). This proximity consequently enables the modern isotope data to be compared with the fossil data, in order to understand how past $\delta^{18}O_{mw}$ values and climatic conditions differed from the present day.

Given that the environmental conditions at the modern sites are integral to the development of a modern calibration between $\delta^{18}O_{rt}$ and $\delta^{18}O_{mw}$, these sites will only be introduced in detail in Chapter 5, which presents the results of the modern analogue study.

3.2.6. Summary and Implications

The $\delta^{18}O$ of precipitation decreases from southwest to northeast Britain due to rainout. The $\delta^{18}O$ of meteoric water parallels the $\delta^{18}O$ of precipitation. Since the $\delta^{18}O$ values of rodent teeth record the $\delta^{18}O$ of local drinking water, $\delta^{18}O$ values of modern rodent teeth from Britain should reflect the spatial pattern in $\delta^{18}O_{mw}$. The $\delta^{18}O$ values of surface meteoric water sources are usually slightly enriched compared to precipitation, but are relatively consistent across the year. Therefore, the average $\delta^{18}O$ of rodent teeth should reflect the mean annual $\delta^{18}O$ of precipitation, which in turn primarily reflects air temperature.

Past changes in temperature are consequently expected to cause increases or decreases in the $\delta^{18}O$ values of meteoric water and rodent teeth, relative to present-day values from the same area.

The average $\delta^{13}C$ values of modern plants in Britain are around -27‰. Modern teeth from herbivorous rodents in Britain should therefore reflect these plant $\delta^{13}C$ values. However, $\delta^{13}C_p$ values have undergone a recent decline due to changes in the $\delta^{13}C$ of atmospheric CO_2. As a consequence, the $\delta^{13}C$ values of modern rodent teeth are likely be lower than the Late Holocene and Pleistocene teeth that have formed under lower atmospheric $\delta^{13}C$ values.

3.3. The British Quaternary record

The Quaternary terrestrial record in Britain offers a valuable framework in which to test the applicability of isotopes in rodent teeth for reconstructing palaeoenvironmental conditions. Firstly, this record has been extensively studied, and consequently the Quaternary stratigraphy of Britain is now relatively well understood. Furthermore, excavations of fluvial sedimentary sequences in southern and eastern England, and cave sequences in southwest and northern Britain, have yielded rich assemblages of fossil remains that have provided a wealth of information about palaeoclimatic changes over the past ~800 thousand years (ka) (e.g. Stuart, 1974; Candy et al., 2010; Coope, 2010b). Therefore, the palaeoenvironmental context of Britain during the Quaternary period is also well understood.

Moreover, the robust biostratigraphy and chronology of the British record has enabled the correlation of individual beds with specific Marine Oxygen Isotope Stages (MIS) (Bridgland, 1994; Keen, 2001; Preece, 2001; Schreve, 2001; Preece & Parfitt, 2008; Penkman et al., 2013). These correlations have demonstrated that every interglacial episode from MIS 17 (~700 ka) to the present day (MIS 1) is represented within the Quaternary deposits in southeast Britain (Penkman et al., 2013). Cave sequences in Britain also preserve palaeoenvironmental and archaeological evidence from multiple interglacial stages as well as the last glacial stage (MIS 2) (Andrews et al., 1999; Currant & Jacobi, 2001). This has consequently enabled the

British terrestrial record to be placed within the context of long-term climatic fluctuations recorded in marine cores, and abrupt climate shifts recorded in high-resolution ice cores (e.g. Candy & Schreve, 2007; Jacobi & Higham, 2009; Candy et al., 2010). The study sites investigated in this thesis are shown against these marine core and ice core records in Figure 3.3.

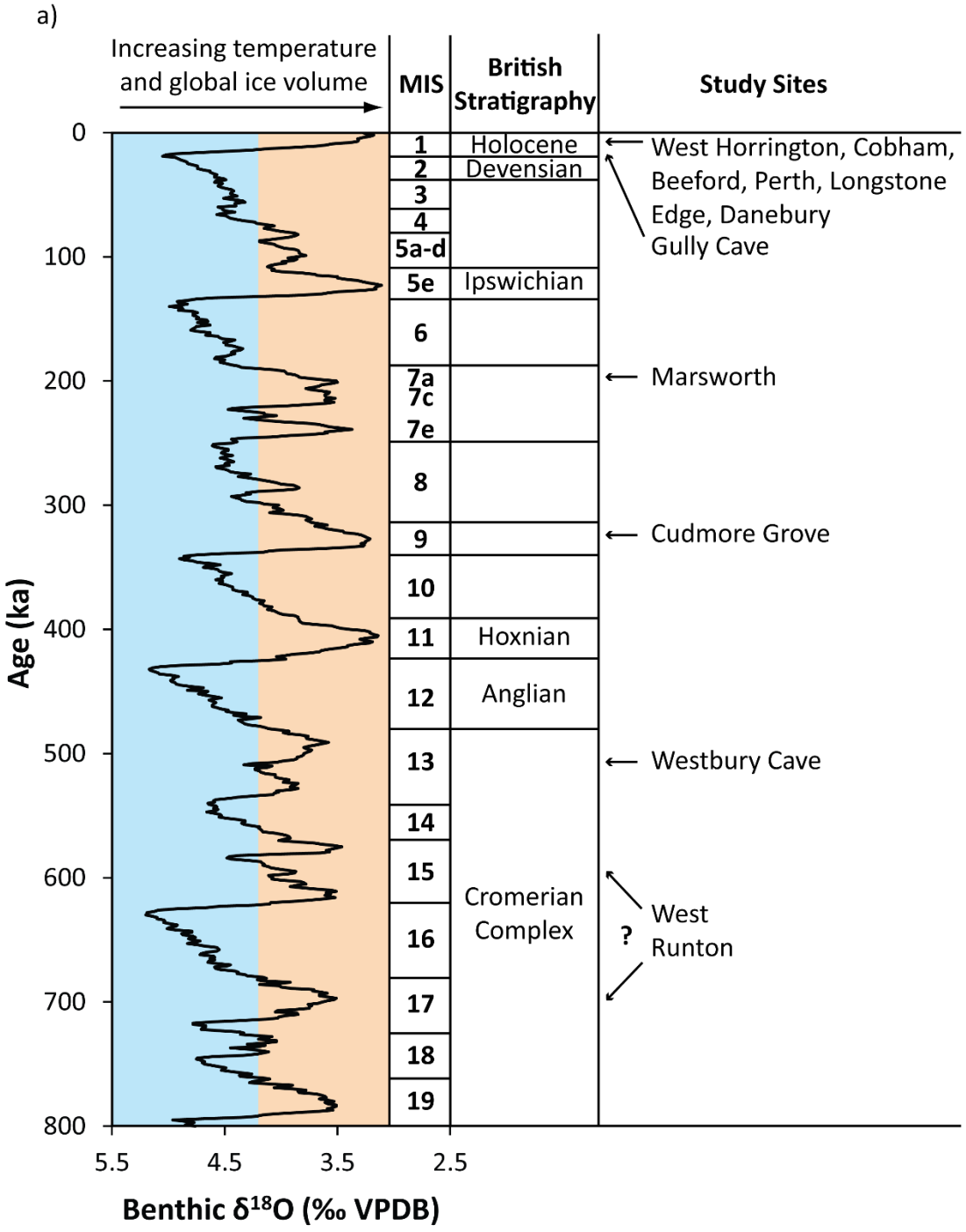

Figure 3.3. *(for caption see overleaf)*

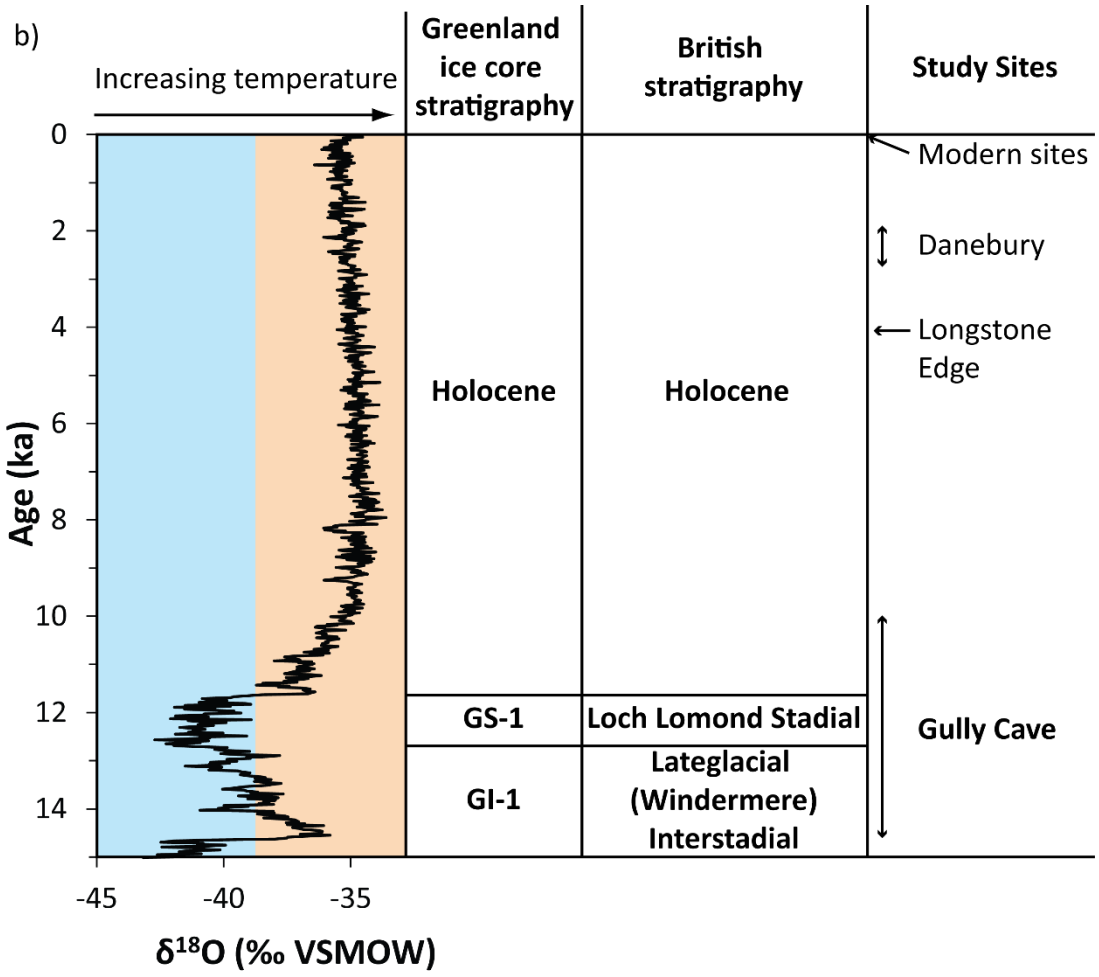

***Figure 3.3**: Correlation of the study sites with the stacked marine benthic oxygen isotope record for the North Atlantic (a), and the NGRIP ice core record on the GICC05 timescale (b). The marine core data were obtained from Lisiecki & Raymo (2009), and the Greenland ice core data are from Vinther et al. (2006) and Rasmussen et al. (2006).*

In addition, abundant mammalian remains and molluscan shells have been recovered from Quaternary fluvial deposits across Britain (e.g. Schreve et al., 2002; Roe et al., 2009). British cave sequences likewise contain large accumulations of small mammal remains (Andrews, 1990). Therefore, abundant fossil remains are available within the British Quaternary record for use in isotopic studies on tooth and shell carbonates.

A diverse range of palaeoecological proxies, including pollen, plant macrofossils, molluscs, ostracods, beetles, and vertebrates, is also preserved within the fluvial sequences in Britain. Consistent palaeoclimate reconstructions have been generated from these proxies, based on the modern biogeographical distributions of the taxa, and quantitative 'Mutual Climatic Range' methods. These methods involve using the overlap of the climatic tolerances of each species present within a fossil assemblage, in order to estimate the average warmest month (July) and coldest month (January) temperatures that existed during the period in which the assemblage lived. These methods include: 1) the Mutual Climatic Range (MCR) method for beetles (Coleoptera) (Atkinson et al., 1987), 2) the Mutual Ostracod Temperature Range (MOTR) method for ostracods (Horne, 2007), and 3) the mutual climatic range method for reconstructing temperatures and precipitation from herpetofaunal (amphibian and reptile) assemblages (Böhme, 1996; Böhme, 2000; Böhme et al., 2006). Climate reconstructions generated from these methods are available for the interglacial study sites investigated in this thesis (see section 3.4). These reconstructions provide a useful record against which the isotope-based temperature reconstructions can be compared and validated.

In summary, the Quaternary record of Britain provides an appropriate setting for addressing the aims of this research, due to 1) the well-understood stratigraphy and chronology of the terrestrial deposits, 2) the abundance of fossil remains on which isotope analyses can be undertaken, and 3) the existence of independent palaeoclimate data with which the isotope data can be compared.

3.4. Pleistocene and Late Holocene study sites

The second part of this thesis aims to apply the modern relationship between the $\delta^{18}O$ values of rodent teeth and meteoric water to reconstruct climatic conditions in Britain during the Pleistocene. This will be explored by: 1) coupling the $\delta^{18}O$ values of rodent teeth and mollusc shells, to generate quantitative estimates of past summer temperatures (Chapter 6), and

2) analysing rodent teeth from stratified cave sequences to reconstruct short-term palaeoclimatic fluctuations (Chapter 7).

To assess the reliability of the coupled isotope approach for reconstructing past summer temperatures, three interglacial fluvial sites were selected: 1) West Runton, Norfolk, 2) Cudmore Grove, Essex, and 3) Marsworth, Buckinghamshire. These sites were chosen for three main reasons. Firstly, fossil rodent teeth and mollusc shells are relatively abundant and well-preserved within the deposits at these sites. Therefore, sufficient fossil material was available for isotopic analysis. Secondly, the main fossil-bearing sediments were deposited fairly rapidly in low-energy depositional environments. As a result, the teeth and shells from these deposits are likely to reflect local environmental conditions during a similar interval of time, enabling their isotope values to be compared. Finally, these sites have been studied in great detail, and robust palaeoclimate evidence is available. The coupled isotope temperature estimates can consequently be validated against existing palaeoclimate reconstructions.

Two study sites were chosen for investigating whether the isotope values of rodent teeth from stratified cave sequences can record short-term climate fluctuations: 1) Westbury Cave, Somerset, and 2) Gully Cave, Somerset. Again, these sites were chosen due to the abundance of well-preserved rodent teeth within the deposits. Palaeoecological evidence from these rodent remains also suggests that short-term climatic changes occurred during the accumulation of the sequences. Thus, the isotope data from the rodent teeth can be directly compared with the faunal assemblages from which the teeth were obtained. This will enable an assessment to be made regarding the reliability of using the isotope values of rodent teeth as palaeoclimate proxies for cave sites.

The final key aim of this thesis is to investigate how the $\delta^{13}C$ values of rodent teeth from Britain have changed during the Late Quaternary period, in order to: 1) assess whether the $\delta^{13}C$ values of fossil teeth have been affected by diagenesis, and 2) investigate how recent anthropogenic impacts on atmospheric CO_2 are reflected in the $\delta^{13}C$ values of rodent teeth. To address this aim, isotope analyses must be undertaken on several teeth from well-dated and recent (Late Holocene) contexts. Archaeological sites can fulfil this

requirement, as abundant mammalian remains are often recovered during archaeological excavations. Additionally, these remains can be relatively precisely dated, through their association with age-diagnostic human artefacts, as well as radiocarbon dating. At present, there are few archaeological sites in Britain from which abundant rodent remains have been collected. However, there are two notable exceptions, from which rodent teeth were obtained for this thesis: 1) Longstone Edge, Derbyshire, and 2) Danebury, Hampshire.

The following sections outline the stratigraphic, palaeoenvironmental, palaeoclimatic and geochronological contexts of these Pleistocene and Late Holocene study sites.

3.4.1. West Runton, Norfolk

3.4.1.1. Site context

West Runton, located on the north Norfolk coast (Figure 3.4), is an internationally important site. The site is famous for its layer of organic, richly fossiliferous muds, known as the West Runton Freshwater Bed (WRFB). These deposits have been studied in great detail, from the original descriptions by Reid (1882; 1890), to the later study by West (1980). West (1980) designated the WRFB as belonging to the Cromer Forest-bed Formation, and named West Runton as the type site for the Middle Pleistocene Cromerian interglacial. Later studies, however, have recognized that multiple temperate stages are represented within the Cromer Forest-bed Formation (Preece & Parfitt, 2000; Preece, 2001; Stuart & Lister, 2001).

The site gained further attention in 1990, due to the discovery of a near-complete skeleton of the extinct steppe mammoth, *Mammuthus trogontherii* (Stuart, 2000; Stuart & Lister, 2010). This discovery provided an opportunity for new, systematic research to be undertaken, which culminated in the publication of a Quaternary International Special Issue in 2010 (Stuart & Lister, 2010).

The WRFB is currently exposed along a ~260 m section of the coast (NGR: TG 186431 to TG 188430) (Gibbard et al., 2010). The bed occurs within

a shallow, channel-shaped depression that is underlain and overlain by a sequence of tidal sands and gravels that form part of the Wroxham Crag Formation (West, 1980; Rose et al., 2008; Gibbard et al., 2010). The Wroxham Crag Formation is overlain by the glacial Cromer Till, which is of Anglian age (MIS 12) (West, 1980; Gibbard et al., 2010).

Studies on the WRFB have been mainly undertaken at two different locations along the coastal exposure of the deposit: 1) at the *M. trogontherii* excavation site (Davies et al., 2000; Rose et al., 2008; Lister & Stuart, 2010), which will henceforth be referred to as WR1, and 2) approximately 50 m west of this site (Rose et al., 2008; Gibbard et al., 2010), which will be referred to as WR2 (Figure 3.4). The isotope data used in this thesis were generated from analyses of fossil material originating from these two locations.

3.4.1.2. Sedimentology and depositional environment

The WRFB comprises a complex sequence of calcareous and organic detritus muds, interspersed with brecciated sediments and lenses of shelly sands (West, 1980; Rose et al., 2008). The sediments gradually fine through the sequence, from silty sands at the base of the bed, to predominantly silts at the top (Rose et al., 2008; Gibbard et al., 2010). The internal stratigraphy of the WRFB is also spatially variable, due to the lateral and vertical discontinuity of individual units (West, 1980; Rose et al., 2008; Gibbard et al., 2010). For example, a diamicton occurs at the base of the sequence at WR2 (Rose et al., 2008). Also, calcareous silts and gravelly sands at the base of the bed are generally restricted to the eastern half of the channel, while the younger, organic, laminated silts are thicker in the west (Gibbard et al., 2010). Due to this spatial variability, the interval of sediment accumulation may differ between different sections along the coastal exposure of the bed (West, 1980; Rose et al., 2008).

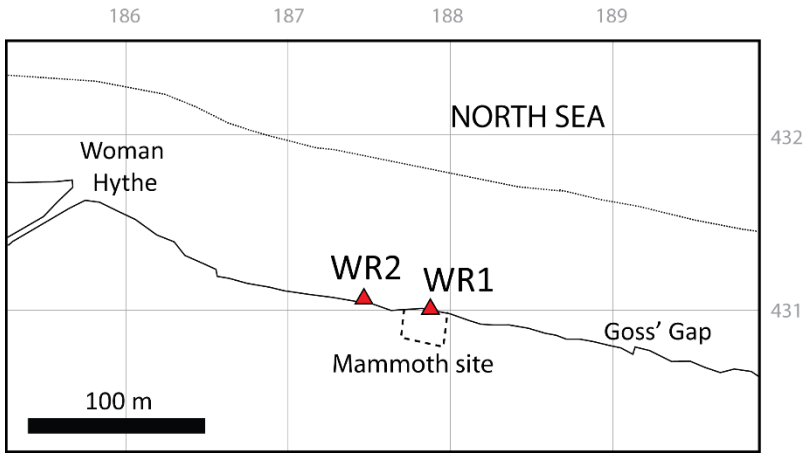

Figure 3.4: *The location of the study sites at West Runton on the North Norfolk coast. Grid reference lines are shown in grey. Modified from Gibbard et al. (2010).*

Nevertheless, the WRFB is relatively thin (maximum of ~1.8 m), and the accumulation of silts via suspension settling is a fairly rapid process (Rose et al., 2008). Furthermore, the completeness of the *M. trogontherii* skeleton indicates that the deposition of the WRFB occurred over a relatively short period of time (Rose et al., 2008). Likewise, other bones and teeth from the bed show no evidence for rounding or subaerial weathering, suggesting that the remains were transported only a short distance before deposition, and were buried rapidly with sediment (Maul & Parfitt, 2010). Therefore, any temporal diachronicity between different sections of the bed is likely to be fairly minor.

The WRFB sequence reflects the infill of a meandering fluvial channel or basin, with variations in the energy of deposition. The fine-grained muds indicate low-energy deposition in a shallow body of standing water, such as a backwater pool near to an active channel (West, 1980; Rose et al., 2008; Gibbard et al., 2010). The presence of calcareous muds suggests that the water in the channel was slow-flowing, and fed by a carbonate-rich spring (Gibbard et al., 2010). The diamictons were likely deposited due to the erosion and collapse of the channel banks (Rose et al., 2008), while the interspersed sand lenses suggest that intermittent but rapid, high-energy flood events

occurred (Gibbard et al., 2010). Towards the top of the sequence, these lenses become less frequent, suggesting that the local landscape and channel stabilised over time (Gibbard et al., 2010), enabling the accumulation of organic detritus silts. These silts progressively infilled the basin, resulting in an ecological succession from an open aquatic environment to a moist, vegetated swamp (Rose et al., 2008; Gibbard et al., 2010).

Evidence from the WRFB also indicates that fossil material from the site is likely to be relatively well-preserved. The presence of reduced iron compounds in the lower part of the bed indicates that conditions are anoxic, and no significant diagenetic modification of the sediments has occurred (Gibbard et al., 2010). Also, the flattened form of the wood fragments suggests that the sediments have been slightly compressed and compacted (Gibbard et al., 2010). As a result, the fine-grained silts are relatively impermeable to oxic groundwaters (Rose et al., 2008).

3.4.1.3. Palaeoenvironmental evidence

The WRFB contains a rich array of biological proxies, including pollen, plant macrofossils, non-marine molluscs, ostracods, beetles, and vertebrates (Stuart, 2000). The fauna suggest the presence of a clean, shallow, well-vegetated, slowly-flowing stream or stagnant pool (De Deckker, 1979; Sparks, 1980; Böhme, 2010; Coope, 2010a). The ostracod assemblage also hints at the presence of a nearby spring (De Deckker, 1979). Furthermore, riffle beetles, which are characteristic of flowing rivers, are absent, suggesting that the water was predominantly sluggish or still (Coope, 2010a).

The banks of the water body were lined with tall marsh and swamp vegetation, including reeds and rushes (De Deckker, 1979; Sparks, 1980; Field & Peglar, 2010). These reed swamps may have been interspersed with areas of alder carr, surrounded by damp grassland (Field & Peglar, 2010). These waterside habitats were likely inhabited by semi-aquatic mammals, such as water voles (*Mimomys savini*), water shrews (*Neomys newtoni*), and beavers (*Castor fiber*) (Stuart, 2000; Maul & Parfitt, 2010). The large concentration of small mammal remains modified by digestion also indicates

that diurnal avian predators, such as the kestrel, may have roosted in trees near to the water body (Mayhew, 1977; Maul & Parfitt, 2010).

Mixed deciduous woodland existed further afield, inhabited by large herbivores such as the fallow deer (*Dama* sp.) (West, 1980; Stuart, 1992; Coope, 2010a; Field & Peglar, 2010). These woodlands were probably fairly open, with patches of dry grasslands (Stuart, 2000; Field & Peglar, 2010) that were inhabited by giant deer (*Megaloceros savini*), horse (*Equus* sp.), and grassland voles (*Microtus* spp.) (Stuart, 1992).

The presence of deciduous woodland is supported by the pollen record, which comprises a large proportion of temperate arboreal taxa (West, 1980). The pollen stratigraphy of the WRFB is divided into two main stages: 1) a *Betula* and *Pinus* woodland, with some *Ulmus* and *Alnus* (Cr I: pre-temperate), which is associated with the basal calcareous silts and gravelly sands, and 2) a temperate deciduous woodland dominated by *Quercus*, *Ulmus*, and *Alnus*, with *Salix* and *Tilia*, which is associated with the shelly sands and fossiliferous muds (Cr II: early temperate) (West, 1980; Field & Peglar, 2010; Gibbard et al., 2010). The pollen record therefore suggests that the entire section of the WRFB accumulated during the early part of an interglacial stage, over a period of ~5-6 ka (Gibbard et al., 2010).

However, changes in the vegetational assemblage are only observed at certain sections of the WRFB. At both WR1 and WR2, the pollen assemblage is consistent throughout the sequence (Rose et al., 2008; Field & Peglar, 2010), and is correlated with the early part of Cr II (Field & Peglar, 2010). Likewise, no stratigraphic changes are observed in the beetle or small mammal faunas at WR1 (Coope, 2010a; Maul & Parfitt, 2010). This suggests that the sequences at WR1 and WR2 were deposited during a period of environmental stability, over a relatively short interval of time, i.e. tens to hundreds of years (Rose et al., 2008; Field & Peglar, 2010; Maul & Parfitt, 2010). Nevertheless, bioturbation due to trampling around the mammoth carcass at WR1 may have caused some mixing of the sediments, which could have obscured any stratigraphic changes in the biological assemblages (Field & Peglar, 2010).

In summary, the fossil assemblages from the WRFB indicate a habitat mosaic consisting of slow-flowing or standing water in a shallow, well-

vegetated pool, surrounded by marshland, reed swamps, alder carr, damp and dry grassland, and mixed deciduous woodland. The sedimentary and palaeoenvironmental evidence are summarised in Table 3.2.

3.4.1.4. Palaeoclimate evidence

The flora and fauna of the WRFB indicate full interglacial conditions (Table 3.3). Table 3.3 shows that the mean warmest month temperature was generally between +16 and +17°C, but may have reached +19°C. These temperature reconstructions are consistent with the mean July temperature in Norfolk at the present day (+16.8°C) (Table 3.1). Conversely, the mean coldest month temperature is around -3 to -1°C, which is cooler than present-day Norfolk (+4.8°C) (Table 3.1). This suggests that the climate was more continental than today. This is supported by the presence of molluscan, herpetile and mammalian taxa that have modern biogeographical distributions that span continental Europe (Table 3.3). Furthermore, the mean annual temperature reconstruction based on the herpetile assemblage is +6-8°C, which is slightly cooler than Norfolk today (+9.9°C) (Böhme, 2010). This cool mean annual temperature is due to the cooler winter temperatures relative to present.

The WRFB fauna also provide an indication of the humidity of the climate. The presence of taxa that require permanent aquatic habitats suggests that the annual precipitation was sufficient to maintain wet environments year-round. This is supported by the mean annual precipitation of 890 ± 255 mm, reconstructed from the herpetile assemblage (Böhme et al., 2006; Böhme, 2010). This precipitation value is significantly higher than the mean annual precipitation in present-day Norfolk (627 mm), and is more typical of the precipitation received in western Britain (Met Office, 2018). This may suggest that the atmospheric circulation during the West Runton interglacial was different to today (Böhme, 2010).

Table 3.2: *Summary of the sedimentary, depositional and palaeoenvironmental context of the West Runton Freshwater Bed. Information summarised from West (1980), Sparks (1980), Stuart (1992), Rose et al. (2008), Böhme (2010), Coope (2010), Field & Peglar (2010), Gibbard et al. (2010), Maul & Parfitt (2010), Preece (2010), and Stewart (2010).*

Sedimentary unit	Depositional interpretations	Pollen stratigraphy	Palaeoenvironmental interpretations
- Fine silt, lacking fossils	- Infilling of a shallow, sluggish pool with fine muds - Leaching of sediments and degradation of fossils by oxic groundwater	Cr II *Quercus*, *Ulmus* and *Alnus* woodland	- Shallow, slow-flowing or still backwater pool, containing abundant aquatic vegetation and inhabited by fishes, amphibians and waterfowl - Marshland, reed swamps and alder carr along the banks of the water body, inhabited by semi-aquatic small mammals - Disturbed areas trampled by large herbivores - Damp and drier grassland inhabited by deer, horses and voles - Mixed deciduous woodland
- Organic detritus muds with shell and wood fragments - Interspersed with shelly sand lenses	- Suspension settling of muds in a shallow, sluggish pool near to an active stream channel - Intermittent flooding, which became less frequent over time		
- Clast-rich diamicton	- Collapse and erosion of the stream channel banks		
- Calcareous detritus mud	- Slow-flowing stream fed by a carbonate spring	Cr I *Betula and Pinus* woodland	- Stream channel fed by a nearby spring

Table 3.3: *Summary of the palaeoclimate evidence from the West Runton Freshwater Bed. T_{max} refers to the mean warmest month (July) temperature, and T_{min} is the mean coldest month (January) temperature. Comparisons with the present-day climate in Norfolk are based on the data in Table 3.1. References: 1) Coope (2000; 2010), 2) De Deckker (1979); T.S. White (pers. comm.), 3) Preece (2010), 4) Böhme (2010), 5) Stewart (2010), 6) Maul & Parfitt (2010), 7) Stuart (2000); Field & Peglar (2010).*

Proxy	**Taxonomic composition of the assemblage**	**Temperature reconstructions**		**Palaeoclimate interpretations**
		T_{max} (°C)	**T_{min} (°C)**	
Beetles[1]	- 100% of taxa are extant in southern Britain today - Lack of thermophilous species typical of climates warmer than today - Presence of taxa that are active in marshy habitats during summer	+16 to +19	-3 to +5	- T_{max} and T_{min} comparable to present - Amount of precipitation during the warmest months was sufficient to maintain a wet environment
Ostracods[2]	- Majority of the taxa are extant in Northern Europe today - Presence of species (e.g. *Ilyocypris gibba*) that live in perennial water bodies	+16 to +19	-5 to +1	- T_{max} comparable to present - T_{min} lower than present - Climate more continental than present - Precipitation sufficient to maintain a small pool year-round
Molluscs[3]	- 91% of the taxa are extant in East Anglia today - Lack of southern thermophilous taxa (e.g. *Corbicula fluminalis*)	-	-	- Climate comparable to present - Climate possibly more continental than present

	- Several species (e.g. *Bithynia troschelii*, *Pisidium clessini* and *Discus ruderatus*) have geographical ranges that extend into Central and Eastern Europe today			
Herpetofauna[4]	- Lack of taxa that are characteristic of interglacial climate optima, e.g. *Emys orbicularis* (the European pond terrapin) - Assemblage comparable to cool interglacial or interstadial faunas from central Europe - 66% of the frog taxa only occur in continental Europe today - Abundance of taxa that require water for spawning	+16 to +17	-6 to -1.4	- T_{max} comparable to present - T_{min} lower than present - Climate more continental than present - Humid climate, with sufficient precipitation to sustain a permanent water body at the site
Fish[4] and birds[5]	- 100% of fish taxa extant in Britain today - 93% of bird taxa extant in Britain today	-	-	- Climate comparable to present
Mammals[6]	- Presence of *Cricetus runtonensis* (hamster), which currently lives in cool, continental grassland and steppe habitats	-	-	- Climate more continental than present
Plants[7]	- Lack of thermophilous species typical of climates warmer than today e.g. *Trapa natans* (water chestnut) or *Salvinia natans* (floating water fern) - Nearly all taxa are extant in Britain today	-	-	- Climate comparable to present

3.4.1.5. Previous isotope research on the site

Isotopic analyses have been undertaken on shells of the freshwater gastropod, *Valvata piscinalis*, from the WR1 and WR2 sections of the WRFB. The $\delta^{18}O$ values of the shells slightly differ between the two sites, with an average of -5.96‰ (1σ = 0.55, n = 75) at WR1 (Davies et al., 2000), and -5.08‰ (1σ = 0.52, n = 64) at WR2 (Rose et al., 2008). Nevertheless, the ranges in $\delta^{18}O_{ms}$ values are uniform throughout the WR1 and WR2 sequences (Davies et al., 2000; Rose et al., 2008). This suggests that climatic conditions were relatively constant during the deposition of the WRFB. Furthermore, the $\delta^{18}O_{ms}$ values are comparable to modern *V. piscinalis* shells from the River Thames and River Gipping in southern England (Davies et al., 2000; Rose et al., 2008; Waghorne et al., 2012). This indicates that environmental and climatic conditions at West Runton were comparable to the present day.

The $\delta^{13}C$ values of the shells are consistent with carbon derived from the soil zone underlying C_3 vegetation (Rose et al., 2008). However, the $\delta^{13}C_{ms}$ values are generally more enriched compared to modern shells, with values between -8 and -13‰ (Rose et al., 2008). These enriched $\delta^{13}C_{ms}$ values are likely related to 1) differences between the modern and past $\delta^{13}C$ value of atmospheric CO_2, and 2) increased equilibration of DIC with the atmosphere, due to the sluggish flow of the West Runton water body (Rose et al., 2008).

3.4.1.6. Age of the deposits

Since the Anglian-age Cromer Till lies stratigraphically above the West Runton sequence, the WRFB must pre-date MIS 12 (Preece & Parfitt, 2008). Palaeomagnetism measurements also demonstrate that the WRFB accumulated during a period of normal polarity (Gibbard et al., 2010). Therefore, the WRFB must fall within the Brunhes Chron, which begins ~780 ka (MIS 19). Additionally, the pollen biostratigraphy suggests that the WRFB corresponds to the early part of an interglacial stage (West, 1980). Consequently, the WRFB is unlikely to correlate with MIS 19, which begins ~790 ka (Lisiecki & Raymo, 2005). This means that the bed must correspond to an interglacial between MIS 13 and MIS 17.

Biostratigraphic evidence likewise demonstrates that the WRFB must pre-date MIS 13 (Preece & Parfitt, 2008). The WRFB faunal assemblages are distinct from other Middle Pleistocene sites in Britain, in that they lack southern thermophilous taxa and include a unique combination of extinct taxa (Coope, 2010a; Preece, 2010). These taxa include: 1) the extinct water vole, *Mimomys savini*, which is thought to have disappeared in Europe in early MIS 15 (Preece & Parfitt, 2008; Markova & Puzachenko, 2016), 2) the extinct vole, *Microtus gregaloides*, which has only been found in European deposits that are MIS 13 or older (Markova & Puzachenko, 2016), and 3) the freshwater molluscan taxa *Borysthenia goldfussiana*, *Tanousia runtoniana*, and *Viviparus viviparus gibbus*, which are only known from earlier sites within the Cromerian Complex, namely West Runton, Pakefield/Kessingland and Sugworth (Preece, 2001). Amino acid racemization data also suggest that the WRFB pre-dates MIS 11 and is older than the sediments at Waverley Wood, which are thought to date to the latter part of the Cromerian Complex (Preece, 2001; Penkman et al., 2010; Penkman et al., 2013). This combined evidence suggests that the WRFB correlates with the early part of MIS 15 or MIS 17 (Preece & Parfitt, 2008).

3.4.1.7. Justification for site choice

The WRFB offers ideal circumstances for coupling the $\delta^{18}O$ values of rodent teeth and freshwater shells. Firstly, the sedimentological and palaeoecological evidence indicates that the WRFB accumulated over a short period of time, during which palaeoclimatic conditions remained relatively stable. Therefore, small mammal teeth and shells from the bed are likely to be coeval, and reflect similar climatic conditions. The WRFB also has a low permeability and is anoxic, and thus the fossil material is unlikely to have been diagenetically modified due to interaction with groundwater. Finally, remains of the ancestral water vole, *Mimomys savini*, are highly abundant in the WRFB (Maul & Parfitt, 2010). Therefore, fossil rodent teeth are available in sufficient numbers to sample for isotopic analyses.

3.4.2. Cudmore Grove, Essex

3.4.2.1. Site context

The highly fossiliferous deposits at Cudmore Grove on Mersea Island, Essex (NGR: TM 065 144 to TM 069 147), are part of the important terrace staircase of fluvial sediments in the Lower Thames Valley of southeast England (Bridgland, 1994). The deposits lie within a channel-like depression, incised into the underlying Eocene-age London Clay Formation (Figure 3.5) (Bridgland, 1994). The sediments in this channel form the Cudmore Grove Member of the Lower Thames Formation (Roe et al., 2009). These sediments were deposited by the diverted course of the River Thames, known as the Thames-Medway (Bridgland, 1994; Roe et al., 2009). The Cudmore Grove Member comprises a thick (up to 20 m) sequence of deposits, containing abundant biological proxies that have provided detailed palaeoenvironmental information (Roe et al., 2009). The following sections summarise this multi-proxy evidence, as described by Roe et al. (2009).

3.4.2.2. Sedimentology and depositional environment

The deposits within the Cudmore Grove Channel have been divided into five stratigraphic units: 1) basal sands and gravels, 2) layered silty clays (comprising sub-units a-d), which represent most of the channel fill, 3) a thin, richly-fossiliferous bed of shelly detritus muds, 4) organic clays that contain abundant wood fragments but lack calcareous fossils, and 5) a thin layer of grey clays (Figure 3.5). This sequence reflects the deposition of fluvial gravels and sands under high-energy conditions, followed by the low-energy accumulation of muds within a fluvio-estuarine environment (Bridgland, 1994). The evidence for the depositional environment is mainly derived from the range of biological proxies preserved within the sediments.

A rich assemblage of faunal remains has been recovered from the detritus muds of Unit 3, including a large number of small vertebrates (Holman et al., 1990; Bridgland, 1994; Roe et al., 2009). The fossil material analysed in this research was derived from these sediments. The following sections

summarise the palaeoenvironmental and palaeoclimatic evidence from Unit 3, as well as the immediately overlying and underlying sediments.

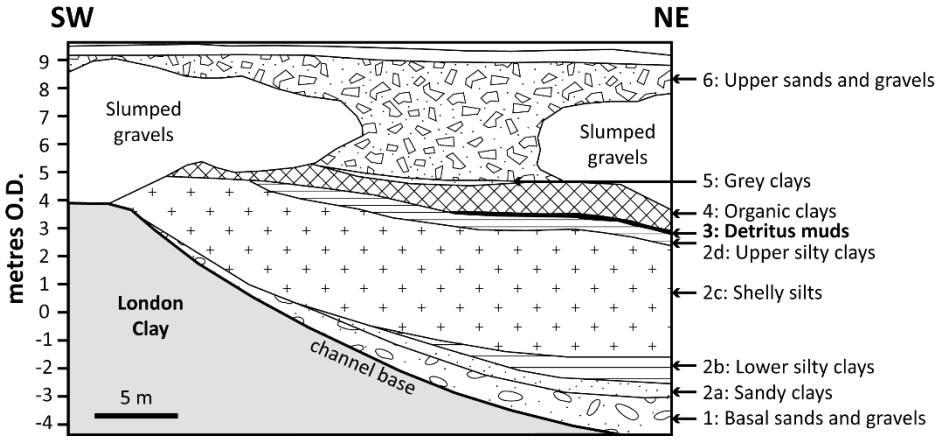

Figure 3.5: *Simplified stratigraphy of the Pleistocene deposits at the western edge of the Cudmore Grove Channel. Modified from Roe et al. (2009).*

3.4.2.3. Palaeoenvironmental evidence

The Cudmore Grove sediments contain abundant fossil remains of plants, diatoms, ostracods, molluscs, beetles and vertebrates. The palaeoenvironmental evidence from Units 2-4 is summarised in Table 3.4.

Key shifts in the floral and faunal assemblages are observed through these units. The diatom and ostracod assemblages from Units 2a-b are indicative of a fluvial environment in the upper reaches of an estuary. In the overlying Units 2c-d, the abundance of freshwater taxa declines, while marine and brackish taxa increase, suggesting a shift to a shallow, intertidal estuarine environment. The estuary was surrounded by mudflats with marginal wetland vegetation and expanding mixed deciduous woodland. The arboreal pollen assemblage from Unit 2 suggests a correlation with the early temperate sub-stage (II) of an interglacial.

The overlying detritus muds of Unit 3 indicate a change in the mode of deposition. These sediments are sandier and contain a rich assemblage of fossil remains from a range of local habitats. Ostracods almost disappear in

this unit, and due to breakage and corrosion, mollusc shells are generally poorly preserved. This suggests that the currents that transported the sand and shell debris to the site were high-energy, and therefore not conducive to the preservation of these fossils.

Conversely, the vertebrate remains from Unit 3 are very well-preserved. For example, fragile herpetile vertebrae (Holman et al., 1990), and small mammal mandibles with teeth *in situ*, have been found within these sediments. The bones also show no evidence for rolling or abrasion. This suggests that the vertebrate remains were transported under low-energy conditions and deposited proximal to their source, with minimal post-depositional disturbance.

The diatom assemblage in Unit 3 is dominated by marine and brackish taxa (> 75%). The molluscan assemblage likewise comprises an abundance of brackish taxa, but also includes a relatively diverse range of freshwater taxa. The freshwater mollusc remains comprise a mixture of species that are typical of slow-flowing waters (e.g. *Valvata piscinalis*) and faster-flowing waters (e.g. *Pisidium amnicum*). The presence of riffle beetles also suggests that running water habitats existed nearby.

Nevertheless, the beetle, herpetofaunal and bird assemblages indicate that sluggish, well-vegetated, freshwater habitats were dominant in the local area. Additionally, beetle and fish taxa that are characteristic of saline conditions are absent. This indicates that the beetle and vertebrate remains originate from freshwater habitats that lay upstream of the tidal influence.

The plant and beetle assemblages also include species characteristic of damp marginal habitats, including reed swamps and alder carr. These wetland habitats were likely inhabited by small mammals such as the water vole (*Arvicola cantiana*) and beaver (*Castor fiber*).

Mixed deciduous woodlands, comprising *Alnus*, *Pinus, Quercus*, *Fraxinus* and *Tilia*, were also present. These tree taxa are consistent with the late temperate sub-stage (III) of an interglacial. The woodlands were inhabited by a diverse range of woodland mammals, including the bank vole (*Myodes glareolus*), wood mouse (*Apodemus sylvaticus*), red squirrel (*Sciurus vulgaris*), and macaque (*Macaca sylvanus*). Local areas of open grassland are also indicated by the presence of the field vole (*Microtus agrestis*) and horse (*Equus* sp.).

This evidence shows that the faunal assemblages in Unit 3 are ecologically heterogeneous, comprising a mixture of brackish, standing and flowing freshwater, marshland, woodland and grassland taxa. Most of the proxies suggest the presence of a slow-flowing freshwater river surrounded by wetlands. The preservation of delicate vertebrate remains suggests that they were washed into the channel from the local landscape. On the other hand, the brackish diatom and molluscan remains may have been re-worked from nearby sources or the underlying estuarine deposits (Unit 2). Unit 3 has therefore been interpreted as a 'lag' deposit, formed via the high-energy erosion and transport of estuarine sediments, followed by the low-energy deposition of local fossil material within a freshwater channel.

The transition from an estuarine to a freshwater environment is further indicated by the clays of Unit 4. The evidence from this unit suggests that the sediments accumulated within a quiet backwater lagoon (Table 3.4).

In summary, the Cudmore Grove sequence reflects a transition from a low-energy fluvial and estuarine environment (Unit 2), to a relatively high-energy fluvial environment (Unit 3), and finally a low-energy lagoonal environment (Unit 4).

3.4.2.4. Palaeoclimate evidence

The palaeoclimate evidence from Cudmore Grove, summarised in Table 3.5, suggests that the sediments accumulated during an interglacial stage. The presence of several exotic 'southern' taxa is a clear indication that the climate was warmer than southern England at the present day. Also, the MCR best estimate for the mean warmest month temperature (19°C) (Roe et al., 2009) is slightly warmer than today (17.8°C) (Table 3.1). Conversely, the best estimate for the mean coldest month temperature (+1°C) (Roe et al., 2009) is slightly colder than today (+4.4°C) (Table 3.1). This suggests that climatic conditions were more continental than present. This is supported by the presence of taxa with modern biogeographical ranges that extend into central and eastern Europe. The climatic regime at Cudmore Grove was therefore warmer and more continental than southern England today.

Table 3.4: *Summary of the sedimentological and palaeoenvironmental evidence from Units 2-4 of the Cudmore Grove Member. All information was obtained from Roe et al. (2009).*

Stratigraphic unit	**Sediment description**	**Depositional interpretations**	**Pollen stratigraphy**	**Palaeoenvironmental interpretations**
Unit 4	- Organic clays with abundant wood fragments, but a lack of shell debris	- Accumulation of muds in a quiet backwater lagoon	Late temperate (III): *Alnus*, *Quercus*, and *Pinus,* with *Corylus, Carpinus* and *Abies*	- Eutrophic, still, body of freshwater, isolated from the estuary - Marine taxa decline from a maximum; freshwater taxa increase in abundance - Mixed deciduous woodland, dominated by *Alnus* - Expansion of coniferous trees
Unit 3	- Shelly detritus muds	- 'Lag' deposit, comprising allochthonous material inwashed from proximal sources - Rapid deposition, probably following an erosive episode	Late temperate (III): *Alnus*, *Quercus*, and *Pinus,* with *Fraxinus* and *Tilia*	- Permanent, eutrophic, slow-flowing or still freshwater in a well-vegetated river near to an estuary - Some evidence for flowing water nearby - Damp, infilled channel colonised by ferns - Surrounding alder carr, marshland and reed swamps - Mixed deciduous woodland with dry, open shrubby areas

Unit 2	c-d	- Shelly silts and silty clays	- Estuarine environment	Early temperate (II): *Quercus*, with *Pinus*, *Fraxinus* and *Tilia*	- Decline in freshwater taxa towards a minimum; gradual increase in brackish and marine taxa - Increase in salinity due to the landward progression of the tidal head, associated with a long-term sea-level rise - Mixed deciduous woodland with shaded forest floor and open grassland habitats
	a-b	- Sandy and silty clays with occasional shell fragments	- Fluvial environment near to an estuary	Early temperate (II): *Pinus* and *Betula* with *Quercus*	- Calm, shallow, eutrophic water surrounded by marshland - Predominantly freshwater, with only a minor brackish influence - Boreal-type woodland

Table 3.5: *Palaeoclimate evidence from Units 2 and 3 of the Cudmore Grove Member. References: 1) Roe et al. (2009), 2) Horne et al. (2012), 3) Holman et al. (1990), 4) Sinka (1993).*

Proxy	**Taxonomic composition of the assemblage**	**Temperature reconstructions**		**Palaeoclimate interpretations**
		T_{max} (°C)	**T_{min} (°C)**	
Beetles[1] (Unit 3)	- 100% of the taxa are exotic to Britain today - These taxa have 'southern' biogeographical distributions at the present day	+16 to +22	-7 to +4	- Climate warmer than southern England today - T_{max} similar or higher than today - T_{min} similar or lower than today
Ostracods[1-2] (Unit 2)	-	+15 to +21	-8 to +4	- T_{max} similar or higher than today - T_{min} similar or lower than today - Climate potentially warmer and more continental than present
Herpetofauna [1, 3-4] (Unit 3)	- 43% of the taxa are exotic to Britain today - Presence of taxa associated with interglacial climate optima e.g. *Emys orbicularis* (European pond terrapin) and *Zamenis longissimus* (aesculapian snake) - Presence of taxa such as *Rana arvalis* (moor frog) that currently live in eastern continental Europe	+17 to +24°C	-6 to +4	- T_{max} similar or higher than today - T_{min} similar or lower than today - Climate possibly more continental than southern England today

	- Abundance of taxa that require water for spawning			- Humid climate, with sufficient precipitation to sustain a permanent water body at the site
Birds[1] (Unit 3)	- Presence of waterfowl such as *Anas querquedula* (garganey), *Anas strepera* (gadwall), and *Porzana parva* (little crake) that currently live in eastern Europe and central Asia	-	-	- Summer temperatures comparable to central Europe today
Mammals[1] (Unit 3)	- Presence of *Crocidura* cf. *leucodon* (white-toothed shrew), which has a modern biogeographical distribution that spans southern and central Europe	-	-	- Climate warmer and possibly more continental than southern England today

3.4.2.5. Previous isotope research on site

Isotope analyses have been undertaken on a small number (n = 27) of *Valvata piscinalis* shells from Unit 3 (Ruddy, 2005). The mean $\delta^{18}O_{ms}$ value is -5.31‰ (1σ = 0.82), which is slightly higher than the mean value for modern *V. piscinalis* shells (Candy et al., 2014). These isotope results are therefore consistent with a climate warmer than today (Table 3.5).

Analyses have also been undertaken on enamel phosphate from 13 *Arvicola cantiana* incisors from Unit 3 (Ruddy, 2005). These analyses generated a median $\delta^{18}O$ value of 15.4‰ (VSMOW). When coupled with the mean $\delta^{18}O$ of the mollusc shells, a mean summer palaeotemperature of +22°C was generated (Ruddy, 2005). This temperature value is consistent with the maximum warmest month temperature reconstructions for Cudmore Grove (Table 3.5).

3.4.2.6. Age of the deposits

The Cudmore Grove sequence was originally correlated with the Hoxnian interglacial stage (MIS 11), based on similarities in the pollen stratigraphy and clast lithology with the nearby site of Clacton-on-Sea, located 10 km west of Cudmore Grove (Bridgland, 1988; Bridgland, 1994). However, biostratigraphic evidence from the mammalian assemblage supports a younger age for the Cudmore Grove deposits. The assemblage lacks the indicator species that are characteristic of the Hoxnian-age Swanscombe Mammal Assemblage Zone (MAZ) (Schreve, 2001). For example, no remains of the extinct small mole (*Talpa minor*) and rabbit (*Oryctolagus cuniculus*) have been discovered in the Cudmore Grove sediments, despite the recovery of more than 1500 remains from the site (Roe et al., 2009). Moreover, the Cudmore Grove mammalian assemblage comprises the extant European beaver (*Castor fiber*) and brown bear (*Ursus arctos*), as opposed to the extinct giant beaver (*Trogontherium cuvieri*) and cave bear (*Ursus spelaeus*) that are characteristic of the Hoxnian (Schreve, 2001). In addition, the *Arvicola cantiana* molars from Cudmore Grove are morphologically advanced compared to those from Swanscombe, but are comparable to molars from sites attributed to MIS 9, such as Purfleet

(Schreve, 2001; Roe et al., 2009). This strongly suggests that the Cudmore Grove Member accumulated during an interglacial stage that is younger than MIS 11 (Roe et al., 2009).

The Cudmore Grove mammalian assemblage is most similar to the Purfleet MAZ (Schreve, 2001). The deposits at Purfleet occur on a terrace of the River Thames that is stratigraphically younger than the Hoxnian sediments at Swanscombe, and which is correlated with MIS 9 (Bridgland, 1994). Independent geochronological evidence from Purfleet, in the form of optically-stimulated luminescence dates, supports a correlation with MIS 9 (Bridgland et al., 2013). Amino acid racemization analyses also place Cudmore Grove within MIS 9 (Penkman et al., 2007; Penkman et al., 2013). Therefore, the available evidence indicates that the Cudmore Grove Member accumulated during MIS 9.

3.4.2.7. Justification for site choice

The sedimentological, taphonomic and palaeoenvironmental evidence from Unit 3 at Cudmore Grove suggest that the vertebrate remains experienced minimal transport before deposition. Due to the predominance of freshwater taxa in these sediments, it is likely that the freshwater mollusc shells were also deposited near to their source. Consequently, the $\delta^{18}O$ values of the fossil rodent teeth and shells are both likely to reflect the $\delta^{18}O$ value of local meteoric water. Also, fossil rodent remains, and particularly the remains of *Arvicola cantiana*, are very abundant within Unit 3 (Roe et al., 2009). Thus, sufficient rodent teeth are available for isotopic analysis. Finally, the consistent palaeotemperature reconstructions from the site (Table 3.5) enable the reliability of isotope-based temperature estimates to be assessed. Cudmore Grove is therefore a suitable site for applying the coupled isotope approach.

3.4.3. Marsworth, Buckinghamshire

3.4.3.1. Site context

The sequence of fluvial deposits near Marsworth in Buckinghamshire is of great importance to the British Quaternary record. The biostratigraphic and geochronological evidence from the site have played key roles in demonstrating that additional, post-Hoxnian (MIS 11) but pre-Ipswichian (MIS 5e) interglacials are represented in the Middle-Late Pleistocene stratigraphy of lowland Britain (Green et al., 1984; Murton et al., 2001; Candy & Schreve, 2007; Murton et al., 2015). Moreover, the wide range of proxies preserved in the Marsworth deposits has enabled the depositional environment and palaeoenvironmental conditions to be reconstructed in great detail (Green et al., 1984; Field, 1993; Murton et al., 2001; Murton et al., 2015).

The deposits occur within a former quarry, which is now the site of the College Lake Wildlife Centre (NGR: SP 933143) (Murton et al., 2001). This site is situated on a platform of Cretaceous Lower Chalk (Sherlock, 1922), ~3-4 km northwest of the Chilterns Hills scarp. The Chiltern Hills are one of the recharge areas for the London Chalk aquifer, and groundwater from this aquifer emerges at the base of the scarp in the form of springs. These springs feed several small streams that have played important roles in the transport and deposition of sediments in the Marsworth area (Murton et al., 2001).

The Pleistocene sequence at Marsworth was first described by Green et al. (1984), following controlled excavations undertaken in 1980-1984 at an area called Site B. The results of multi-proxy analyses on the deposits at this site were presented by Murton et al. (2001), and other Pleistocene deposits within the quarry were later investigated by Murton et al. (2015). Three major sedimentological phases have been identified at Marsworth: 1) the deposition of gravelly sands and spatially-restricted organic muds within a ‘Lower Channel’ feature cut into the chalk (Unit B2), 2) the accumulation and deformation of colluvial deposits, formed under periglacial conditions (Unit B3), and 3) the deposition of gravels, sands and silts in an ‘Upper Channel’ feature (Green et al., 1984; Murton et al., 2001). All material analysed in this research originates from the Lower Channel. The following review summarises the evidence from this channel, as reported in Murton et al. (2001).

3.4.3.2. Sedimentology and depositional environment

The basal sediments in the Lower Channel comprise a layer of gravelly calcareous sands (Level 3) (Figure 3.6), containing abundant bone fragments and tufa clasts. Tufa is calcium carbonate that precipitates in streams that are rich in calcium and bicarbonate ions due to the dissolution of carbonate bedrock (Andrews, 2006). The presence of abundant tufa clasts therefore suggests that the Lower Channel was located near to a carbonate spring. This spring likely emerged at the foot of the chalk scarp in the nearby Chiltern Hills.

At the base of the Lower Channel, the tufa clasts are preserved as angular, boulder-sized fragments, suggesting that these clasts are *in situ* or located proximal to the site of formation. Some of the tufa clasts may also be annually laminated. This suggests that the discharge of groundwater at the spring was perennial, enabling tufa precipitation throughout the year. Therefore, the sedimentological evidence indicates that Level 3 accumulated in a relatively low-energy, spring-fed, perennial stream located proximal to its source.

Level 3 is locally overlain by organic muds (Level 2) (Figure 3.6) that are rich in the fossil remains of various plants and animals. The following section summarises the palaeoenvironmental evidence derived from these fossil remains.

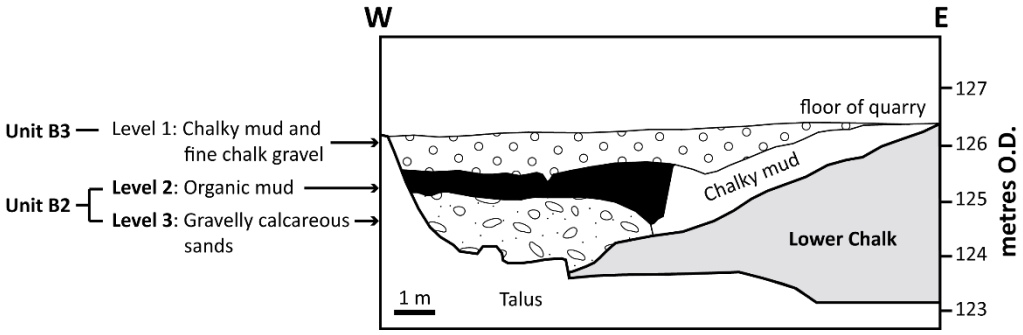

Figure 3.6: *Simplified stratigraphy of the Middle Pleistocene sequence at Marsworth. Modified from Murton et al. (2001).*

3.4.3.3. Palaeoenvironmental evidence

A wide range of biological proxies is preserved in the Lower Channel, including pollen, plant macrofossils, molluscs, ostracods, beetles and vertebrates. No major stratigraphic shifts are observed in the pollen, molluscan, beetle, and mammalian assemblages through Levels 3 and 2. This suggests that environmental conditions were fairly stable during the infilling of the Lower Channel (Table 3.6). Therefore, in the following review, the evidence from Levels 3 and 2 will be considered together.

The aquatic pollen, ostracod and beetle remains from the Lower Channel are dominated by taxa characteristic of shallow, sluggish, perennially-flowing streams. The presence of water vole (*Arvicola cantiana*) remains supports this evidence, as this rodent commonly live on the banks of small streams or ponds (MacDonald & Barrett, 1993). The aquatic mollusc assemblage also comprises slum species such as *Galba truncatula*, which are commonly found in small, muddy, stagnant ponds that are prone to drying.

The slow-flowing stream was fringed by marshland vegetation comprising reeds and sedges. Beyond these wetlands lay open calcareous grasslands, colonised by molluscs such as *Trochulus hispidus*, and mammals such as wild horse (*Equus ferus*) and woolly mammoth (*Mammuthus* sp.). The rodent assemblage is also dominated by the remains of the northern vole (*Microtus oeconomus*), which is found today in wet, grassy, tundra environments in continental Europe (MacDonald & Barrett, 1993).

The presence of taxa such as *Palaeoloxodon antiquus* (straight-tusked elephant) suggests that woodland habitats were additionally present in the local area. However, arboreal and shrub taxa (*Betula*, *Alnus*, *Juniperus* etc.) constitute only a minor component of the pollen assemblages from Levels 3 and 2. Moreover, mollusc taxa that prefer shaded habitats are infrequent in the deposits, and tree-dependent beetles are entirely absent. Therefore, woodland habitats probably only consisted of small stands of scattered trees.

In summary, the palaeoenvironmental evidence indicates that the Lower Channel deposits accumulated within a small, slow-flowing, well-vegetated, perennial stream, surrounded by muddy pools, marshland, open calcareous grasslands, and small patches of woodland further afield.

3.4.3.4. Palaeoclimate evidence

The palaeoclimate evidence from the Lower Channel deposits is summarised in Table 3.7. Quantitative temperature estimates based on the beetle and ostracod assemblages indicate mean summer temperatures between +15 and +16°C, which are similar to or slightly cooler than Marsworth at the present day (16.8°C) (Table 3.1). The mean coldest month temperatures fall between -4 and +1°C, which are again slightly cooler than today (4.0°C) (Table 3.1). The most likely figures for the T_{max} and T_{min} are +15°C and -5°C, respectively (Murton et al., 2001). These reconstructions suggest that the climate at Marsworth was temperate, but slightly cooler and more continental than today.

The abundance of aquatic and marshland species also suggests that the climate was relatively humid. Furthermore, the homogeneity in the floral and faunal assemblages throughout the Lower Channel suggests that the climate remained relatively stable during the period of deposition. Therefore, the overall indication is that the deposits accumulated during a humid, temperate episode.

However, the fossil assemblages from the Lower Channel are fairly unusual for an interglacial stage, as many species that are characteristic of temperate woodland environments are notably absent. Middle and Late Pleistocene interglacial sequences in Britain usually preserve an abundance of temperate woodland taxa (Stuart, 1974). In contrast, the fossil assemblages from Marsworth are dominated by grassland taxa, which is a feature normally associated with cool, interstadial-like conditions. Nevertheless, the lack of cold-adapted species, the presence of taxa with southern distributions, and the reconstruction of temperatures that are comparable to today, indicates that the open environment at Marsworth did not result from a cold climate. Instead, it is likely that the deposits represent an interval towards the end of an interglacial stage, when climatic conditions were slightly cooler, and the vegetation more open. This interpretation is supported by the presence of pollen and beetle taxa that are characteristic of cool, boreal-montane conditions in the uppermost Lower Channel deposits, suggesting that the climate began to cool towards the top of Level 2.

Table 3.6: *Summary of the sedimentological and palaeoenvironmental evidence from Levels 3 and 2 in the Lower Channel at Marsworth. Information obtained from Murton et al. (2001).*

Stratigraphic Unit	Sediment description	Depositional interpretations	Palaeoenvironmental interpretations
Level 2	- Organic muds	- Suspension settling of fine organic muds in a still or slow-flowing stream	- Shallow, slow-flowing perennial stream containing dense aquatic vegetation - Temporary, stagnant, muddy ponds nearby - Dense marshland vegetation along the margins of the stream - Open dry grasslands dominated the landscape - Scattered patches of mixed deciduous woodland
Level 3	- Gravelly calcareous sands - Contain abundant bone fragments and laminated tufa clasts	- Sands and gravels eroded and transported from a nearby chalk scarp - Tufa precipitated in a low-energy, spring-fed carbonate stream - Tufa locally re-worked and re-deposited into the Lower Channel	

Table 3.7: *Palaeoclimate evidence from Levels 3 and 2 in the Lower Channel at Marsworth. Information obtained from Murton et al. (2001). The Mutual Ostracod Temperature Range reconstruction is from Horne (2007).*

Proxy	**Taxonomic composition of the assemblage**	**Temperature reconstructions**		**Palaeoclimate interpretations**
		T_{max} (°C)	**T_{min} (°C)**	
Beetles	- Lack of obligate cold-adapted taxa - Presence of taxa with relatively southern and eastern European distributions e.g. *Stomoides gyrosicollis*, which is found today as far north as eastern Austria and the Czech Republic - Abundance of marshland species but a lack of taxa typical of running water	+15 to +17	-9 to +1	- T_{max} similar to or slightly cooler than present - T_{min} cooler than present - Temperate climate comparable to central England today - Climate possibly more continental than present - Climate sufficiently humid to support damp habitats, but the stream and local ponds may have dried during the summer
Ostracods	- None of the taxa indicate temperatures different to Marsworth today	+16 to +19	-4 to +4	- T_{max} similar to present - T_{min} similar to or cooler than present
Molluscs	- Lack of obligate cold-adapted taxa - Presence of species with relatively 'southern' distributions e.g. *Azeca goodalli* - Diverse aquatic fauna	-	-	- Temperate climate - Climate sufficiently humid to support damp habitats

Mammals	- Presence of taxa that only occur in Britain during interglacial stages e.g. *Palaeoloxodon antiquus* (straight-tusked elephant) - Abundance of open grassland taxa, including species that currently live in tundra and taiga habitats in eastern Europe and Asia (e.g. *Microtus oeconomus*)	-	-	- Temperate climate - Climate possibly more continental than today

3.4.3.5. Age of the deposits

Obtaining reliable age estimates for the Marsworth deposits initially proved problematic. Uranium-Thorium (U-Th) dating has been undertaken on several tufa clasts from Level 3, with varying degrees of success. Green et al. (1984) produced dates between 171 and 149 ka, with broad 1σ errors of 15-30 ka. These dates suggest that tufa formation occurred during the penultimate glacial stage, MIS 6. However, given that the Lower Channel deposits contain temperate-adapted floras and faunas, this scenario seems highly unlikely.

Murton et al. (2001) undertook additional U-Th dating on the tufa clasts in an attempt to refine the age constraints for the Lower Channel. However, this dating also produced broad age ranges between > 360 and 156 ka. Moreover, several samples were found to be contaminated with detrital thorium derived from Chalk debris, leading to overestimations in the ages of the clasts. As a result, Murton et al. (2001) deemed the U-Th ages unreliable.

Amino acid racemization analyses, undertaken on molluscs from the Lower Channel, are likewise difficult to interpret. Comparison of the amino acid ratios for Marsworth with those derived for other British interglacial sites suggests that Level 2 accumulated during or after MIS 5e (Murton et al., 2001; Murton et al., 2015).

However, these dates are incompatible with the biostratigraphic evidence from the site. The mammalian assemblage from Marsworth, which is dominated by open grassland indicators such as *Mammuthus* sp., *Equus ferus*, and a relatively large form of *Microtus oeconomus*, is characteristic of the Sandy Lane Mammal Assemblage Zone (Schreve, 2001). This zone has been correlated with the latter part of MIS 7 (Schreve, 2001). This means that the tufa clasts, which are deposited at the base of the Lower Channel and therefore pre-date Levels 3 and 2, must have formed during an earlier warm episode within MIS 7. The dominance of arboreal pollen within the tufa clasts (Murton et al., 2001) suggests a correlation with the Ponds Farm MAZ, which is characterised by an abundance of temperate woodland indicators (Schreve, 2001).

This biostratigraphic evidence has been corroborated by further U-Th dating of the tufa clasts (Candy & Schreve, 2007), as well as optically-stimulated luminescence dating of quartz grains from Level 3 (Murton et al., 2015). Optical dates for the Lower Channel sands range from 208 to 255 ka (Murton et al., 2015). According to the marine benthic $\delta^{18}O$ record, MIS 7 spanned ~243 to 191 ka (Lisiecki & Raymo, 2005). The optical ages consequently suggest that Level 3 accumulated during MIS 7.

The U-Th dates for the tufa clasts fall within two distinct clusters: 1) between 254 and 234 ka, and 2) between 220 and 208 ka (Candy & Schreve, 2007). These clusters correlate with substages MIS 7e and MIS 7c, respectively (Candy & Schreve, 2007). Given that the tufa was reworked and deposited within the Lower Channel, the Lower Channel sediments must post-date MIS 7c. This, in combination with the biostratigraphic evidence, suggests that the Lower Channel sediments were deposited during MIS 7a.

3.4.3.6. Justification for site choice

The Lower Channel sediments contain relatively abundant rodent teeth and mollusc shells. The rodent assemblage is dominated by *M. oeconomus*, and therefore sufficient rodent teeth belonging to a single taxon are available for isotopic analysis. In addition, the Lower Channel deposits, and particularly the organic muds in Level 2, accumulated under relatively low-energy conditions. Therefore, the fossil material is unlikely to have undergone long-distance transport or significant re-working. Furthermore, there are no stratigraphic changes in the fossil assemblages through the Lower Channel sequence. This suggests that the sediments accumulated over a relatively short interval of time (perhaps a few thousand years). Therefore, the $\delta^{18}O$ values of the teeth and shells are likely to reflect similar $\delta^{18}O$ values of local meteoric water. Consistent palaeotemperature reconstructions are also available (Table 3.7), for comparison with the isotope-based temperature estimates. The Lower Channel at Marsworth is consequently suitable for applying the coupled isotope approach.

3.4.4. Westbury Cave, Somerset

3.4.4.1. Site context

The Pleistocene deposits at Westbury Cave are exposed on the northeast face of a limestone quarry in the Mendip Hills, located near to Westbury-sub-Mendip in Somerset (NGR: ST 508 504). The cave comprises two chambers: 1) a large Main Chamber, situated at the southeastern end of the cave system, and 2) a smaller Side Chamber on the northwest side of the cave (Andrews, 1990). The site was first investigated by Bishop (1974), who divided the sequence into two main groups: 1) the Siliceous Member, which occurs at the base of the sequence and contains a rich assemblage of Early Pleistocene mammals (Adams, 2017), and 2) the Calcareous Member, which comprises a thick, well-stratified sequence of limestone breccias, containing abundant Middle Pleistocene mammalian remains.

Further excavations at the site were undertaken by the Natural History Museum, London, between 1976 and 1984 (Andrews et al., 1999). During these excavations, 20 stratigraphic units were identified, 19 of which occur within the Calcareous Member (Figure 3.7) (Andrews, 1990). These units have yielded a large number of small mammal remains, dominated by isolated vole teeth (Andrews, 1990). Stratigraphic changes in the small mammal faunas indicate that short-term paleoenvironmental and palaeoclimatic changes may have occurred during the accumulation of the sequence (Stringer et al., 1996). Moreover, the occupation of early humans at the site has been proposed due to the presence of possible Acheulean flint tools and cut-marked bones within the deposits (Bishop, 1974; Bishop, 1975; Andrews et al., 1999). Westbury Cave is therefore an important site for understanding short-term palaeoclimatic fluctuations during the Middle Pleistocene, as well as the palaeoclimatic context for the early human occupation of Britain. The following sections summarise the main findings from the Natural History Museum excavations, as published in Andrews (1990) and Andrews et al. (1999).

3.4.4.2. Site stratigraphy

The key stratigraphic units within the Main Chamber and Side Chamber at Westbury Cave are illustrated in Figure 3.7. Major units have been divided into sub-units, which each represent a separate depositional event. However, some of these units occur within different sections of the chambers, and cannot necessarily be correlated. Thus, while unit numbers generally denote stratigraphic succession, this is not always the case. Unit 1, the Siliceous Member, is the only unit that is common to both chambers. Units 3, 4, 6 and 7 in the Side Chamber are unfossiliferous, water-lain silts, while Units 2 and 5 primarily contain the remains of cave bears (*Ursus deningeri*) (Bishop, 1974; Andrews, 1990). Therefore, the following reviews will only focus on Units 8 and above. These are the units from which the rodent teeth were obtained for isotopic analysis.

Of the two chambers, the Side Chamber sequence is the longest (Figure 3.7), and contains the richest assemblages of small mammal remains. This sequence has been studied at three main sections (W2, W2/9 and W9), between which individual units have been laterally correlated. Unit 8 is a layer of fossil-bearing water-lain sediments, while Units 9 and 10 comprise re-worked, water-lain siliceous sediments that are mostly unfossiliferous. The overlying Units 11-15 consist of a series of limestone breccias, which have been sub-divided based on their colour and bone content. There are two notable concentrations of highly abundant small mammal remains within these breccias: 1) Unit 12, which has been named the ‘Mole layer’, and 2) Unit 15/8, which is named the Rodent Earth.

A different sedimentary sequence is seen in the Main Chamber (Figure 3.7), suggesting that these deposits were derived from an independent source. The deposits have been studied at three main sections (W1, W10 and W5). Within the Main Chamber, Unit 1 is overlain by Units 17-20, which are a series of limestone breccias. The sediments in Units 18-19 are thought to have been brought into the cave via mudflows. A large concentration of small mammal remains occurs within sub-unit 19/14 (the Rodent Breccia), although most of Unit 19 contains little skeletal material. Unit 20 also contains few fossils.

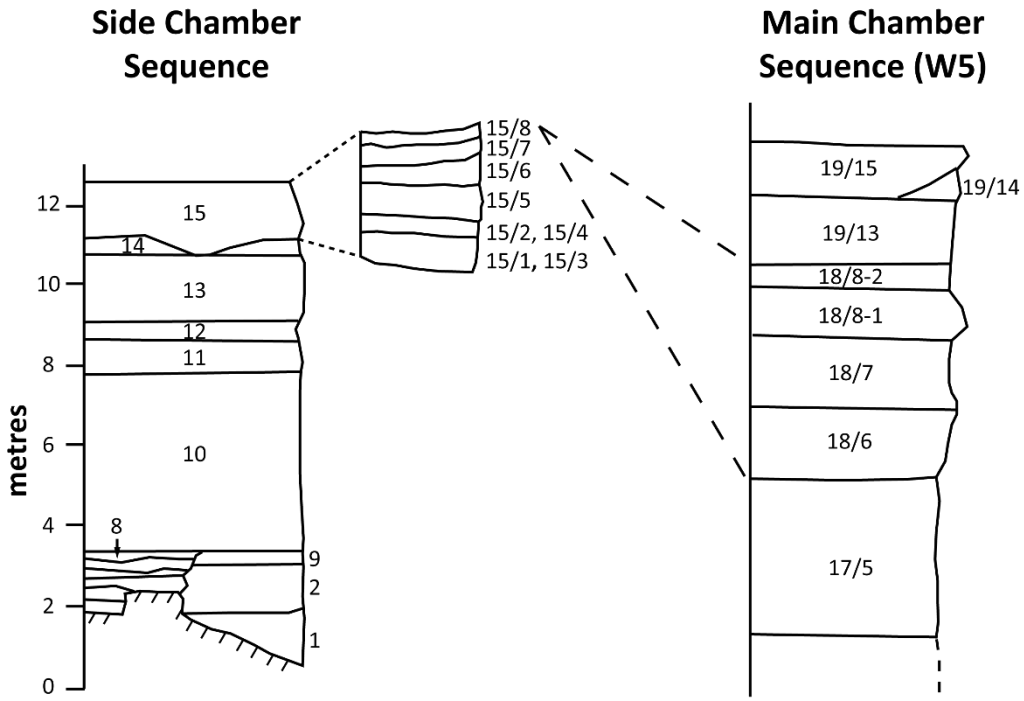

Figure 3.7: *Summary of the stratigraphic sequences in the Side Chamber and Main Chamber of Westbury Cave. The dashed lines indicate the suggested correlation between the sequences in the two chambers. Diagrams modified from Andrews (1990).*

3.4.4.3. Small mammal remains

Small mammal remains are abundant throughout much of the Calcareous Member. However, the relative abundances of each species vary through the sequence (Table 3.8). The small mammal assemblages are primarily dominated by the extinct narrow-headed vole *Microtus (Pitymys) gregaloides*, and the extant voles *Microtus agrestis/arvalis* (Table 3.8). However, in Units 13, 14, 15/8 and 18, lemmings (e.g. *Dicrostonyx torquatus*, the collared lemming) are also present. Furthermore, in Units 15/2, 15/4 and 15/5, the extinct pine vole *Pitymys arvaloides* (now referred to as *Microtus arvalidens*) replaces *M. gregaloides* as the dominant species.

The mammalian assemblages from Units 15/8 and 18 are very similar, suggesting that they may have been deposited during similar time intervals. These units have therefore been tentatively correlated (Figure 3.7). This correlation between the Side Chamber and Main Chamber sequences has

enabled a composite stratigraphic and palaeoenvironmental record to be generated for Westbury Cave (Table 3.8).

The processes responsible for accumulating the small mammal remains also vary between the different units (Table 3.8). The remains from Unit 8 are dominated by teeth that are broken and rounded due to physical attrition during transport. The majority of these remains are also stained black with manganese dioxide. This evidence suggests that the material was primarily transported and deposited by running water.

In contrast, the remains from Unit 11 are well-preserved, and are locally abundant within small pockets of sediment. Within these pockets, bones and teeth are concentrated into small, oval-shaped patches that resemble the pellets of avian predators. The bones and teeth also show evidence of corrosion due to digestion. Therefore, the remains from this unit were probably accumulated by an avian predator, and most likely an owl.

Owls were also the primary accumulating agents of the rodent remains in Units 12-15. However, the degree of digestion, and thus the owl species responsible for depositing the rodent remains, differs between each stratigraphic sub-unit. The identified predators include the barn owl, European eagle owl and long-eared owl. Conversely, the presence of strongly digested bones in sub-unit 15/5 suggests that this material originated from common buzzard pellets.

In the Main Chamber sequence, rodent remains are less abundant, and are evenly distributed throughout the sediments. The taphonomic evidence indicates that these remains originated from mammalian carnivore scats (Units 18/2 and 18/3), and owl pellets (Units 18/4 and 19/15), but were later transported and re-deposited within the cave via mudflows. Unit 19/14 is the exception to this, as the remains from these sediments are highly concentrated within pockets. This indicates that these remains accumulated due to the direct deposition of owl pellets within the cave or near the cave entrance.

Table 3.8: *Summary of the stratigraphy, small mammal assemblages and palaeoenvironmental reconstructions from the Middle Pleistocene sequence at Westbury Cave. Only the units that are relevant to the material analysed in this thesis are shown. Stratigraphic units that are shown with two different sub-units (e.g. 11/1 & 11/3) refer to the equivalent sedimentary layers in the W9 and W2 sections (Side Chamber), or the W10 and W5 sections (Main Chamber), respectively. The information is sourced from Andrews (1990).*

Stratigraphic Unit	**Unit name**	**Sub-unit name or description**	**Rodent fauna**	**Depositional processes and sources of rodent remains**	**Palaeoenvironmental reconstruction**
19/15	Yellow Breccias	-	- *M. agrestis/arvalis* dominant - *P. gregaloides* also present	- Mudflows - Barn owl pellets - Natural mortality	- Deciduous woodland and boreal forest - Cool, dry temperate climate
19/14		Rodent breccia	- *P. gregaloides* dominant - Large concentrations of remains	- Barn owl pellets	
18/4 & 18/7	Grey Breccia	Cobble bed containing intrusive pink breccia with rodent remains	- *P. gregaloides* dominant - *M. agrestis/arvalis* is the only other species present in large numbers - *Dicrostonyx torquatus* present	- Mudflows - Owl pellets	- Tundra and boreal forest - Very cold climate
18/2-18/3 & 18/6		-		- Mudflows - Scats of a vole-specialist predator (probably a stoat)	

15/8	Red Breccia	Rodent Earth	- Very large concentrations of remains - *P. gregaloides* dominant - Remaining material largely from *M. agrestis/arvalis* - Lemmings present in small numbers	- Barn owl pellets - Pitfall-trapped animals	- Tundra and boreal forest - Very cold climate
15/5		Intermediate Silts	- *P. arvaloides* most common - *M. agrestis/arvalis* present	- Common buzzard pellets	- Cool moorland or tundra environment
15/2 & 15/4		Dark Silts with ‘mole layer’	- *P. arvaloides* dominant - *M. agrestis/arvalis* present	- Possibly barn owl (15/2) and European eagle owl (15/4) pellets - Pitfall-trapped animals	- Deciduous woodland - Warm climate, similar to interglacial optima
15/1 & 15/3		Lower Breccia	- *P. gregaloides* abundant - *M. agrestis/arvalis* present	- Mixed assemblage of prey from different owl species - Pitfall-trapped animals	- Deciduous woodland - Warming climate
14/1 & 14/2	Grey Silty Breccia	-	- *P. gregaloides* dominant - *Cricetulus migratorius* abundant - *M. agrestis/arvalis* present - Lemmings present	- Barn owl pellets - Deposition under wet conditions	- Deciduous and boreal forest - Cold, dry, continental climate

13/1 & 13/2	Brown Breccia	-	- *P. gregaloides* dominant - *M. agrestis/arvalis* present - Shrews abundant - *D. torquatus* present	- Barn owl (13/1) and long-eared owl (13/2) pellets - Pitfall-trapped animals	- Deciduous and boreal forest - Cool, dry, continental climate
12/1 & 12/2	Dark Brown Breccia	-	- *P. gregaloides* and *M. agrestis/ arvalis* dominant - *Apodemus sylvaticus* present	- Long-eared owl pellets - Pitfall-trapped animals	- Deciduous woodland - Warm, humid climate
11/2 & 11/4	Pink Silt	Cemented stalagmite horizon	- *M. agrestis/arvalis* common - *P. gregaloides* absent	- European eagle owl pellets	- Deciduous woodland - Warm, humid climate - Interglacial optima
11/1 & 11/3	Pink Breccia	-	- *P. gregaloides* and *M. agrestis/ arvalis* dominant	- Owl pellets (vole specialist predator)	
10	Yellow Silty Breccia	-	- Voles dominant - Unit poorly fossiliferous	- Water-lain towards base of unit - Animals living in the cave	- Deciduous and boreal woodland - Cool temperate climate
8	Red Silt and Bone gravel	-	- *P. gregaloides* dominant - *Microtus agrestis/arvalis* present	- Water-lain material - Owl pellets - Animals living in the cave	- Warm, humid climate

3.4.4.4. Palaeoenvironmental and palaeoclimatic evidence

The palaeoenvironmental record from Westbury Cave is currently based upon ecological interpretations of the small vertebrate faunas (Andrews, 1990; Holman, 1993; Stringer et al., 1996). Palaeoenvironmental changes through the cave sequence have been reconstructed via a method known as the Taxonomic Habitat Index (THI) (Andrews, 1990). The THI was created by assigning a score to each rodent species based on its modern distribution within major habitat types (tundra, boreal forest, deciduous forest, Mediterranean, steppe, forest and steppe, arid, tropical and montane). The average habitat preferences for all taxa within each stratigraphic unit were then added together, to provide an indication of the dominant habitats that existed proximal to the site (Andrews, 1990). These habitat reconstructions have been used to infer the broad-scale climatic conditions during the period in which the sediments were deposited (Andrews, 1990). Herpetile remains have also been used to reconstruct the palaeoenvironmental conditions at Westbury (Holman, 1993).

The small mammal fauna from Unit 8 is too limited to produce a THI reconstruction. However, the presence of *Emys orbicularis*, which requires mean summer temperatures of at least +17-18°C, suggests that the climate was comparable to or warmer than the present day (Andrews, 1990; Holman, 1993). The THI reconstructions indicate that warm, humid conditions continued in Units 11 and 12 (Figure 3.8). This evidence therefore suggests that Units 8 and 11-12 accumulated during peak interglacial conditions, with a climate comparable to south-central Europe today (Andrews, 1990; Stringer et al., 1996).

In Units 13 and 14, however, the proportions of boreal and tundra elements increase, suggesting a shift towards a drier, cooler and more continental climate. The presence of *Cricetulus migratorius*, which is currently found in dry grassland and steppe environments in the Middle East and Asia, supports this interpretation.

The evidence from Units 15/1-4 indicates a return to temperate deciduous woodland. The climatic conditions were likely as warm as present, and close to the peak interglacial conditions.

Unit 15/5 marks a return to cool, tundra conditions. The diverse faunas from Units 15/8 and 18 comprise an abundance of tundra, boreal and steppe elements, which are indicative of dry, cold, continental conditions similar to northern Scandinavia today (Andrews, 1990; Stringer et al., 1996). The THI from Unit 19 indicates a decline in tundra and boreal elements, and thus a slight climatic amelioration. Conditions during this stage were likely cool and dry, similar to southern Scandinavia today (Andrews, 1990; Stringer et al., 1996).

In summary, the palaeoecological evidence suggests that two main temperate episodes and two cold episodes are represented within the Westbury Cave sequence. These stratigraphic and palaeoenvironmental changes are summarised in Figure 3.8 and Table 3.8.

Stratigraphic Unit	Dominant Habitat	Inferred climate
19	Boreal + Deciduous forest	
15/8 +18	Boreal + Deciduous forest + Tundra	
15/5	-	
15/2+4	Deciduous woodland	
15/1+3	Deciduous woodland	
14	Boreal + Deciduous forest + Steppe	
13	Boreal + Deciduous forest	
12	Deciduous woodland	
11	Deciduous woodland	
10	Boreal forest	
8	-	

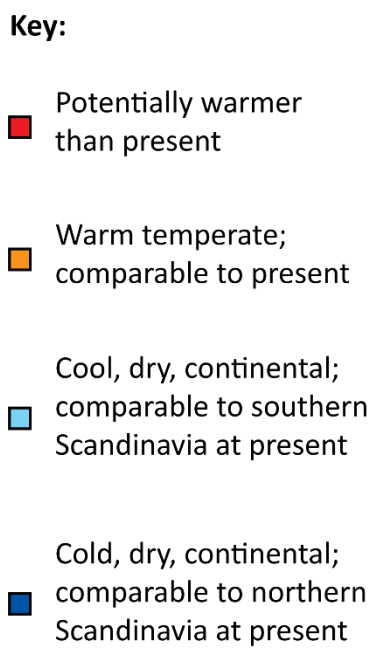

Figure 3.8: *Summary of the palaeoclimate evidence from the Taxonomic Habitat Index scores generated for the rodent faunas from the Westbury Cave sequence. Information from Andrews (1990) and Stringer et al. (1996).*

3.4.4.5. Age of the deposits

The taxonomic compositions of the small mammal faunas suggest that the Calcareous Member correlates with the Cromerian Complex (Andrews, 1990; Stringer et al., 1996). However, the Calcareous Member contains the remains of the advanced water vole, *Arvicola cantiana*, suggesting that these deposits must post-date sites at which *M. savini* remains have been found (e.g. West Runton) (Stringer et al., 1996). In Western Europe, the transition between *M. savini* and *A. cantiana* occurs in early MIS 15 (Preece & Parfitt, 2008; Markova & Puzachenko, 2016). This suggests that the Westbury deposits correspond to the latter part of MIS 15, or MIS 13. However, the Westbury sequence appears to record two major temperate peaks, separated by a cold episode (Figure 3.8) (Andrews, 1990; Stringer et al., 1996). While it is possible that the two temperate peaks correspond to MIS 15 and MIS 13, respectively, the palaeoenvironmental record from Westbury is not consistent with interglacial-glacial scale climatic variability (Schreve et al., 1999; Preece & Parfitt, 2012; Candy et al., 2015).

In addition, the small mammal faunas from Westbury are very similar to those from Boxgrove in West Sussex (Stringer et al., 1996; Schreve et al., 1999; Roberts & Parfitt, 1999). Notably, both sites preserve the remains of *A. cantiana* instead of *M. savini*. This suggests that these sites could record the same interglacial stage (Stringer et al., 1996). However, the assemblages at Westbury contain *M. gregaloides*, whereas at Boxgrove, only its evolutionary descendant, *M. gregalis*, is present (Andrews, 1990; Roberts & Parfitt, 1999). Despite this, it has been argued that all pre-Anglian faunas containing *A. cantiana* correlate with MIS 13 (Preece & Parfitt, 2012; Candy et al., 2015). The Middle Pleistocene deposits at Westbury Cave have therefore been assigned to the Cromerian Complex Interglacial IV (Stringer et al., 1996; Schreve et al., 1999), which has been correlated with MIS 13 (Candy et al., 2015). If this correlation is correct, the palaeoclimatic changes through the Westbury sequence must reflect sub-stage climatic fluctuations within this interglacial episode.

3.4.4.6. Justification for site choice

Westbury Cave contains a well-stratified sequence of deposits with abundant rodent remains. Consequently, sufficient rodent teeth are available from each stratigraphic level for isotopic analysis. The palaeoenvironmental evidence from the small mammal assemblages indicates that significant, sub-stage climatic fluctuations occurred during the accumulation of the sequence. However, this evidence provides only a qualitative reconstruction of the climatic changes i.e. warm and humid vs. cold and dry. Isotope analyses of rodent teeth can potentially provide a more quantitative climate record for Westbury Cave. Westbury Cave is therefore an ideal site for investigating whether the isotope values of rodent teeth can record temporal climatic changes at a single location.

3.4.5. Gully Cave, Somerset

3.4.5.1. Site context

Gully Cave is situated on the eastern side of Ebbor Gorge in the Mendip Hills area of Somerset (Schreve, 2006). Excavations have been undertaken at the cave since 2006. The site has been divided into a series of grid squares, and sediments systematically excavated from each square in 10 cm vertical spits (Schreve, 2010). The depth of each spit has been measured relative to a Ordnance Datum point, which lies at 143.71 m O.D. (Schreve, 2011).

The excavations at Gully Cave have yielded a rich assemblage of vertebrate remains that span the period from the last glacial stage (Devensian) to the early Holocene (Schreve, 2006, 2007, 2010, 2011, 2012a, 2012b, 2014, 2015, 2016). The upper deposits in the cave correspond to the Lateglacial period (Schreve, 2012a). This time interval is characterised by a series of abrupt climatic changes from the extreme cold of the Last Glacial Maximum (Dimlington Stadial), to the cool-temperate climate of the Lateglacial Interstadial, followed by a return to cold conditions in the Loch Lomond Stadial (or Younger Dryas), and finally a climatic amelioration into the early Holocene (Figure 3.3b). Gully Cave is therefore an important site for understanding the palaeoenvironmental context of Britain during the Lateglacial period.

3.4.5.2. Site stratigraphy

Near the top of the cave lies a highly-cemented calcium carbonate flowstone (Schreve, 2006). Below this flowstone is a thin layer of tufaceous sediment, underlain by a thick sequence of red breccias comprising abundant fossil remains, including a large assemblage of mammalian bones and teeth, as well as bird bones and mollusc shells (Schreve, 2006; Schreve, 2010; Schreve, 2012a). Below these red breccias is a layer of very coarse deposits that lacks mammalian remains (Schreve, 2014), which is underlain by further fossiliferous sediments (Schreve, 2015; Schreve, 2016). The sediments slope downwards from the south to the north of the cave (Schreve, 2012b), and thus time-equivalent deposits occur at different depths (up to 1 m different) in each grid square (Schreve, 2015).

The rodent teeth analysed in this thesis originate from the red breccias. These breccias are comprised of limestone clasts, formed by the frost shattering of local bedrock under cold climatic conditions (Schreve, 2006; Schreve, 2014). The limestone clasts are surrounded by a fine-grained silt and clay matrix. This fine material is typically generated through the chemical weathering of limestone bedrock by acidic water. This process is usually associated with warm, humid conditions that promote the dissolution of bedrock (Schreve, 2014). Stratigraphic shifts in the relative proportions of the limestone clasts and fine matrix therefore enable broad-scale climatic changes to be inferred. There are two main units that are dominated by coarse red breccia, and these have been interpreted as cold-climate deposits (Schreve, 2014). These breccias are separated by matrix-rich deposits, which are suggested to have formed under more temperate climatic conditions (Schreve, 2014). These interpretations are supported by the faunal evidence, described in the following sections.

3.4.5.3. Small mammal remains

Small mammal bones and teeth constitute the majority of the vertebrate remains from the red breccias (Schreve, 2007; Schreve, 2010). The small mammal assemblages comprise a diverse mixture of species, including

lemmings (*Lemmus lemmus* and *Dicrostonyx torquatus*), various vole taxa (*Microtus* spp., *Arvicola terrestris*, *Myodes* sp.), wood mice (*Apodemus sylvaticus*), and shrews (Soricidae) (Schreve, 2012a). *Microtus agrestis/arvalis* and *M. gregalis* are the dominant taxa within the matrix-rich sediments (Schreve, 2012a; Schreve, 2012b), while lemmings, the northern vole (*M. oeconomus*) and the narrow-skulled vole (*M. gregalis*) dominate the upper clast-rich breccia (Schreve, 2015). These shifts in the relative abundances of the rodent species suggest that palaeoenvironmental changes occurred during the accumulation of the Gully Cave sequence (Table 3.9).

The small mammal remains from Gully Cave occasionally occur within concentrated pockets, suggesting that the remains accumulated due to the deposition of avian raptor pellets or small carnivore scats (Schreve, 2007). Evidence for the digestive corrosion of the remains supports this interpretation (Schreve, 2006; Schreve, 2012a). The small mammal material is predominantly lightly digested, which indicates that most of the remains were accumulated by a predator such as the barn owl (Schreve, 2012a). In addition, the remains of predatory birds, including the long-eared owl and kestrel, have been discovered at the site (Schreve, 2010). These predators may have also contributed to the accumulation of the rodent remains within Gully Cave.

3.4.5.4. Palaeoenvironmental and palaeoclimatic evidence

The small mammal remains from the red breccias indicate the presence of open grassland, steppe and tundra habitats (Table 3.9). In the matrix-rich deposits, the presence of species such as *Microtus gregalis* and *M. oeconomus*, which are typically found in tundra and taiga zones of continental Europe today, suggests that climatic conditions were sub-optimal (Schreve, 2006; Schreve, 2010). Conversely, in the overlying clast-rich breccias, the faunal assemblage is dominated by cold-climate indicators, including lemmings and reindeer (Table 3.9). This suggests that the climate had deteriorated. Towards the top of these breccias, the relative abundances of species that prefer temperate shrubland and woodland habitats (e.g. *Myodes*) gradually increase, indicating that the climate began to warm

(Schreve, 2015). Nevertheless, cold-climate indicators remain, suggesting that open grassland habitats persisted through the early stages of the warm episode (Schreve, 2015). Therefore, the upper sequence in Gully Cave records three climatic intervals: 1) a cool temperate episode, 2) a cold episode, and 3) a temperate episode.

3.4.5.5. Previous isotope research on site

Isotope analyses have been previously undertaken on 15 *A. terrestris* incisors from the Gully Cave sequence (Peneycad, 2013). The $\delta^{18}O$ values of the incisors show an overall trend from high values at the base of the sequence, lower values in the middle of the sequence, and higher values at the top of the sequence (Peneycad, 2013). These changes were interpreted as reflecting climatic shifts, with lower values indicating colder conditions, and higher values indicating warmer climates (Peneycad, 2013). These interpretations are consistent with the faunal evidence, which suggests that two relatively warm episodes, separated by a cold episode, are represented within the Gully Cave sequence (Table 3.9). However, the existing isotope dataset is based upon the analyses of only 1-2 teeth per stratigraphic level. Therefore, further data are needed in order to confirm the patterns observed in this initial study.

3.4.5.6. Age of the deposits

Several radiocarbon dates have been generated via the Accelerator Mass Spectrometry dating of collagen in mammalian bones from the red breccia deposits (Schreve, 2012b). These dates indicate that the red breccias span the period from the Lateglacial Interstadial to the Early Holocene (Schreve, 2012b). The faunas within the matrix-rich sediments correlate with the Lateglacial Interstadial (~14.7-12.9 ka), the upper red breccias correlate with the Loch Lomond Stadial (~12.9-11.7 ka), and the warm-climate faunas at the top of the breccias correlate with the early Holocene (~11.7-10 ka) (Schreve, 2012a). This chronological evidence is consistent with the palaeoecological evidence from the mammalian faunas (Table 3.9).

Table 3.9: *Summary of the sedimentary, palaeoecological and palaeoclimatic evidence from the upper sequence at Gully Cave. Information from Schreve (2006, 2007, 2010, 2011, 2012a, 2012b, 2014, 2015, 2016).*

Sedimentary unit	**Depositional interpretations**	**Key mammal taxa**		**Habitat interpretations**	**Palaeoclimatic interpretations**	**Climate interval**
		Latin name	**Common name**			
Loose, open-framework limestone breccia	Frost-shattered limestone bedrock transported into the cave	*Arvicola terrestris*	Water vole	- Persistence of open grassland areas - Development of shrubby vegetation and woodland - Slow-flowing water source	- Warming climate	Early Holocene
		Microtus oeconomus	Northern vole			
		Sorex araneus	Common shrew			
		Myodes sp.	Bank vole			
		Lemmus lemmus	Northern lemming			
		Microtus gregalis	Narrow-skulled vole	- Open grassland - Steppe-tundra	- Cold climate	Loch Lomond Stadial (Younger Dryas)
		Microtus oeconomus	Northern vole			
		Dicrostonyx torquatus	Collared lemming			
		Lemmus lemmus	Northern lemming			
		Rangifer tarandus	Reindeer			

Matrix-rich pebbly breccia	Matrix formed by chemical dissolution of limestone bedrock	*Microtus agrestis/arvalis*	Field vole or common vole	- Damp, open grassland - Some shrub and tree cover - Boreal forest, tundra and steppe habitats - Slow-flowing water source	- Cool temperate climate	Lateglacial (Windermere) Interstadial
		Microtus gregalis	Narrow-skulled vole			
		Microtus oeconomus	Northern vole			
		Arvicola terrestris	Water vole			
		Equus ferus	Wild horse			
Limestone breccia with minimal matrix	Frost-shattered limestone bedrock transported into the cave	Fossil remains lacking		-	- Very cold climate	Last Glacial Maximum (Dimlington Stadial)

3.4.5.7. Justification for site choice

The sediments at Gully Cave contain abundant rodent remains that can potentially be utilized for isotopic studies. The small mammal faunas and radiocarbon dates suggest that the sediments span the interval of abrupt climatic fluctuations from the Lateglacial Interstadial to Early Holocene. The existing isotope data appear to mirror this pattern. However, additional analyses are needed on rodent teeth sampled at higher stratigraphic resolutions in order to assess whether these results are reliable. Gully Cave is therefore a useful site for investigating the applicability of the $\delta^{18}O$ values of rodent teeth for reconstructing short-term climatic variability.

3.4.6. Longstone Edge, Derbyshire

3.4.6.1. Site context

Longstone Edge, Derbyshire, is a site comprising two Bronze-age barrow mounds that are located on a limestone escarpment in the Peak District National Park (NGR: SK 2088 7841) (Last, 2014). The escarpment lies on the edge of a former quarry that has gradually collapsed, causing the subsidence and fissuring of the mounds. The site was consequently excavated in 1995-1996 in order to preserve the archaeological material. These excavations yielded a rich assemblage of small mammal remains in association with human bones and archaeological artefacts (Last, 2014).

The rodent teeth investigated in this thesis were obtained from Barrow 1. The main phase of archaeological activity at this site occurred in the Bronze Age, during which several graves were dug into the limestone bedrock and later covered by a burial mound (Last, 2014). The sampled rodent teeth originate from the deposits associated with this phase of activity. The following sections summarise the existing research on these deposits.

3.4.6.2. Site stratigraphy

At the base of Barrow 1 lie 2-3 rock-cut graves, which are each covered by a series of limestone slabs to form burial cists (Last, 2014). The central grave contained two, incomplete human skeletons, buried by two distinct layers of sediment: 1) a layer of firm, clayey silt (context 1060), overlain by 2) a layer of loose silt (context 1059). Both of these layers contain a large number of small mammal remains, which constitute up to 80% of the deposits (Last, 2014). The remains analysed in thesis were derived from context 1060.

The graves are covered by a mound consisting of limestone fragments, mixed with soil (Last, 2014). A food vessel containing cremated remains was also discovered at the base of the mound near to the main cist grave. The stone mound was later extended, and human bones and artefacts from pre-mound contexts were randomly re-deposited and incorporated into the new mound structure (Last, 2014). This re-use of the site caused some disturbance to the Barrow, resulting in the mixing of later Iron Age and Romano-British pottery with earlier Bronze Age artefacts (Last, 2014). The mixing of archaeological remains may have also been caused by bioturbation within the soil, or by the gravitational settling of the mound, which caused later material to fall into the spaces between the limestone slabs of the cist (Last, 2014).

3.4.6.3. Small mammal remains

Small mammal remains are extremely abundant within the Barrow 1 sediments; more than 5300 rodent molars have been recovered from the main cist grave (Andrews & Fernandez-Jalvo, 2012). The remains of *Arvicola terrestris* and *Microtus agrestis* together constitute 80-90% of the small mammal assemblage (Andrews & Fernandez-Jalvo, 2012). This level of abundance can only be achieved by the activities of predators that accumulate the remains of their prey via the deposition of pellets (Andrews, 1990). This interpretation is supported by the taphonomic evidence from the teeth in the cist grave; the teeth show a degree of digestion consistent with a predator such as the short-eared owl (Andrews & Fernandez-Jalvo, 2012).

Many of the bones also show evidence for extensive root damage and sub-surface corrosion, indicating that the barrow sediments have been affected by bioturbation (Andrews & Fernandez-Jalvo, 2012). The abundance of the remains additionally suggests that the predators occupied the site for a number of years. Therefore, the rodent assemblage within the cist grave may span a period of several decades, and may also include intrusive material from the overlying mound, due to the mixing of sediments via bioturbation.

3.4.6.4. Age of the deposits

The human skeletons within the main cist grave have been radiocarbon dated using Accelerator Mass Spectrometry (Marshall et al., 2014). Charred remains from the food vessel found at the base of the barrow mound have also been dated. The results of these dates are shown in Table 3.10.

The dates obtained from the human skeletons are similar at around 2200-2000 BC. Various sherds of Beaker pottery, which date to around 2300-2000 BC, were also discovered within and beneath the Barrow 1 mound (Beswick, 2014). This suggests that the main cist grave and the associated sediments date to ~2300-2000 BC.

In contrast, the dates from the food vessel remains are slightly younger, at ~2000-1800 BC. The typology of the food vessel also indicates an Early Bronze Age date of ~2000-1900 BC (Beswick, 2014). Since the food vessel occurs at the base of the barrow mound, the construction of the first stone mound must have occurred after these dates.

This means that the rodent remains within the cist grave likely date to between 2200 and 1800 BC (or ~4200-3700 yr BP). However, due to the disturbance of the deposits, caused by the slumping of the underlying bedrock and bioturbation, the contemporaneity of the small mammal remains and archaeological artefacts has been called into question. Therefore, as part of this thesis, radiocarbon dating was undertaken on three *Arvicola terrestris* mandibles from context 1060. The dating results are presented in Chapter 8.

***Table 3.10**: Results of the radiocarbon dating undertaken on human bone collagen from the cist grave and food vessel from Barrow 1 at Longstone Edge. The dates are from Marshall et al. (2014), and were calibrated using OxCal version 4.3 and the IntCal13 calibration curve (Bronk Ramsey, 2009; Reimer et al., 2013). The calibrated dates are shown on both the BC (before 0 AD) and BP (before 1950 AD) timescales.*

Lab number	Sample context	Radiocarbon date (yr BP)	Calibrated date range (95% confidence)	
			yr BC	yr BP
OxA-13449	Cist grave skeleton	3771 ± 29	2290-2057	4239-4006
OxA-13448	Cist grave skeleton	3691 ± 29	2196-1978	4145-3927
OxA-14087	Food vessel cremation	3560 ± 40	2023-1772	3972-3721
GrA-26548	Food vessel cremation	3555 ± 40	2020-1768	3969-3717

3.4.6.5. Justification for site choice

At Longstone Edge, abundant rodent remains occur in close stratigraphic association with precisely-dated human bones. Furthermore, the remains from context 1060 are contained within a firm and relatively consolidated deposit at the base of the main cist grave. Consequently, these remains are less likely to have experienced significant disturbance, and may be approximately contemporaneous with the human skeletons. Therefore, Longstone Edge provides the rodent material and robust chronology required in order to compare the $\delta^{13}C$ values of Late Holocene rodent teeth with atmospheric CO_2 records.

3.4.7. Danebury, Hampshire

3.4.7.1. Site context

Danebury, located in Central Hampshire, is the site of a well-preserved Iron Age hillfort. Excavations undertaken at the site between 1969 and 1988 have yielded a wealth of information about Iron Age communities in Britain (Cunliffe, 1984a; Cunliffe, 1984b; Cunliffe & Poole, 1991a; Cunliffe & Poole, 1991b; Cunliffe, 1995). The archaeological evidence indicates that the main period of occupation spanned from ~470 to 50 BC (Cunliffe, 1995). The most prominent features within the hillfort are the storage pits; more than 2000 pits have been discovered inside the main rampart of the fort (Cunliffe, 1995). These pits were found to contain abundant pottery fragments, animal bones and charred grains (Cunliffe, 1971), and are the source of the rodent teeth analysed in this thesis.

3.4.7.2. Site stratigraphy and chronology

Establishing the stratigraphy and chronology of the site has proven rather difficult, as a large number of the features are unstratified, and the processes involved in the deposition of the archaeological material are complex (Cunliffe, 1995). However, a chronology has been generated for the hillfort, based on: 1) the typology of the pottery fragments within individual pits and sedimentary layers, and 2) the stratigraphic relationships between the pits (Cunliffe, 1995). This chronological evidence has enabled the period of human occupation to be divided into several ‘ceramic phases’ (Table 3.11). The broad-scale boundaries of these phases have been estimated by applying Bayesian modelling to 70 radiocarbon dates (Cunliffe, 1995). Each pit has been assigned to a preferred ceramic phase, and categorised according to the reliability of this chronological assignment. The reliability assessment is based on the number of diagnostic and datable pottery sherds plus the presence of potentially intrusive sherds within the pit (Cunliffe, 1995).

For many of the pits, the assigned ceramic phase may be unreliable. This is because the pottery sherds within a pit need not necessarily be contemporaneous with other material from the same context (Cunliffe, 1995). Indeed, taphonomic evidence suggests that the pottery and animal bones may

have had different pre-depositional histories (Lock & Brown, 1995). The re-use of older pottery, the stockpiling of material in middens, plus the removal and re-deposition of rubbish from other areas of the site, means that the pottery sherds may be significantly older than the pit sediments in which they were deposited (Cunliffe, 1995).

Due to these issues of residuality, there is some uncertainty in the site chronology (Brown, 1995). Nevertheless, > 99% of the pottery sherds can be attributed to the Iron Age (Brown, 1995). The evidence also indicates that the pits were created throughout the period of hillfort occupation (Cunliffe, 1976). In geological terms, the occupation of the hillfort spanned a relatively short interval of time (~500 years). Therefore, the material within the pits can be dated to a relatively small time window, during which environmental conditions were unlikely to have undergone any large changes.

Table 3.11: *Summary of the occupation phases at Danebury Hillfort (from Cunliffe, 1995).*

Ceramic phase	Stage of hillfort development	Age range	
		yr BC/AD	yr BP (before 1950 AD)
1	Early hillfort	800 – 650 BC	2750 – 2600
3	Developed hillfort	470 – 360 BC	2420 – 2310
4-5		360 – 270 BC	2310 – 2220
6-7	Late hillfort	270 – 50 BC	2220 – 2000
8-9	End of hillfort occupation	50 BC – 50 AD	2000 – 1900

3.4.7.3. Small mammal remains

Small assemblages of vertebrate remains have been found in several of the pits (Coy, 1982). These assemblages are dominated by the remains of short-tailed field voles (*Microtus agrestis*), wood mice (*Apodemus sylvaticus*) and water voles (*Arvicola terrestris*) (Coy, 1982; Browne, 1995). These remains were originally thought to have accumulated due to the deposition of owl or

buzzard pellets (Coy, 1982), but subsequent analyses suggest that this is unlikely (Browne, 1995). The remains are generally very well-preserved, with all skeletal elements present, and there is minimal evidence for digestion by a predator (Browne, 1995). Moreover, the rodent assemblages are generally small, comprising an average of only 2-3 individuals per pit (Browne, 1995). In contrast, assemblages derived from the deposition of owl pellets are usually quite substantial (e.g. Andrews, 1990; Andrews & Fernandez-Jalvo, 2012). Therefore, it is more likely that the rodent material accumulated as a result of individuals falling into the pits and becoming trapped (Browne, 1995).

3.4.7.4. Justification for site choice

The rodent remains at Danebury are fairly abundant, and occur within relatively well-dated contexts. The remains primarily accumulated due to individuals falling into storage pits, and thus the material is likely to be *in situ*. While the pottery sherds within the pits may not necessarily be contemporaneous with the rodent material, due to the relatively short duration of the hillfort occupation, the ages of the rodent teeth can be estimated to within ± 250 years. This level of precision is sufficient for assessing how the $\delta^{13}C$ values of Late Holocene rodent teeth reflect environmental conditions. Danebury is therefore a useful source of rodent teeth for undertaking isotopic analyses to address this research aim.

3.5. Summary

In this thesis, rodent teeth were sampled from multiple modern, Late Holocene and Pleistocene study sites in order to explore the applicability of the $\delta^{18}O$ and $\delta^{13}C$ values of rodent teeth for reconstructing palaeoenvironmental conditions. The key information relating to these study sites, and their relevance to the research aims, is summarised in Table 3.12.

The next chapter outlines, reviews and justifies the sampling strategies employed for the rodent teeth and mollusc shells, and describes the laboratory and analytical methods applied to the sample material.

Table 3.12: *Summary of the study sites investigated in this thesis. In the climatic conditions column, T_{max} refers to the mean temperature of the warmest month, and T_{min} refers to the mean temperature of the coldest month.*

	Site name	Relevance to research aims	Depositional environment	Climatic conditions	Age
1	West Horrington, Somerset	- Establishing the modern relationship between $\delta^{18}O_{rt}$ and $\delta^{18}O_{mw}$ - Investigating $\delta^{18}O$ and $\delta^{13}C$ variability in modern rodent populations	- Modern barn owl pellets from roosting and nesting sites	- T_{max} = ~17°C - T_{min} = ~5°C	Modern
2	Cobham, Surrey				
3	Beeford, East Yorkshire			- T_{max} =~15°C - T_{min} = ~4°C	
4	Perth, Perthshire				
5	West Runton, Norfolk	- Testing the reliability of coupling the $\delta^{18}O$ values of rodent teeth and shells for reconstructing past summer temperatures	- Shallow backwater pool	- T_{max} comparable to today - T_{min} < today	MIS 15 or 17
6	Cudmore Grove, Essex		- Fluvial channel near an estuary	- T_{max} ≥ today - T_{min} ≤ today	MIS 9
7	Marsworth, Buckinghamshire		- Shallow, slow-flowing stream	- T_{max} ≤ today - T_{min} < today	MIS 7a
8	Westbury Cave, Somerset	- Investigating whether short-term climatic fluctuations are recorded in the $\delta^{18}O$ values of rodent teeth from stratified cave sequences	- Cave - Rodent remains accumulated by avian predators	- 2 temperate episodes, similar to or warmer than today, separated by 1 cool-temperate episode - 1 cold episode at top of sequence	MIS 13
9	Gully Cave, Somerset			- 1 cool-temperate episode - 1 cold episode - 1 warm temperate episode	15-10 ka before present

10	Longstone Edge, Derbyshire	- Assessing the influence of diagenesis and recent changes in atmospheric CO_2 on the $\delta^{13}C$ values of rodent teeth	- Cist grave in a Bronze-Age barrow	- Conditions comparable to today	~ 4 ka before present
11	Danebury, Hampshire		- Storage pits in an Iron Age hillfort		~ 2 ka before present

4. Sampling, Laboratory and Analytical Methods

4.1. Introduction

The following chapter reviews and outlines the sampling, laboratory, and analytical methods that were applied to the modern and fossil tooth and shell carbonates. Isotope analyses were undertaken on rodent teeth from arvicoline taxa belonging to the genera *Microtus* and *Arvicola*, as well a small number of fossil shells from aquatic mollusc taxa. The first part of this chapter discusses the rationale for sampling these materials for isotopic analyses, by outlining key aspects of small mammal and molluscan ecology and taphonomy in the context of the isotopic values of tooth and shell biominerals. The second part of the chapter reviews the biominerals chosen for isotopic analysis, and provides an assessment of the potential for the diagenetic alteration of the fossil carbonates. Finally, the pre-treatment procedures used on the teeth and shells are reviewed and outlined, and the analytical methods are described.

4.2. Small mammal and molluscan ecologies and their significance for the sampling and stable isotope analyses of rodent teeth and mollusc shells

4.2.1. Rodent taxa

Analyses for this thesis were undertaken on rodents belonging to the tribe Arvicolini Gray, 1821 (Class: Mammalia L. 1758; Order: Rodentia Bowdich, 1821; Family: Cricetidae Fischer, 1817; Subfamily: Arvicolinae Gray, 1821). Species within the genera *Microtus* Schrank, 1798 and *Arvicola* Lacépède, 1799 were chosen as the focus of this research, for several reasons. Firstly, the fossil teeth of arvicoline rodents, and in particular members of the genus *Microtus*, are highly abundant in Quaternary deposits in the Northern

Hemisphere, and this is especially true for European cave sites (Andrews, 1990; Navarro et al., 2004; Sesé & Villa, 2008; López-García et al., 2015; Fernández-García et al., 2016; Royer et al., 2016). Secondly, the modern biogeographical distributions of arvicoline rodents are broad, spanning much of Europe and western Asia (Table 4.1). As a result, these rodents are found in a range of climate zones, and are capable of inhabiting Europe during both temperate interglacial and interstadial stages, and cold stadial stages (Sutcliffe & Kowalski, 1976; Fernández-García et al., 2016; Royer et al., 2016). Arvicoline remains are consequently abundantly preserved in a variety of depositional settings (e.g. fluvial and cave environments) and geographical areas, across different climatic intervals (Sutcliffe & Kowalski, 1976; Andrews, 1990; Maul & Parfitt, 2010; Royer et al., 2013b). Therefore, isotope analyses of arvicoline teeth can potentially provide large environmental datasets for Quaternary sites across Europe, allowing spatial and temporal patterns of palaeoenvironmental changes to be investigated.

In addition, Royer et al. (2013a) demonstrated that the $\delta^{18}O$ values of *Microtus* spp. and *Arvicola terrestris* teeth can provide reliable estimates for the mean annual $\delta^{18}O$ of meteoric water in mid-latitude regions. However, *M. agrestis/arvalis* teeth often have slightly higher $\delta^{18}O$ values compared to *A. terrestris* teeth from the same site (Gehler et al., 2012; Royer et al., 2013a; Royer et al., 2014). In contrast, species that inhabit regions with broad seasonal ranges in temperature (i.e. high-latitude, high-altitude or continental areas), such as the European snow vole [*Chionomys nivalis* (Martins, 1842)], have $\delta^{18}O_{rt}$ values that appear to reflect the mean $\delta^{18}O_{mw}$ during the warmest months of the year (Royer et al., 2013a). These observations can be linked to the ecological characteristics of the rodent taxa.

4.2.1.1. Stable isotopes and rodent ecology

In present-day Britain, the European water vole, *A. terrestris*, has a close connection to meteoric water (MacDonald & Barrett, 1993). This species inhabits the banks of slow-flowing rivers, feeding on grasses and sedges growing along the margins of the water body (Boyce, 1991). As a result,

A. terrestris obtains its food and drinking water directly from major surface water sources. Since the $\delta^{18}O$ values of these sources are likely to be analogous to the $\delta^{18}O$ of local precipitation, the $\delta^{18}O$ values of *A. terrestris* teeth can provide a proxy for mean $\delta^{18}O_{pt}$.

On the other hand, *Microtus agrestis* typically inhabits moist, open grassland habitats, where it feeds on the leaves and stems of grasses (Ferns, 1976; Alibhai & Gipps, 1991). *M. arvalis*, *M. oeconomus* and *M. (T.) subterraneus* have similar habitat and dietary preferences (Table 4.1). These species may live in areas located at a distance from major surface water sources such as rivers. As a result, food resources are derived from open areas, and drinking water sources are likely obtained from small, isolated water bodies such as ditches and ponds. These water sources are generally more susceptible to evaporative enrichment compared to rivers. Consequently, within the same local area, the food and drinking water sources consumed by *Microtus* spp. may be isotopically enriched relative to those of *A. terrestris*. Indeed, Royer et al. (2014) interpret enriched $\delta^{18}O$ values of fossil *Microtus* teeth as resulting from a greater intake of evaporated water compared to *A. terrestris*. The $\delta^{18}O$ values of *Microtus* teeth may, therefore, be sensitive to changes in aridity (Royer et al., 2014). Nevertheless, while the $\delta^{18}O$ values of the drinking water sources consumed by *Microtus* and *Arvicola* are likely to differ, the slope of the fractionation relationship between the $\delta^{18}O$ of bioapatite and the mean annual $\delta^{18}O_{mw}$ is considered to be comparable in both genera (Longinelli et al., 2003; Royer et al., 2013a).

In contrast, *M. gregalis* typically lives in continental and mountainous habitats (Table 4.1). The ecological characteristics of this species are similar to *Chionomys nivalis* (Amori, 1999). Royer et al. (2013a) found that the $\delta^{18}O$ values of *C. nivalis* teeth tend to overestimate the mean annual $\delta^{18}O_{mw}$. This is likely because in continental and mountainous environments, rodent tooth mineralization is strongly biased towards the warm and dry summer months, when $\delta^{18}O_{mw}$ values are enriched (Royer et al., 2013). The $\delta^{18}O$ values of *Microtus* teeth that have formed during periods of cold and/or continental conditions may also be biased towards enriched summer $\delta^{18}O_{mw}$ values. This will be taken into consideration when examining the isotope data from the fossil *Microtus* teeth from Westbury Cave and Gully Cave (Chapter 7).

Table 4.1: *The ecological characteristics of the arvicoline rodent taxa that were investigated in this research. References: 1) Shenbrot & Krasnov (2005), 2) Alibhai & Gipps (1991), 3) MacDonald & Barrett (1993), 4) Hansson (1971), 5) Ferns (1976), 6) Gorman (1991), 7) Tast (1966), 8) Batasaikhan et al. (2016), 9) Kryštufek (1999), 10) Butet & Delettre (2011), 11) Boyce (1991).*

Taxon		**Modern biogeographical distribution**	**Habitats**	**Diet**
Common name	**Latin name**			
Short-tailed field vole	*Microtus agrestis* (Linnaeus, 1761)	- Widespread across the Palaearctic, from western Europe to Lake Baikal[1] - Absent from Ireland and southern Europe[1]	- Mainly ungrazed grasslands[2-3] - Also woodlands, peat bogs, heaths, dunes[2-3] - Favours damp areas[3]	- Green leaves and stems of grasses[2] - Increased proportions of herbaceous plants, mosses and fungi during summer and autumn[4-5]
Common vole	*Microtus arvalis* (Pallas, 1778)	- Across much of Europe, southwest Russia, and the Middle East[1] - Absent from Britain (except Orkney and Guernsey), Fennoscandia, and the northern Mediterranean[3]	- Mainly open habitats (meadows, pastures, moorland)[3] - Also marshes and moist forests[6]	- Green leaves, stems and roots of grasses and herbaceous plants[6]
Northern or Root vole	*Microtus oeconomus* (Pallas, 1776)	- Holarctic distribution[1] - In Europe, the species mainly occurs east of Germany and Sweden[1,3]	- Damp habitats with dense, tall vegetation[7]	- Sedges and grasses; aquatic plants[3,7]

			- Moist grasslands and meadows, marshes, bogs, riverbanks[3,7]	- Subterranean parts of sedges and grasses in winter[7] - Green parts of sedges in summer[7]
Narrow-headed vole	*Microtus gregalis* (Pallas, 1779)	- Tundra along the northern and southern edges of Russia[8] - Steppes of Kazakhstan, Mongolia, and northern China[8]	- Tundra plains, mountain steppes, meadows[8] - Open grassy areas of forests and semi-deserts[8]	- Wild and cultivated plants; prefers legumes[8]
European Pine vole	*Microtus (Terricola) subterraneus* (de-Selys-Longchamps, 1836)	- Across central continental Europe, from the Atlantic coast of France to western Russia[1]	- Damp and dry areas[13] - Woodlands, meadows, pastures, rocky areas in high mountains[9]	- Mainly the green parts of plants, but also some seeds, fruits, and mosses[10]
European Water vole	*Arvicola terrestris* (Linnaeus, 1758)	- Widespread across most of Europe, parts of the Middle East, and southwest and central Russia[1,3] - Absent from Ireland and Spain[3]	- In Britain: steep, densely-vegetated banks of ditches, slow-flowing lowland rivers, and lakes[3,11] - In continental Europe: favours pastures, and has a fossorial lifestyle[3]	- Mainly grasses, sedges and roots[3,11] - Sometimes eats insects and small fish[3]

Inter-species differences in ecology could also influence the $\delta^{13}C$ values of arvicoline teeth. Nevertheless, in present-day Europe, the average $\delta^{13}C$ values of *Microtus* spp. and *A. terrestris* teeth are generally comparable (Gehler et al., 2012). This is because the diets of these taxa are similar, consisting primarily of grasses and sedges (Table 4.1). It can therefore be assumed that any variations in $\delta^{13}C_{rt}$ values are mainly due to environmental changes, rather than inter-taxon differences in dietary preferences. Moreover, because these taxa predominantly feed on leaves, as opposed to $\delta^{13}C$-enriched sources such as seeds and roots, the $\delta^{13}C$ values of their teeth can potentially provide an accurate proxy for the mean $\delta^{13}C$ of local vegetation.

4.2.1.2. Evolution of arvicoline rodents

During the Early Middle Pleistocene, the water vole followed an evolutionary trend from the extinct species, *Mimomys savini*, to an intermediate form, *Arvicola cantiana,* and finally to the modern species, *Arvicola terrestris* (von Koenigswald & van Kolfschoten, 1996). Although the precise ecologies of extinct water vole species are unknown, fossil remains of water voles are abundant in freshwater deposits at several British Quaternary sites (e.g. Roe et al., 2009; Maul & Parfitt, 2010). This implies that the extinct species, to a certain extent, also lived near to surface water sources. Therefore, in this research, it is assumed that the $\delta^{18}O$ values of *M. savini* and *A. cantiana* teeth provide an accurate record of the mean annual $\delta^{18}O$ of meteoric water.

Species within the genus *Microtus* have also evolved during the Quaternary period. For example, *M. gregalis* evolved from *M. gregaloides* (Hinton, 1923) (formerly known as *Pitymys gregaloides*), and *M. subterraneus* evolved from *M. arvalidens* Kretzoi, 1958 (also known as *Pitymys arvaloides*) (Maul et al., 2007; Markova & Puzachenko, 2016). Again, extinct species in the *Microtus* lineages are assumed to have had similar ecological preferences as their modern descendants, and therefore tooth $\delta^{18}O$ values that accurately reflect the mean $\delta^{18}O_{mw}$.

4.2.2. Role of predators in the accumulation of rodent remains

Understanding the taphonomic processes involved in the accumulation of skeletal remains is also important for interpreting the isotope values of rodent teeth. Rodent mortality can result from several factors, including: 1) natural causes (e.g. old age), 2) falling into a pitfall trap, such as a cave, or 3) predation (Andrews, 1990). Predators, and specifically avian raptors (owls, kestrels, buzzards), play the greatest role in generating accumulations of rodent skeletal remains (Mayhew, 1977; Andrews, 1990).

Avian raptors usually swallow their prey whole, and then regurgitate indigestible material in the form of pellets (Figure 4.1a). Rodents are the primary source of prey for many owl species (Mikkola, 1983), and the pellet remains from these raptors are often very well preserved (Mayhew, 1977; Andrews, 1990). Consequently, owls are frequently the key predators responsible for pellet-derived accumulations of rodent skeletal material (Mayhew, 1977; Andrews, 1990; Andrews & Fernandez-Jalvo, 2012). Owl pellets are often found in large numbers in a single area, due to the species' strong preferences for roosting and nesting sites (Andrews, 1990). Skeletal material derived from the pellets can consequently accumulate near to these sites, and become later incorporated into sedimentary deposits (e.g. Mayhew, 1977; Andrews, 1990). Additionally, owl roosting and nesting sites are often situated within caves, and thus stratified cave deposits containing abundant rodent remains can accumulate over time.

However, predation often causes the modification of skeletal material (Andrews, 1990). Acidic conditions in the predator's stomach result in the dissolution of bioapatite. This digestion is usually greatest on the external surfaces of the bones and teeth. Tearing of the prey prior to ingestion can also cause the breakage and loss of skeletal elements (Andrews, 1990). The extent of these modifications varies depending on the predator species (Table 4.2). Detailed taphonomic studies can therefore enable the identification of the predator(s) responsible for the accumulation of rodent remains.

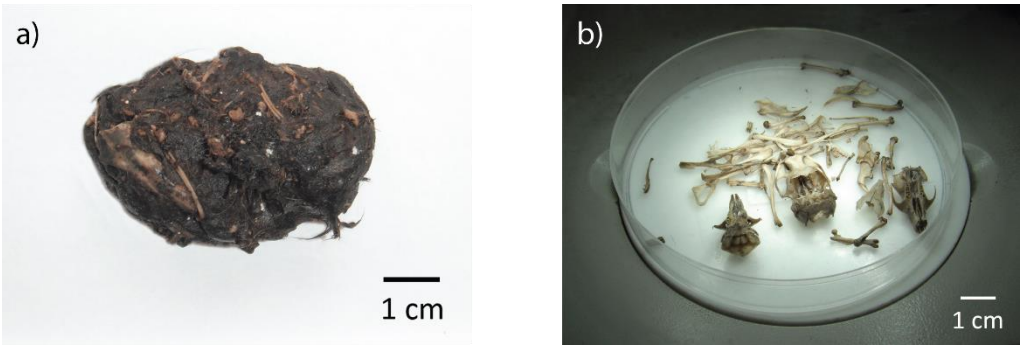

Figure 4.1: *a) Photograph of a modern barn owl pellet, with visible rodent skeletal remains. b) Photograph showing well-preserved rodent remains that have been extracted from a modern barn owl pellet.*

The predator that causes the least breakage and digestion of small mammal remains is the barn owl [*Tyto alba* (Scopoli, 17690] (Andrews, 1990). Barn owl pellets can be easily identified, due to their compact ovular shape and black, shiny surface (Figure 4.1a), and skeletal material from barn owl pellets is usually intact and readily identifiable (Figure 4.1b) (Taylor, 1994). Across Northwest Europe today, the barn owl's diet predominantly consists of the short-tailed field vole, *Microtus agrestis*, or the common vole, *Microtus arvalis* (continental Europe only) (Andrews, 1990; Taylor, 1994). As aforementioned, *Microtus* remains are often abundant in Quaternary fossil assemblages. Therefore, modern barn owl pellets offer a valuable source of material for investigating the modern isotope ecology of these important arvicoline species.

Moreover, the barn owl has a relatively restricted home range, typically spanning 1-2 km during summer, and up to 5 km in winter (Taylor, 1994). Therefore, the isotope values of rodent teeth from barn owl pellets reflect environmental conditions within a limited geographical area. However, because owl pellets accumulate gradually over time, rodent remains within a single sample or sedimentary deposit will represent a time-averaged record of local environmental conditions.

Table 4.2: *Taphonomic modifications to rodent teeth resulting from ingestion by predators. Modifications are divided into the categories established by Andrews (1990). Percentages indicate the typical proportions of skeletal elements that are modified in each category.*

Category	**Predator species**	**Modifications to molars**		**Modifications to incisors**	
		Digestion	Breakage (%)	Digestion	Breakage (%)
1	- Barn owl - Short-eared owl - Long-eared owl - Snowy owl	0-3% Light rounding of occlusal corners of salient angles	0	10-20% Slight to moderate pitting over enamel surface	0-5
2	- Long-eared owl - Snowy owl - Great grey owl	4-6% Moderate rounding and flattening of salient angles	0	20-30% Enamel removed at incisor tip; wavy outline of dentine	0
3	- Spotted eagle owl - European eagle owl - Tawny owl	10-30% Strong rounding of corners; enamel penetrated along salient angles	< 5	40-70% Enamel reduced to small islands; surface of dentine pitted and wavy	5-10
4	- Little owl - Kestrel - Peregrine falcon	50-70% Severe rounding of corners; enamel entirely removed from salient angles; some dissolution of dentine	15	60-80% Extensive dissolution of enamel and dentine; enamel often entirely removed	10-30
5	- Buzzard - Hen harrier - Red kite	50-100% Enamel and dentine largely removed from salient angles	> 10	100%	> 10

Barn owl digestion has been shown to cause a slight depletion (~0.7‰) in the $\delta^{18}O$ values of rodent teeth relative to undigested control samples (Barham et al., 2017). Nevertheless, fossil rodent assemblages are frequently accumulated due to the deposition of owl pellets. Likewise, modern isotope fractionation equations are often derived from analyses of pellet-derived rodent material. Therefore, isotopic modifications due to digestion are likely to be comparable in both modern and fossil rodent teeth.

In summary, fossil rodent remains are primarily accumulated due to the activities of owls. Modern barn owl pellets can consequently provide a useful analogue for understanding and interpreting data from Quaternary accumulations of rodent remains. Barn owl pellets were therefore collected for the modern analogue study in Chapter 5. The characteristic appearance of barn owl pellets (Figure 4.1a) enabled the sampled pellets to be definitively attributed to this predator species. Additionally, given the dominance of *M. agrestis* in modern barn owl pellets from Britain, this species was chosen as the focus of the modern analogue study.

4.2.3. Temporal bias of rodent teeth due to tooth mineralization periods and predators

In order to understand the environmental meaning of the tooth isotopic values, the timing of tooth mineralization must also be considered (Ruddy, 2005; Royer et al., 2013a; Jeffrey et al., 2015). In both *Microtus* and *Arvicola*, the molars and incisors grow continuously, but over slightly different intervals of time. Daily laminations within *A. terrestris* incisors indicate that these teeth span ~50 days (Ruddy, 2005). Conversely, rodents in the genus *Microtus* have smaller teeth relative to *Arvicola*. As a consequence, *Microtus* incisors mineralize over a shorter period of ~30-40 days (Klevezal et al., 1990), whereas *Microtus* molars represent growth within ~50-80 days (von Koenigswald & Golenishev, 1979). These differences in the mineralization periods may lead to offsets in the isotope values of molars and incisors from the same rodent population (Royer et al., 2013a; Jeffrey et al., 2015). Inter-

tooth isotope differences are consequently investigated in the modern analogue study (Chapter 5).

These mineralization periods also mean that $\delta^{18}O_{rt}$ and $\delta^{13}C_{rt}$ values reflect the average isotope values of food and water sources consumed during the final 1-2 months before death. Therefore, the isotope values of teeth within an owl pellet will be influenced by the environmental conditions prior to predation (Ruddy, 2005; Gehler et al., 2012). Theoretically, a rodent may be predated at any time of the year. Consequently, the average $\delta^{18}O_{rt}$ of a sample should reflect the mean annual $\delta^{18}O$ of meteoric water, while the range in $\delta^{18}O_{rt}$ values represents the seasonal amplitude in $\delta^{18}O_{mw}$ (Royer et al., 2013a). Likewise, the average $\delta^{13}C_{rt}$ value of a sample should reflect the mean seasonal $\delta^{13}C$ of the diet (Calandra et al., 2015). Royer et al. (2013a) also suggest that due to their smaller sizes and shorter mineralization periods, *Microtus* teeth can provide higher resolution records compared to *Arvicola* teeth. As a result, *Microtus* teeth can potentially be used to reconstruct seasonal variations in $\delta^{18}O_{mw}$ and dietary $\delta^{13}C$ (Royer et al., 2013a; Royer et al., 2013b, Royer et al., 2014).

However, rodent predation is often seasonally biased. Vole populations increase in size at the start of the breeding season in early spring, and reach an annual peak in late summer (Corbet & Harris, 1991; MacDonald & Barrett, 1993; Weber et al., 2002). Predator numbers track variations in the population size of their prey (Salamolard et al., 2000; Norrdahl & Korpimaki, 2002; Weber et al., 2002), and thus the period of greatest rodent predation is also at the end of the summer. Therefore, raptor pellets are deposited in greater numbers during the warmest months of the year (Gehler et al., 2012). Correspondingly, the mean isotope value of any sample of vole teeth is likely to be biased towards the summer isotope compositions of food and water sources (Ruddy, 2005). However, in British lowland river systems at the present day, $\delta^{18}O_{mw}$ values remain relatively constant across the year (Darling et al., 2003; Waghorne et al., 2012). Consequently, the mean $\delta^{18}O_{rt}$ value of a modern vole population should reflect the mean annual $\delta^{18}O$ of meteoric water, regardless of the exact month during which tooth mineralization occurred. Moreover, as noted by Gehler et al. (2012), modern and fossil rodent remains both primarily accumulate due to the deposition of raptor pellets. Therefore, any seasonal

bias in the $\delta^{18}O$ and $\delta^{13}C$ values of modern rodent teeth will likewise be reflected in isotope data from fossil rodent assemblages. This means that the isotope values of modern and fossil rodent teeth can be directly compared.

In summary, the $\delta^{18}O$ and $\delta^{13}C$ values of a rodent tooth record environmental conditions over a period of 1-2 months prior to death. Therefore, different teeth within a sample may have different isotope values, depending on the season during which the rodents were predated. At the present day, the average $\delta^{18}O_{rt}$ and $\delta^{13}C_{rt}$ values of a sample reflect the mean annual $\delta^{18}O_{mw}$ and $\delta^{13}C$ of the diet, but with a small bias towards the warmest months of the year (spring-autumn) due to the seasonal activities of predators.

4.2.4. Sampling the rodent teeth for isotope analyses

The review of rodent ecology in Section 4.2.1. indicates that in order to reconstruct the mean $\delta^{18}O$ of past meteoric water, analyses should be undertaken on taxa that are closely associated with surface water sources (Grimes et al., 2008). Likewise, in order to reconstruct the mean $\delta^{13}C$ of local vegetation, analyses should ideally be undertaken on rodent taxa that are primarily herbivorous. Both *Microtus* and *Arvicola* fulfil these requirements.

Therefore, in this thesis, isotope analyses were undertaken on *Microtus* and *Arvicola* teeth. The taxon chosen for analysis at each study site was dependent on the availability of the fossil remains. Also, due to the dramatic decline in water vole populations over the past century, *Microtus* spp. is significantly more abundant than *A. terrestris* in Britain at the present day (Strachan & Jefferies, 1993). Therefore, *Microtus agrestis* teeth were chosen as the focus of the modern analogue study.

In order to obtain representative values for the mean $\delta^{18}O$ of meteoric water and the mean $\delta^{13}C$ of the diet, multiple teeth were selected for analysis. Gehler et al. (2012) recommend that a minimum of 4 teeth must be analysed per stratigraphic unit in order to estimate the mean $\delta^{18}O$ of a population. Conversely, Royer et al. (2013a) suggest that a larger sample, of around 10 teeth per unit, is required in order to: 1) obtain a normal distribution in the $\delta^{18}O$ values of the rodent teeth, and 2) investigate the variability in $\delta^{18}O_{rt}$ values within a sample. Royer et al. (2013a) indicate that the data must be normally

distributed if the mean $\delta^{18}O_{rt}$ value of the sample is to be interpreted as the mean annual $\delta^{18}O_{mw}$. Determining the maximum variability in $\delta^{18}O_{rt}$ values within the sampled population is also essential for reconstructing the past seasonal amplitude in $\delta^{18}O_{mw}$ values (Royer et al., 2013a).

Therefore, the general consensus is that ~5-10 rodent teeth should be sampled per sedimentary level for isotopic analyses. The appropriateness of this sample size will be assessed in Chapter 5, using the isotope data collected from the modern rodent teeth from Britain.

4.2.5. Molluscan taxa

The isotope data used in this thesis were obtained from analyses of freshwater gastropod mollusc shells (Phylum: Mollusca Linnaeus, 1958; Class: Gastropoda Cuvier, 1795). Freshwater molluscs were chosen because the $\delta^{18}O$ values of their shells are a function of: 1) the $\delta^{18}O$ of the meteoric water in which the shells mineralized, and 2) the temperature at which shell mineralization occurred (Fritz & Poplawski, 1974). Freshwater shells are therefore ideal for use in the coupled isotope approach (see section 2.4.2.1). In addition, the shells of non-marine molluscs are often highly abundant in Quaternary deposits, and especially fluvial sediments dating to interglacial stages (Sparks, 1964; Keen, 2001). Moreover, many freshwater molluscan taxa have broad ecological tolerances (Table 4.3), and are found in a wide range of environments and climatic intervals during the Quaternary period (Sparks, 1964). Gastropod species within the genera *Valvata* (O. F. Müller, 1773) and *Bithynia* Leach, 1818 are particularly dominant in freshwater deposits in Britain; their presence has been recorded in every known interglacial stage over the past 800 thousands years (Keen, 2001; Preece, 2001).

The two gastropod species that were specifically investigated in this thesis are *Valvata piscinalis* and *Galba truncatula* (Table 4.3). The shells of both taxa are composed entirely of aragonite (Linz & Müller, 1981). This aragonitic habit is comparable to that of *Radix peregra*, which is the species upon which the modern relationship between shell $\delta^{18}O$, $\delta^{18}O_{mw}$ and temperature is based (Equation 2.5). *V. piscinalis* and *G. truncatula* were also

chosen due to the relative abundance of their shells at the interglacial study sites (*V. piscinalis* at West Runton and Cudmore Grove; *G. truncatula* at Marsworth). Both species are widely distributed across Europe, and are found in various freshwater habitats (Table 4.3). The shells of these gastropods can consequently be found in similar environments to arvicoline rodent taxa that live in moist habitats (e.g. *A. terrestris*, *M. oeconomus*). This means that gastropod shells and arvicoline teeth have the potential to provide directly comparable proxies for the $\delta^{18}O$ of local meteoric water.

4.2.6. Temporal bias of mollusc shells due to shell mineralization periods

The $\delta^{18}O$ and $\delta^{13}C$ values of a whole shell reflect the average isotope values of meteoric water and DIC, integrated over the lifespan of the organism (Jones et al., 2002). The main period of shell growth in *Valvata piscinalis* spans from June to September (Table 4.3). Correspondingly, the $\delta^{18}O$ values of *V. piscinalis* shells are consistent with mean $\delta^{18}O_{mw}$ values and water temperatures between May and September (Waghorne et al., 2012). *G. truncatula* is likewise predominantly active during summer, with a comparable breeding season from April-September (Table 4.3). Therefore, the $\delta^{18}O$ values of *V. piscinalis* and *G. truncatula* shell aragonite provide a seasonal signal of $\delta^{18}O_{mw}$ and temperature.

Moreover, both *V. piscinalis* and *G. truncatula* are annual species, which means that they have lifespans of approximately 1 year (Table 4.3). As a result, the bulk isotope values of their shells record the average $\delta^{18}O$ and $\delta^{13}C$ values of the water source across a single year. In large river systems, which are the main habitats of *V. piscinalis*, $\delta^{18}O_{mw}$ values remain relatively constant across the year, and thus shell $\delta^{18}O$ values are primarily dictated by variations in water temperature (Waghorne et al., 2012). On the other hand, moisture levels in the habitats of *G. truncatula* are generally more variable than in the habitats of *V. piscinalis* (Table 4.3). Therefore, the $\delta^{18}O$ values of *G. truncatula* shells may be affected by the evaporative enrichment of the water source, in addition to temperature.

Table 4.3: *The ecological characteristics of the molluscan species that were analysed in this research. References: 1) Ellis (1926), 2) Fretter & Graham (1978), 3) Young (1975), 4) Kerney (1999), 5) McMillan (1968), 6) Heppleston (1972).*

Taxon	**Modern biogeographical distribution**	**Habitat**	**Life cycle**
Valvata piscinalis (O.F. Müller, 1774)	- Widespread across Europe, the Caucasus and western Asia[1]	- Most commonly found in a range of freshwater environments, including rivers, streams, ditches, and canals[1-2] - Prefers a relatively large, eutrophic, slow-flowing water body with a muddy substrate[2] - Less common in small, quiet ponds and lakes[2]	- Breeding occurs from April-September[2] - Period of greatest growth is during summer[2-3] - Lifespan ~1-3 years[2-3]
Galba truncatula (O.F. Müller, 1774)	- Widely distributed across the Holarctic region (throughout Europe, North Africa, Asia, North America)[1]	- Slum species, tolerant of poorly-vegetated and disturbed habitats[4] - Common in shallow, well-aerated water bodies; in marshes; on wet mud beside rivers and lakes; in small, temporary pools and ditches; water meadows[1,5] - Mostly found in permanent habitats (areas that remain damp year-round e.g. springs); less common in temporary habitats (areas that are dry during summer)[6] - Occurrence affected by temperature and moisture levels[6] - Amphibious rather than strictly aquatic; is often found out of water in moist habitats, rather than submerged[1,5] - Species is generally sedentary[6]	- Generally only active when temperatures are > 10°C[6] - Breeding occurs from April-September[6] - Main period of growth from June-September[6] - Lifespan up to 1 year[6]

4.2.7. Sampling the shells for isotope analyses

Jones et al. (2002) suggest that a minimum of 6 shells should be analysed per stratigraphic level in order to obtain an accurate range in isotope values for the period of time represented by the sample. These recommendations were adopted when sampling the fossil shells from Marsworth; a total of 17 shells were analysed. The *V. piscinalis* isotope datasets from West Runton (Davies et al., 2000; Rose et al., 2008) and Cudmore Grove (Ruddy, 2005), are also based on the analyses of large numbers of shells (139 and 27 shells, respectively).

4.2.8. Summary of sampling the rodent teeth and mollusc shells

Multiple *Microtus* or *Arvicola* teeth were sampled from every modern context or stratigraphic level for isotopic analysis. Several *G. truncatula* shells were also sampled from the deposits at Marsworth. These species were chosen because: 1) their fossil remains are abundant in Quaternary deposits, 2) they can be found in a wide range of environments, and 3) the $\delta^{18}O$ values of their remains are a close reflection of the mean $\delta^{18}O$ value of local meteoric water. Rodent remains in modern and past environments are primarily accumulated due to the deposition of owl pellets over a number of years. Therefore, *M. agrestis* teeth were sampled from modern barn owl pellets in order to investigate the variability in the $\delta^{18}O$ and $\delta^{13}C$ values of arvicoline teeth in modern populations. Mollusc shells also accumulate in fluvial environments over several years. As a consequence, sedimentary deposits containing rodent teeth and mollusc shells reflect time-averaged records of local environmental conditions. Due to a seasonal bias in rodent mortality and shell mineralization, the $\delta^{18}O$ and $\delta^{13}C$ values of rodent teeth and mollusc shells primarily reflect environmental conditions during summer. Since rodent teeth and gastropod shells record similar seasonal intervals, a direct comparison can be made between the isotope values of these materials.

4.3. Sampling of the tooth and shell biominerals

4.3.1. Carbonate in tooth bioapatite

In this thesis, all isotopic analyses on the rodent teeth were undertaken on the carbonate component of bulk (enamel and dentine) bioapatite. Carbonate was chosen instead of phosphate for several reasons. Firstly, carbonate isotope measurements are quicker and easier to undertake for large numbers of samples. Also, in general, less sample material is needed for each carbonate analysis. Therefore, each tooth can be analysed individually, rather than pooling several teeth into a single sample, as is sometimes required for phosphate isotope analyses (e.g. Royer et al., 2013a). Moreover, two stable isotopes within carbonate, oxygen and carbon, can be measured simultaneously. These isotopes provide two different indicators of environmental conditions: 1) the $\delta^{18}O$ of meteoric water, and 2) the average $\delta^{13}C$ of the whole diet. Consequently, isotope analyses on carbonates can generate more detailed palaeoenvironmental information compared to phosphates.

In previous studies on fossil mammalian bioapatite, however, enamel phosphate or bulk tooth phosphate (for $\delta^{18}O$), and bone or dentine collagen (for $\delta^{13}C$), have been the preferred materials for isotopic analysis (Bocherens et al., 1995; Drucker et al., 2003; Grimes et al., 2004; Stevens & Hedges, 2004; Héran et al., 2010; Fabre et al., 2011). This is due to the relative resistance of these materials to diagenetic alteration. Enamel phosphate is thought to be the most resistant material (Ayliffe et al., 1994; Sharp et al., 2000; Tütken et al., 2008). This is because: 1) the phosphate-oxygen bond is strong, and consequently oxygen in phosphate is generally resistant to inorganic isotopic exchange with aqueous fluids at surface temperatures (Blake et al., 1997; Lecuyer et al., 1999), 2) enamel has large and regularly-structured crystallites (Ayliffe et al., 1994; Hillson, 2005), and thus the surface area that is available for alteration is small relative to the volume of each crystallite, and 3) enamel has a low organic content (Williams & Elliott, 1989; Ayliffe et al., 1994). The degradation of organic material by microbes leads to the production of acids, which can cause the dissolution and remineralization

of bioapatite (Hare, 1980). Therefore, a low organic content reduces the likelihood of this occurring.

On the other hand, bone bioapatite and tooth dentine are often argued to be more susceptible to post-mortem diagenetic alteration, as they have smaller crystallites, a porous structure, and a greater organic content (Nelson et al., 1986; Ayliffe et al., 1994; Wang & Cerling, 1994; Kohn et al., 1999). Carbonate is also thought to be less resistant to alteration compared to phosphate. This is because the carbonate-oxygen bond is weaker than the phosphate-oxygen bond (Newesely, 1989), and carbonate constitutes only a small proportion (up to ~5%) of the mineral structure within bioapatite (Rink et al., 1996; Zazzo et al., 2004a). This means that carbonate in bioapatite is more liable to undergo dissolution and recrystallization (Newesely, 1989), and any diagenetic alteration of the carbonate will have a greater influence on measured isotope values.

Despite this, there has been much disagreement as to the isotopic integrity of carbonate in bioapatite, particularly in relation to $\delta^{13}C$ values (Sullivan & Krueger, 1981; Schoeninger & DeNiro, 1982; Lee-Thorp & van der Merwe, 1991; Lee-Thorp, 1989). Alteration of bioapatite may occur via two main processes: 1) the recrystallization of existing hydroxyapatite crystals, and 2) the adsorption or secondary deposition of exogenous carbonates within the crystal matrix (Krueger, 1991). For example, interaction with environmental aqueous fluids (seawater or groundwater) can lead to the dissolution of bioapatite, isotopic exchange with the fluid, and the re-precipitation of diagenetic apatite (Schoeninger & DeNiro, 1982; Wang & Cerling, 1994; Tütken et al., 2008). Microbial activity has also been shown to cause isotopic exchange between bioapatite and environmental water (Blake et al., 1997; Zazzo et al., 2004b).

Nonetheless, the $\delta^{18}O$ and $\delta^{13}C$ values of bioapatite are not always modified when exposed to microbes (Brady et al., 2008). In addition, Krueger (1991) undertook an experiment to examine the effects of isotopic exchange between bioapatite and synthetic groundwater. The results indicate that while the $\delta^{13}C$ of bioapatite gradually increased over time, less than 0.1% of the carbon in bioapatite had exchanged with the groundwater (Krueger, 1991). Moreover, the $\delta^{13}C$ of bioapatite can potentially provide a more useful

measure of diet than collagen, as it records the average $\delta^{13}C$ value of the diet, rather than the $\delta^{13}C$ of dietary protein (Ambrose & Norr, 1993). Furthermore, collagen undergoes fairly rapid degradation over time, and is generally not available for analysis in samples older than 30 ka (Bada et al., 1999). Therefore, the $\delta^{13}C$ of carbonate within fossil bioapatite can potentially provide a useful and reliable indication of the past $\delta^{13}C$ composition of the diet.

Also, ~90% of the carbonate within bioapatite is structural (Type B) carbonate, which resides within the phosphate bonding sites (Elliott et al., 1985). Kohn et al. (1999) suggests that since these bonding sites are generally resistant to alteration, it is likely that structural carbonate is also fairly resistant. The remaining 10% of the carbonate (Type A), is weakly-bonded in the hydroxyl sites. This carbonate may be more vulnerable to isotopic exchange due to the weaker bond with the bioapatite lattice, although pre-treatment procedures may be capable of removing any exogenous carbonates from these sites (Koch et al., 1997). Furthermore, since Type A carbonate constitutes only a small proportion of the total carbonate within bioapatite, any alteration of this carbonate will have a relatively minor (up to ± 1‰) influence on the $\delta^{18}O$ composition of bulk tooth carbonate (Kohn et al., 1999). Consequently, in most cases, the $\delta^{18}O$ values of carbonate in recent bioapatite are unlikely to have undergone significant modification due to diagenesis.

4.3.2. Mollusc shell aragonite

Most mollusc shells are composed of the mineral aragonite, which is a metastable polymorph of calcium carbonate. This mineral is replaced by calcite during the dissolution and recrystallization of carbonate (Bischoff & Fyfe, 1968; Al-Aasm & Veizer, 1986a). Aragonitic shells that have undergone recrystallization are consequently susceptible to isotopic exchange with the burial environment, and especially aqueous solutions (Al-Aasm & Veizer, 1986b; Buchardt & Weiner, 1981). The measured isotope ratios of shells can also be modified due to the attachment or adsorption of exogenous contaminants (e.g. calcite from local bedrock) onto the surfaces of shells.

X-ray diffraction (XRD) analysis is a common technique that can be used to assess whether fossil aragonitic shells contain calcite (e.g. Davies & Hooper, 1963; Sepulcre et al., 2009; Douka et al., 2010; Collins, 2012). XRD enables the determination of the crystallinity and mineral composition of geological materials. Therefore, the presence of exogenous contaminants within shells can be identified using this technique. XRD analyses were consequently undertaken on the shells from Marsworth to test for the diagenetic alteration of carbonates at this site (see Section 4.5.3. for methods).

4.3.3. Preservation of fossil carbonates analysed in this research

There are no standardised procedures for assessing the diagenetic alteration of the stable isotope compositions of fossil carbonates, and especially carbonate within bioapatite. This is because there are few analytical methods that can satisfactorily detect diagenesis, especially on small samples such as those from rodent teeth. Consequently, no diagenetic tests were undertaken on the rodent teeth sampled for this thesis.

Nevertheless, it can be argued that significant diagenetic alteration of the samples is unlikely, for the following reasons. Firstly, XRD analyses on the shells from West Runton (Davies et al., 2000; Rose et al., 2008) and Marsworth (see Chapter 6) indicate that no recrystallization to calcite has occurred. This suggests that the shells are unlikely to have experienced isotopic exchange with the burial environment. Moreover, the fossiliferous sediments at West Runton have a low permeability, and consequently act as an aquitard (Gibbard et al., 2010). Therefore, the fossil carbonates from these sediments are unlikely to have come into contact with permeating groundwater, with which isotopic exchange could have occurred. Furthermore, when directly compared in this study, the $\delta^{18}O$ offsets between the carbonate and phosphate components of the rodent teeth from Cudmore Grove are ~8-10‰ (see Chapter 6). These values are entirely consistent with isotopic offsets measured in modern, unaltered mammalian bioapatite (Iacumin et al., 1996; Martin et al., 2008; Pellegrini et al., 2011). Since phosphate is generally considered to be resistant to alteration, and the carbonate-phosphate offsets

are consistent with modern samples, it can be argued that the rodent teeth from Cudmore Grove are unlikely to have been diagenetically altered.

The possibility of diagenetic alteration is more difficult to assess for the rodent teeth from the cave sites. However, at all of the study sites, including Westbury Cave and Gully Cave, the isotope values of the rodent teeth retain a large degree of variation that is compatible with the variability observed in modern rodent populations. In addition, the $\delta^{18}O$ and $\delta^{13}C$ values of the fossil teeth are consistent with independent palaeoenvironmental evidence from the study sites (see Chapter 7). This suggests that the original isotopic values of the teeth have been preserved. The recent rodent teeth from Longstone Edge and Danebury are also expected to have undergone no alteration. This is because these teeth are relatively young, and their $\delta^{18}O$ values are comparable to modern teeth from southern Britain.

Consequently, it is proposed that the fossil biogenic carbonates have experienced minimal diagenetic alteration to their isotopic values. The preservation of the fossil rodent teeth and mollusc shells will be discussed in more detail in Chapters 6-8.

4.4. Laboratory methods

4.4.1. Identification and recording of biological remains

The modern and fossil rodent teeth were identified by comparing the size and morphology of the molars with diagrams in Hillson (2005). However, molars within the genus *Microtus* have very similar morphologies, and can often only be distinguished based on the morphology of the lower first molar (e.g. for distinguishing *M. agrestis/arvalis* from *M. oeconomus*) or the upper second molar (*M. agrestis* has an additional posterior loop compared to other species of *Microtus*). In instances in which these teeth were unavailable, the molars were labelled as *Microtus* sp. Likewise, vole incisors are very similar in their morphology, and thus could only be assigned to a genus (e.g. *Microtus* or *Arvicola*) or subfamily (Arvicolinae), based on 1) their relative size (*Arvicola* is larger than *Microtus*), and 2) the taxonomic representation of rodents within the fossil assemblage, which was determined from the dental elements that

are species-diagnostic. All shells were identified by Dr Tom White (Life Sciences Department, Natural History Museum).

The preservation and completeness of all analysed material were also recorded. For pre-modern teeth, taphonomic observations included: disarticulation, breakage, evidence for predatory digestion (localised pitting and rounding of edges), and other surface features (scratches, large-scale pitting, chipping, rounding, and flaking). All taphonomic descriptions are based on the work by Andrews (1990). Modifications due to predation were classified according to the categories listed in Table 4.2.

4.4.2. Pre-treatment of tooth carbonate

4.4.2.1. Review of published treatment methods

One approach to limit the potential for diagenetic alteration to effect the measured isotopic values of fossil carbonates is to use rigorous cleaning methods prior to isotopic analysis. Various pre-treatment procedures have been suggested for the removal of exogenous contaminants, although the most commonly applied method is that of Koch et al. (1997), which was developed from the original work by Lee-Thorp (1989). This method involves two stages: 1) treatment with a bleaching agent (sodium hypochlorite, NaClO, or hydrogen peroxide, H_2O_2), followed by 2) treatment with an acetic acid solution. Bleaching agents are used to oxidize organic compounds within bioapatite or on the outer surfaces of bones and teeth. Conversely, dilute acetic acid is used to dissolve exogenous carbonates that are absorbed onto the surfaces of hydroxyapatite crystals (Koch et al., 1997).

Koch et al. (1997) experimented with differing concentrations of the bleaching agents and acetic acid solutions, in order to assess the effects that these chemicals have on the isotope values of modern bioapatite. These experiments showed that the bleaching stage had no appreciable effect on the isotope values of enamel carbonate. With the addition of the acetic acid treatment, the $\delta^{18}O$ of enamel became enriched, while the $\delta^{13}C$ of enamel became depleted, relative to untreated samples. These isotopic shifts, which are usually around 1-2‰, have also been observed in other studies that have

used the acetic acid treatment on mammalian bones and teeth (Lee-Thorp & van der Merwe, 1991; Garvie-Lok et al., 2004; Yoder & Bartelink, 2010; Pellegrini et al., 2011; Crowley & Wheatley, 2014). Koch et al. (1997) suggests that these isotopic shifts are due to the partial dissolution of carbonate from more weakly bonded sites within the hydroxyapatite structure (i.e. Type A carbonate). The use of unbuffered or concentrated acetic acid has also been shown to result in the loss or recrystallization of bioapatite, as well as the formation of secondary phosphate minerals such as brushite (Lee-Thorp & van der Merwe, 1991; Koch et al., 1997; Garvie-Lok et al., 2004). Consequently, Koch et al. (1997), recommend using treatments that produce the lowest isotopic shifts and least recrystallization of modern bioapatite. These treatments are: 1) a dilute solution of NaClO or H_2O_2, followed by 2) a 1M acetic acid solution buffered with calcium acetate, or 0.1M acetic acid.

Several subsequent studies have applied the treatment methods suggested by Koch et al. (1997) to the preparation of modern and Pleistocene bioapatite. However, these studies have often varied the method in terms of the oxidizing agent used, the concentrations of the reagents, the temperature during treatment, and the duration in which the samples remained soaked within the reagents (Fraser et al., 2008; Clementz et al., 2009; Blaise & Balasse, 2011; Gehler et al., 2012; Kovács et al., 2012). This is a potential problem, as different treatment methodologies may have different effects on the isotope values of bones and teeth. Crowley & Wheatley (2014) therefore examined the isotopic offsets induced by each treatment step individually, and by different treatment conditions. These authors concluded that the treatment methods that produce the “best” results for tooth enamel and dentine, in terms of the lowest isotopic shifts caused by the treatment chemicals and the minimum loss of bioapatite, are: 1) 30% H_2O_2, followed by 2) a 1M acetic acid solution buffered with calcium acetate to a pH of ~5. Therefore, the methods recommended by Crowley & Wheatley (2014), outlined in more detail below, were used on all rodent teeth analysed for this thesis.

However, a more recent study by Pellegrini & Snoeck (2016) demonstrated that this method can cause variable $\delta^{18}O$ and $\delta^{13}C$ offsets (generally within ± 1.5‰) compared to untreated bioapatite. Furthermore, H_2O_2, a weak acid, was found to be inefficient at removing organic material

(Snoeck & Pellegrini, 2015). This reagent also causes the partial dissolution of carbonate in bioapatite, leading to the loss of sample.

Despite these potential limitations, it was decided that all samples should be prepared using the methods recommended by Crowley & Wheatley (2014), for four main reasons. Firstly, the majority of the sampled teeth have been ingested by owls, and have consequently been exposed to digestive conditions that are much more acidic than applied during pre-treatment. Secondly, the use of acetic acid was considered important for removing potential carbonate contaminants from the fossil teeth originating from carbonate-rich sedimentary contexts (Marsworth, Westbury Cave, and Gully Cave). Indeed, acetic acid has been shown to be effective at removing exogenous carbonates (Krueger, 1991). Thirdly, the majority of studies that have investigated the effects of pre-treatment methods have found no significant or consistent isotopic offsets between different treatment methodologies (Passey et al., 2002; Clementz et al., 2009; Yoder & Bartelink, 2010; Chenery et al., 2012; Jeffrey et al., 2015). Finally, maintaining consistency in the treatment procedures ensures that all isotope data collected during this research, and all published data generated using similar methods (e.g. Gehler et al., 2012), can be compared. However, it is acknowledged that the chemical treatments may have slightly altered the $\delta^{18}O$ and $\delta^{13}C$ values of the teeth relative to original biological values.

4.4.2.2. Treatment methods used in this research

Firstly, each tooth was placed in a small glass vial and covered with 0.5% sodium hexametaphosphate. The vials were then placed in an ultrasonic bath for 10 minutes. This enabled any remaining pellet material or sediment to be dislodged from the surfaces of the modern and fossil teeth. The teeth were then rinsed with deionised water and air-dried at room temperature. Once dry, the teeth were crushed into a fine powder using an agate pestle and mortar. Given the small size of the specimens, it was not possible to mechanically separate the dentine from the enamel while also retaining sufficient sample powder for isotopic analysis. Therefore, all teeth were crushed in bulk.

The teeth were subsequently pre-treated in order to remove detrital organic and carbonate material. The samples were first soaked in 30% H_2O_2 for 24 hours at room temperature (~20-25°C), and then rinsed 4 times with deionised water. Next, the samples were soaked in a 1M acetic acid–calcium acetate buffer solution (pH ~5) for 24 hours at room temperature, and then rinsed 5 times in deionised water. During each stage of pre-treatment, approximately 0.05 ml of chemical solution (H_2O_2 or acetic acid buffer) was used per milligram of sample powder. Finally, the samples were left to dry in a fume cupboard at room temperature.

4.4.3. Pre-treatment of shells

Each shell was placed in a small glass vial and covered with 0.5% sodium hexametaphosphate. The vials were then placed in an ultrasonic bath for approximately 10 minutes to dislodge any detrital sediment on or inside the shell. However, the shells were small (< 2 mm) and fragile, and the ultrasonic bath caused them to gradually disintegrate. Therefore, the samples were carefully monitored whilst in the ultrasonic bath to ensure that most of the visible sediment had been removed without the complete destruction of the shell. Nevertheless, some shells were removed from the ultrasonic bath before 10 minutes and may not have been fully cleaned of sediment.

The shells were subsequently rinsed with deionised water and left to air-dry at room temperature. Once dry, each shell was crushed using an agate pestle and mortar, and the powder added to a clean glass vial. Shells are sometimes treated with hydrogen peroxide prior to isotopic analysis to remove detrital organic material (e.g. Waghorne et al., 2012). However, there is typically some sample loss during this treatment, due to the transfer of the sample between tubes. Therefore, to prevent this and ensure that sufficient material remained for analysis, no further treatment methods were performed on the shells. This lack of further treatment should not have had a great effect on the results. This is because shells are 90-100% carbonate, and thus the presence of a small amount of detrital sediment would have only a minor influence on the isotope values.

4.5. Analytical methods

4.5.1. $\delta^{18}O$ and $\delta^{13}C$ analyses of tooth and shell carbonates

4.5.1.1. Analyses of samples and standards

The majority of the samples were analysed in the Department of Earth Sciences at Royal Holloway. Approximately 2-4 mg of each powdered tooth sample, and 0.3-0.4 mg of each shell sample, was weighed for isotope analysis using a Mettler Toledo XP6 microbalance. For some samples (primarily the modern second and third molars, or the fragmented fossil teeth), only 0.5-2 mg of powder remained following pre-treatment. Therefore, the entirety of each of these samples was weighed for analysis.

Once weighed, the samples were reacted with 100% orthophosphoric acid at 90°C to produce carbon dioxide gas. The oxygen and carbon isotope ratios of the gas were analysed using a GV Instruments Multiflow preparation system connected to an IsoPrime mass spectrometer. Internal (3 x RHBNC-PRISM) and external (NBS-19 and LSVEC) standards were analysed for every 18 samples (Table 4.4). Oxygen and carbon isotope ratios of the standards and samples were normalized to the international carbonate standard, Vienna Pee Dee Belemnite (VPDB), using the equations below:

$$\delta^{18}O\ (‰) = [(^{18}O/^{16}O_{sample} \div {}^{18}O/^{16}O_{VPDB}) - 1] \times 1000 \quad (4.1).$$

$$\delta^{13}C\ (‰) = [(^{13}C/^{12}C_{sample} \div {}^{13}C/^{12}C_{VPDB}) - 1] \times 1000 \quad (4.2).$$

The calibration of sample isotope values was based on a two-point linear regression between NBS-19 and LSVEC. The average internal precision (1σ standard deviation) for individual measurements of NBS-19 during the sample analysis period was ± 0.04‰ for $\delta^{18}O$ and ± 0.02‰ for $\delta^{13}C$. The average internal precision for LSVEC was ± 0.02‰ for $\delta^{18}O$ and ± 0.05‰ for $\delta^{13}C$. Analytical uncertainties (1σ standard deviation) on the isotope measurements of the samples are also typically less than ± 0.1‰ for both $\delta^{18}O$ and $\delta^{13}C$. The results of the three replicate analyses of RHBNC during each analytical run were used to assess the internal precision for each run and the external

precision across multiple runs. The average internal precision (1σ standard deviation) for the runs undertaken during this thesis was ± 0.05‰ for $\delta^{18}O$, and ± 0.02‰ for $\delta^{13}C$, and the external precision (1σ standard deviation) was ± 0.08‰ for $\delta^{18}O$ and ± 0.04‰ for $\delta^{13}C$.

Table 4.4: *Accepted oxygen and carbon isotopic values for the carbonate standards that were used in this study for the calibration of the isotope ratios of the samples.*

Carbonate standard	$\delta^{18}O$ (‰ VPDB)	$\delta^{13}C$ (‰ VPDB)
NBS-19	-2.20	+1.95
LSVEC	-26.70	-46.50
BDH	-1.97	+1.95

The teeth from the two archaeological sites (Longstone Edge and Danebury) and from Gully Cave were analysed at the Bloomsbury Environmental Isotope Facility, University College London. Approximately 1.5-1.6 mg of each sample from the archaeological sites, and ~2.0-2.3 mg of each sample from Gully Cave, was weighed using a Mettler Toledo XP6 microbalance. Each sample was subsequently reacted with 100% orthophosphoric acid at 45°C, and analysed using a Thermo Delta Plus XP mass spectrometer connected to a Thermo Finnigan Gas Bench II. Isotope values were calibrated against the internal standard BDH (Table 4.4). One BDH standard was analysed for every three samples to correct for measurement drift, and one additional standard was analysed for every five samples to correct for the influence of sample volume on the isotope measurements. The internal precision (1σ standard deviation) on individual measurements of the BDH standard is typically within ± 0.05‰ for both $\delta^{18}O$ and $\delta^{13}C$.

Three analyses of the external standard, NBS-19, were also undertaken per run of 56 samples. The isotope values of the samples were corrected for the average offsets (generally ≤ 0.15‰) between the measured and known (Table 4.4) $\delta^{18}O$ and $\delta^{13}C$ values for this standard. The internal

precision (1σ standard deviation) for an analytical run is generally better than ± 0.10‰ for $\delta^{18}O$ and ± 0.05‰ for $\delta^{13}C$. The external precision for the runs undertaken during this research is ± 0.17‰ for $\delta^{18}O$ and ± 0.03‰ for $\delta^{13}C$.

Further information on the analytical methods, the calibration of sample isotope ratios, and the performance of the RHUL and BEIF labs during the sample analysis periods is provided in Appendix B.

4.5.1.2. Outliers and replicate analyses

Some of the analysed teeth yielded oxygen isotope values that lie significantly outside the main cluster of data for the study site in question. These values were consequently considered outliers. In most cases, the outlying values result from the analysis of a small quantity of powder, which generated insufficient carbon dioxide for the accurate and precise measurement of isotopic ratios. However, occasionally, analyses of the modern teeth produced $\delta^{18}O$ values consistently around -3 to -2‰. These values lie outside the ranges of the modern tooth datasets. The cause of these anomalous measurements is unclear, as re-analyses of these samples produced $\delta^{18}O$ values that are significantly lower and generally consistent with the results obtained from other modern teeth. Therefore, any outlying values of around -2‰ were excluded from the modern dataset.

Other sample measurements that were identified as being potentially anomalous (e.g. due to issues with the flushing of the sample gas to the mass spectrometer during analysis), and that had sufficient sample powder remaining, were also re-analysed. The data generated from the replicate analyses were used to estimate the 1σ standard deviation precision on an individual measurement of a sample of bioapatite carbonate (see section B.3 of Appendix B for further details). The precision on a single measurement of bioapatite carbonate is typically better than ± 0.5‰ for $\delta^{18}O$, and ± 0.18‰ for $\delta^{13}C$. The lower precision on measurements of tooth carbonate relative to pure carbonates (e.g. NBS-19) is attributed to internal variations in the isotope composition of a tooth (e.g. Passey & Cerling, 2006).

Therefore, in cases where the $\delta^{18}O$ value obtained during re-analysis was less than around 1‰ different from the value obtained during initial analysis, the isotope values of the two analyses were averaged. The standard error on the values obtained from the two analyses was additionally calculated as a measure of the uncertainty on the mean isotope value of the sample.

In a few cases, however, the re-analysis of a sample generated an outlying $\delta^{18}O$ value that was greater than 1‰ different from the value obtained during the first analysis. Consequently, the value from the first analysis was used in the subsequent exploration of the data. Samples with outlying values and insufficient material for re-analysis were excluded from the dataset.

4.5.2. $\delta^{18}O$ and δD analyses of modern water

A small number of water samples were obtained from modern rivers and ditches to compare with the isotope data from the modern rodent teeth (Chapter 5). These samples were collected by submerging a small, air-tight Teflon bottle into the water body, until the bottle was completely filled with water. The samples were submitted to the Stable Isotope Facility at the British Geological Survey in Keyworth, Nottingham, for isotopic analysis. Oxygen isotope ratios were measured using an Isoprime 100 mass spectrometer with Aquaprep, and hydrogen isotope ratios were measured by an Isoprime mass spectrometer with EuroPyrOH. All water isotope values in this thesis are expressed in ‰ relative to Vienna Standard Mean of Ocean Water (VSMOW).

4.5.3. X-ray Diffraction analyses of shells

The shells analysed in this thesis originate from a carbonate-rich burial environment located near to groundwater, and thus it was considered important to test for the recrystallization or contamination of these shells. Therefore, XRD analyses were undertaken on the 5 largest shell samples from Marsworth, in the Department of Earth Sciences at Royal Holloway. Each powdered shell was transferred to a separate glass slide using a glass pipette and deionised water. The glass slides were then left to dry in a drying cabinet

at 40°C. The samples were analysed using a Phillips PW1830/3020 spectrometer with copper Kα X-rays. Samples were run at diffraction angles of 4° to 50° (2θ) at a rate of 1° per minute. Mineral peaks were then identified manually, and compared to the XRD patterns for pure aragonite and pure calcite, using the RRUFF Project database (Lafuente et al., 2015).

4.6. Summary

Oxygen and carbon isotope analyses were undertaken on modern and fossil *Microtus* and fossil *Arvicola* dental carbonate. Modern *Microtus agrestis* teeth were obtained from barn owl pellets, to examine the modern isotopic ecology of arvicoline rodents. Most of the fossil rodent remains also likely accumulated due to the activities of avian predators. The $\delta^{18}O$ values of the rodent teeth reflect the mean $\delta^{18}O$ of meteoric water, but with a bias towards summer isotopic compositions due to a seasonal dominance in rodent predation. The $\delta^{13}C$ values of the rodent teeth record the mean seasonal $\delta^{13}C$ of the diet, which reflects the mean $\delta^{13}C$ composition of local vegetation. The rodent teeth were pre-treated according to standard methods recommended for carbonate within bioapatite.

Fossil *Galba truncatula* shells were also sampled for oxygen and carbon isotope analyses and XRD analyses. The $\delta^{18}O$ values of the shells reflect the temperature and average $\delta^{18}O$ of meteoric water during the period of shell mineralization. Freshwater gastropod shells mainly grow during summer. Therefore, the $\delta^{18}O$ values of rodent teeth and shells can be compared, as they mineralize within a similar temporal period.

Although dental carbonate is potentially susceptible to post-mortem alteration, it is argued that the fossil rodent teeth analysed in this thesis have experienced minimal diagenetic alteration, because: 1) XRD analyses indicate that the fossil shells from West Runton and Marsworth have not undergone diagenetic recrystallization to calcite, 2) the $\delta^{18}O$ offsets between the dental carbonate and phosphate from Cudmore Grove are comparable to published offsets recorded in modern bioapatite, and 3) the isotopic values of the teeth are consistent with independent palaeoenvironmental proxies from each site.

Oxygen and hydrogen isotope analyses were additionally undertaken on a small number of modern water samples, to enable comparison with the $\delta^{18}O$ values of the modern *M. agrestis* teeth. The following chapter presents the results of this modern study, which investigates the relationships between isotopic variability in modern rodent teeth and local environmental conditions across Britain.

5. Variability in the stable isotope values of modern rodent dental carbonate from Britain: implications for palaeoenvironmental reconstructions

5.1. Introduction

This chapter presents the results of the modern analogue study on the isotope values of rodent teeth from Britain. This study aimed to investigate the significance of isotopic variability between: 1) different teeth within a single individual, 2) different individuals within a population, and 3) different populations from multiple locations across Britain. Assessing this variability is critical for: 1) identifying the teeth (molars or incisors) that most reliably reflect the average $\delta^{18}O$ and $\delta^{13}C$ values of a rodent population, 2) determining the number of teeth that must be analysed in order to generate accurate and precise mean isotope values for a population, and 3) understanding how tooth isotopic values correlate with local environmental factors. The study also aimed to develop a new calibration for the relationship between the $\delta^{18}O$ of rodent bioapatite and the $\delta^{18}O$ of local water in mid-latitude regions.

To achieve these aims, *Microtus agrestis* teeth were sampled from modern barn owl pellets collected from four sites across Britain: 1) West Horrington, Somerset, 2) Cobham, Surrey, 3) Beeford, East Yorkshire, and 4) Perth, Perthshire. These teeth were analysed to determine the oxygen and carbon isotope values of bioapatite carbonate. Firstly, the isotope values of molars and incisors from different individuals are compared, in order to assess the significance of isotopic variability within each rodent population. Secondly, the $\delta^{18}O$ values of rodent tooth carbonate ($\delta^{18}O_{rt}$) are compared with the $\delta^{18}O$ values of local surface water ($\delta^{18}O_{mw}$) and precipitation ($\delta^{18}O_{pt}$), to generate

regression equations for the relationships between $\delta^{18}O_{rt}$ and the $\delta^{18}O$ of environmental water. These equations are the first to be generated for the $\delta^{18}O$ of dental carbonate, and for the $\delta^{18}O$ of bioapatite in a single species of rodent. The relationships are evaluated against published calibrations, in order to assess their applicability for reconstructing $\delta^{18}O_{mw}$ from the $\delta^{18}O$ values of rodent teeth. The $\delta^{13}C$ values of the teeth ($\delta^{13}C_{rt}$) are also interpreted in terms of the $\delta^{13}C$ of the diet ($\delta^{13}C_{d}$). Finally, the implications of the results for using the $\delta^{18}O$ and $\delta^{13}C$ values of rodent tooth bioapatite for palaeoenvironmental reconstructions are discussed, and recommendations are made on appropriate strategies for sampling fossil rodent teeth for isotopic analysis.

5.2. Study sites

The locations of the four study sites are illustrated in Figure 5.1, and their environmental contexts are summarised in Table 5.1. These sites were chosen because they lie along a gradient in the mean $\delta^{18}O$ of meteoric water (see section 3.2.3), and span nearly the maximum range in $\delta^{18}O_{mw}$ values across modern Britain. The data from the sites therefore enable the relationship between the $\delta^{18}O$ values of rodent teeth and meteoric water to be investigated and quantified. West Horrington and Beeford are also located proximal to important Quaternary sites [Westbury Cave, Somerset (Andrews et al., 1999); Gully Cave, Somerset (Schreve, 2006); Star Carr, Yorkshire (Clark, 1954)]. The data from the modern rodent teeth can consequently provide a useful comparison with isotope values of fossil teeth from the nearby Pleistocene localities.

5.2.1. West Horrington, Somerset

The first site is West Horrington, Somerset, which is located on the southeastern edge of the Mendip Hills Area of Outstanding Natural Beauty (Figure 5.2). The site is also situated near to the limestone gorges of Cheddar Gorge and Ebbor Gorge (Figure 5.2), where several important Late Pleistocene cave sites have been discovered, containing abundant

mammalian remains and important evidence for Upper Palaeolithic human occupation (e.g. Currant, 1986; Jacobi, 2004). The Pleistocene sites of Westbury Cave and Gully Cave (Ebbor Gorge), are respectively located just 5 and 7 km northwest of West Horrington.

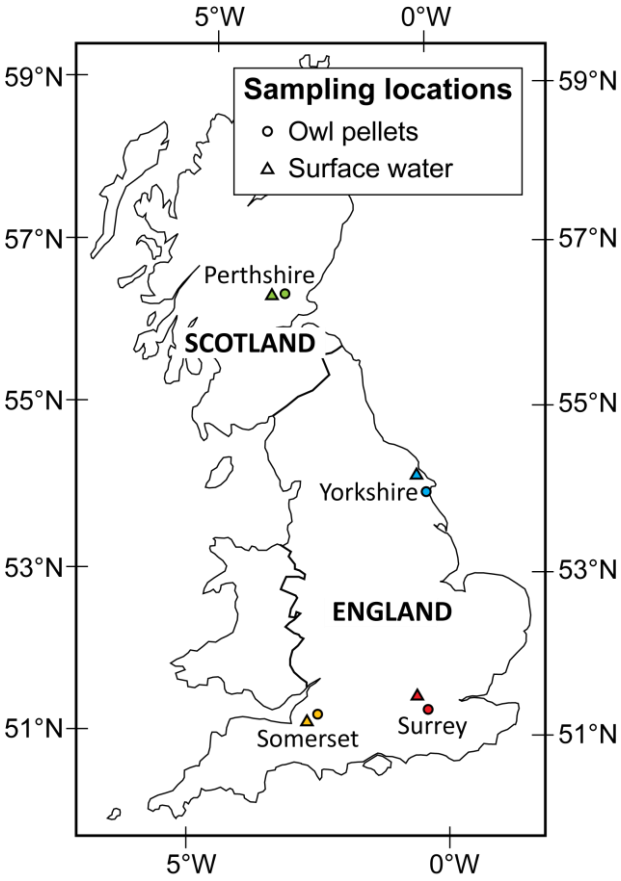

Figure 5.1: *Map showing the locations of the modern study sites.*

Owl pellets were collected from West Horrington in September-October 2015. A small stream flows through the woodland to the west of West Horrington, although the nearest major stream is Keward Brook (Figure 5.2). This stream is sourced by natural springs and is a tributary of the River Sheppey, which flows through the centre of the nearby town of Wells. The average $\delta^{18}O$ value of local groundwater varies between -7.0 and -6.5‰ (Darling et al., 2003), and the modelled mean annual $\delta^{18}O$ of precipitation is likewise around -7‰ (Table 5.1). However, due to evaporation, the average $\delta^{18}O$ value of water in British rivers is usually ~0.5‰ more enriched than that of the underlying groundwater (e.g. Darling & Bowes, 2016). Therefore, the average $\delta^{18}O$ value of surface waters near to West Horrington is estimated to lie between -6.5 and -6.0‰.

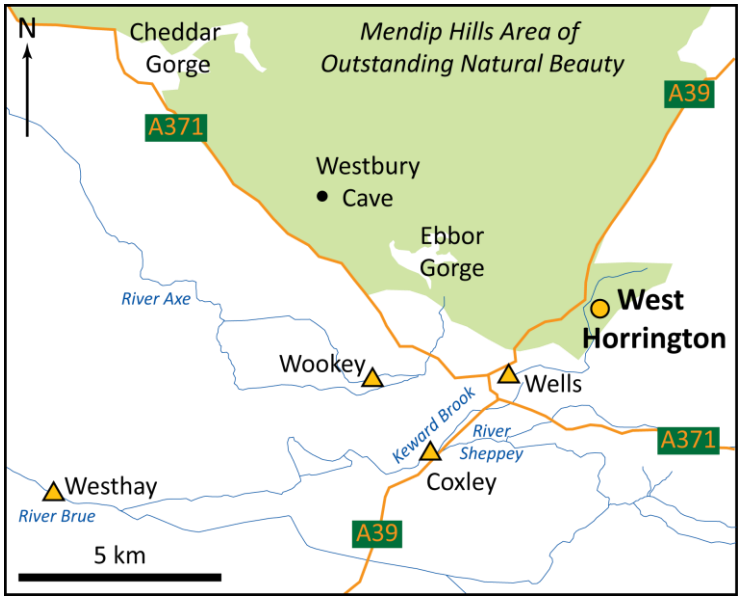

Figure 5.2: *Map showing the locations of the owl pellet (yellow circle) and water (triangles) sampling sites in Somerset. The locations of key Pleistocene sites are also shown.*

5.2.2. Cobham, Surrey

The second site is Cobham in northwest Surrey (Figure 5.3). The sampled barn owl pellets were collected in April 1973. The River Mole, a tributary of the River Thames, flows through Cobham and converges with the Thames near Hampton Court Palace (Figure 5.3). Precipitation in Cobham, and groundwater in the Runnymede area (Figure 5.3), have similar mean annual $\delta^{18}O$ values of -7.0 ± 0.1‰ (Bowen, 2017), and -7.1‰, respectively (Bearcock & Smedley, 2010). The $\delta^{18}O_{mw}$ of the River Thames varies between -8.0 and -6.0‰, but with relatively enriched annual average values of around -6.5‰ (Davies, 1999; Sherriff, 2016). During 2011-2013, the $\delta^{18}O$ of the Thames at Runnymede varied between -8.0 and -6.2‰, with an average of -6.8‰ (Darling & Bowes, 2016). Seasonal and inter-annual fluctuations in the $\delta^{18}O_{mw}$ of the River Thames are relatively small, reaching a maximum of ~1‰ (Darling & Bowes, 2016). Therefore, it is expected that water sources near to Cobham would have had average $\delta^{18}O$ values of approximately -7 to -6‰ during the period in which the sampled teeth mineralized.

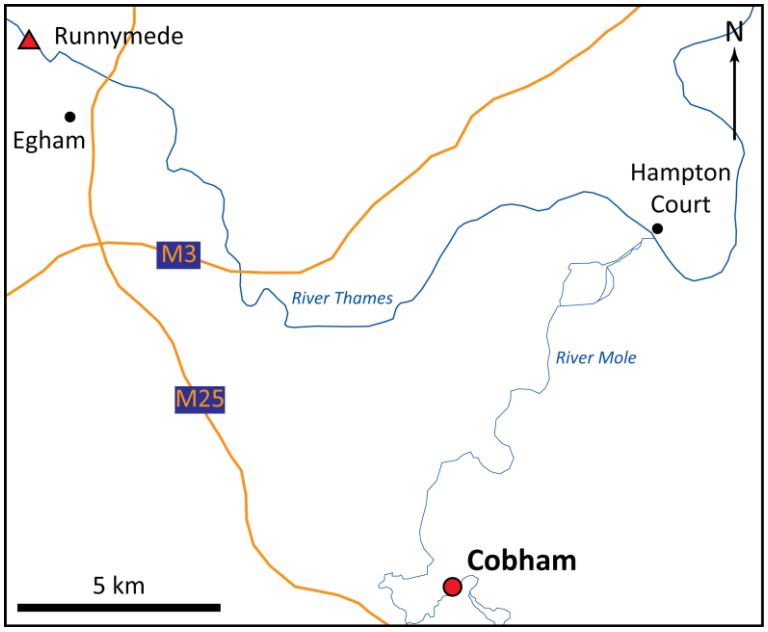

***Figure 5.3**: Map showing the locations of the owl pellet (red circle) and water (triangle) sampling sites in Surrey.*

5.2.3. Beeford, East Yorkshire

The third study site is Woodhouse Farm, which lies ~2 km north of Beeford in East Yorkshire, and approximately 25 km south-southeast of the famous Mesolithic and Palaeolithic site of Star Carr in North Yorkshire (Figure 5.4). Owl pellets were collected from Woodhouse Farm in March 2015. The main surface water bodies in the area are field drains and small ponds, such as the Pitwherry Drain and Old Howe Drain that surround the farm. The modelled mean annual $\delta^{18}O$ of precipitation for the site is -8.3 ± 0.3‰ (Bowen, 2017). Local groundwater has a similar average $\delta^{18}O$ value of between -7.8‰ (Darling et al., 2003) and -8.1‰ (Brown et al., 2011). Analyses of water collected from ditches, field drains and rivers in the Star Carr area during October-December 2009 yielded a higher average $\delta^{18}O$ value of -7.3‰ (Brown et al., 2011). Surface water sources in East Yorkshire are therefore expected to have comparable $\delta^{18}O$ values of between -8 and -7‰.

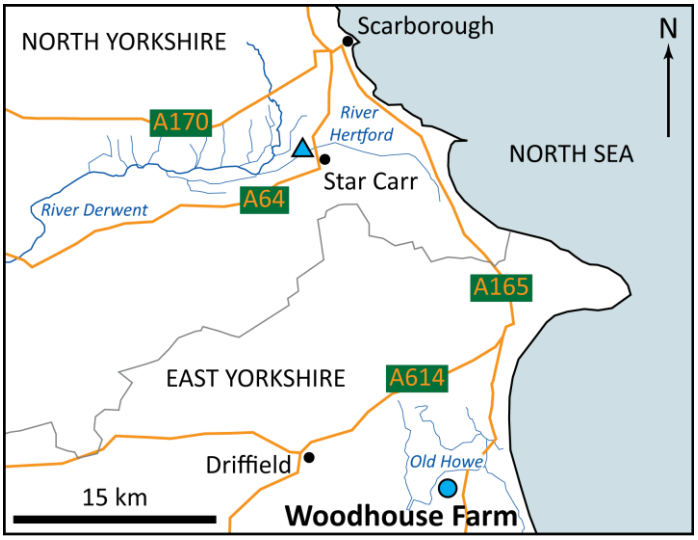

***Figure 5.4**: Map showing the locations of the owl pellet (blue circle) and water (triangle) sampling sites in Yorkshire.*

5.2.4. Perth, Perthshire

The final study area is Perthshire, in eastern Scotland. Barn owl pellets were collected from two nest sites in this area in November-December 2016 (labelled Site A and Site B in Figure 5.5). Small streams flow eastward through Perthshire towards the Firth of Tay (Figure 5.5). Sites A and B are also respectively located 8.5 and 12 km north of the River Tay, which is the major source of water in the area (Figure 5.5).

The modelled $\delta^{18}O$ of precipitation for the area is around -6.5‰ (Table 5.1). The modelled $\delta^{18}O_{pt}$ values for Sites A and B are identical within uncertainties, and thus teeth from these sites would be expected to have comparable $\delta^{18}O$ values that are representative of the local *Microtus agrestis* population. In contrast, the $\delta^{18}O$ value of groundwater in Perthshire is much more depleted at between -8.5 and -8.0‰ (Darling et al., 2003). However, as aforementioned, surface water is generally ~0.5‰ enriched compared to groundwater, and thus local surface water sources likely have $\delta^{18}O$ values of around -8.0 to -7.5‰.

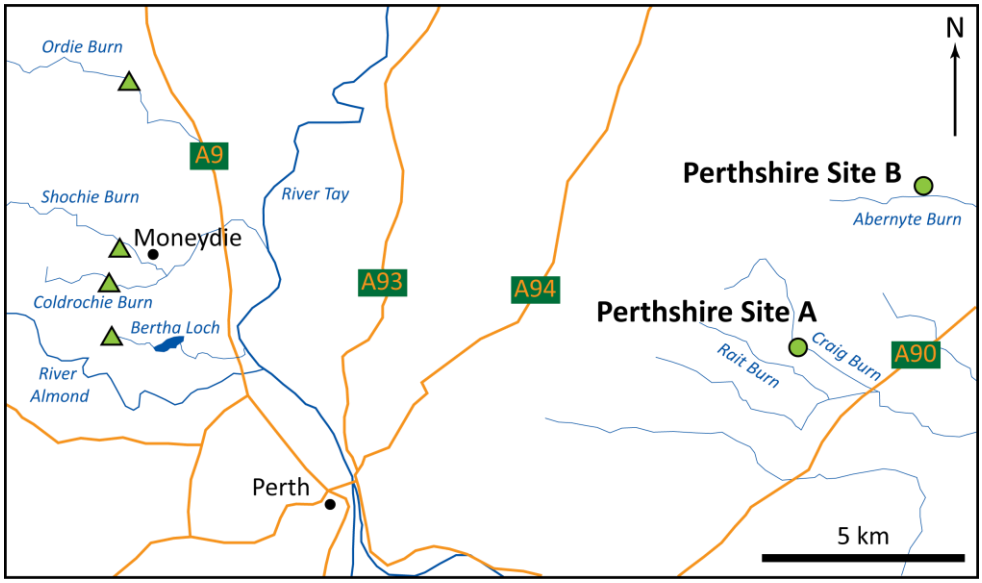

Figure 5.5: *Map showing the locations of the owl pellet (green circles) and water (triangles) sampling sites in Perthshire.*

5.3. Sampling strategies

5.3.1. Rodent teeth

In order to determine the magnitude of isotopic variability in modern rodent populations, 9-10 *Microtus agrestis* individuals, derived from multiple barn owl pellets, were selected from each study area. The owl pellets were dissected in deionised water, and skulls from different individuals were placed in separate glass vials. The skeletal remains were left to air-dry, and were subsequently identified under a low-powered optical microscope.

Following identification, one *M. agrestis* right mandible was selected from each of 9 different pellets from Somerset, Surrey and East Yorkshire (Figure 5.6). Five *M. agrestis* right mandibles were selected from each nest site in Perthshire. Well-preserved mandibles were preferentially chosen to ensure that 1) all four teeth in each mandible were *in situ* and belonged to a single individual, and 2) all teeth were complete for isotopic analysis.

Table 5.1: *Summary of the geographic locations, $\delta^{18}O$ values of precipitation, and measured or estimated $\delta^{18}O$ values of local surface water sources for the four study sites. Grid references for Cobham and Perth are approximate. Modelled mean annual $\delta^{18}O$ values of precipitation were obtained using the Online Isotopes in Precipitation Calculator (Bowen, 2017), and uncertainties on these values indicate 95% confidence intervals around the mean (Bowen & Revenaugh, 2003). Measured $\delta^{18}O$ values of local meteoric water are from: [a]Davies (1999); Sherriff (2016); [b]Darling & Bowes (2016); [c]Brown et al. (2011).*

Site name		National Grid Reference	Latitude (°)	Longitude (°)	Elevation (m above sea level)	Modelled mean annual $\delta^{18}O$ of precipitation (‰ VSMOW)	Measured or estimated $\delta^{18}O$ of local surface water (‰ VSMOW)
West Horrington, Somerset		ST 57180 47430	51.22	-2.61	159	-7.2 ± 0.1	-6.0 to -6.5
Cobham, Surrey		TQ 10725 59521	51.32	-0.41	22	-7.0 ± 0.1	-6.5[a] to -6.8[b]
Beeford, East Yorkshire		TA 11996 55585	53.98	-0.29	9	-8.3 ± 0.3	-7.3[c]
Perth, Perthshire	Site A	NO 23000 27000	56.43	-3.25	33	-6.5 ± 0.5	-7.5 to -8.0
	Site B	NO 26000 31000	56.47	-3.20	103	-6.6 ± 0.6	

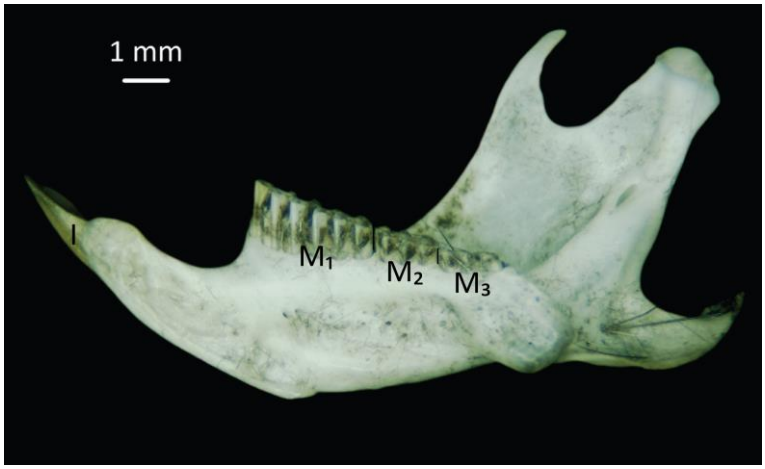

Figure 5.6: *Photograph of a modern* Microtus agrestis *right mandible from Surrey. The four teeth (I, M_1, M_2 and M_3) are labelled.*

To investigate isotopic offsets between different tooth types, the incisor (I), first molar (M_1), second molar (M_2), and third molar (M_3) from each mandible were analysed (Figure 5.6). The lower left and upper teeth from one individual from Somerset (Individual 3), Surrey (Individual 9) and East Yorkshire (Individual 1) were additionally analysed to assess the magnitude of isotopic variability between all teeth within a single individual. The M_1 was missing from the right mandible of Individual 5 from Surrey, and thus analyses could only be undertaken on the I, M_2, and M_3 from this specimen. The samples selected for analysis are summarised in Table 5.2.

Offsets between the measured isotope values of different teeth may partly result from variations in the isotope compositions of different aliquots of a single sample of rodent tooth bioapatite. This isotope variability within a sample of tooth bioapatite is related to changes in the isotope values of the water and dietary sources consumed by an individual during the period of tooth mineralization. In order to assess the uncertainty on a individual isotopic measurement of rodent bioapatite, several teeth were analysed twice (Analysis 1 and Analysis 2), with each analysis undertaken on a different day (see Appendix B). Replicate analyses on the modern teeth were specifically undertaken on the lower M_1 and incisors from Somerset, and the lower incisors and upper teeth from Surrey. The $\delta^{18}O$ values of the lower first molars and

incisors obtained during Analysis 2 were generally within 1‰ of the values from Analysis 1. This is also the case for the upper second molars from Surrey. Differences in the measured $\delta^{13}C$ values between analyses were mostly within 0.4‰. In contrast, the measured $\delta^{18}O$ values of the upper first molars and incisors from Surrey were consistently 2-3‰ more depleted in Analysis 2 relative to Analysis 1. The 1σ standard deviation precision on a single measurement of rodent tooth carbonate, calculated from the replicate analyses, is ± 0.50‰ for $\delta^{18}O$, and ± 0.18‰ for $\delta^{13}C$. The magnitude and significance of isotopic differences between modern rodent teeth must, therefore, be considered in the context of this measurement uncertainty. This will be taken into account in the following discussion of the results.

Table 5.2: *Summary of the numbers of* Microtus agrestis *teeth sampled from the modern study sites.*

Site name		**Number of barn owl pellets**	**Number of *Microtus agrestis* individuals**	**Total number of teeth analysed**
West Horrington, Somerset		9	9	48
Cobham, Surrey		9	9	47
Beeford, East Yorkshire		9	9	48
Perth, Perthshire	Site A	Unknown	5	20
	Site B		5	20

5.3.2. Meteoric water

In order to assess the relationship between $\delta^{18}O_{rt}$ and $\delta^{18}O_{mw}$, the oxygen isotope values of local water sources must be known. Bioapatite-water fractionation equations are commonly generated using modelled $\delta^{18}O$ values

of precipitation. Therefore, mean annual $\delta^{18}O_{pt}$ values were estimated for each study site using the Online Isotopes in Precipitation Calculator (Table 5.1) (Bowen & Revenaugh, 2003; Bowen, 2017). This calculator is based upon a model that accounts for the variation in $\delta^{18}O_{pt}$ with latitude and altitude, resulting from the temperature-dependent fractionation of oxygen isotopes in water (Bowen & Wilkinson, 2002). Variations in $\delta^{18}O_{pt}$ due to non-temperature effects are accounted for by using spatial interpolation between $\delta^{18}O_{pt}$ measurements derived from the Global Network of Isotopes in Precipitation (GNIP) (IAEA/WMO, 2018). However, isotope data for precipitation in Britain are limited, and there are significant gaps in the spatial distribution of the data (IAEA/WMO, 2018). Data are especially sparse in southwest England and Scotland. As a result, the modelled $\delta^{18}O_{pt}$ values may not precisely reflect the $\delta^{18}O$ of local water at the study sites.

To address this issue, $\delta^{18}O$ and δD data were obtained for surface meteoric water sources located proximal to each site. Published water isotope data were used for Surrey and Yorkshire. The data for Surrey consist of 26 monthly or bi-monthly measurements on water from the River Thames at Runnymede, which were collected between October 2011 and May 2013 (Darling & Bowes, 2016). The data for East Yorkshire comprise 38 measurements on water from various rivers, surface ditches and field drains in the Hertford Catchment, collected during October-November 2009 (Brown et al., 2011).

Data for surface water sources proximal to Somerset and Perthshire are currently unavailable. Therefore, four water samples were collected in October 2016 from various rivers located ~2-14 km southwest of West Horrington (Figure 5.2). Four water samples were also collected from small tributary streams that flow into the River Tay in Perthshire (Figure 5.5). The sampling locations in Perthshire are situated ~16-19 km west of the two owl nesting sites, and ~3-4 km west of the main channel of the River Tay (Figure 5.5). These samples were collected in early April 2017. Details of the water sampling locations are summarised in Table 5.3.

Table 5.3: *Summary of the sampling locations and dates of collection for the water samples from Somerset and Perthshire.*

Study site	Sampling location	National Grid Reference	Elevation (m above sea level)	Collection date
West Horrington, Somerset	River Sheppey (Keward Brook), Wells Market Cross fountain	ST 54987 45758	45	11/10/2016
	River Sheppey, Mill Lane, Coxley	ST 53039 43809	15	11/10/2016
	River Axe, Wookey	ST 51581 45656	21	12/10/2016
	River Brue, Westhay	ST 43717 42668	5	12/10/2016
Perth, Perthshire	Ordie Burn, on National Cycle Route 77	NO 07045 33689	52	Early April 2017
	Shochie Burn, near Moneydie	NO 06659 29773	58	
	Coldrochie Burn, south of Moneydie	NO 06382 28599	68	
	Stream near Cotterton	NO 06394 27667	71	

5.4. Statistical methods

Various statistical tests were applied to the data in order to assess the isotopic variability within the *Microtus agrestis* populations. Firstly, linear regression analyses were used to determine the significance of the correlation between the $\delta^{18}O$ and $\delta^{13}C$ values of the teeth, and the $\delta^{18}O$ and δD values of meteoric water, for each study site. Pearson's r^2 values and significance levels (*p*) were calculated for the linear regressions. Shapiro-Wilk tests were also undertaken to determine whether the data follow a Gaussian (normal) distribution. The significance of isotopic differences between the molars and incisors, and

between different individuals in each population, was assessed using one-way analyses of variance (ANOVA), followed by post-hoc Tukey's Q tests for pairwise comparisons. In cases where the assumption of a normal distribution was violated, a Kruskal-Wallis non-parametric ANOVA was performed (with Mann-Whitney pairwise comparisons). Levene's tests were also used to assess whether the variance in isotope values between each tooth type and individual are statistically different. The confidence level was set at 95% ($\alpha = 0.05$) for all tests.

Additionally, in order to assess whether isotopic offsets between molars and incisors from the same individual are systematic, the $\delta^{18}O$ value of the incisor was subtracted from the $\delta^{18}O$ values of the molars, after the methods of Jeffrey et al. (2015):

$$\Delta^{18}O_{M\text{-}I} = \delta^{18}O_{Molar} - \delta^{18}O_{Incisor} \quad (5.1).$$

Two-sample Student's T-tests (or Mann-Whitney tests if the data were non-normal) were also used to assess whether the average isotope values of the vole populations and meteoric water sources are significantly different between the sites.

The relationships between the mean $\delta^{18}O$ values of the rodent teeth and the mean $\delta^{18}O$ values of meteoric water and precipitation were determined using least-squares linear regression analyses. The strength of each relationship was quantified by calculating Pearson's r^2 and *p* values. Regression equations were generated for the linear relationships in the form:

$$y = ax + b \quad (5.2)$$

where *y* is the population mean $\delta^{18}O$ value of the rodent teeth, *x* is the population mean $\delta^{18}O$ value of meteoric water, *a* is the slope coefficient, and *b* is the y-intercept coefficient (the *y* value when $x = 0$). The 1σ standard deviation uncertainty (δy) on the least-squares fit of the regression line was calculated for various *x* ($\delta^{18}O_{mw}$) values using the following equations, as published in Pryor et al. (2014):

$$\delta y = \sqrt{\left(\delta b^2 + \delta a^2 \, (x - \bar{x})^2\right)} \quad (5.3)$$

$$\delta b = \frac{Sy/x}{\sqrt{n}} \quad (5.4)$$

$$\delta a = \frac{Sy/x}{\sqrt{\Sigma(x_i - \bar{x})^2}} \quad (5.5)$$

where δb is the uncertainty in the least-squares fit at $x = \bar{x}$, $\bar{x}$ is the mean *x* value for the regression (the mean $\delta^{18}O_{mw}$ across all study sites), δa is the uncertainty on the slope coefficient, n is the number of data points (or in this case study sites) used in the regression analysis, x_i is the sample *x* value (the mean $\delta^{18}O_{mw}$ for the study site), and Sy/x is:

$$Sy/x = \sqrt{\frac{\Sigma \, (y_i - ax_i - b)^2}{n-2}} \quad (5.6)$$

where y_i is the sample *y* value (mean $\delta^{18}O_{rt}$ value for the study site), a is the slope coefficient and b is the y-intercept coefficient.

In order to aid comparison with published regression equations that are based on the $\delta^{18}O$ values of phosphate in rodent bioapatite (relative to VSMOW), the $\delta^{18}O$ values of the teeth were also converted from the VPDB to the VSMOW scale using the following equation of Coplen et al. (1983):

$$\delta^{18}O \text{ (VSMOW)} = 1.03091 \times \delta^{18}O \text{ (VPDB)} + 30.91 \quad (5.7).$$

All statistical tests were performed using the free software program, PAST, version 3.11 (Hammer et al., 2001). The original isotope data for the modern teeth are provided in Appendix C.

5.5. Results

5.5.1. West Horrington, Somerset

5.5.1.1. $\delta^{18}O$ of teeth

All oxygen and carbon isotope results for the teeth from Somerset are plotted in Figure 5.7. There is no significant correlation between the $\delta^{18}O_{rt}$ and $\delta^{13}C_{rt}$ values ($r^2 = 0.04$, $p > 0.05$).

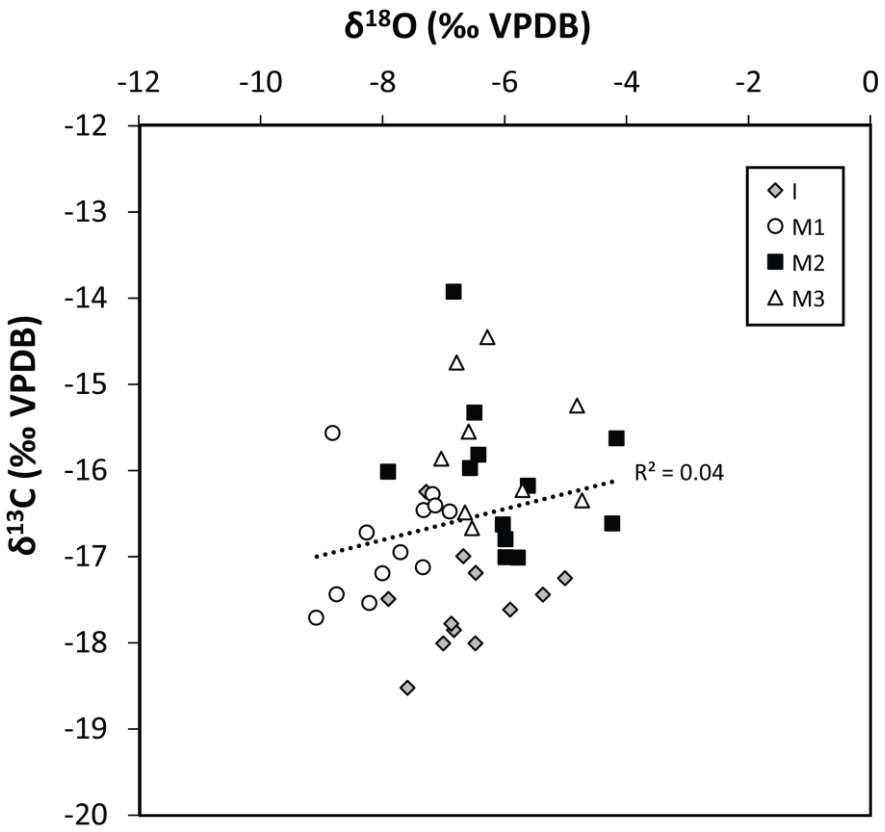

Figure 5.7: *The oxygen and carbon isotope results for the* M. agrestis *teeth from Somerset, plotted according to tooth type.*

Two of the samples produced anomalous $\delta^{18}O$ results. Firstly, the initial analysis of the lower incisor from Individual 7 generated an enriched value of -2.7‰. This sample was re-analysed twice, yielding consistent values of -5.7‰ and -5.0‰ that were averaged. Secondly, the lower M_3 from Individual 9

generated a depleted value of -11.8‰, which likely results from the small quantity of sample analysed (878 µg), and the resultant small peak (0.65 nA) of CO_2 that was produced. This value was considered unreliable and was therefore excluded from the dataset. Additionally, the lower M_3 from Individual 5 yielded insufficient sample powder for the accurate determination of isotopic ratios, and thus was not submitted for analysis.

The overall range in $\delta^{18}O$ values of the remaining lower right teeth is 4.9‰, between a minimum of -9.1‰ and a maximum of -4.2‰ (Figure 5.7). The mean $\delta^{18}O$ value is -6.60‰ (1σ standard deviation = 1.27‰), and the median is -6.58‰. The data for the lower M_1 and lower incisors are normally distributed (Shapiro-Wilk, $p > 0.05$), whereas the data for the lower M_2 and M_3 are positively skewed (Shapiro-Wilk, $p < 0.05$). Given that the data are variably distributed, the median values were chosen as the measures of central tendency in the following descriptions of the results.

As shown in Table 5.4, the $\delta^{18}O$ values of the M_2, M_3 and incisors are relatively similar. Mann-Whitney tests demonstrate that the population average $\delta^{18}O$ values for these teeth are statistically equivalent at 95% confidence. Also, intra-population ranges in the $\delta^{18}O$ values of each tooth type are fairly narrow at around 2‰ (Table 5.4), although these ranges exceed the typical uncertainty for a single measurement of tooth bioapatite (± 0.5‰). Nevertheless, the Levene's test shows that there are no statistically significant differences in the variance in $\delta^{18}O$ values between each tooth type ($p > 0.05$). Average $\delta^{18}O$ values of the teeth from each individual (Table 5.5) are also not statistically different (Kruskal-Wallis, $p > 0.05$).

When examined in further detail, the $\delta^{18}O$ value of the M_2 from each individual is ~0.2-1.0‰ more enriched than both the M_3 and incisor, whilst the $\delta^{18}O$ of the M_3 is ~0.2-1.0‰ more enriched relative to the incisor (Figure 5.8). The magnitudes of these inter-tooth differences are similar to or slightly greater than the typical measurement uncertainty for a single sample of bioapatite (± 0.5‰). In contrast, the average $\delta^{18}O$ of the M_1 and the average $\delta^{18}O$ values of the M_2, M_3 and incisors are statistically different (Mann-Whitney, $p < 0.05$). The $\delta^{18}O$ values of the first molars are ~1-3‰ more depleted compared to the $\delta^{18}O$ values of the other tooth types (Figure 5.8; Table 5.4). These large inter-tooth offsets are further illustrated in Table 5.5, which shows that intra-jaw $\delta^{18}O$

ranges are between 1.4 and 3.5‰ for all individuals in the population. The data for the first molars contribute significantly to these ranges; removing these data results in intra-jaw ranges of only 0.1-1.6‰ (Table 5.5).

Table 5.4: *Averages and intra-population ranges in the $\delta^{18}O$ values of the lower right teeth from Somerset.*

Tooth type	Mean $\delta^{18}O$ value (‰ VPDB)	1σ standard deviation (‰)	Median $\delta^{18}O$ value (‰ VPDB)	Range in $\delta^{18}O$ values (‰)	No. of teeth
I	-6.46	0.87	-6.68	2.59	9
M_1	-8.15	0.66	-8.22	1.91	9
M_2	-5.65	0.88	-5.98	2.40	9
M_3	-5.97	0.89	-6.53	2.06	7

One possible cause of these inter-tooth differences may be errors in the isotopic measurements of the first molars. The first molars from Somerset were analysed in a different batch of samples to the second molars, third molars and incisors. The isotopic differences may therefore relate to the specific conditions during the analyses of different sample batches. To investigate this issue, the first molars and incisors were re-analysed. The results of these re-analyses are presented in Table 5.6. For the first molars, the $\delta^{18}O$ results from Analysis 2 are generally ≤ 1‰ more depleted than the results from Analysis 1. For the incisors, the $\delta^{18}O$ values obtained during Analysis 2 are up to ± 0.7‰ different from the results of Analysis 1. These isotopic differences between replicate analyses are acceptable given the estimated 1σ standard deviation uncertainties on individual $\delta^{18}O$ measurements of rodent tooth bioapatite (± 0.5‰). The relative consistency in the results of the replicate analyses consequently suggests that the observed offsets between the $\delta^{18}O$ values of the different tooth types are genuine. Therefore, in general, $M_1 < I < M_3 < M_2$ for the $\delta^{18}O$ values of lower right teeth from Somerset.

Table 5.5: *Median $\delta^{18}O$ values for the lower right teeth from each* M. agrestis *individual from Somerset. Intra-jaw ranges in $\delta^{18}O$ values are also shown, using the values for all four teeth (I, M_1, M_2, and M_3), and for the second molar, third molar and incisor only.*

M. agrestis **individual number**	**Median $\delta^{18}O$ value of all available teeth in mandible (‰ VPDB)**	**Intra-jaw range in $\delta^{18}O$ values for all teeth (‰)**	**Intra-jaw range in $\delta^{18}O$ values for M_2, M_3 and incisor only (‰)**
1	-7.04	2.33	0.79
2	-6.71	2.64	1.21
3	-4.91	3.02	0.84
4	-6.13	2.51	0.77
5	-6.03	1.43	0.12
6	-7.12	3.11	1.61
7	-5.05	3.47	1.14
8	-6.77	2.77	1.02
9	-6.68	1.44	0.11

Inter-tooth $\delta^{18}O$ differences of similar magnitudes are observed between the upper and lower teeth from Individual 3 (see Table C.3 of Appendix C). In general, $\delta^{18}O$ offsets between upper and lower teeth of the same type (e.g. upper and lower M_1), and left and right teeth of the same type, are ≤ 1.5‰. Lower teeth are consistently enriched compared to upper teeth of the same type, and right teeth are generally enriched relative to left teeth. Additionally, the lower right M_2, M_3 and incisor are substantially (~2-3‰) more enriched than all other teeth from the individual. As a result, the average $\delta^{18}O$ value of the lower right teeth is higher than that of the lower left, upper right and upper left teeth, although these differences are not statistically significant (Mann-Whitney, $p > 0.05$). Again, these inter-tooth $\delta^{18}O$ differences are generally similar to or greater than the measurement precision for a single

sample of tooth bioapatite (± 0.5‰). The overall range in tooth $\delta^{18}O$ values for Individual 3 is 3.7‰.

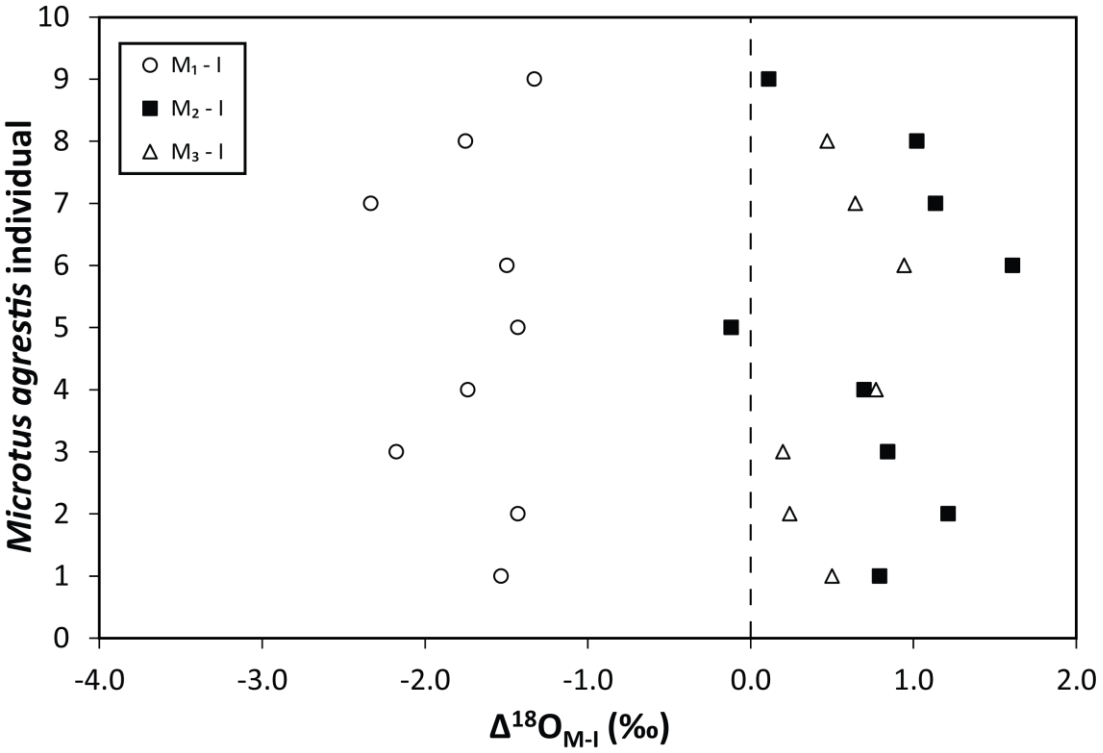

Figure 5.8: *Offsets between the oxygen isotope values of the molars and incisor for each* M. agrestis *individual from Somerset. The dashed line indicates a zero offset between the $\delta^{18}O$ value of the molar and the $\delta^{18}O$ value of the incisor.*

5.5.1.2. $\delta^{13}C$ of teeth

The $\delta^{13}C$ values of the teeth from Somerset fall within a range of 4.6‰, between a minimum of -18.5‰ and a maximum of -13.9‰ (Figure 5.7). The mean $\delta^{13}C$ value of the lower right teeth is -16.73‰ (1σ = 0.89‰), and the median value is -16.76‰. The carbon isotope data for each tooth type and the population as a whole are normally distributed (Shapiro-Wilk, $p > 0.05$). Differences in the $\delta^{13}C$ results between Analyses 1 and 2 are generally less than ± 0.3‰.

Table 5.6: *Oxygen isotope results for Analysis 1 and Analysis 2 on the first molars and incisors from Somerset. Rows marked with a dash indicate samples for which insufficient powder remained for re-analysis.*

M. agrestis **Individual number**	**$\delta^{18}O$ of first molar (‰)**			**$\delta^{18}O$ of incisor (‰)**		
	Analysis 1 (A1)	**Analysis 2 (A2)**	**$\Delta^{18}O_{A1-A2}$**	**Analysis 1**	**Analysis 2**	**$\Delta^{18}O_{A1-A2}$**
1	-8.4	-9.2	0.8	-7.1	-7.5	0.5
2	-7.9	-8.6	0.8	-6.7	-6.9	0.2
3	-6.6	-7.7	1.1	-5.2	-4.9	-0.3
4	-7.7	-8.8	1.1	-6.3	-6.7	0.5
5	-7.3	-	-	-5.9	-	-
6	-8.6	-9.6	1.0	-7.4	-7.8	0.4
7	-7.7	-7.7	0.0	-5.7	-5.0	-0.7
8	-8.4	-9.1	0.7	-7.0	-7.0	0.0
9	-8.0	-	-	-6.8	-6.6	-0.2

In contrast to the oxygen isotope results, no statistically significant differences are observed between the average $\delta^{13}C$ values of the M_1, M_2 and incisors (Tukey's Q, $p > 0.05$). The average $\delta^{13}C$ of the M_3, however, is significantly more enriched than the average $\delta^{13}C$ values of the M_1 and incisors (Table 5.7) (Tukey's Q, $p < 0.05$). The average $\delta^{13}C$ of the M_2 is also significantly more enriched than that of the incisors.

The calculated inter-tooth $\delta^{13}C$ offsets for each individual confirm these observations. The $\delta^{13}C$ values of the M_1 are generally ~0.5-1.1‰ more enriched than the incisors, the M_2 are ~1.0-1.5‰ more enriched than the incisors, and the M_3 are ~1.3-2.3‰ more enriched than the incisors (Figure 5.9). These inter-tooth $\delta^{13}C$ differences exceed the estimated uncertainty on a single measurement of tooth bioapatite (± 0.18‰). Thus, overall, $I < M_1 < M_2 < M_3$ for the $\delta^{13}C$ values of the teeth from Somerset (Figure 5.9).

Table 5.7: *Average $\delta^{13}C$ values and intra-population ranges in the $\delta^{13}C$ values of the lower right teeth from Somerset.*

Tooth type	Mean $\delta^{13}C$ value (‰ VPDB)	1σ standard deviation (‰)	Median $\delta^{13}C$ value (‰ VPDB)	Range in $\delta^{13}C$ values (‰)	No. of teeth
I	-17.55	0.67	-17.61	2.28	9
M_1	-16.94	0.68	-17.12	2.14	9
M_2	-16.35	0.61	-16.61	1.68	9
M_3	-15.89	0.72	-16.22	1.92	7

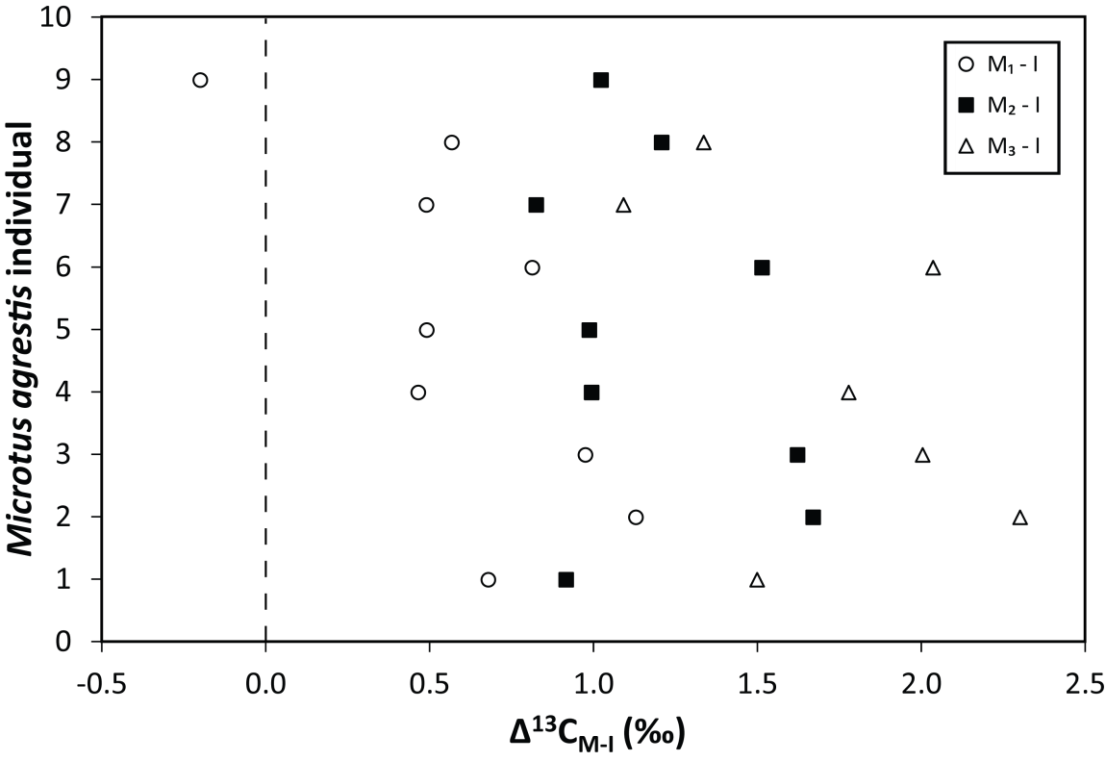

Figure 5.9*: Offsets between the carbon isotope values of the molars and incisors for each* M. agrestis *individual from Somerset.*

The $\delta^{13}C$ offsets between upper and lower teeth of the same type and left and right teeth of the same type from Individual 3 are of similar magnitude (Table C.4 in Appendix C). Most offsets are less than 1‰, although the $\delta^{13}C$ values of the upper right M^2 and M^3 are ~2-4‰ more enriched than all other teeth. The $\delta^{13}C$ value of the lower right M_3 is likewise 2-3‰ heavier than the incisors. On average, right teeth are enriched relative to left teeth, and upper teeth are more enriched than lower teeth, although these differences are not statistically significant (Student's T-tests, $p > 0.05$). The overall range in $\delta^{13}C_{rt}$ values for Individual 3 is 3.9‰.

Tooth $\delta^{13}C$ values also differ between individuals in the population. For example, the mean $\delta^{13}C$ values of the teeth from Individuals 1 and 6 are significantly different (Tukey's Q, $p < 0.05$). Conversely, the Levene's tests show that there are no statistically significant differences in the variance in $\delta^{13}C$ values between each tooth type, and between each individual ($p > 0.05$). Intra-population (Table 5.7) and intra-jaw (Table 5.8) ranges in $\delta^{13}C_{rt}$ values are fairly narrow at between ~1 and 2‰ (Table 5.8). Nevertheless, these ranges are greater than the estimated 1σ uncertainty on a single $\delta^{13}C$ measurement of tooth bioapatite (± 0.18‰), and thus intra-population $\delta^{13}C_{rt}$ variability is significant.

5.5.1.3. $\delta^{18}O$ and δD of water

The mean $\delta^{18}O$ value of the four water samples from Somerset is -6.0‰ (1σ = 0.41‰), and the mean δD is -37.7‰ (1σ = 1.75‰). This measured mean $\delta^{18}O$ value is consistent with the estimated $\delta^{18}O$ values for meteoric water sources in Somerset (Table 5.1). The ranges in $\delta^{18}O$ and δD values are 0.9‰ and 3.6‰, respectively. There is a strong positive correlation between $\delta^{18}O$ and δD ($r^2 = 0.99$, $p < 0.01$), and the data lie close to the Global Meteoric Water Line of Craig (1961) (Figure 5.10). However, the slope of the relationship between $\delta^{18}O$ and δD for the Somerset samples (4.2) is shallower than the GMWL (8.0). In fact, the slope is more closely comparable with the line for the River Thames at Wallingford (5.3), determined by Darling & Bowes (2016).

Table 5.8: *Medians and intra-jaw ranges in the $\delta^{13}C$ values of the lower right teeth from each individual from Somerset.*

M. agrestis **individual number**	**Median $\delta^{13}C$ value of all available teeth in mandible (‰ VPDB)**	**Intra-jaw range in $\delta^{13}C$ values (‰)**
1	-15.45	1.50
2	-16.45	2.30
3	-15.95	2.01
4	-17.27	1.78
5	-17.12	0.99
6	-17.36	2.04
7	-16.78	1.09
8	-17.12	1.34
9	-16.99	1.22

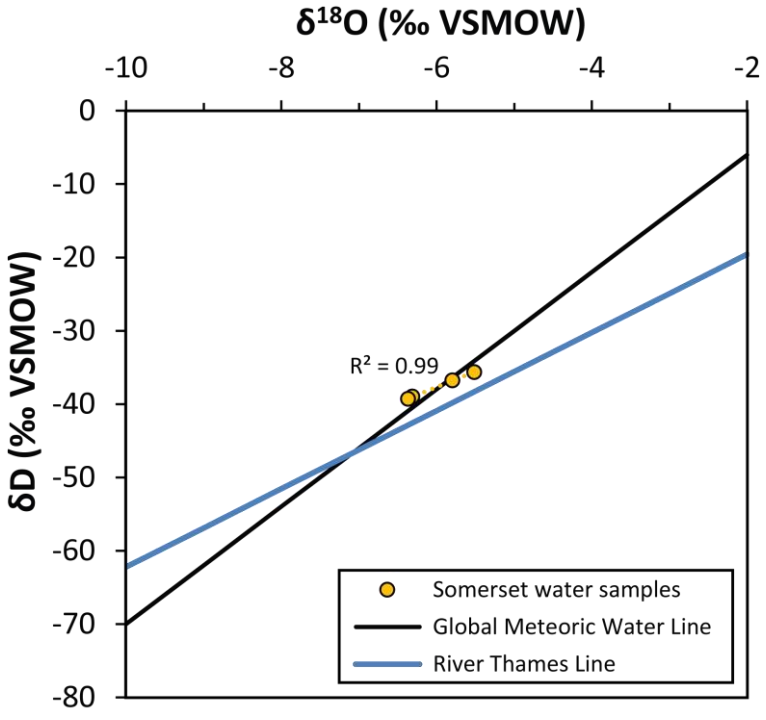

Figure 5.10: *Plot of the oxygen and hydrogen isotope results for the meteoric water samples from Somerset. The Global Meteoric Water Line of Craig (1961) and the River Thames Line of Darling & Bowes (2016) are shown for comparison.*

5.5.2. Cobham, Surrey

5.5.2.1. $\delta^{18}O$ of teeth

The oxygen and carbon isotope data for the teeth from Surrey are plotted in Figure 5.11. The $\delta^{18}O$ and $\delta^{13}C$ values are not significantly correlated (r^2 = 0.08, p > 0.05). There is one notable outlier, with a $\delta^{18}O$ value of -2.2‰ (Individual 4, M_1). This sample was re-analysed, yielding a value of -10.3‰, which is the lowest value of all lower right teeth in the population. This secondary value is therefore a potential outlier. Nevertheless, the results of a Grubbs' test on the data for the lower M_1 (n = 8) indicates that the value for Individual 4 (-10.3‰) is not a significant outlier (p > 0.05). This value was consequently retained in the dataset.

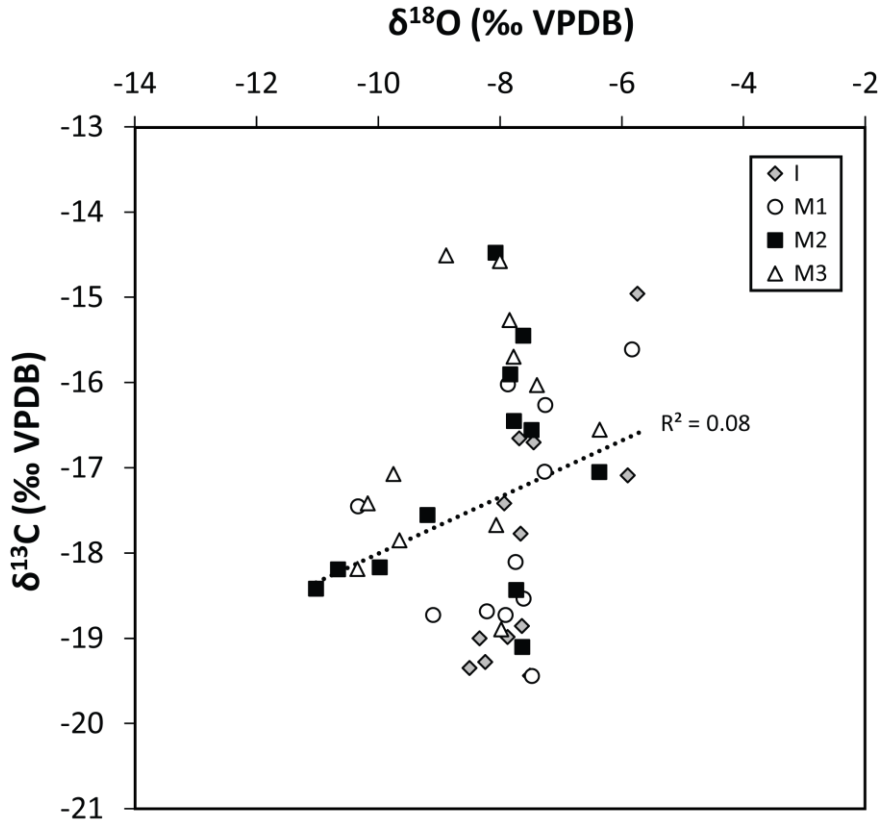

Figure 5.11: *The oxygen and carbon isotope results for the* M. agrestis *teeth from Surrey, plotted according to tooth type.*

The range in $\delta^{18}O$ values of the lower right teeth is 4.6‰, between a minimum of -10.3‰ and a maximum of -5.7‰. The mean $\delta^{18}O$ value of all lower right teeth is -7.75‰ (1σ = 0.98‰), and the median value is -7.77‰. The data for all lower right teeth are negatively skewed, the data for the incisors are positively skewed (Shapiro-Wilk, $p < 0.05$), while the data for the molars are normally distributed (Shapiro-Wilk, $p > 0.05$).

As shown in Table 5.9, the median $\delta^{18}O$ values of the four tooth types are relatively similar, falling between -8.0 and -7.7‰. Differences in these values are not statistically significant (Kruskal-Wallis, $p > 0.05$). The median $\delta^{18}O$ values of different individuals in the population are likewise relatively comparable, at between -8 and -7‰ (Table 5.10). However, the $\delta^{18}O$ values of the teeth from Individual 5 are relatively enriched compared to other individuals in the population, whereas the $\delta^{18}O$ values of the teeth from Individual 7 are relatively depleted (Table 5.10). Nevertheless, the Kruskal-Wallis results demonstrate that the average $\delta^{18}O_{rt}$ values for different individuals are not significantly different at 95% confidence.

Although the average $\delta^{18}O_{rt}$ values are similar, intra-population ranges in values are fairly broad, varying from ~3.0‰ for the M_2, M_3 and incisor, to 4.5‰ for the M_1 (Table 5.9). Nevertheless, the variances in $\delta^{18}O$ values are not statistically different between each tooth type (Levene's test, $p > 0.05$). The larger range in values for the M_1 is due to the low $\delta^{18}O$ value for Individual 4; exclusion of this value results in an intra-population range of 3.3‰.

Table 5.9: *Average $\delta^{18}O$ values and intra-population ranges in the $\delta^{18}O$ values of the lower right teeth from Surrey.*

Tooth type	Mean $\delta^{18}O$ value (‰ VPDB)	1σ standard deviation (‰)	Median $\delta^{18}O$ value (‰ VPDB)	Range in $\delta^{18}O$ values (‰)	No. of teeth
I	-7.37	0.93	-7.67	2.76	9
M_1	-7.88	1.34	-7.68	4.50	8
M_2	-7.75	0.72	-7.74	2.82	9
M_3	-8.01	0.93	-7.98	3.39	9

Table 5.10: *Medians and intra-jaw ranges in the $\delta^{18}O$ values of the lower right teeth from each individual from Surrey.*

M. agrestis **individual number**	**Median $\delta^{18}O$ value of all available teeth in mandible (‰ VPDB)**	**Intra-jaw range in $\delta^{18}O$ values (‰)**
1	-7.81	1.03
2	-7.84	0.42
3	-7.65	0.52
4	-7.89	2.67
5	-6.37	0.47
6	-6.95	3.14
7	-9.15	2.24
8	-7.44	0.66
9	-7.90	0.33

On the other hand, for most individuals, the intra-jaw ranges in $\delta^{18}O_{rt}$ values are ≤ 1‰ (Table 5.10). Conversely, for Individuals 4, 6 and 7, the intra-jaw ranges are much broader at ~2-3‰ (Figure 5.12; Table 5.10). As a result, the variance in $\delta^{18}O_{rt}$ values is significantly different between individuals (Levene's test, $p < 0.05$). The depleted value of the M_1 from Individual 4 is the cause of the large intra-jaw $\delta^{18}O$ range in this individual. For Individual 6, the $\delta^{18}O$ values of the M_1 and incisor are enriched (~ -5.8‰) compared to the M_2 and M_3 (~ -8.5‰), whereas for Individual 7, the $\delta^{18}O$ values of the molars are ~1.5-2‰ more depleted than the $\delta^{18}O$ of the incisor. Re-analysis of the M_1 from Individual 7 and the lower right incisors from all individuals produced values consistent (within 1‰) with the first analysis. These intra-jaw isotopic differences are therefore likely to be accurate.

Excluding Individuals 4, 6 and 7, $\delta^{18}O$ offsets between the molars and incisor from each mandible are within ± 1‰ (Figure 5.12). The $\delta^{18}O$ values of the molars in each mandible are also very similar, falling within ± 0.5‰ of each other. These inter-tooth differences are comparable to the estimated measurement uncertainty for a single sample of bioapatite (± 0.5‰). Also,

there is no consistency in the magnitude or direction of the $\delta^{18}O$ offsets between the molars and incisor from each individual (Figure 5.12).

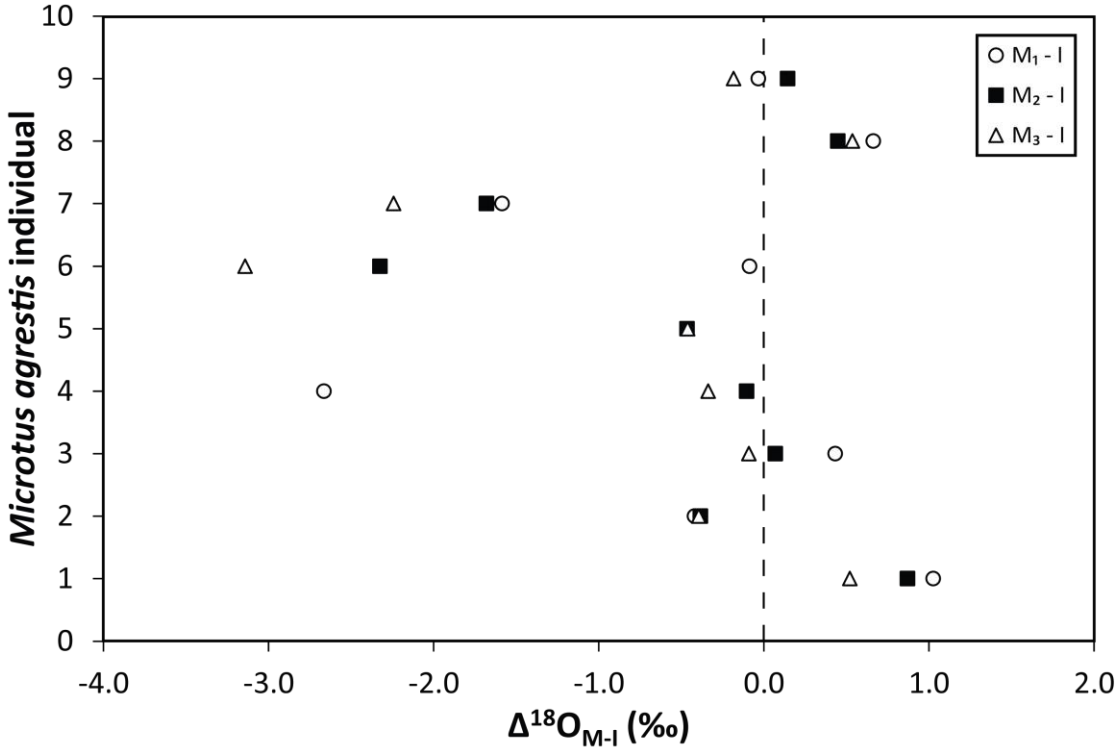

Figure 5.12: *Offsets between the oxygen isotope values of the molars and incisor for each* M. agrestis *individual from Surrey.*

Nevertheless, as indicated by the results from Individuals 4, 6 and 7, teeth from the same individual may have significantly different $\delta^{18}O$ values that exceed the estimated uncertainty for a single measurement of bioapatite. This is likewise seen in the data for Individual 9. The upper and lower left M_2 and M_3 are 2-3‰ more depleted compared to all other teeth from this individual (see Table C.5 of Appendix C). Consequently, right teeth are generally enriched compared to left teeth of the same type, and lower teeth are generally enriched compared to upper teeth. Nevertheless, only the differences between the lower right and lower left teeth are statistically significant (Mann-Whitney, $p < 0.05$). The overall range in tooth $\delta^{18}O$ values for Individual 9 is 3.0‰.

The $\delta^{18}O$ values of the lower left M_2 and M_3 and upper M^2 and M^3 from Individual 9 (-11.0 to -9.7‰) also fall outside the range of most of the data from the Surrey population. Re-analyses of the upper first molars and incisors produced values that are 2-3‰ more depleted than the values obtained in Analysis 1 (see Appendix B). Conversely, the re-analysis of the lower incisor produced a value (-8.5‰) that is only 1.3‰ more depleted than in Analysis 1, and is consistent with the results from other individuals in the population. This may suggest that the teeth from Individual 9 mineralized during a season (probably early spring) when the $\delta^{18}O$ of local water varied greatly between depleted values, reflecting colder temperatures and possibly snowmelt, and enriched values, reflecting warmer temperatures and evaporation. This variation may have resulted in large differences between the measured $\delta^{18}O$ values of different aliquots of the same sample, as well as a large variability in the average $\delta^{18}O$ values of teeth with different mineralization periods. This variability is clearly observed in the results for Individual 9.

5.5.2.2. $\delta^{13}C$ of teeth

The carbon isotope data range between -19.4 and -14.5‰ (range = 5.0‰) (Figure 5.11), with a mean $\delta^{13}C$ value of -17.00‰ (1σ = 1.49‰) and a median of -17.04‰. The data are normally distributed (Shapiro-Wilk, $p > 0.05$). The $\delta^{18}O$ value of the M_1 from Individual 4 was previously identified as a potential outlier. However, the $\delta^{13}C$ value of this tooth is consistent with the $\delta^{13}C$ values of the incisor and M_2 from this individual. Isotopic differences between the first and second analyses are generally less than ± 0.4‰.

As shown in Table 5.11, the average $\delta^{13}C$ values of the four tooth types are fairly similar, varying between -17.5 and -16.0‰. Differences in these mean values are not statistically significant (ANOVA: F statistic = 1.59, F critical = 2.91, $p > 0.05$). Also, intra-jaw ranges in $\delta^{13}C$ values are relatively narrow, and generally vary between 0.5 and 1.5‰, except for Individuals 4 and 7 where the ranges reach 3.2 and 2.4‰, respectively. Consequently, inter-individual differences in the variance in $\delta^{13}C_{rt}$ values are statistically significant (Levene's test, $p < 0.05$).

In contrast, intra-population ranges in $\delta^{13}C$ values for each tooth type are comparatively large, reaching a maximum of 4.5‰ (Table 5.11). This variability is further demonstrated in Table 5.12. Differences in the mean $\delta^{13}C$ values between individuals are statistically significant (ANOVA: F statistic = 13.24, F critical = 2.32, $p < 0.05$). Tukey's Q pairwise comparisons indicate that the mean $\delta^{13}C_{rt}$ value of Individual 1 is significantly different to all other analysed specimens, excepting Individuals 7 and 9. The mean $\delta^{13}C_{rt}$ values of Individuals 7 and 9 are also significantly different to the mean values of Individuals 2, 3 and 6.

Table 5.11: *Average $\delta^{13}C$ values and intra-population ranges in the $\delta^{13}C$ values of the lower right teeth from Surrey.*

Tooth type	Mean $\delta^{13}C$ value (‰ VPDB)	1σ standard deviation (‰)	Median $\delta^{13}C$ value (‰ VPDB)	Range in $\delta^{13}C$ values (‰)	No. of teeth
I	-17.60	1.47	-17.42	4.48	9
M_1	-17.41	1.43	-17.25	3.83	8
M_2	-16.78	1.45	-16.56	4.63	9
M_3	-16.25	1.46	-16.03	4.39	9

While the $\delta^{18}O$ results indicate no consistent or significant isotopic offsets between the molars and incisors, clearer patterns of intra-jaw variation are observed in the carbon isotope data. In nearly all individuals (except for Individuals 1 and 6), the $\delta^{13}C$ value of the incisor is more depleted than the $\delta^{13}C$ values of the molars (Figure 5.13). The $\delta^{13}C$ offset between the M_1 and incisor is generally +0.2-0.7‰, the offset between the M_2 and incisor varies between 0 and +1.9‰, and the offset between the M_3 and incisor varies between +0.5 and +2.4‰. These offsets generally exceed the typical precision on an individual $\delta^{13}C$ measurement of rodent bioapatite (± 0.18‰). Therefore, in general, $I < M_1 < M_2 < M_3$ for the $\delta^{13}C$ values of the teeth from Surrey.

Table 5.12: *Medians and intra-jaw ranges in the $\delta^{13}C$ values of the teeth from each individual from Surrey.*

M. agrestis **individual number**	**Median $\delta^{13}C$ value of all available teeth in mandible (‰ VPDB)**	**Intra-jaw range in $\delta^{13}C$ values (‰)**
1	-19.23	0.55
2	-15.96	1.43
3	-15.98	1.20
4	-16.95	3.20
5	-17.05	0.54
6	-14.73	1.14
7	-18.14	2.36
8	-16.80	1.39
9	-18.58	1.31

The intra-individual $\delta^{13}C_{rt}$ differences for Individual 9 are likewise greater than the typical measurement uncertainty for tooth bioapatite (± 0.18‰), and generally range between 0.3 and 1.3‰ (Table C.6 of Appendix C). Average $\delta^{13}C$ values of the left and right teeth and upper and lower teeth are comparable, and offsets between teeth of the same type are not consistent in magnitude or direction. Additionally, in contrast to the $\delta^{18}O$ results, the re-analyses of the upper molars generated $\delta^{13}C$ values that are consistent (within ± 0.4‰) with Analysis 1 (Appendix B). The overall range in $\delta^{13}C_{rt}$ values for Individual 9 is 1.9‰.

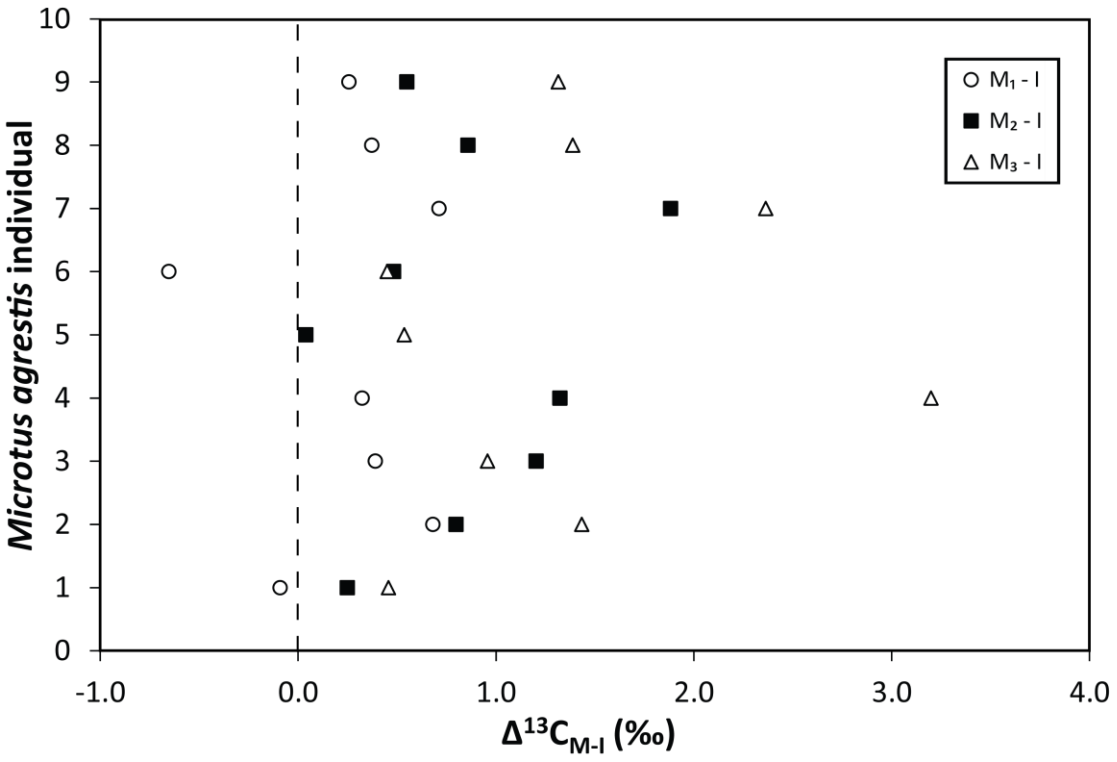

Figure 5.13: *Offsets between the carbon isotope values of the molars and incisor for each* M. agrestis *individual from Surrey.*

5.5.3. Beeford, East Yorkshire

5.5.3.1. $\delta^{18}O$ of teeth

The oxygen and carbon isotope data for the teeth from East Yorkshire are presented in Figure 5.14. The $\delta^{18}O$ and $\delta^{13}C$ values of the teeth are significantly correlated ($p < 0.05$). However, the data are fairly scattered, and consequently the r^2 value is small (0.18).

The M_1 from Individual 2 produced an anomalous $\delta^{18}O$ result of -2.9‰, and was therefore re-analysed. Analysis 2 yielded a value of -10.0‰, which falls at the lower end of the range in values within the population. Nevertheless, the results of a Grubbs' test demonstrate that this second value is not an outlier ($p > 0.05$), and thus this value was retained in the dataset.

The overall mean $\delta^{18}O$ value of the lower right teeth is -8.30‰ (1σ = 0.76‰), the median value is -8.23‰, and the range in values is 3.03‰. The data are normally distributed for all tooth types (Shapiro-Wilk, $p > 0.05$).

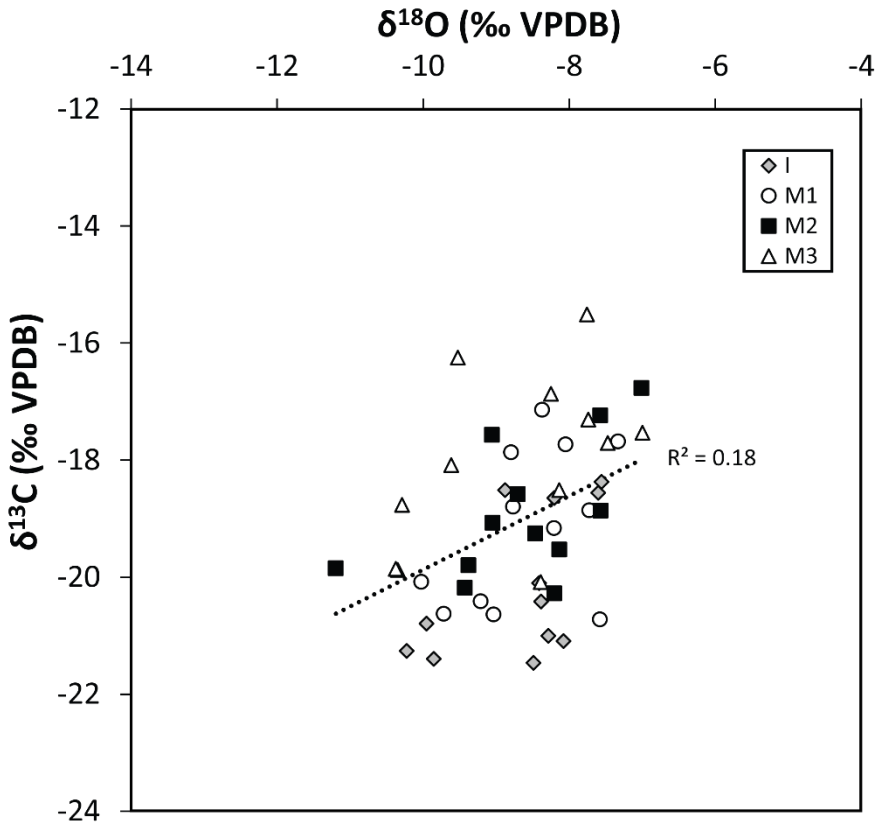

***Figure 5.14**: The oxygen and carbon isotope results for the* M. agrestis *teeth from East Yorkshire, plotted according to tooth type.*

The mean $\delta^{18}O$ values of the four tooth types are very similar (Table 5.13), and are not statistically different (ANOVA: F statistic = 0.18, F critical = 2.90, $p > 0.05$). Intra-population ranges in $\delta^{18}O_{rt}$ values are likewise comparable, at between 2.1 and 2.7‰ (Table 5.13). A Levene's test confirms that the variances in $\delta^{18}O$ values are not statistically different between each tooth type ($p > 0.05$). Conversely, the average $\delta^{18}O$ values of different individuals are significantly different (ANOVA: F statistic = 4.56, F critical = 2.31, $p < 0.05$) (Table 5.14). Specifically, the mean $\delta^{18}O_{rt}$ values of Individuals 5 and 7 are significantly depleted compared to the values of Individuals 3 and 4 (Tukey's Q, $p < 0.05$).

Table 5.13: *Averages and intra-population ranges in the $\delta^{18}O$ values of the lower right teeth from East Yorkshire.*

Tooth type	Mean $\delta^{18}O$ value (‰ VPDB)	1σ standard deviation (‰)	Median $\delta^{18}O$ value (‰ VPDB)	Range in $\delta^{18}O$ values (‰)	No. of teeth
I	-8.42	0.71	-8.39	2.40	9
M_1	-8.37	0.86	-8.21	2.70	9
M_2	-8.20	0.71	-8.21	2.05	9
M_3	-8.21	0.88	-8.14	2.62	9

While the intra-population ranges in $\delta^{18}O_{rt}$ values are relatively consistent, intra-jaw ranges are more variable, at between 0.2 and 2.2‰ (Table 5.14). Nevertheless, inter-individual differences in the variance in $\delta^{18}O$ values are not statistically significant (Levene's test, $p > 0.05$). The fairly large intra-jaw range for Individual 1 is due to the enriched value of the M_3 (-7.0‰). The sample from this tooth was relatively small, and thus the measured isotopic ratios may not be entirely accurate. The relatively large intra-jaw range for Individual 2 results from the low $\delta^{18}O$ value of the M_1. However, in the context of the population as a whole, these $\delta^{18}O$ values are not outliers.

Intra-jaw variation is also seen in Figure 5.15. On the whole, inter-tooth offsets in $\delta^{18}O$ values are < 1.5‰. Differences between the M_1 and incisor are ± 1.6‰, offsets between the M_2 and incisor range from -0.3 to +0.9‰, and offsets between the M_3 and incisor range from -0.7 to +1.5‰. The magnitudes of these offsets are similar to or greater than the typical 1σ uncertainty on a single measurement of tooth bioapatite (± 0.5‰). Nevertheless, there are generally no consistent patterns in the direction of inter-tooth offsets. The exception to this is that in 7 of the 9 individuals, the $\delta^{18}O$ of the M_2 is slightly enriched relative to the M_3 and incisor.

Table 5.14: *Averages and intra-jaw ranges in the $\delta^{18}O$ values of the lower right teeth from each individual from East Yorkshire.*

M. agrestis **individual number**	**Median $\delta^{18}O$ value of all available teeth in mandible (‰ VPDB)**	**Intra-jaw range in $\delta^{18}O$ values (‰)**
1	-8.48	2.22
2	-8.26	1.89
3	-7.67	0.17
4	-7.45	0.74
5	-9.33	1.58
6	-8.13	0.67
7	-8.97	0.73
8	-8.25	0.81
9	-8.31	1.24

In most cases, isotopic offsets between the upper and lower teeth from Individual 1 are also < 1.5‰ (Table C.7 in Appendix C). Nonetheless, the $\delta^{18}O$ value of the left M^2 is ~2‰ depleted compared to all other teeth from the individual, while the $\delta^{18}O$ values of the right M_2 and M_3 are ~2-4‰ enriched relative to all other teeth. As aforementioned, the $\delta^{18}O$ value of the right M_3 may be inaccurate due to the small sample size. On average, right teeth are enriched compared to left teeth, and lower teeth are more enriched than upper teeth of the same type. However, these differences are not statistically significant (Student's T-tests, $p > 0.05$). The overall range in $\delta^{18}O_{rt}$ values for Individual 1 is 4.2‰.

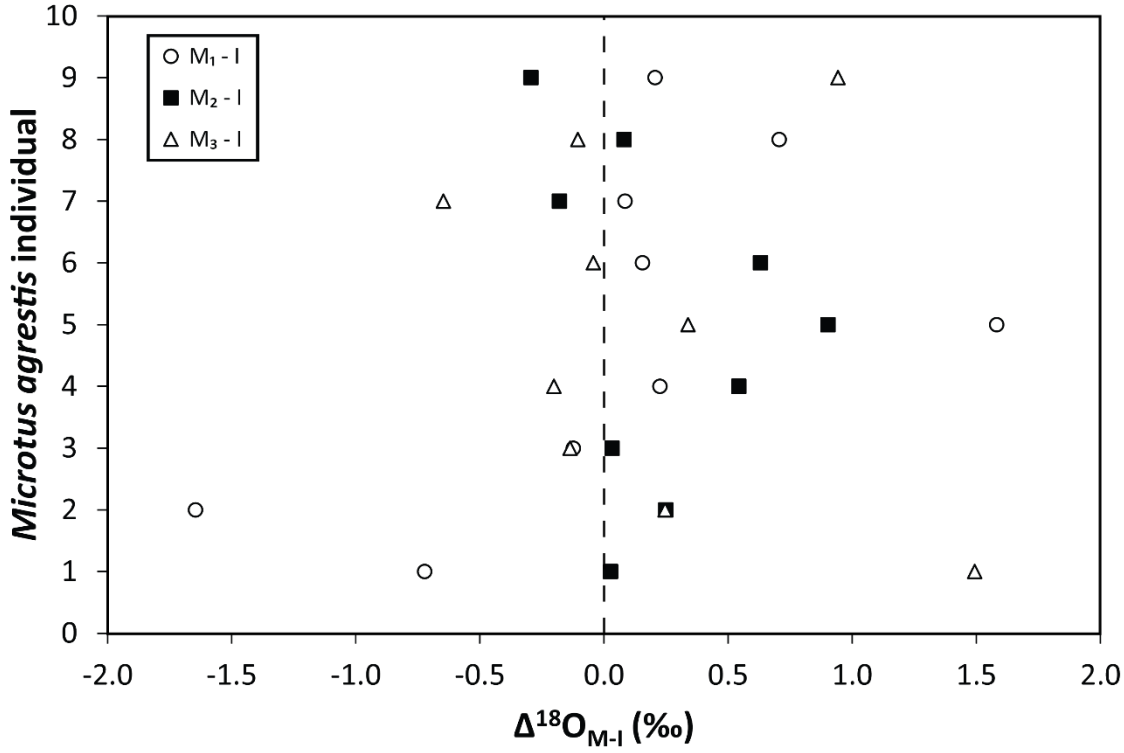

***Figure 5.15**: Offsets between the oxygen isotope values of the molars and incisor for each* M. agrestis *individual from East Yorkshire.*

5.5.3.2. δ13C of teeth

The $\delta^{13}C$ values of the lower right teeth span a relatively broad range of 6.0‰ (Figure 5.14), with a mean value of -18.68‰ (1σ = 1.45), and a median of -18.57‰. The data for each tooth type and the dataset as a whole are normally distributed (Shapiro-Wilk, $p > 0.05$).

The average $\delta^{13}C$ values of the molars and incisors vary between -19.8‰ and -17.5‰ (Table 5.15). Tukey's Q pairwise comparisons indicate that the mean $\delta^{13}C$ value of the incisors is significantly depleted compared to the mean $\delta^{13}C$ of the M_3 ($p < 0.05$). Inter-individual $\delta^{13}C$ differences are likewise statistically significant; the mean $\delta^{13}C_{rt}$ for Individual 8 is significantly depleted relative to Individuals 4, 6 and 7 (Tukey's Q, $p < 0.05$).

Table 5.15: *Averages and intra-population ranges in the $\delta^{13}C$ values of the lower right teeth from East Yorkshire.*

Tooth type	Mean $\delta^{13}C$ value (‰ VPDB)	1σ standard deviation (‰)	Median $\delta^{13}C$ value (‰ VPDB)	Range in $\delta^{13}C$ values (‰)	No. of teeth
I	-19.76	1.24	-20.10	3.09	9
M_1	-18.85	1.33	-18.85	3.59	9
M_2	-18.57	1.16	-18.86	3.51	9
M_3	-17.54	1.32	-17.53	4.57	9

These inter-individual isotopic differences are reflected in the broad intra-population ranges in the $\delta^{13}C$ values of the four tooth types (Table 5.15). The intra-jaw ranges in $\delta^{13}C$ values are also fairly large (Table 5.16), and are variable between different individuals in the population, although the differences in $\delta^{13}C_{rt}$ variance are not statistically significant (Levene's test, $p > 0.05$). The large intra-jaw variation mainly results from the enriched $\delta^{13}C$ values of the third molars. The $\delta^{13}C$ value of the M_3 is 1-4‰ higher than the incisor in all individuals (Figure 5.16). All third molars from East Yorkshire yielded small quantities of powder, and as a consequence, peak height ratios for most of these samples were ≤ 1.0 nA. Therefore, the measured isotope ratios for the M_3 may be inaccurate.

In addition, in all but one individual, the $\delta^{13}C$ of the M_1 is enriched relative to the incisor, and the magnitude of this enrichment is generally 0.3-1.1‰ (Figure 5.16). Similarly, the $\delta^{13}C$ values of the M_2 are ~0.7-1.7‰ enriched relative to the incisors. These differences are greater than the estimated 1σ uncertainty for a single $\delta^{13}C$ measurement of tooth bioapatite (± 0.18‰). The M_1 and M_2 are both consistently isotopically depleted relative to the M_3 (Figure 5.16). Therefore, overall, $I < M_1 < M_2 < M_3$ for the $\delta^{13}C$ values of the teeth from East Yorkshire.

Table 5.16: *Medians and intra-jaw ranges in the $\delta^{13}C$ values of the lower right teeth from each individual from East Yorkshire.*

M. agrestis **individual number**	**Median $\delta^{13}C$ value of all available teeth in mandible (‰ VPDB)**	**Intra-jaw range in $\delta^{13}C$ values (‰)**
1	-19.83	3.93
2	-19.80	1.91
3	-18.70	1.55
4	-17.22	2.86
5	-18.58	3.66
6	-17.48	1.78
7	-17.71	2.27
8	-20.50	0.92
9	-18.87	2.39

Intra-individual offsets in the $\delta^{13}C$ values of the teeth from Individual 1 are also generally within ± 1.6‰ (Table C.8 in Appendix C). Nevertheless, larger isotopic offsets of ~2-4‰ occur between the right M_3 and all other teeth, and the right M_1, right M_2, left M^3 and the incisors. Despite this, only the difference between the average $\delta^{13}C$ values of the M_3 and incisors is statistically significant (Student's T-test, $p < 0.05$). Furthermore, there is no consistency in the magnitude or direction of isotopic offsets between right and left teeth or lower and upper teeth of the same type. The overall range in $\delta^{13}C_{rt}$ values for Individual 1 is 3.9‰.

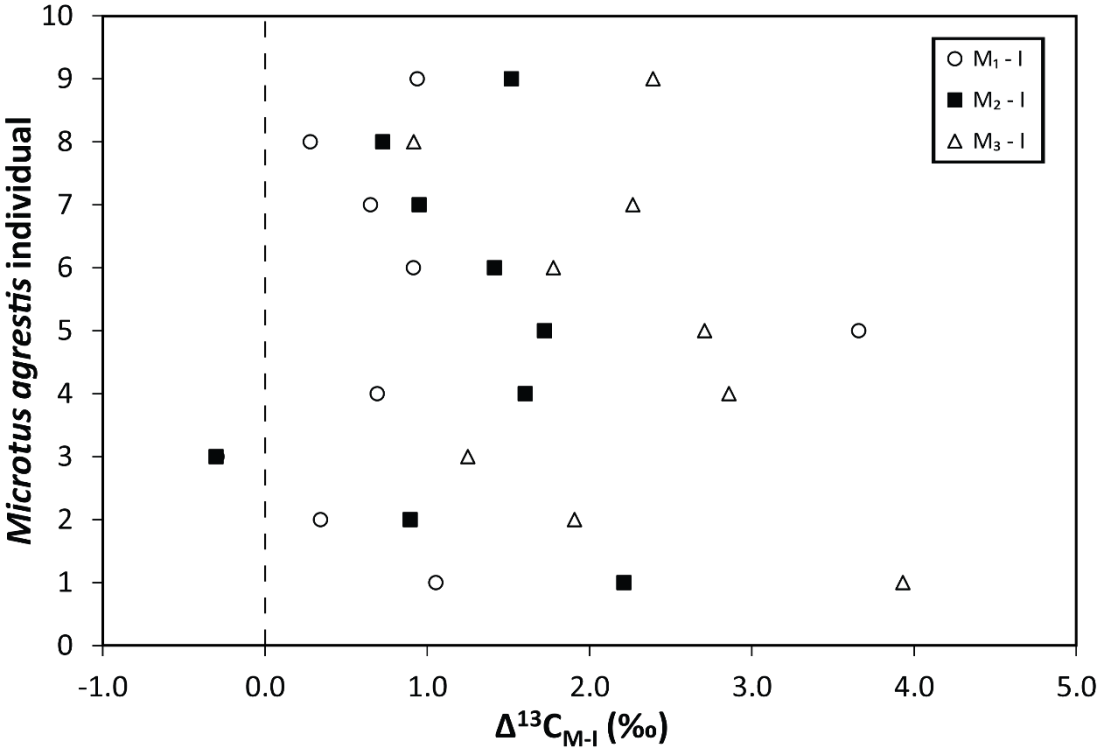

Figure 5.16: *Offsets between the carbon isotope values of the molars and incisor for each* M. agrestis *individual from East Yorkshire.*

5.5.4. Perth, Perthshire

5.5.4.1. δ18O of teeth

All oxygen and carbon isotope results for the teeth from Perthshire are displayed in Figure 5.17. There is a slight negative correlation between the $\delta^{18}O$ and $\delta^{13}C$ values of the teeth ($r^2 = 0.07$), although this correlation is not statistically significant ($p > 0.05$).

The overall mean $\delta^{18}O$ value of the lower right teeth is -7.21‰ (1σ = 0.65), and the median is -7.25‰. The data as a whole are normally distributed (Shapiro-Wilk, $p > 0.05$), the data for the M_1 are significantly positively skewed, and the data for the M_3 are negatively skewed (Shapiro-Wilk, $p < 0.05$). The $\delta^{18}O$ values span a total range of 3.4‰, between a minimum of -8.8‰ and a maximum of -5.4‰ (Figure 5.17). The average $\delta^{18}O$ values of the teeth from the two nest sites, A (median = -7.08‰) and B (median = -7.28‰), are statistically equivalent (Mann-Whitney, $p > 0.05$), and span identical ranges

(2.6‰). Therefore, the data from these two sites will henceforth be regarded as belonging to a single population.

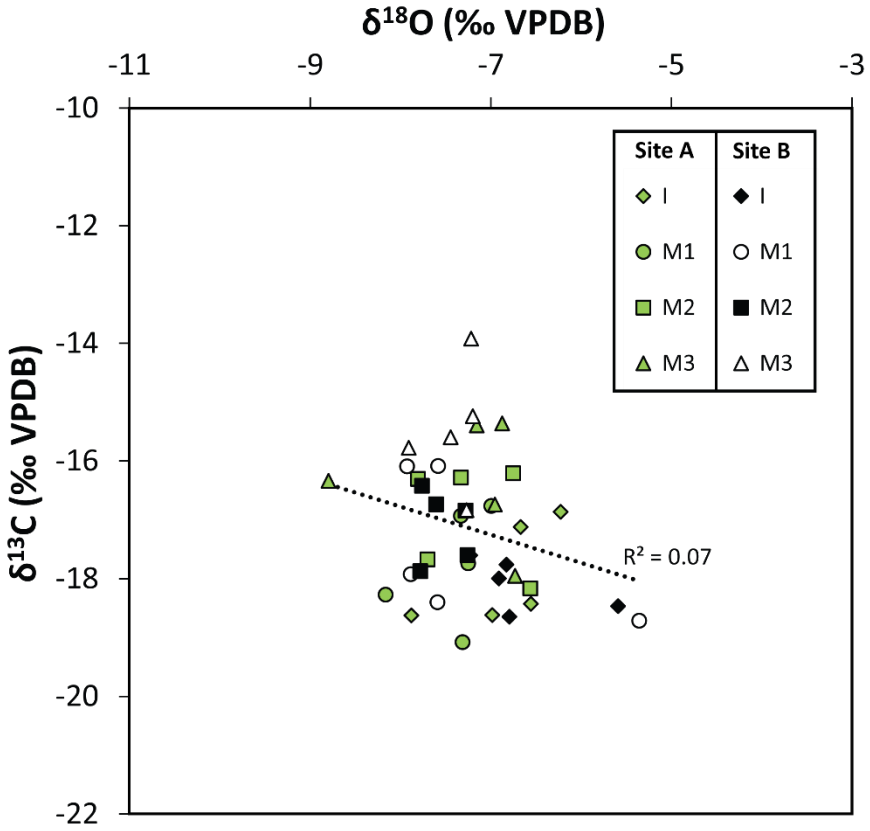

Figure 5.17: *The oxygen and carbon isotope results for the* M. agrestis *teeth from Perthshire, plotted according to the nest site and tooth type.*

Table 5.17 shows that the average $\delta^{18}O$ values of the M_1, M_2 and M_3 are very similar. In contrast, the average $\delta^{18}O$ value of the incisors is relatively enriched. These inter-tooth differences are statistically significant (Kruskal-Wallis, $p < 0.05$). Inter-individual differences in average $\delta^{18}O$ values are likewise significant (Kruskal-Wallis, $p < 0.05$). Mann-Whitney pairwise comparisons indicate that the mean $\delta^{18}O_{rt}$ value of Individual 5 is significantly depleted compared to Individuals 1-4 and 7-8.

Table 5.17: *Averages and intra-population ranges in the $\delta^{18}O$ values of the lower right teeth from Perthshire.*

Tooth type	Mean $\delta^{18}O$ value (‰ VPDB)	1σ standard deviation (‰)	Median $\delta^{18}O$ value (‰ VPDB)	Range in $\delta^{18}O$ values (‰)	No. of teeth
I	-6.77	0.60	-6.81	2.29	10
M_1	-7.34	0.78	-7.46	2.81	10
M_2	-7.38	0.44	-7.47	1.24	10
M_3	-7.36	0.60	-7.21	2.06	10

Despite this, intra-population ranges in $\delta^{18}O_{rt}$ values are relatively narrow, varying between 1.2 and 2.8‰ (Table 5.17). Differences in the variance in $\delta^{18}O_{rt}$ values between each tooth type are not statistically significant (Levene's test, $p > 0.05$). Intra-jaw ranges in tooth $\delta^{18}O$ values are similarly narrow, at ≤ 1‰ for nearly all individuals (Table 5.18), although inter-individual differences in $\delta^{18}O$ variances are statistically significant (Levene's test, $p < 0.05$). The larger intra-jaw range for Individual 9 is because the $\delta^{18}O$ values of the M_1 and incisor are relatively enriched compared to the M_2 and M_3 (Figure 5.18).

Small inter-tooth ranges in $\delta^{18}O$ values are also observed in Figure 5.18. In general, the $\delta^{18}O$ offset between the M_1 and incisor is -0.3 to -1.1‰, the offset between the M_2 and incisor varies from 0 to -1.7‰, and the offset between the M_3 and incisor is -0.2 to -0.9‰. Conversely, the offsets between the $\delta^{18}O$ values of the molars are variable in magnitude and direction, and are generally < 1‰. These offsets are comparable to or larger than the estimated 1σ uncertainty for a single $\delta^{18}O$ measurement of tooth bioapatite (± 0.5‰). Thus, overall, molars < incisor for the $\delta^{18}O$ values of the teeth from Perthshire.

Table 5.18: *Medians and intra-jaw ranges in the $\delta^{18}O$ values of the teeth from each individual from Perthshire.*

M. agrestis **individual number**	**Median $\delta^{18}O$ value of all available teeth in mandible (‰ VPDB)**	**Intra-jaw range in $\delta^{18}O$ values (‰)**
1	-7.24	0.66
2	-6.82	0.77
3	-7.12	0.75
4	-6.65	0.76
5	-8.02	0.99
6	-7.60	0.70
7	-7.40	0.70
8	-7.43	0.99
9	-6.43	2.55
10	-7.24	1.06

5.5.4.2. $\delta^{13}C$ of teeth

The mean and median $\delta^{13}C$ values of the teeth from Perthshire are -17.13 and -17.03‰, respectively. The range in $\delta^{13}C$ values is 5.2‰, and the data are normally distributed (Shapiro-Wilk, $p > 0.05$). The mean $\delta^{13}C$ for nest Site A is -17.24‰, and the mean for nest Site B is -17.03‰. These average values are not statistically different (Student's T-test, $p > 0.05$).

The average $\delta^{13}C$ values of the molars and incisors are relatively variable, spanning a range of ~2‰ between -18.0 and -15.9‰ (Table 5.19). Tukey's Q pairwise comparisons indicate that the mean $\delta^{13}C$ of the M_3 is significantly enriched relative to that of the M_1 and incisor ($p < 0.05$). In contrast, average $\delta^{13}C$ values of different individuals within the population are not significantly different (Table 5.20) (ANOVA: F statistic = 2.22, F critical = 2.21, $p = 0.05$).

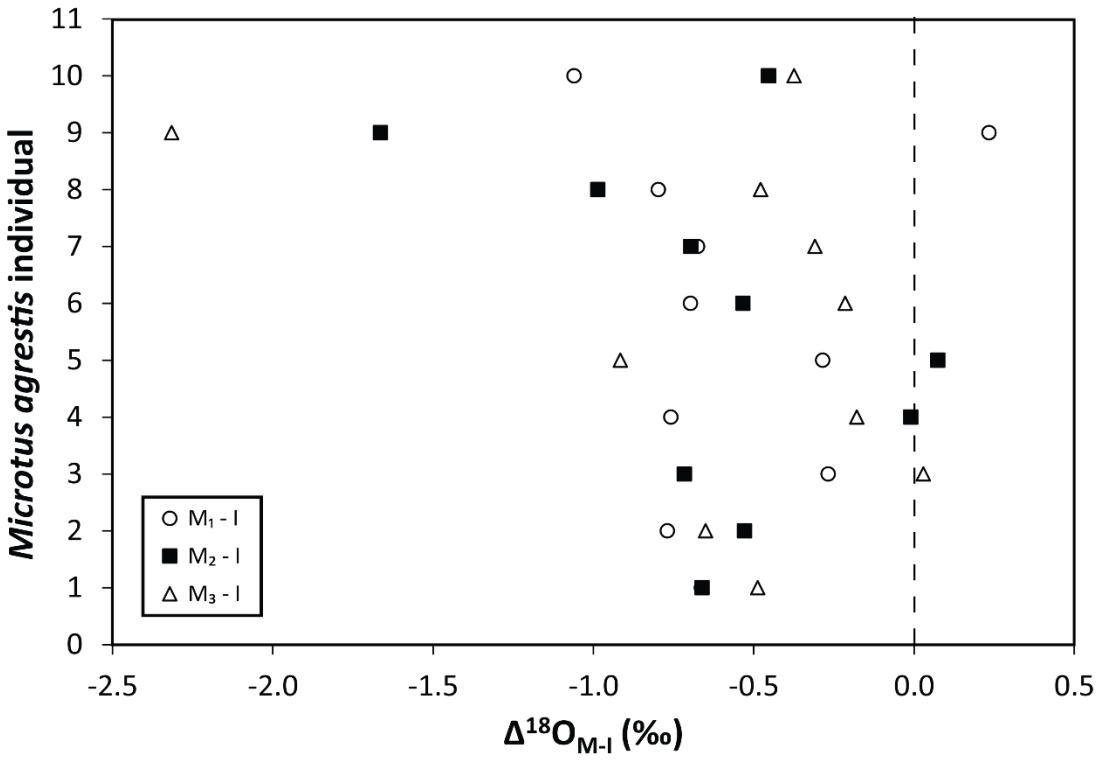

Figure 5.18: *Offsets between the oxygen isotope values of the molars and incisors for each* M. agrestis *individual from Perthshire.*

Intra-population (Table 5.19) and intra-jaw (Table 5.20) ranges in the $\delta^{13}C$ values of the teeth are also fairly broad and variable, ranging from 1.1‰ to 4.1‰. However, the differences between the variances in $\delta^{13}C$ values for each tooth type and individual are not statistically significant (Levene's test, $p > 0.05$). The large isotopic ranges for the M_3 and Individual 7 are due to the enriched $\delta^{13}C$ value of the M_3 from Individual 7 (-13.9‰) (Figure 5.19). Statistically, this enriched value is not an outlier (Grubbs' test, $p > 0.05$). Excluding this value, the intra-population and intra-jaw ranges are all < 3‰.

As illustrated in Figure 5.19, for most individuals, the $\delta^{13}C$ value of the M_1 is 0.1-1.9‰ enriched compared to the incisor, the M_2 is 0.3-2.3‰ enriched relative to the incisor, while the M_3 is 0.5-4.1‰ enriched relative to the incisor. These offsets exceed the estimated 1σ uncertainty on an individual $\delta^{13}C$ measurement of tooth bioapatite (± 0.18‰). Moreover, the $\delta^{13}C$ values of the M_3 are consistently higher than the M_1 and M_2. Therefore, in general, $I < M_1 < M_2 < M_3$ for the $\delta^{13}C$ values of the teeth from Perthshire.

Table 5.19: *Averages and intra-population ranges in the $\delta^{13}C$ values of the teeth from Perthshire.*

Tooth type	Mean $\delta^{13}C$ value (‰ VPDB)	1σ standard deviation (‰)	Median $\delta^{13}C$ value (‰ VPDB)	Range in $\delta^{13}C$ values (‰)	No. of teeth
I	-18.01	0.65	-18.21	1.78	10
M_1	-17.60	1.07	-17.83	2.99	10
M_2	-17.01	0.74	-16.79	1.95	10
M_3	-15.91	1.10	-15.68	4.03	10

Table 5.20: *Medians and intra-jaw ranges in the $\delta^{13}C$ values of the teeth from each individual from Perthshire.*

M. agrestis individual number	Median $\delta^{13}C$ value of all available teeth in mandible (‰ VPDB)	Intra-jaw range in $\delta^{13}C$ values (‰)
1	-16.61	1.73
2	-16.48	1.50
3	-17.71	1.88
4	-18.29	1.13
5	-17.30	2.32
6	-16.26	2.01
7	-16.41	4.08
8	-18.14	1.81
9	-18.03	2.94

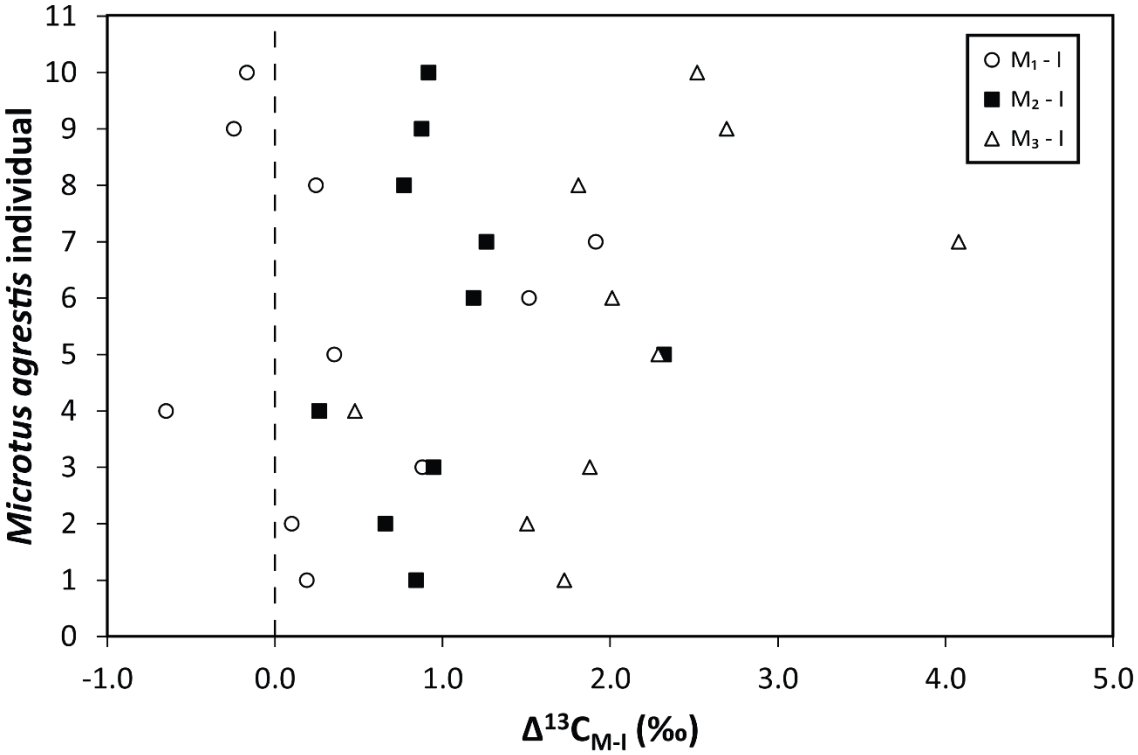

Figure 5.19: *Offsets between the carbon isotope values of the molars and incisor for each* M. agrestis *individual from Perthshire.*

5.5.4.3. δ18O and δD of water

The mean $\delta^{18}O$ and δD values of the water samples are -7.99‰ and -51.92‰, respectively. The measured mean $\delta^{18}O$ value is consistent with the predicted average $\delta^{18}O$ value for meteoric water sources in Perthshire (Table 5.1). The ranges in $\delta^{18}O$ and δD values are 0.2‰ and 1.9‰, respectively. There is a relatively strong, positive correlation between $\delta^{18}O$ and δD ($r^2 = 0.47$), although this correlation is not statistically significant ($p > 0.05$). The data lie slightly above the Global Meteoric Water Line, and fall along the line for the River Thames at Wallingford (Figure 5.20).

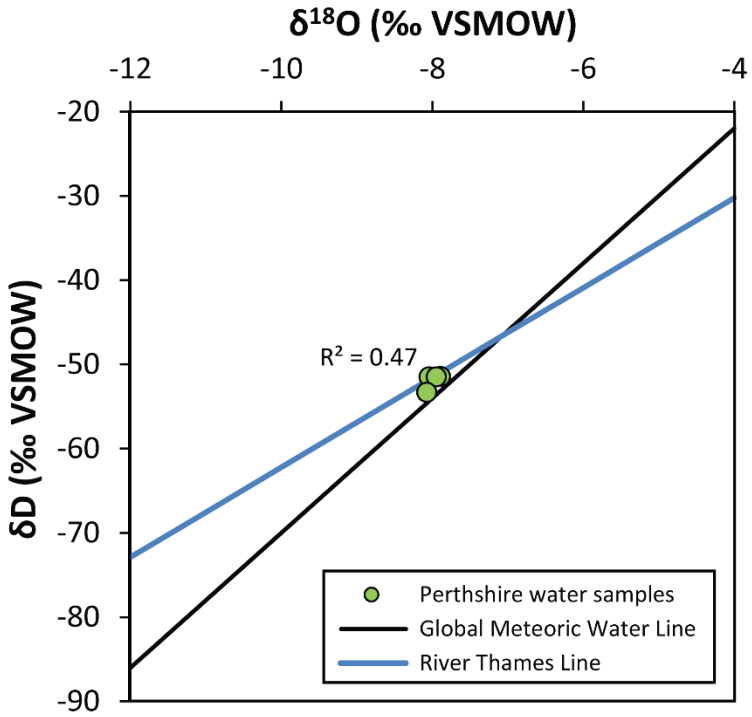

Figure 5.20: *Plot of the oxygen and hydrogen isotope results for the meteoric water samples from Perthshire. The Global Meteoric Water Line of Craig (1961) and the River Thames Line of Darling & Bowes (2016) are shown for comparison.*

5.5.5. Inter-site comparisons

5.5.5.1. Intra-population and inter-tooth variability in $\delta^{18}O$ values

In general, intra-population ranges in the $\delta^{18}O$ values of the *Microtus agrestis* incisors, M_1, M_2, and M_3 are between 2 and 3‰ (Figure 5.21). Occasionally, the intra-population range is < 2‰ (e.g. the M_2 from East Yorkshire) or > 3‰ (e.g. the M_1 from Surrey). This isotopic variability within a population results from inter-individual differences in tooth $\delta^{18}O$ values. In most cases, the average $\delta^{18}O$ values of incisors and molars from the same population are not significantly different. The exceptions to this are the depleted first molars from Somerset and the enriched incisors from Perthshire (Figure 5.21). The $\delta^{18}O$ values of lower and upper teeth are also not statistically different, although right teeth are generally slightly enriched compared to left teeth, and lower

teeth are slightly enriched compared to upper teeth. Moreover, the 1σ standard deviations and inter-quartile ranges in the $\delta^{18}O$ values of the teeth are typically ≤ 1‰ for all sites (Figure 5.21). This indicates that the average $\delta^{18}O_{rt}$ of a *M. agrestis* population can be precisely estimated (to within ± 0.5‰) using the $\delta^{18}O$ values of teeth sampled from 9 individuals. This precision is comparable to the estimated 1σ measurement uncertainty for a single sample of tooth bioapatite.

Moreover, in general, the $\delta^{18}O$ data are normally distributed, and in instances where the data are skewed, there is no consistent pattern in the direction of skew. For example, as seen in Figure 5.21, the $\delta^{18}O$ values of the M_2 and M_3 from Somerset and the M_1 from Perthshire are significantly positively skewed, due to a small number of teeth with enriched values. Conversely, the $\delta^{18}O$ data for the M_3 from Perthshire and all teeth from Surrey are negatively skewed. This suggests that in most *M. agrestis* populations, the majority of the teeth will have $\delta^{18}O$ values that fall close to the population mean (within ~1‰). However, there may be a small number of teeth that have extreme $\delta^{18}O$ values (either highly enriched or highly depleted) that can positively or negatively skew the distribution.

Intra-jaw and intra-individual offsets in $\delta^{18}O_{rt}$ values are also relatively comparable between the sites. The $\delta^{18}O$ values of different teeth from the same mandible typically fall within ~2‰ of each other, and differences between molars are usually less than ± 1.5‰. However, in some instances, inter-tooth $\delta^{18}O$ offsets are between 2 and 4‰. This is especially evident in the Somerset population, where the first molars have significantly depleted values compared to all other teeth from the site. Nevertheless, large inter-tooth offsets are often due to enriched or depleted values of the lower or upper M_2 or M_3. As a result, the total range in $\delta^{18}O$ values of all teeth (upper and lower) from the same individual is usually 3-4‰. Overall, however, the magnitudes and directions of inter-tooth $\delta^{18}O$ offsets do not follow any consistent pattern.

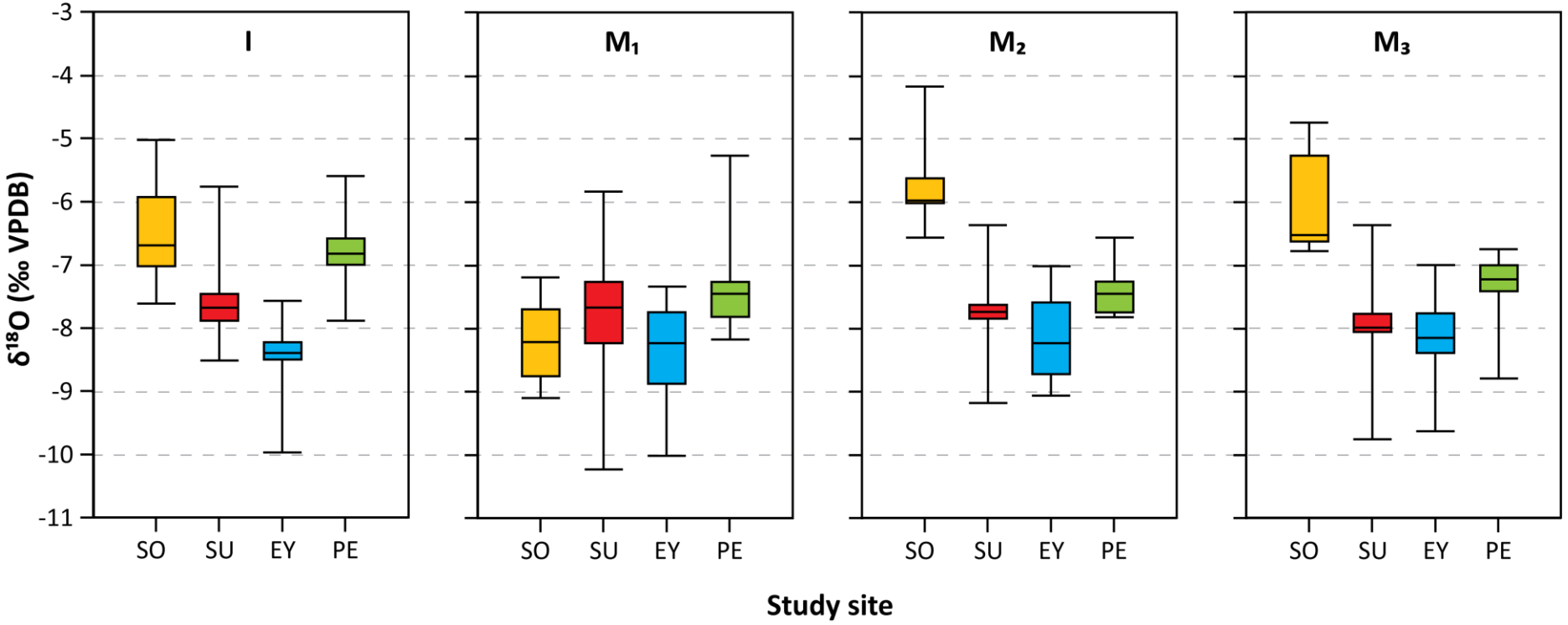

Figure 5.21: *Box and whisker plots showing the oxygen isotope results for the* M. agrestis *lower right incisors (I), first molars (M_1), second molars (M_2) and third molars (M_3) from each study site. Study sites: SO = Somerset, SU = Surrey, EY = East Yorkshire, PE = Perthshire. The box within each box and whisker plot represents the inter-quartile range in the $\delta^{18}O$ values, and the horizontal line in each box represents the median $\delta^{18}O$ value. The whiskers mark the maximum and minimum $\delta^{18}O$ values for each dataset.*

5.5.5.2. Intra-population and inter-tooth variability in $\delta^{13}C$ values

Intra-population ranges in the $\delta^{13}C$ values of *M. agrestis* teeth are generally broader and more variable than the ranges in $\delta^{18}O$ values. Ranges in $\delta^{13}C_{rt}$ values typically vary between ~1.6 and 4.6‰ (Figure 5.22). The Somerset and Perthshire populations have the smallest intra-population ranges of 1.7-3.0‰, whereas the Surrey and East Yorkshire populations have larger ranges of 3.1-4.6‰ (Figure 5.22). As with the $\delta^{18}O$ data, this isotopic variability within a population results from inter-individual differences in $\delta^{13}C_{rt}$ values. Nevertheless, while the average $\delta^{18}O$ values of the molars and incisors are generally similar, the $\delta^{13}C$ values of these teeth are often statistically different. For example, the average $\delta^{13}C$ of the M_3 is significantly enriched in the Somerset, East Yorkshire and Perthshire populations (Figure 5.22).

These observations are supported by the inter-tooth offset calculations. For all four study sites, a consistent pattern of $\delta^{13}C$ offsets is observed between the molars and incisors, whereby $I < M_1 < M_2 < M_3$. This pattern is clearly evident in Figure 5.22, and is also observed in both the lower and upper tooth rows. As a result of these inter-tooth isotopic differences, the total intra-population ranges in $\delta^{13}C_{rt}$ values (including all teeth) are 3.8-6.0‰. Ranges in the $\delta^{13}C$ values of different teeth from the same individual are also fairly variable, generally falling between ~1.0 and 3.0‰, with a maximum of 4.0‰. Despite this variability, 1σ standard deviations in the $\delta^{13}C$ values for each population are ≤ 1.5‰. In addition, all $\delta^{13}C$ data from the *M. agrestis* populations follow a normal distribution. Therefore, the mean $\delta^{13}C$ values of the sampled *M. agrestis* teeth (n = 36) can provide accurate values for the population mean, within a precision of ± 0.25‰. This precision is comparable to the estimated 1σ measurement uncertainty for an individual sample of tooth bioapatite (± 0.18‰).

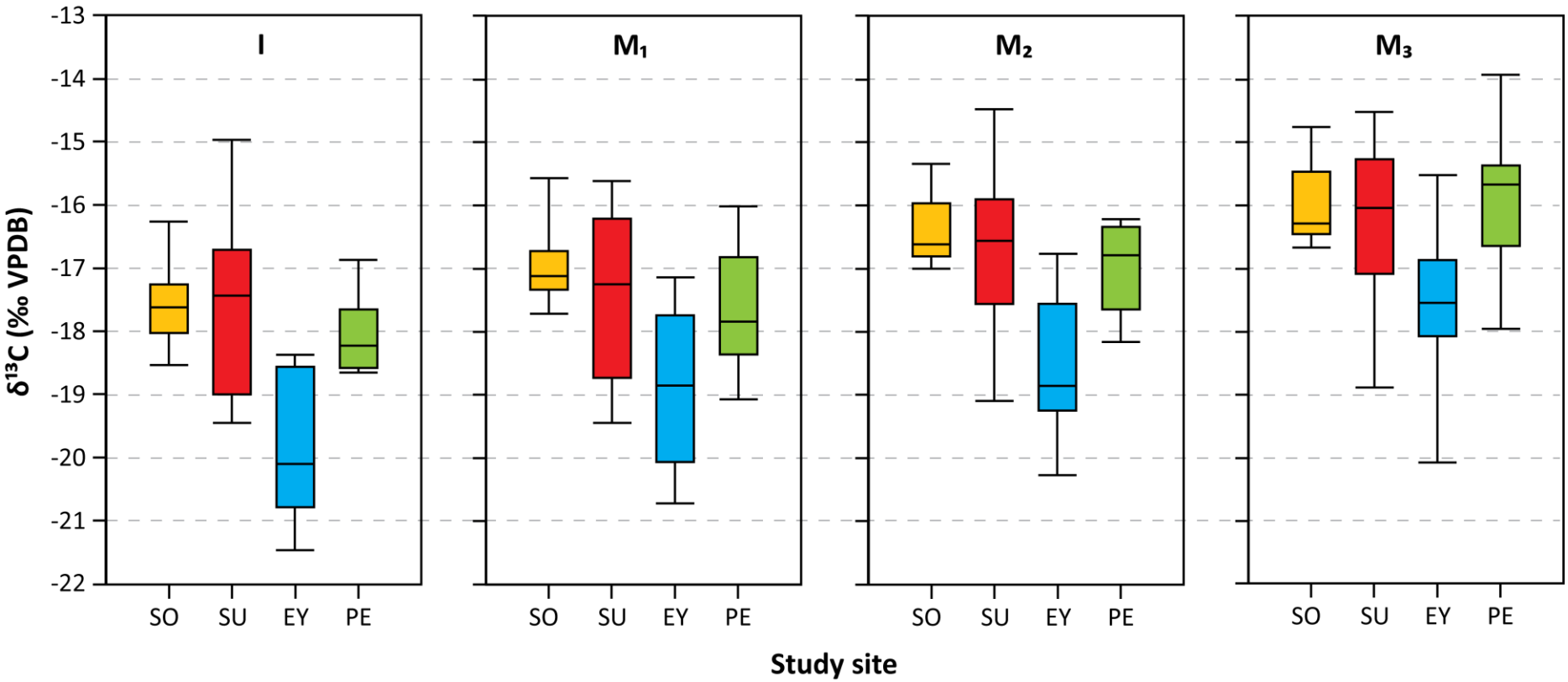

Figure 5.22: *Box plots showing the carbon isotope results for the* M. agrestis *lower right incisors (I), first molars (M_1), second molars (M_2) and third molars (M_3) from each study site. Study sites: SO = Somerset, SU = Surrey, EY = East Yorkshire, PE = Perthshire. The box within each box and whisker plot represents the inter-quartile range in the $\delta^{13}C$ values, and the horizontal line in each box represents the median $\delta^{13}C$ value. The whiskers mark the maximum and minimum $\delta^{13}C$ values for each dataset.*

5.5.5.3. Spatial patterns in tooth $\delta^{13}C$ values

In addition to intra-population isotopic differences, the average $\delta^{13}C$ values of the teeth also differ between the four study sites (Figure 5.23). Specifically, the $\delta^{13}C$ values of the teeth from East Yorkshire are depleted compared to the other three populations. The results of Student's T-tests indicate that these differences are statistically significant at 95% confidence (Table 5.21). These results are consistent across all tooth types, except for the third molars from Surrey and East Yorkshire ($p = 0.07$). Conversely, the $\delta^{13}C_{rt}$ values for Somerset, Surrey and Perthshire are relatively comparable (Figure 5.23), and are not statistically different (Table 5.21).

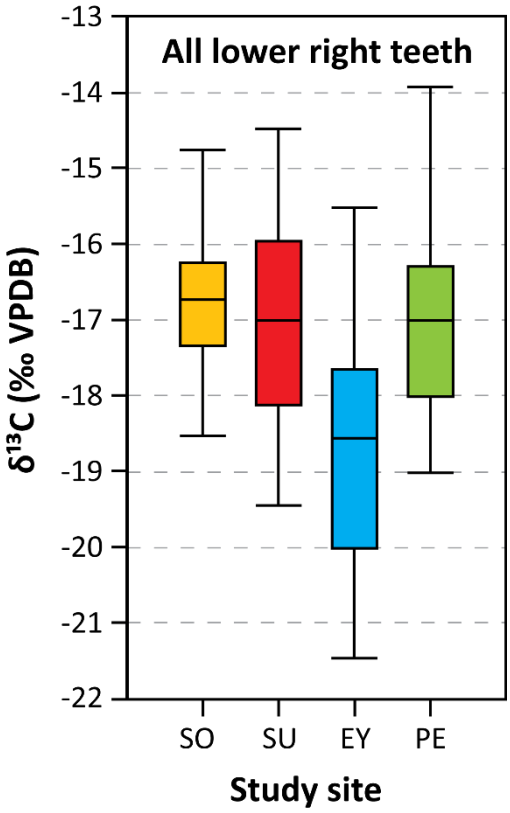

Figure 5.23: *Box plots showing the carbon isotope results for all lower right* M. agrestis *teeth from each study site.*

Table 5.21: *Results of two-tailed Student's T-tests comparing the mean $\delta^{13}C$ values of all lower right teeth from the four study sites. The figures in the upper half of the table are the calculated* p *values for each test. A* p *value > 0.05 indicates no statistically significant difference between the average tooth $\delta^{13}C$ values for the two sites, whereas a* p *value < 0.05 indicates a statistically significant difference at 95% confidence. The lower half of the table shows whether there is no statistical difference (N) or a statistically significant difference (Y) in the average $\delta^{13}C$ values. SO = Somerset, SU = Surrey, EY = East Yorkshire, PE = Perthshire.*

All lower right teeth	**SO**	**SU**	**EY**	**PE**
SO	-	0.35	< 0.01	0.09
SU	N	-	< 0.01	0.67
EY	Y	Y	-	< 0.01
PE	N	N	Y	-

5.5.5.4. Spatial patterns in tooth $\delta^{18}O$ values

The average $\delta^{18}O_{rt}$ values likewise differ between the four study populations. As illustrated in Figure 5.21, the $\delta^{18}O$ values of the teeth from Somerset are ~1-2‰ enriched compared to the other three sites for all tooth types except the M_1. Similarly, the average $\delta^{18}O$ values of the teeth from Surrey are generally ~0.5‰ enriched relative to the teeth from East Yorkshire. This suggests that there is an overall trend of decreasing average $\delta^{18}O_{rt}$ values from Somerset, in the southwest of England, to East Yorkshire, in the northeast. However, this trend does not continue into Scotland. In general, the average $\delta^{18}O_{rt}$ values for the Perthshire population are similar to the values for Somerset and Surrey (Figure 5.21).

To examine these spatial differences in $\delta^{18}O_{rt}$ values in further detail, two-tailed Mann-Whitney tests were performed to compare the average $\delta^{18}O$ values of each tooth type between the four sites. The results of these tests are presented in Tables 5.22-5.25.

Table 5.22: *Results of two-tailed Mann-Whitney tests, used to assess the statistical significance of differences in the average $\delta^{18}O$ values of the* M. agrestis *incisors from Somerset, Surrey, East Yorkshire and Perthshire. For an explanation of the table contents see the caption for Table 5.21.*

Incisor	**SO**	**SU**	**EY**	**PE**
SO	-	0.03	< 0.01	0.66
SU	Y	-	0.02	0.08
EY	Y	Y	-	< 0.01
PE	N	N	Y	-

Table 5.23: *Results of Mann-Whitney tests comparing the $\delta^{18}O$ values of the first molars from the four study sites. For an explanation of the table contents see the caption for Table 5.21.*

First molar	**SO**	**SU**	**EY**	**PE**
SO	-	0.48	0.73	0.02
SU	N	-	0.24	0.57
EY	N	N	-	0.01
PE	Y	N	Y	-

Table 5.24: *Results of Mann-Whitney tests comparing the $\delta^{18}O$ values of the second molars from the four study sites. For an explanation of the table contents see the caption for Table 5.21.*

Second molar	**SO**	**SU**	**EY**	**PE**
SO	-	< 0.01	< 0.01	< 0.01
SU	Y	-	0.30	0.18
EY	Y	N	-	0.03
PE	Y	N	Y	-

Table 5.25: *Results of Mann-Whitney tests comparing the $\delta^{18}O$ values of the third molars from the four study sites. For an explanation of the table contents see the caption for Table 5.21.*

Third molar	SO	SU	EY	PE
SO	-	< 0.01	< 0.01	< 0.01
SU	Y	-	0.80	0.04
EY	Y	N	-	0.02
PE	Y	Y	Y	-

The results in these Tables confirm that the average $\delta^{18}O_{rt}$ values of the M_2, M_3 and incisors from Somerset are significantly enriched compared to the $\delta^{18}O_{rt}$ values for the other three sites. In contrast, there is no statistically significant difference between the average $\delta^{18}O$ of the M_1 from Somerset, relative to the M_1 from Surrey and East Yorkshire (Table 5.23). This is due to the depleted $\delta^{18}O$ values of the first molars from Somerset. Similarly, the significantly enriched $\delta^{18}O$ values of the incisors from Perthshire are similar to the average $\delta^{18}O$ values of the incisors from Somerset, resulting in no statistical difference between these datasets (Table 5.22).

Generally, the average $\delta^{18}O_{rt}$ values for Surrey and East Yorkshire are not statistically different. Likewise, for three of the four tooth types (excepting the M_3), there is no significant difference between the average $\delta^{18}O_{rt}$ values for Surrey and Perthshire. Conversely, the average $\delta^{18}O_{rt}$ values for East Yorkshire are consistently and significantly more depleted than the average values for Perthshire.

These results indicate that although the average $\delta^{18}O$ values of molars and incisors from the same population are generally statistically comparable, the significance of the statistical differences between populations varies depending on the tooth type being considered. This shows that inter-tooth isotopic differences can influence comparisons between datasets. Differences between the $\delta^{18}O$ values of different tooth types also result in larger intra-population ranges of 3-5‰, when all tooth data from the populations are

considered (Figure 5.24). To account for this variability in $\delta^{18}O_{rt}$ values within a population, the average values for all analysed lower right teeth from each site were also compared using Mann-Whitney tests. The results of these tests are shown in Table 5.26.

Table 5.26 demonstrates that when the data from each population are considered as a whole, differences in the average $\delta^{18}O_{rt}$ values between all study sites are highly statistically significant ($p < 0.01$ in all cases). This is also illustrated in Figure 5.24. A clearly defined pattern of decreasing average $\delta^{18}O$ values from Somerset to East Yorkshire is seen, whereas the average $\delta^{18}O$ value for Perthshire lies between that for Somerset and Surrey. This shows that by averaging the isotopic data from all lower right teeth, the influence of extreme sample values on the average $\delta^{18}O_{rt}$ of each population is reduced. As a result, the average $\delta^{18}O_{rt}$ values for each site are more representative of the population mean, enabling true statistical differences between the populations to be identified. Samples sizes can therefore have an important impact on the interpretation of the results. Consequently, the average $\delta^{18}O_{rt}$ values for all analysed teeth from each population will be used in the following interpretations of the data.

Table 5.26: *Results of Mann-Whitney tests comparing the average $\delta^{18}O$ values of all analysed lower right teeth from the four study sites. For an explanation of the table contents see the caption for Table 5.21.*

All lower right teeth	**SO**	**SU**	**EY**	**PE**
SO	-	< 0.01	< 0.01	< 0.01
SU	Y	-	< 0.01	< 0.01
EY	Y	Y	-	< 0.01
PE	Y	Y	Y	-

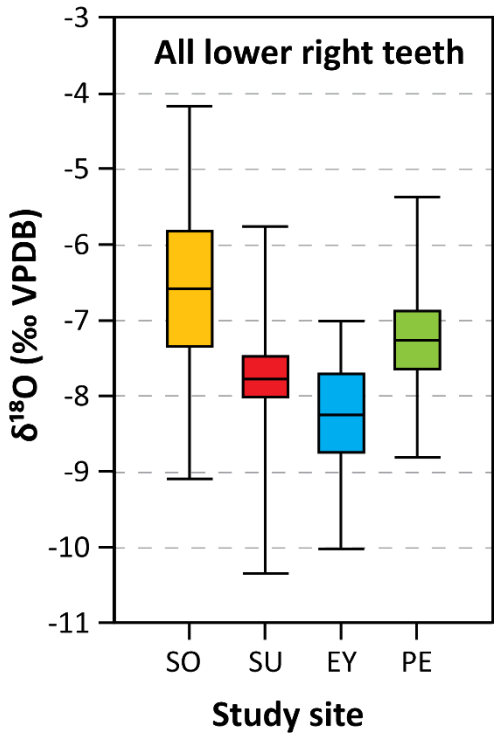

Figure 5.24: *Box plots showing the oxygen isotope results for all lower right* M. agrestis *teeth from each study site.*

5.5.5.5. Spatial patterns in water isotope values

As illustrated in Figure 5.25, the $\delta^{18}O$ and δD values for the meteoric water samples from the four study locations are strongly correlated ($r^2 = 0.85$). The data fall near to the Global Meteoric Water line, but lie along a slightly shallower slope of 6.27. This slope is similar to that of the line generated by Darling & Bowes (2016) for the River Thames at Wallingford, and is therefore consistent with other surface water sources in Britain.

Figure 5.25 also shows that there is a gradual decline in the $\delta^{18}O$ and δD values of meteoric waters from Somerset to Perthshire. This suggests a north-eastward depletion in the isotopic values of meteoric water across Britain. In addition, isotopic differences between all four sites are statistically significant (Table 5.27).

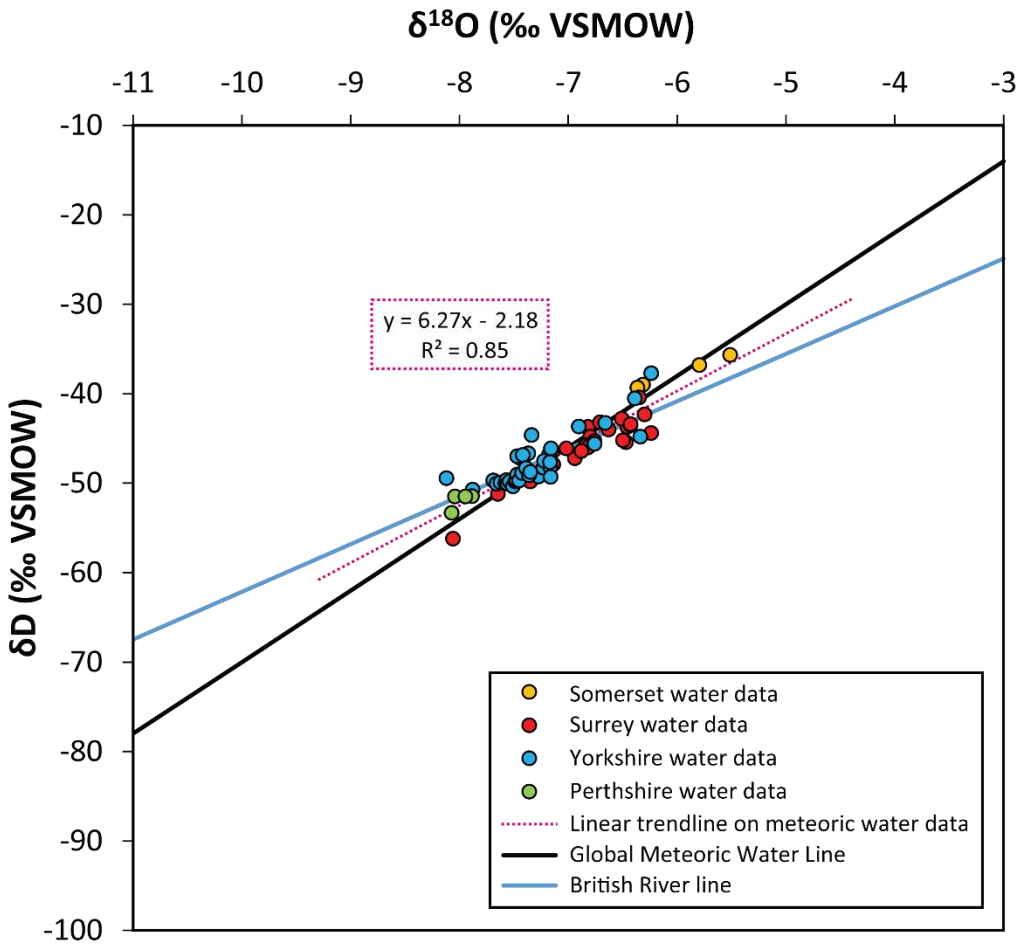

Figure 5.25: *Plot of the oxygen and hydrogen isotope values of meteoric water sources at the four study sites. The Global Meteoric Water Line of Craig (1961) and the River Thames Line of Darling & Bowes (2016) are shown for comparison.*

The modelled mean $\delta^{18}O$ values of precipitation (Table 5.1) follow a similar pattern to the measured meteoric water values, but with a few notable differences (Figure 5.26). The modelled $\delta^{18}O$ of precipitation decreases by ~1‰ from southern to northern England, in parallel with the $\delta^{18}O$ of meteoric water. However, the average $\delta^{18}O_{mw}$ values for sites in England are up to 1‰ more enriched than the average $\delta^{18}O$ of precipitation. Additionally, the $\delta^{18}O_{pt}$ for Somerset is slightly depleted compared to Surrey, whereas the $\delta^{18}O_{mw}$ in Somerset is significantly enriched compared to Surrey. Also, the mean annual $\delta^{18}O_{pt}$ values for Perthshire are enriched compared to the other three sites

(Figure 5.26). This is in opposition to the pattern observed in the meteoric water data. Nevertheless, uncertainties on the modelled $\delta^{18}O_{pt}$ values for Perthshire are relatively large, and the values do not fall along the Global Meteoric Water Line (Figure 5.26).

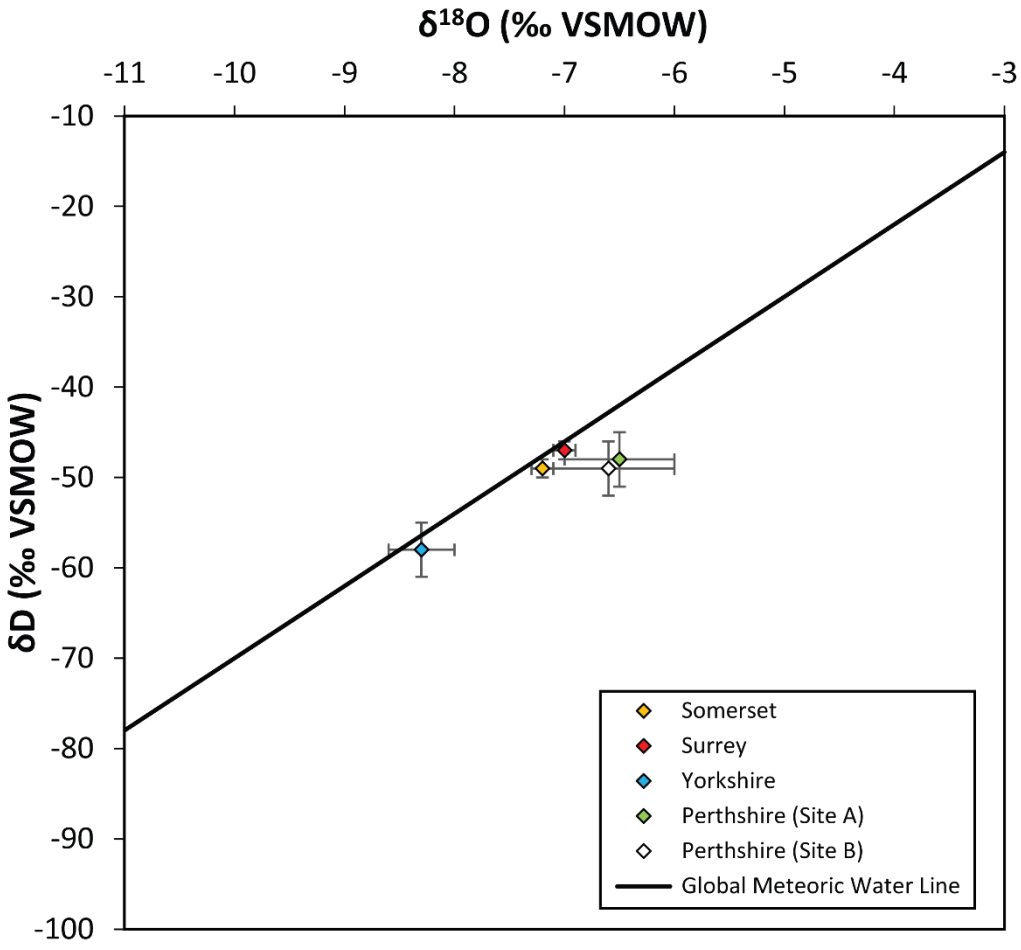

Figure 5.26: *Plot of the modelled oxygen and hydrogen isotope values of precipitation for the four study sites. The Global Meteoric water Line of Craig (1961) is also shown for comparison.*

Table 5.27: *Results of Mann-Whitney tests comparing the average $\delta^{18}O$ values of the meteoric water sources at the four study sites. For an explanation of the table contents see the caption for Table 5.21.*

	SO	**SU**	**EY**	**PE**
SO	-	< 0.01	< 0.01	< 0.01
SU	Y	-	< 0.01	< 0.01
EY	Y	Y	-	< 0.01
PE	Y	Y	Y	-

5.5.5.6. Relationships between tooth and water $\delta^{18}O$ values

The mean $\delta^{18}O_{rt}$ values of the sampled *M. agrestis* populations and the mean $\delta^{18}O$ values of the sampled surface water sources are assumed here to provide accurate estimates of the population mean isotope values for the four study sites. This assumption is likely to be valid, as large datasets were used in the calculation of the mean $\delta^{18}O$ values. Therefore, although the ranges in $\delta^{18}O$ values at each site are relatively large and overlapping, the correlation between the mean $\delta^{18}O_{rt}$ and mean $\delta^{18}O_{mw}$ is expected to provide an accurate reflection of the true relationship between these variables.

The correlation between the mean $\delta^{18}O_{rt}$ and mean $\delta^{18}O_{mw}$ across the four sites is statistically insignificant (r^2 = 0.19, p = 0.56) (Figure 5.27a). Nevertheless, the $\delta^{18}O_{rt}$ and $\delta^{18}O_{mw}$ values for the sites in England (Somerset, Surrey, and Yorkshire) follow a similar trend of isotopic depletion from the southwest to the northeast of the country. In contrast, the results for Perthshire, Scotland, deviate from this trend. This is because the $\delta^{18}O_{rt}$ values for Perthshire are comparable to the sites in southern England, while the $\delta^{18}O_{mw}$ compositions are depleted compared to all other sites. When only the data from sites in England are considered, a strong positive correlation is observed between the mean $\delta^{18}O_{rt}$ and mean $\delta^{18}O_{mw}$ (r^2 = 0.99) (Figure 5.27b), although this correlation is not statistically significant at 95% confidence (p = 0.06). This lack of significance is likely due to the small number

of sites (n = 3) used in the linear regression analysis. The forward fit linear regression for the data from the sites in England generates the following equation:

$$\delta^{18}O_{rt}\ (VPDB) = 1.31 \times \delta^{18}O_{mw} + 1.23 \qquad (5.8).$$

The 1σ uncertainties on the fit of this regression line are shown in Table 5.28. The uncertainties are less than ± 0.5‰ across the range in $\delta^{18}O$ values of meteoric water sources in Britain at the present day. Within the range in mean $\delta^{18}O_{mw}$ values used in the development of the regression equation (-7.3 to -6.0‰), uncertainties are within ± 0.2‰. However, outside of this range, uncertainties are greater, as the $\delta^{18}O_{mw}$ values are extrapolated beyond the boundaries of the regression line. The uncertainty in the slope coefficient (δa in Equation 5.5) is 0.11.

Table 5.28: *Uncertainties (δy) in the fit of the regression between $\delta^{18}O_{rt}$ and $\delta^{18}O_{mw}$ for Equation 5.8. These uncertainties were calculated using Equations 5.3-5.6, for the different $\delta^{18}O_{mw}$ positions along the regression line.*

$\delta^{18}O_{mw}$ value (‰ VSMOW)	**± 1σ uncertainty in the least-squares fit (‰)**
-3	0.43
-4	0.32
-5	0.20
-6	0.10
-7	0.07
-8	0.16
-9	0.27
-10	0.38

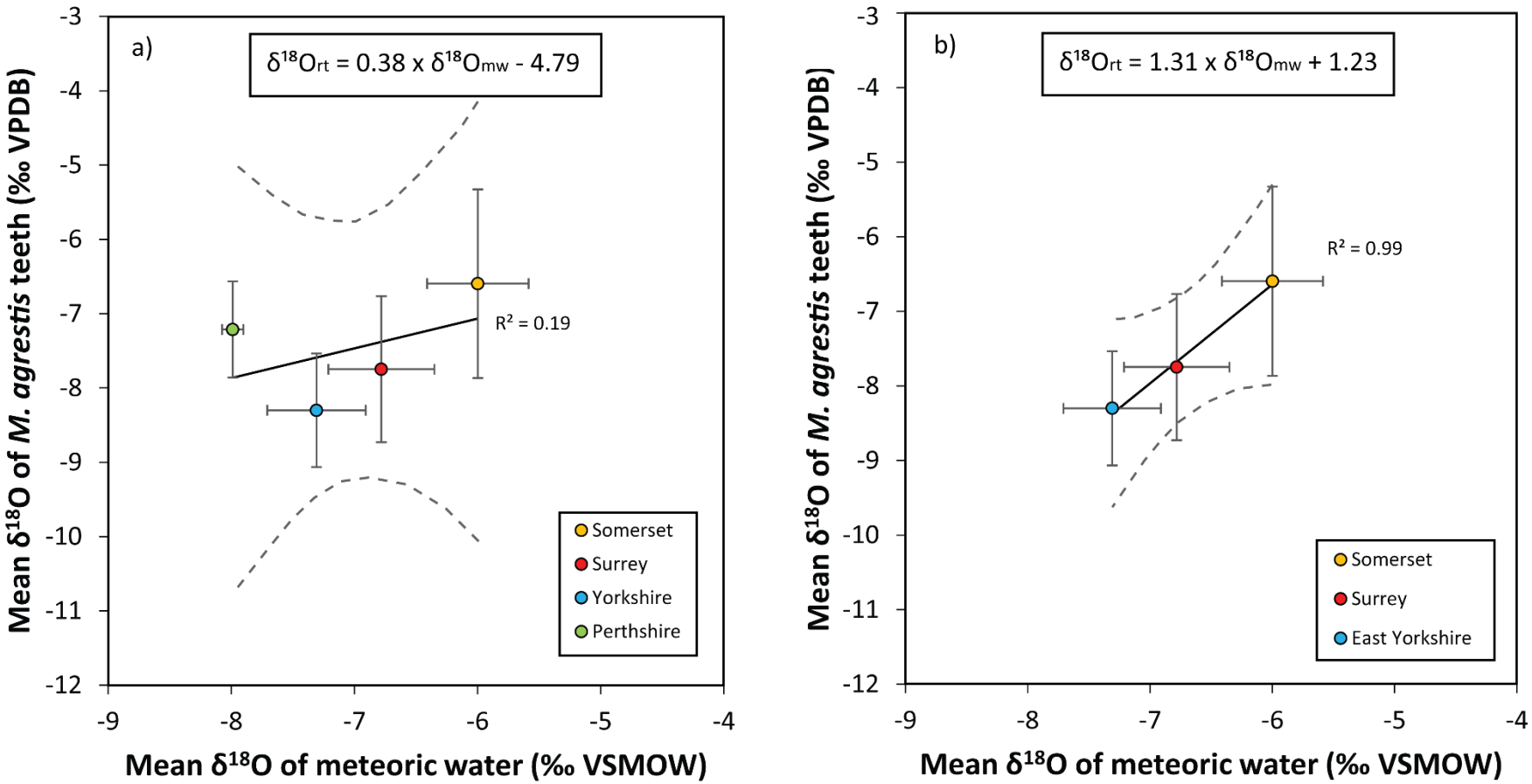

Figure 5.27: *Relationships between the mean oxygen isotope values of* M. agrestis *teeth and meteoric water for a) all study sites, and b) only the study sites in England. The dashed lines represent the 95% confidence intervals around each regression line.*

The $\delta^{18}O_{rt}$ values for sites in England were also converted to the VSMOW scale to produce the equation below:

$$\delta^{18}O_{rt}\ (VSMOW) = 1.36 \times \delta^{18}O_{mw} + 32.22 \quad (5.9).$$

The correlation between the mean $\delta^{18}O_{rt}$ and the modelled mean annual $\delta^{18}O$ of precipitation across all four sites is also statistically insignificant ($r^2 = 0.39$, $p = 0.33$) (Figure 5.28a). This is because the spatial trend in the modelled $\delta^{18}O_{pt}$ values between Somerset and Surrey (i.e. Somerset < Surrey) opposes the trend observed in the $\delta^{18}O_{rt}$ data (Somerset > Surrey). If the data from Somerset are excluded, the correlation between $\delta^{18}O_{rt}$ and $\delta^{18}O_{pt}$ increases in strength ($r^2 = 0.94$) (Figure 5.28b), although is not statistically significant ($p = 0.16$). The forward fit linear regression model for the Surrey, East Yorkshire and Perthshire data generates the following equation:

$$\delta^{18}O_{rt}\ (VPDB) = 0.57 \times \delta^{18}O_{pt} - 3.62 \quad (5.10).$$

The $\delta^{18}O_{pt}$ value used for Perthshire is -6.5‰. The 1σ uncertainties in the fit of this regression line are similar to those for Equation 5.8, with values of less than ± 0.2‰ within the range of the $\delta^{18}O_{pt}$ data (-8.3 to -6.5‰), and ± 0.2-0.6‰ for extrapolated $\delta^{18}O_{pt}$ values. The 1σ uncertainty on the slope coefficient is 0.14. The equivalent equation for $\delta^{18}O_{rt}$ values on the VSMOW scale is as follows:

$$\delta^{18}O_{rt}\ (VSMOW) = 0.59 \times \delta^{18}O_{pt} + 27.17 \quad (5.11).$$

Equation 5.10 does not differ significantly if the data from Somerset are included in the regression analysis (Figure 5.28a); the probability that the two regressions have the same slope is 0.96. Conversely, the slopes of Equations 5.8 and 5.10 are significantly different at 90% confidence ($p = 0.07$).

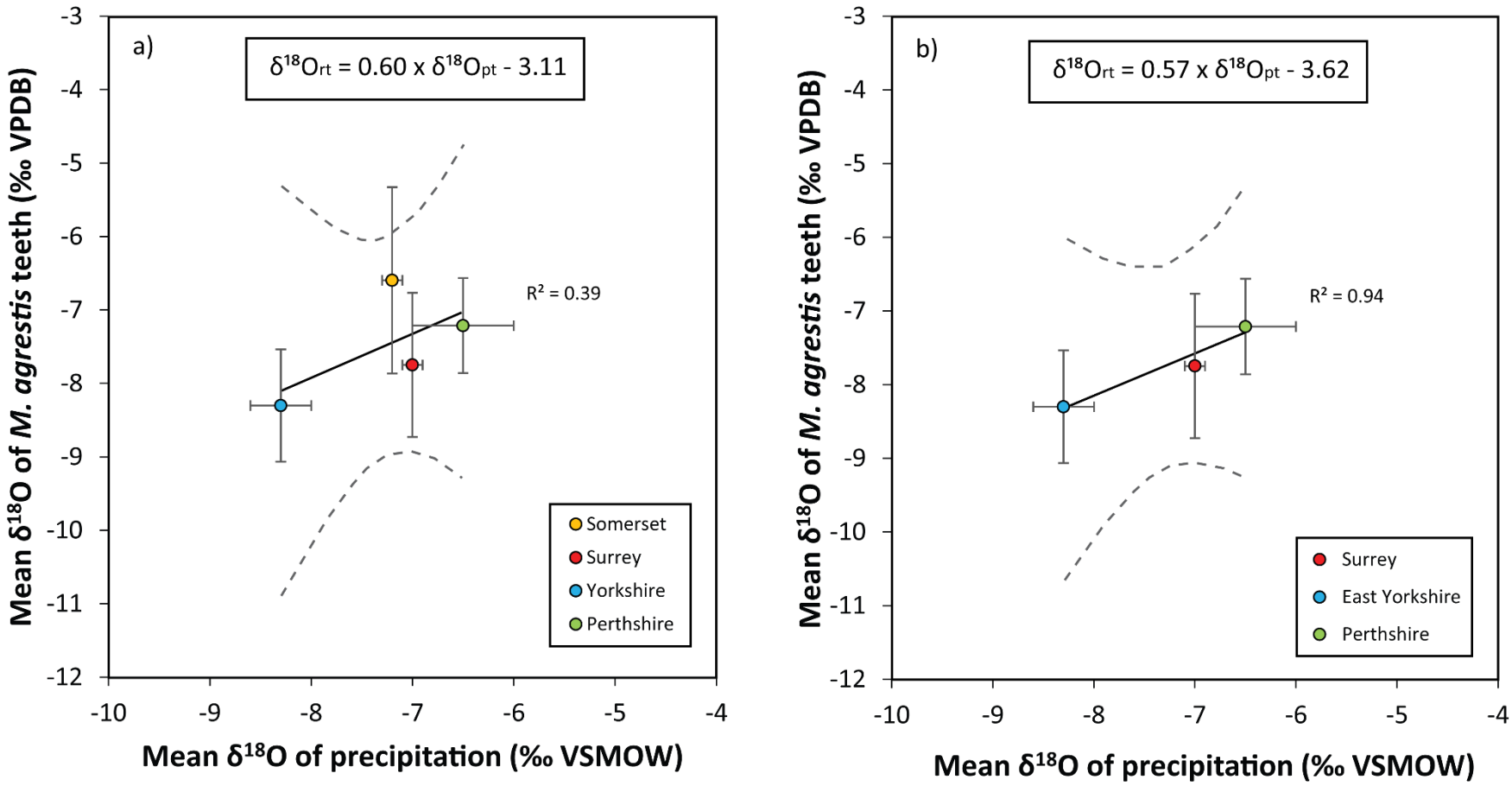

***Figure 5.28**: Relationships between the mean oxygen isotope values of* M. agrestis *teeth and precipitation for a) all study sites, and b) Surrey, East Yorkshire and Perthshire only.*

5.6. Interpretations and Discussion

5.6.1. Isotope variability in rodent populations

5.6.1.1. Intra-population variability in $\delta^{18}O$ values

Intra-population ranges in the $\delta^{18}O$ values of *Microtus agrestis* teeth are relatively consistent across Britain, and generally fall between 2 and 3‰ for a single tooth type (Table 5.29). Gehler et al. (2012) report a comparable intra-population range of 2.9‰ for *M. agrestis* incisors from northwest Germany (Table 5.29). This suggests that the intra-population variability in the $\delta^{18}O$ values of modern *M. agrestis* teeth is consistent across northwest Europe. Other vole species, such as *M. arvalis* and *Arvicola terrestris*, have larger ranges of 3.5-3.9‰ (Table 5.29). Therefore, in general, modern intra-population ranges in the $\delta^{18}O$ values of vole teeth are ~2-4‰, although are usually less than 3‰ for the species *Microtus agrestis*.

This variability in $\delta^{18}O_{rt}$ values within a population can be largely explained by spatial and temporal variations in the $\delta^{18}O$ values of drinking water sources (Royer et al., 2013a). Each individual in a population is likely to consume different water sources in the local area. Differential evaporation, and variations in the residence times of these waters, can lead to small differences in their $\delta^{18}O_{mw}$ values. For example, evaporative enrichment has a greater influence on isolated, ephemeral water bodies, such as ponds and ditches, compared to perennial streams that are sustained by runoff and base flow (Darling et al., 2003; Darling, 2004). Differences between the $\delta^{18}O$ values of food water sources, due to variations in the degree of evapo-transpiration, may additionally contribute to intra-population $\delta^{18}O_{rt}$ variability (Royer et al., 2013a). These spatial variations in the $\delta^{18}O$ of ingested water will consequently result in differences between the $\delta^{18}O_{rt}$ values of individuals that are captured from different locations within an owl's hunting range.

The $\delta^{18}O$ values of precipitation and surface water can also fluctuate significantly on daily and seasonal timescales (e.g. Soulsby et al., 2000; Darling & Talbot, 2003; Darling et al., 2003; Darling & Bowes, 2016). For instance, stream waters in Britain tend to be isotopically depleted during winter and relatively enriched in summer, due to seasonal changes in air temperature

and evaporative potential (Darling et al., 2003; Darling & Talbot, 2003; Darling & Bowes, 2016). As a consequence, the average $\delta^{18}O_{mw}$ recorded within a rodent tooth will be dependent on the interval during which the animal lived prior to predation. Since barn owls often use the same roosting and nesting sites throughout their lives (Andrews, 1990; Taylor, 1994), the pellets sampled in this study likely comprise rodents that were eaten over a period of several weeks or months. Therefore, rodent teeth from different owl pellets will reflect different $\delta^{18}O_{mw}$ values, resulting in isotopic variability within the sampled population. As suggested by Royer et al. (2013a), this temporal variability may also mean that the range in $\delta^{18}O_{rt}$ values within a sample reflects the seasonal variation in the average $\delta^{18}O$ of local meteoric water.

Table 5.29: *Intra-population ranges in the $\delta^{18}O$ values of teeth from modern voles. The isotope data for the vole teeth from Germany are sourced from Gehler et al. (2012).*

Study site	**Species**	**Tooth type**	**Intra-population range in $\delta^{18}O_{rt}$ (‰)**
West Horrington, Somerset	*Microtus agrestis*	Molars and incisors	1.9 – 2.6
Cobham, Surrey	*Microtus agrestis*	Molars and incisors	2.8 – 4.5
Beeford, East Yorkshire	*Microtus agrestis*	Molars and incisors	2.1 – 2.7
Perthshire, Scotland	*Microtus agrestis*	Molars and incisors	1.2 – 2.8
North Rhine-Westphalia, Germany	*Microtus agrestis*	Incisors	2.9
	Microtus arvalis		3.8
	Arvicola terrestris		3.9
	Myodes glareolus		3.5

5.6.1.2. Inter-tooth variability in $\delta^{18}O$ values

In general, the $\delta^{18}O$ values of the *M. agrestis* molars from Britain fall within ± 1.5‰ of each other, and differences between molars and incisors from the same mandible are less than 2‰. These inter-tooth ranges are consistent with modern *A. terrestris* specimens from Germany (Table 5.30). This suggests that $\delta^{18}O$ offsets between teeth from the same individual may be relatively comparable across different vole species.

However, occasionally, differences between the $\delta^{18}O$ values of *M. agrestis* teeth are greater than those reported by Gehler et al. (2012) for *A. terrestris*. For example, inter-tooth ranges of 2-4‰ are observed for the Somerset population, due to the depleted $\delta^{18}O$ values of the first molars. Likewise, ranges in the $\delta^{18}O$ values of upper and lower teeth from the same individual can reach up to ~3-4‰. The magnitude of this variability within an individual is comparable to the intra-population ranges in $\delta^{18}O$ values for a single tooth type. This demonstrates that inter-tooth differences can contribute significantly to the variability in $\delta^{18}O_{rt}$ values within a sample. Consequently, the precision of the calculated average $\delta^{18}O_{rt}$ value for a population is likely to be lower for samples that comprise both molars and incisors.

Nevertheless, across the four study sites, there is no consistency in the direction of the $\delta^{18}O$ offsets between molars and incisors from the same individual. This is in contrast to the findings of Gehler et al. (2012), who report that the $\delta^{18}O$ values of *A. terrestris* incisors are typically slightly enriched compared to the molars. The only *M. agrestis* population in Britain for which this pattern is observed is Perthshire. However, for Somerset, Surrey and East Yorkshire, the M_2 or M_3 are generally slightly enriched or depleted relative to the other teeth from the same individual. This may partly result from small inaccuracies in the isotopic measurements of these molars, due to the small sizes of the samples.

Despite this, in most cases, the average $\delta^{18}O$ values of *Microtus* molars and incisors from the same population are not statistically different. These results are in agreement with the findings of Royer et al. (2013a), who examined composite $\delta^{18}O$ data from multiple vole species and populations. Navarro et al. (2004) likewise suggest that inter-tooth isotopic variations are

likely to be insignificant in arvicoline rodents. Nevertheless, the depleted first molars from Somerset and enriched incisors from Perthshire demonstrate that although inter-tooth $\delta^{18}O$ offsets are generally minor and follow no consistent pattern, occasionally, the $\delta^{18}O$ values of certain teeth can vary widely from the population as a whole.

Table 5.30: *Intra-jaw variation in tooth $\delta^{18}O$ values for modern voles. The data from Germany were sourced from Gehler et al. (2012).*

Study site	**Species**	**Intra-jaw range in $\delta^{18}O_{rt}$ (‰)**
West Horrington, Somerset	*Microtus agrestis*	1.4 – 3.5
Cobham, Surrey	*Microtus agrestis*	0.3 – 3.1
Beeford, East Yorkshire	*Microtus agrestis*	0.2 – 2.2
Perthshire, Scotland	*Microtus agrestis*	0.7 – 2.6
North Rhine-Westphalia, Germany	*Arvicola terrestris*	0.3 – 1.9

These variations in the $\delta^{18}O$ values of molars and incisors can be attributed to differences in the periods of tooth mineralization (Royer et al., 2013a). As aforementioned, $\delta^{18}O_{mw}$ varies seasonally, and thus teeth that mineralize during different seasons will record different average $\delta^{18}O$ values of drinking water. In vole species such as *M. agrestis* and *A. terrestris*, molars and incisors grow continuously throughout the life of the animal in order to replenish tooth surfaces lost through wear (Alibhai & Gipps, 1991). As a consequence, the $\delta^{18}O$ values of these teeth will reflect the average $\delta^{18}O$ of water ingested during the interval preceding the animal's death (Navarro et al., 2004). Vole incisors are typically renewed every ~6-8 weeks (Klevezal et al., 1990; Ruddy, 2005), whereas the complete regeneration of *Microtus* molars occurs within 8-12 weeks (von Koenigswald & Golenishev, 1979). These small offsets in the period of mineralization may therefore lead to differences between the $\delta^{18}O$ values of molars and incisors.

Additionally, Royer et al. (2013a) suggest that the smaller teeth of *Microtus* may provide a shorter averaged record of $\delta^{18}O_{mw}$ compared to the larger teeth of *A. terrestris*. Therefore, the $\delta^{18}O$ values of *M. agrestis* teeth may be more sensitive to short-term fluctuations in $\delta^{18}O_{mw}$. This may explain why some *M. agrestis* individuals have relatively large inter-tooth $\delta^{18}O$ offsets compared to the *A. terrestris* individuals investigated by Gehler et al. (2012) (Table 5.30).

5.6.1.3. Variability in tooth and dietary $\delta^{13}C$ values

Intra-population ranges in the $\delta^{13}C$ values of modern *M. agrestis* teeth from Britain are generally 2-4‰ (Table 5.31). Gehler et al. (2012) found similar ranges for vole teeth from Germany (Table 5.31), although intra-jaw $\delta^{13}C$ ranges are often broader in *M. agrestis* than *A. terrestris* (Table 5.32). The pattern of increasing $\delta^{13}C$ values from the incisor to the third molar (i.e. from the proximal to the distal end of the tooth row), which is consistently observed in the British *M. agrestis* datasets, is likewise seen in the *A. terrestris* data from Gehler et al. (2012). The $\delta^{13}C$ values of *A. terrestris* incisors are typically 0.5-1‰ more depleted than the molars, whereas *M.* agrestis incisors are generally 0.5-2‰ more depleted relative to the molars. Again, this suggests that the $\delta^{13}C$ values of *M. agrestis* teeth are more variable compared to *A. terrestris* teeth.

This inter-tooth variability in $\delta^{13}C$ values reflects spatial and temporal variations in the $\delta^{13}C$ compositions of the rodents' diets. The composition of the diet will vary depending on the availability of food resources within the home range of each rodent (Ferns, 1976). *M. agrestis* predominantly feeds on the stems and leaves of grasses (Hansson, 1971; Ferns, 1976; Alibhai & Gipps, 1991; Butet & Delettre, 2011). However, the $\delta^{13}C$ values of these grasses are likely to be spatially heterogeneous due to: 1) variations between plants in the degree of carbon isotope fractionation during photosynthesis, and 2) local variations in environmental factors, such as light and moisture availability (O'Leary, 1981; Tieszen, 1991). These variations will be correspondingly recorded in the $\delta^{13}C$ values of the *M. agrestis* teeth.

Table 5.31: *Intra-population ranges in the $\delta^{13}C$ values of modern vole teeth. The isotope data for Germany are from Gehler et al. (2012).*

Study site	Species	Tooth type	Intra-population range in $\delta^{13}C_{rt}$ (‰)
West Horrington, Somerset	*Microtus agrestis*	Molars and incisors	1.7 – 2.3
Cobham, Surrey	*Microtus agrestis*	Molars and incisors	3.8 – 4.6
Beeford, East Yorkshire	*Microtus agrestis*	Molars and incisors	3.1 – 4.6
Perthshire, Scotland	*Microtus agrestis*	Molars and incisors	1.8 – 4.0
North Rhine-Westphalia, Germany	*Microtus agrestis*	Incisors	1.9
	Microtus arvalis		4.0
	Arvicola terrestris		1.8
	Myodes glareolus		2.2

Table 5.32: *Intra-jaw ranges in the $\delta^{13}C$ values of modern vole teeth. The isotope data for Germany are from Gehler et al. (2012).*

Study site	Species	Intra-jaw range in $\delta^{13}C_{rt}$ (‰)
West Horrington, Somerset	*Microtus agrestis*	1.0 – 2.3
Cobham, Surrey	*Microtus agrestis*	0.5 – 3.2
Beeford, East Yorkshire	*Microtus agrestis*	0.9 – 3.9
Perthshire, Scotland	*Microtus agrestis*	1.1 – 4.1
North Rhine-Westphalia, Germany	*Arvicola terrestris*	0.3 – 1.5

The diet of *M. agrestis* also varies seasonally. Herbaceous plants, mosses, fungi and insects constitute an increased proportion of the diet during summer and autumn, whereas graminoids (grasses and sedges) are the dominant component of the diet during winter (Hansson, 1971; Ferns, 1976). Graminoids, mosses and fungi have slightly different $\delta^{13}C$ compositions, and thus seasonal variations in the relative consumption of these food sources will lead to temporal differences in the $\delta^{13}C$ values of *M. agrestis* teeth (Calandra et al., 2015). Indeed, Calandra et al. (2015) found that the $\delta^{13}C$ values of *M. agrestis* incisors from Finnish Lapland differed depending on the season of tooth mineralization. Teeth that mineralized during winter-spring had $\delta^{13}C$ values that were 1-2‰ higher than teeth that formed during summer-autumn.

This may provide an explanation for the consistent patterns of inter-tooth differences observed for the vole populations from Britain and Germany, whereby $\delta^{13}C_{incisor} < \delta^{13}C_{molar}$. As aforementioned, molars and incisors mineralize over slightly different periods of time, with incisors representing a more recent interval prior to death relative to the molars. Vole populations increase in size during spring and summer (Alibhai & Gipps, 1991), and thus the sampled populations may be predominantly comprised of individuals that were predated during these seasons. The trend from the enriched $\delta^{13}C$ values of the molars to the depleted incisors may therefore reflect a transition from the isotopically-enriched diets consumed during spring, to the more diverse and isotopically-depleted diets of summer.

Variations in the duration of tooth mineralization may also contribute to the differences in the ranges in $\delta^{13}C_{rt}$ values between *M. agrestis* and *A. terrestris*. As suggested for the $\delta^{18}O$ results, *M. agrestis* teeth may provide a higher resolution record of changing environmental conditions, due to their smaller size relative to *A. terrestris* teeth (Royer et al. 2013a). The dampening of short-term variations in dietary $\delta^{13}C$ values is consequently less pronounced within *M. agrestis* teeth, and as a result, inter-tooth $\delta^{13}C$ variability is greater. Moreover, *M. agrestis* typically consumes a more diverse range of food items compared to *A. terrestris*, including mosses, fungi and insects (Hansson, 1971; Butet & Delettre, 2011). This may additionally contribute to the broader inter-tooth $\delta^{13}C$ ranges in *M. agrestis*.

Given that the $\delta^{13}C$ value of mammalian bioapatite has a known relationship with the average $\delta^{13}C$ of the diet ($\delta^{13}C_d$), the carbon isotope results from the *M. agrestis* teeth can also be used to calculate the mean $\delta^{13}C$ value of the rodents' diets. The average $\delta^{13}C$ enrichment between bioapatite and the diet in modern vole teeth is +11.5‰ (Passey et al., 2005). The $\delta^{13}C_d$ values for the sampled *M. agrestis* individuals from Britain therefore range between around -33.0 and -25.5‰. The mean $\delta^{13}C$ values of the diet for the Somerset, Surrey and Perthshire populations fall between -28.6 and -28.2‰, while the mean $\delta^{13}C_d$ for East Yorkshire is -30.2‰. These values suggest that the rodents solely consumed C_3 plants. This is consistent with our knowledge of the modern vegetation in Britain. Inter-site differences in the mean $\delta^{13}C_{rt}$ values likely result from the natural variability in the $\delta^{13}C$ values of C_3 plants (Figure 2.2).

5.6.2. Relationship between the $\delta^{18}O$ values of rodent teeth and local water

In order to utilize the $\delta^{18}O$ values of rodent teeth for reconstructing past climatic conditions, the relationship between the $\delta^{18}O$ of rodent tooth carbonate and the $\delta^{18}O$ of local water must first be quantified and understood. The results of this modern analogue study suggest that the mean $\delta^{18}O$ values of *M. agrestis* teeth and meteoric water are spatially related, but only for sites in England (Figure 5.27). This spatial relationship results from the close connection between the average $\delta^{18}O$ of local precipitation and the average $\delta^{18}O$ values of meteoric water sources, from which rodents obtain their drinking water. In Britain, the north-eastward depletion in the average $\delta^{18}O$ of surface meteoric waters (Figure 5.25) is paralleled by the spatial trend in the $\delta^{18}O$ values of precipitation and groundwater (Figure 3.2) (Darling et al., 2003; Darling & Talbot, 2003). This trend results from the progressive rainout of the heavier ^{18}O isotope as moisture travels north-eastwards from its Atlantic Ocean source (Darling & Talbot, 2003).

The $\delta^{18}O$ of precipitation also varies at a single location, due to daily and seasonal changes in temperature (Darling & Talbot, 2003). In contrast,

intra-annual variability in the $\delta^{18}O$ values of rivers is significantly dampened, due to the contribution of groundwater discharge to the total river flow (Darling et al., 2003; Darling & Bowes, 2016). In lowland England, the average $\delta^{18}O$ of groundwater is similar to the mean annual $\delta^{18}O$ of precipitation (Darling et al., 2003; Brown et al., 2011). As a result, average $\delta^{18}O$ values of surface water sources are a close reflection of the mean annual $\delta^{18}O_{pt}$, but with an evaporative enrichment of ~1‰. Since rodents inherit the $\delta^{18}O$ values of their drinking water sources, the average $\delta^{18}O$ values of the *M. agrestis* teeth follow a spatial trend that is comparable to meteoric water and precipitation, whereby values gradually decrease from Somerset to East Yorkshire (Figure 5.24). A strong positive linear relationship is consequently generated between mean $\delta^{18}O_{rt}$ and mean $\delta^{18}O_{mw}$ across lowland England (Figure 5.27b).

Conversely, in highland areas of Scotland, the hydrological controls on $\delta^{18}O_{mw}$ are more complex. Groundwater recharge can be greatest during the coldest months of the year, due to the high levels of precipitation during winter, followed by the melting of snow in early spring (Soulsby et al., 2000). The $\delta^{18}O$ values of streams and groundwaters in these areas are therefore influenced by the input of isotopically-depleted water during winter and spring (Soulsby et al., 2000; Speed et al., 2011). As a consequence, average $\delta^{18}O_{mw}$ values can be depleted relative to the mean annual $\delta^{18}O$ of precipitation. This has been observed in the Allt a' Mharcaidh catchment, which is located in the western Cairngorm Mountains ~80 km northwest of Perthshire (Soulsby et al., 2000). This pattern is also evident in the Perthshire data, as the measured $\delta^{18}O$ values of meteoric water (Figure 5.25) are significantly lower than the modelled mean $\delta^{18}O_{pt}$ (Figure 5.26).

Nevertheless, in the Dee Catchment, ~70 km north of Perthshire, average $\delta^{18}O_{mw}$ values are generally 0.5-1‰ more enriched than the mean $\delta^{18}O_{pt}$ (Speed et al., 2011). Thus in Scotland, $\delta^{18}O_{mw}$ values may not always parallel the mean annual $\delta^{18}O_{pt}$. Also, since the water samples from Perthshire were collected during spring, their $\delta^{18}O$ values may reflect a short-term depletion in $\delta^{18}O_{mw}$ due to the input of snowmelt. Therefore, the average $\delta^{18}O$ value of the water samples may not provide an accurate value for the mean annual $\delta^{18}O_{mw}$.

While the $\delta^{18}O_{mw}$ value for Perthshire is depleted, the average $\delta^{18}O_{rt}$ and modelled $\delta^{18}O_{pt}$ values for this site are comparatively enriched. This may suggest that the $\delta^{18}O$ values of the rodent teeth reflect the average annual $\delta^{18}O$ of precipitation. Alternatively, since the owl pellets were collected in November, the sampled teeth may have predominantly mineralized during late summer and autumn, when $\delta^{18}O_{mw}$ compositions might have been relatively enriched. The tooth data may therefore be biased towards enriched values that are not representative of the mean annual $\delta^{18}O$ of local meteoric water. Despite this, the $\delta^{18}O_{rt}$ dataset from Perthshire is large and normally distributed, and thus any seasonal bias in the data is likely to be fairly minor.

The discrepancy between the $\delta^{18}O_{mw}$ and $\delta^{18}O_{pt}$ values for Perthshire may also be due to uncertainties in the modelled mean $\delta^{18}O$ values of precipitation. The prediction error on modelled $\delta^{18}O_{pt}$ values is greater in areas with fewer GNIP stations to use in the spatial interpolation of $\delta^{18}O_{pt}$ data (Bowen & Revenaugh, 2003). There are very few stations in northern Europe with long-term measurement records; the nearest stations to Perthshire are Armagh in northern Ireland (340 km SW of Perthshire), Keyworth in Nottingham (440 km SSE), and a former station near to Vestbygd on the southwestern tip of Norway (600 km ENE) (IAEA/WMO, 2018). Due to this low spatial resolution in the data, the 95% confidence intervals on mean annual $\delta^{18}O_{pt}$ estimates are relatively high for northern Europe (Bowen & Revenaugh, 2003).

This is seen with the modelled $\delta^{18}O_{pt}$ data for Perthshire. As shown in Figure 5.24, the $\delta^{18}O$ values of the teeth from Perthshire are similar to those from Surrey. Conversely, the modelled $\delta^{18}O$ of precipitation for Perthshire is much more enriched than for Surrey, and does not lie on the GMWL (Figure 5.26). Nevertheless, the 95% confidence intervals on the $\delta^{18}O_{pt}$ for Perthshire are large, and the lower boundaries of these uncertainties overlap with the $\delta^{18}O_{pt}$ for Surrey (Figure 5.26). Thus, the true mean annual $\delta^{18}O_{pt}$ for Perthshire could potentially lie closer to that for Surrey at around -7‰.

Furthermore, the $\delta^{18}O_{pt}$ spatial model, developed by Bowen & Wilkinson (2002), does not account for local rainout effects. This model is primarily based upon variations in $\delta^{18}O_{pt}$ with latitude and altitude, while local $\delta^{18}O_{pt}$ variability is accounted for by the spatial interpolation of data between

measurement stations (Bowen & Wilkinson, 2002). As aforementioned, few GNIP stations currently exist in northern Europe, and thus local $\delta^{18}O_{pt}$ variability in this region is poorly represented by the model. Moreover, in addition to the latitude, altitude and continental effects, the $\delta^{18}O$ of precipitation in eastern Scotland is influenced by orographic effects induced by the Scottish Highlands to the west (Darling et al., 2003). As a consequence, $\delta^{18}O_{mw}$ values in eastern Scotland are ~2‰ lower than in western Scotland (Darling et al., 2003). In contrast, the $\delta^{18}O_{pt}$ model predictions for eastern Scotland are comparable to or ~1‰ higher than those for western Scotland (Bowen & Revenaugh, 2003; Bowen, 2017; Bowen, 2018). This clearly indicates that the modelled $\delta^{18}O_{pt}$ values for Perthshire are likely to be inaccurate as well as imprecise.

Inaccuracies in the modelled mean annual $\delta^{18}O_{pt}$ values may also partly explain why the slopes of the relationships between $\delta^{18}O_{rt}$ and $\delta^{18}O_{mw}$ (Equation 5.8, Figure 5.27b), and $\delta^{18}O_{rt}$ and $\delta^{18}O_{pt}$ (Equation 5.10, Figure 5.28b), are significantly different. These differences are discussed further in the following section.

In summary, the mismatch between the $\delta^{18}O$ values of the teeth and the $\delta^{18}O$ of local water from Perthshire may be due to a combination of three factors: 1) the measured $\delta^{18}O$ values of meteoric water are depleted relative to the mean annual $\delta^{18}O_{mw}$, due to the input of isotopically-depleted snowmelt during spring, 2) the measured mean $\delta^{18}O_{rt}$ may be enriched relative to the mean annual $\delta^{18}O_{rt}$ because of a seasonal bias in mineralization, and 3) the modelled $\delta^{18}O$ of precipitation is an inaccurate and imprecise estimate for the mean annual $\delta^{18}O_{pt}$. These findings consequently highlight the need for additional, higher-resolution isotope data for rodent teeth and meteoric water sources from Scotland. A higher spatial resolution in the isotope measurements on precipitation is also required in order to improve the reliability of modelled $\delta^{18}O_{pt}$ values for this region.

5.6.3. Regression equations

5.6.3.1. Slope coefficient

Several linear regression equations have been developed for the relationship between the $\delta^{18}O$ of phosphate in rodent bioapatite and the $\delta^{18}O$ of environmental water (Luz & Kolodny, 1985; D'Angela & Longinelli, 1990; Longinelli et al., 2003; Navarro et al., 2004; Royer et al., 2013a). However, this is the first study to have generated equations for the $\delta^{18}O$ of mammalian tooth carbonate from mid-latitude regions. The regression for the relationship between the $\delta^{18}O$ of *M. agrestis* tooth carbonate and the $\delta^{18}O$ of meteoric water (Equation 5.9) is compared with published calibration lines in Figure 5.29a. Within the 1σ uncertainties, the slope coefficient for the *M. agrestis* regression (1.36 ± 0.11) is comparable to the slopes of the calibration lines generated by Royer et al. (2013a) for vole teeth from across Europe (1.14 ± 0.18), and Longinelli et al. (2003) for mice and vole bones from central Europe (1.14) (Figure 5.29a). This suggests that the slope of the relationship between the $\delta^{18}O$ of rodent bioapatite and the $\delta^{18}O$ of environmental water is relatively consistent across Europe.

The slightly higher slope for the *M. agrestis* regression may be due to three key reasons. Firstly, there is often a fair degree of scatter in the relationship between $\delta^{18}O_{rt}$ and the $\delta^{18}O$ of local water (Royer et al., 2013a). This scatter may result from small differences between the $\delta^{18}O$ of the rodents' drinking water and the measured or modelled mean $\delta^{18}O$ of environmental water. Secondly, only three sites were used in the linear regression analysis, and thus the *M. agrestis* regression may reflect this variability in the relationship between $\delta^{18}O_{rt}$ and $\delta^{18}O_{mw}$. Lastly, the slope of the regression may vary as a result of inter-species differences in the degree of oxygen isotope fractionation between drinking water and body water. This variation in fractionation could be due to differences in the contribution of food water to the total oxygen flux (Royer et al., 2013a). For example, Velivetskaya et al. (2014) demonstrated that the slope of the calibration between $\delta^{18}O_{rt}$ and temperature differs between *Microtus* spp. and other species of voles and mice.

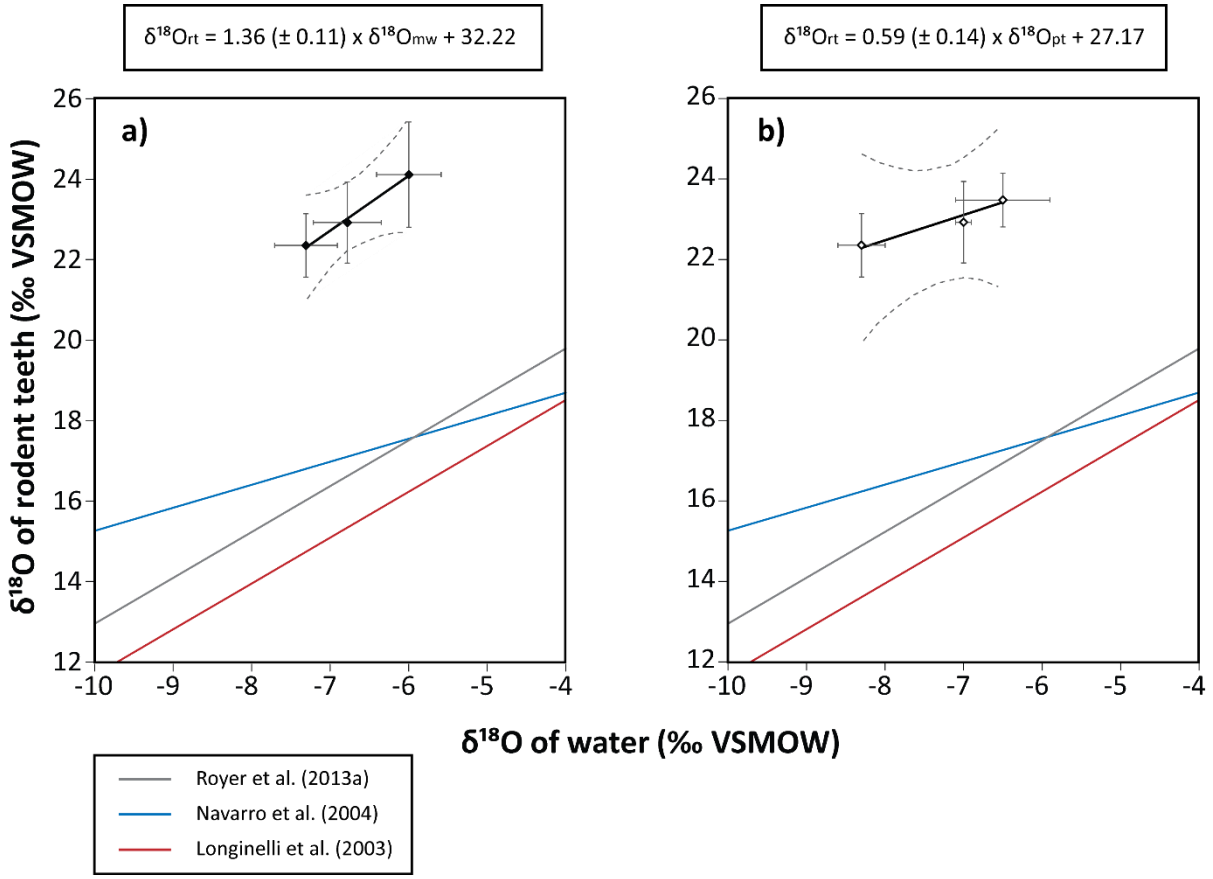

Figure 5.29: *Regressions between a) the $\delta^{18}O$ of* M. agrestis *tooth carbonate and meteoric water, and b) the $\delta^{18}O$ of* M. agrestis *tooth carbonate and precipitation. The regressions are compared with published calibrations for the $\delta^{18}O$ of rodent phosphate.*

On the other hand, the slope of the regression between *M. agrestis* $\delta^{18}O_{rt}$ and $\delta^{18}O_{mw}$ differs significantly from the slope of the calibration produced by Navarro et al. (2004) (0.57 ± 0.07) (Figure 5.29a). This equation relates the $\delta^{18}O$ of vole tooth phosphate to the measured $\delta^{18}O$ of precipitation, and thus would be expected to be comparable to the other published calibrations for rodent phosphate. Despite this, the relationship between *M. agrestis* $\delta^{18}O_{rt}$ and the modelled $\delta^{18}O$ of precipitation has a similar slope of 0.59 ± 0.14 (Figure 5.29b). This demonstrates that the data selected for the $\delta^{18}O$ of environmental water (measured surface water vs. measured or modelled precipitation) can have a significant influence on the modelled slope of a regression.

Longinelli et al. (2003) also found that errors in the slope coefficient of a regression can potentially arise from the use of inaccurate $\delta^{18}O$ values of environmental water. The relationship between the $\delta^{18}O$ of mice bone phosphate and $\delta^{18}O_{pt}$ for central Europe was first investigated by D'Angela & Longinelli (1990). This study yielded an equation with a slope coefficient of 0.79. However, subsequent improvements in our knowledge of the $\delta^{18}O$ values of precipitation in Europe showed that for certain sites, the original $\delta^{18}O_{pt}$ estimates were unreliable (Longinelli et al., 2003). The regression was therefore re-quantified using updated $\delta^{18}O_{pt}$ data, generating a relationship with a significantly different slope of 1.14. This shows that the differences in the slopes of the relationships between *M. agrestis* $\delta^{18}O_{rt}$ and $\delta^{18}O_{mw}$, and $\delta^{18}O_{rt}$ and $\delta^{18}O_{pt}$, may partly result from unreliable $\delta^{18}O_{pt}$ estimates. As aforementioned, the mean $\delta^{18}O_{pt}$ for Perthshire may be particularly unreliable. Given these possible inaccuracies in the $\delta^{18}O_{pt}$ values, the strong correlation observed between $\delta^{18}O_{rt}$ and $\delta^{18}O_{pt}$ (Figure 5.29b) may be simply coincidental. In addition, since the regression between *M. agrestis* $\delta^{18}O_{rt}$ and $\delta^{18}O_{mw}$ (Figure 5.29a) is broadly comparable to published calibrations that are based upon reliable $\delta^{18}O_{pt}$ values (Longinelli et al., 2003; Royer et al., 2013a), it can be argued that this regression provides a more accurate reflection of the true relationship between the $\delta^{18}O$ of arvicoline tooth carbonate and the $\delta^{18}O$ of environmental water in mid-latitude regions.

Nevertheless, small differences between equations that use meteoric water or precipitation data might be expected. This is because the influence of

evaporative enrichment causes the $\delta^{18}O$ values of meteoric water to deviate from the Global Meteoric Water Line (Figure 5.25). Furthermore, the degree of evaporative enrichment varies depending on the geographic location. For example, water bodies in southern Britain may be expected to experience a slightly greater evaporative enrichment than those in northern Britain, due to warmer temperatures and lower relative humidities. Indeed, increased evaporation in southwest Britain may explain why $\delta^{18}O_{mw}$ values in Somerset are enriched compared to those in Surrey (Figure 5.25), while $\delta^{18}O_{pt}$ values for these sites are comparable (Figure 5.26). Moreover, water bodies in highland areas are additionally affected by inputs of $\delta^{18}O$-depleted snowmelt. Therefore, across a geographic region, the offset between $\delta^{18}O_{mw}$ and $\delta^{18}O_{pt}$ is likely to vary. The $\delta^{18}O$ values of rodent teeth will consequently have slightly different relationships with the mean $\delta^{18}O$ values of meteoric water and precipitation. Since rodents drink from surface water sources, the $\delta^{18}O$ values of their teeth are more directly linked to the $\delta^{18}O$ of meteoric water than the $\delta^{18}O$ of precipitation. It is therefore suggested that the modern *M. agrestis* relationship between $\delta^{18}O_{rt}$ and $\delta^{18}O_{mw}$ (Equations 5.8 and 5.9) is more appropriate for reconstructing past environmental conditions than the relationship between $\delta^{18}O_{rt}$ and $\delta^{18}O_{pt}$.

5.6.3.2. Y-Intercept

The y-intercepts for the regressions based on *M. agrestis* tooth carbonate (Equation 5.9) and rodent phosphate (D'Angela & Longinelli, 1990; Longinelli et al., 2003; Navarro et al., 2004; Royer et al., 2013a) are offset by a factor of between 7.9 and 11.2‰ (Figure 5.29a). These offsets are consistent with the measured $\delta^{18}O$ differences between the carbonate and phosphate ions of modern rodent bioapatite (8.5-11.4‰) (Kirsanow & Tuross, 2011; Gehler et al., 2012). This indicates that both carbonate and phosphate in bioapatite have comparable fractionation relationships with the $\delta^{18}O$ of drinking water. This is to be expected, as carbonate and phosphate mineralize in isotopic equilibrium with the same water source (body water), but the isotopic fractionation during mineralization differs depending on the mineral ion (Iacumin et al., 1996). As

a result, both the $\delta^{18}O$ of rodent tooth carbonate and the $\delta^{18}O$ of rodent phosphate can potentially be used to reconstruct palaeoenvironmental conditions. This is provided that no diagenetic alteration of the fossil carbonate has occurred.

5.6.3.3. Uncertainties in the regression line

The uncertainties in the fit of the regression between $\delta^{18}O_{rt}$ and $\delta^{18}O_{mw}$ have implications for the application of this regression for reconstructing past $\delta^{18}O_{mw}$ values. The uncertainties are generally within ± 0.2‰ (Table 5.28), and thus are much smaller than the ranges in $\delta^{18}O_{rt}$ values within a modern vole population (Table 5.29). However, when extrapolating $\delta^{18}O_{mw}$ values beyond the regression line, the uncertainties are greater (up to ± 0.5‰). Consequently, for sites with $\delta^{18}O_{rt}$ values similar to today, the uncertainties in the calculated $\delta^{18}O_{mw}$ values will primarily result from variations in the $\delta^{18}O$ values of the sampled teeth, rather than uncertainties in the modern calibration (Pryor et al., 2014). Conversely, for sites with $\delta^{18}O_{rt}$ values much higher or lower than today, uncertainties in the modern calibration will have a greater influence on the overall uncertainty in the calculated $\delta^{18}O_{mw}$. This may prove to be a particular issue for reconstructing $\delta^{18}O_{mw}$ values from the cold climatic intervals of Westbury Cave and Gully Cave.

5.7. Conclusions: Implications for using $\delta^{18}O$ and $\delta^{13}C$ values of rodent teeth as palaeoenvironmental proxies

5.7.1. Implications of intra-population isotope variability

Previous studies on stable isotopes in rodent teeth have emphasized the importance of understanding modern isotope variability for the interpretation of isotope data from fossil teeth (Gehler et al., 2012; Royer et al., 2013a; Jeffrey et al., 2015). The results of this modern analogue study have shown that intra-population ranges in the $\delta^{18}O$ and $\delta^{13}C$ values of *Microtus agrestis* teeth are relatively broad, in agreement with previous research on vole teeth

from Europe. Spatial and temporal differences in the $\delta^{18}O$ values of local water sources and $\delta^{13}C$ values of plants are the most likely causes of this intra-population isotopic variability. This variability may reduce the precision with which the average $\delta^{18}O$ of past meteoric waters and the average $\delta^{13}C$ of past rodent diets can be reconstructed. In addition, differences in average isotope values between individuals within a population are sometimes statistically significant. Consequently, several teeth must be analysed per stratigraphic unit in order to capture the natural isotopic variability within a population, and to ensure that the average isotope values for the sampled teeth accurately and precisely reflect the population mean.

Moreover, as suggested by Royer et al. (2013a), variations in the ranges in $\delta^{18}O_{rt}$ values could potentially provide information on past changes in the seasonality of the climate. Obtaining a representative sample of teeth for isotopic analyses is consequently essential for this purpose. Royer et al. (2013a) recommend that a minimum of 5 teeth, and ideally up to 10 teeth should be analysed per stratigraphic unit, to account for the isotopic variability between individuals within a population. The data obtained from the modern *M. agrestis* teeth support this recommendation. Therefore, where possible, this sample size recommendation was adopted for the following chapters on the isotope values of fossil rodent teeth from Britain.

5.7.2. Implications of inter-tooth isotope variability

The investigation on inter-tooth isotope variability has shown that, in general, the average $\delta^{18}O$ values of *M. agrestis* molars and incisors are not statistically different. This indicates that generally, arvicoline molars and incisors can both provide accurate values for the average $\delta^{18}O_{rt}$ of a population. This is important, as some fossil localities may preserve insufficient numbers of either tooth type for isotopic analysis.

Nevertheless, it is suggested that, where possible, analyses should be restricted to a single tooth type. This is because offsets in the period of tooth mineralization result in inter-tooth $\delta^{18}O$ and $\delta^{13}C$ differences. Consequently, mixed samples of molars and incisors have broader intra-population ranges in

isotope values. As aforementioned, this variability can reduce the precision of palaeoenvironmental reconstructions.

Additionally, fossil teeth should ideally be sampled and analysed separately, rather than being analysed as single bulk samples comprising multiple different teeth (e.g. Navarro et al., 2004; Royer et al., 2013a). This is because isotope variability between fossil teeth can result from: 1) natural inter-individual differences in $\delta^{18}O$ and $\delta^{13}C$ values within a population, 2) re-working and mixing of teeth from different time periods, or 3) diagenetic alteration. By combining teeth into a single bulk sample, isotope variability within the sample is averaged. As a result, potential outliers in the dataset are more difficult to identify, and the influences of re-working or diagenetic alteration cannot be fully assessed.

In order to analyse fossil teeth individually, a sufficient sample quantity must be obtained from each tooth for isotopic analysis. In this study, the *M. agrestis* second and third molars sometimes produced unreliable $\delta^{18}O$ results due to the small sizes of the samples. It is therefore recommended that larger *Microtus* sp. teeth, and specifically the lower or upper first molars or incisors, should be the preferred teeth for analysis. These sampling recommendations were consequently applied to the studies on Pleistocene rodent teeth from Britain, presented in the following chapters.

This study has also demonstrated that occasionally, the average $\delta^{18}O_{rt}$ of a sample may be significantly enriched or depleted compared to the population mean (i.e. the first molars from Somerset and incisors from Perthshire). Royer et al. (2013a) suggest that the mean $\delta^{18}O_{rt}$ of a dataset can only be interpreted as reflecting the mean annual $\delta^{18}O_{mw}$ if the dataset is normally distributed. Both the Somerset and Perthshire datasets are normally distributed (Figure 5.21). Therefore, a normal distribution does not necessarily indicate that the average $\delta^{18}O_{rt}$ of a dataset is an accurate reflection of the mean $\delta^{18}O_{rt}$ of the population, and the mean annual $\delta^{18}O_{mw}$. Therefore, caution must be taken when interpreting $\delta^{18}O$ data from a single tooth type.

While the average $\delta^{18}O$ values of vole molars and incisors are usually comparable, the $\delta^{13}C$ values of these teeth are consistently and significantly different. This is due to temporal variability in the $\delta^{13}C$ composition of the rodents' diet, and spatial heterogeneity in the local environmental conditions

that influence the $\delta^{13}C$ values of C_3 plants. Thus, when comparing $\delta^{13}C$ datasets based on the analyses of different tooth types, inter-tooth differences in $\delta^{13}C$ values should be taken into account. This is especially important for studies intending to use the $\delta^{13}C$ values of fossil vole teeth to reconstruct long-term temporal changes in palaeodiet or vegetation. The results also show that carbon isotope analyses of both molars and incisors may be useful for investigating seasonal shifts in the $\delta^{13}C$ value of the diet.

5.7.3. Relationship between the $\delta^{18}O$ of rodent bioapatite and $\delta^{18}O$ of environmental water

The mean $\delta^{18}O$ values of modern *M. agrestis* tooth carbonate show a strong relationship with the mean $\delta^{18}O$ values of local meteoric water sources in Britain (Equation 5.8, Figure 5.29a). The $\delta^{18}O$ of *Microtus* tooth carbonate can consequently be used as a proxy for reconstructing the past $\delta^{18}O$ of meteoric water. Moreover, although the modern calibration generated in this study is based upon data from only three sites, this calibration is considered valid and applicable to fossil arvicoline rodent teeth from northwest Europe, due to three key reasons. Firstly, the sites sampled in this study span a range in $\delta^{18}O_{mw}$ values across Britain of ~2‰. Across this limited variation in $\delta^{18}O_{mw}$, the mean $\delta^{18}O$ values of *M. agrestis* teeth show statistically significant differences between sites. The spatial differences in $\delta^{18}O_{rt}$ are consistent with the spatial variation in mean $\delta^{18}O_{mw}$ values, indicating that $\delta^{18}O_{rt}$ and $\delta^{18}O_{mw}$ are well correlated, even at small spatial scales (across ~5° of latitude). Secondly, although only four sites were studied, extensive numbers of teeth were analysed from each site. Given the scatter in $\delta^{18}O_{rt}$ values within rodent populations, generating a calibration based on large datasets from only a few sites is considered preferable to producing a calibration based on a few samples from many sites, as several previous modern analogue studies have done (e.g. Royer et al., 2013a). Finally, the regression for *M. agrestis* tooth carbonate parallels published calibrations that relate the $\delta^{18}O$ of rodent phosphate to the $\delta^{18}O$ of precipitation in Europe. This regression therefore supports previous studies, and demonstrates that the relationship between the

mean $\delta^{18}O$ of rodent bioapatite and the mean $\delta^{18}O$ of environmental water is relatively consistent across Europe. Consequently, Equation 5.8 will be used in the following chapters in order to quantify past $\delta^{18}O_{mw}$ values.

The small differences between Equation 5.8 and the published calibrations may suggest that inter-species differences in isotopic fractionation can influence the slope of a calibration. These differences may consequently be reflected in the existing calibrations that use the $\delta^{18}O$ values of tooth phosphate from multiple rodent taxa. Additional fractionation equations based on single rodent species are therefore needed to determine the importance of potential inter-species differences.

The results also show that the accuracy and precision of the $\delta^{18}O$ values of environmental water have an important influence on the slope coefficient of a regression line. The relationship between $\delta^{18}O_{rt}$ and the mean annual $\delta^{18}O$ of precipitation differs significantly from the relationship between $\delta^{18}O_{rt}$ and the mean $\delta^{18}O$ of meteoric water (Figure 5.29). This may be due to several reasons, including inaccurate and imprecise $\delta^{18}O_{pt}$ measurements, and variable offsets between $\delta^{18}O_{mw}$ and $\delta^{18}O_{pt}$ due to the influence of evaporation on meteoric water. Unreliable $\delta^{18}O_{pt}$ estimates, as well as seasonal snowmelt inputs, are also likely to be responsible for the mismatch between the $\delta^{18}O_{rt}$, $\delta^{18}O_{mw}$ and $\delta^{18}O_{pt}$ values for Perthshire. This demonstrates that a detailed understanding of the hydrological controls on the $\delta^{18}O$ values of drinking water sources, and the relationship between drinking water and precipitation $\delta^{18}O$ values, is essential for generating accurate isotope calibrations based on field data. Furthermore, high spatial and temporal resolutions in the isotope measurements of environmental water are important for obtaining accurate and precise mean annual $\delta^{18}O$ values of meteoric water and precipitation.

In summary, the $\delta^{18}O$ and $\delta^{13}C$ values of rodent tooth carbonate can potentially provide useful proxies for environmental conditions in mid-latitude regions. However the provisos outlined above should be taken into careful consideration when applying and interpreting these proxies. In the following chapter, the modern isotope relationship is applied to the $\delta^{18}O$ values of fossil rodent teeth from three interglacial sites in Britain, in order to reconstruct past $\delta^{18}O_{mw}$ values and mean summer palaeotemperatures.

6. Coupling the $\delta^{18}O$ values of rodent tooth and mollusc shell carbonates: testing a novel approach to reconstructing Pleistocene interglacial temperatures

6.1. Introduction

This chapter explores the applicability of coupling the $\delta^{18}O$ values of rodent teeth and mollusc shell carbonates for reconstructing Quaternary palaeotemperatures. This coupled isotope approach is applied to three Middle Pleistocene interglacial sites in Britain: 1) West Runton, Norfolk, 2) Cudmore Grove, Essex, and 3) Marsworth, Buckinghamshire. The locations of these study sites, plus other comparative sites mentioned in this chapter, are illustrated in Figure 6.1. The modern isotope relationship, developed in Chapter 5, is used to reconstruct the average $\delta^{18}O$ value of meteoric water ($\delta^{18}O_{mw}$) for each site from measured $\delta^{18}O$ values of fossil rodent teeth ($\delta^{18}O_{rt}$). The reconstructed $\delta^{18}O_{mw}$ values are then combined with measured or published $\delta^{18}O$ values of coeval mollusc shells ($\delta^{18}O_{ms}$), in order to calculate average growing season palaeotemperatures. These estimated temperatures are then compared with the published palaeoclimate evidence from each site to assess the consistency between the different approaches to palaeotemperature quantification. Carbon isotope results are also briefly described and interpreted in terms of past vegetation.

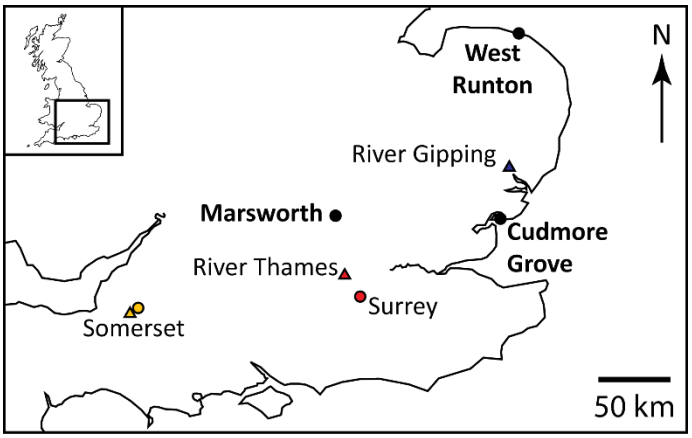

***Figure 6.1**: Locations of the sites mentioned in this chapter. The Pleistocene study sites are shown in bold. Modern* Microtus agrestis *tooth sampling sites are indicated by coloured circles, and modern sites from which mollusc shell and surface water isotope data were obtained are indicated by coloured triangles.*

6.2. Requirements and assumptions of the coupled isotope approach

As discussed in Section 2.4.2, Grimes et al. (2003) created an approach for obtaining palaeotemperature estimates, by combining the $\delta^{18}O_{mw}$ value calculated from rodent bioapatite, with the $\delta^{18}O$ values of co-existing freshwater proxies, such as mollusc shells. However, there are certain requirements for the application of this approach that must first be met. These requirements have been highlighted by Grimes et al. (2003; 2008), and are addressed here.

Firstly, in order for the $\delta^{18}O$ of meteoric water to be calculated from the $\delta^{18}O$ of rodent bioapatite, it must be demonstrated that the majority of the rodent's water intake was derived from drinking water rather than food water. The ecological preferences of the rodent taxa analysed in this research (*Arvicola* and selected species of *Microtus*) were reviewed in Section 4.2. This review demonstrated that these taxa typically live in humid environments, and thus are likely to obtain most of their water directly from surface water sources.

Consequently, the average $\delta^{18}O$ values of *Arvicola* and *Microtus* teeth can provide an accurate estimate of the average $\delta^{18}O$ of local meteoric water.

Coupling the $\delta^{18}O$ values of rodent bioapatite and freshwater mollusc shells is additionally dependent upon the assumption that these biominerals have precipitated from water with comparable $\delta^{18}O_{mw}$ values. For this assumption to be valid, the rodents must have primarily ingested water from the same local water source in which the freshwater shells mineralized. The teeth and shells must also be coeval. Therefore, the teeth and shells must have experienced minimal transport or post-depositional re-working, and must have accumulated during a short period of time, or an interval with relatively stable environmental conditions. Consequently, fossil remains from deposits that accumulated relatively quickly in a low-energy environment are the most suitable for use in the coupled isotope approach. As outlined in Chapter 3, West Runton, Cudmore Grove and Marsworth fulfil these requirements.

A third requirement of the approach is that the teeth and shells selected for isotopic analysis have not been diagenetically altered. The likelihood of alteration was addressed in Section 4.2.6. Evidence for the preservation of original isotopic signatures is also provided in the results section of this chapter. For all three study sites, it can be argued that the fossil material has experienced minimal diagenetic alteration.

Also, in order to calculate palaeotemperatures from the $\delta^{18}O$ values of fossil biominerals, modern calibrations that are specific to the biomineral and taxon being investigated are needed. In this study, the measured $\delta^{18}O$ values of fossil arvicoline tooth carbonate are used with the modern calibration relationship generated in Chapter 5 to calculate the mean $\delta^{18}O$ of past meteoric water. The mean $\delta^{18}O_{mw}$ value and the mean $\delta^{18}O$ value of the mollusc shells are then substituted into the calibration of White et al. (1999), in order to estimate the mean summer water temperature. As water temperatures for modern British lowland rivers closely match prevailing air temperatures (Waghorne et al., 2012), summer water temperatures calculated via the coupled isotope approach can potentially provide estimates for past summer air temperatures.

Finally, in order to test the reliability of the coupled isotope approach, and assess whether the aforementioned assumptions are valid, reconstructed

palaeotemperatures must be validated against independent temperature estimates (Fricke and Wing, 2004; Peneycad, 2013). As summarised in Chapter 3, a wealth of palaeoclimate information is available from the study sites, against which isotope-based temperature reconstructions can be compared.

In summary, the fossil material and study sites chosen for this research meet all of the requirements for the application of the coupled isotope approach. The following sections introduce the materials that were sampled for analysis, and the statistical methods that were applied to the isotope results.

6.3. Materials

6.3.1. West Runton, Norfolk

6.3.1.1. Sediment samples and sample processing

The rodent teeth for this study were obtained from sediment samples that were collected from site WR2 (Figure 3.4) by the Department of Geography at Royal Holloway University of London (Juby, 2004). The sediments were sampled every 5 cm through the West Runton Freshwater Bed (WRFB). The samples analysed for this thesis comprise nine small bags of sediment that range from 10-120 cm above the base of the WRFB. Each sample was soaked in warm water overnight, in order to disaggregate the sediment. The sediments were then washed through a stack of 2 mm, 1 mm and 0.5 mm sieves. The sieved residues were left to dry overnight at 50°C. Once dry, the > 2 mm and 1-2 mm residues were sorted under a low-powered optical microscope. Further details on the sediment samples are provided in Appendix D.

6.3.1.2. Rodent teeth selected for analysis

Only three of the nine sediment samples (30-35 cm, 40-45 cm and 50-55 cm) yielded small mammal teeth. These teeth were identified as: 1) an *Apodemus sylvaticus* upper molar, 2) a *Mimomys savini* lower first molar (M_1), 3) an upper

second molar (M^2), attributed to *M. savini*, and 4) a fragment of an upper incisor from a medium-sized rodent. The *A. sylvaticus* molar was considered too small for isotopic analysis, and thus analyses were only undertaken on teeth 2-4.

The *M. savini* M_1 is unrooted and has the distinctive '*Mimomys* fold' morphological feature (Figure 6.2a), whereas the upper second molar is rooted (Figure 6.2b). Only three small mammal taxa in the WRFB have rooted molars: 1) *M. savini*, which is the most abundant taxa at the site, 2) *Clethrionomys hintonianus* Kretzoi, 1958, and 3) *Pliomys episcopalis* Méhely, 1914 (Maul & Parfitt, 2010). Both *C. hintonianus* and *P. episcopalis* have relatively small teeth, while *M. savini* has comparatively large teeth (Maul & Parfitt, 2010). The length of the M^2 recovered in this study is larger than most of the *C. hintonianus* and *P. episcopalis* teeth from the WRFB, and thus the tooth has been attributed to *M. savini*.

The incisor fragment (Figure 6.2c) cannot be identified to species level. However, the width of the incisor is fairly narrow (1.3 mm), and is smaller than the widths of *M. savini* incisors from the WRFB (~1.6-2.1 mm) (Peneycad, 2013). This suggests that the incisor belongs to a smaller rodent taxon (e.g. *C. hintonianus*, *P. episcopalis* or *Microtus* sp.).

The two *M. savini* molars and incisor selected for analysis are well-preserved, and the broken edges of the incisor are unrounded. The good preservation of these teeth indicates that they did not undergo high-energy or long-distance transport before deposition.

6.3.1.3. Existing isotope data for West Runton

Nine *M. savini* upper incisors were analysed in a pilot study by Peneycad (2013). The incisors were collected in the early 1900s, and the section of the WRFB from which the teeth originate is unknown. However, given that the WRFB is thought to have accumulated fairly rapidly during an interval in which environmental conditions remained relatively stable (see Section 3.4.1), the isotope values of the three additional teeth are expected to be comparable to the values of the nine incisors.

Figure 6.2: *Photographs of the rodent teeth from West Runton that were selected for analysis: a) occlusal (left) and lingual (right) views of the* Mimomys savini *first lower molar, b) occlusal (left) and lingual (right) view of the* M. *cf.* savini *upper second molar, and c) the unidentified rodent upper incisor.*

Nevertheless, the nine incisors were pre-treated using different methods than the teeth in the current research. The incisors were treated with 10% hydrogen peroxide, rather than 30%, and no additional acetic acid treatment was used. To assess the impact of these differences in treatment methods on the isotope values of the teeth, three *Microtus agrestis* incisors were selected from the modern study sites (1 incisor each from, Somerset, Surrey, and East Yorkshire). Each tooth was crushed in bulk, and the powder divided into two samples. The first sample was soaked in 10% hydrogen peroxide for 24 hours (Treatment 1). The second sample was soaked in 30% hydrogen peroxide for 24 hours, rinsed 4 times with deionised water, and then treated with 1M acetic acid buffer solution for a further 24 hours (Treatment 2). Once treated, the samples were analysed at the Bloomsbury Environmental Isotope Facility (BEIF) to obtain oxygen and carbon isotope values.

The results in Table 6.1 show that isotopic differences between samples prepared using the two treatment methods generally fall within the 1σ uncertainties for measurements of rodent bioapatite at BEIF [± 0.20‰ for $\delta^{18}O$, and ± 0.12‰ for $\delta^{13}C$ (see Appendix B)]. Moreover, the $\delta^{18}O$ and $\delta^{13}C$ values of the teeth are comparable to the mean isotope values of the modern teeth from Somerset, Surrey and East Yorkshire (Chapter 5). Therefore, any larger isotopic offsets between the nine incisors analysed by Peneycad (2013) and the three additional teeth analysed for this thesis cannot be attributed to the differences in the treatment methods that were applied to the teeth.

Isotope analyses have also been undertaken on *Valvata piscinalis* shells from two sections of the WRFB: 1) 75 shells from the mammoth site at WR1 (Davies et al., 2000), and 2) 64 shells from ~50 m to the west at WR2 (Rose et al., 2008). The shells from WR2 originate from the same sediment sections as the two *M. savini* molars and the incisor fragment (Figure 6.2).

The isotope data from the *M. savini* incisors and *V. piscinalis* shells will be briefly presented in the results section of this chapter, to provide a context for the calculation of the palaeotemperatures using the coupled isotope approach. The data from the nine incisors will henceforth be referred to as Sample 1, and the data from the three additional teeth will be referred to as Sample 2.

Table 6.1: *Oxygen and carbon isotope results from modern* Microtus agrestis *lower incisors treated using 1) 10% hydrogen peroxide only, and 2) 30% hydrogen peroxide followed by 1M acetic acid buffer solution. The 1σ errors are the analytical uncertainties on the isotopic measurements.*

Site	**Treatment 1 (T1) (‰ VPDB)**				**Treatment 2 (T2) (‰ VPDB)**				**Difference in $\delta^{18}O$ (‰) (T1-T2)**	**Difference in $\delta^{13}C$ (‰) (T1-T2)**
	$\delta^{18}O$	**1σ Error**	**$\delta^{13}C$**	**1σ Error**	**$\delta^{18}O$**	**1σ Error**	**$\delta^{13}C$**	**1σ Error**		
Somerset	-6.1	0.10	-16.3	0.03	-6.1	0.10	-17.2	0.03	-0.1	0.8
Surrey	-7.8	0.10	-16.4	0.03	-7.9	0.10	-16.4	0.03	0.1	0.0
East Yorkshire	-7.3	0.10	-18.4	0.03	-7.4	0.10	-18.3	0.03	0.2	-0.2

6.3.2. Cudmore Grove, Essex

6.3.2.1. Rodent teeth selected for analysis

Fifteen *Arvicola cantiana* upper incisors from Unit 3 at Cudmore Grove were previously selected for analysis by Ruddy (2005). Ruddy (2005) analysed thirteen of these teeth to determine the $\delta^{18}O$ value of the enamel phosphate. Remaining small fragments of enamel from three of these incisors, plus the two complete incisors that were not originally analysed (Figure 6.3), were available for analysis in the current research.

The majority of the teeth analysed by Ruddy (2005) were well-preserved, with minimal breakage or rounding. Most of the teeth also showed evidence for digestion by a predator. Ruddy (2005) cleaned the teeth prior to analysis by placing each specimen in a glass vial containing deionised water, and then placing the vial within an ultrasonic bath. The teeth were subsequently dried at 90°C for ~1 minute. The dentine was separated from the enamel using a small rotary tool with a diamond-studded drill bit. These procedures are consistent with standard methods, and are unlikely to have affected the isotope values of the teeth.

The remaining enamel fragments and two complete teeth were further pre-treated and analysed according to the methods in Chapter 4. The complete teeth were crushed in bulk because: 1) all other teeth in this thesis were analysed in bulk, and 2) the isotope results from the complete teeth can be compared with the data obtained from the enamel fragments, in order to assess whether the dentine has experienced significant diagenetic alteration. If the dentine is well-preserved, the isotope values of the enamel fragments and bulk teeth should be comparable.

Comparison with the existing $\delta^{18}O$ data for enamel phosphate also enables the preservation of the enamel carbonate to be assessed. The $\delta^{18}O$ values of carbonate and phosphate in modern rodent bioapatite are typically offset by +8.5-11.4‰ (Gehler et al., 2012; Kirsanow & Tuross, 2011). Therefore, if the original isotopic values of the fossil enamel carbonate have been retained, the $\delta^{18}O$ offsets between the enamel carbonate and phosphate should be consistent with these published values.

Figure 6.3: *Photograph of one of the complete* Arvicola cantiana *incisors from Cudmore Grove (CG-4).*

6.3.2.2. Existing isotope data for Cudmore Grove

In addition to analysing the $\delta^{18}O$ of *A. cantiana* enamel phosphate, Ruddy (2005) also obtained $\delta^{18}O$ data from 27 *Valvata piscinalis* shells from Unit 3 at Cudmore Grove. As the tooth phosphate and shell isotope data are important for the interpretation of the tooth carbonate results in this study, and for the application of the coupled isotope approach, these data will be presented in the results section of this chapter.

6.3.3. Marsworth, Buckinghamshire

6.3.3.1. Sediment samples and sample processing

Sediment samples from Level 3 and Level 2 in the Lower Channel deposits at Marsworth were provided by the Buckinghamshire County Museum Resource Centre for this research. The sediments were collected during controlled excavations undertaken in 1981-1984, and the samples originate from a series of 1 m grid squares at site P3 (Murton et al., 2001). Four bags of sediment were obtained from Level 3 and ten bags were obtained from Level 2. All sediment samples were individually wet-sieved, and the > 2 mm, 1-2 mm,

0.5-1 mm and 0.25-0.5 mm size fractions retained. The > 2 mm and 1-2 mm residues from each sample were sorted under a low-powered optical microscope for mammalian and molluscan remains. Further details on the sediment samples are provided in Appendix D.

6.3.3.2. Rodent teeth selected for analysis

Complete teeth were absent from the deposits, and thus only tooth fragments could be analysed. Twelve molar and incisor fragments from Level 3 and eight fragments from Level 2 were selected for analysis. The largest tooth fragments were preferentially chosen to ensure that sufficient material could be obtained for isotopic analysis. Most of the teeth were too fragmented to enable identification to species level. However, all of the molars have the characteristic morphology of vole taxa belonging to the tribe Arvicolini. The molars are also unrooted and relatively small, and have therefore been attributed to the genus *Microtus*. The anterior cap is preserved on three of the selected first lower molars, and the morphology of this cap is characteristic of the species *Microtus oeconomus* (Figure 6.4a-b). Although rodent incisors are not generally diagnostic to species, all of the incisors are likewise relatively small. Given the dominance of molars attributable to *Microtus* sp., it is likely that most (if not all) of the incisors also originate from individuals of this genus.

As the selected teeth vary in terms of the tooth type (lower and upper molars and incisors) and the size of the fragment, it is unlikely that the period of time represented by each fragment is equivalent. Nevertheless, the results of the modern study (Chapter 5) indicate that $\delta^{18}O$ variability between *Microtus agrestis* molars and incisors from the same population is generally unsystematic. Therefore, the $\delta^{18}O$ values of the selected teeth are likely to be relatively comparable.

The taphonomic evidence from the mammalian remains indicates that the rodent teeth accumulated via various depositional agents (see Appendix D for full review). Evidence for digestion (Figures 6.4c-d) suggests that the deposition of pellets by Category 1-2 predators (e.g. the short-eared owl) likely contributed to the accumulation of the remains. The high degree of breakage

and slight rounding also suggests that the teeth may have been primarily transported and deposited into the Lower Channel during flood events. Since owls hunt over a restricted geographical area, and flood events are usually fairly rapid, the selected teeth likely record local environmental conditions over a relatively short period of time.

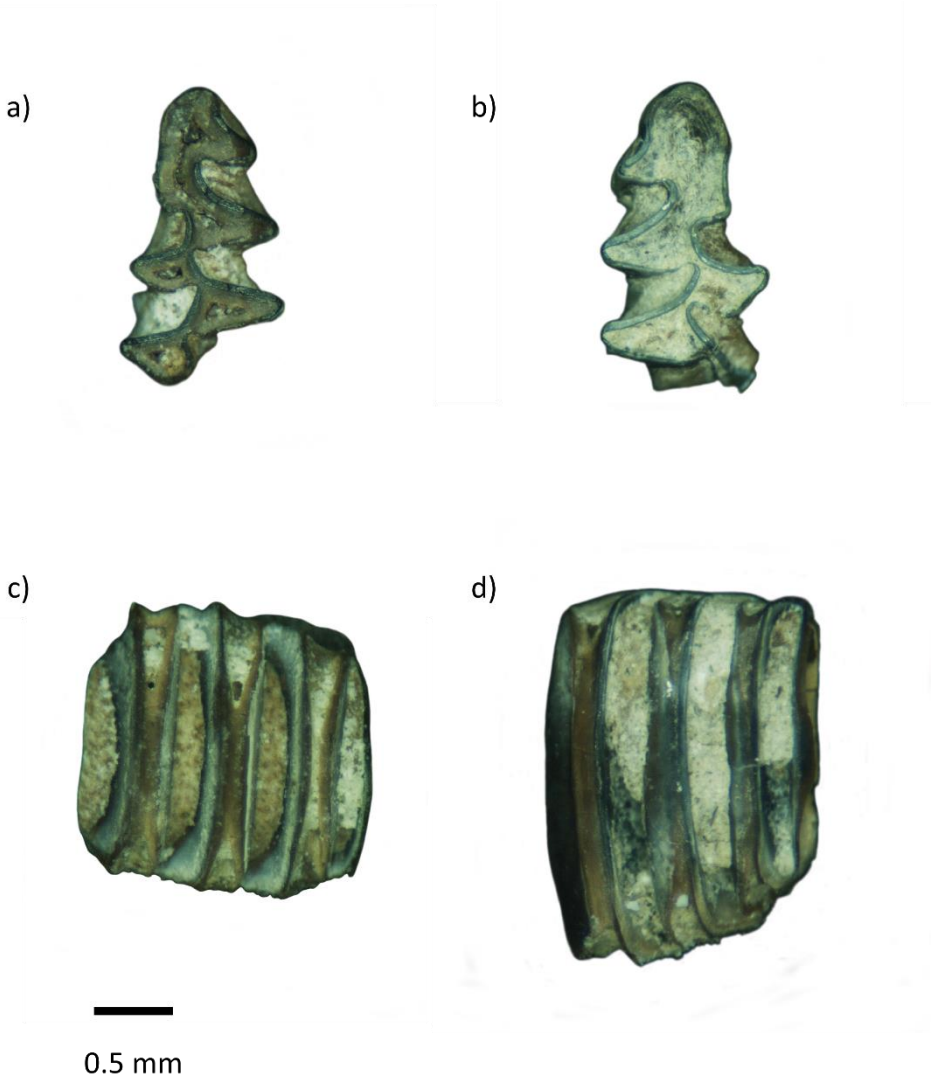

Figure 6.4: *Photographs of some of the rodent molars from Marsworth: a) fragment of a* Microtus oeconomus *lower left first molar from Level 3 (occlusal view), b) fragment of a* M. oeconomus *lower right first molar from Level 2 (occlusal view), c) a* Microtus *sp. lower right first molar from Level 3, which shows evidence for heavy digestion along the salient angles with the enamel largely removed, d) a* Microtus *sp. upper left third molar from Level 2, with evidence of moderate digestion along the salient angles.*

6.3.3.3. Mollusc shells selected for analysis

Isotope analyses on mollusc shells from Marsworth have not been previously undertaken. Thus, a small number of shells were selected for analysis in this study. The only aquatic or amphibious species that was abundant in both Levels 3 and 2 is *Galba truncatula*. Analyses were therefore undertaken on two *G. truncatula* shell fragments from Level 3, and eighteen shell fragments from Level 2 (Figure 6.5). All shell fragments consist of 3-4 whorls at the apex of the shell, representing shell aragonite that mineralized in the first few weeks after hatching during spring.

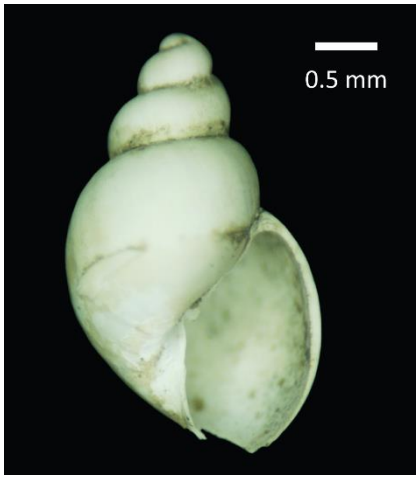

Figure 6.5: *Photograph of a* Galba truncatula *shell from Level 2 at Marsworth (MA-2-G13).*

6.4. Methods

The rodent teeth and mollusc shells were analysed to determine their oxygen and carbon isotope values. X-Ray Diffraction analyses were also undertaken on the 5 largest shell samples from Marsworth (1 shell from Level 3, 4 shells from Level 2). All pre-treatment and analytical procedures are described in Chapter 4. The following section outlines the statistical methods used in order to calculate the mean $\delta^{18}O$ value of meteoric water and mean summer palaeotemperature for the three study sites.

6.4.1. Descriptive statistics

Basic descriptive statistics were generated for all isotope datasets. Shapiro-Wilk tests were undertaken to determine whether the datasets are normally distributed, and Grubbs' tests were undertaken to identify potential outliers. Correlations between the $\delta^{18}O$ and $\delta^{13}C$ data were assessed by calculating the Pearson's correlation coefficient (r^2) and associated significance level (*p*). The statistical significance of the differences in mean isotope values between WR1 and WR2 at West Runton, and Levels 3 and 2 at Marsworth, was calculated using T-tests (for normally distributed data) or Mann-Whitney tests (skewed data). The confidence level was set at 95% ($\alpha = 0.05$) for all tests. The tests were performed using the free software program PAST (Hammer et al., 2001). The $\delta^{13}C$ compositions of the rodent diet were also calculated using an enrichment factor between bioapatite and the diet of 11.5‰ (Passey et al., 2005).

6.4.2. Calculating the $\delta^{18}O$ of meteoric water

The $\delta^{18}O$ of meteoric water ($\delta^{18}O_{mw}$) was calculated from the measured $\delta^{18}O$ values of rodent tooth carbonate ($\delta^{18}O_{rt}$) using the modern *Microtus agrestis* equation developed in Chapter 5 (Equation 5.8). Pryor et al. (2014) recommend using an inverted form of a forward fit least-squares regression, as this the most statistically appropriate method for calculating $\delta^{18}O_{mw}$. Equation 5.8 was therefore re-arranged to generate a relationship in the form $x = (y - b)/a$:

$$\delta^{18}O_{mw} = (\delta^{18}O_{rt} - 1.2289) / 1.3109 \quad (6.1).$$

The uncertainty on the mean $\delta^{18}O_{mw}$ value for each site, resulting from the uncertainty in the fit of the modern calibration (Equation 6.1), was calculated using the following equation of Pryor et al. (2014):

$$\delta x_o = \frac{Sy/x}{a} \sqrt{\left[\frac{1}{m} + \frac{1}{n} + \frac{(y_o - \bar{y})^2}{a^2 \Sigma(x_i - \bar{x})^2}\right]} \quad (6.2)$$

where $S_{y/x}$ is the standard deviation of the natural variability in the calibration line (calculated using Equation 5.6), *a* is the slope of the calibration line (1.3109), *m* is the number of fossil rodent teeth in the sample, *n* is the number of data points in the modern calibration (3), y_o is the mean $\delta^{18}O$ of the sample of fossil teeth, $\bar{y}$ is the mean $\delta^{18}O_{rt}$ of the calibration line, x_i is the $\delta^{18}O_{mw}$ of each data point used in the calibration line (i.e. mean $\delta^{18}O_{mw}$ of each modern study site), and $\bar{x}$ is the mean $\delta^{18}O_{mw}$ of the calibration line. The 1σ standard error around the mean $\delta^{18}O_{mw}$ value was added to the uncertainty calculated from Equation 6.2, in order to account approximately for the sample variability in $\delta^{18}O_{rt}$ values.

For Cudmore Grove, the mean $\delta^{18}O$ of local water was also calculated using the *A. cantiana* enamel phosphate data generated by Ruddy (2005). Three different calibration equations for the $\delta^{18}O$ of rodent tooth phosphate (VSMOW) were used. The first equation is a modified version of the Navarro et al. (2004) calibration. Ruddy (2005) re-plotted the $\delta^{18}O$ values of arvicoline tooth phosphate, produced by Navarro et al. (2004), against measured mean $\delta^{18}O$ values of local summer precipitation. The resulting regression equation is shown below:

$$\delta^{18}O_{mw} = (\delta^{18}O_{phosphate} - 19.98) / 0.80 \quad (6.3).$$

The second equation is from Longinelli et al. (2003), and describes the relationship between the $\delta^{18}O$ values of rodent (mouse and vole) bone phosphate and the modelled mean annual $\delta^{18}O$ of local precipitation:

$$\delta^{18}O_{mw} = (\delta^{18}O_{phosphate} - 23.07) / 1.14 \quad (6.4).$$

The third equation, by Royer et al. (2013a), relates the mean $\delta^{18}O$ of arvicoline tooth phosphate with the modelled mean annual $\delta^{18}O$ of precipitation:

$$\delta^{18}O_{mw} = (\delta^{18}O_{phosphate} - 24.35) / 1.14 \quad (6.5).$$

6.4.3. Calculating past summer temperature

The mean $\delta^{18}O_{mw}$ values were subsequently coupled with the mean $\delta^{18}O$ value of the mollusc shells ($\delta^{18}O_{ms}$) to calculate the mean water temperature during the period of shell mineralization. The following equation of White et al. (1999) was used for these calculations:

$$T°C = 21.36 - 4.83 (\delta^{18}O_{ms} - \delta^{18}O_{mw}) \quad (6.6).$$

This was considered the most appropriate equation, as it is based upon the $\delta^{18}O$ values of aragonitic shells from a modern gastropod species, *Radix peregra*. The mollusc data used in this chapter were obtained from the analyses of shells from two gastropod taxa: *Valvata piscinalis* and *Galba truncatula*. The temperature-dependent fractionation between shell $\delta^{18}O$ and $\delta^{18}O_{mw}$ is very similar across different mollusc taxa (White et al., 1999; Bugler et al., 2009), and therefore Equation 6.6 is deemed applicable to both *V. piscinalis* and *G. truncatula*.

The 1σ standard error uncertainties on the calculated temperatures (S_T) were estimated using a standard propagation of error equation, following the methods of Grimes et al. (2003). This equation is shown below:

$$S_T = \sqrt{\left[(S_{ms} \times \frac{\partial T}{\partial ms})^2 + (S_{mw} \times \frac{\partial T}{\partial mw})^2\right]} \quad (6.7)$$

where S_{ms} is the 1σ standard error on the shell $\delta^{18}O$ dataset, S_{mw} is the 1σ uncertainty on the mean calculated $\delta^{18}O_{mw}$ value, and ∂_T/∂_{ms} and ∂_T/∂_{mw} are the partial derivatives of T with respect to $\delta^{18}O_{ms}$ and $\delta^{18}O_{mw}$, determined from Equation 6.6.

6.5. Results: West Runton, Norfolk

6.5.1. $\delta^{18}O$ of teeth

The $\delta^{18}O$ results for the nine *Mimomys savini* incisors (Sample 1) and three additional teeth (Sample 2) from West Runton are shown in Figure 6.6. The $\delta^{18}O$ values of the teeth from Sample 1 span a narrow range of 1.0‰, between -8.3 and -7.3‰. The data are normally distributed (Shapiro-Wilk, $p > 0.05$), and the mean $\delta^{18}O$ value is -7.77‰ ($1\sigma = 0.29$).

The $\delta^{18}O$ values of the teeth from Sample 2 are more enriched, varying from -7.1 to -5.7‰ (range = 1.4‰), with a mean value of -6.25‰ ($1\sigma = 0.74$‰). These teeth were re-analysed to assess the consistency in the results. The $\delta^{18}O$ values generated from the two analyses are within 1‰ of each other and were consequently averaged.

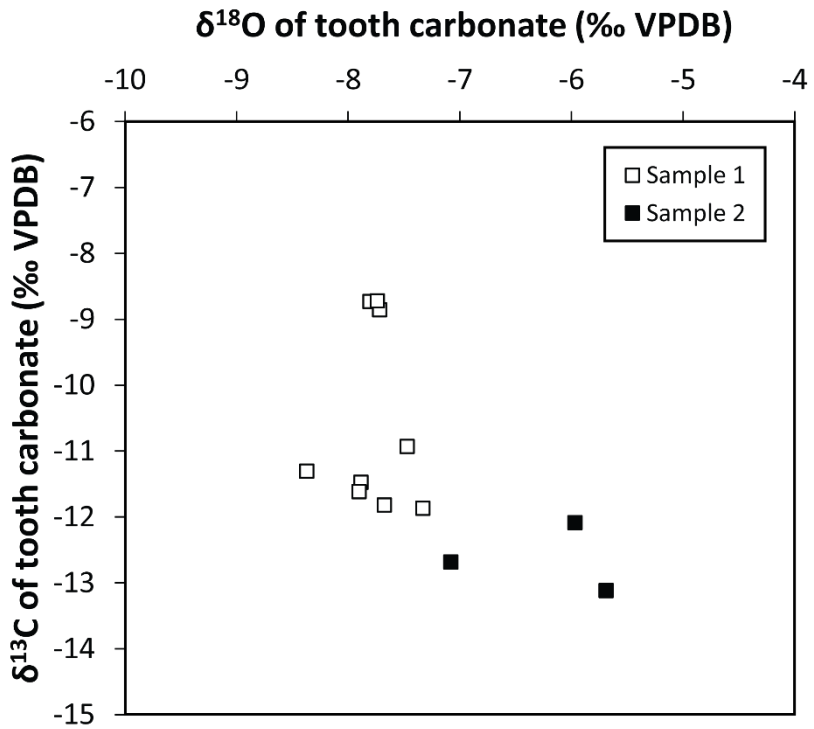

***Figure 6.6**: Oxygen and carbon isotope results for the fossil rodent teeth from West Runton. The results for Sample 1 are from Peneycad (2013).*

The mean $\delta^{18}O$ values of Samples 1 and 2 were compared using a two-sample T-test, assuming unequal variances. The results show that the difference in the mean $\delta^{18}O$ values of the two samples is close to statistical significance ($p = 0.06$). These samples are therefore considered separately in the following calculations.

6.5.2. $\delta^{13}C$ of teeth

The $\delta^{13}C$ data for the teeth from Sample 1 fall into two groups: 1) with values between -12 and -11‰, and 2) with values between -8.9 and -8.7‰ (Figure 6.6). The data are significantly positively skewed (Shapiro-Wilk, $p < 0.05$). The mean value is -10.59‰ (1σ = 1.39‰), and the range is 3.2‰.

The $\delta^{13}C$ values of the teeth from Sample 2 are slightly lower than those from Sample 1 (Figure 6.6). The values range from -13.1 to -12.1‰, with a mean of -12.63‰ (1σ standard deviation = 0.52‰). The re-analyses of the teeth generated $\delta^{13}C$ values within ± 0.3‰ of the first analysis.

The median $\delta^{13}C$ values of the teeth from Samples 1 and 2 are significantly different (Mann-Whitney, $p < 0.05$). Also, there is no significant correlation between the $\delta^{18}O$ and $\delta^{13}C$ values of the teeth in Sample 1 ($r^2 = 0.00$, $p = 0.98$) or Sample 2 ($r^2 = 0.01$, $p = 0.94$).

6.5.3. $\delta^{18}O$ and $\delta^{13}C$ of mollusc shells

The isotope values of the shells from WR1 and WR2 are displayed in Figure 6.7. The $\delta^{18}O$ values of the shells from WR1 range from -6.8 to -4.4‰ (range = 2.4‰), with a mean value of -5.96‰ (1σ standard deviation = 0.55‰, 1σ standard error = 0.06‰). The $\delta^{18}O$ data are significantly positively skewed (Shapiro-Wilk, $p < 0.05$). The mean $\delta^{13}C$ value of the shells from WR1 is -11.06‰ (1σ standard deviation = 1.18‰).

The average $\delta^{18}O$ and $\delta^{13}C$ values of the shells from WR2 are significantly more enriched than the shells from WR1 (Mann-Whitney tests, $p < 0.05$). The $\delta^{18}O$ values of the WR2 shells range between -6.3 and -3.9‰ (range = 2.4‰), with a mean of -5.08‰ (1σ standard deviation = 0.52‰, 1σ

standard error = 0.06‰). The mean $\delta^{13}C$ value is -9.96‰ (1σ standard deviation = 0.77‰).

The correlations between the $\delta^{18}O$ and $\delta^{13}C$ values of the shells from WR1 ($r^2 = 0.26$, $p < 0.01$) and WR2 ($r^2 = 0.18$, $p < 0.01$) are statistically significant but relatively weak. In addition, no major shifts in the $\delta^{18}O_{ms}$ values are observed through the two sediment sections (Figure 6.8). Therefore, the mean $\delta^{18}O_{ms}$ values for the entire WR1 and WR2 datasets will be used in the following temperature calculations.

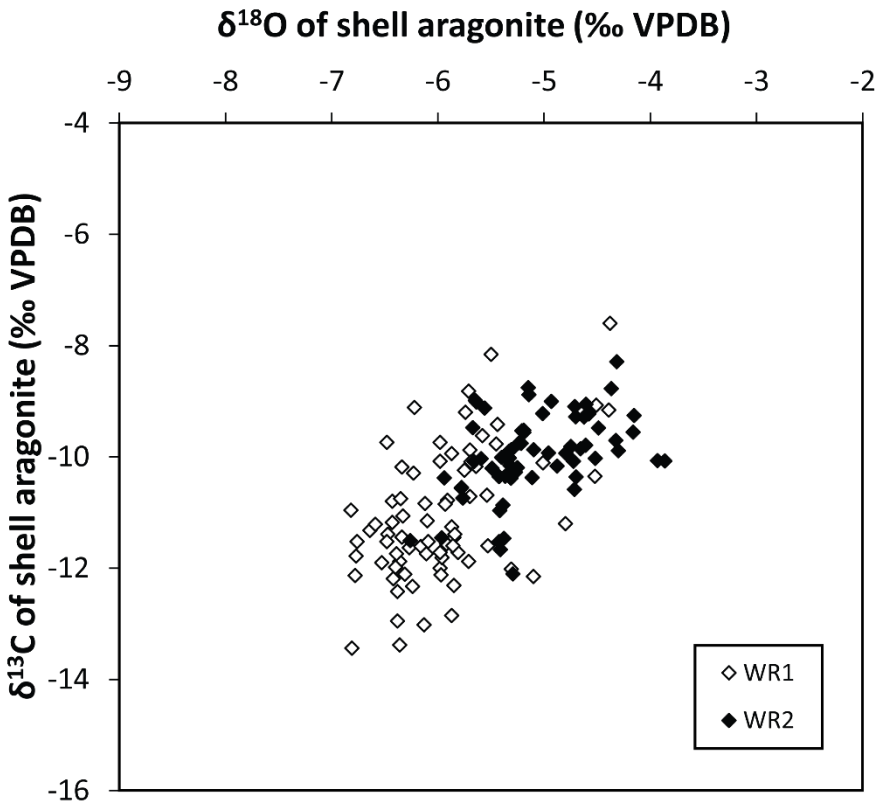

Figure 6.7: *Oxygen and carbon isotope data for the* Valvata piscinalis *shells from West Runton. The data for WR1 are from Davies et al. (2000) and the data for WR2 are from Rose et al. (2008).*

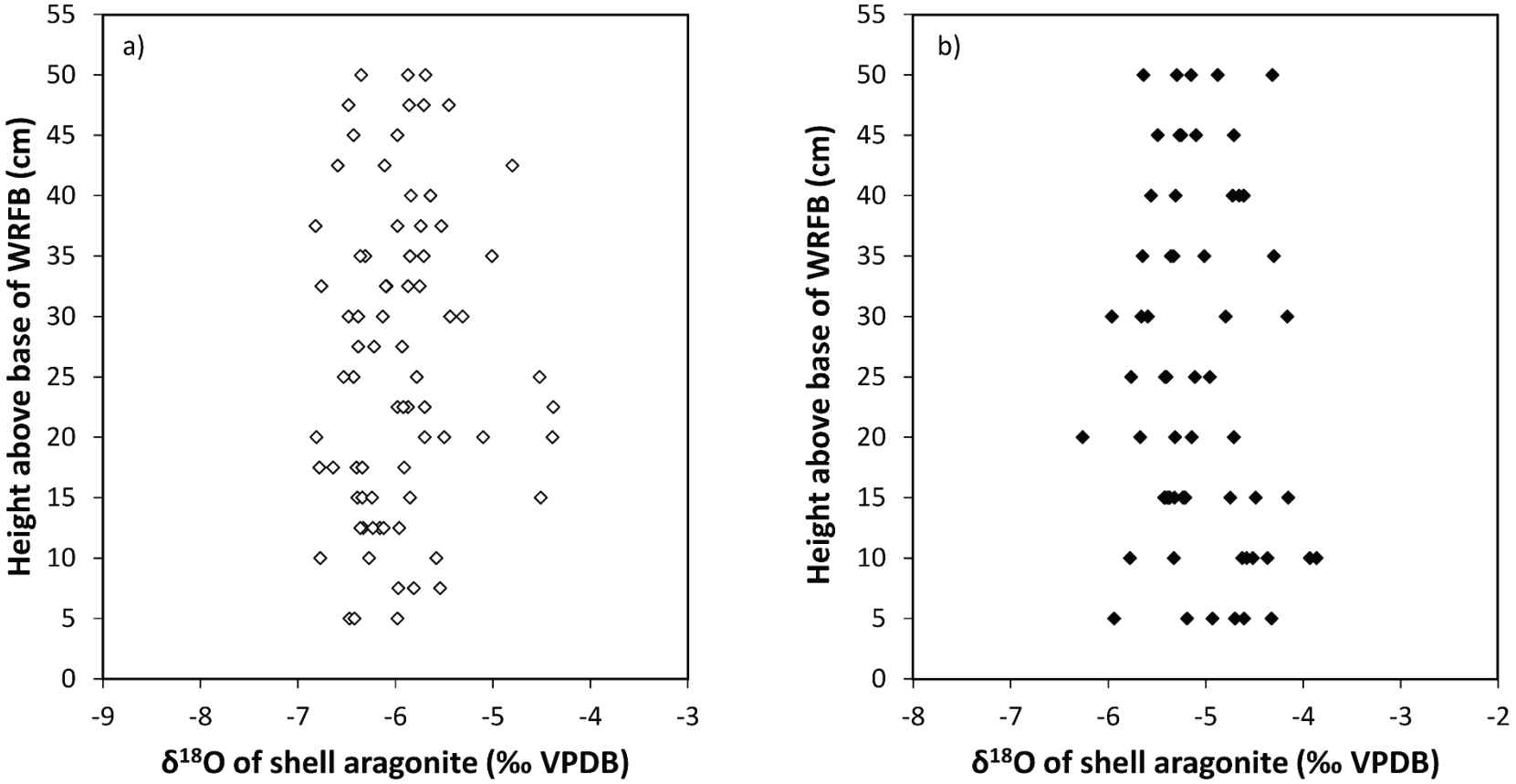

Figure 6.8: *Oxygen isotope data for the* V. piscinalis *shells from a) WR1 (Davies et al., 2000), and b) WR2 (Rose et al., 2008) at West Runton. The data are plotted by height above the base of the West Runton Freshwater Bed.*

6.5.4. $\delta^{18}O$ of meteoric water

The $\delta^{18}O$ values of meteoric water, calculated from the $\delta^{18}O$ values of the teeth in Samples 1 and 2, are shown in Figure 6.9. The mean $\delta^{18}O_{mw}$ value for Sample 1 is -6.86‰, and the 1σ uncertainty is ± 0.13‰ (± 0.06‰ uncertainty from the calibration, plus a 1σ standard error of 0.07‰ on the calculated $\delta^{18}O_{mw}$ values). The mean $\delta^{18}O_{mw}$ value for Sample 2 is -5.70 ± 0.42‰ (calibration uncertainty = 0.10‰; 1σ standard error = 0.32‰). The uncertainty on the mean value for Sample 2 is larger due to the small sample size (n = 3).

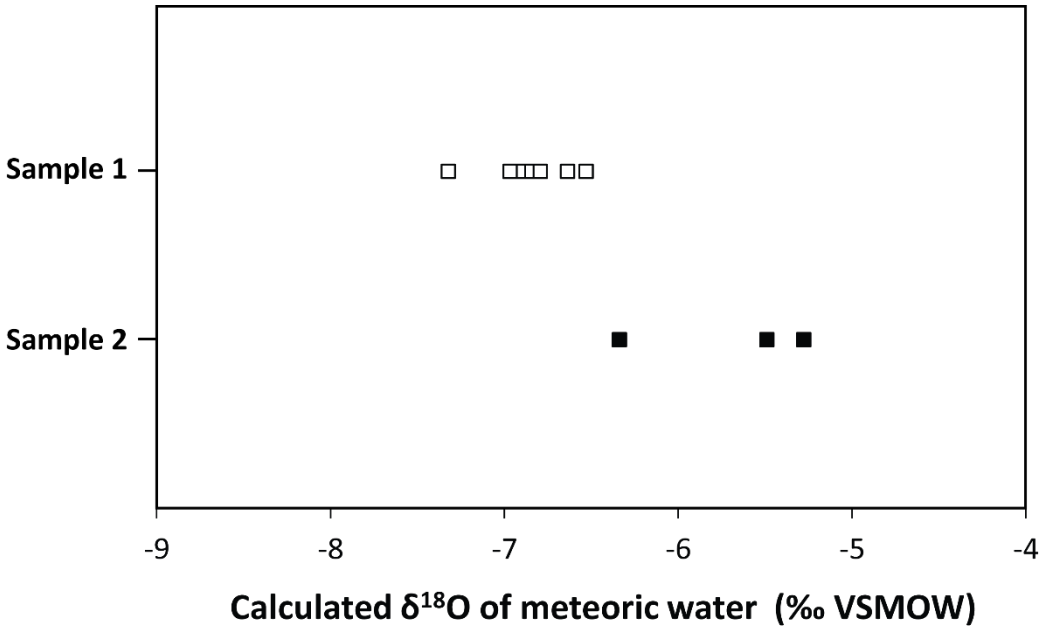

Figure 6.9: *Oxygen isotope values of meteoric water, calculated from the $\delta^{18}O$ values of the rodent teeth from Samples 1 and 2 at West Runton.*

6.5.5. Summer temperature

The calculated mean summer temperatures are summarised in Table 6.2. The mean temperatures range from ~12 to 22°C. Since the rodent teeth in Sample 2 originate from sediments at WR2, the temperature estimate calculated by coupling the $\delta^{18}O$ values of the teeth and shells from this site is considered to be the most reliable. This is because the teeth and shells are derived from the same deposits, and thus their $\delta^{18}O$ values likely reflect comparable palaeoenvironmental conditions. Therefore, the temperature calculated by combining the $\delta^{18}O$ values of the Sample 2 teeth and WR1 shells will not be considered further.

On the other hand, the section of the WRFB from which the rodent teeth in Sample 1 were collected is not known. As a consequence, the likely contemporaneity of these rodent teeth with the WR1 or WR2 shells is unclear. However, the comparisons with the published palaeotemperature reconstructions for West Runton in the following section may help to resolve this issue. The temperatures quantified using Sample 1 coupled with WR1, and Sample 2 coupled with WR2, are illustrated in Figure 6.10.

Table 6.2: *Mean summer temperatures for West Runton, calculated by coupling the mean $\delta^{18}O_{mw}$ values for the rodent teeth from Samples 1 and 2, with the mean $\delta^{18}O$ values of the mollusc shells from sites WR1 and WR2. Temperatures are shown in °C with ± 1σ standard error uncertainties.*

Shell dataset →	**WR1**	**WR2**
Tooth dataset ↓		
Sample 1	17. 00 ± 0.70	12.73 ± 0.70
Sample 2	22.60 ± 2.08	18.34 ± 2.08

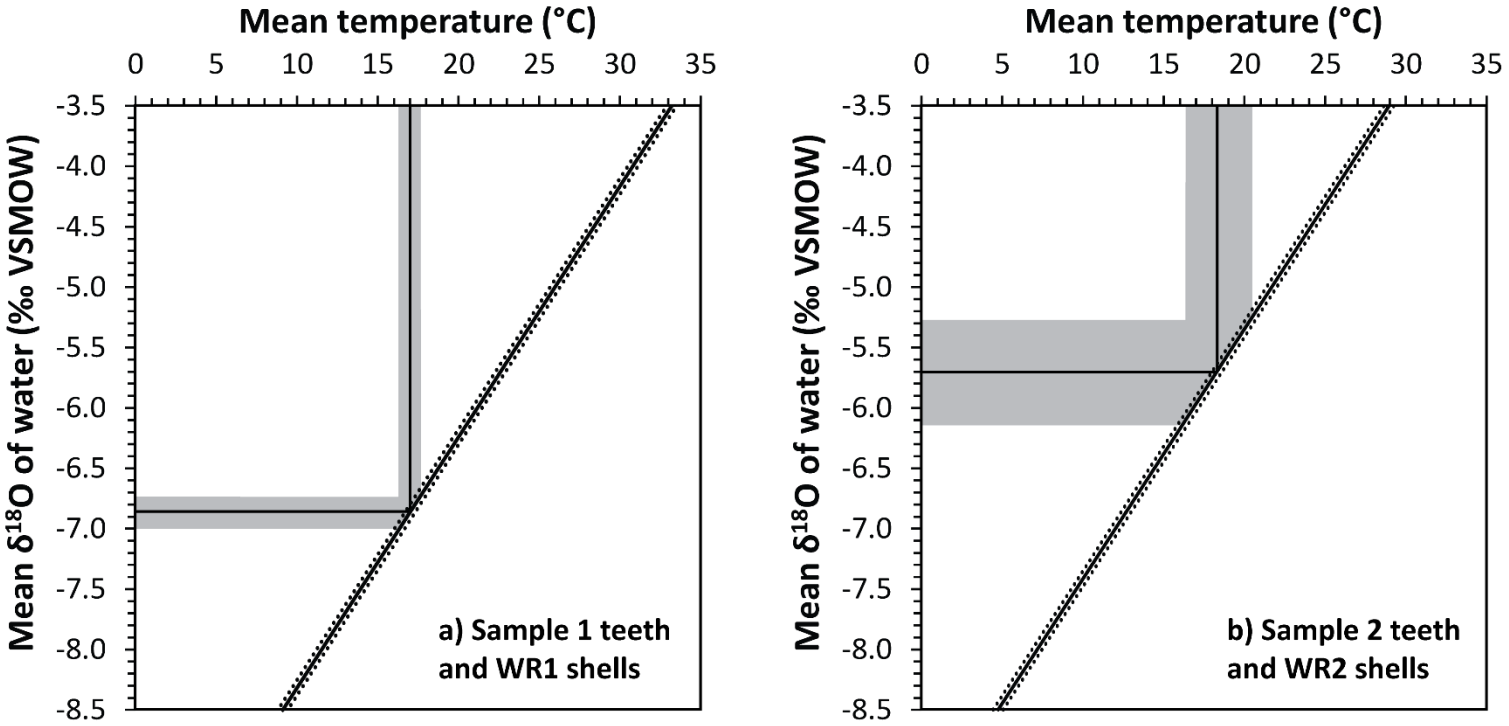

Figure 6.10: *Graphs illustrating the calculation of mean summer temperatures from the mean calculated $\delta^{18}O$ of meteoric water and the mean $\delta^{18}O$ of the* V. piscinalis *shells for sites WR1 (a) and WR2 (b). The mean $\delta^{18}O$ of the shells is represented by the straight black line, and the dotted lines indicate the 1σ standard error around this mean value. The grey shaded areas represent the 1σ uncertainties around the meteoric water and temperature values.*

6.5.6. Interpretations and Discussion

6.5.6.1. $\delta^{18}O$ and $\delta^{13}C$ of teeth

The mean $\delta^{18}O$ value of the *Mimomys savini* incisors from Sample 1 is almost identical to the mean $\delta^{18}O$ value of modern *Microtus agrestis* teeth from Surrey (Figure 6.11). This suggests that the $\delta^{18}O$ of meteoric water during the formation of the incisors was comparable to southeast Britain at the present day. In contrast, the mean $\delta^{18}O_{rt}$ of Sample 2 is closer to the mean $\delta^{18}O$ composition of modern *M. agrestis* teeth from Somerset, in southwest Britain (Figure 6.11). This indicates that the meteoric water consumed by the Sample 2 rodents was isotopically enriched relative to southeast Britain today.

The $\delta^{13}C$ values of the West Runton teeth (~ -13 to -8‰) are also substantially more enriched than modern *M. agrestis* teeth from southern Britain (~ -18 to -16‰). The calculated mean $\delta^{13}C$ values of the diet are -22.1‰ for Sample 1 and -24.1‰ for Sample 2. These values are consistent with a diet comprising only C_3 plants. However, the values lie at the upper end of the range in $\delta^{13}C$ compositions of modern C_3 plants (Figure 2.2).

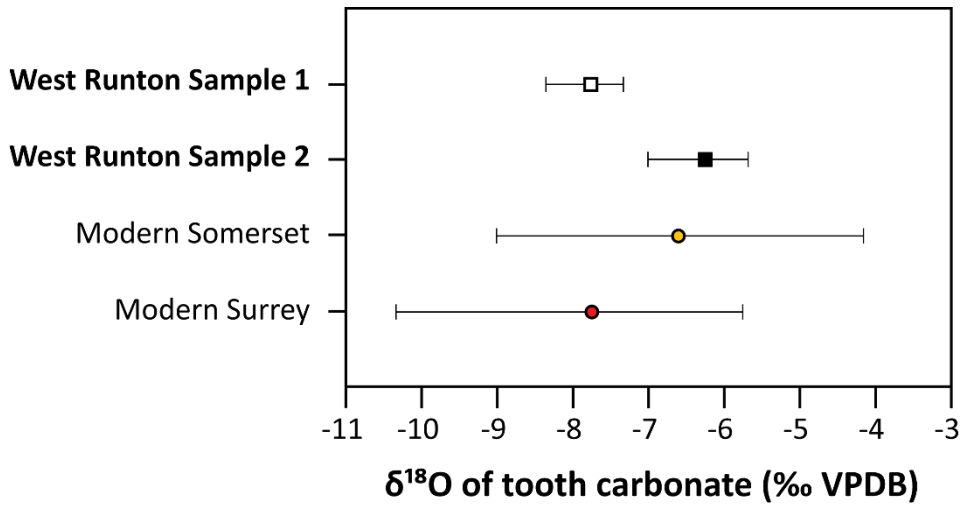

Figure 6.11: *Comparison of the mean $\delta^{18}O$ values of the rodent teeth from West Runton, with the modern $\delta^{18}O$ compositions of* Microtus agrestis *teeth from southern Britain (Chapter 5). The error bars represent the ranges in tooth $\delta^{18}O$ values at each site.*

6.5.6.2. $\delta^{18}O$ and $\delta^{13}C$ of mollusc shells

The $\delta^{18}O$ values of the mollusc shells from WR1 and WR2 are consistent with the $\delta^{18}O$ values of modern *Valvata piscinalis* shells from rivers in southeast Britain (Figure 6.12). This suggests that climatic conditions at West Runton were comparable to the present day. The mean $\delta^{18}O_{ms}$ for WR1 is closest to the mean $\delta^{18}O$ value of modern shells from the River Thames at Runnymede in Surrey (Figure 6.12). At present, the mean $\delta^{18}O_{mw}$ value of the River Thames is around -6.8 to -6.5‰ (Davies, 1999; Darling & Bowes, 2016).

In contrast, the mean $\delta^{18}O_{ms}$ value for WR2 is relatively enriched, and is most similar to the mean $\delta^{18}O$ of modern shells from the River Gipping in Suffolk (Figure 6.12). The River Gipping currently has an average $\delta^{18}O_{mw}$ composition of approximately -6.3‰ (Waghorne et al., 2012), and is therefore isotopically enriched compared to the River Thames. This implies that the differences between the $\delta^{18}O$ values of the shells from WR1 and WR2 may primarily result from variability in the $\delta^{18}O$ of local meteoric water, rather than differences in the water temperature at which the shells mineralized. The data indicate that the WR2 shells precipitated within meteoric water with a relatively enriched $\delta^{18}O$ value. This enrichment likely results from evaporation.

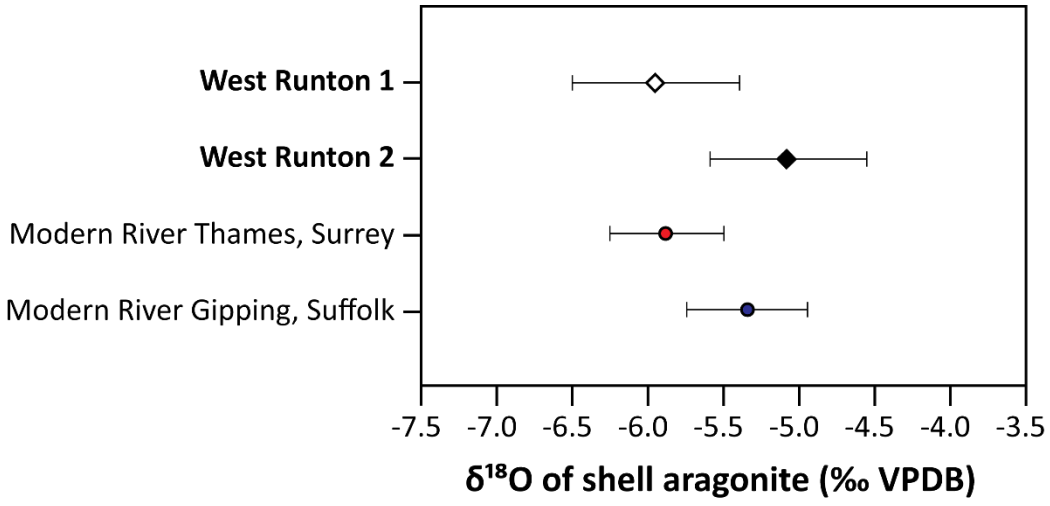

Figure 6.12: *Comparison of the mean $\delta^{18}O$ values of the* V. piscinalis *shells from West Runton with the mean $\delta^{18}O$ values of modern* V. piscinalis *shells from southern Britain. The data for the River Thames are from Davies (1999) and the data for the River Gipping are from Waghorne et al. (2012). The error bars represent the 1σ standard deviations on the datasets.*

This interpretation is supported by the carbon isotope data from the fossil shells. The $\delta^{13}C$ values of the WR2 shells are significantly enriched compared to the WR1 shells (Figure 6.7). The $\delta^{13}C$ of mollusc shell aragonite mainly reflects the $\delta^{13}C$ composition of DIC (Fritz & Poplawski, 1974). As discussed in Section 2.2.2.5, the $\delta^{13}C$ of DIC can become enriched due to equilibration with atmospheric CO_2. This generally occurs in water bodies with longer residence times, as a decrease in the inflow of water to the basin plus increased evaporation leads to the degassing of CO_2 (Talbot, 1990). This may suggest that the residence time of the water body was longer during the deposition of the WR2 sediments than the WR1 sediments. This idea is discussed further in the following section.

6.5.6.3. Reconstructed $\delta^{18}O$ of meteoric water

The $\delta^{18}O$ of meteoric water, calculated from the teeth in Sample 1, is consistent with the mean $\delta^{18}O_{mw}$ of the modern River Thames (Figure 6.13). In contrast, the $\delta^{18}O_{mw}$ calculated from Sample 2 is more enriched, and is similar to modern $\delta^{18}O_{mw}$ values in Somerset. As the $\delta^{18}O$ values of rodent teeth and mollusc shells both reflect the $\delta^{18}O$ of meteoric water, and the teeth and shells from WR2 are isotopically enriched compared to Surrey at the present day (Figures 6.11 and 6.12), the water source from which these biominerals mineralized must have also been enriched. This is reflected in the calculated $\delta^{18}O_{mw}$ value for WR2 (Figure 6.13).

Conversely, the $\delta^{18}O$ values of the fossil teeth and shells from Sample 1 and WR1 are similar to modern teeth and shells from Surrey (Figures 6.11 and 6.12). This suggests that these biominerals mineralized from a water source with a $\delta^{18}O$ composition similar to the modern River Thames. At the present day, the $\delta^{18}O$ values of groundwater sources in Norfolk are similar to the $\delta^{18}O$ values of groundwaters in Surrey (see Figure 3.2). Therefore, if palaeoclimatic conditions at West Runton were similar to the present day, $\delta^{18}O_{mw}$ values at this site would be relatively similar to modern $\delta^{18}O_{mw}$ values for the River Thames in Surrey. The data from Sample 1 and WR1 are consistent with this interpretation (Figures 6.12 and 6.13).

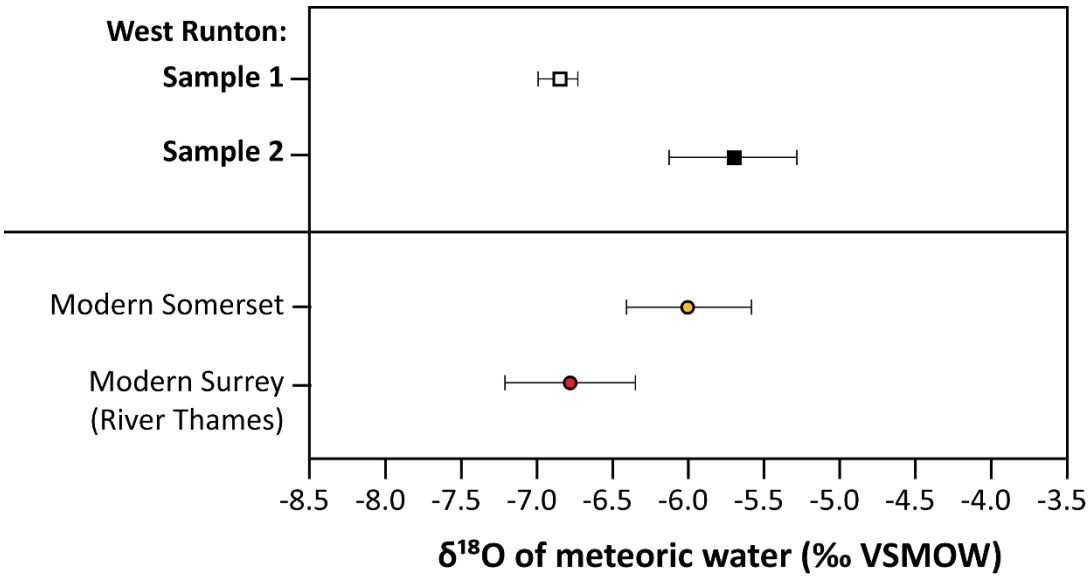

Figure 6.13: *Comparisons of the mean $\delta^{18}O$ values of meteoric water calculated from the West Runton rodent teeth, with the modern $\delta^{18}O$ compositions of surface water sources in southern Britain. The modern data for Somerset are from Chapter 5, and the modern data for Surrey are from Darling & Bowes (2016) for the River Thames at Runnymede.*

These differences in the $\delta^{18}O_{mw}$ values between WR1 and WR2 can be related to the sedimentology of the WRFB. Due to lateral changes in the WRFB stratigraphy, it is likely that the sediments at WR1 and WR2 accumulated during slightly different intervals of time (Rose et al., 2008). However, the proxy evidence from these sections indicates that climatic conditions remained relatively stable during the accumulation of the sediments (see Section 3.4.1). Therefore, the difference in the mean $\delta^{18}O_{mw}$ values between WR1 and WR2 is unlikely to result from a significant change in average temperature.

The basal sediments at WR1 comprise coarse, pebbly sands and silts, whereas the basal 50 cm at WR2 consists of upward-fining silts, interspersed with sand lenses that decrease in frequency up-sequence (Rose et al., 2008). The upward-fining silts are generally thought to have been deposited after the coarser sands and gravels (Rose et al., 2008; Gibbard et al., 2010). Gibbard et al. (2010) also note that the youngest sediments of the WRFB are generally restricted to the western half of the coastal exposure. Consequently, the basal

50 cm of the section at WR2, which lies to the west, probably post-dates the basal 50 cm at WR1. The upward-fining silts are interpreted as reflecting the infill of the lake basin, with intermittent flood events that became less frequent over time (Rose et al., 2008; Gibbard et al., 2010). The gradual reduction in the inflow to the basin would have led to an increase in the residence time of the water body. Also, as the lake infilled, and the volume of the water decreased, evaporation would have likely had a greater influence on the average $\delta^{18}O$ of the water. Evaporation leads to an enrichment in $\delta^{18}O_{mw}$ values. This enrichment would consequently be reflected in the $\delta^{18}O$ values of the teeth and shells from WR2, and this is indeed the case. However, small temporal changes in temperature might have also contributed to the difference in $\delta^{18}O_{mw}$ values between WR1 and WR2.

6.5.6.4. Reconstructed mean summer temperatures

The calculated mean summer temperatures for West Runton are shown against published palaeotemperature estimates in Figure 6.14. The mean temperatures calculated by coupling the $\delta^{18}O$ data from Sample 1 with WR1, and Sample 2 with WR2, are entirely consistent with the palaeoecological-based temperature estimates for the site. Conversely, the temperature calculated by coupling the Sample 1 teeth with the WR2 shells significantly underestimates the mean summer temperature. This suggests that the teeth in Sample 1 may originate from the eastern half of the WRFB, near to WR1. This is supported by the fact that the mean summer temperature for Sample 1 coupled with WR1 is identical to the maximum temperature estimate derived from the herpetofaunal assemblage at WR1 (Figure 6.14).

Moreover, the similarity in the calculated temperatures for WR1 and WR2 suggests that palaeoclimatic changes of no more than 1-2°C occurred during the accumulation of the WRFB. This is consistent with the floral and faunal evidence from the site (Rose et al., 2008; Coope, 2010a; Field, 2010; Maul & Parfitt, 2010). However, the slightly higher temperature for WR2 (Figure 6.14) may imply that mean summer temperatures were marginally warmer during the latter half of the interval represented by the WRFB.

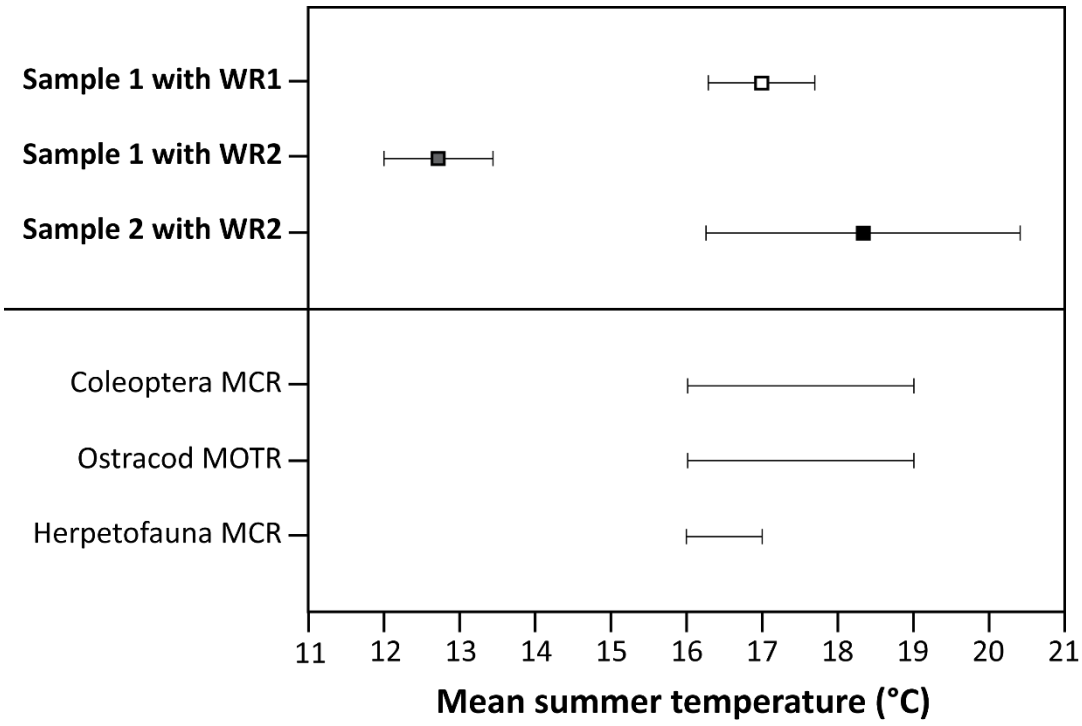

Figure 6.14: *Comparisons of the mean summer temperatures calculated using the coupled isotope approach, with the mean summer temperatures derived from the palaeoecological proxies from West Runton. The beetle (Coleoptera) Mutual Climatic Range (MCR) data are from Coope (2010a), the ostracod Mutual Ostracod Temperature Range is from T.S. White (pers. comm.) and the herpetofauna MCR is from Böhme (2010).*

6.5.7. Summary

The $\delta^{18}O$ values of the rodent tooth and mollusc shell carbonates from the West Runton Freshwater Bed are comparable to the $\delta^{18}O$ values of modern teeth and shells from southern Britain. The calculated $\delta^{18}O$ values of local meteoric water are likewise consistent with modern $\delta^{18}O_{mw}$ values for southern Britain. These results therefore suggest that climatic conditions at West Runton were similar to the present day. This interpretation is in agreement with the wealth of palaeoclimate evidence previously obtained from the WRFB (see section 3.4.1).

The $\delta^{18}O$ values of the teeth and shells from WR2 are significantly enriched compared to those from WR1. These differences suggest that the deposits at WR1 and WR2 represent different intervals of time within the same

interglacial stage. The $\delta^{18}O$ composition of the water body at West Runton was more depleted during the deposition of the older, coarser sediments at WR1, than during the deposition of the younger, fine-grained sediments at WR2. This temporal change in $\delta^{18}O_{mw}$ is thought to result from: 1) the gradual decrease in the frequency of inflow events, and consequent increase in the residence time of the water body, 2) the infilling of the basin and resultant reduction in water volume, which led to 3) increased evaporation and a greater equilibration of DIC with atmospheric CO_2. This resulted in relatively enriched $\delta^{18}O$ values of the teeth and enriched $\delta^{18}O$ and $\delta^{13}C$ values of the shells from WR2.

The mean summer temperatures calculated for West Runton using the coupled isotope approach are equivalent, within uncertainties, to the published palaeotemperature estimates derived from the beetle, ostracod and herpetofaunal assemblages from the WRFB. This demonstrates that the coupled isotope approach has the potential to provide accurate and relatively precise temperature estimates for past interglacial stages.

6.6. Results: Cudmore Grove, Essex

6.6.1. $\delta^{18}O$ of teeth

The $\delta^{18}O$ results for the *A. cantiana* tooth carbonate and phosphate are shown in Figure 6.15. One of the samples of enamel fragments yielded insufficient material for analysis. The carbonate $\delta^{18}O$ values (VPDB) of the 4 remaining samples vary from -6.4 to -4.7‰ (range = 1.7‰), with a mean value of -5.30‰ (1σ = 0.77‰). Ruddy (2005) identified one outlier in the phosphate isotope data, and this data point was therefore excluded. The phosphate $\delta^{18}O$ (VSMOW) values of the remaining teeth range from 14.7 to 17.3‰ (range = 2.6‰), with a mean of 15.88‰ (1σ = 0.93‰). The phosphate $\delta^{18}O$ data are normally distributed (Shapiro-Wilk, $p > 0.05$).

The carbonate $\delta^{18}O$ values of the two enamel samples were converted from the VPDB to the VSMOW scale using the equation of Coplen et al. (1983) (Equation 5.7), in order to enable comparison with the phosphate data. The carbonate $\delta^{18}O$ values of the samples are 25.8‰ and 25.6‰, while the

phosphate $\delta^{18}O$ values are 16.0‰ and 17.3‰, respectively. Therefore, the $\delta^{18}O$ offsets between enamel carbonate and phosphate are 9.8‰ and 8.3‰. These offsets are consistent with measured isotopic differences between carbonate and phosphate in modern mammalian teeth (Figure 6.16). This suggests that the enamel carbonate has undergone negligible diagenetic alteration. Moreover, the carbonate $\delta^{18}O$ values of the bulk teeth are comparable to the $\delta^{18}O$ values of the enamel fragments, suggesting that these teeth are likewise well-preserved.

6.6.2. $\delta^{13}C$ of teeth

The $\delta^{13}C$ values of the teeth range from -12.7 to -8.2‰ (range = 4.5‰) (Figure 6.15a), with a mean value of -10.84‰ (1σ = 2.24‰). There is no significant correlation between the $\delta^{18}O$ and $\delta^{13}C$ values of the teeth ($r^2 = 0.51$, $p = 0.29$).

6.6.3. $\delta^{18}O$ of mollusc shells

The isotope data for the *V. piscinalis* mollusc shells from Cudmore Grove were unavailable for presentation in this thesis, although summary statistics are provided by Ruddy (2005). The mean $\delta^{18}O$ value of the mollusc shells is -5.31‰ (VPDB), the 1σ standard deviation is 0.82‰, and the 1σ standard error is 0.16‰.

6.6.4. $\delta^{18}O$ of meteoric water

The calculated $\delta^{18}O$ values of meteoric water for the *A. cantiana* incisor carbonate and phosphate are shown in Figure 6.17 and Table 6.3. The mean $\delta^{18}O_{mw}$ value calculated from the incisor carbonate is -4.98‰, and the total 1σ uncertainty is ± 0.46‰ (calibration uncertainty = 0.16‰, 1σ standard error = 0.29‰). These uncertainties are fairly large because the mean $\delta^{18}O_{mw}$ is based upon data from only four samples, and the calculation of $\delta^{18}O_{mw}$ required extrapolation beyond the range of the modern calibration line.

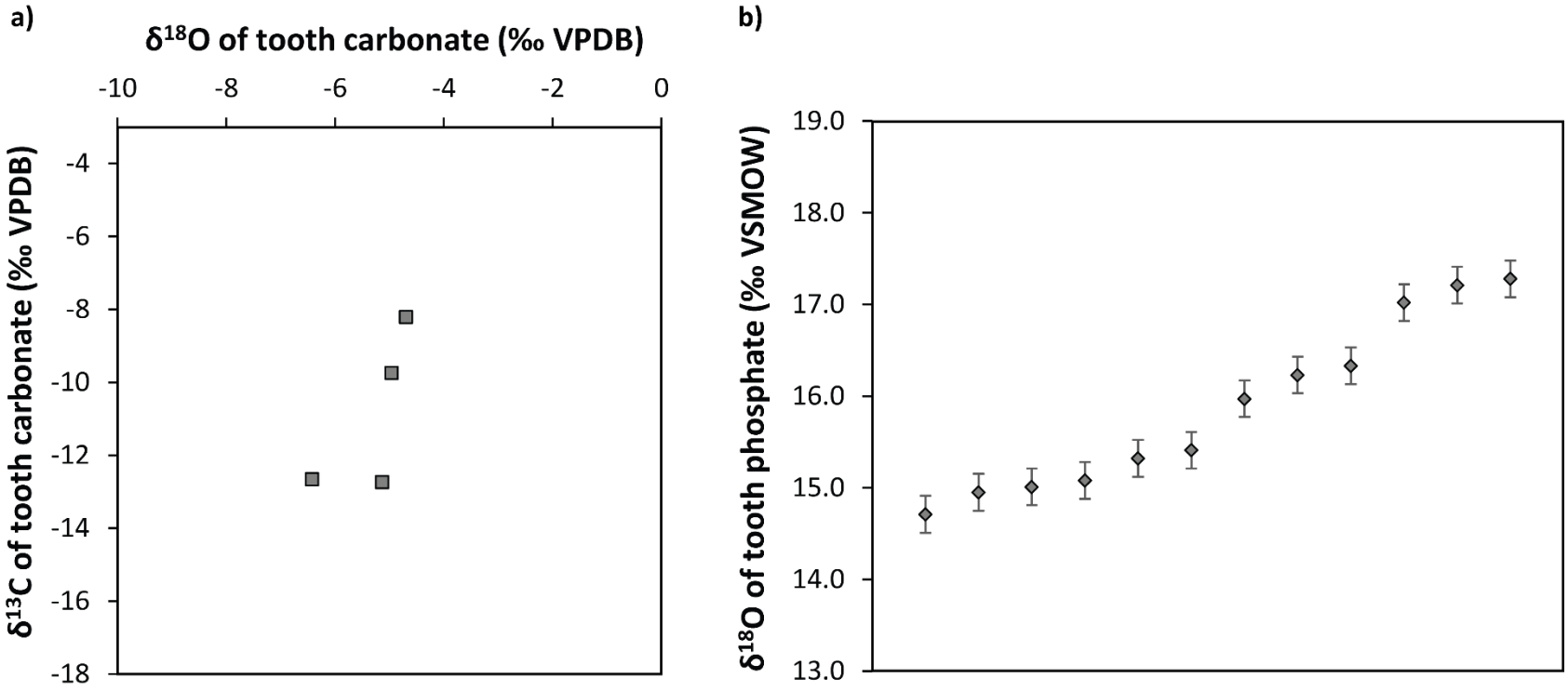

Figure 6.15: *Isotope results for the* Arvicola cantiana *tooth carbonate (a) and phosphate (b) from Cudmore Grove. The tooth phosphate data are from Ruddy (2005), and the error bars on these data represent analytical uncertainties.*

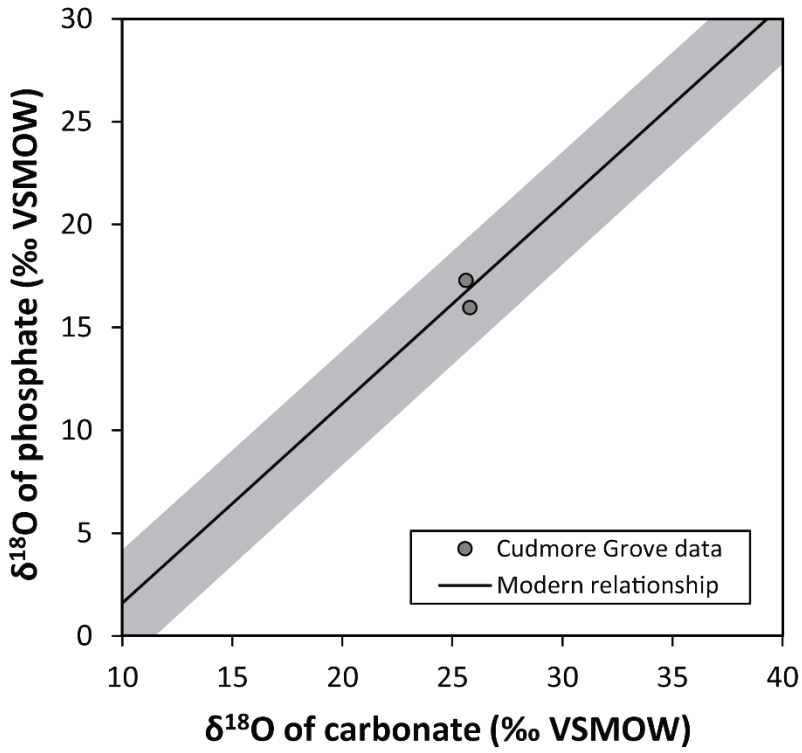

Figure 6.16: *Correlation between the oxygen isotope values of tooth carbonate and tooth phosphate for Cudmore Grove, shown against the modern calibration line from Figure 2.6. The grey shaded area represents the range in the isotope values of the modern mammalian teeth.*

The mean $\delta^{18}O$ of summer precipitation calculated using the modified Navarro et al. (2004) equation is consistent, within uncertainties, with the mean $\delta^{18}O_{mw}$ value generated from the carbonate data (Table 6.3). The results of a T-test confirm that these $\delta^{18}O$ values are not significantly different (p = 0.75). In contrast, the $\delta^{18}O_{pt}$ values calculated using the Longinelli et al. (2003) and Royer et al. (2013a) equations are significantly more depleted than those generated from the carbonate equation and modified Navarro et al. (2004) equation (T-tests, $p < 0.01$).

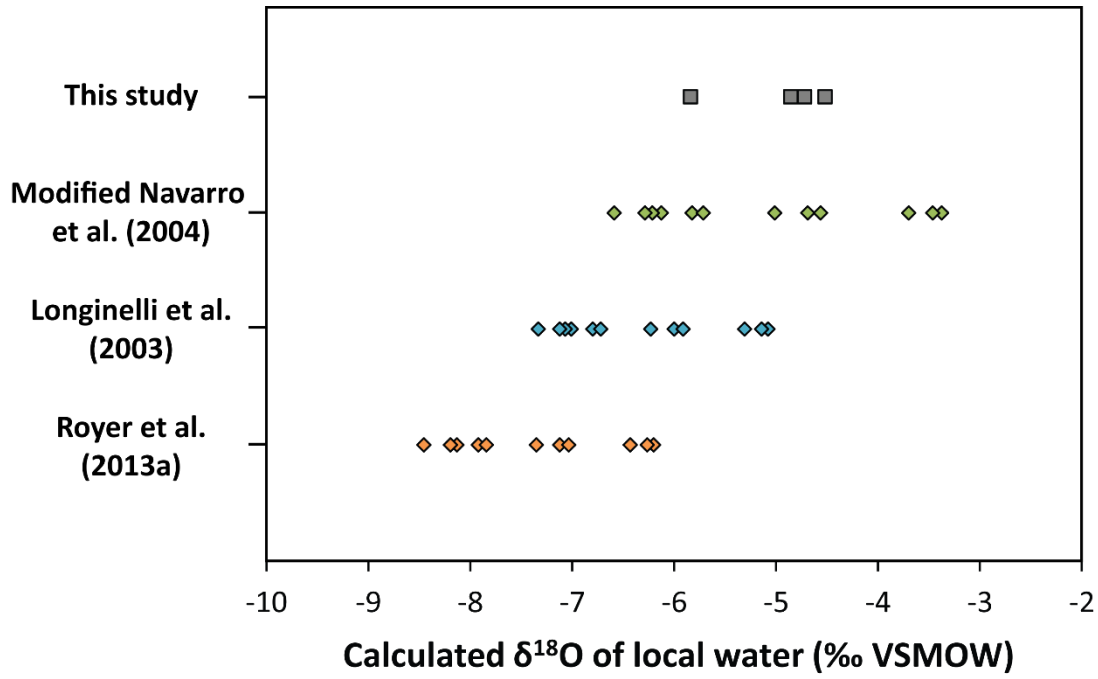

Figure 6.17: *Oxygen isotope values of local water for Cudmore Grove, calculated using four different modern calibration equations.*

Table 6.3: *Mean $\delta^{18}O$ values of local water, calculated from the $\delta^{18}O$ values of fossil* A. cantiana *tooth carbonate and phosphate from Cudmore Grove. These values were calculated using four different modern calibration equations (Equations 6.1, 6.3, 6.4 and 6.5).*

Modern calibration	Mineral ion in bioapatite	Mean $\delta^{18}O$ of local water ± 1σ uncertainty (‰ VSMOW)
This study (Chapter 5)	Carbonate	-4.98 ± 0.46
Navarro et al. (2004), modified by Ruddy (2005)	Phosphate	-5.13 ± 0.34
Longinelli et al. (2003)	Phosphate	-6.31 ± 0.24
Royer et al. (2013a)	Phosphate	-7.43 ± 0.24

6.6.5. Summer temperature

The mean summer palaeotemperatures, calculated from the $\delta^{18}O$ values of *A. cantiana* tooth carbonate and phosphate coupled with the mean $\delta^{18}O$ value of the shells, are shown in Figure 6.18 and Table 6.4. The mean summer palaeotemperatures reconstructed from the carbonate and modified Navarro et al. (2004) equations are comparable at ~22°C. Conversely, the mean temperatures calculated from the Longinelli et al. (2003) and Royer et al. (2013a) equations are much lower at between ~11 and 16°C. However, the uncertainties on the palaeotemperature estimates are relatively broad at around ± 1.4-2.3°C. Consequently, for the tooth carbonate data, the mean temperature value may lie anywhere between 20.61°C and 25.26°C.

Table 6.4: *Mean summer palaeotemperatures for Cudmore Grove, calculated by coupling the mean $\delta^{18}O_{mw}$ values generated from the* A. cantiana *tooth carbonate and phosphate $\delta^{18}O$ data, with the mean $\delta^{18}O$ value of fossil shell aragonite.*

Modern calibration	Mineral phase of bioapatite	Mean summer temperature ± 1σ uncertainty (°C)
This study (Chapter 5)	Carbonate	22.93 ± 2.33
Navarro et al. (2004), modified by Ruddy (2005)	Phosphate	22.23 ± 1.79
Longinelli et al. (2003)	Phosphate	16.53 ± 1.37
Royer et al. (2013a)	Phosphate	11.11 ± 1.37

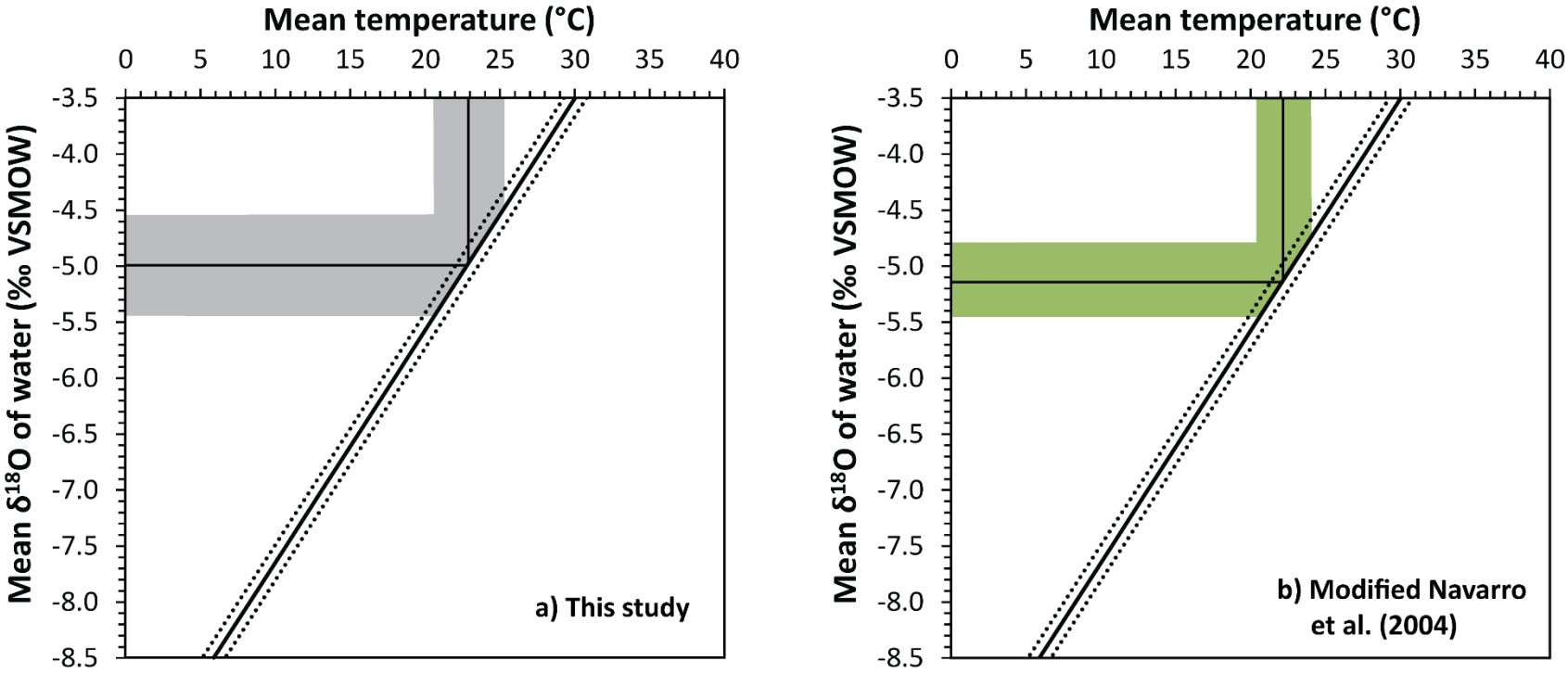

Figure 6.18: *Graphs illustrating the calculation of the mean palaeotemperatures for Cudmore Grove, from the mean $\delta^{18}O$ of local water calculated using the four different calibrations (a-d), coupled with the mean $\delta^{18}O$ value of the shells (solid straight line). The dotted lines indicate the 1σ standard error on the mean shell $\delta^{18}O$ value, and the shaded areas indicate the 1σ standard error uncertainties on the calculated mean $\delta^{18}O$ of local water and mean temperature values.*

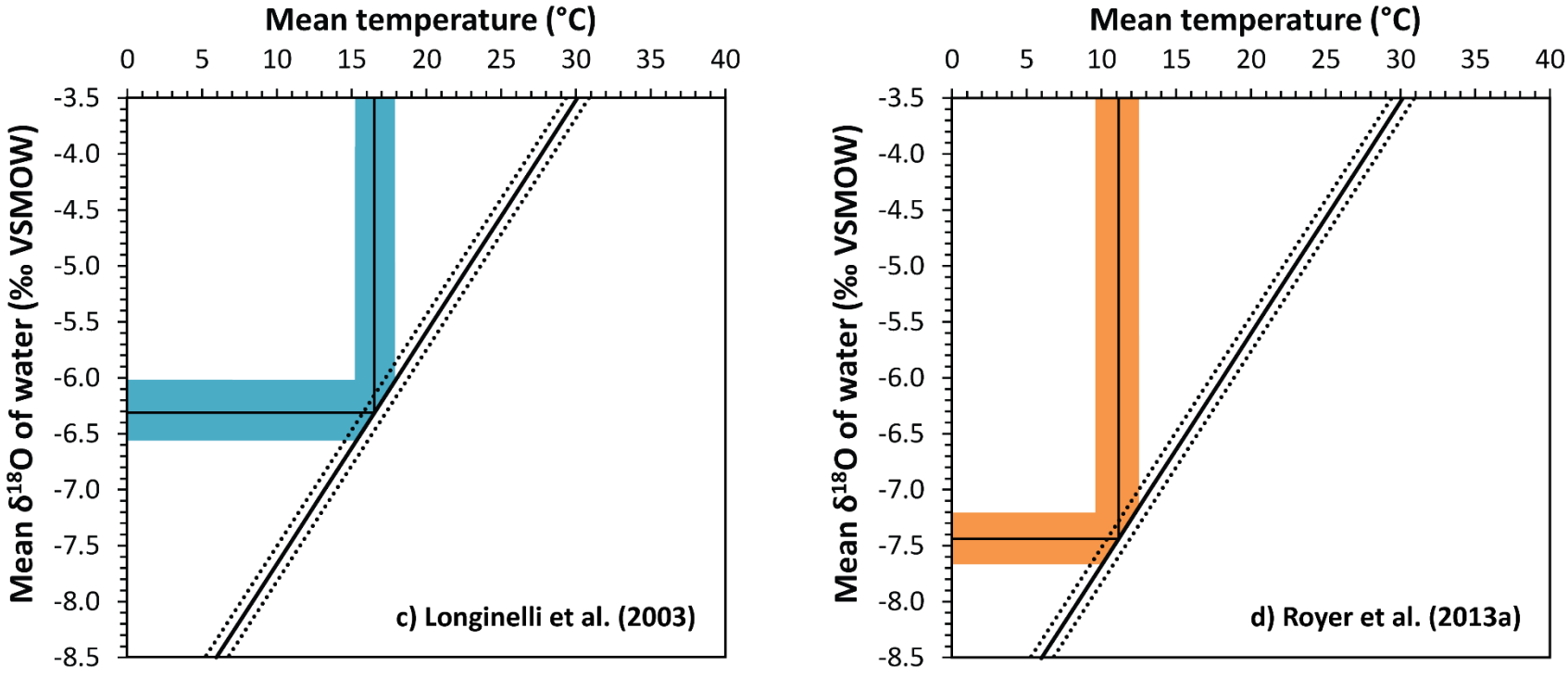

Figure 6.18: *For caption see previous page.*

6.6.6. Interpretations and Discussion

6.6.6.1. $\delta^{18}O$ and $\delta^{13}C$ of teeth

The mean $\delta^{18}O$ value of *A. cantiana* tooth carbonate (-5.30‰) is much higher than the mean $\delta^{18}O$ values of modern *Microtus agrestis* teeth from southern Britain, although is consistent with the highest $\delta^{18}O_{rt}$ values for Somerset (Figure 6.19). This indicates that the fossil teeth from Cudmore Grove reflect $\delta^{18}O_{mw}$ values that are significantly enriched relative to southern Britain today.

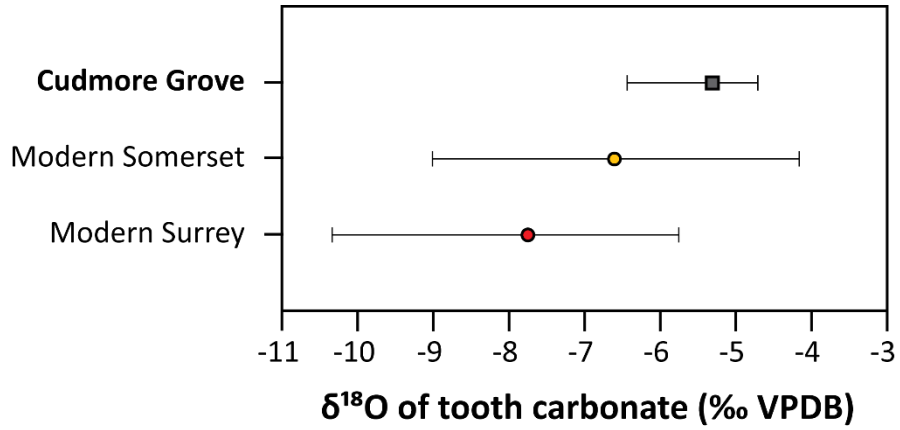

Figure 6.19: *Comparison of the mean $\delta^{18}O$ value of the fossil* A. cantiana *tooth carbonate from Cudmore Grove, with the mean $\delta^{18}O$ values of modern* M. agrestis *tooth carbonate from sites in southern Britain. The error bars represent the ranges in the tooth $\delta^{18}O$ values for each site.*

The mean $\delta^{18}O$ value of *A. cantiana* tooth phosphate (15.88‰) is also slightly enriched compared to modern $\delta^{18}O$ values of *Arvicola* spp. teeth from lowland areas of northwest Europe. *Arvicola* teeth from northern France and Sweden generally have phosphate $\delta^{18}O$ values of ~9-14‰, whereas teeth from southern France, Spain and Portugal have $\delta^{18}O$ values of ~15-20‰, although there is some variability in this overall pattern (Royer et al., 2013a). The tooth phosphate data from Cudmore Grove therefore suggest that the mean $\delta^{18}O$ value of meteoric water at Cudmore Grove was similar to west-central or southern Europe today. This indicates that climatic conditions at the site may have been warmer than present.

The mean $\delta^{13}C$ value of the Cudmore Grove teeth (-10.84‰) is also significantly more enriched than the mean $\delta^{13}C$ values of modern *M. agrestis* teeth from Britain (-18 to -16‰). The calculated mean $\delta^{13}C$ composition of the rodents' diet is -22.4‰, which is consistent with a diet consisting of C_3 plants.

6.6.6.2. Reconstructed mean $\delta^{18}O$ of meteoric water

The mean $\delta^{18}O_{mw}$ value, quantified using the modern *M. agrestis* carbonate equation, is significantly more enriched than the measured $\delta^{18}O$ compositions of surface meteoric waters in southern Britain at the present day (Figure 6.20). Some of the highest $\delta^{18}O_{mw}$ values in Britain today (-5.4 and -5.0‰) are recorded in the far southwest corner of England (Figure 3.2). The reconstructed $\delta^{18}O_{mw}$ value for Cudmore Grove in eastern England is therefore approximately equivalent to modern $\delta^{18}O_{mw}$ values in southwest England. Given that modern $\delta^{18}O_{mw}$ values in mid-latitude regions are related to air temperature (Rozanski et al., 1993), the $\delta^{18}O_{mw}$ data for Cudmore Grove imply that palaeotemperatures may have been considerably warmer than today.

Enriched $\delta^{18}O$ values of surface waters can also result from evaporation. Increased evaporation can occur due to low humidities or the hydrological isolation of the water body (e.g. Darling, 2004). The Cudmore Grove deposits accumulated within a major river (Roe et al., 2009), and thus evaporation due to hydrological isolation seems unlikely. Therefore, an alternative explanation for the enriched $\delta^{18}O_{mw}$ values may be that the climate at Cudmore Grove was drier than today.

However, the enriched mean $\delta^{18}O_{mw}$ value may also result from a bias in the $\delta^{18}O_{rt}$ data. The data are skewed towards enriched $\delta^{18}O_{rt}$ values (skewness = -1.67), and as a consequence, this skew is also reflected in the $\delta^{18}O_{mw}$ estimates (Figures 6.15a and 6.20). Additionally, only four teeth were analysed, and thus the uncertainties on the mean $\delta^{18}O_{mw}$ value are relatively broad. Furthermore, the calculated $\delta^{18}O_{mw}$ values were extrapolated from the modern calibration. The modern relationship between the $\delta^{18}O$ of rodent tooth carbonate and $\delta^{18}O_{mw}$ may vary, and thus there is some uncertainty regarding the accuracy and precision of the extrapolated $\delta^{18}O_{mw}$ values.

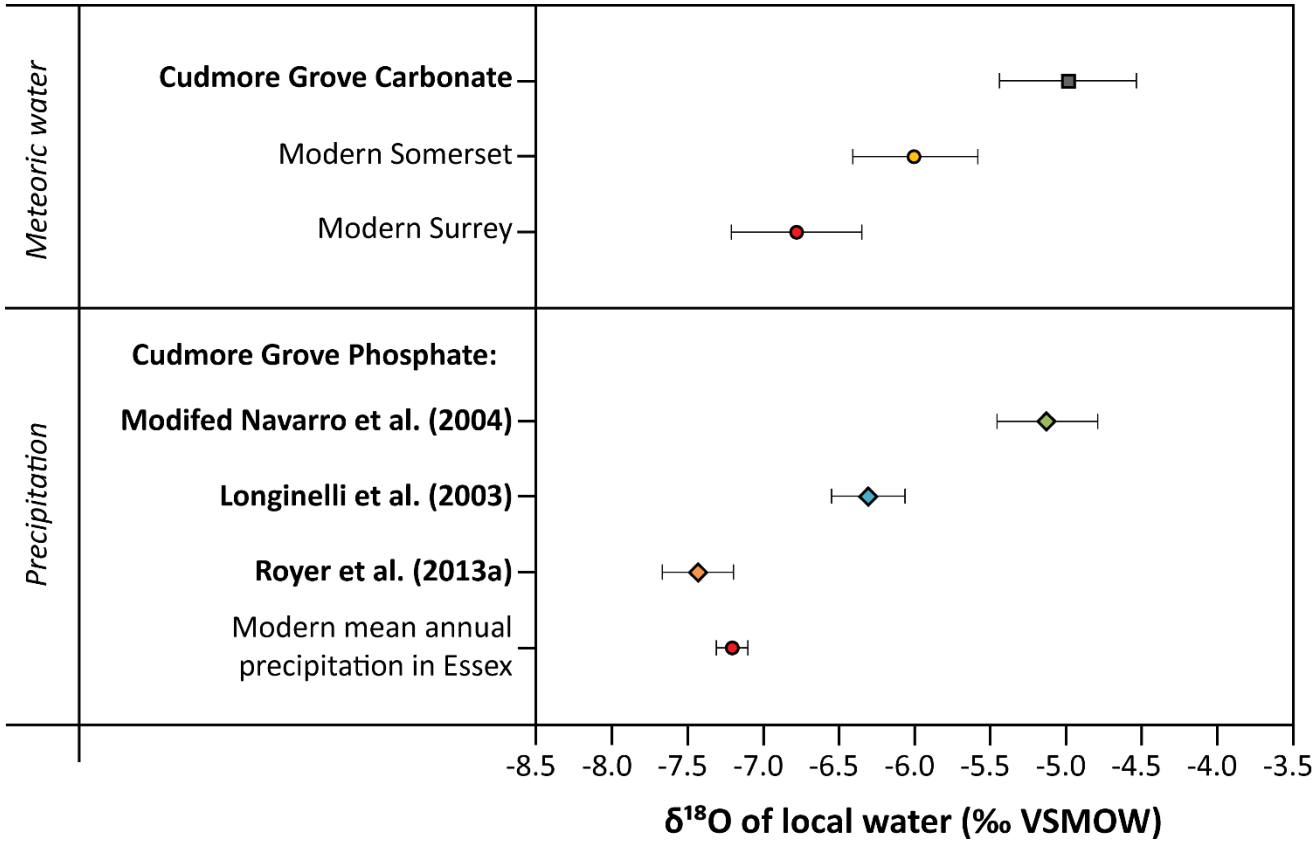

Figure 6.20: *Comparison of the mean $\delta^{18}O$ values of local water, calculated using the fossil rodent tooth data from Cudmore Grove (bold), with the mean $\delta^{18}O$ values of modern meteoric water and precipitation from southern Britain. The modern $\delta^{18}O$ values of meteoric water for Somerset and Surrey are from Chapter 5 and Darling & Bowes (2016), respectively. The modern $\delta^{18}O$ of mean annual precipitation for Essex was calculated using the Online Isotopes in Precipitation Calculator (Bowen et al., 2003; Bowen, 2017).*

Despite this, the mean annual $\delta^{18}O_{pt}$ value calculated using the Longinelli et al. (2003) equation is also more enriched than modern $\delta^{18}O_{pt}$ values in southern Britain, while the mean $\delta^{18}O_{pt}$ value calculated using the Royer et al. (2013a) equation is comparable to today (Figure 6.20). Therefore, the $\delta^{18}O_{pt}$ reconstructions also suggest that the climate at Cudmore Grove was similar to or warmer than present.

The mean $\delta^{18}O$ of summer precipitation, generated using the modified Navarro et al. (2004) equation, is likewise comparable to or slightly higher than southeast Britain today (Figure 6.21). The similarity in the $\delta^{18}O$ values generated using the carbonate and modified Navarro et al. (2004) equations (Figure 6.20) indicates that the mean $\delta^{18}O_{mw}$ at Cudmore Grove was comparable to the summer $\delta^{18}O_{pt}$. In present-day Britain, the mean $\delta^{18}O_{mw}$ value of the River Thames is ~0.5‰ lower than the mean $\delta^{18}O$ of precipitation during summer, although the ranges in $\delta^{18}O_{mw}$ and $\delta^{18}O_{pt}$ values overlap (Figure 6.21) (Darling et al., 2003; Darling & Bowes, 2016). This suggests that surface water at Cudmore Grove may have experienced increased evaporation due to drier climatic conditions, resulting in $\delta^{18}O_{mw}$ values that are comparable to the mean $\delta^{18}O$ of summer precipitation.

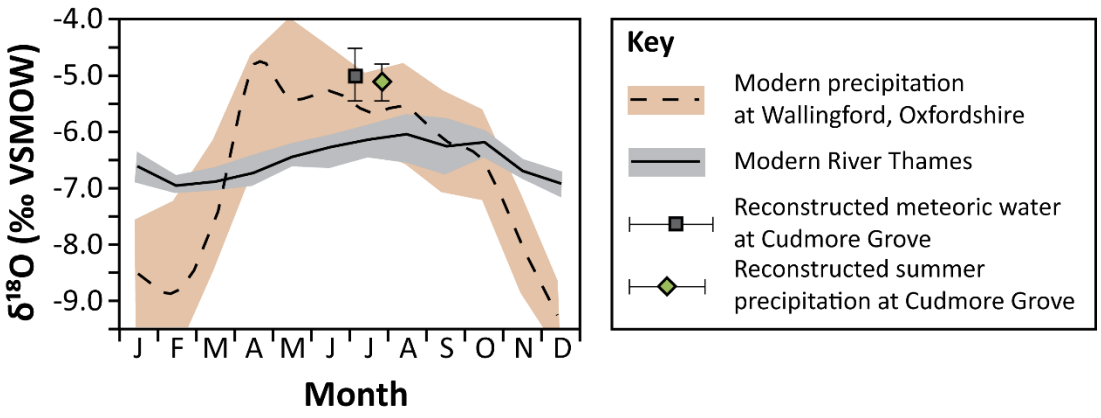

***Figure 6.21**: Comparison of the reconstructed $\delta^{18}O$ values of meteoric water and summer precipitation for Cudmore Grove, with mean monthly $\delta^{18}O$ values of modern meteoric water and precipitation from southeast Britain. This diagram is adapted from Figure 3d in Darling & Bowes (2016). The shaded areas indicate the inter-quartile ranges in the river water and precipitation data.*

The differences in the $\delta^{18}O$ values of local water reconstructed using the various equations (Table 6.3) result from the differences in the data used to generate the calibrations. The Longinelli et al. (2003) and Royer et al. (2013a) calibrations are based upon the mean annual $\delta^{18}O$ of precipitation, the modified Navarro et al. (2004) equation is based on the mean $\delta^{18}O$ of summer precipitation, and the *M. agrestis* carbonate equation uses measured $\delta^{18}O$ values of surface meteoric waters. Due to the dominant influence of temperature on $\delta^{18}O_{pt}$ in mid-latitude regions, the $\delta^{18}O$ of precipitation is more enriched during summer than during winter (Dansgaard, 1964; Rozanski et al., 1993; Darling & Talbot, 2003). Surface water sources in Britain are also typically enriched compared to the mean annual $\delta^{18}O$ of precipitation (e.g. Darling & Bowes, 2016). As a result, the carbonate and modified Navarro et al. (2004) equations yield higher $\delta^{18}O_{mw}$ values relative to the Longinelli et al. (2003) and Royer et al. (2013a) equations (Table 6.3).

In order to apply the coupled isotope approach, however, the reconstructed $\delta^{18}O_{mw}$ value must accurately reflect the summer $\delta^{18}O$ composition of the surface water source in which the mollusc shells mineralized. The Longinelli et al. (2003) and Royer et al. (2013a) equations, which generate mean annual $\delta^{18}O$ values of precipitation, are therefore likely to underestimate the $\delta^{18}O$ composition of this water source. On the other hand, the $\delta^{18}O$ values derived from the carbonate and Navarro et al. (2004) equations are likely to provide a more accurate reflection of the summer $\delta^{18}O_{mw}$ value. This will consequently be taken into consideration when assessing the reliability of the reconstructed temperatures in the following section.

6.6.6.3. Reconstructed mean summer temperatures

The summer palaeotemperatures, reconstructed using the coupled isotope approach, are shown alongside published mean summer temperature estimates in Figure 6.22. The temperatures calculated from the mean $\delta^{18}O_{mw}$ and summer $\delta^{18}O_{pt}$ values are consistent, within uncertainties, with the maximum mean summer temperatures (T_{max}) generated from the coleopteran,

ostracod and herpetofaunal assemblages. The fact that the coupled isotope temperature estimates lie towards the higher end of the existing reconstructions may be due to the aforementioned factors, such as: 1) the influence of evaporation on the $\delta^{18}O$ of meteoric water, and particularly the $\delta^{18}O$ of food and drinking water, 2) a negative skew in the $\delta^{18}O_{rt}$ data, and 3) uncertainties in the mean $\delta^{18}O_{mw}$ due to potential variability in the modern calibration.

The mean annual $\delta^{18}O_{pt}$ derived from the Longinelli et al. (2003) equation generates a mean temperature value that is comparable to the lower T_{max} estimates from the palaeoecological proxies (Figure 6.22). Conversely, the $\delta^{18}O_{pt}$ from the Royer et al. (2013a) equation produces a mean temperature that is significantly lower than all other palaeoclimate reconstructions. This supports the argument that calibrations based on mean annual $\delta^{18}O_{pt}$ data tend to underestimate the $\delta^{18}O$ value of surface meteoric water. Since the Longinelli et al. (2003) equation produces temperatures that overlap with the existing palaeoclimate evidence from Cudmore Grove, this equation may provide reliable values for the $\delta^{18}O$ of meteoric water.

Nevertheless, the mean $\delta^{18}O_{pt}$ calculated using the Royer et al. (2013a) equation could provide an estimate for the mean annual temperature. Modern rodent teeth with average phosphate $\delta^{18}O$ values similar to those from Cudmore Grove, at ~15.5‰, occur in areas with mean annual temperatures of around 11-12°C (Royer et al., 2013a). The mean annual temperature at Cudmore Grove today is around 10.6°C (Met Office, 2018). The $\delta^{18}O_{pt}$ value reconstructed using the Royer et al. (2013a) equation may therefore indicate that the past mean annual temperature at Cudmore Grove was slightly warmer than today.

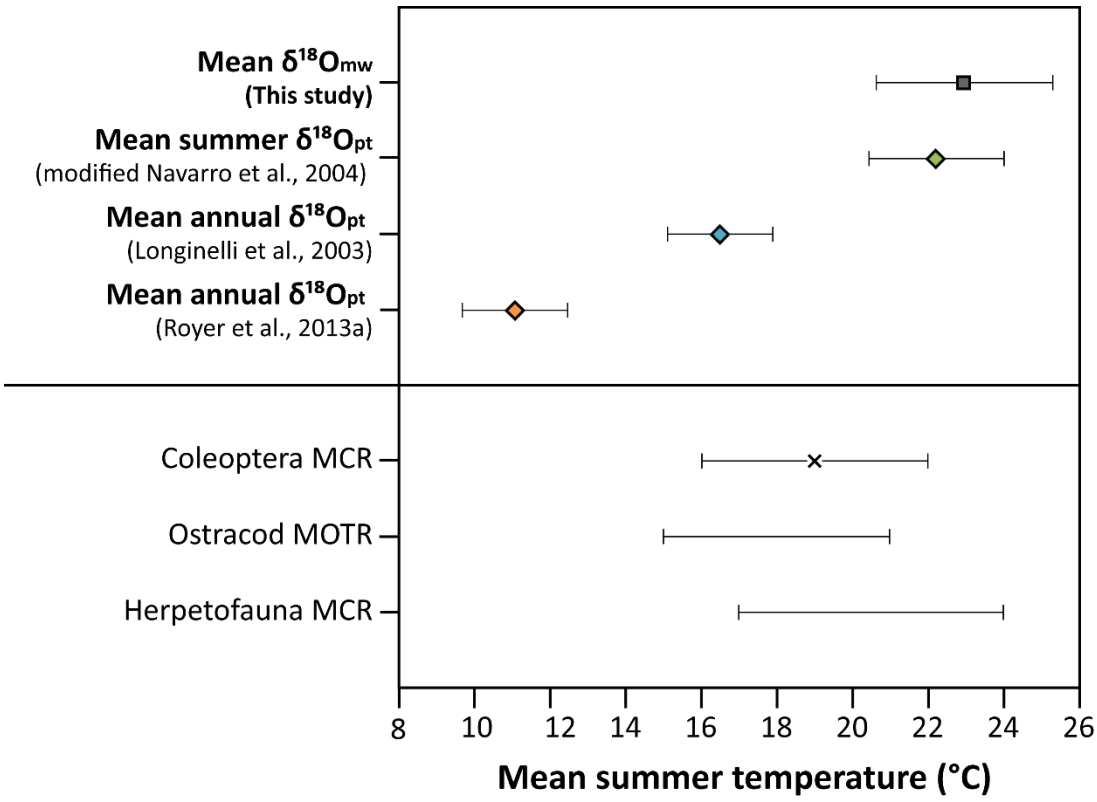

Figure 6.22: *Comparison of the mean temperatures for Cudmore Grove, calculated using the coupled isotope approach, with published palaeotemperature estimates for the site. The beetle-based (Coleoptera) mean summer temperature estimates are from Roe et al. (2009), the ostracod-based temperature estimates are from Horne et al. (2012), and the herpetofauna-based temperature estimates are from Sinka (1993). The cross on the Coleoptera MCR reconstruction indicates the most likely mean summer temperature.*

6.6.7. Summary

The $\delta^{18}O$ values of the *A. cantiana* tooth carbonate and phosphate, and the reconstructed mean $\delta^{18}O$ value of surface meteoric water, both suggest that the climate at Cudmore Grove was warmer than southern Britain at the present day. The reconstructed mean $\delta^{18}O$ of summer precipitation likewise indicates that climatic conditions were similar to or warmer than today. The highly enriched mean $\delta^{18}O_{mw}$ value may also suggest that the climate was slightly drier than the present day.

The summer palaeotemperatures generated via the coupled isotope approach overlap with the existing temperature estimates derived from the faunal assemblages at Cudmore Grove. This suggests that the coupled isotope approach can provide accurate summer temperature reconstructions for past interglacial stages. However, due to the small number of teeth sampled for carbonate analyses, and the need to extrapolate $\delta^{18}O_{mw}$ values beyond the modern calibration, the uncertainties on the temperature estimates are fairly large, and the mean calculated temperature is slightly higher than suggested by the faunal evidence. These issues highlight the need for analyses to be undertaken on > 4 teeth per site in order to obtain an accurate and precise mean $\delta^{18}O_{rt}$ value for the local rodent population. Moreover, analyses of rodent teeth from additional modern sites are needed to extend the modern calibration to encompass the potential range in past $\delta^{18}O_{mw}$ values.

Conversely, the calculated mean annual $\delta^{18}O_{pt}$ values generally underestimate the mean summer temperature. This is because the mean annual $\delta^{18}O$ of precipitation is typically depleted relative to the mean $\delta^{18}O$ compositions of the surface water sources from which rodent teeth and mollusc shells mineralize. Therefore, when applying the coupled isotope approach using the $\delta^{18}O$ values of rodent tooth phosphate, it is recommended that a summer-specific calibration, such as the modified version of the Navarro et al., (2004) equation produced by Ruddy (2005), should be used. Despite this, the Longinelli et al. (2003) equation seems to generate fairly accurate mean $\delta^{18}O_{mw}$ values. Furthermore, mean annual $\delta^{18}O_{pt}$ values, generated using the Royer et al. (2013a) equation, may be useful for reconstructing past mean annual temperatures.

6.7. Results: Marsworth, Buckinghamshire

6.7.1. $\delta^{18}O$ of teeth

The $\delta^{18}O$ values of the teeth from Level 3 vary between -8.0‰ and -3.6‰ (range = 4.4‰), although the majority of the data lie between -8 and -6‰ (Figure 6.23). The data are significantly positively skewed (Shapiro-Wilk,

$p < 0.05$). However, there is one possible outlier with a value of -3.6‰. This sample, plus two others, were re-analysed to check the consistency of the results. The secondary analyses generated values that were within 0.4‰ of the values from Analysis 1 (Table 6.5). These differences fall within the estimated 1σ precision on individual $\delta^{18}O$ measurements of rodent bioapatite (± 0.5‰). Therefore, the values from the two analyses were averaged. The results of a Grubbs' test suggest that the enriched value of -3.7‰ is a significant outlier ($p < 0.05$). This value was consequently excluded from the dataset. The mean value, excluding this outlier, is -7.11‰ (1σ standard deviation = 0.86‰) and the median is -7.54‰ (range = 2.25‰).

The $\delta^{18}O$ data for the teeth from Level 2 range between -9.2 and -5.9‰, with the majority of samples also falling between -8 and -6‰ (Figure 6.23). The data are normally distributed (Shapiro-Wilk, $p > 0.05$), and there are no outliers. Two samples were re-analysed, and the results are broadly consistent (Table 6.5). The mean value of the teeth from Level 2 is -7.41‰ (1σ = 0.96‰), and the median is -7.49‰ (range = 3.1‰).

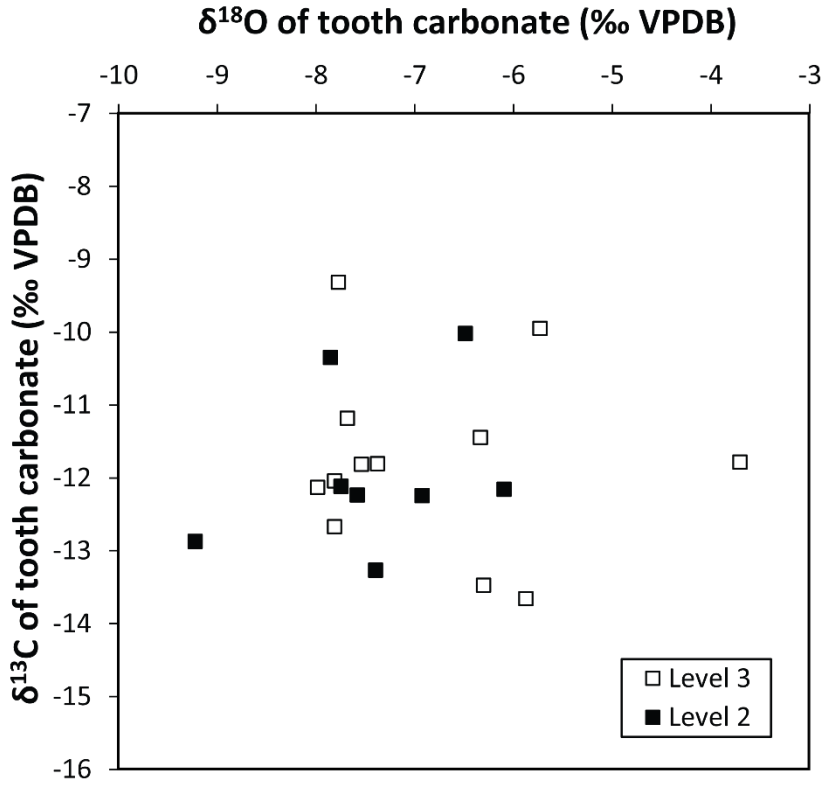

Figure 6.23: *Oxygen and carbon isotope results for the fossil rodent teeth from Level 3 and Level 2 at Marsworth.*

As is evident in Figure 6.23, the ranges in $\delta^{18}O$ values of the teeth from Levels 3 and 2 are very similar. The results of a Mann-Whitney test confirm that there is no statistically significant difference between the average $\delta^{18}O$ values of the teeth from these sedimentary layers ($p > 0.05$). The $\delta^{18}O_{rt}$ datasets from Levels 3 and 2 can therefore be combined. The overall mean $\delta^{18}O$ value is -7.24‰ (1σ = 0.89), and the median is -7.54‰ (range = 3.49‰). The data are normally distributed (Shapiro-Wilk, $p > 0.05$). This combined dataset will be used in the following calculations of the $\delta^{18}O$ of meteoric water.

Table 6.5: *Oxygen isotope results from the first and second analyses of the teeth from Levels 3 and 2 at Marsworth.*

Specimen code	**$\delta^{18}O$ (‰ VPDB)**			
	Analysis 1 (A1)	**Analysis 2 (A2)**	**Difference (A1-A2)**	**Average (A1+A2)/2**
MA-3-J9-T1	-3.6	-3.8	0.2	-3.7
MA-3-J10-T2	-7.5	-7.9	0.4	-7.7
MA-3-J16-T2	-7.6	-7.9	0.3	-7.8
MA-2-L10-T4	-5.9	-6.3	0.4	-6.1
MA-2-L11-T1	-6.5	-7.8	1.3	-7.1

6.7.2. $\delta^{13}C$ of teeth

The carbon isotope values of the teeth from Level 3 vary between -13.7‰ and -9.3‰ (range = 4.3‰) (Figure 6.23). The data are normally distributed (Shapiro-Wilk, $p > 0.05$). The re-analyses of the three teeth from Level 3 generated values within 1‰ of Analysis 1. Therefore, the results from the two analyses were averaged. The mean value for Level 3 is -11.86‰ (1σ = 1.31‰).

The $\delta^{13}C$ values of the teeth from Level 2 span a narrower range of 3.4‰, between values of -13.3 and -9.9‰ (Figure 6.23). The data are normally distributed (Shapiro-Wilk, $p > 0.05$). Re-analyses of the teeth from Level 2

produced values within 0.3‰ of the results from Analysis 1. The mean $\delta^{13}C$ value for Level 2 is -11.91‰ (1σ = 1.14).

As with the $\delta^{18}O$ results, the mean $\delta^{13}C$ values of the teeth from Levels 3 and 2 are very similar. The results of a T-test show that there is no statistically significant difference between the mean $\delta^{13}C_{rt}$ values of these datasets ($p > 0.05$). The overall mean $\delta^{13}C_{rt}$ value is -11.83‰ (1σ = 1.21). Furthermore, there is no significant correlation between the $\delta^{18}O$ and $\delta^{13}C$ values of the teeth ($r^2 = 0.003$, $p = 0.86$).

6.7.3. Mineralogy of the mollusc shells

The X-ray Diffraction patterns (diffractograms) for the 5 shell samples are shown in Figure 6.24. Comparison of the major diffraction peaks with XRD crystallography data for pure minerals (Figure 6.24a-b) indicates that all of the shells are composed of aragonite. However, sample MA-2-G4 (Figure 6.24d) has an additional peak at 29.5° 2θ, which corresponds with the main diffraction peak of calcite (Figure 6.24b). Also, some of the minor peaks in the calcite diffractogram occur at similar values of 2θ as aragonite (i.e. ~36°, ~43°, ~48.5°), and thus these peaks may be masked by the dominant aragonite signal. Nevertheless, the minor calcite peaks at 39.5° 2θ, and 47.5° 2θ are not seen in the XRD results for sample MA-2-G4. This suggests that the sample is predominantly composed of aragonite.

In order to test this interpretation, the relative calcite content in sample MA-2-G4 was calculated using the calibration curve of Douka et al. (2010). This curve relates the relative peak heights of calcite and aragonite in XRD spectra to the percentage calcite content by weight within the sample (Figure 6.25). To calculate the relative peak heights, the following equation was used:

$$\text{Peak height ratio} = \frac{H_c}{H_c + H_a} \qquad (6.8)$$

where H_c is the height of the ~29.4° 2θ calcite peak minus the background noise, and H_a is the height of the ~33° 2θ aragonite peak minus the background noise. The calculated peak height ratio for sample MA-2-G4 is

0.53. The conversion of this ratio to an approximate percentage calcite value is shown in Figure 6.25. This figure shows that the calcite concentration in the sample is, on average, ~16.5% by weight. This means that the sample contains ~83.5% aragonite by weight.

These XRD results indicate that the majority of the shells have retained their original aragonitic composition, while one sample may have undergone recrystallization to calcite. However, it is also possible that the presence of calcite in MA-2-G4 may result from contamination, due to the insufficient cleaning of the sample prior to analysis. The sediments at Marsworth are carbonate-rich, due to the erosion and dissolution of the local Chalk bedrock (Murton et al., 2001). Thus, the presence of a small amount of detrital calcium carbonate in the sample is not implausible. Also, as mentioned in Section 4.4.3., the fragile nature of the shells prevented the use of rigorous cleaning methods, and consequently, some of the shells may not have been fully cleaned of sediment.

In addition, proportional mixtures of aragonite and calcite (e.g. 80% aragonite, 20% calcite), analysed via X-ray diffraction, Raman spectrometry and Fourier Transform spectrometry methods, typically produce smaller and broader aragonite peaks compared to samples comprising 100% aragonite (Davies & Hooper, 1963; Kontoyannis & Vagenas, 2000; Loftus et al., 2015). This is because the replacement of aragonite with calcite leads to a reduction in the measured signal intensity of aragonite. However, in the XRD diffractogram for sample MA-2-G4, all of the peaks corresponding to aragonite have a high intensity and are comparable in shape to the other shell samples consisting of pure aragonite (Figure 6.24). This strongly suggests that the calcite within this sample originates from detrital calcite contamination rather than the alteration of the shell aragonite. Nevertheless, a small degree of aragonite recrystallization in some of the analysed shells cannot be entirely ruled out.

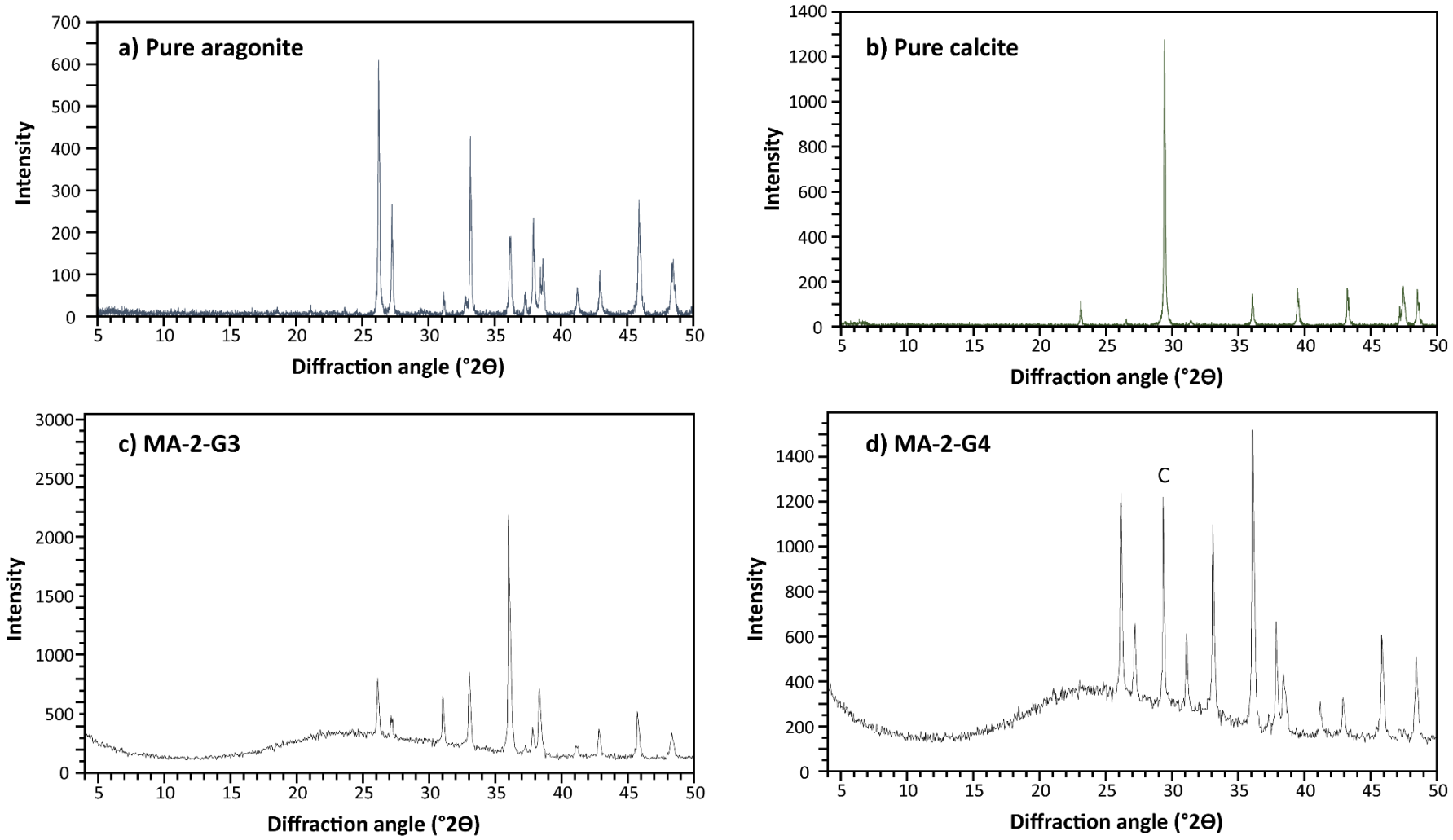

Figure 6.24. *(for caption see overleaf)*

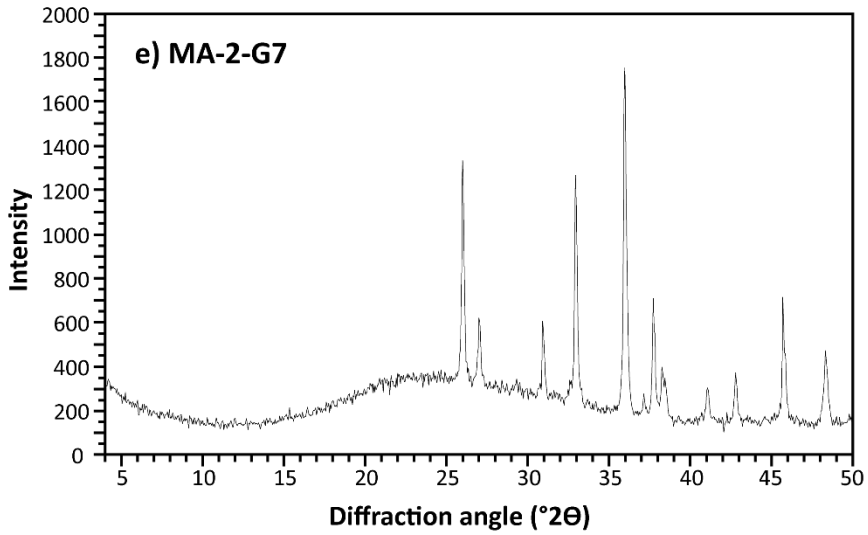

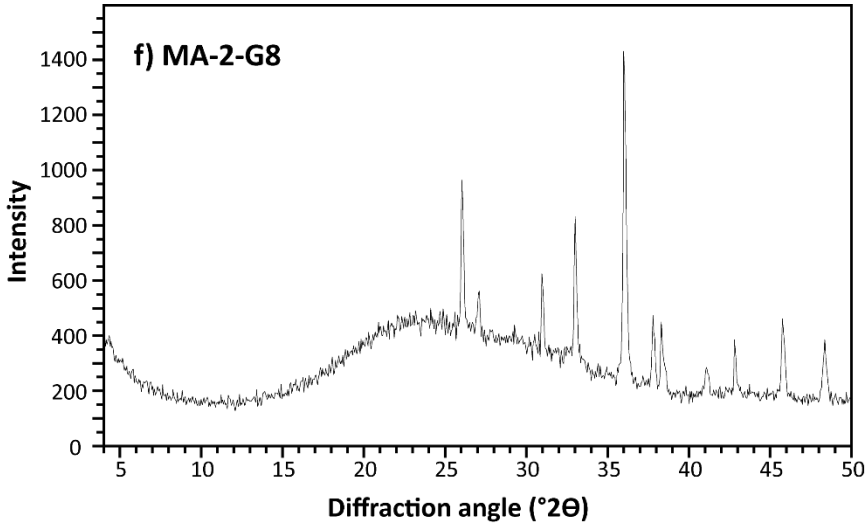

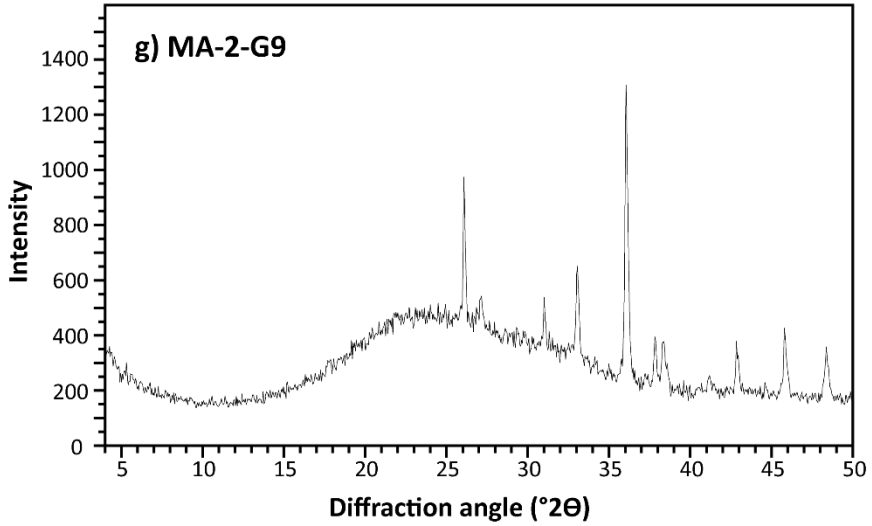

Figure 6.24: *X-ray diffractograms for a) pure aragonite (from Aragon, Spain), b) pure calcite (from Catalonia, Spain), and c-g) the fossil* Galba truncatula *shells from Marsworth. The data for the pure aragonite and calcite samples were obtained from Lafuente et al. (2015). The calcite peak in sample MA-2-G4 is labelled 'C'.*

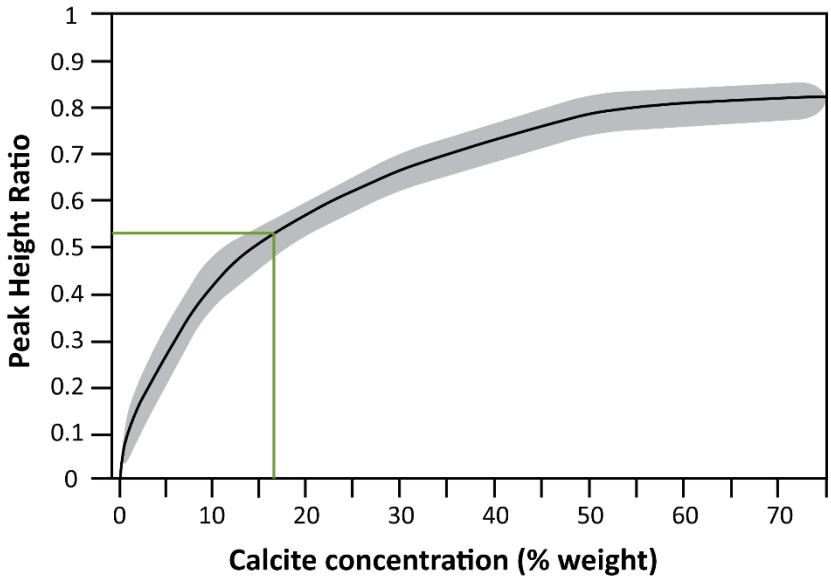

Figure 6.25: *The calibration curve of Douka et al. (2010), for converting the peak height ratio of aragonite and calcite peaks in an X-ray diffractogram from a carbonate sample, to the calcite concentration within the sample. The grey shading represents the uncertainties around the calibration line (black), and the green line shows the results for sample MA-2-G4 from Marsworth.*

6.7.4. $\delta^{18}O$ and $\delta^{13}C$ of mollusc shells

The oxygen and carbon isotope results for the mollusc shells are shown in Figure 6.26. One shell from Level 2 generated insufficient material for analysis. Four of the shells also failed to produce reliable results during initial analysis, and thus three of these samples, which had sufficient material remaining, were re-analysed. The re-analyses generated isotope values that are consistent with the dataset as a whole.

The $\delta^{18}O$ values of the two shells from Level 3 are very similar, with a mean value of -4.47‰. The $\delta^{13}C$ values of these shells are -8.6‰ and -12.0‰.

In contrast, the $\delta^{18}O$ values of the shells from Level 2 are variable, ranging from a minimum of -4.8‰ to a maximum of -0.6‰ (range = 4.2‰) (Figure 6.26). The mean $\delta^{18}O$ value is -2.83‰. The $\delta^{13}C$ values of the shells from Level 2 are similar to those from Level 3, with values varying between -12.1 and -8.1‰ (Figure 6.26). The mean $\delta^{13}C$ value of the Level 2

shells is -9.95‰. The $\delta^{18}O$ and $\delta^{13}C$ data for Level 2 are normally distributed (Shapiro-Wilk, $p > 0.05$).

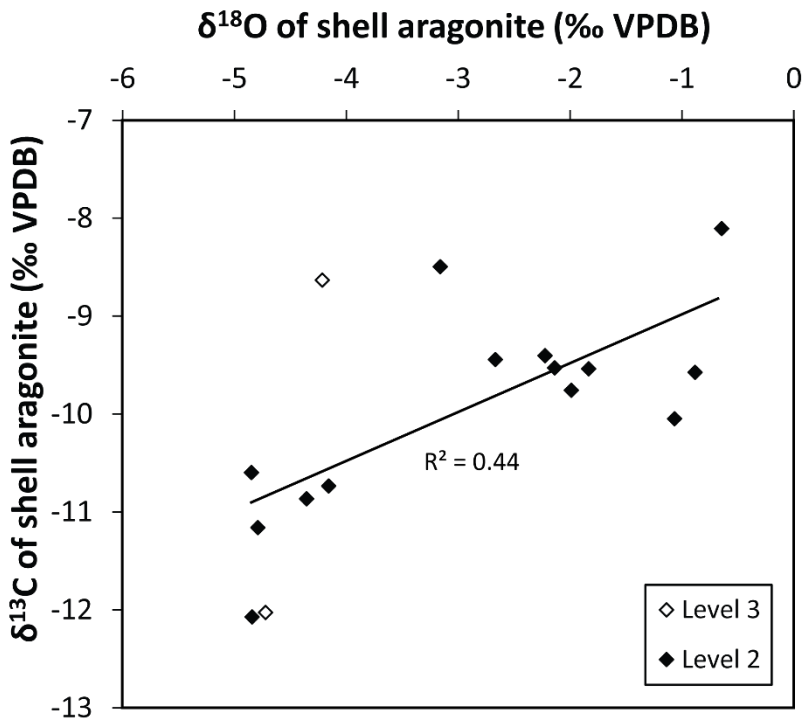

Figure 6.26: *Oxygen and carbon isotope results for the fossil* G. truncatula *shells from Levels 3 and 2 at Marsworth.*

The presence of detrital calcite in sample MA-2-G4 (Figure 6.24d) may have influenced the isotope results for this shell. The major source of calcite proximal to Marsworth is the Cretaceous Chalk bedrock. This marine limestone has typical $\delta^{18}O$ values of around -4 to -1‰, and $\delta^{13}C$ values of around +1 to +5‰ (Hudson, 1977; Jenkyns et al., 1994). Therefore, it would be expected that shell samples containing detrital calcite, or shells that have undergone partial recrystallization to calcite, would have relatively enriched $\delta^{18}O$ and $\delta^{13}C$ values. The $\delta^{18}O$ value of sample MA-2-G4 is -2.2‰ and thus is relatively enriched. However, the $\delta^{13}C$ value of this sample is -9.4‰, and thus is not consistent with substantial contamination from the local bedrock. Moreover, three of the four shells that comprise pure aragonite have $\delta^{18}O$ and

$\delta^{13}C$ values comparable to sample MA-2-G4. This suggests that potential detrital contamination has had a minimal impact on the isotope results of the shells.

Since the $\delta^{18}O$ and $\delta^{13}C$ values of the shells from Levels 3 and 2 overlap, the datasets from these layers have been combined. The overall mean $\delta^{18}O$ value is -3.03‰ (1σ = 1.53‰) and the mean $\delta^{13}C$ value is -10.00‰ (1σ = 1.17). However, Figure 6.26 shows that there is a fairly weak but statistically significant correlation between the $\delta^{18}O$ and $\delta^{13}C$ values of the shells (r^2 = 0.44, p = 0.006). As mentioned in Section 2.2.2.5, covariance in the $\delta^{18}O$ and $\delta^{13}C$ values of lacustrine carbonates is often associated with the hydrological closure and evaporation of a water body (Talbot, 1990; Li & Ku, 1997). Therefore, as it is likely that the water body that the Marsworth shells precipitated within was affected by evaporation, the lowest shell $\delta^{18}O$ value (-4.8‰) has been selected for the following temperature calculations. This is because the minimum $\delta^{18}O_{ms}$ value is likely to provide the closest reflection of the calculated mean $\delta^{18}O$ of local meteoric water. The 1σ uncertainty for the $\delta^{18}O_{ms}$ value is the measurement error on the isotopic analysis (± 0.09‰).

6.7.5. $\delta^{18}O$ of meteoric water

The calculated $\delta^{18}O_{mw}$ values for Levels 3 and 2 are shown in Figure 6.27. The overall mean value is -6.46 ± 0.21‰ (calibration uncertainty = 0.05‰, 1σ standard error = 0.16‰). The mean $\delta^{18}O_{mw}$ value for Level 3 is -6.36 ± 0.26‰, and the mean value for Level 2 is -6.59 ± 0.31‰.

6.7.6. Summer temperature

The mean summer temperature, calculated by coupling the overall mean $\delta^{18}O_{mw}$ value with the minimum shell $\delta^{18}O$ value, is illustrated in Figure 6.28. The mean summer temperatures for Level 3, Level 2 and the dataset as a whole are also compared in Table 6.6. The temperatures, including uncertainties, range from ~11-15°C. The mean value for Level 2 is slightly less

than that for Level 3, although there is no statistically significant difference between these temperature estimates (Mann-Whitney, $p > 0.05$).

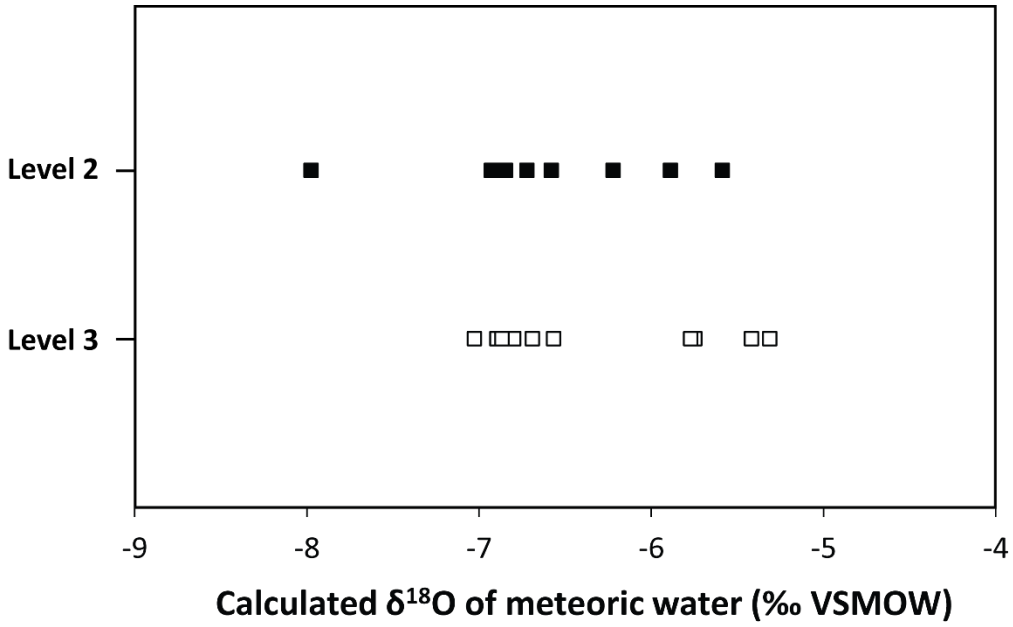

Figure 6.27: *Oxygen isotope values of meteoric water, calculated from the $\delta^{18}O$ values of the rodent teeth from Levels 3 and 2 at Marsworth.*

Table 6.6: *Calculated mean summer temperatures for Marsworth, using the mean $\delta^{18}O$ values of meteoric water for Level 3, Level 2 and both levels combined.*

$\delta^{18}O$ data	**Mean summer temperature ± 1σ uncertainty (°C)**
Level 3	14.04 ± 1.33
Level 2	12.92 ± 1.58
All data	13.57 ± 1.11

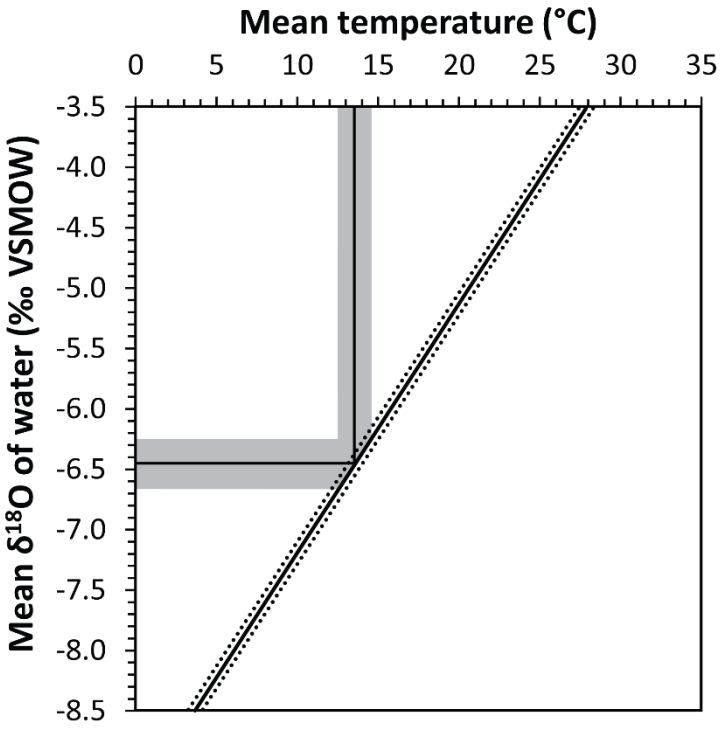

Figure 6.28: *Graph illustrating the calculation of the mean summer temperature for Marsworth, by coupling the mean calculated $\delta^{18}O$ of meteoric water with the minimum $\delta^{18}O$ value of the mollusc shells (solid black straight line). The dotted lines represent the 1σ analytical error on the $\delta^{18}O$ value of the shell, and the grey shading indicates the 1σ standard error uncertainties on the calculated meteoric water and temperature values.*

6.7.7. Interpretations and Discussion

6.7.7.1. $\delta^{18}O$ and $\delta^{13}C$ of teeth

The mean $\delta^{18}O$ value of the *Microtus* sp(p). teeth from Marsworth is comparable to the $\delta^{18}O$ values of modern *M. agrestis* teeth from southern Britain (Figure 6.29). This suggests that the $\delta^{18}O_{mw}$ compositions and palaeoclimatic conditions at Marsworth were similar to southern Britain at the present day.

As with West Runton and Cudmore Grove, the mean $\delta^{13}C$ value of the teeth from Marsworth (-11.83‰) is more enriched than modern *M. agrestis*

teeth from Britain (-18 to -16‰). The calculated mean $\delta^{13}C$ of the diet is -23.3‰, which is consistent with a pure C_3 diet.

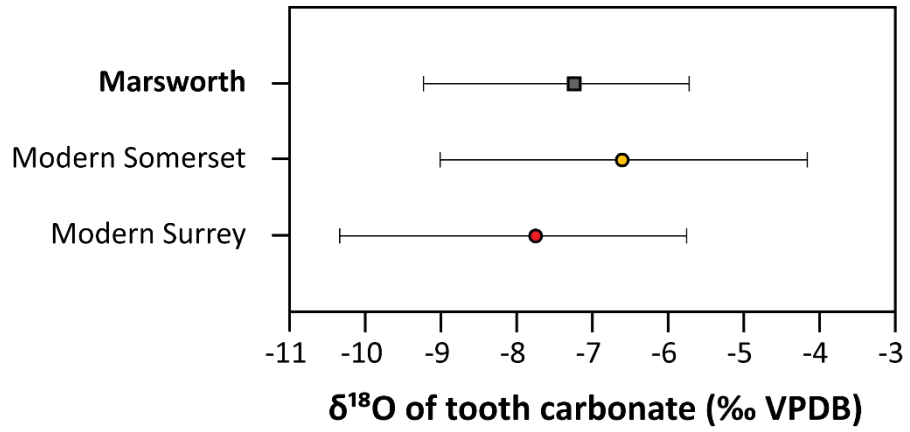

Figure 6.29: *Comparison of the mean $\delta^{18}O$ of rodent tooth carbonate for Marsworth, with the mean $\delta^{18}O$ values of modern* M. agrestis *teeth from southern Britain. The error bars indicate the range in tooth $\delta^{18}O$ values for each site.*

6.7.7.2. $\delta^{18}O$ and $\delta^{13}C$ of mollusc shells

The $\delta^{18}O$ values of the *Galba truncatula* shells from Marsworth are significantly enriched compared to the mean $\delta^{18}O$ values of modern freshwater gastropod shells from southern Britain (Figure 6.30). Since the $\delta^{18}O$ values of mollusc shells reflect $\delta^{18}O_{mw}$, these results might suggest that $\delta^{18}O_{mw}$ values at Marsworth were more enriched than the present day.

The mean $\delta^{13}C$ value of the *G. truncatula* shells (-10‰) is also more enriched than modern shells from the River Thames (-16 to -14‰) (Davies, 1999), and River Gipping (-12 to -11‰) (Waghorne et al., 2012) in southeast Britain. The $\delta^{13}C$ values of aquatic mollusc shells reflect the $\delta^{13}C$ of DIC, plus metabolic carbon derived from the molluscs' diet (Fritz & Poplawski, 1974; McConnaughey & Gillikin, 2008). Therefore, the differences between the $\delta^{13}C$ values of the modern (*G. truncatula*) and fossil (*Valvata piscinalis*, *Bithynia tentaculata*, and *Sphaerium corneum*) shells may partly result from differences

in the dietary preferences of the gastropod species. However, no modern analogue studies have been undertaken on the isotopic values of *G. truncatula* shells, and thus it is not currently possible to assess this hypothesis. The relatively depleted $\delta^{13}C$ values of the modern shells could also result from the recent decline in the $\delta^{13}C$ value of atmospheric CO_2. The water body at Marsworth may have also experienced greater equilibration with atmospheric CO_2 compared to the modern rivers. This interpretation is supported by the observed correlation between the $\delta^{18}O_{ms}$ and $\delta^{13}C_{ms}$ values (Figure 6.26).

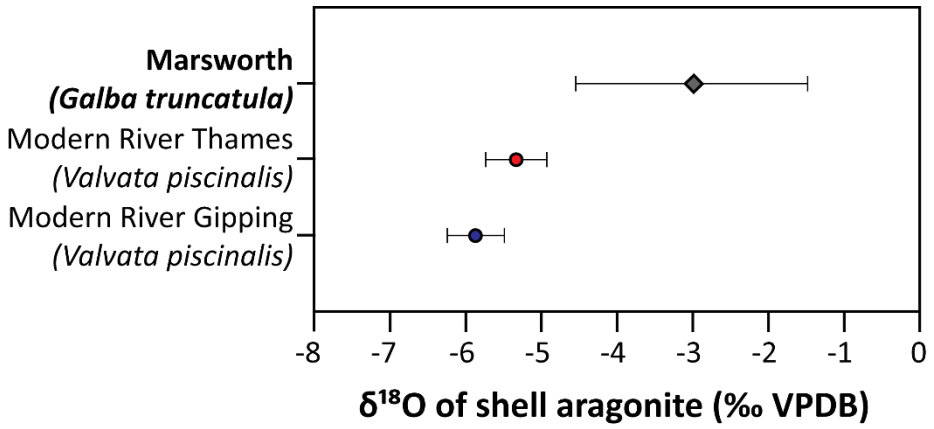

Figure 6.30: *Comparison of the mean $\delta^{18}O$ values of the fossil* G. truncatula *shells from Marsworth, with the mean $\delta^{18}O$ values of modern* V. piscinalis *shells from the River Thames, Surrey (Davies, 1999), and the River Gipping, Suffolk (Waghorne et al., 2012). The error bars represent the 1σ standard deviations on the datasets.*

The covariance between the $\delta^{18}O$ and $\delta^{13}C$ values of the shells can be related to the depositional environment of Marsworth, plus the ecological preferences of *Galba truncatula.* The Level 3 and Level 2 sediments at Marsworth were deposited by a spring-fed stream (Murton et al., 2001). The likely source of this stream is the Chiltern scarp, which occurs ~2 km to the southeast of Marsworth (Murton et al., 2001). Seasonal and inter-annual fluctuations in groundwater levels, due to variations in the amount of precipitation, would have led to variations in the quantity of groundwater

emerging from the spring. This would, in turn, have resulted in fluctuations in stream discharge. During periods of reduced discharge, the stream at Marsworth would be more susceptible to evaporation. This evaporation would cause enrichment in the $\delta^{18}O$ value of the water body and the $\delta^{13}C$ of DIC, due to the preferential loss of the ^{16}O isotope, and the equilibration of DIC with the atmosphere via the preferential degassing of $^{12}CO_2$ from the water (e.g. Andrews et al., 1993; Talbot, 1990).

Temporal changes in stream flow are supported by the sedimentological evidence from Marsworth (Murton et al., 2001). The coarse sands and gravels of Level 3 are consistent with a relatively high stream discharge. Although only two shells were analysed from these sediments, the $\delta^{18}O$ values of both shells are relatively depleted (Figure 6.26). These results imply that the stream experienced limited evaporation during the mineralization of the shells. This interpretation is also consistent with the palaeoecological proxies from Level 3, which suggest the presence of a perennially-flowing stream at the site (Murton et al., 2001).

In contrast, the fine-grained sediments of Level 2 may represent a period of reduced discharge. The abundant presence of palaeoecological proxies within Level 2 that are characteristic of shallow, stagnant water bodies is consistent with this evidence (Murton et al., 2001). Moreover, the $\delta^{18}O$ values of the shells from Level 2 are fairly variable (Figure 6.30) and there is a strong and statistically significant correlation between the $\delta^{18}O_{ms}$ and $\delta^{13}C_{ms}$ values (Figure 6.26). This suggests that the shells from Level 2 mineralized within an evaporating body of water.

The depositional environment at Marsworth is compatible with the ecological preferences of *Galba truncatula*. This species is not strictly aquatic, but is an amphibious mollusc that is often found on wet mud rather than submerged within water (Ellis, 1926). A study on modern *G. truncatula* populations in Orkney showed that fewer than 10% of the snails inhabited permanent habitats that remained wet or damp throughout the year (Heppleston, 1972). The remaining ~90% of the population resided in temporary habitats, such as small patches of mud near to areas of standing water, which often dried up during summer (Heppleston, 1972). *G. truncatula* is therefore typically found in environments that experience fluctuations in

moisture. Moreover, since *G. truncatula* shells primarily grow during summer, when small pools and muddy banks are likely to be particularly susceptible to evaporation (Heppleston, 1972), the $\delta^{18}O$ and $\delta^{13}C$ values of the shells may be significantly enriched. This also means that the $\delta^{18}O$ values of the shells are likely to be enriched relative to the mean $\delta^{18}O_{mw}$ value recorded by the rodent teeth.

In summary, while the palaeoenvironmental proxies indicate that no significant change in climatic conditions occurred during the deposition of Levels 3 and 2 (Murton et al., 2001), the isotopic evidence from the *G. truncatula* shells hint at a change in the local hydrology, from 1) a perennial, slow-flowing stream, to 2) a still or sluggish stream that experienced periodic isolation and drying. The change in the sedimentology from the widespread fluvial sands and gravels of Level 3, to the localised fine-grained muds of Level 2 (Murton et al., 2001), support a shift from higher energy flow within a fluvial channel to low-energy deposition in an isolated basin. The results also demonstrate that *G. truncatula* is perhaps not an ideal species for use in the coupled isotope approach. However, shells of 'true' aquatic species were comparatively rare in the sediment samples investigated in this study. Consequently, *G. truncatula* shells were selected for analysis in order to ensure that the dataset was large enough to record the range in isotopic values for the site. The likely influence of evaporative enrichment on the isotopic values of the shells will therefore be taken into consideration when interpreting the palaeotemperature results.

6.7.7.3. Reconstructed mean $\delta^{18}O$ of meteoric water

The calculated mean $\delta^{18}O_{mw}$ is consistent, within uncertainties, with the modern $\delta^{18}O$ values of surface water sources in southern Britain (Figure 6.31). The mean $\delta^{18}O_{mw}$ value is slightly higher than the mean $\delta^{18}O_{mw}$ of the modern River Thames, which currently lies ~40 km south of Marsworth. This suggests that the climate at Marsworth may have been slightly warmer or drier than present, resulting in a slight enrichment in $\delta^{18}O_{mw}$ relative to today. The

palaeoecological proxies from Marsworth also indicate that local streams and ponds may have dried during the summer (Murton et al., 2001).

In addition, the mean $\delta^{18}O_{mw}$ value for Level 3 is closer to the modern mean value for Somerset, whereas the mean $\delta^{18}O_{mw}$ value for Level 2 is closer to the modern mean value for Surrey (Figure 6.31). This may suggest that palaeoclimatic conditions during the interval represented by Level 3 were slightly warmer than during Level 2. This idea is explored further in the following section.

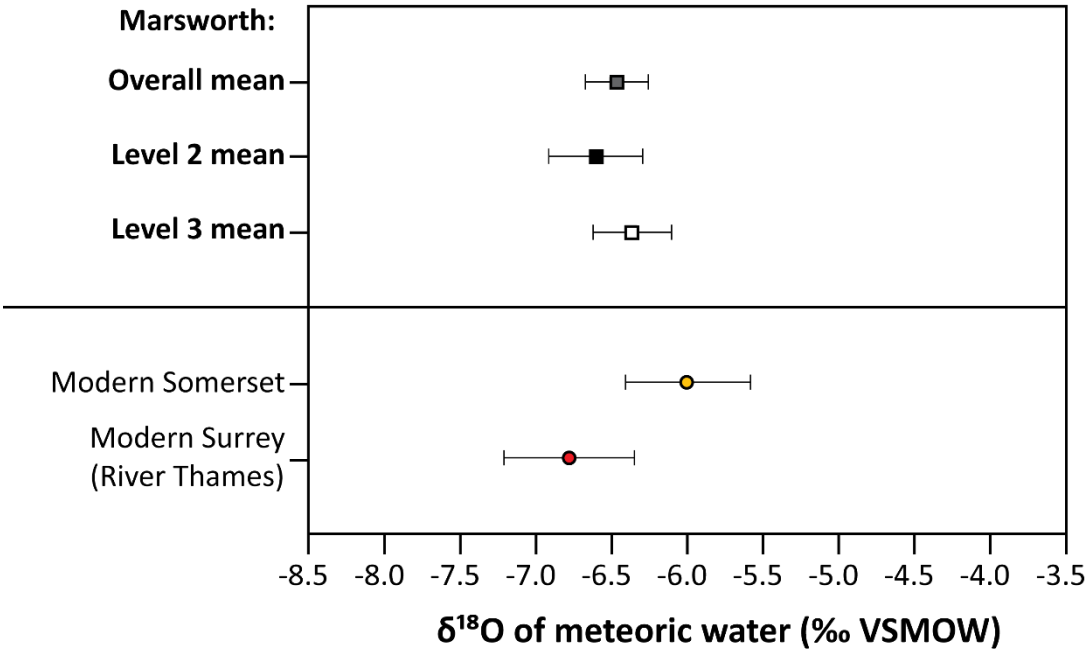

Figure 6.31: *Comparison of the mean calculated $\delta^{18}O$ values of meteoric water for Marsworth, with modern $\delta^{18}O$ values of surface waters in southern Britain. The modern data for Somerset are from Chapter 5, and the modern data for the River Thames at Runnymede are from Darling & Bowes (2016).*

6.7.7.4. Reconstructed mean summer temperature

Figure 6.32 shows that the mean summer temperatures calculated using the coupled isotope approach underestimate the mean summer temperatures

generated from the coleopteran and ostracod assemblages from Marsworth. This is likely due to the mollusc shells having mineralized in an evaporating water body, which has a $\delta^{18}O$ value that is enriched relative to the mean $\delta^{18}O$ values of local meteoric water and summer precipitation.

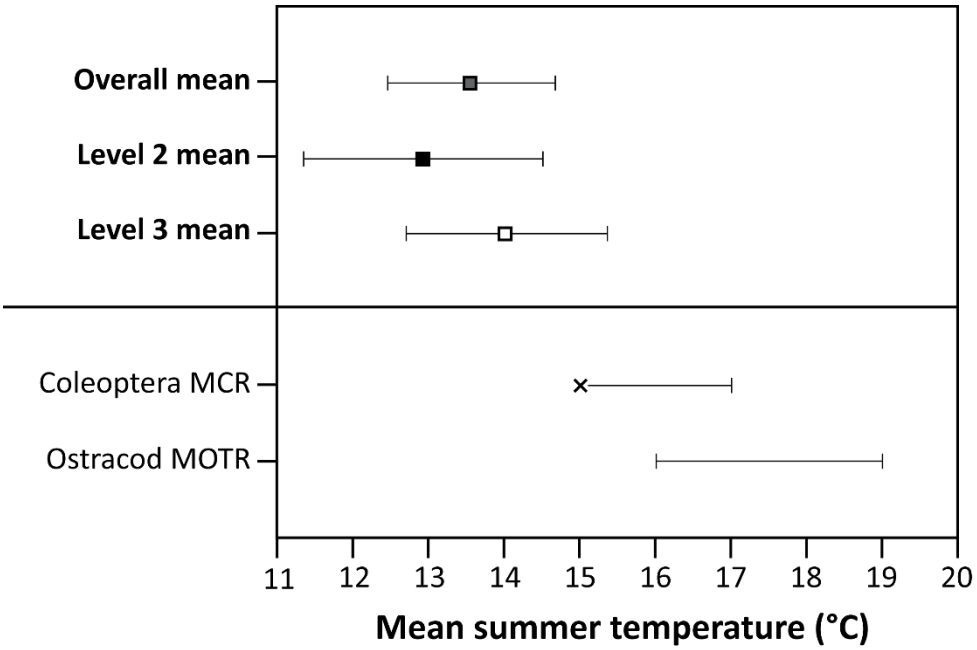

Figure 6.32: *Comparison of the mean summer temperatures for Marsworth, calculated using the coupled isotope approach (bold) and the coleopteran and ostracod assemblages from the site. The coleoptera MCR data are from Murton et al. (2001), and the ostracod data are from Horne (2007). The cross on the coleopteran temperature reconstruction indicates the best estimate for the mean summer temperature value.*

Nevertheless, the uncertainties on the isotope-based temperature estimate for Level 3 overlap with the minimum MCR summer temperature value (Figure 6.32). Also, the temperature estimate for Level 3 is slightly higher than that for Level 2. Similarly, the summer temperature reconstruction based on the ostracod remains from Level 3 is higher than the beetle-based temperature reconstruction for Level 2 (Figure 6.32). This suggests that the mean $\delta^{18}O_{mw}$ values calculated using the rodent teeth from Levels 3 and 2

provide an accurate reflection of the climatic changes through the Marsworth sequence, even though the absolute temperature values are underestimated. The isotope values of the rodent teeth therefore indicate that the climate gradually cooled through Levels 3 and 2. This cooling trend is supported by the occurrence of pollen and beetle taxa that are typical of cool, boreal-montane habitats in the uppermost samples from Level 2 (Murton et al., 2001). However, the uncertainties in the mean $\delta^{18}O_{mw}$ and temperature values for Level 3 and Level 2 overlap, and thus the observed patterns through the sequence may be coincidental.

By substituting the MCR and MOTR temperature reconstructions and the calculated $\delta^{18}O_{mw}$ values into Equation 6.6, it is possible to estimate the $\delta^{18}O$ values of aquatic mollusc shells that have precipitated within a water body that has not been significantly affected by evaporation. The results of these calculations are shown in Table 6.7.

Table 6.7: *Estimated $\delta^{18}O$ values of aquatic mollusc shells for Levels 3 and 2 at Marsworth, calculated by combining the mean $\delta^{18}O$ values of meteoric water generated from the fossil rodent teeth, with the ostracod MOTR and Coleoptera MCR temperature reconstructions from Horne (2007) and Murton et al. (2001), respectively.*

Unit	Mean $\delta^{18}O_{mw}$ (‰ VSMOW)	Mean summer temperature (°C)			Estimated $\delta^{18}O$ of mollusc shell aragonite (‰ VPDB)	
		Method	Min.	Max.	Min.	Max.
Level 3	-6.36	MOTR	+16	+19	-5.87	-5.25
Level 2	-6.59	MCR	+15	+17	-5.69	-5.28

The estimated $\delta^{18}O_{ms}$ values are similar for both Level 3 and Level 2, and vary between -5.3 and -5.9‰. These values are consistent with the modern $\delta^{18}O$ values of freshwater gastropods from southern Britain (Figure 6.30). The $\delta^{18}O_{ms}$ values are also ~0.5-1‰ more depleted than the minimum measured $\delta^{18}O$ values of the *G. truncatula* shells from Marsworth. This equates to a minimum enrichment in the $\delta^{18}O$ of meteoric water of between 0.2 and 1.2‰. This indicates that the evaporation of the water source had a considerable effect on the $\delta^{18}O$ values of the sampled shells. Therefore, caution must be taken when applying the coupled isotope approach to sites where local water sources may have experienced substantial evaporation.

6.7.8. Summary

The $\delta^{18}O$ values of the fossil rodent teeth from Marsworth, and the mean $\delta^{18}O_{mw}$ compositions calculated from these values, are comparable to southern Britain at the present day. This indicates that mean summer temperatures at Marsworth were similar to today.

In contrast, the $\delta^{18}O$ values of the fossil *Galba truncatula* shells are significantly enriched compared to modern shells from southern Britain. The results of X-ray Diffraction analyses demonstrate that the shells have not undergone diagenetic recrystallization. Therefore, the enriched isotopic values are unlikely to result from post-depositional alteration. Instead, it is thought that the shells formed within a water body that experienced evaporation and CO_2 degassing. The relatively strong and statistically significant correlation between the $\delta^{18}O$ and $\delta^{13}C$ values of the shells from Level 2 provides support for this interpretation. Strong positive correlations between $\delta^{18}O$ and $\delta^{13}C$ values are typically observed in carbonates that have precipitated within hydrologically isolated and evaporating water bodies. This suggests that the water body at Marsworth was isolated from the local stream during the accumulation of Level 2.

The enriched isotope values of the shells are also consistent with the habitat preferences of *G. truncatula*. This species primarily lives in temporary, small water bodies and wet patches that are susceptible to evaporation.

Therefore, the $\delta^{18}O$ values of *G. truncatula* shells may not always provide an accurate reflection of the mean $\delta^{18}O$ compositions of the water sources from which rodents obtain their drinking water. It is therefore concluded that this species is unsuitable for use in the coupled isotope approach. As demonstrated by the results from West Runton and Cudmore Grove, strictly aquatic gastropods, such as *Valvata piscinalis*, are more likely to provide an accurate record of the mean $\delta^{18}O_{mw}$.

Due to the enriched $\delta^{18}O$ values of the shells, the calculated mean summer temperatures are lower than the existing palaeoclimate reconstructions for Marsworth. Nevertheless, the mean $\delta^{18}O_{mw}$ values and temperatures for Levels 3 and 2 accurately record the pattern of climatic changes through the Marsworth sequence. The isotope-based temperatures are slightly higher for Level 3 than for Level 2. A parallel trend is seen in the palaeoecologically-based temperature estimates, from higher values of 16-19°C in Level 3, to slightly lower values of 15-17°C in Level 2. Therefore, the mean $\delta^{18}O$ values of the rodent teeth from Marsworth have provided useful palaeoclimate information, despite the fact that the temperatures calculated via the coupled isotope approach underestimate the likely temperatures at the site. This shows that the coupled isotope approach has the potential to generate reliable mean summer temperature reconstructions, provided that shells from suitable mollusc taxa can be analysed.

6.8. Discussion and Conclusions: Reliability of the coupled isotope approach for reconstructing past interglacial temperatures

The research undertaken by Grimes et al. (2003; 2004; 2005; 2008) highlighted the potential value of coupling the $\delta^{18}O$ values of fossil rodent teeth with the $\delta^{18}O$ values of coexisting palaeoproxies to estimate past seasonal temperatures. Although Grimes et al. (2004) suggested that this approach can be applied to the Quaternary period, the method has not been widely utilized in Quaternary studies thus far (cf. Ruddy, 2005; Peneycad, 2013). The results in this chapter demonstrate that the approach can generate accurate mean

summer temperatures for Quaternary interglacial stages, provided that certain conditions, outlined below, are met.

Firstly, the fossil teeth and shells must have mineralized during similar intervals of time. Therefore, the fossil material must ideally originate from sediments that were deposited 1) relatively rapidly, and 2) in a low-energy depositional environment, whereby the fossil material has been transported a limited distance prior to deposition. The fossil material must have also experienced minimal post-depositional disturbance or alteration, in order to ensure that the teeth and shells are coeval and retain their original isotopic signatures. The isotopic differences between the fossil material from sites WR1 and WR2 at West Runton clearly illustrate the importance of using teeth and shells derived from the same sedimentary sections when applying the coupled isotope approach.

Secondly, analyses must be undertaken on appropriate sample sizes. The results from Sample 2 at West Runton and the tooth carbonate from Cudmore Grove show that when the sample comprises ≤ 4 rodent teeth, the propagated uncertainties on the calculated mean temperatures are relatively large (> 2°C). Nevertheless, the mean $\delta^{18}O_{mw}$ values and mean summer temperatures calculated from these samples are consistent with the published palaeoclimate reconstructions for the sites. This suggests that small sample sizes can provide accurate mean $\delta^{18}O_{rt}$ values, although the precision on these mean values is relatively poor. Therefore, to obtain precise temperature estimates, > 4 rodent teeth should be analysed per sedimentary layer. This is especially important for studies aiming to examine minor palaeoclimatic changes between different layers within a stratigraphic sequence.

Analyses must also be undertaken on suitable sample materials. The results obtained from the Marsworth shells imply that amphibious taxa, such as *Galba truncatula*, are unsuitable for the coupled isotope approach, due to their preference for habitats that are liable to evaporation. As a result, the $\delta^{18}O$ values of their shells may record $\delta^{18}O_{mw}$ values that are enriched relative to the meteoric water sources from which rodents drink. This shows that the coexistence of fossil rodent teeth and shells within the same deposits does not guarantee that these biominerals reflect comparable $\delta^{18}O_{mw}$ values. It also

demonstrates that a detailed understanding of rodent and mollusc ecology is required in order to accurately interpret isotopic data from fossil rodent teeth and mollusc shells.

Finally, in order to generate accurate estimates for the mean $\delta^{18}O$ of surface water, appropriate and robust modern calibrations must be used. The various modern calibrations for vole tooth bioapatite generated significantly different $\delta^{18}O$ values of local water for Cudmore Grove. Equations based on the mean $\delta^{18}O$ of surface meteoric water or the mean $\delta^{18}O$ of summer precipitation produced consistent calculated $\delta^{18}O_{mw}$ values. These $\delta^{18}O_{mw}$ values generated mean summer temperatures that are consistent with published palaeotemperature reconstructions for Cudmore Grove.

Conversely, equations based on the mean annual $\delta^{18}O$ of precipitation generally underestimate the mean $\delta^{18}O_{mw}$ and summer temperature values. Aquatic gastropod shells primarily grow during summer (e.g. Waghorne et al., 2012). In order to couple the $\delta^{18}O$ values of rodent teeth with the $\delta^{18}O$ values of aquatic gastropod shells, the mean $\delta^{18}O$ of surface water during summer must be quantified. Calibrations based on the mean annual $\delta^{18}O_{pt}$ are therefore unsuitable for use in the coupled isotope approach. It is consequently recommended that equations that reconstruct the $\delta^{18}O$ of surface meteoric water (Equation 6.1) or the mean $\delta^{18}O$ of summer precipitation (e.g. Equation 6.3) should be used to calculate $\delta^{18}O_{mw}$ when applying this approach. Equations that reconstruct the $\delta^{18}O$ of surface water are preferable, as the relative similarity between the mean $\delta^{18}O_{mw}$ and mean summer $\delta^{18}O_{pt}$, which is observed at the present day and at Cudmore Grove (Figure 6.21), may not necessarily be consistent across all interglacial stages.

Despite these limitations of the coupled isotope approach, valuable palaeoclimate information can be gained from the isotope data and temperature estimates generated via this approach. These benefits are briefly highlighted in the following sections.

6.8.1. Significance of the $\delta^{18}O$ of rodent bioapatite as a palaeoclimate proxy

For all three study sites, the $\delta^{18}O$ values of rodent bioapatite are consistent with the existing proxy evidence from the sites. At West Runton and Marsworth, the palaeoclimate evidence suggests that mean summer temperatures were comparable to the present day (Murton et al., 2001; Coope, 2010a). Similarly, the $\delta^{18}O$ values of the rodent teeth from these sites are comparable to the $\delta^{18}O$ values of modern teeth from southern Britain. Conversely, the faunal evidence from Cudmore Grove indicates that mean summer temperatures were warmer than southern Britain today (Roe et al., 2009). The $\delta^{18}O_{rt}$ values for this site are likewise more enriched than the present day.

Furthermore, isotope data from different sedimentary layers or sections at the same site can potentially provide insights on local hydrological changes or regional climatic variations. For example, at West Runton, the differences between the $\delta^{18}O$ values of the rodent teeth from WR1 and WR2 reflect the local stabilisation of the landscape and infilling of the lake basin. Also, the small decrease in the $\delta^{18}O$ values of the rodent teeth from Level 3 to Level 2 at Marsworth may reflect a gradual cooling of the climate over time, although the isotope values from these layers are not statistically different.

These results clearly show that regardless of the accuracy and precision of the palaeotemperature estimates generated using the coupled isotope approach, the $\delta^{18}O$ values of rodent bioapatite can provide useful and accurate palaeoenvironmental information.

6.8.2. Reliability of mean palaeotemperatures generated from the coupled isotope approach

Provided that the conditions outlined above are met, the coupled isotope approach can produce reliable average summer palaeotemperature estimates. The reconstructed mean temperatures for both West Runton and Cudmore Grove are equivalent, within uncertainties, to published palaeotemperature estimates for the sites. With large isotope datasets (> 4

rodent teeth), the uncertainties on the coupled isotope temperatures are similar to the uncertainties on temperatures reconstructed using mutual climatic range methods applied to faunal assemblages. Thus, in conclusion, the coupled isotope approach can provide accurate and reasonably precise mean summer palaeotemperatures for past interglacial stages.

In the next chapter, the $\delta^{18}O$ values of fossil rodent teeth from stratified cave sites are utilized to reconstruct short-term palaeoclimatic fluctuations.

7. Reconstructing millennial-scale climatic changes using the $\delta^{18}O$ values of rodent teeth from caves

7.1. Introduction

The aim of this chapter is to examine whether the $\delta^{18}O$ values of fossil rodent teeth can provide palaeoclimate records for cave sequences. This aim is addressed by investigating the stable isotope values of rodent teeth from stratified Pleistocene deposits in two caves located in Somerset, southwest Britain: 1) Westbury Cave, and 2) Gully Cave. The locations of these study sites are shown in Figure 7.1a.

This chapter begins with an explanation of the rationale behind the interpretation of the tooth $\delta^{18}O$ values, before outlining the materials and methods used in this study. The isotope results are then presented and discussed. Stratigraphic patterns in the mean stable isotope values of the rodent teeth are examined qualitatively and statistically. The tooth $\delta^{18}O$ values are also converted to $\delta^{18}O$ values of meteoric water using the modern equation from Chapter 5. The calculated $\delta^{18}O$ values of meteoric water are compared with the $\delta^{18}O$ values of modern water sources from southwest Britain (Figure 7.1a), in order to assess how palaeoclimatic conditions differed from the present day. The $\delta^{13}C$ values of the teeth are also briefly interpreted in terms of past changes in rodent diet, atmospheric CO_2, and climate. Finally, the isotope data from the caves are validated against regional proxy climate records (Figure 7.1b). The Westbury Cave data are also compared with the faunal evidence from this site. These comparisons are used to assess whether the isotopic values of the rodent teeth can provide accurate and meaningful records of the short-term climatic fluctuations that occurred during the intervals in which the cave sequences accumulated.

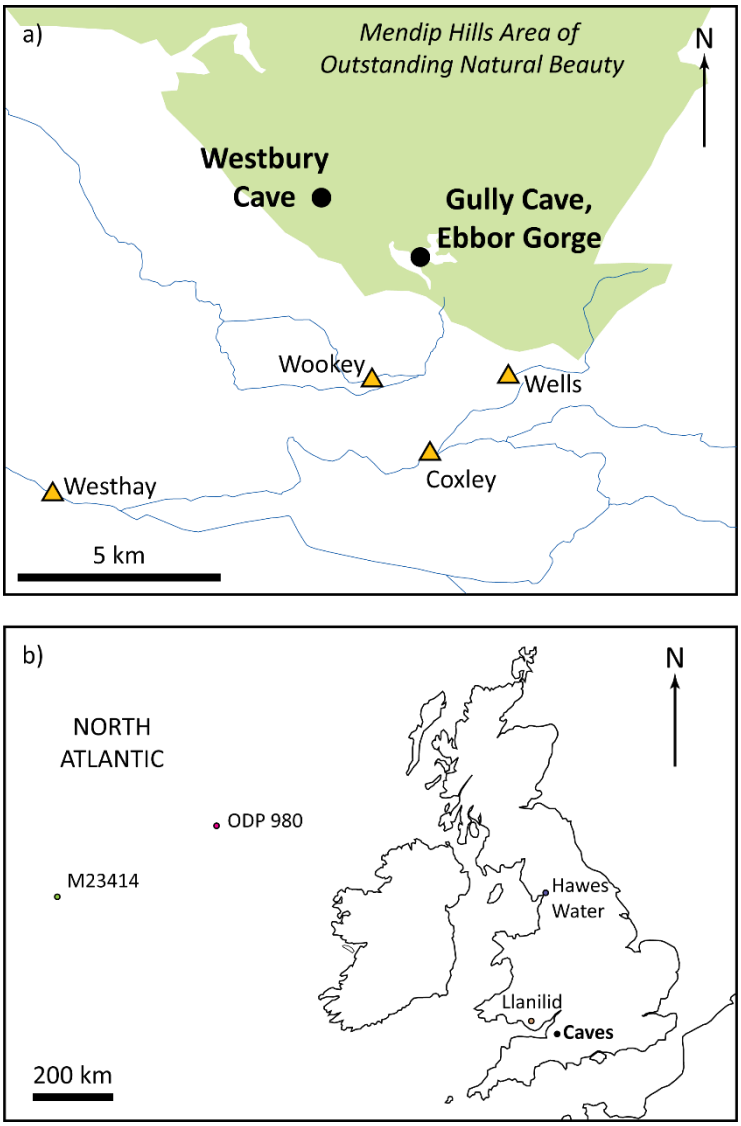

Figure 7.1: *a) Locations of the cave sites investigated in this study (black dots), and the sampling locations for the modern water sources investigated in Chapter 5 (yellow triangles), in Somerset. b) Locations of the sites of regional proxy records. The isotope records from the two caves (labelled with a black dot) are validated against these proxy records in the discussion section of this chapter.*

7.2. Rationale

The utilization of the $\delta^{18}O$ of rodent teeth as a palaeoclimate proxy is based upon the principle that the mean $\delta^{18}O$ of rodent bioapatite ($\delta^{18}O_{rt}$) is positively correlated with the mean $\delta^{18}O$ of meteoric water ($\delta^{18}O_{mw}$) (Figure 5.29a). Since $\delta^{18}O_{mw}$ in mid-latitude areas is also positively correlated with air temperature (Rozanski et al., 1993; Fricke & O'Neil, 1999), mean $\delta^{18}O_{rt}$ values are expected to be relatively enriched during warmer intervals (interglacials and interstadials) and relatively depleted during cooler intervals (glacials and stadials). Therefore, the $\delta^{18}O$ values of rodent teeth from stratified depositional sequences can potentially be used to reconstruct temporal changes in $\delta^{18}O_{mw}$ and climate.

Due to the deposition of pellets by avian predators, rodent remains can accumulate over time to form stratified deposits within caves (Andrews, 1990). If major climatic changes occurred during the accumulation of these deposits, mean $\delta^{18}O_{rt}$ values would likely vary through the depositional sequence. Both Westbury Cave and Gully Cave are known to span time intervals during which the climate fluctuated on millennial to multi-millennial timescales (Andrews et al., 1999; Schreve, 2012a; Schreve, 2012b). Stratigraphic changes in the $\delta^{18}O$ values of the rodent teeth from these caves are consequently expected to parallel the climatic fluctuations.

As recognised by Royer et al. (2013b; 2014), the range in $\delta^{18}O_{rt}$ values within each stratigraphic level is also an important consideration for the interpretation of this proxy. Since a rodent may be predated during any month of the year, the range in $\delta^{18}O_{rt}$ values within a sample can potentially provide a measure of the seasonal variability in the $\delta^{18}O$ value of local meteoric water, and by extension, air temperature (Royer et al., 2013a). For example, Royer et al. (2013b; 2014) interpret an increase in the variability in $\delta^{18}O_{rt}$ values during the Last Glacial Stage in France as resulting from a more continental climate. This continental climate was characterised by cold winters combined with relatively warm and arid summers. The cold temperatures during winter would have led to relatively depleted $\delta^{18}O_{mw}$ values, whereas the warm and arid conditions during summer would have resulted in the increased evaporation and $\delta^{18}O$ enrichment of meteoric water.

Royer et al. (2013b; 2014) also propose that a greater seasonal bias in predation can influence the mean $\delta^{18}O_{rt}$ values of samples from colder climatic intervals. Increased snow cover during winter can reduce the survival of rodents (Korslund & Steen, 2006) and limit the access of predators to their prey (Duchesne et al., 2011). As a result, the predation of rodents is likely to be primarily restricted to the warmest months of the year, when $\delta^{18}O_{mw}$ values reach their annual maximum (Royer et al., 2013b; 2014). This means that during cold periods in which snow cover is thick and extensive, mean $\delta^{18}O_{rt}$ values will be relatively enriched. If conditions during summer are also fairly arid, this enrichment is likely to be enhanced. In contrast, during cold periods in which the snow cover is limited, mean $\delta^{18}O_{rt}$ values are likely to be relatively depleted. This is because predators are able to capture their prey more readily throughout the year. As a consequence, the mean $\delta^{18}O$ values of the rodent teeth reflect $\delta^{18}O_{mw}$ values averaged over summer and winter. Mean $\delta^{18}O_{rt}$ values during warm interstadial and interglacial stages are also likely to reflect the mean annual $\delta^{18}O_{mw}$.

Taking all of these factors into consideration, the mean $\delta^{18}O$ values of the rodent teeth from Westbury Cave and Gully Cave are hypothesised to be: 1) relatively enriched during warm interglacial and interstadial stages, 2) relatively depleted and variable during cold stadial or glacial stages that had limited snow cover, and 3) relatively enriched during stadials or glacials in which the snow cover was extensive.

7.3. Materials

7.3.1. Westbury Cave

Permission was obtained from the Natural History Museum, London, for the destructive sampling of 110 rodent teeth from Westbury Cave. These teeth originate from most of the major stratigraphic units and sub-units in the Side Chamber and Main Chamber sequences of the cave (Table 7.1). For some sub-units, the teeth were selected from two different sediment samples, referred to as sample groups A and B (Table 7.1).

Table 7.1: *Summary of the numbers of rodent teeth sampled for isotopic analysis from each stratigraphic sub-unit in Westbury Cave.*

	Sub-unit	Sub-unit description	No. of teeth	Additional comments
Main Chamber	19/15	Lower Yellow Breccia	6	- 3 teeth selected from each of 2 different sediment samples (19/15A and 19/15B)
	19/14	Rodent Breccia	10	- 5 teeth selected from each of 2 different sediment samples (19/14A and 19/14B)
	18	Cobble bed or brown breccia with pink silty matrix	6	- 3 teeth selected from each of 2 different sediment samples (18A and 18B) - Samples probably from sub-unit 18/4
	18/6	Grey silty breccia	3	-
Side Chamber	15/8	Rodent Earth	12	-
	15/5	Brown weathered horizon	6	-
	15/2	Mole layer	8	-
	15/3	Light red-brown layer	4	-
	14	Grey-green layer	15	- 10 teeth from 14/1 at section W9 - 5 teeth from 14/2 at section W2
	13	Lower part of Brown Silt	10	- Teeth from sediment sample 219 in Unit 13/1
	12	Dark Brown Breccia	10	-
	11	Pink Breccia	15	- 10 teeth from the top of the unit at the western end of the exposure (11A) - 5 teeth from a bulk sample of unknown origin within the unit (11B)
	8	Bone gravel	5	-

As suggested by the results of the modern analogue study (Chapter 5), and from the application of the coupled isotope approach (Chapter 6), 5-10 teeth must be sampled per stratigraphic unit in order to ensure that the average measured $\delta^{18}O_{rt}$ values are accurate and precise representations of each unit as a whole. These sample sizes were achieved for most sub-units in the Westbury sequence (Table 7.1). However, due to the limited numbers of rodent teeth available from Units 8, 15/3, and 18/6, only 3-5 teeth were sampled from these layers. Also, no teeth were available from Unit 10.

All of the selected teeth are upper first molars that have been identified as belonging to the genus *Microtus*. These teeth were chosen for several reasons. Firstly, isolated *Microtus* molars form the dominant component of the fossil assemblages in almost all major sub-units in the Westbury Cave sequence (Andrews, 1990). Secondly, upper first molars are large enough to allow sufficient material to be obtained for isotopic analysis. Thirdly, the results from the modern *M. agrestis* teeth (Chapter 5) demonstrate that isotopic differences between upper and lower teeth are generally minor (≤ 1.5‰) and not statistically significant. Therefore, the isotope values of upper first molars can be considered to be representative of the average $\delta^{18}O_{rt}$ and $\delta^{13}C_{rt}$ values of the *Microtus* assemblages in each stratigraphic unit. Finally, upper first molars are not diagnostic to species, and so these teeth were chosen instead of lower first molars. This is because lower first molars are taxonomically informative and are consequently valuable for morphometric analyses. It was therefore concluded that these teeth should not be destructively sampled.

Although the upper first molars cannot be identified to species level, members of the genus *Microtus* in Britain have comparable ecological preferences, and thus likely record similar mean $\delta^{18}O$ values of local meteoric water (see section 4.2.1.1). Therefore, differences in the species represented within each sub-unit will likely have a minimal influence on the isotopic differences between the sampled teeth. However, the assemblages at Westbury are dominated by the species *Microtus* (*Pitymys*) *gregaloides*. The extant descendant of this species, *M. gregalis*, lives in relatively dry, steppic environments (Batasaikhan et al., 2016), where meteoric water sources may be affected by evaporative enrichment. Consequently, the $\delta^{18}O$ values of the

M. gregaloides teeth from Westbury may be slightly enriched relative to teeth from species such as *M. agrestis*, which generally inhabit damper environments (MacDonald & Barrett, 1993). These inter-species differences would result in increased variability in the $\delta^{18}O$ values of the teeth from sub-units in which *M. gregaloides* and *M. agrestis/arvalis* are similarly abundant (e.g. 12, 19/14 and 19/15). This factor will consequently be assessed when interpreting the isotope results from Westbury Cave.

The selected teeth additionally include both left and right upper molars. Therefore, it is possible that certain pairs of left and right teeth may originate from the same individual. However, for several of the units, the numbers of teeth available were insufficient to enable the tooth selection to be restricted to a single side (left or right). Also, due to the mixing of the fossil remains within each sample during sorting, it is likely that most of the selected teeth originate from different individuals.

Where possible, well-preserved teeth were chosen for analysis, although most of the selected teeth are broken. The majority of the teeth show no evidence for digestion by a predator. The light modifications on the few teeth that have been digested are consistent with a Category 1 predator such as the barn owl or long-eared owl. These observations are consistent with the previous taphonomic work on the rodent assemblages from Westbury Cave (Andrews, 1990).

7.3.2. Gully Cave

7.3.2.1. Rodent teeth analysed in previous research

A pilot study was carried out by Peneycad (2013) on the $\delta^{18}O$ and $\delta^{13}C$ values of *Arvicola terrestris* incisors from Gully Cave. Analyses were undertaken on fifteen teeth from spits spanning -130 to +30 cm relative to the established site datum point (Table 7.2). Faunal associations and radiocarbon dates on mammalian bones indicate that these spits encompass three climatic intervals: 1) the Lateglacial Interstadial, 2) the Loch Lomond Stadial, and 3) the early Holocene (Table 7.2). Stratigraphic shifts in the mean $\delta^{18}O$ values of the *A. terrestris* teeth appear to parallel the climatic changes between these

intervals (Peneycad, 2013). However, only 1-2 teeth were analysed per level, and the data are relatively scattered. Consequently, the significance of the isotopic shifts could not be fully assessed. To address this, large numbers of *Microtus* teeth were analysed for this thesis (see below). To provide a comparison with the new results obtained from these teeth, the *Arvicola* data from Peneycad (2013) are re-presented in the results section of this chapter, and are reinterpreted alongside the new data in the light of the latest knowledge of the Gully Cave sequence and its chronology (Table 7.2).

7.3.2.2. Rodent teeth analysed in this study

Due to the potential indicated by the results of the pilot study, additional rodent teeth were sampled from Gully Cave at higher stratigraphic, and therefore temporal, resolutions (Table 7.3). The teeth originate from spits that are chronologically well-constrained due to the radiocarbon dating of mammalian bones from the same spit or an adjacent spit. The radiocarbon dates have been used to correlate each spit with the major climatic intervals during the Lateglacial to early Holocene period (Table 7.3). The isotope data from the *Microtus* sp(p). teeth will be presented according to these correlations.

A total of 79 teeth were selected for analysis, consisting of 4-5 teeth per spit. All of the teeth are upper first molars (Figure 7.2). The justification for selecting this tooth type was discussed in section 7.3.1. The majority of the teeth show no evidence for digestion. However, ~25% of the teeth are lightly digested, while 6% are moderately digested. These modifications suggest digestion by a Category 1-2 predator such as the long-eared owl. This is consistent with the presence of long-eared owl remains within the cave (Schreve, 2010).

Table 7.2: *Stratigraphic and geochronological information for the* Arvicola terrestris *incisors from Gully Cave, which were analysed in a pilot study by Peneycad (2013). Correlations with the climatic intervals are shown based on the evidence from the radiocarbon dating of mammalian bones (Schreve, 2012b), and the palaeoclimatic interpretations of the molluscan assemblages from the site (Schreve, 2015).*

Sample number	Grid square	Depth relative to datum (cm)	Inferred climatic interval	
			Radiocarbon dating	Mollusc assemblages
GC-1a	G0	+30 to +20	-	Probably Holocene
GC-1b				
GC-2	F0	+20 to +10	Probably Holocene	Holocene
GC-3	G0	-20 to -30	Loch Lomond Stadial or younger	-
GC-4	F2	-33 to -50	Loch Lomond Stadial or younger	-
GC-5	G2	-40	-	-
GC-6a	G0	-40 to -60	Lateglacial Interstadial - Loch Lomond Stadial boundary	-
GC-6b				
GC-7a	G3	-40 to -50	Probably Holocene	Holocene
GC-7b				
GC-8	G3	-50 to -60	Probably Holocene	Holocene
GC-9	G3	-70 to -100	Probably Holocene	Holocene
GC-10	E2	-115 to -125	-	Lateglacial Interstadial
GC-11	F2	-120 to -130	Probably Lateglacial Interstadial	Lateglacial Interstadial
GC-12	G3	-120 to -130	Late Loch Lomond Stadial	Holocene

Microtus was chosen as the target genus for this study, as fossil *Microtus* teeth are more abundant in the Gully Cave deposits than *Arvicola* teeth. *Microtus* remains from the cave have been identified as belonging to four different species: 1) *M. agrestis*, 2) *M. arvalis*, 3) *M. gregalis* and 4) *M. oeconomus* (Schreve, 2012a). *M. agrestis/arvalis* and *M. gregalis* are the dominant species at the site (Schreve, 2012a; Schreve, 2012b), and thus the majority of the selected molars likely belong to these taxa. *M. gregalis* declines in abundance from the Lateglacial Interstadial to the early Holocene, while *M. agrestis/arvalis* increases in abundance during this period (Schreve, 2012a; Schreve, 2012b). Therefore, a greater proportion of the selected teeth from the Lateglacial Interstadial deposits likely belong to *M. gregalis*. Conversely, most of the teeth from the Loch Lomond Stadial and early Holocene deposits likely belong to *M. agrestis/arvalis*. As aforementioned, these taxa have different ecological preferences, which may result in increased variability in the $\delta^{18}O$ values of the teeth. This factor will therefore be taken into consideration when interpreting the results from the site.

Isotopic differences may also occur between the *Arvicola* and *Microtus* teeth from Gully Cave. Since the $\delta^{18}O$ values of *Arvicola* and *Microtus* teeth both reflect the mean $\delta^{18}O$ of meteoric water (Royer et al., 2013a), stratigraphic changes in the $\delta^{18}O_{rt}$ values of these taxa are expected to be similar. However, as mentioned in section 4.2.1.1, the $\delta^{18}O$ values of *Microtus* teeth are often isotopically enriched compared to *Arvicola* teeth, due to the greater intake of evaporated water sources by *Microtus* (Royer et al., 2013a; Royer et al., 2014). Changes in aridity may consequently have a greater influence on the $\delta^{18}O$ values of *Microtus* teeth (Royer et al., 2014). This is particularly relevant for Gully Cave, as sedimentological and palaeoecological evidence from northwest Europe indicate that conditions were relatively arid during the Lateglacial period (e.g. Kasse, 2002; Birks & Birks, 2014). Therefore, the potential influence of aridity on the $\delta^{18}O$ values of the *Microtus* teeth will be assessed in the results section for Gully Cave.

Table 7.3: *Stratigraphic and geochronological information for the* Microtus *sp(p). upper molars from Gully Cave. Correlations with the climatic intervals are based upon radiocarbon dates undertaken on mammalian bones from the same spit or an adjacent spit (Schreve, 2012b). The radiocarbon dates were calibrated using OxCal version 4.3 and the IntCal13 calibration curve (Bronk Ramsey, 2009; Reimer et al., 2013), and were compared with the dates of the GI-1, GS-1 and Holocene climatic transitions in the NGRIP ice core record, according to the GICC05 timescale (Rasmussen et al., 2006). It is acknowledged that the timings of the climatic changes in Britain may differ slightly from those in Greenland, and therefore the dates from the NGRIP record are considered here as approximations for the likely dates of the Lateglacial Interstadial, Loch Lomond Stadial and Holocene climatic intervals in Britain. The climatic intervals inferred from the mollusc assemblages at Gully Cave are also shown for comparison (Schreve, 2015). The sample groups are listed in order of the relative stratigraphy and age of each spit.*

Sample group number	**Grid square**	**Depth relative to datum (cm)**	**No. of *Microtus* sp(p). teeth sampled for analysis**	**Inferred climatic interval**	
				Radiocarbon dating	**Mollusc assemblages**
GCEG-1	G4	-60 to -100	5	early Holocene	-
GCEG-2	G4	-140 to -150	5	earliest Holocene	-
GCEG-3	G3	-110 to -120	5	Loch Lomond Stadial - Holocene boundary	Holocene
GCEG-4	G3	-120 to -130	5	late Loch Lomond Stadial	Holocene
GCEG-6	F0	-10 to -20	4	late Loch Lomond Stadial	Holocene
GCEG-7	F0	-20 to -30	5		Holocene
GCEG-5	G3	-130 to -140	5	middle Loch Lomond Stadial	-
GCEG-8	F0	-30 to -40	5	early-middle Loch Lomond Stadial	Holocene
GCEG-9	F0	-40 to -50	5		Loch Lomond Stadial

GCEG-10	F0	-50 to -60	5	late Lateglacial Interstadial	Loch Lomond Stadial
GCEG-11	F0	-60 to -70	5	-	
GCEG-12	F0	-70 to -80	5	-	
GCEG-13	F0	-80 to -90	5	-	
GCEG-14	F2	-140 to -150	5	early Lateglacial Interstadial	early Lateglacial Interstadial
GCEG-15	F2	-150 to -160	5		
GCEG-16	D3	-175 to -215	5		

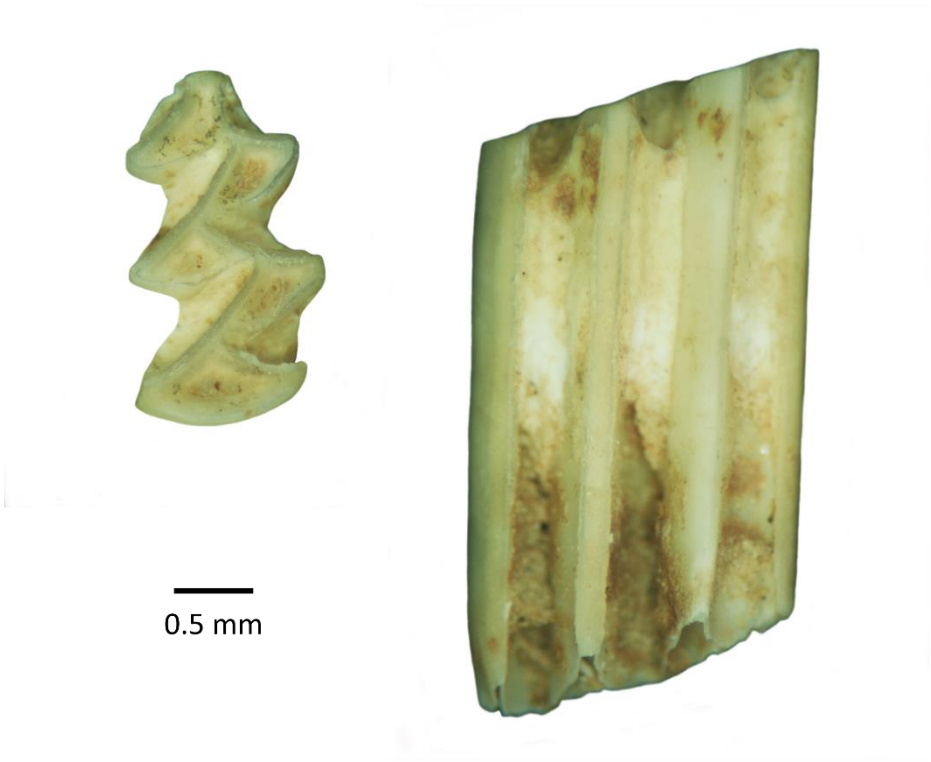

Figure 7.2: *Photographs of a* Microtus *sp(p). upper first molar from Gully Cave. The occlusal (left) and lingual (right) views are shown.*

7.4. Methods

7.4.1. Isotope analyses

Analyses of the rodent teeth from Westbury Cave were largely undertaken in the Department of Earth Sciences at Royal Holloway, University of London (RHUL). Due to issues regarding the availability of the stable isotope laboratory at RHUL, the remaining teeth from the site (5 of the 8 teeth from sub-unit 15/2, all of the teeth from sub-unit 15/5, and 5 of the 12 teeth from sub-unit 15/8) were analysed at the Bloomsbury Environmental Isotope Facility (BEIF), University College London. The isotopic measurements from both laboratories were calibrated against the same international carbonate standard, NBS-19, and thus inter-laboratory differences in the isotope results are assumed to be minimal. This assumption is supported by the comparability in the isotope values of different teeth from sub-units 15/2 and 15/8 that were analysed at RHUL and BEIF (Figure 7.3).

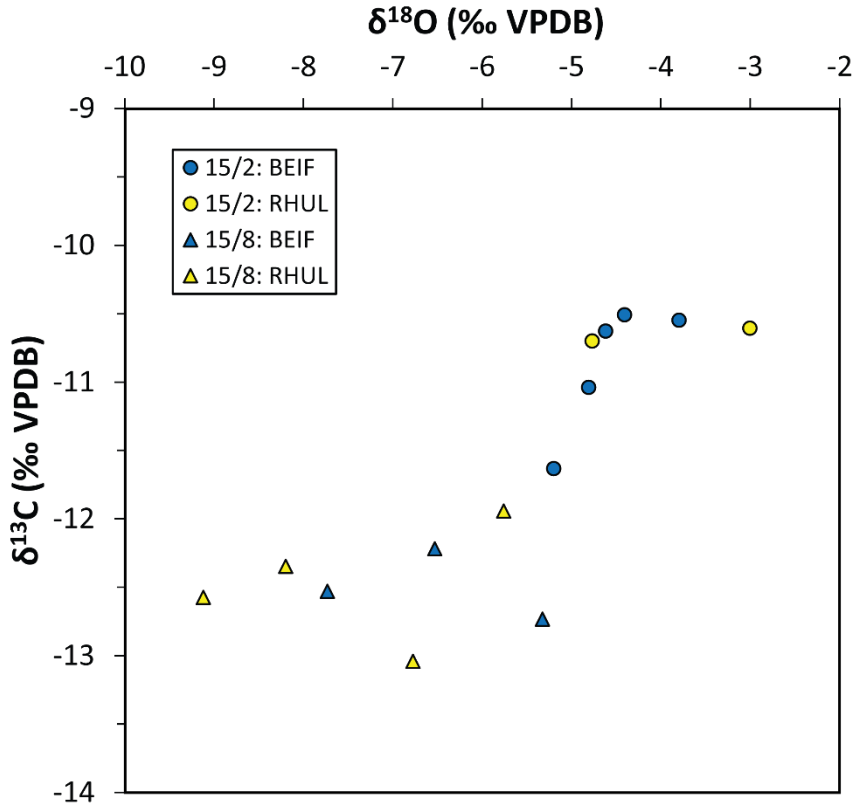

Figure 7.3: *Graph comparing the oxygen and carbon isotope results obtained from two isotope laboratories (BEIF and RHUL) on analyses of teeth from Westbury Cave. A different set of teeth from each stratigraphic unit (15/2 and 15/8) was analysed at each laboratory. Different sets of teeth from the same unit are expected to have similar means and distributions in isotopic values, as the teeth likely mineralized during the same climatic interval.*

Analytical issues (a blockage in the needle supplying the sample to the spectrometer, and the contamination of a sample with air), resulted in five of the samples from Westbury being lost (three from Unit 12, one from 15/2, and one from 15/5). In addition, some of the samples were too small following pre-treatment to enable reliable isotopic measurements to be obtained. Consequently, two samples from sub-unit 15/8 were not submitted for analysis. Isotope results from samples that generated peak heights of < 1 nA (one from 14/2, two from 15/8, and one from 19/15A) were also considered unreliable, and were therefore excluded from the dataset. Nevertheless, the numbers of teeth analysed from each sub-unit are sufficient that these losses are not likely to significantly affect the interpretations of the results. The remaining dataset comprises results from 99 teeth.

All of the *Microtus* teeth from Gully Cave were analysed at BEIF, whereas all of the *Arvicola* teeth sampled by Peneycad (2013) were analysed at RHUL. Three teeth (one each from GCEG-1, GCEG-6, and GCEG-13) generated insufficient material for analysis. Therefore, the *Microtus* dataset comprises results from 76 teeth.

Due to issues encountered during the analyses of some of the samples from Gully Cave, the internal measurement precision on the $\delta^{18}O$ values was relatively poor (0.17‰). Twenty-six samples were therefore re-analysed at BEIF. The $\delta^{18}O$ and $\delta^{13}C$ values obtained during Analysis 2 were respectively within ± 1‰ and ± 0.6‰ different from the results of Analysis 1 (see Appendix B). The results from the two analyses were consequently averaged. All specimen and isotope data for the two cave sites are provided in Appendix E.

7.4.2. Statistical methods

7.4.2.1. Descriptive statistics

For each stratigraphic level in the two caves, basic descriptive statistics (mean, standard deviation, range etc.) for the $\delta^{18}O$ and $\delta^{13}C$ data were calculated. Grubbs' tests were used to identify outliers, and Shapiro-Wilk tests were undertaken to determine whether the data are normally distributed at 95% confidence. T-tests (or Mann-Whitney tests for non-normally distributed data) were used to assess whether the isotope values of teeth from different sample groups within the same stratigraphic unit are statistically different. Regression statistics (Pearson's r^2 and significance values) were also calculated for the correlation between the $\delta^{18}O$ and $\delta^{13}C$ values of the teeth from each level.

7.3.2.2. Assessing the statistical significance of stratigraphic shifts in isotopic values

In order to investigate the statistical significance of differences in the mean isotope values between each stratigraphic unit, one-way Analyses of Variance (ANOVA) were undertaken. Due to the differences in the sample sizes for each unit at Westbury Cave, and the possible shifts in the ranges in isotope values

between different climatic intervals, the variance in isotopic values is likely to differ between each unit or sample group. Levene's tests were therefore used to determine whether the isotopic variances of the sample groups are statistically different at 95% confidence. For cases in which the variances are not statistically different (Levene's test, $p > 0.05$), and the data are normally distributed (Shapiro-Wilk, $p > 0.05$), a classic parametric ANOVA was used, with post-hoc Tukey's Q tests for pairwise comparisons. For cases in which the variances are statistically different ($p < 0.05$), and the data are normally distributed, a Welch's ANOVA was used, with Games-Howell post-hoc tests. All tests were undertaken using the free software program, PAST (Hammer et al., 2001), except for the Games-Howell tests, which were undertaken in Microsoft Excel.

7.4.2.3. Calculating the $\delta^{18}O$ of meteoric water and $\delta^{13}C$ of diet

Mean $\delta^{18}O$ values of meteoric water were calculated from the mean $\delta^{18}O$ values of the teeth from each stratigraphic level, using the inverted forward fit least-squares regression of the modern correlation generated in Chapter 5. This regression equation is shown again below:

$$\delta^{18}O_{mw} = (\delta^{18}O_{rt} - 1.2289) / 1.3109 \quad (7.1).$$

The calibration uncertainties on the mean $\delta^{18}O_{mw}$ values were calculated using Equation 6.2. Since the variability in $\delta^{18}O_{rt}$ values may provide an indication of the relative continentality of the climate, the standard deviation in the $\delta^{18}O_{mw}$ values was also calculated for each unit, as a measure of the spread in the data. This standard deviation was added to the uncertainties calculated from Equation 6.2.

The $\delta^{13}C$ values of the rodent teeth were converted to dietary $\delta^{13}C$ values ($\delta^{13}C_d$) using an enrichment factor between vole bioapatite and the diet of 11.5‰ (Passey et al., 2005).

7.5. Results: Westbury Cave

7.5.1. $\delta^{18}O$ of teeth

The oxygen isotope results for the rodent teeth from Westbury Cave are plotted in Figure 7.4. The $\delta^{18}O$ data are very scattered, varying across a range of 6.1‰, from a minimum of -9.1‰ to a maximum of -3.0‰. However, as shown in Figure 7.5a, the $\delta^{18}O$ values of the teeth differ between the stratigraphic units, with relatively depleted values in Units 8 to 15/3 and 15/8 to 19, and relatively enriched values in sub-units 15/2 and 15/5. The descriptive statistics for each sub-unit are summarised in Table 7.4.

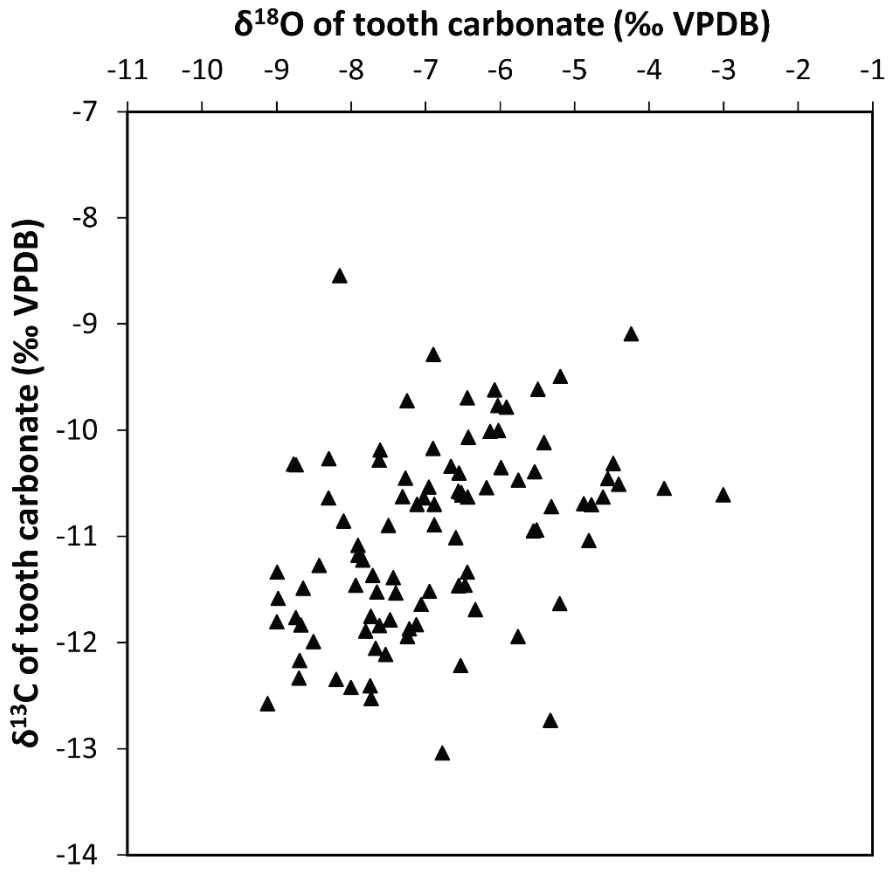

Figure 7.4: *Plot of the oxygen and carbon isotope values of the rodent teeth from Westbury Cave, excluding outliers.*

One sample from Unit 8 generated an outlying $\delta^{18}O$ value of -3.9‰ (Grubbs' test, $p < 0.05$), which was excluded from the dataset (Figure 7.5a). This sample was relatively small, and consequently the isotopic measurements for this sample are likely to be inaccurate. The mean $\delta^{18}O$ value of the remaining teeth is -7.75‰.

A small sample from Unit 11, with a $\delta^{18}O$ value of -10.6‰, is likewise identified as an outlier (Grubbs' test, $p < 0.05$). The median $\delta^{18}O$ values of the teeth from sample groups 11A (-7.31‰) and 11B (-7.12‰) are not statistically different (Mann-Whitney, $p > 0.05$), and therefore the data for these groups were combined. The overall mean $\delta^{18}O$ value for Unit 11 is -7.41‰, which is slightly higher than the mean for Unit 8. The mean $\delta^{18}O$ value for Unit 12 is slightly higher again at -7.24‰. This increasing trend reaches a peak in Unit 13, with a mean $\delta^{18}O$ value of -6.80‰.

The mean $\delta^{18}O_{rt}$ value subsequently declines to a minimum of -8.05‰ in Unit 14. There is no statistically significant difference between the mean $\delta^{18}O$ values of the teeth from sub-units 14/1 (-8.13‰) and 14/2 (-7.83‰) (T-test, $p > 0.05$), and thus the data for these sub-units were combined.

The mean $\delta^{18}O_{rt}$ increases to a maximum in sub-unit 15/2 with a value of -4.37‰, before declining through sub-units 15/5 and 15/8 towards values that are comparable to those at the base of the sequence (Figure 7.5a). One sample from sub-unit 15/8 produced an enriched $\delta^{18}O$ value of -2.2‰, which was identified as a possible outlier (Figure 7.5a). The results of a Grubbs' test indicate that statistically, this value is not an outlier when only the data from sub-unit 15/8 are considered (G = 2.00, G critical = 2.03, $p = 0.12$). Nevertheless, this value is an outlier in terms of the dataset as a whole, and was therefore excluded as a likely anomalous result. Excluding this value, the mean $\delta^{18}O_{rt}$ for sub-unit 15/8 is -7.06‰, and the range is 3.80‰. This range is broader than the ranges in the $\delta^{18}O_{rt}$ values for Units 8 to 15/5, which are generally < 3‰ (Table 7.4).

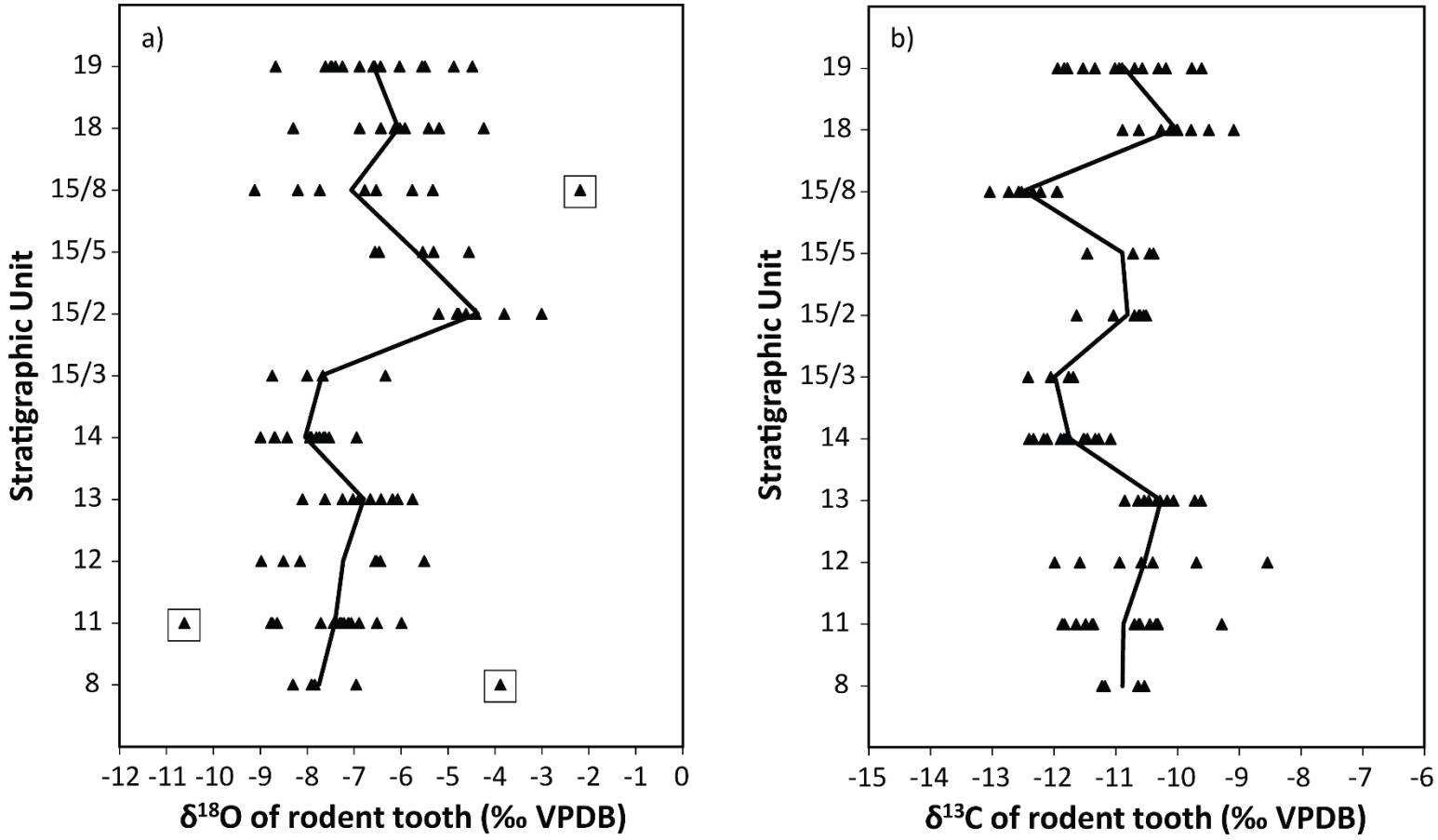

Figure 7.5: *The oxygen (a) and carbon (b) isotope values of the rodent teeth from Westbury Cave, plotted by stratigraphic unit. Outliers in the oxygen isotope data are highlighted with a box. The thick black lines indicate changes in the mean isotope values through the sequence.*

The average $\delta^{18}O_{rt}$ increases slightly in Unit 18. The median $\delta^{18}O$ values of the teeth from the three sample groups (18A, 18B and 18/6) are -6.13‰, -5.19‰ and -6.02‰, respectively. These values are not statistically different (Mann-Whitney tests, $p > 0.05$), and therefore the data for Unit 18 are considered as a whole. The overall mean value is -6.06‰, and the range is 4.06‰, which is again broader than for Units 8 to 15/5.

The range in the $\delta^{18}O$ values of the teeth from Unit 19 is also relatively broad at 4.19‰ (Figure 7.5a). There are no statistically significant differences between the mean $\delta^{18}O_{rt}$ values of the two sample groups from sub-unit 19/14 (A = -6.34‰, B = -7.10‰), and the two groups from sub-unit 19/15 (A = -6.02‰, B = -6.51‰) (T-tests, $p > 0.05$). Likewise, the mean $\delta^{18}O$ values of the teeth from sub-units 19/14 (-6.72‰) and 19/15 (-6.32‰) are not statistically different (T-test, $p > 0.05$). Therefore, the isotope data for all of the teeth from Unit 19 were combined into a single dataset. The overall mean value is -6.59‰, which is similar to units 15/8 and 18.

The shifts in the ranges in $\delta^{18}O$ values through the sequence (Table 7.4) could be related to the differences in the sample sizes from each stratigraphic unit. In order to test whether the range in isotope values is dependent on sample size, a regression analysis was performed. The results show that the ranges are not significantly correlated with the number of teeth analysed from each unit ($r^2 = 0.14$, $p = 0.26$). The results of the Levene's test also show that differences between the variance in $\delta^{18}O$ values within each unit are not statistically significant ($p = 0.16$).

To further investigate the differences in the mean $\delta^{18}O_{rt}$ values between the units, a one-way ANOVA was performed. The results of the ANOVA indicate that there is a statistically significant difference between the mean $\delta^{18}O_{rt}$ values of the units; the F statistic (9.62) is much greater than the F critical value (1.94), and the p value is < 0.05. Post-hoc Tukey's Q tests show that the mean $\delta^{18}O_{rt}$ value for sub-unit 15/2 is significantly different from the mean $\delta^{18}O_{rt}$ values of all other units except for 15/5 (Table 7.5). Also, the mean $\delta^{18}O_{rt}$ of sub-unit 15/5 is significantly different from Units 8, 11, 14 and 15/3, while the mean $\delta^{18}O_{rt}$ of Unit 18 is significantly different from Units 8 and 14. These results confirm that the $\delta^{18}O_{rt}$ values of sub-units 15/2 and 15/5 are significantly enriched relative to the other units in the sequence (Figure 7.5a).

Table 7.4: *Summary statistics for the oxygen isotope data from the rodent teeth from each stratigraphic sub-unit at Westbury Cave, excluding outliers. The normal distribution column is based on the results of Shapiro-Wilk tests undertaken at 95% confidence.*

Sub-unit	No. of teeth	Mean $\delta^{18}O$ (‰ VPDB)	Standard deviation (‰)	Median $\delta^{18}O$ (‰ VPDB)	Range (‰)	Normally distributed?
19	15	-6.59	1.14	-6.59	4.19	Yes
18	9	-6.06	1.14	-6.02	4.06	Yes
15/8	7	-7.06	1.36	-6.77	3.80	Yes
15/5	5	-5.68	0.84	-5.54	2.00	Yes
15/2	7	-4.37	0.74	-4.62	2.19	Yes
15/3	4	-7.69	1.01	-7.83	2.41	Yes
14	14	-8.05	0.61	-7.86	2.05	Yes
13	10	-6.80	0.73	-6.78	2.35	Yes
12	7	-7.24	1.30	-6.55	3.47	Yes
11	14	-7.41	0.82	-7.24	2.78	Yes
8	4	-7.75	0.57	-7.87	1.35	Yes

7.5.2. $\delta^{13}C$ of teeth

The carbon isotope results for the rodent teeth from Westbury Cave are displayed in Figures 7.4 and 7.5b. The $\delta^{13}C$ data for all stratigraphic units span a range of 4.5‰, from a minimum of -13.0‰ to a maximum of -8.5‰. The $\delta^{13}C_{rt}$ values fluctuate through the sequence in a broadly similar pattern to the $\delta^{18}O$ data (Figure 7.5). The mean $\delta^{13}C$ values are relatively enriched in Units 8-13, 15/2, 15/5 and 18-19, and relatively depleted in Units 14, 15/3 and 15/8 (Figure 7.5b, Table 7.6). Nevertheless, for most stratigraphic units, the $\delta^{18}O$ and $\delta^{13}C$ values of the teeth are not significantly correlated (r^2 values generally < 0.2, and $p > 0.05$). However, there are significant positive correlations between the $\delta^{18}O$ and $\delta^{13}C$ values for Units 15/5 ($r^2 = 0.79$, $p = 0.04$), 18 ($r^2 = 0.52$, $p = 0.03$) and 19 ($r^2 = 0.33$, $p = 0.02$).

Table 7.5: *Results of the Tukey's Q tests comparing the mean $\delta^{18}O$ values of the teeth from the different stratigraphic units at Westbury Cave. The table shows the* p *values calculated from the tests, and the shading indicates whether the differences are statistically significant (orange) or not statistically significant (blue) at 95% confidence.*

	11	**12**	**13**	**14**	**15/3**	**15/2**	**15/5**	**15/8**	**18**	**19**
8	1	0.99	0.73	1	1	< 0.01	< 0.01	0.96	< 0.05	0.45
11		1	0.98	0.97	1	< 0.01	0.04	1	0.23	0.87
12			1	0.88	1	< 0.01	0.10	1	0.43	0.97
13				0.34	0.81	< 0.01	0.52	1	0.93	1
14					1	< 0.01	< 0.01	0.69	< 0.01	0.15
15/3						< 0.01	< 0.01	0.98	0.07	0.54
15/2							0.28	< 0.01	< 0.05	< 0.01
15/5								0.21	1	0.79
15/8									0.67	1
18										1

Similar to the $\delta^{18}O$ data, the mean $\delta^{13}C$ values of the teeth gradually increase through Units 8 to 13 (Figure 7.5b). The mean $\delta^{13}C$ values of the two sample groups from Unit 11 (A = -10.52‰, B = -11.51‰) are significantly different (T-test, $p < 0.05$). However, this difference may be coincidental due to the small number of teeth analysed from 11B. Since both sample groups originate for the same stratigraphic unit, and the mean $\delta^{18}O_{rt}$ values of the groups are comparable, the $\delta^{13}C$ data for Unit 11 are regarded as a single dataset.

The mean $\delta^{13}C_{rt}$ value subsequently declines in Units 14 and 15/3 (Figure 7.5b). The $\delta^{13}C$ values of the teeth from sub-units 14/1 and 14/2 are not significantly different (T-test, $p > 0.05$). The mean $\delta^{13}C$ increases again in sub-units 15/2 and 15/5, before declining towards a minimum of -12.48‰ in sub-unit 15/8. The mean $\delta^{13}C_{rt}$ subsequently increases to a maximum of -10.01‰ in Unit 18, and then decreases slightly into Unit 19. There are no statistically significant differences between the average $\delta^{13}C$ values of the teeth from the three sample groups from Unit 18 (Mann-Whitney, $p > 0.05$), and from sub-units 19/14 and 19/15 (T-test, $p > 0.05$).

The data were further tested to assess the statistical significance of the changes in mean $\delta^{13}C_{rt}$ values through the sequence. The Levene's test shows that there are statistically significant differences in the variance in $\delta^{13}C$ values between each stratigraphic unit ($p < 0.05$), although the data are normally distributed (Shapiro-Wilk, $p > 0.05$). Therefore, a Welch's test was used. The results of this test indicate that the mean $\delta^{13}C_{rt}$ values of the stratigraphic units are significantly different (F statistic = 20.63, F critical = 2.24, $p < 0.05$). Post-hoc Games-Howell tests show that at 95% confidence, there are statistically significant differences between the mean $\delta^{13}C_{rt}$ value of sub-unit 15/8, and the mean $\delta^{13}C_{rt}$ values of all other units except for 12 and 15/3 (Table 7.7). In addition, the mean $\delta^{13}C_{rt}$ values of Units 14 and 15/3 are significantly different from the mean values of 11, 13, 15/2, 18 and 19. These results support the observations from Figure 7.5b, whereby the mean $\delta^{13}C$ values of the teeth from Units 14, 15/3 and 15/8 are relatively depleted compared to all other units.

Table 7.6: *Summary statistics for the carbon isotope data from the rodent teeth from each stratigraphic sub-unit in Westbury Cave (excluding outliers).*

Sub-unit	No. of teeth	Mean $\delta^{13}C$ (‰ VPDB)	Standard deviation (‰)	Median $\delta^{13}C$ (‰ VPDB)	Range (‰)	Normally distributed?
19	15	-10.88	0.72	-10.90	2.33	Yes
18	9	-10.03	0.55	-10.01	1.80	Yes
15/8	7	-12.48	0.36	-12.53	1.10	Yes
15/5	5	-10.90	0.53	-10.72	1.07	Yes
15/2	7	-10.81	0.40	-10.63	1.12	No
15/3	4	-11.98	0.33	-11.91	0.73	Yes
14	14	-11.75	0.41	-11.78	1.32	Yes
13	10	-10.27	0.39	-10.31	1.24	Yes
12	7	-10.53	1.16	-10.59	3.45	Yes
11	14	-10.87	0.74	-10.66	2.58	Yes
8	4	-10.89	0.36	-10.91	0.69	Yes

7.5.3. $\delta^{18}O$ of meteoric water

The calculated mean $\delta^{18}O$ values of meteoric water vary across a range of 2.8‰, from a minimum of -7.1‰ in Unit 14, to a maximum of -4.3‰ in Unit 15/2 (Figure 7.6). For most of the stratigraphic units, the mean $\delta^{18}O_{mw}$ value lies between -6 and -7‰. The ranges in $\delta^{18}O_{mw}$ values within Units 8 to 15/5 are generally 1.3-2.5‰. The ranges for Units 15/8, 18 and 19 are slightly broader at between 3.4 and 3.6‰.

Table 7.7: *Results of the Games-Howell Q tests comparing the mean $\delta^{13}C$ values of the teeth from the different stratigraphic units at Westbury Cave. The table shows the significance (*p*) values calculated from the Q statistic values. The shading indicates whether the differences are statistically significant (orange) or not statistically significant (blue) at 95% confidence.*

	11	**12**	**13**	**14**	**15/3**	**15/2**	**15/5**	**15/8**	**18**	**19**
8	1	1	0.30	0.10	0.06	1	1	< 0.01	0.14	1
11		1	0.31	0.03	0.03	1	1	< 0.01	0.13	1
12			1	0.35	0.22	1	1	0.06	0.98	1
13				< 0.01	< 0.01	0.28	0.50	< 0.01	1	0.26
14					0.96	< 0.01	0.21	0.02	< 0.01	0.02
15/3						0.02	0.11	0.50	< 0.01	0.02
15/2							1	< 0.01	0.12	1
15/5								0.01	0.26	1
15/8									< 0.01	< 0.01
18										0.10

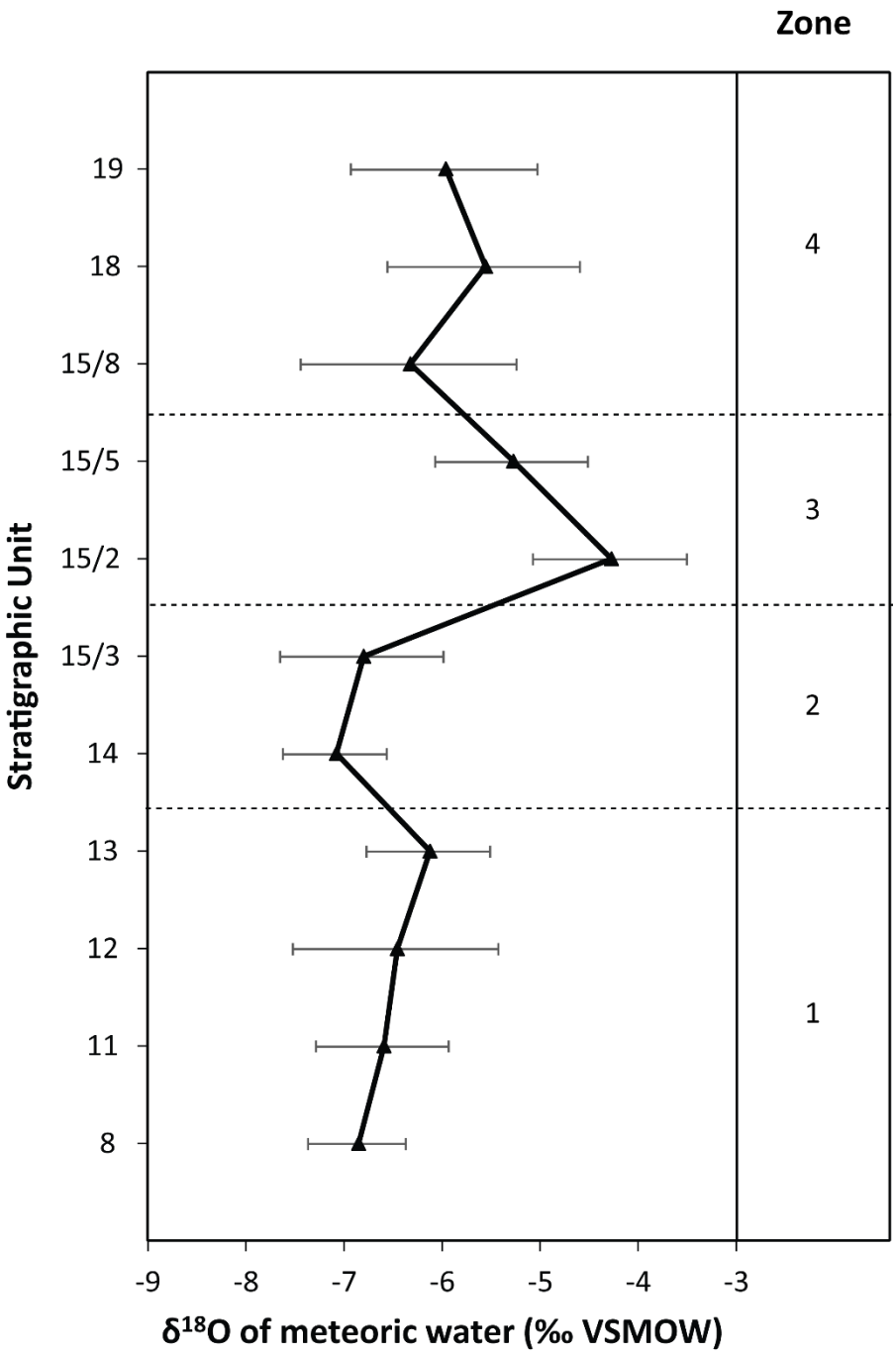

Figure 7.6: *The mean $\delta^{18}O$ values of meteoric water for each stratigraphic unit in Westbury Cave, calculated from the mean $\delta^{18}O$ values of the rodent teeth. The error bars represent the 1σ standard deviation uncertainties on the mean $\delta^{18}O$ values for each stratigraphic unit. The four 'climatic' zones identified in the data are also indicated.*

7.5.4. Interpretations and Discussion

7.5.4.1. $\delta^{18}O$ of teeth

If the mean $\delta^{18}O$ values of the rodent teeth are assumed to parallel changes in temperature, the data from Westbury Cave can be divided into four zones characterised by different climatic conditions: 1) a gradual warming through Units 8 to 13, 2) a cooler climate during Units 14 and 15/3, 3) a significant warm peak in Unit 15/2, followed by a slight cooling into 15/5, and 4) cooler climatic conditions during Units 15/8, 18 and 19 (Figure 7.6).

The ranges in $\delta^{18}O_{rt}$ values may also provide information on the continentality of the climate. The broader ranges through Units 15/8 to 19 suggest that the climate may have been slightly more continental than during the lower half of the sequence. Additionally, the $\delta^{18}O$ ranges (~4‰) for these units are slightly broader than the typical intra-population ranges for modern *Microtus agrestis* teeth from Britain (~2-3‰). This also suggests that the climate may have been more continental than today.

Alternatively, the larger ranges for Unit 19 may be related to the differences in the ecological preferences of *M. gregaloides* and *M. agrestis/arvalis*. Both taxa are likely to be represented within the sample of teeth from Unit 19. As aforementioned, the $\delta^{18}O$ values of *M. gregaloides* teeth may be slightly enriched compared to *M. agrestis/arvalis* teeth. The presence of both taxa within Unit 19 may therefore result in a larger overall range in $\delta^{18}O$ values. The relatively broad range in values for Unit 12 may also result from increased continentality, or the mixture of *M. gregaloides* and *M. agrestis/arvalis* remains within the sample from this unit.

7.5.4.2. $\delta^{13}C$ of teeth

The mean $\delta^{13}C$ values of the teeth from Westbury Cave (-12 to -10‰), are significantly higher than the mean $\delta^{13}C$ values of modern *M. agrestis* teeth from southern Britain (-18 to -16‰). This offset likely results from the recent decline in the $\delta^{13}C$ of atmospheric CO_2 (Figure 2.4b), plus temporal differences in the partial pressure of CO_2 (pCO_2). The Middle Pleistocene sequence at Westbury Cave is thought to correlate with Marine Isotope Stage (MIS) 13

(Candy et al., 2015). Atmospheric CO_2 levels during MIS 13 varied between ~230 and 250 ppm (Siegenthaler et al., 2005), whereas modern pCO_2 values are ~400 ppm (NOAA, 2018). Plant $\delta^{13}C$ values increase with decreasing pCO_2 (Schubert & Jahren, 2012). The enriched $\delta^{13}C$ values of the rodent teeth from Westbury Cave are therefore consistent with a lower concentration of atmospheric CO_2.

The calculated $\delta^{13}C$ values of the diet range from -24.5 to -20.0‰. These values are close to the maximum $\delta^{13}C$ compositions of modern C_3 plants (Figure 2.2). This suggests that the $\delta^{13}C_{rt}$ fluctuations through the Westbury sequence reflect changes in the $\delta^{13}C$ of local C_3 plants.

The similar stratigraphic patterns observed in the $\delta^{18}O$ and $\delta^{13}C$ data (Figure 7.5) suggests that these isotopes are responding to the same environmental forcing factor. Since $\delta^{18}O_{rt}$ is thought to reflect climate, the changes in the $\delta^{13}C$ values of the plants that the rodents are consuming must also be driven by climate. As outlined in Section 2.2.2, the $\delta^{13}C$ values of C_3 plants ($\delta^{13}C_p$) are influenced by various environmental factors, including the $\delta^{13}C$ value and partial pressure of atmospheric CO_2, precipitation, and temperature. Atmospheric CO_2 levels, moisture levels, and air temperatures are higher during warm stages than during cold stages (e.g. Petit et al., 1999). All of these environmental factors are negatively correlated with plant $\delta^{13}C$ values (Table 2.1). Consequently, if these factors had a dominant influence on $\delta^{13}C_p$ values at Westbury, the $\delta^{13}C$ values of the rodent teeth would be relatively depleted during warm intervals, when $\delta^{18}O_{rt}$ values are enriched.

However, the opposite is seen in the Westbury Cave data (Figure 7.5). Therefore, another environmental factor, namely the $\delta^{13}C$ value of atmospheric CO_2 ($\delta^{13}C_a$), must be responsible for the fluctuations in the $\delta^{13}C_{rt}$ values. In general, $\delta^{13}C_a$ is relatively enriched during warm stages, due to an increase in the photosynthesis and storage of $^{12}CO_2$ by plants (Marino et al., 1992). Changes in $\delta^{13}C_a$, in response to changes in climate, may therefore explain the parallel trends in the oxygen and carbon isotope data through the Westbury Cave sequence. The significant correlations between $\delta^{18}O_{rt}$ and $\delta^{13}C_{rt}$ within units corresponding to major isotopic transitions (e.g. sub-unit 15/5) also demonstrate the key influence of climate on the $\delta^{18}O$ and $\delta^{13}C$ values of the teeth.

7.5.4.3. $\delta^{18}O$ of meteoric water

Figure 7.7a shows that the calculated mean $\delta^{18}O$ values of meteoric water for Units 8, 11, 14 and 15/3 are slightly depleted relative to the $\delta^{18}O$ values of water sources in Somerset today. This suggests that climatic conditions during these intervals were slightly cooler than present. On the other hand, the mean $\delta^{18}O_{mw}$ values for Units 12, 13, 15/8, 18 and 19, are comparable to the present day. The mean $\delta^{18}O_{mw}$ values for sub-units 15/2 and 15/5 are much higher than present, indicating that the climate may have been warmer and possibly more arid than today. Therefore, the data suggest that the sequence spans the following climatic intervals: 1) a cool climatic interval (Units 8-11) that gradually transitioned into a warm stage with conditions similar to today (Units 12-13), 2) a cool climatic interval (Units 14-15/3), 3) a temperate stage with a climate that was warmer and possibly drier than today (Units 15/2-15/5), and 4) a warm stage with a climate comparable to today (Units 15/8-19). Nevertheless, as outlined in the rationale, extensive snow cover during glacial and stadial stages can result in an enhanced summer bias in the mean $\delta^{18}O_{rt}$ values of rodent assemblages accumulated by avian predators. This means that units with relatively enriched $\delta^{18}O_{mw}$ values may in fact correspond to a cold stage. These interpretations are tested in the following section, by comparing the isotope data with the associated faunal assemblages from Westbury Cave.

7.5.4.4. Comparisons between the isotope and faunal records from Westbury Cave

The current palaeoclimate record for Westbury Cave is based upon Taxonomic Habitat Indices (THI) calculated for the rodent faunal assemblages from each stratigraphic unit (Andrews, 1990; Stringer et al., 1996). A diagrammatic representation of this THI record is shown in Figure 7.7b. This record suggests that the Westbury Cave sequence spans two temperate episodes and two cooler episodes. The temperate episodes correspond to Units 8-12 and 15/2 to 15/3, respectively. These episodes are separated by a cool interval spanning Units 13-14. The second temperate episode is

succeeded by a climatic decline into a cold stage through Units 15/5 to 19. The patterns in the mean $\delta^{18}O$ values of the rodent teeth are generally consistent with the THI record for the two temperate stages and cool interval (Units 8 to 15/5), but different from the THI during the cold stage (15/8-19). The following discussion will compare the isotope and THI records according to these two parts of the sequence.

At the base of the sequence, the $\delta^{18}O_{mw}$ values indicate that climatic conditions were slightly cooler than today. In contrast, the presence of *Emys orbicularis* in Unit 8 suggests that the climate was warmer than present (Andrews, 1990; Holman, 1993). However, the fossil material in Unit 8 was transported into the cave by water (Andrews, 1990). Therefore, it is possible that this unit contains a mixture of remains that were deposited during intervals with different climatic conditions. Also, the mean $\delta^{18}O_{mw}$ for Unit 8 is based on only four teeth, and thus may not provide an accurate reflection of the mean $\delta^{18}O_{mw}$ for this unit.

The rodent faunas from Units 11-12 indicate that temperate conditions continued (Andrews, 1990). The faunas are characteristic of deciduous woodlands in central Europe today, and are therefore indicative of peak interglacial conditions (Andrews, 1990). Although the mean $\delta^{18}O_{mw}$ values for Units 11-12 are slightly less than today, the ranges in values overlap with the modern mean $\delta^{18}O$ of meteoric water in southwest Britain. Therefore, the $\delta^{18}O$ data for these units are consistent with warm climatic conditions, comparable to today.

In Unit 13, however, a discrepancy occurs between the $\delta^{18}O_{mw}$ and THI records (Figure 7.7). The isotope and THI data for this unit are based upon rodent remains from the same sediment sample (Sample 219), and thus the two proxy records should reflect similar climatic conditions. The rodent assemblage from Sample 219 comprises taxa typical of tundra habitats, such as the collared lemming (*Dicrostonyx torquatus*) and the grey hamster (*Cricetulus migratorius*), suggesting that conditions were cool, dry and continental (Andrews, 1990). Conversely, the $\delta^{18}O_{mw}$ values are comparable to the present day. This discrepancy may be due to the evaporation of local water sources under an arid climate. This would have led to relatively enriched $\delta^{18}O_{mw}$ values. Alternatively, the enriched values may be related to a seasonal

bias in the accumulation of the rodent remains. Sample 219 occurred as an isolated pocket of concentrated remains within Unit 13. Andrews (1990) suggests that this sample represents the prey assemblage of a single predator (a long-eared owl) that inhabited the cave for a limited period of time. As outlined in Section 7.2, the predation of rodents and deposition of pellets during cold stages is likely to be biased towards the summer months. Therefore, it is possible that the majority of Sample 219 comprises teeth that mineralized during a time of the year in which $\delta^{18}O_{mw}$ values were relatively enriched.

The THI record indicates that climatic conditions remained cool and dry into Unit 14. The depleted $\delta^{18}O_{mw}$ values in this unit are consistent with this evidence. The decrease in $\delta^{18}O_{mw}$ from Unit 13 to Unit 14 may be due to a shift from a summer-biased assemblage to an assemblage that more closely reflects the mean annual $\delta^{18}O_{mw}$.

A second discrepancy is observed in sub-unit 15/3; the THI indicates temperate conditions, whereas the $\delta^{18}O_{mw}$ values are relatively depleted. Again, only four teeth from sub-unit 15/3 were analysed, and thus the mean $\delta^{18}O_{mw}$ may not be accurate. Despite this, *Microtus oeconomus* and *C. migratorius* are present within the rodent assemblage from this sub-unit, suggesting that fairly cool, continental conditions persisted (Andrews, 1990). It should also be noted that the mean $\delta^{18}O_{mw}$ values for Units 8 and 15/3 are comparable, and according to the faunal evidence, both of these units accumulated during temperate climatic stages.

The subsequent climatic warming in 15/2, and cooling in 15/5, is reflected in both the $\delta^{18}O_{mw}$ and THI records (Figure 7.7). The rodent faunal assemblage from sub-unit 15/2 is consistent with an interglacial climate that is comparable to today but slightly cooler than the interglacial peak of Unit 11 (Andrews, 1990). The assemblage from 15/5, although limited, is suggestive of cooler conditions (Andrews, 1990). In contrast, the mean $\delta^{18}O_{mw}$ values for sub-units 15/2 and 15/5 are both significantly more enriched than the values for Unit 11 and for the present day. This enrichment may result from the evaporation of meteoric water under relatively arid climatic conditions. Alternatively, this enrichment could be related to the species present within the rodent assemblages. The remains of *Microtus arvalidens* (formerly *Pitymys*

arvaloides) dominate the assemblages from sub-units 15/2 and 15/5, whereas all other units are dominated by the remains of *M. gregaloides* and *M. agrestis/arvalis* (Andrews, 1990). Inter-species differences in the relationship between $\delta^{18}O_{rt}$ and $\delta^{18}O_{mw}$ may therefore explain the enhanced enrichment in $\delta^{18}O_{rt}$ values during sub-units 15/2 and 15/5 only.

While the relative changes in $\delta^{18}O_{mw}$ values through Units 8 to 15/5 are generally consistent with the THI record, the $\delta^{18}O_{mw}$ values for Units 15/8 to 19 suggest warmer conditions than indicated by the rodent faunal assemblages. The presence of lemmings in Units 15/8 to 19 is indicative of a cold, dry and continental climate comparable to northern Scandinavia today (Andrews, 1990). Conversely, the $\delta^{18}O_{mw}$ values are similar to the present day. This may be due to the evaporation of meteoric water under arid climatic conditions. The enriched $\delta^{18}O_{rt}$ values may additionally relate to a summer bias in predation, due to the presence of thick snow during a glacial stage. The increased ranges in $\delta^{18}O$ values within Units 15/8 to 19 may also suggest that the temperature or humidity varied during this cold period.

Figure 7.7 *(overleaf): Comparison between the rodent isotope and faunal records from Westbury Cave and the regional proxy records for MIS 13. The grey dashed lines mark the tentative correlations made between these records. a) The record of mean $\delta^{18}O$ values of meteoric water for Westbury Cave, generated from the mean $\delta^{18}O$ values of the rodent teeth. The error bars on the mean $\delta^{18}O$ values represent the 1σ standard deviation uncertainties. The black dashed line indicates the mean $\delta^{18}O$ of modern meteoric water sources in Somerset, and the grey shading indicates the range in $\delta^{18}O$ values around this mean. b) The climatic changes through the Westbury Cave sequence, inferred from the Taxonomic Habitat Indices (THI) for the rodent faunal assemblages (Andrews, 1990). c) Mean annual and mean summer sea surface temperature (SST) records from the North Atlantic marine cores ODP 980 and M23414 (Candy & Alonso-Garcia, 2018). d) The stacked $\delta^{18}O$ record for benthic foraminifera from Atlantic marine cores (Lisiecki & Raymo, 2009). The Marine Oxygen Isotope Stages (MIS) are labelled.*

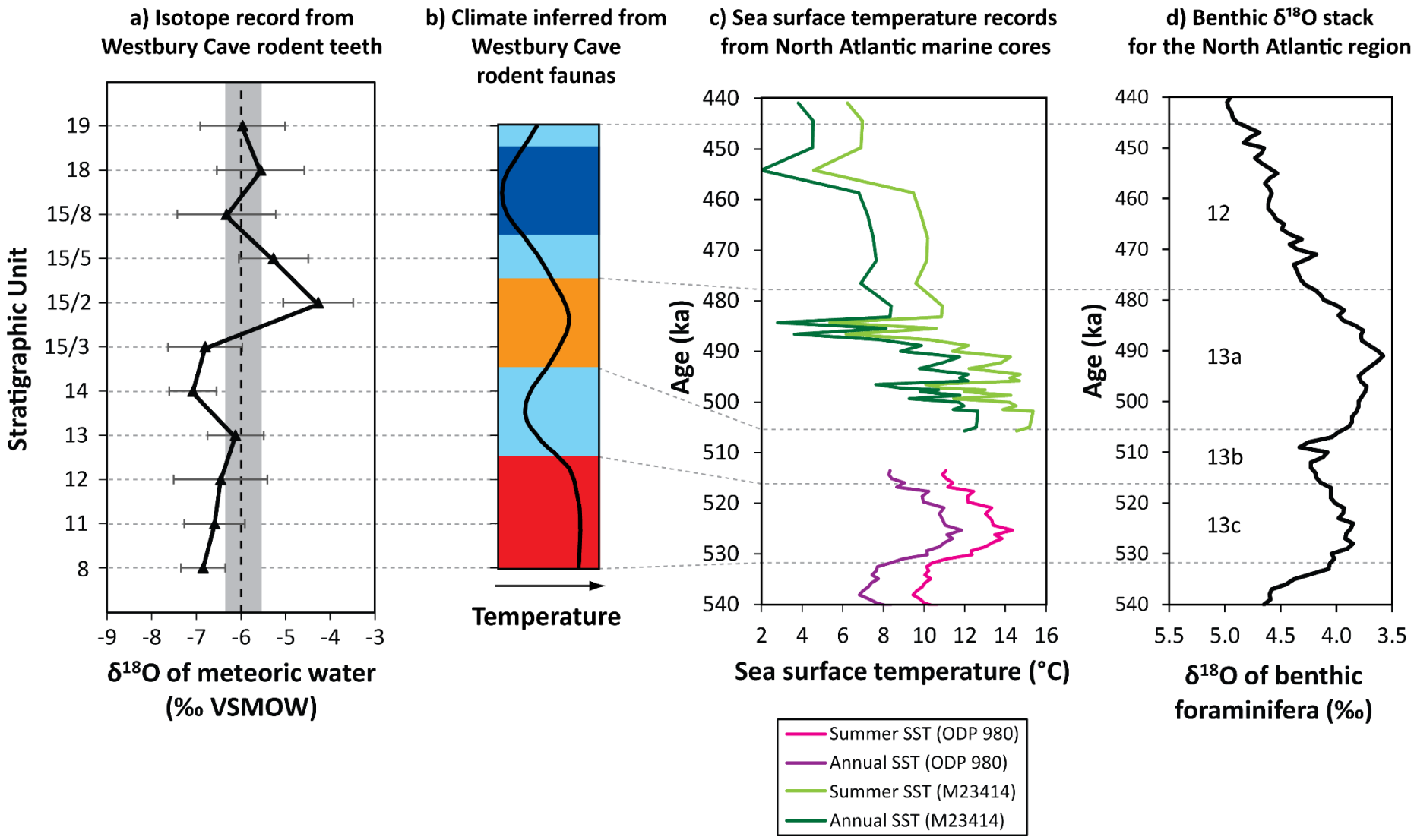
a) Isotope record from Westbury Cave rodent teeth
b) Climate inferred from Westbury Cave rodent faunas
c) Sea surface temperature records from North Atlantic marine cores
d) Benthic δ18O stack for the North Atlantic region
Stratigraphic Unit
19
18
15/8
15/5
15/2
15/3
14
13
12
11
8
-9 -8 -7 -6 -5 -4 -3
δ18O of meteoric water (‰ VSMOW)
Temperature
Age (ka)
440 450 460 470 480 490 500 510 520 530 540
2 4 6 8 10 12 14 16
Sea surface temperature (°C)
Summer SST (ODP 980)
Annual SST (ODP 980)
Summer SST (M23414)
Annual SST (M23414)
12
13a
13b
13c
5.5 5.0 4.5 4.0 3.5
δ18O of benthic foraminifera (‰)

In summary, the patterns in the mean $\delta^{18}O$ values of the rodent teeth through the Westbury Cave sequence are similar to the climatic changes inferred from the faunal record. This suggests that fluctuations in air temperature had a key influence on the $\delta^{18}O$ values of local meteoric water, which were in turn recorded in the $\delta^{18}O$ values of the rodent teeth. However, the relative shifts in the $\delta^{18}O_{mw}$ values between the stratigraphic units are not always consistent with the magnitudes of the climatic changes suggested by the rodent THI record. During the temperate episodes, both the $\delta^{18}O_{mw}$ and THI records are consistent with climates comparable to or warmer than today. In contrast, during the cold stages, $\delta^{18}O_{mw}$ values are more enriched than expected for intervals with low mean air temperatures. Therefore, other factors must have also played a role in influencing the $\delta^{18}O_{rt}$ values. These factors include: 1) changes in the season during which the rodent remains accumulated, 2) variations in the rodent species represented within the samples of teeth selected for analysis, and 3) temporal shifts in humidity, which led to variations in the degree of evaporation of meteoric water.

7.5.4.5. Comparisons between the isotope data from Westbury Cave and North Atlantic marine core records

The $\delta^{18}O$ values of the rodent teeth from Westbury Cave indicate that the climatic structure of MIS 13 in Britain consisted of two discrete temperate episodes (Units 8-13 and 15/2-15/5), separated by a slightly cooler episode (Units 14-15/3). The relative magnitudes of the $\delta^{18}O_{rt}$ peaks suggest that the thermal regime of the first temperate episode was comparable to today, whereas the second episode was substantially warmer than present. This pattern is consistent with records of MIS 13 from the North Atlantic region, adjacent to Britain (Figures 7.7c and 7.7d), and from global marine core, ice core and terrestrial records that span this interglacial stage (Lang & Wolff, 2011). The rodent isotope and faunal records from Westbury Cave can therefore be tentatively correlated with regional records for MIS 13 (Figure 7.7).

One of the most notable features in the $\delta^{18}O_{mw}$ record from Westbury Cave is the enriched values corresponding to the second temperate peak in sub-unit 15/2. The Atlantic marine core records (Figure 7.7c-d), and the deuterium-based temperature record from the EPICA Dome C ice core (Jouzel et al., 2007), suggest that minimum ice volumes and maximum temperatures were reached during the second temperate peak of MIS 13. The enriched $\delta^{18}O_{mw}$ values for sub-unit 15/2 at Westbury Cave are therefore consistent with warmer climatic conditions during MIS 13a. This suggests that any differences in species ecology likely had a minimal impact on the mean $\delta^{18}O$ values of the teeth from sub-units 15/2 and 15/5.

Following MIS 13a, the sea surface temperature (SST) gradually declines towards the MIS 12 glacial stage (Figure 7.7c). This change is also reflected in the $\delta^{18}O_{mw}$ and THI records from Units 15/5 to 19 in Westbury Cave. However, as aforementioned, the $\delta^{18}O_{mw}$ values for Units 15/8-19 are comparable to the present day, and are therefore more enriched than would be expected for a glacial climate. This enrichment is interpreted as resulting from a summer bias in the accumulation of the rodent assemblages during the cold stage (MIS 12). Conversely, the assemblages from the interglacial stage (MIS 13) are generally thought to provide a record of mean annual $\delta^{18}O_{mw}$ values. These interpretations are supported by the SST data from the North Atlantic. The annual SST values during MIS 13c are comparable to the summer SST values during MIS 12 (Figure 7.7c). Similarly, the mean $\delta^{18}O_{mw}$ values for Units 8-12 (correlated with MIS 13c) are similar to the mean $\delta^{18}O_{mw}$ values for Units 15/8-19 (correlated with MIS 12) (Figure 7.7a). This suggests that the rodent teeth from the interglacial stage reflect mean annual temperatures, whereas the rodent teeth from the glacial stage reflect mean summer temperatures.

These comparisons demonstrate that the isotopic and faunal records from Westbury Cave are consistent with regional climate records spanning MIS 13-12. The $\delta^{18}O$ values of the rodent teeth from the cave consequently provide a coherent record of the climatic fluctuations that occurred during this time period.

7.5.5. Summary

The mean $\delta^{18}O$ and $\delta^{13}C$ values of the fossil *Microtus* sp(p). teeth from Westbury Cave fluctuate significantly through the stratigraphic sequence. The $\delta^{18}O_{rt}$ values indicate that the sequence spans two temperate and two cold stages. The parallel shifts in the $\delta^{18}O_{rt}$ and $\delta^{13}C_{rt}$ values suggest that the $\delta^{13}C$ of local vegetation fluctuated in response to climatically-driven variations in the $\delta^{13}C$ of atmospheric CO_2. The stratigraphic patterns in the isotope values are consistent with the rodent faunal assemblages from Westbury Cave, as well as regional and global climate records for MIS 13. This indicates that the isotope values of the rodent teeth reliably record the structure of the climatic fluctuations that occurred during the accumulation of the Westbury Cave sequence. Comparisons with marine records suggest that the two $\delta^{18}O_{rt}$ peaks correlate with MIS 13c and 13a, and the two $\delta^{18}O_{rt}$ troughs correlate with MIS 13b and 12.

Although the pattern of climatic changes is accurately reflected in the $\delta^{18}O_{rt}$ data, the $\delta^{18}O$ values during the glacial stage are more enriched than expected for a cold climatic regime. This is suggested to result from a summer bias in predation, which led to the rodent remains being dominated by teeth that reflect meteoric water sources with enriched $\delta^{18}O$ values. Increased aridity may have also contributed to these enriched $\delta^{18}O_{mw}$ values. Despite this, the increased ranges in $\delta^{18}O_{mw}$ values during the glacial stage are consistent with a greater instability of the climate.

In conclusion, the results from Westbury Cave demonstrate that the mean $\delta^{18}O$ values of rodent teeth from cave sites have the potential to offer valuable records of palaeoclimatic fluctuations during interglacial stages. Nevertheless, the complexities in the data highlight the fact that a clear understanding of 1) rodent ecology, 2) the taphonomic context of the fossil rodent remains, and 3) the general climatic context of the interval being investigated, are all necessary for the meaningful interpretation of the stable isotope values of rodent teeth from cave sequences. The third point is especially important for sites in which the chronology of the sequence is poorly constrained.

7.6. Results: Gully Cave

7.6.1. *Arvicola terrestris* teeth

7.6.1.1. $\delta^{18}O$ of teeth

The $\delta^{18}O$ values of the *A. terrestris* incisors vary from -13.3 to -7.7‰ (range = 5.6‰). The data are plotted in Figure 7.8a, according to the inferred correlations of the spits with the Lateglacial Interstadial (LGI), Loch Lomond Stadial (LLS), and Holocene climatic intervals (Table 7.2), and the relative depths of the spits within each of these intervals. The data have been divided into three groups, corresponding to the three climatic intervals. The descriptive statistics for these groups are summarised in Table 7.8.

The mean $\delta^{18}O$ values of the teeth for the LGI and Holocene are comparable at -8 to -9‰ (Figure 7.8a). In contrast, the mean $\delta^{18}O_{rt}$ value for the LLS is relatively depleted at -10.60‰. The ranges in $\delta^{18}O_{rt}$ values also differ between the climatic intervals; the range for the Holocene is less than half the range for the LLS (Table 7.8).

Proxy records from northwest Europe indicate that a climatic shift occurred in the middle of the LLS or Younger Dryas cold period, from cold and humid conditions, to slightly warmer and drier conditions (e.g. Walker, 1995; Bakke et al., 2009; Lane et al., 2013). Therefore, the $\delta^{18}O$ data from the LLS levels of Gully Cave were divided into 'early' and 'late' sub-groups, based upon the stratigraphic associations between the spits from which the teeth were recovered. The mean $\delta^{18}O_{rt}$ value of the 'early' sub-group is -10.05‰, whereas the mean value of the 'late' sub-group is slightly lower at -10.97‰. However, these mean values are based upon data from only 2-3 teeth, and thus the statistical significance of these differences cannot be assessed.

The mean $\delta^{18}O$ values of the teeth from the three climatic intervals were compared using a Welch's ANOVA (Levene's test, $p < 0.05$). The results of this test indicate that there are no significant differences between the mean $\delta^{18}O_{rt}$ values (F statistic = 5.01, F critical = 5.14), although the *p* value is close to statistical significance at 95% confidence ($p = 0.053$). This lack of statistical significance may result from the small size of the dataset.

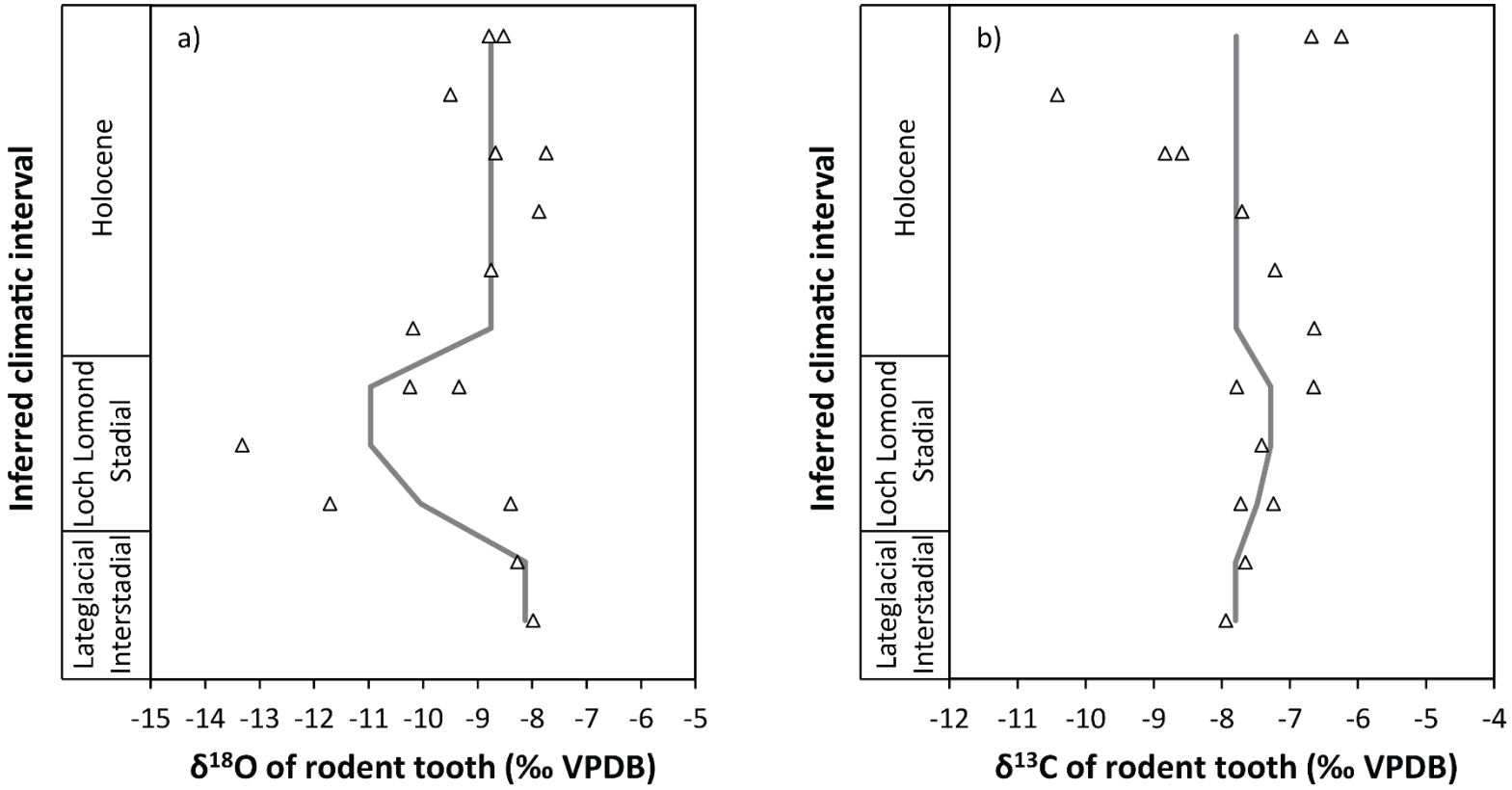

Figure 7.8: *The oxygen (a) and carbon (b) isotope data for the* Arvicola terrestris *incisors from Gully Cave, plotted against the inferred correlations with the climatic intervals. The grey lines indicate the mean values for each interval. The data are from Peneycad (2013).*

Table 7.8: *Summary statistics for the oxygen isotope values of the* Arvicola terrestris *teeth from Gully Cave. The normal distribution column is based on the results of Shapiro-Wilk tests undertaken at 95% confidence.*

Inferred climatic interval	No. of teeth	Mean $\delta^{18}O$ (‰ VPDB)	Standard deviation (‰)	Median $\delta^{18}O$ (‰ VPDB)	Range (‰)	Normally distributed?
Holocene	8	-8.75	0.80	-8.71	2.44	Yes
Loch Lomond Stadial	5	-10.60	1.95	-10.24	4.93	Yes
Lateglacial Interstadial	2	-8.12	0.21	-8.12	0.29	-

7.6.1.2. $\delta^{13}C$ of teeth

The $\delta^{13}C$ values of the teeth vary from a minimum of -10.4‰ to a maximum of -6.2‰ (range = 4.2‰). The mean $\delta^{13}C_{rt}$ values for the LGI and Holocene groups are comparable, while the mean $\delta^{13}C_{rt}$ for the LLS is slightly enriched (Table 7.9, Figure 7.8b). Nevertheless, the results of a Welch's ANOVA (Levene's test, p = 0.05) show that the mean $\delta^{13}C_{rt}$ values for the three intervals are not significantly different (F statistic = 1.43, F critical = 5.14, p = 0.31). Furthermore, the oxygen and carbon isotope values of the teeth from each group are not significantly correlated ($r^2 < 0.1$, $p > 0.05$).

7.6.1.3. $\delta^{18}O$ of meteoric water

The calculated mean $\delta^{18}O_{mw}$ values for the climatic intervals are shown in Table 7.10. The mean $\delta^{18}O_{mw}$ values for the LGI and Holocene are similar at between -7 and -8‰, whereas the mean values for the LLS are 1-2‰ more depleted. However, the mean $\delta^{18}O_{mw}$ values for the three climatic intervals overlap within the 1σ uncertainties.

Table 7.9: *Summary statistics for the carbon isotope values of the* Arvicola terrestris *teeth from Gully Cave.*

Inferred climatic interval	No. of teeth	Mean $\delta^{13}C$ (‰ VPDB)	Standard deviation (‰)	Median $\delta^{13}C$ (‰ VPDB)	Range (‰)	Normally distributed?
Holocene	8	-7.79	1.41	-7.46	4.17	Yes
Loch Lomond Stadial	5	-7.36	0.45	-7.41	1.13	Yes
Lateglacial Interstadial	2	-7.80	0.20	-7.80	0.29	-

Table 7.10: *Mean $\delta^{18}O$ values of meteoric water for the major climatic intervals during the Lateglacial and Holocene period, calculated from the mean $\delta^{18}O$ values of the* Arvicola terrestris *teeth from Gully Cave. The 1σ standard deviation uncertainties on the mean values are also shown.*

Inferred climatic interval		Mean $\delta^{18}O$ of meteoric water (‰ VSMOW)	1σ standard deviation uncertainty (‰)
Holocene		-7.61	0.71
Loch Lomond Stadial	late	-9.30	1.83
	early	-8.60	1.97
Lateglacial Interstadial		-7.13	0.24

7.6.2. *Microtus* sp(p). teeth

7.6.2.1. $\delta^{18}O$ of teeth

The $\delta^{18}O$ values of the *Microtus* sp(p). molars from Gully Cave span a broad range of 9.7‰, between a minimum of -8.4‰ and a maximum of 1.3‰ (Figure 7.9). Despite this large degree of scatter, clear stratigraphic patterns can be seen in the mean $\delta^{18}O$ values of the teeth (Figure 7.10a). Towards the base of the sequence, in spits corresponding the early part of the LGI, the $\delta^{18}O_{rt}$ values are relatively enriched. The mean $\delta^{18}O_{rt}$ reaches a peak in sample group 14 with a value of -0.68‰. Following this peak, the mean $\delta^{18}O_{rt}$ declines to a value of -5.55‰ in group 11, before increasing slightly to -4.08‰ in group 10. The mean $\delta^{18}O_{rt}$ values remain between -4.0 and -5.5‰ throughout the latter part of the LGI (groups 10-11) and the early-middle stages of the LLS (groups 9, 8 and 5), with only minor fluctuations during this part of the sequence (Figure 7.10a). The mean $\delta^{18}O_{rt}$ subsequently declines to a minimum of -7.21‰ in group 7, and remains relatively depleted in group 6 at a value of -6.09‰. At approximately the LLS-Holocene boundary, in groups 3-4, the mean $\delta^{18}O_{rt}$ increases to around -3.5‰. The mean $\delta^{18}O_{rt}$ remains between -3 and -4‰ during the early Holocene at the top of the sequence (groups 1-2).

A parametric ANOVA was undertaken to compare the mean $\delta^{18}O$ values of the teeth from each sample group (Levene's test, $p = 0.88$). The results of this test indicate that there are statistically significant differences between the mean $\delta^{18}O_{rt}$ values (F statistic = 4.10, F critical = 1.84, $p < 0.05$). Post-hoc Tukey's Q tests reveal that these differences occur between the enriched mean $\delta^{18}O$ value of group 14, and the relatively depleted values of groups 6-9, 11 and 12 (Table 7.11). The mean $\delta^{18}O_{rt}$ of group 6 is also significantly different from group 15, while the mean value of group 7 is significantly different from groups 13 and 15. These results show that statistically significant differences occur between the groups with the highest (groups 13-15) and lowest (groups 6-7) mean $\delta^{18}O_{rt}$ values. These groups correspond with the LGI peak and LLS trough, respectively.

To highlight the major patterns in the $\delta^{18}O_{rt}$ values, data from stratigraphically superposed spits that have mean $\delta^{18}O_{rt}$ values that are not

significantly different (Table 7.11) were averaged. The descriptive statistics for the averaged groups are shown in Table 7.12. The ranges in $\delta^{18}O_{rt}$ values within the groups generally vary from ~4 to 6‰, and there a no clear patterns in these ranges through the sequence.

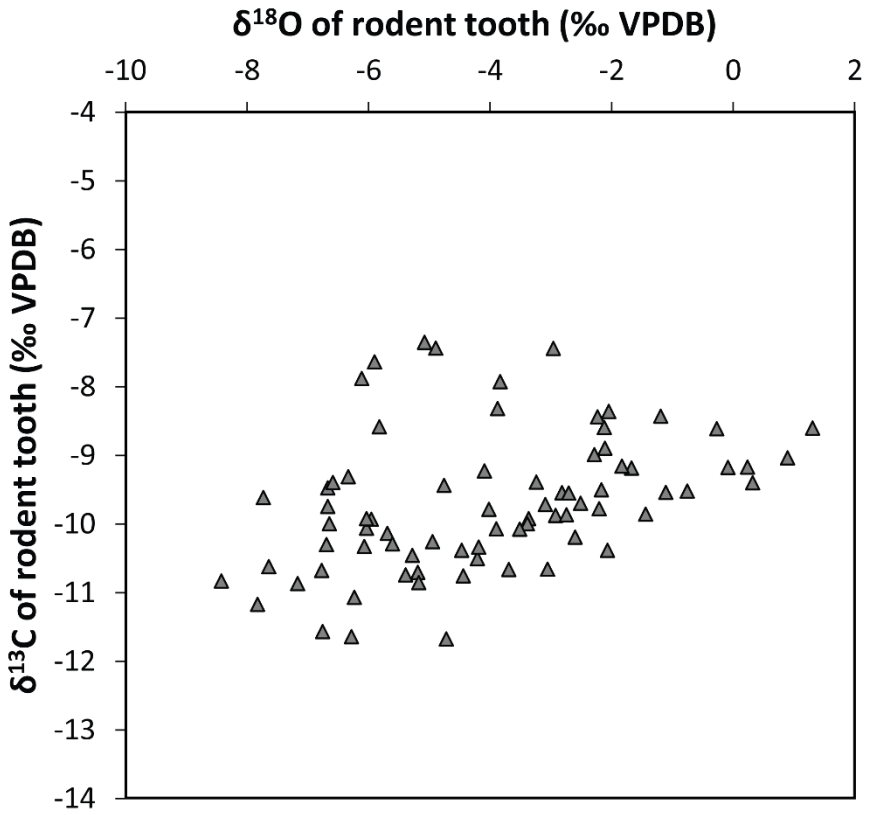

Figure 7.9: *Plot of the oxygen and carbon isotope data for the* Microtus *sp(p). teeth from Gully Cave.*

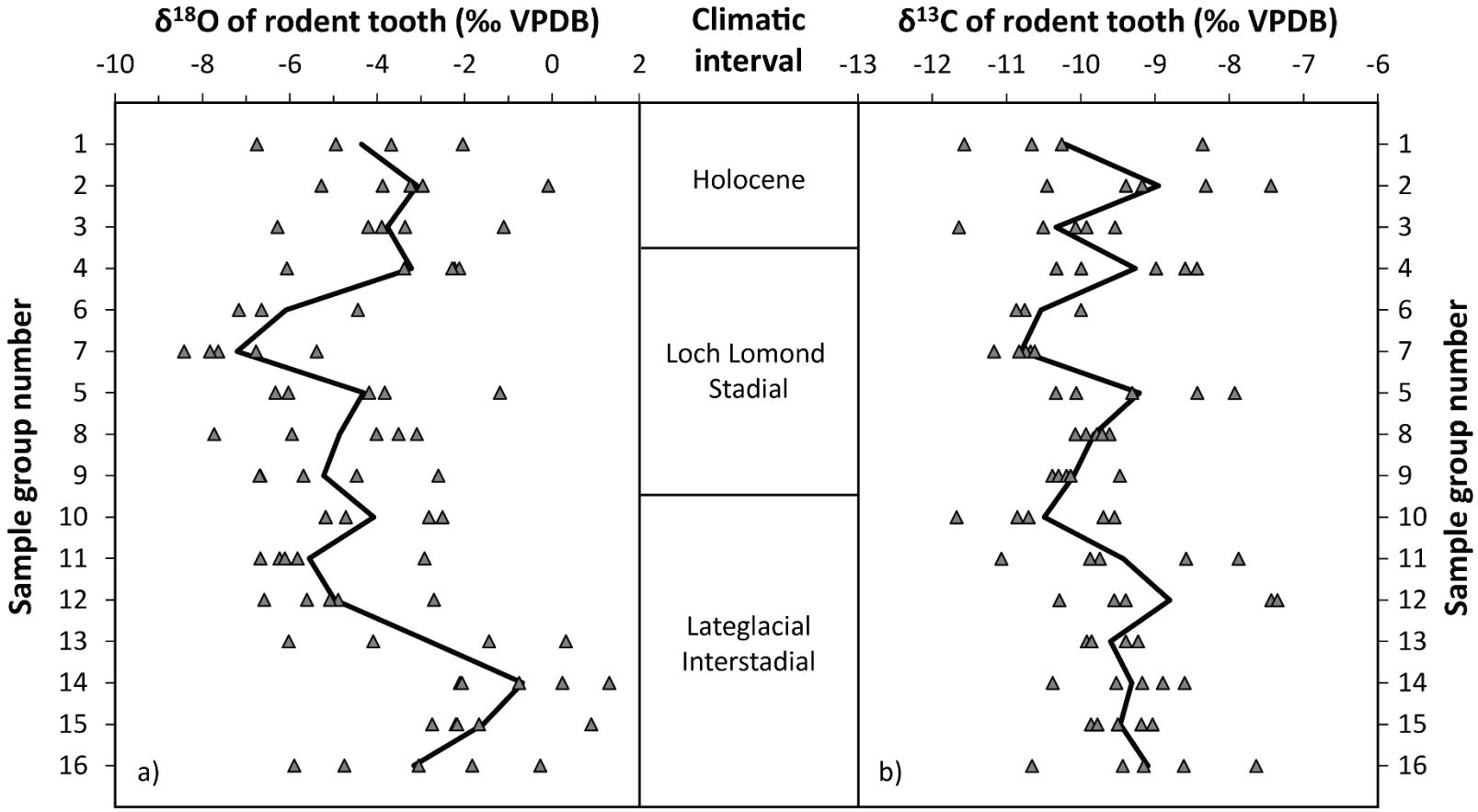

Figure 7.10: *The oxygen (a) and carbon (b) isotope values of the* Microtus *sp(p). teeth from Gully Cave, plotted by sample group number and climatic interval. The black lines indicate the mean values for each sample group.*

Table 7.11: *Results of the Tukey's Q tests undertaken on the* $\delta^{18}O$ *values of the* Microtus *sp(p). teeth from the 16 sample groups from Gully Cave. The results are shown as* p *values, with blue shading indicating no statistically significant difference at 95% confidence, and orange shading indicating a statistically significant difference at 95% confidence.*

	2	**3**	**4**	**5**	**6**	**7**	**8**	**9**	**10**	**11**	**12**	**13**	**14**	**15**	**16**
1	1	1	1	1	0.98	0.52	1	1	1	1	1	1	0.14	0.56	1
2		1	1	1	0.44	0.06	0.98	0.90	1	0.76	0.96	1	0.78	0.99	1
3			1	1	0.82	0.22	1	1	1	0.98	1	1	0.38	0.87	1
4				1	0.51	0.07	0.99	0.93	1	0.82	0.98	1	0.71	0.99	1
5					0.98	0.50	1	1	1	1	1	0.99	0.15	0.59	1
6						1	1	1	0.93	1	1	0.29	<0.01	0.02	0.48
7							0.81	0.94	0.37	0.99	0.86	0.03	<0.01	<0.01	0.07
8								1	1	1	1	0.92	<0.05	0.29	0.98
9									1	1	1	0.78	0.02	0.15	0.92
10										1	1	1	0.24	0.73	1
11											1	0.59	<0.01	0.08	0.79
12												0.88	0.04	0.24	0.97
13													0.90	1	1
14														1	0.74
15															0.99

Table 7.12: *Summary statistics for the oxygen isotope data from the* Microtus *sp(p). molars from Gully Cave. The normally distributed column is based upon Shapiro-Wilk tests undertaken at 95% confidence.*

Sample group numbers	Inferred climatic interval	No. of teeth	Mean $\delta^{18}O$ (‰ VPDB)	Standard deviation (‰)	Median $\delta^{18}O$ (‰ VPDB)	Range (‰)	Normally distributed?
1	Holocene	4	-4.36	1.99	-4.32	4.71	Yes
2	Holocene	5	-3.09	1.90	-3.24	5.19	Yes
3-4	Loch Lomond Stadial-Holocene boundary	10	-3.49	1.69	-3.38	5.18	Yes
6-7	late Loch Lomond Stadial	8	-6.79	1.32	-6.97	3.98	Yes
5	Loch Lomond Stadial	5	-4.32	2.06	-4.19	5.14	Yes
8-9	early Loch Lomond Stadial	10	-5.04	1.74	-5.08	5.13	Yes
10	middle-late Lateglacial Interstadial	5	-4.08	1.31	-4.72	2.68	Yes
11-12		10	-5.26	1.42	-5.72	3.97	Yes
13		4	-2.81	2.81	-2.77	6.35	Yes
14-15	early Lateglacial Interstadial	10	-1.13	1.45	-1.87	4.05	Yes
16		5	-3.16	2.25	-3.05	5.63	Yes

7.6.2.2. $\delta^{13}C$ of teeth

The $\delta^{13}C$ data span a range of 4.3‰, between a minimum of -11.7‰ and a maximum of -7.4‰ (Figure 7.9). The mean $\delta^{13}C_{rt}$ values generally vary between -11 and -9‰ (Table 7.13), and there are no clear stratigraphic patterns that correspond to the three climatic intervals (Figure 7.10b). Also, in general, the $\delta^{13}C$ fluctuations do not parallel the stratigraphic changes in the $\delta^{18}O$ data (Figure 7.10a). The exceptions to this occur in the top half of the sequence; the major $\delta^{18}O$ depletion in groups 6 and 7 is also reflected in the $\delta^{13}C$ data. The small fluctuations in mean $\delta^{18}O$ during the Holocene are likewise seen in the $\delta^{13}C$ data, although the $\delta^{13}C$ changes are of a larger magnitude (Figure 7.10b).

To assess whether the fluctuations in mean $\delta^{13}C_{rt}$ are statistically significant, a Welch's ANOVA was performed (Shapiro-Wilk, $p > 0.05$; Levene's test, $p < 0.05$). The results of this test indicate that there are statistically significant differences between the mean $\delta^{13}C$ values of the groups (F statistic = 5.62, F critical = 2.18, $p < 0.05$). These differences occur between group 7 and groups 8, 13, and 15 (Games-Howell, $p < 0.05$).

For most sample groups, the $\delta^{18}O$ and $\delta^{13}C$ values are not significantly correlated (Pearson's r^2 values < 0.3, $p > 0.05$). However, for groups, 1, 3, 4, 10, and 15, strong positive correlations occur between the $\delta^{18}O$ and $\delta^{13}C$ values of the teeth (r^2 = 0.7-0.9). The correlation in the group 3 data is statistically significant at 95% confidence ($p < 0.05$), whereas the correlations for groups 1, 4, 10 and 15 are statistically significant at 90% confidence ($0.05 < p < 0.1$). However, these correlations are based upon data from only 4-5 teeth, and thus may disappear with data from additional samples.

Table 7.13: *Summary statistics for the carbon isotope data from the* Microtus *sp(p). molars from Gully Cave.*

Sample group numbers	Inferred climatic interval	No. of teeth	Mean $\delta^{13}C$ (‰ VPDB)	Standard deviation (‰)	Median $\delta^{13}C$ (‰ VPDB)	Range (‰)	Normally distributed?
1	Holocene	4	-10.21	1.35	-10.46	3.21	Yes
2	Holocene	5	-8.95	1.14	-9.17	3.02	Yes
3	Loch Lomond Stadial-Holocene boundary	5	-10.33	0.81	-10.07	2.10	Yes
4		5	-9.27	0.85	-8.99	1.89	Yes
6	late Loch Lomond Stadial	3	-10.54	0.47	-10.75	0.87	Yes
7		5	-10.81	0.22	-10.74	0.55	Yes
5	Loch Lomond Stadial	5	-9.21	1.03	-9.31	2.41	Yes
8	early Loch Lomond Stadial	5	-9.82	0.18	-9.78	0.46	Yes
9		5	-10.10	0.36	-10.19	0.91	Yes
10	middle-late Lateglacial Interstadial	5	-10.49	0.88	-10.71	2.13	Yes
11		5	-9.43	1.24	-9.74	3.19	Yes
12		5	-8.80	1.33	-9.39	2.94	Yes
13		4	-9.60	0.34	-9.62	0.69	Yes
14	early Lateglacial Interstadial	5	-9.31	0.69	-9.17	1.78	Yes
15		5	-9.47	0.36	-9.50	0.83	Yes
16		5	-9.10	1.11	-9.15	3.02	Yes

7.6.2.3. $\delta^{18}O$ of meteoric water

The calculated mean $\delta^{18}O$ values of meteoric water range from a minimum of -6.12‰ in sample groups 6-7, to a maximum of -1.80‰ in groups 14-15 (Figure 7.11). The mean $\delta^{18}O_{mw}$ values for all other sample groups vary between -5 and -3‰. However, since the mean $\delta^{18}O$ values of the *Microtus* teeth from Gully Cave (generally -1 to -6‰) are enriched compared to the mean $\delta^{18}O$ values of the modern *M. agrestis* teeth from Britain upon which the regression equation is based (-6.6 to -8.3‰), the calibration uncertainties on the mean calculated $\delta^{18}O_{mw}$ values are relatively large (0.2-0.4‰). Also, due to the large scatter in the $\delta^{18}O$ data from each sample group, the standard deviations in the $\delta^{18}O_{mw}$ values are broad, reaching up to 2‰ (Figure 7.11). As a result, the calculated mean $\delta^{18}O_{mw}$ values for the Gully Cave sequence are relatively imprecise.

7.6.3. Comparisons between the *Arvicola* and *Microtus* data

7.6.3.1. $\delta^{18}O$ of teeth

The broad-scale stratigraphic patterns in the $\delta^{18}O$ values of the *Arvicola* and *Microtus* teeth are similar (Figure 7.12). In both taxa, the $\delta^{18}O_{rt}$ values are relatively enriched during the LGI and Holocene, and relatively depleted during the LLS. Both taxa also have relatively enriched mean $\delta^{18}O_{rt}$ values during the early LLS compared to the latter part of this interval. However, the $\delta^{18}O$ values of the *Microtus* teeth are significantly more enriched than the *Arvicola* teeth (Figure 7.12). The degree of enrichment varies between 4 and 6‰.The magnitudes of the $\delta^{18}O_{rt}$ shifts between the three climatic intervals are also slightly higher in *Microtus* than in *Arvicola* (Table 7.14).

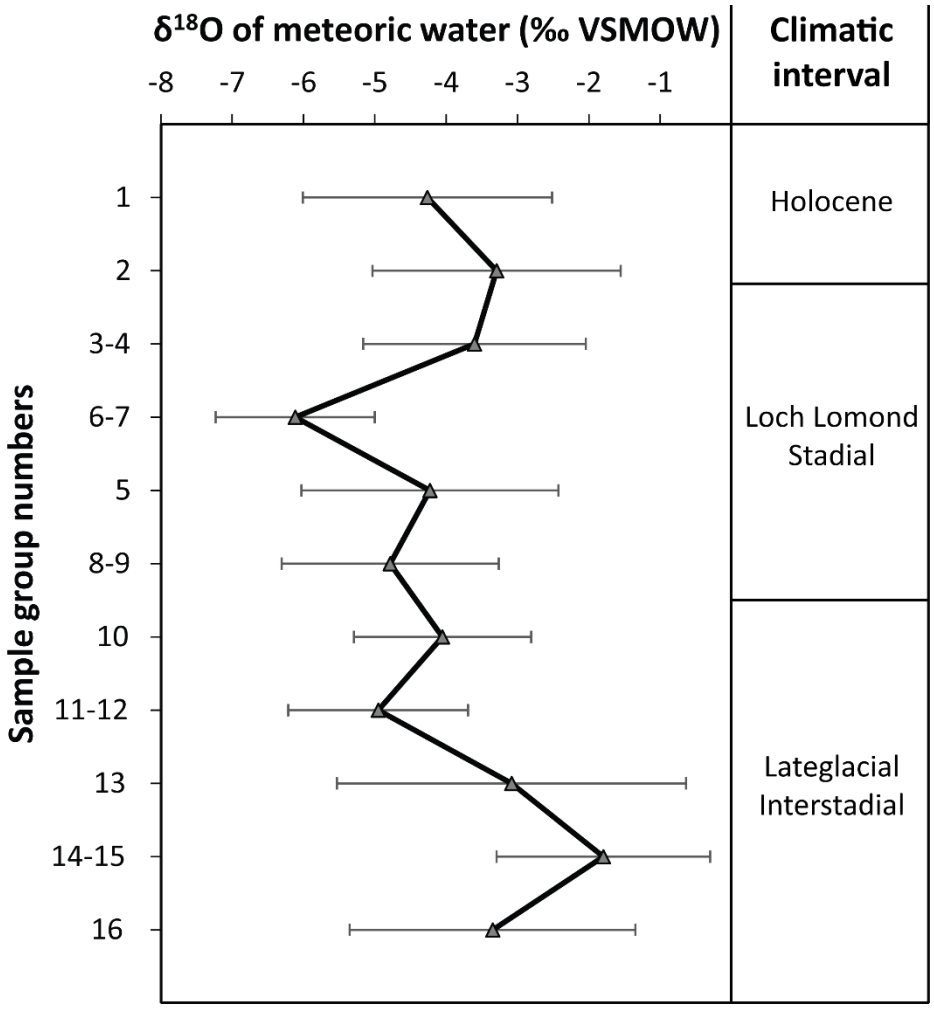

Figure 7.11: *The mean $\delta^{18}O$ values of meteoric water, calculated from the mean $\delta^{18}O$ values of the* Microtus *sp(p). teeth from Gully Cave. The error bars represent the 1σ standard deviation uncertainties on the mean values. The inferred climatic intervals for the sample groups are also shown.*

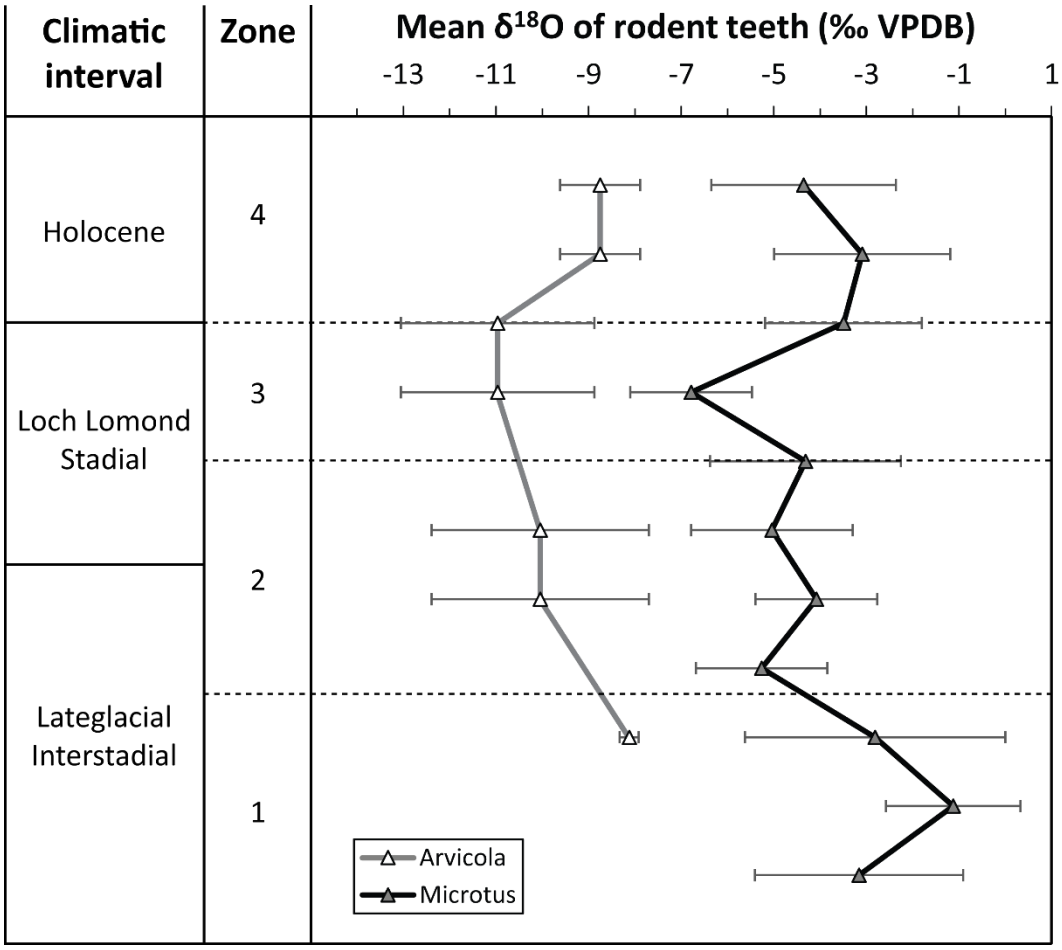

Figure 7.12: *Variations in the mean oxygen isotope values of the* Arvicola *and* Microtus *teeth through the Gully Cave sequence. The inferred correlations with the climatic intervals, and the four zones identified in the data, are indicated. The error bars represent the 1σ standard deviations for each stratigraphic interval. The* Arvicola *and* Microtus *samples are correlated based on their relative stratigraphic positions within the Gully Cave sequence.*

Table 7.14: *Magnitudes of the shifts in the mean $\delta^{18}O$ values of the* Arvicola *and* Microtus *teeth from Gully Cave across the Lateglacial and early Holocene period.*

Climatic intervals	Difference in mean $\delta^{18}O_{rt}$ values (‰)	
	Arvicola	***Microtus***
early Holocene – late Loch Lomond Stadial	2.21	3.29
late Loch Lomond Stadial – early Loch Lomond Stadial	0.92	1.75
early Loch Lomond Stadial – late Lateglacial Interstadial	1.92	2.23

7.6.3.2. $\delta^{13}C$ of teeth

While the mean $\delta^{18}O$ values of the *Microtus* teeth are enriched compared to the *Arvicola* teeth, the opposite is observed in the $\delta^{13}C$ data (Figure 7.13). The mean $\delta^{13}C$ values of the *Microtus* teeth from the Holocene and LGI are ~1.7-2.7‰ depleted relative to the *Arvicola* teeth. Conversely, the mean $\delta^{13}C$ values of the *Microtus* teeth from the LLS are ~2.5-3.5‰ more depleted than the *Arvicola* teeth. No comparable stratigraphic patterns are seen in the *Microtus* and *Arvicola* $\delta^{13}C_{rt}$ data.

7.6.4. Interpretations and Discussion

7.6.4.1. $\delta^{18}O$ of teeth

If the stratigraphic fluctuations in the mean $\delta^{18}O$ values of the *Arvicola* and *Microtus* teeth are interpreted as reflecting changes in mean air temperature, the data from Gully Cave can be divided into four climatic zones: 1) warm climatic conditions at the base of the sequence, 2) a relatively cooler climate in the middle of the sequence, 3) a cold interval, and 4) a return to a warm climate at the top of the sequence (Figure 7.12). Zones 1 and 4 correspond to spits that have been dated to the LGI and Holocene intervals, respectively.

Zone 2 spans the latter part of the LGI and the early half of the LLS, whereas Zone 3 is restricted to the end of the LLS.

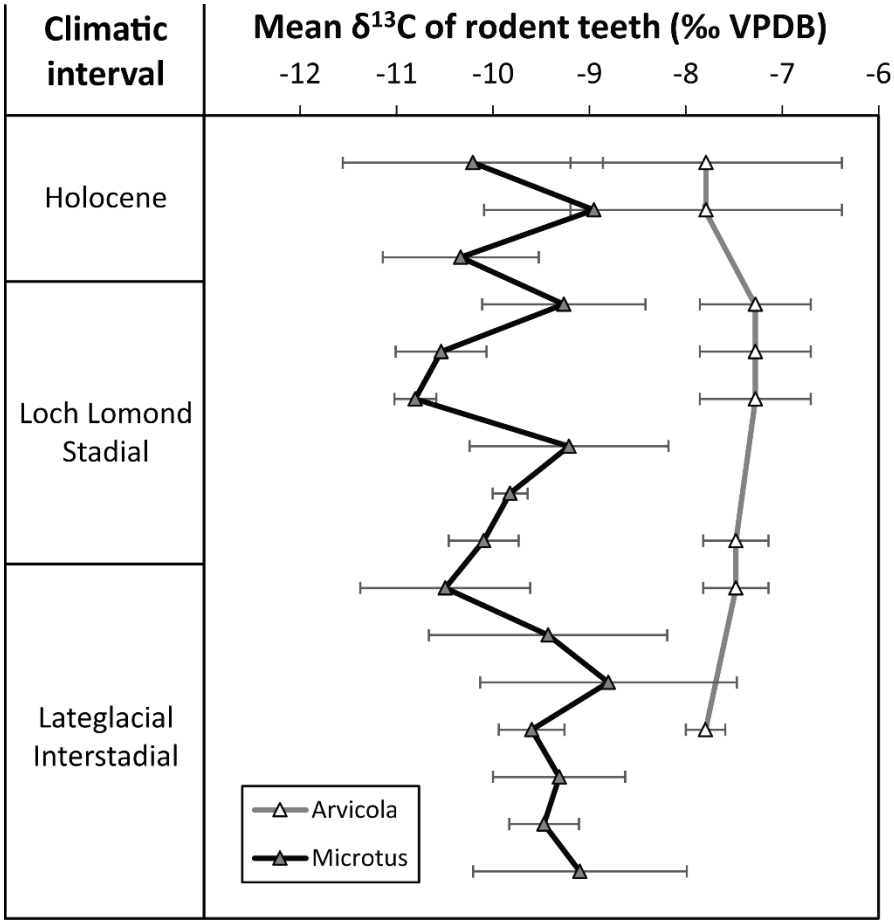

Figure 7.13: *Variations in the mean carbon isotope values of the* Arvicola *and* Microtus *teeth from Gully Cave, plotted by inferred climatic interval. The error bars represent the 1σ standard deviations for the data from each level.*

The mean $\delta^{18}O_{rt}$ reaches a peak in the LGI, with values that are more enriched than in the Holocene (Figure 7.12). This relative enrichment during the LGI may result from: 1) higher temperatures, 2) the consumption of evaporatively-enriched water sources by the rodents, or 3) an enrichment in the $\delta^{18}O$ value of the ocean moisture source. Lateglacial records from Britain

indicate that mean temperatures during the LGI were comparable to or lower than in the Holocene (Walker et al., 2003; Lang et al., 2010; Brooks et al., 2012). This suggests that the enriched $\delta^{18}O_{rt}$ values during the LGI are unlikely to result from higher temperatures. This enrichment can therefore be attributed to an increase in the $\delta^{18}O$ of the source water.

As mentioned in section 7.3.2.2, the rodent assemblages from the LGI are dominated by *Microtus gregalis*, whereas the Holocene assemblages are dominated by *M. agrestis/arvalis*. *M. gregalis* generally lives in relatively dry habitats, whereas *M. agrestis/arvalis* prefers humid habitats. As a consequence, the $\delta^{18}O$ values of the water sources ingested by *M. gregalis* are likely to be more greatly affected by evaporative enrichment. This ecological factor may have contributed to the enriched $\delta^{18}O_{rt}$ values during the LGI.

In addition, during the Last Glacial Maximum, the $\delta^{18}O$ value of seawater in the North Atlantic was approximately 0.7-0.8‰ enriched compared to the Holocene (Schrag et al., 2002). This is because the growth of global ice sheets led to extraction of ^{16}O from the oceans. Since precipitation in Britain is primarily derived from water vapour that has evaporated from the North Atlantic Ocean (Darling & Talbot, 2003), an enrichment in the $\delta^{18}O$ of seawater would also be reflected in the $\delta^{18}O$ values of meteoric water sources in southwest Britain. Rodents drinking these sources would therefore have enriched $\delta^{18}O_{rt}$ values. The calculated mean $\delta^{18}O_{mw}$ values for the LGI peak are up to 1.5‰ higher than in the early Holocene (Figure 7.11). Therefore, the higher $\delta^{18}O_{rt}$ values during the LGI compared to the Holocene can be partly explained by the difference in the $\delta^{18}O$ of seawater.

The decrease in the mean $\delta^{18}O$ values of the *Microtus* teeth from -2‰ in the early LGI, to -5‰ in the late LGI, suggests that the climate significantly cooled. Mean $\delta^{18}O_{rt}$ values of ~ -5‰ continue into the early LLS, implying that climatic conditions during the late interstadial and early stadial were comparable. This inferred similarity in the climatic conditions may result from differences in the seasons reflected by the mean $\delta^{18}O_{rt}$ values during the late LGI and early LLS. Under the warm climatic conditions of the interstadial, the predation of rodents was likely frequent during both summer and winter. This means that the mean $\delta^{18}O_{rt}$ values of the LGI samples likely reflect the mean

annual $\delta^{18}O$ of meteoric water. The depleted mean $\delta^{18}O_{rt}$ values in the late LGI would therefore indicate that the mean annual temperature declined towards the LLS, following the early LGI peak. On the other hand, cold conditions during the early LLS would have likely led to significant snow cover, which may have reduced the frequency of predation during winter. As a result, the rodent assemblages from this interval may be biased towards the warm and arid summer months, when $\delta^{18}O_{mw}$ values would be relatively enriched.

Changes in the seasonal accumulation of the rodent assemblages may also provide an explanation for the notable bipartite structure in the $\delta^{18}O_{rt}$ data from the LLS section of the sequence. A climatic shift in the mid-LLS (or Younger Dryas), from cold, humid conditions to relatively warmer and drier conditions, has been observed in several proxy records from northwest Europe (Walker, 1995; Isarin et al., 1998; Bakke et al., 2009; Lane et al., 2013). This shift is thought to result from the gradual northward progression in the average position of the polar front, coincident with the climatic amelioration at the end of the glacial stage (Lane et al., 2013). After the polar front had moved northwards of Gully Cave, the snow cover during winter may have declined, enabling predators to hunt more readily throughout the year. The mean $\delta^{18}O_{rt}$ values during this period would therefore reflect the mean annual $\delta^{18}O_{mw}$. A shift from summer-biased $\delta^{18}O$ values to mean annual $\delta^{18}O$ values would result in a drop in the $\delta^{18}O$ values of the teeth from the early to the late LLS. This pattern is clearly evident in the $\delta^{18}O_{rt}$ data from Gully Cave (Figure 7.12). The climatic amelioration may also explain why the mollusc assemblages from the late LLS in Gully Cave suggest warmer conditions consistent with the Holocene (Table 7.3).

The relatively broad ranges in the $\delta^{18}O$ values of the teeth within each stratigraphic level at Gully Cave may also suggest that climatic conditions were relatively continental. In particular, the increased variability in the $\delta^{18}O$ values of the *Arvicola* teeth during the LLS (Figure 7.12) is suggestive of an increase in the seasonal range in temperature or humidity during this interval. This suggestion of increased continentality is consistent with the existing palaeoclimate reconstructions for the Younger Dryas cold stage (e.g. Atkinson et al., 1987; Isarin et al., 1998).

7.6.4.2. $\delta^{13}C$ of teeth

The $\delta^{13}C$ values of the *Arvicola* teeth from Gully Cave are ~1-3‰ enriched compared to the *Microtus* teeth (Figure 7.13). The mean $\delta^{13}C$ values of modern *A. terrestris* teeth from northwest Germany are likewise ~1-2‰ enriched compared to *Microtus* spp. teeth from the same site (Gehler et al., 2012). This consistency in the $\delta^{13}C$ offset between the two taxa may suggest that the magnitude of isotopic fractionation between the diet and bioapatite is greater in *Arvicola* than in *Microtus*. Small differences between the dietary preferences of these taxa may also contribute to this $\delta^{13}C$ offset.

The mean $\delta^{13}C$ values of both the *Arvicola* (-7 to -8‰) and *Microtus* (-9 to -11‰) teeth are also significantly more enriched than the $\delta^{13}C$ values of modern *M. agrestis* teeth from Britain (-16 to -18‰). The calculated dietary $\delta^{13}C$ values range from -21.92 to -17.74‰ for *Arvicola*, and from -23.17 to -18.85‰ for *Microtus*. The minimum $\delta^{13}C_d$ values overlap with the modern $\delta^{13}C$ compositions of C_3 plants (Figure 2.2). Conversely, the maximum $\delta^{13}C_d$ values are more enriched than the maximum $\delta^{13}C$ value of modern C_3 plants, which is around -20‰ (Kohn, 2010). These enriched $\delta^{13}C$ values likely result from two factors.

Firstly, the $\delta^{13}C$ values of C_3 plants have declined over the past ~200 years (e.g. Stuiver et al., 1984; Young et al., 2012) due to a ~2‰ decrease in the $\delta^{13}C$ of atmospheric CO_2 since the Industrial Revolution (Graven et al., 2017). Consequently, the $\delta^{13}C$ values of pre-industrial C_3 plants are expected to be ~1-2‰ enriched relative to modern plants. Secondly, the $\delta^{13}C$ values of plant and mammalian tissues are typically slightly enriched during the Last Glacial Stage compared to the early Holocene (Richards & Hedges, 2003; Stevens & Hedges, 2004; Hare et al., 2018). This is because lower atmospheric CO_2 concentrations during glacial stages result in increased plant $\delta^{13}C$ values. Low temperatures and moisture levels during glacial stages may have additionally contributed to the enriched $\delta^{13}C_p$ values (see Table 2.1). These factors may also explain the slight enrichment in the $\delta^{13}C$ values of the *Arvicola* teeth during the LLS.

In contrast, the parallel changes in the $\delta^{18}O$ and $\delta^{13}C$ values of the *Microtus* teeth during the late LLS and early Holocene (Figure 7.10) can be

attributed climatically-driven fluctuations in the $\delta^{13}C$ of atmospheric CO_2. This is because $\delta^{13}C_a$ is the only major environmental factor that is positively correlated with both the $\delta^{13}C$ values of C_3 plants and temperature (Figure 2.4b).

7.6.4.3. Differences between the $\delta^{18}O$ values of meteoric water calculated from the Arvicola *and* Microtus *teeth*

Figure 7.14 shows that the mean $\delta^{18}O_{mw}$ values calculated from the *Microtus* teeth are generally enriched relative to the mean $\delta^{18}O_{mw}$ values of modern water sources in southwest Britain. In contrast, the mean $\delta^{18}O_{mw}$ values calculated from the *Arvicola* teeth are depleted relative to today. These inter-species $\delta^{18}O_{mw}$ offsets likely relate to the ecological preferences of these taxa. As summarised in Section 4.2, members of the genus *Microtus* generally live in open grassland areas, where the $\delta^{18}O$ values of food and drinking water sources are likely to be affected by evaporative enrichment. Conversely, *Arvicola terrestris* in Britain generally lives in riparian habitats. The constant flow of a river reduces the impact of evaporation on the $\delta^{18}O$ of the river water. As a result, the $\delta^{18}O$ values of the water sources consumed by *Arvicola* are likely to be close to the $\delta^{18}O$ of precipitation.

These ecological differences have two implications for the $\delta^{18}O$ values of *Microtus* and *Arvicola* teeth. Firstly, the $\delta^{18}O$ values of the water sources consumed by *Microtus* are likely to be enriched compared to the water sources consumed by *Arvicola*. This pattern is seen in the Gully Cave data; mean $\delta^{18}O_{mw}$ values for *Microtus* are ~3-5‰ enriched compared to those for *Arvicola* (Figure 7.14). Secondly, the $\delta^{18}O$ values of *Arvicola* teeth are likely to primarily reflect changes in temperature, whereas the $\delta^{18}O$ values of *Microtus* teeth are likely to reflect changes in relative humidity as well as temperature. This means that the $\delta^{18}O$ values of *Microtus* teeth may be particularly enriched during periods of enhanced aridity, and specifically during glacial and stadial stages. Relatively arid conditions during the LGI and LLS may consequently explain the highly enriched $\delta^{18}O$ values of the *Microtus* teeth from Gully Cave. These interpretations are supported by previous research on the $\delta^{18}O$ values

of rodent teeth from glacial stages. For example, a study on a cave site in France found that during the Last Glacial Stage, the $\delta^{18}O$ values of *Microtus* teeth were ~0.5-2.5‰ higher than *Arvicola* teeth (Royer et al., 2014). The results from Westbury Cave likewise show that the $\delta^{18}O$ values of *Microtus* teeth in Britain were anomalously enriched during the MIS 12 glacial stage (Figure 7.7).

The sensitivity of *Microtus* to fluctuations in humidity may also explain the broad ranges in the $\delta^{18}O_{rt}$ values within each sample from Gully Cave (Table 7.12). Additionally, the larger magnitudes of the $\delta^{18}O_{rt}$ shifts in *Microtus* (Table 7.14) may result from the shorter tooth mineralization periods in this taxon compared to *Arvicola* (Royer et al., 2013a; 2014).

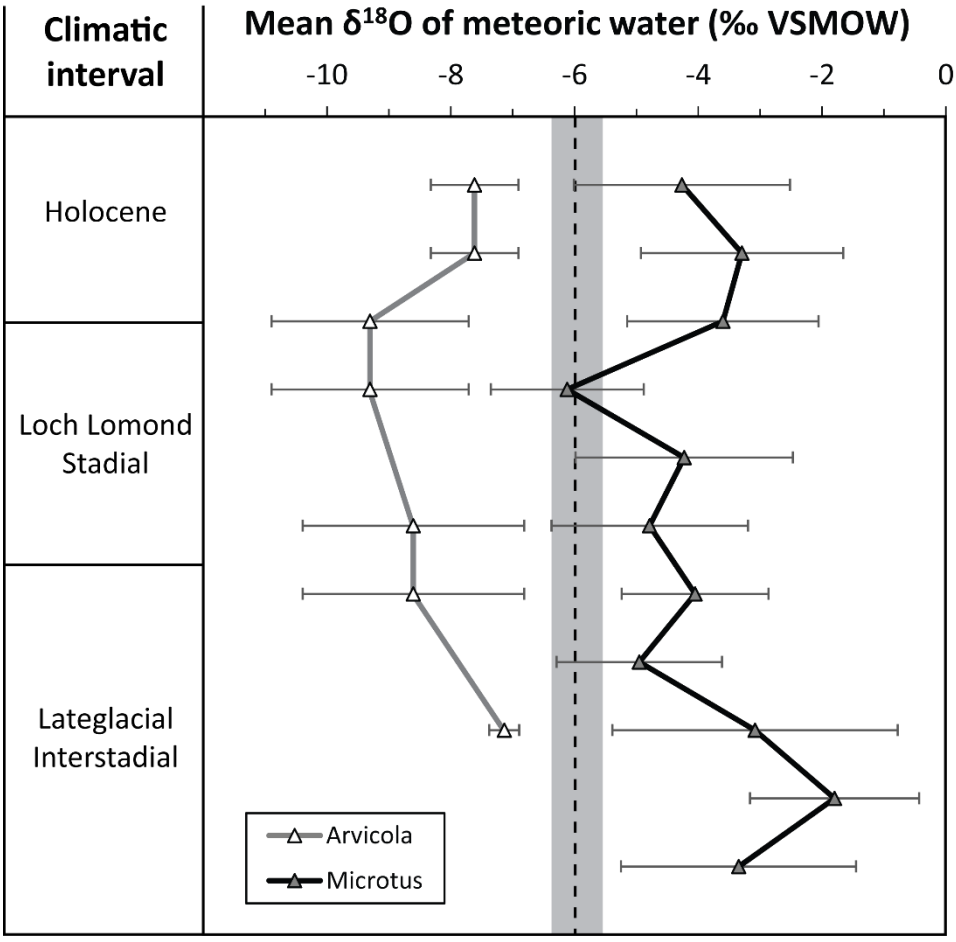

Figure 7.14: *Stratigraphic variations in the mean $\delta^{18}O$ values of meteoric water, calculated from the mean $\delta^{18}O$ values of the* Arvicola *and* Microtus *teeth from Gully Cave.*

While the absolute $\delta^{18}O$ values of the *Microtus* teeth reflect increased aridity, the $\delta^{18}O$ values of the *Arvicola* teeth appear to reflect the reduced temperatures during the Lateglacial period. The $\delta^{18}O_{mw}$ values calculated from the *Arvicola* teeth suggest that between the LGI and early Holocene, $\delta^{18}O_{mw}$ values were ~1-3‰ lower than in southwest Britain at the present day (Figure 7.14). The $\delta^{18}O$ values of groundwater sources in Britain that date to the end of the Last Glacial Stage are also ~1.0-2.5‰ more depleted than in the Holocene (Darling et al., 2003). This suggests that the $\delta^{18}O$ values of the *Arvicola* teeth from Gully Cave provide an accurate reflection of the shifts in the mean $\delta^{18}O$ of precipitation, and therefore mean air temperature, between the LLS and the present day.

7.6.4.4. Comparisons with regional proxy records

Since the isotopic record from the *Microtus* teeth is more stratigraphically complete and chronologically well-constrained compared to the record from the *Arvicola* teeth, only the *Microtus* data are considered in this section. The *Microtus* $\delta^{18}O_{mw}$ data are plotted in Figure 7.15a, according to the calibrated radiocarbon dates from each spit. These data are shown alongside isotopic and temperature records from Britain and Greenland in Figures 7.15b-d.

Figure 7.15 demonstrates that the fluctuations in the $\delta^{18}O_{mw}$ values through the Gully Cave sequence parallel many of the major shifts in the regional proxy records. For example, the $\delta^{18}O_{mw}$ peak in the early LGI is of a similar age to the GI-1a isotope event in the Greenland ice core record. During Greenland Interstadial 1, ice core $\delta^{18}O$ values reach their peak in GI-1a (Figure 7.15d). Likewise, the highest $\delta^{18}O_{mw}$ peak in the LGI section of the Gully Cave record occurs in the early part of this climatic interval. This indicates that the $\delta^{18}O_{rt}$ data from Gully Cave provide an accurate record of the regional climatic shifts that occurred during the Lateglacial Interstadial.

The early interstadial peak at Gully Cave is followed by relatively depleted $\delta^{18}O_{mw}$ values. The mean July temperature record from the nearby site of Llanilid shows a similar warm peak followed by relatively cooler climatic conditions (Figure 7.15c). This suggests that the $\delta^{18}O_{rt}$ values from Gully Cave also accurately reflect the local temperature changes during the LGI.

The Hawes Water (Figure 7.15b) and NGRIP (Figure 7.15d) records show that additional climatic fluctuations occurred during the LGI and GI-1 intervals. The small peak in mean $\delta^{18}O_{mw}$ at ~13.3 ka in the Gully Cave record may correspond to event GI-1c. However, this small $\delta^{18}O_{mw}$ increase may alternatively result from the large variability in the $\delta^{18}O$ values of the small number of teeth (n = 5) that were analysed from this level within the cave (sample group 10).

Figure 7.15 *(overleaf): Comparison between the rodent isotope record from Gully Cave and regional proxy records for the Lateglacial and early Holocene. Grey dashed lines show the correlations between the records. The arrows in a and b highlight the common trend of isotopic depletion seen in both records. a) The record of mean $\delta^{18}O$ values of meteoric water for the* Microtus *teeth from Gully Cave, plotted according to the calibrated radiocarbon dates for each spit. For spits that did not correspond with a radiocarbon date, linear interpolation was used between dates from overlying and underlying spits. The error bars indicate the average ranges in the calibrated radiocarbon dates for the spits. b) The $\delta^{18}O$ record from lake carbonates at Hawes Water in northwest England. The Lateglacial and early Holocene records from Marshall et al. (2002) and Marshall et al. (2007), respectively, were stitched together. c) The Mutual Climatic Range temperature record from Llanilid in South Wales, which is based on coleopteran assemblages from a lake core (Walker et al., 2003). d) The NGRIP ice core record from Rasmussen et al. (2006). The Greenland climate events and British climatic intervals are also labelled.*

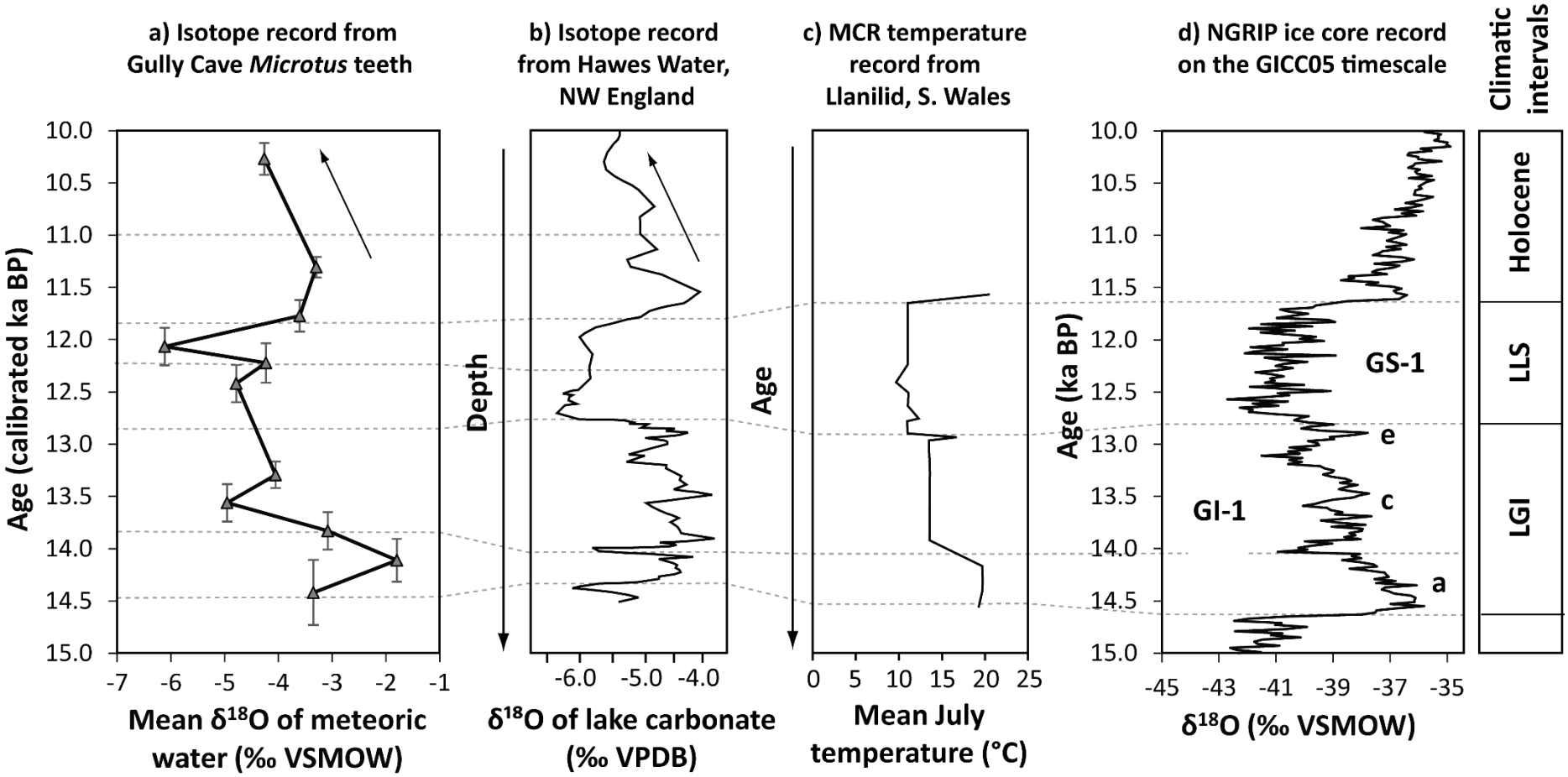
a) Isotope record from Gully Cave *Microtus* teeth
b) Isotope record from Hawes Water, NW England
c) MCR temperature record from Llanilid, S. Wales
d) NGRIP ice core record on the GICC05 timescale
Climatic intervals
Holocene
LLS
LGI
Age (calibrated ka BP)
Depth
Age
Age (ka BP)
GS-1
GI-1
e
c
a
Mean δ18O of meteoric water (‰ VSMOW)
δ18O of lake carbonate (‰ VPDB)
Mean July temperature (°C)
δ18O (‰ VSMOW)

All three regional records show an abrupt climatic decline at the end of the interstadial (Figures 7.15b-d). This is not observed in the $\delta^{18}O_{mw}$ data from Gully Cave. Nevertheless, the bipartite structure within the LLS is seen in both the Gully Cave and Hawes Water records. At Gully Cave, the $\delta^{18}O_{mw}$ values decline in the late LLS, whereas at Hawes Water, the $\delta^{18}O$ values of the lake carbonates increase. The $\delta^{18}O$ values of lake carbonates reflect both the temperature and $\delta^{18}O$ value of the water in which the carbonates precipitated (Leng & Marshall, 2004). Therefore, the increase in $\delta^{18}O$ values at Hawes Water suggests that the temperature and/or $\delta^{18}O_{mw}$ value increased in the late LLS. Since the $\delta^{18}O$ values of rodent teeth also reflect $\delta^{18}O_{mw}$ and temperature, the $\delta^{18}O_{mw}$ data from Gully Cave should also increase in the late LLS. The opposing trend observed in the Gully Cave data suggests that a localized or specific factor must have influenced the $\delta^{18}O$ values of the rodent teeth at this site. As discussed in the previous sections, this factor is likely to be the dominant season during which the rodent assemblages were accumulated by predators.

The abrupt increase in $\delta^{18}O_{mw}$ at ~11.7 ka is consistent with the onset of the Holocene (Figure 7.15). However, during the early Holocene, the trends in the British and NGRIP isotope records differ. At both Gully Cave and Hawes Water, the Lateglacial climatic stratigraphy is clearly recorded in the $\delta^{18}O$ values of the fossil carbonates. During the earliest Holocene, the $\delta^{18}O$ values of the rodent teeth and lake carbonates are enriched. Following this early peak, however, the $\delta^{18}O$ values in both records decline, reaching values that are consistent with those during the Loch Lomond Stadial. In contrast, the $\delta^{18}O$ values in the NGRIP record gradually increase through the early Holocene.

This early Holocene $\delta^{18}O$ depletion has also been recognised in other lake records from Britain (Candy et al., 2015), indicating that this isotopic shift is not a localized phenomenon. Candy et al. (2015) attribute this shift to a change in the seasonality of precipitation. Pollen records indicate that in the earliest Holocene, the climate in Western Europe was relatively continental (Davis et al., 2003). In continental areas, the amount of precipitation increases during the summer months, whereas in maritime climates, monthly precipitation amounts are relatively constant throughout the year (Darling, 2004). Therefore, under a continental climate, the mean annual $\delta^{18}O$ values

of surface water sources are likely to be biased towards the enriched $\delta^{18}O$ values of summer precipitation. Conversely, under a maritime precipitation regime, $\delta^{18}O_{mw}$ values will reflect the mean annual $\delta^{18}O$ of precipitation. Continental climatic conditions may consequently account for the relatively enriched $\delta^{18}O$ values in the Gully Cave and Hawes water records from the earliest Holocene. A continental climate may also explain the large ranges in the $\delta^{18}O$ values of the *Microtus* teeth from this interval. The subsequent $\delta^{18}O$ decline suggests a shift towards a more maritime climate, coincident with the progressive rise in sea level (Candy et al., 2015). The data from Gully Cave therefore support this hypothesis for a shift in the seasonality of precipitation during the early Holocene.

7.6.5. Summary

The $\delta^{18}O$ values of the rodent teeth from Gully Cave indicate that the sequence spans two warm intervals separated by a cold interval. The radiocarbon chronology for the site indicates these intervals approximately correspond with the Lateglacial Interstadial (warm), Loch Lomond Stadial (cold) and early Holocene (warm) climatic stages. The stratigraphic fluctuations in the $\delta^{18}O$ data from the *Arvicola* and *Microtus* teeth are comparable, indicating that both taxa record consistent climatic trends. However, the mean $\delta^{18}O$ values of the *Microtus* teeth are significantly enriched compared to the *Arvicola* teeth. This $\delta^{18}O_{rt}$ offset is attributed to the ecological differences between these taxa. The enriched $\delta^{18}O$ values of the *Microtus* teeth reflect the influence of glacial aridity on the $\delta^{18}O$ values of the water sources ingested by this taxon.

Despite this, the fluctuations in the mean $\delta^{18}O$ values of the *Microtus* and *Arvicola* teeth from Gully Cave are consistent with published proxy records spanning the Lateglacial to early Holocene period. This shows that while the absolute $\delta^{18}O$ values of the teeth may be offset, the stratigraphic changes in mean $\delta^{18}O_{rt}$ values provide a coherent record of the millennial-scale climatic fluctuations that occurred during this period. The $\delta^{13}C$ values of the teeth are also consistent with the temporal changes in the $\delta^{13}C$ value and concentration

of atmospheric CO_2. The consistent $\delta^{13}C$ offsets between the *Arvicola* and *Microtus* teeth may reflect ecological differences between these taxa.

The data also suggest that shifts in the seasonal accumulation of rodent assemblages have a key influence on mean $\delta^{18}O_{rt}$ values. During the Lateglacial Interstadial, late Loch Lomond Stadial and Holocene, the $\delta^{18}O_{rt}$ values are interpreted as reflecting the mean annual $\delta^{18}O$ of meteoric water. In contrast, relatively enriched $\delta^{18}O_{rt}$ values during the early Loch Lomond Stadial are thought to result from a summer bias in predation, caused by the presence of extensive snow cover under cold climatic conditions. The large ranges in $\delta^{18}O_{rt}$ values through the Gully Cave sequence additionally suggest that the climate was relatively continental during the Lateglacial and early Holocene period. The decline in $\delta^{18}O_{rt}$ values during the early Holocene may also relate to changes in the seasonality of precipitation.

In summary, the results from Gully Cave show that the $\delta^{18}O$ values of *Microtus* and *Arvicola* teeth can accurately record the pattern of millennial-scale climatic fluctuations between interstadial and stadial stages. However, caution should be taken when interpreting the absolute $\delta^{18}O$ values of rodent teeth in terms of the $\delta^{18}O$ of meteoric water and temperature. This is because a variety of factors can influence the mean $\delta^{18}O$ values of rodent teeth, and this is especially true for samples dating to glacial and stadial stages. These factors include changes in: 1) humidity, and thus the evaporation and $\delta^{18}O$-enrichment of the food and drinking water sources consumed by rodents, 2) the continentality of the climate and seasonality of precipitation, 3) the $\delta^{18}O$ value of the ocean moisture source, and 4) the degree of snow cover, which can affect the season in which the rodents are predominantly predated.

7.7. Discussion and Conclusions: Validity of using the $\delta^{18}O$ values of rodent teeth from caves for reconstructing millennial-scale climatic fluctuations

The results from Westbury Cave and Gully Cave have demonstrated that the mean $\delta^{18}O$ values of rodent teeth from stratified cave sequences can provide accurate records of millennial-scale climatic fluctuations. The patterns in the

$\delta^{18}O$ data at both sites are consistent with our understanding of the climatic changes that occurred during the intervals in which the cave sequences accumulated. The $\delta^{13}C$ data from Westbury Cave and the upper part of the Gully Cave sequence also show that the $\delta^{13}C$ values of rodent teeth from interglacial and stadial stages have the potential to provide valuable records of short-term climatic changes.

Nevertheless, this study has also shown that in order to interpret the isotope values of rodent teeth from caves, a clear understanding is required of the ecological, taphonomic and environmental contexts of the fossil assemblages from which the sampled teeth are derived. For example, the comparisons between the isotope and faunal records from Westbury Cave reveal that changes in the mean $\delta^{18}O_{rt}$ values through a stratigraphic sequence can differ from the expected shifts in climatic conditions between interglacial and stadial stages. This is largely due to changes in humidity and the seasonality of predation. The pattern of enriched mean $\delta^{18}O_{rt}$ values during the glacial and stadial stages is observed in both the Westbury Cave (MIS 13b and MIS 12) and Gully Cave (Loch Lomond Stadial) records. In the absence of the faunal record from Westbury Cave, and the chronology from Gully Cave, these enriched values may be erroneously interpreted as reflecting warm mean annual temperatures corresponding to an interglacial or interstadial stage. This shows that a summer bias in predation and increased aridity have major effects on the mean $\delta^{18}O$ values of rodent teeth from cold stages. These findings also illustrate that comparative ecological information from faunal assemblages is important for placing the isotope data within a broad-scale climatic context, especially if the cave sequence lacks a robust chronology.

Royer et al. (2013b) likewise emphasise that information on the taphonomy and taxonomy of the rodent remains, plus qualitative knowledge of the environmental context, are important for making valid climatic reconstructions from the mean $\delta^{18}O$ values of rodent teeth from caves. These workers also suggest that the variability in the $\delta^{18}O$ values of rodent teeth (and particularly *Microtus* teeth) within a stratigraphic unit can be used to infer changes in the seasonal range in temperatures. The large ranges in $\delta^{18}O$ values in units corresponding to the glacial stage at Westbury Cave, and the Lateglacial sequence at Gully Cave, are consistent with continental climatic

conditions during these intervals. However, shifts in the isotopic ranges may additionally be affected by changes in the species represented within the samples of rodent teeth. Therefore, climatic interpretations of the ranges in $\delta^{18}O_{rt}$ values should also take into account the taxonomy of the rodent assemblages.

In conclusion, the $\delta^{18}O$ values of rodent teeth from cave sequences can provide useful records of millennial-scale climatic fluctuations, provided that the taphonomic, ecological and environmental or chronological contexts are satisfactorily understood.

In the following chapter, the carbon isotope results from the modern and fossil rodent teeth are examined in further detail. The influences of environmental factors on changes in the $\delta^{13}C$ of C_3 vegetation during the Pleistocene and Holocene in Britain are assessed. Isotope results from late Holocene rodent teeth are also presented in order to evaluate the potential impacts of diagenesis and recent changes in atmospheric CO_2 on temporal differences in the $\delta^{13}C$ values of rodent teeth from Britain.

8. Assessing the influences of environmental factors on temporal variations in the $\delta^{13}C$ values of rodent teeth from Britain

8.1. Introduction

The overall aim of this chapter is to assess the influences of environmental factors on temporal variations in the $\delta^{13}C$ values of rodent dental carbonate ($\delta^{13}C_{rt}$) from Britain. To address this aim, the carbon isotope data that were initially presented in Chapters 5-7 are examined in further detail. This chapter begins by highlighting the significant offset that has been observed between the $\delta^{13}C$ values of the modern and fossil rodent teeth. This offset may result from variations in environmental factors such as atmospheric CO_2 and climate, or diagenetic alteration. The rationale behind the potential contributions of these factors to the variations in $\delta^{13}C_{rt}$ values is explained. The investigations used to assess the influences of these factors on the $\delta^{13}C_{rt}$ data from Britain are subsequently introduced.

The first of these investigations involved the analyses of rodent teeth from two Late Holocene archaeological sites: 1) Longstone Edge, Derbyshire, and 2) Danebury, Hampshire. These analyses were specifically undertaken in order to assess whether diagenesis may have contributed to the differences between the $\delta^{13}C$ values of the modern and fossil rodent teeth. If diagenesis has occurred, the $\delta^{18}O$ data from the fossil rodent teeth could be called into question. To address this, well-preserved rodent teeth were analysed in order to quantify the magnitude of the recent changes in $\delta^{13}C_{rt}$ values that result from factors other than diagenesis. The results of these analyses are presented in the second part of this chapter.

In the third part of the chapter, two published models are utilized in order to estimate the changes in the $\delta^{13}C$ values of C_3 plants over the past 14,500 years. The modelled shifts in the plant $\delta^{13}C$ values are compared with the measured shifts in the $\delta^{13}C$ values of the rodent teeth from Britain. These comparisons are used to interpret the temporal variations in $\delta^{13}C_{rt}$ values in terms of changes in rodent diet, the $\delta^{13}C$ and partial pressure of atmospheric CO_2, and mean annual precipitation. Finally, the variations in the $\delta^{13}C$ values of the rodent teeth from Britain are discussed in the context of previous research on the $\delta^{13}C$ values of Quaternary mammalian tissues.

8.2. Context

8.2.1. The $\delta^{13}C$ values of Quaternary rodent teeth from Britain

Thus far in this thesis, carbon isotope data have been presented for a large number of rodent teeth from Britain, including: 1) modern rodent teeth from owl pellets collected at four different sites (Chapter 5), 2) fossil rodent teeth from fluvial deposits at three different sites, corresponding to MIS 17/15 (West Runton), MIS 9 (Cudmore Grove), and MIS 7 (Marsworth), respectively (Chapter 6), and 3) fossil rodent teeth from two cave sites, corresponding to MIS 13-12 (Westbury Cave) and late MIS 2 to early MIS 1 (Gully Cave) (Chapter 7). The examination of these data reveals that the mean $\delta^{13}C$ values of the fossil *Microtus* and *Arvicola* teeth are significantly enriched compared to the mean $\delta^{13}C$ values of the modern *Microtus agrestis* teeth (Figure 8.1). As illustrated in Figure 8.1, this pattern of enrichment is consistent across all fossil rodent teeth, regardless of the rodent taxon being investigated, the age and depositional context of the study site, and the climatic conditions during the period of tooth formation. The mean $\delta^{13}C$ offsets between the fossil and modern teeth vary from around +5 to +10‰ (Table 8.1), and the overall mean offset is ~7‰. In addition, the $\delta^{13}C$ values of the modern teeth vary between -21.5 and -13.9‰, whereas the $\delta^{13}C$ values of the fossil teeth range from a minimum of -13.7‰ at Marsworth, to a maximum of -6.2‰ in the early Holocene levels at Gully Cave. There is, therefore, no overlap between the

measured $\delta^{13}C$ values of the modern and fossil teeth that have been investigated in this thesis so far (Figure 8.1).

The $\delta^{13}C$ values of the rodents' diets ($\delta^{13}C_d$), calculated from the $\delta^{13}C$ values of the fossil rodent teeth, also differ from the modern $\delta^{13}C$ values of C_3 plants (Figure 8.2). Since rodents in the genera *Arvicola* and *Microtus* are primarily herbivorous (Table 4.1), the $\delta^{13}C$ values of their teeth reflect variations in the $\delta^{13}C$ values of local plants. During the Quaternary period, vegetation in northwest Europe has consisted solely of C_3 plants (Collins & Jones, 1986; Rao et al., 2012). Therefore, for all rodent teeth analysed in this thesis, the $\delta^{13}C$ values of the diet should be consistent with the range in $\delta^{13}C$ values of C_3 plants. The $\delta^{13}C_d$ values for the modern teeth overlap with the $\delta^{13}C$ values of modern C_3 plants (Figure 8.2). Moreover, the modern mean $\delta^{13}C$ value of the diet (-28.9‰) is similar to the global mean $\delta^{13}C$ of C_3 plants (-28.5‰) (Figure 8.2). In contrast, the mean $\delta^{13}C_d$ value for the fossil rodent teeth (-22‰) is close to the maximum $\delta^{13}C$ of C_3 plants at the present day (-20‰). As a result, the maximum $\delta^{13}C_d$ value (-17.7‰) lies outside of the range in $\delta^{13}C$ values of modern C_3 plants (Figure 8.2).

These observations suggest that the $\delta^{13}C$ values of rodent teeth and C_3 plants in Britain underwent a significant shift, from relatively enriched values throughout the Middle and Late Pleistocene (MIS 17 to MIS 2) and early Holocene (MIS 1), to relatively depleted values at the present day. Figure 8.1 also shows that the mean $\delta^{13}C$ values of the rodent teeth underwent smaller fluctuations during the Pleistocene. In particular, the mean $\delta^{13}C_{rt}$ values for the interglacial stages (between -12.6 and -10.6‰) are ~3‰ more depleted than the mean $\delta^{13}C_{rt}$ values for the Lateglacial and early Holocene levels at Gully Cave (-9.7 to -7.7‰). The potential causes of these temporal changes in $\delta^{13}C$ values are outlined in the following section.

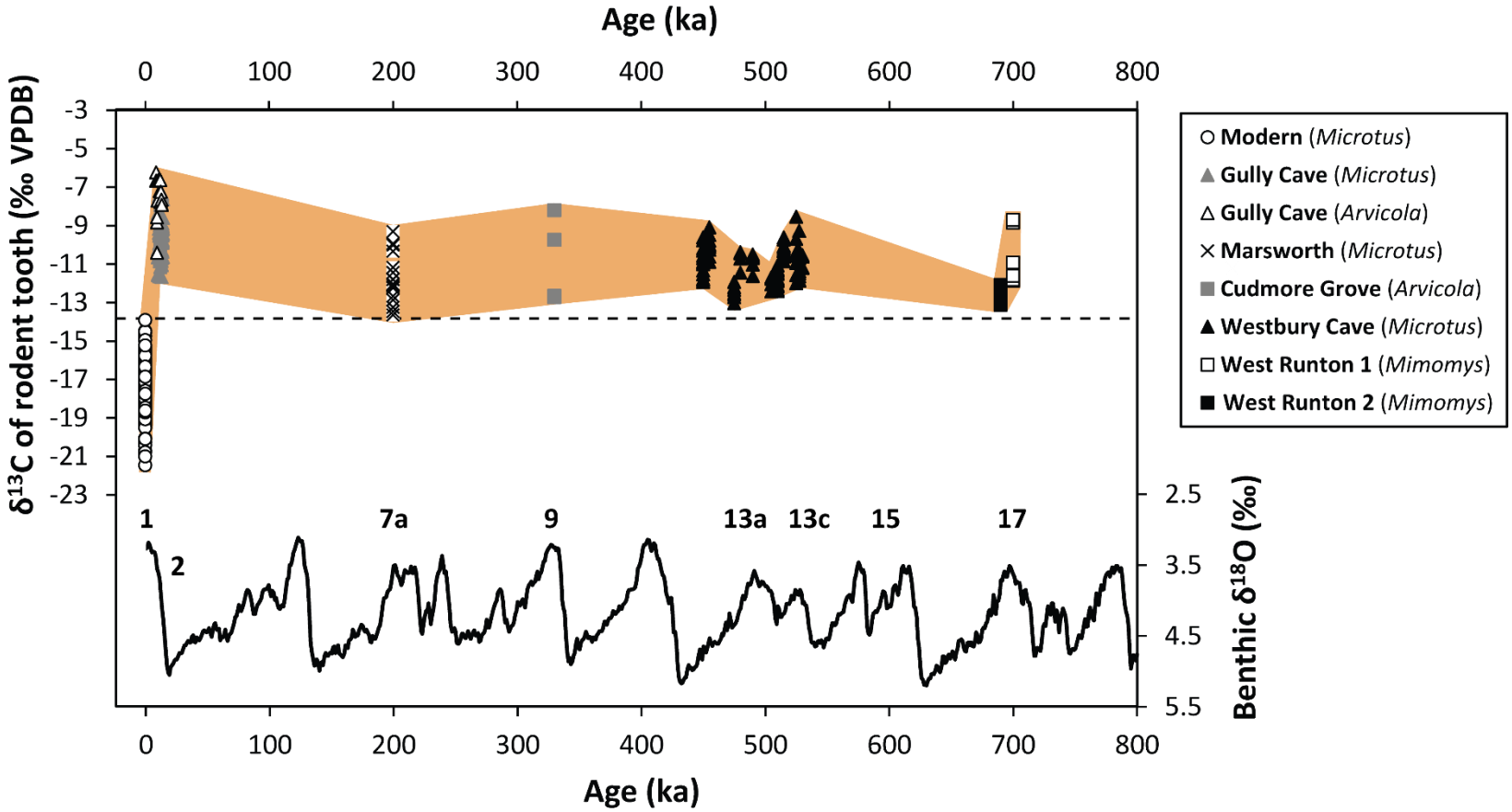

Figure 8.1: *Carbon isotope values of the rodent teeth from Britain (upper), shown against the marine benthic $\delta^{18}O$ record for the North Atlantic (lower) (Lisiecki & Raymo, 2009). The Marine Isotope Stages are labelled in bold. The dashed line marks the separation between the $\delta^{13}C$ values of the modern and fossil rodent teeth.*

Table 8.1: *Calculated offsets between 1) the mean $\delta^{13}C$ value of all of the sampled modern* M. agrestis *teeth from Britain ($\delta^{13}C_{modern}$), and 2) the mean $\delta^{13}C$ value of the fossil rodent teeth from each pre-modern study site investigated in this thesis ($\delta^{13}C_{fossil}$).*

Study site	Average $\delta^{13}C_{rt}$ difference from modern (‰) ($\delta^{13}C_{fossil} - \delta^{13}C_{modern}$)
Gully Cave (*Microtus*)	7.70
Gully Cave (*Arvicola*)	9.74
Marsworth	5.56
Cudmore Grove	6.55
Westbury Cave	6.39
West Runton (Sample 1)	6.55
West Runton (Sample 2)	4.76

8.2.2. Potential causes of temporal variations in tooth $\delta^{13}C$ values

The $\delta^{13}C$ values of C_3 plants ($\delta^{13}C_p$) are influenced by multiple environmental factors, including: 1) the $\delta^{13}C$ value of atmospheric CO_2 ($\delta^{13}C_a$), 2) the partial pressure of atmospheric CO_2 (pCO_2), 3) precipitation amount, 4) the canopy effect, and 5) temperature (see section 2.2.2). The temporal shifts in the $\delta^{13}C$ values of the rodent teeth from Britain (Figure 8.1) are therefore likely to reflect changes in these environmental factors. However, there has been much debate regarding the relative magnitude of the effect that each environmental factor has on $\delta^{13}C_p$ values. For example, Arens et al. (2000) suggest that > 90% of the variation in the $\delta^{13}C$ values of C_3 plants can be explained by changes in $\delta^{13}C_a$, while pCO_2 has no significant influence on $\delta^{13}C_p$ values. In contrast, Schubert & Jahren (2012; 2015) argue that once changes in the $\delta^{13}C$ value of atmospheric CO_2 have been accounted for, pCO_2 can be demonstrated as having a significant and quantifiable effect on the $\delta^{13}C$ values of C_3 plants.

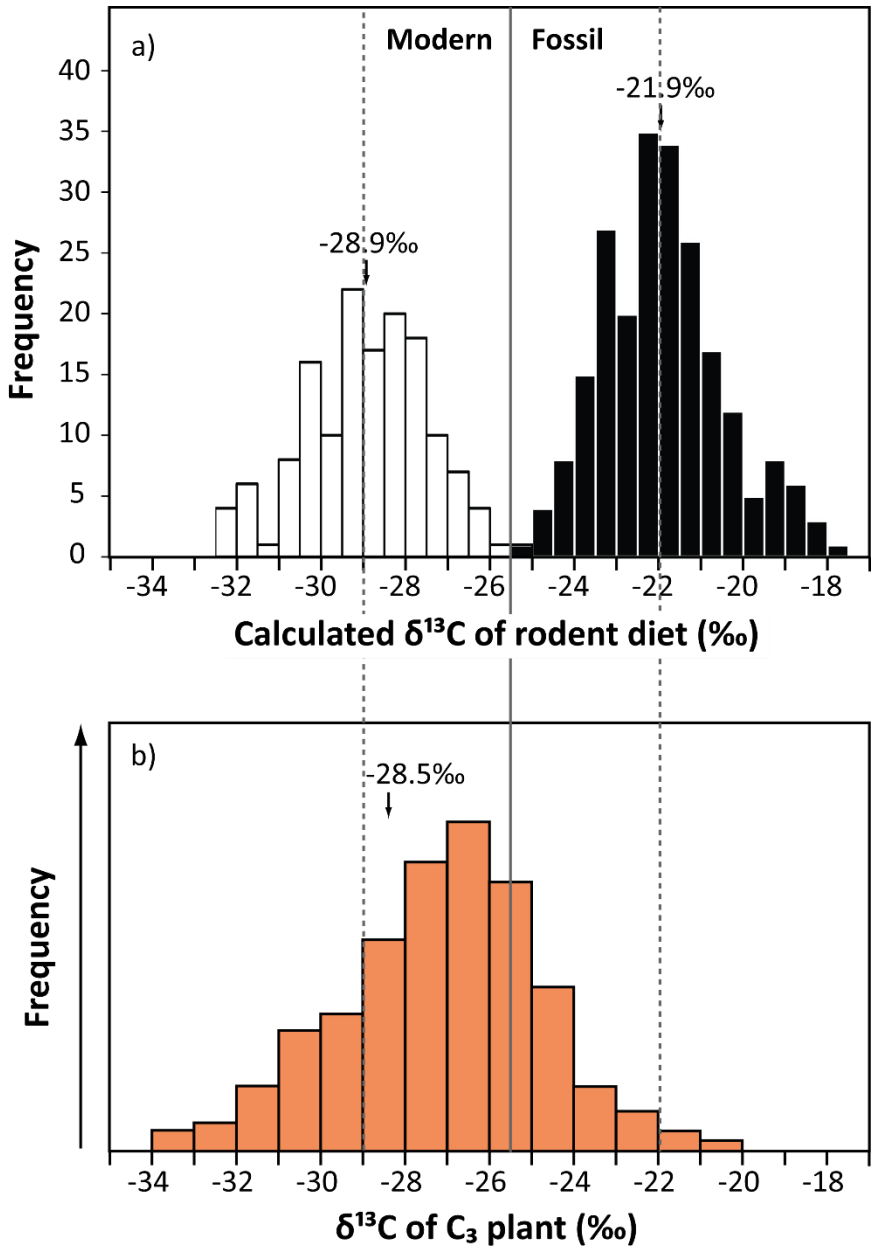

Figure 8.2: *a) Histograms showing the carbon isotope values of the modern and fossil rodents' diets, calculated from the $\delta^{13}C$ values of the rodent bioapatite from Britain, using an average bioapatite-diet offset of 11.5‰ (Passey et al., 2005). b) Measured $\delta^{13}C$ values of C_3 plants, corrected to a $\delta^{13}C$ value of atmospheric CO_2 of -8.0‰ (from Kohn, 2010). The mean $\delta^{13}C$ values are indicated with arrows and dashed lines. The division between the $\delta^{13}C$ values of the modern and fossil teeth is indicated with a grey solid line.*

Several studies have also suggested that variations in the $\delta^{13}C$ value and partial pressure of atmospheric CO_2 have had the greatest influences on the $\delta^{13}C$ values of C_3 plants during the Quaternary period (Krishnamurthy & Epstein, 1990; Richards & Hedges, 2003; Stevens & Hedges, 2004; Bump et al., 2007; Hare et al., 2018). An increase in $\delta^{13}C_a$ results in an increase in $\delta^{13}C_p$ (Arens et al., 2000; Jahren et al., 2008), whereas an increase in pCO_2 results in a decrease in $\delta^{13}C_p$ (Polley et al., 1993; Schubert & Jahren, 2012). In general, both $\delta^{13}C_a$ and pCO_2 are higher during warm stages than during cold stages (Figures 8.3 and 8.4), and thus the opposing effects of these variables on $\delta^{13}C_p$ values have the potential to cancel each other out. Nevertheless, the temporal shifts in $\delta^{13}C_a$ and pCO_2 often differ in magnitude (Figures 8.3 and 8.4). Relative differences in the $\delta^{13}C_a$ and pCO_2 changes are therefore likely to result in temporal variations in the $\delta^{13}C$ values of C_3 plants, and the tissues from mammals that consume C_3 plants.

The most notable change in atmospheric CO_2 over the last glacial-interglacial cycle has occurred within the past ~200 years, due to the anthropogenic burning of fossil fuels since the Industrial Revolution (Figures 8.3 and 8.4). This change involves a decrease in $\delta^{13}C_a$ of ~2‰ (Figure 8.3) and a rise in pCO_2 of ~120 ppm (Figure 8.4). These shifts in $\delta^{13}C_a$ and pCO_2 are of particular importance for understanding the $\delta^{13}C$ data from the British rodent teeth. A decrease in $\delta^{13}C_a$ and increase in pCO_2 will both result in a depletion in $\delta^{13}C_p$ values. Indeed, tree ring records from Britain show that plant $\delta^{13}C$ values have paralleled the trends in atmospheric CO_2 since 1850 AD (e.g. Young et al., 2012). The recent change in atmospheric CO_2 may, therefore, explain why the modern rodent teeth from Britain have significantly depleted $\delta^{13}C$ values compared to the fossil rodent teeth (Figure 8.1).

The ~3‰ difference between the $\delta^{13}C$ values of the rodent teeth from the interglacial stages and the Lateglacial period at Gully Cave (Figure 8.1) may also relate to changes in atmospheric CO_2. As shown in Figure 8.4, pCO_2 levels during the Lateglacial period (~11.7-14.5 ka BP) are lower than during the Holocene (< 11.7 ka BP). Lower pCO_2 levels cause a relative increase in $\delta^{13}C_p$ values (Schubert & Jahren, 2012). Therefore, the enriched $\delta^{13}C$ values of the teeth from Gully Cave might result from a reduction in pCO_2.

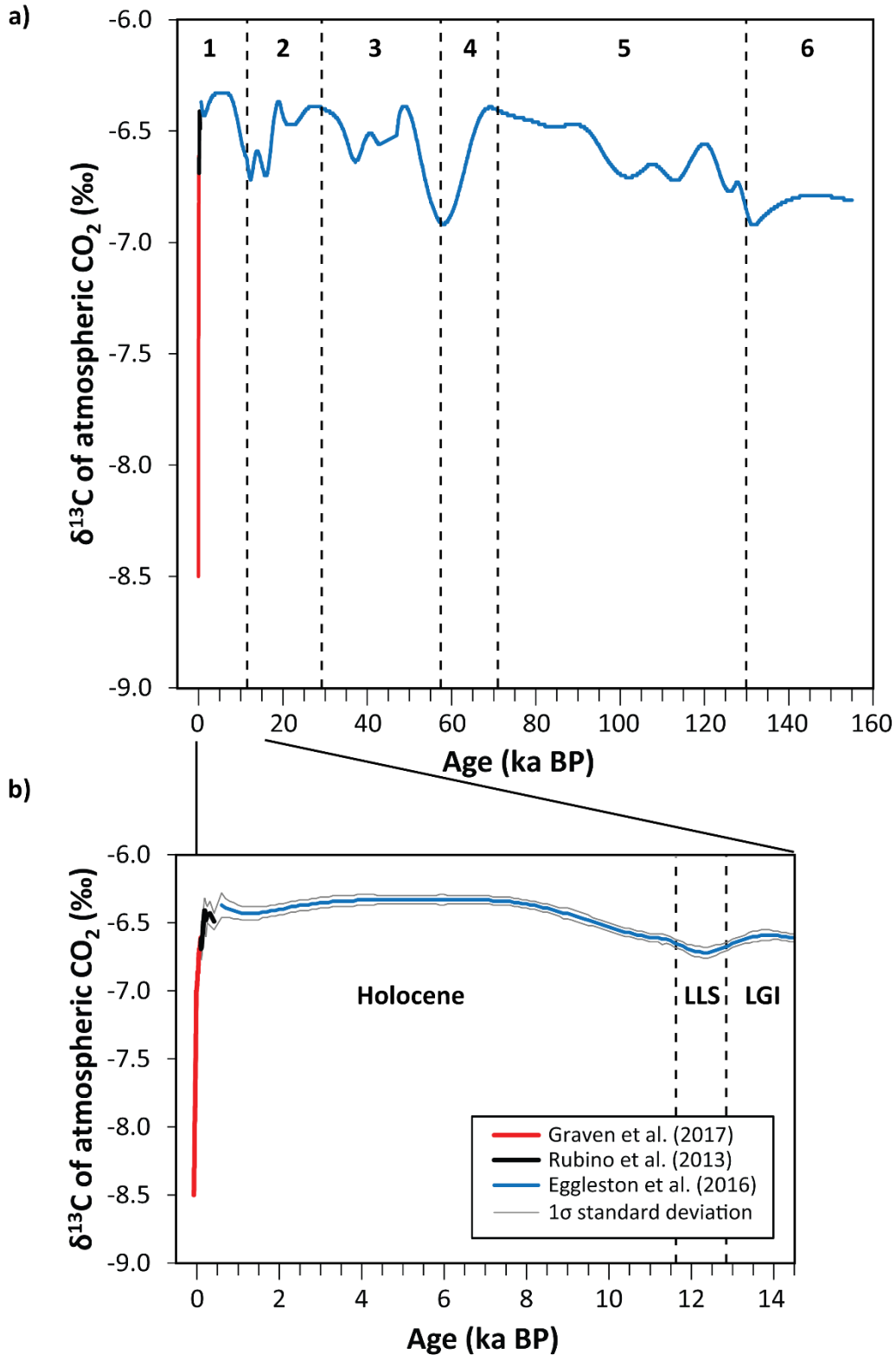

Figure 8.3: *Variations in the global mean $\delta^{13}C$ value of atmospheric CO_2 over the past 160 thousand years (a) and past 14.5 thousand years (b). The data are from recent flask measurements of atmospheric CO_2 (Graven et al., 2017) and Antarctic ice core records (Rubino et al., 2013; Eggleston et al., 2016). The Marine Isotope Stages are labelled in a, and climatic stages are labelled in b (LLS = Loch Lomond Stadial, LGI = Lateglacial Interstadial).*

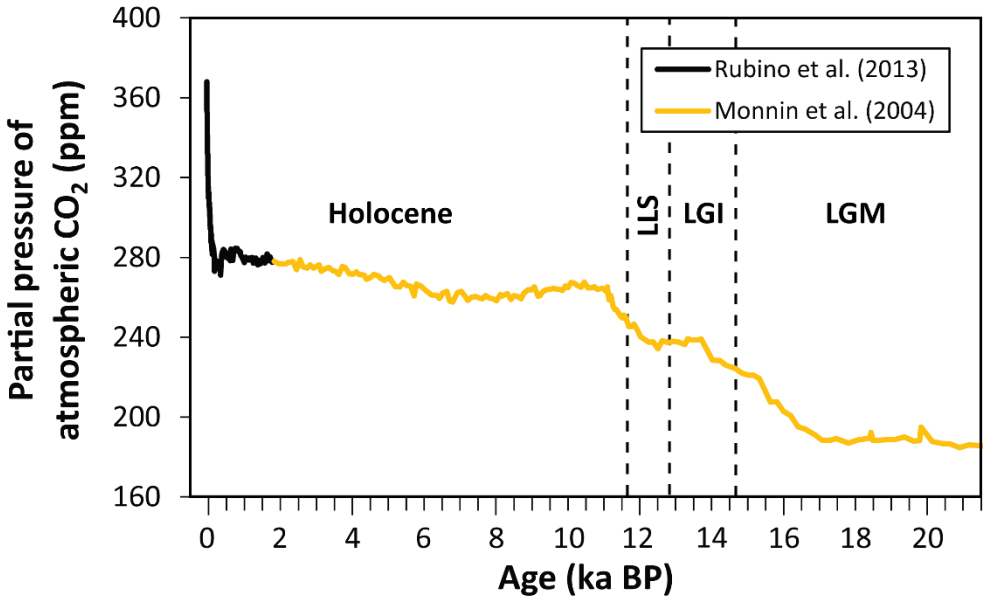

Figure 8.4: *Variations in the partial pressure of atmospheric CO_2 over the past 25 thousand years. The data are from Antarctic ice core records. LLS = Loch Lomond Stadial, LGI = Lateglacial Interstadial, LGM = Last Glacial Maximum.*

Nevertheless, Kohn (2016) disputes the influence of pCO_2 changes on $\delta^{13}C_p$ values, on the basis that: 1) changes in $\delta^{13}C_p$ values between the Last Glacial Maximum and Holocene are entirely explainable by changes in Mean Annual Precipitation (MAP), and 2) $\delta^{13}C_p$ values that have been corrected for changes in pCO_2 do not overlap with dietary $\delta^{13}C$ values calculated from fossil herbivore tissues. The $\delta^{13}C$ values of C_3 plants are negatively correlated with MAP (Diefendorf et al., 2010; Kohn, 2010; Rao et al., 2017), and thus a reduction in MAP could result in an increase in tooth $\delta^{13}C$ values. Proxy records from northwest Europe generally indicate that the climate during the Lateglacial period was fairly arid (Kasse, 2002; Birks & Birks, 2014). Consequently, the relatively enriched $\delta^{13}C$ values of the rodent teeth from Gully Cave may reflect a decrease in MAP, in addition to or instead of a decrease in pCO_2.

Temporal shifts in the $\delta^{13}C$ values of tissues from herbivorous mammals have additionally been attributed to changes in the dominance of the canopy effect (Drucker et al., 2008). The canopy effect results in a

depletion in the $\delta^{13}C$ values of understorey plants (Medina & Minchin, 1980; Schleser & Jayasekera, 1985). This effect is therefore likely to be greater during intervals with extensive woodland cover, than during intervals with limited tree cover. However, since members of the genus *Microtus* live in open grassland environments (Table 4.1), this effect is likely to have had a minimal impact of the $\delta^{13}C$ values of the *Microtus* teeth analysed in this thesis.

The final environmental factor, temperature, has received comparatively little attention within the published literature. Nevertheless, a few studies have shown that there is a significant negative correlation between the $\delta^{13}C$ values of modern C_3 plants and mean annual temperature (Körner et al., 1988; Körner et al., 1991; Rao et al., 2012). Consequently, the offset between the $\delta^{13}C$ values of the rodent teeth from the interglacial and glacial stages may, in part, be due to differences in temperature. Despite this, the correlation between $\delta^{13}C_p$ and temperature is relatively weak (r^2 = -0.38) compared to the correlation between $\delta^{13}C_p$ and MAP (r^2 = -0.68) (Rao et al., 2017). Therefore, changes in precipitation are likely to have had a greater influence on temporal variations in $\delta^{13}C_{rt}$ values than changes in temperature.

In addition to variations in environmental factors, the $\delta^{13}C$ values of fossil bioapatite may also be affected by diagenetic alteration. The isotopic values of bioapatite can be altered via various processes, including: 1) the incorporation of exogenous carbonates from the environment, and 2) the dissolution and re-mineralization of bioapatite following isotopic exchange with groundwater (Sponheimer & Lee-Thorp, 1999). Some of the fossil rodent teeth analysed in this thesis originate from sites underlain by marine carbonate bedrock. These sites include Gully Cave, Marsworth and Westbury Cave. In Britain, marine limestones have enriched $\delta^{13}C$ values of around +1 to +5‰ (Hudson, 1977; Jenkyns et al., 1994). The incorporation of marine carbonates may consequently have contributed to the enriched $\delta^{13}C$ values of the fossil teeth (Figure 8.1).

In summary, there are a variety of factors that may have contributed to the temporal variations in the $\delta^{13}C$ values of the rodent teeth from Britain. In order to evaluate the relative contribution of each factor to these variations, two requirements must be met. Firstly, isotope data must be obtained from fossil rodent teeth that have undergone negligible diagenetic alteration. Secondly, proxy records must be available in order to correct for temporal fluctuations in the key environmental variables. The two variables for which the highest resolution and most precise records are available are $\delta^{13}C_a$ and pCO_2 (Figures 8.3 and 8.4). The $\delta^{13}C_a$ record only spans the past ~160 ka (Figure 8.3), and thus corrections for this factor can only be made for rodent teeth that date within this period i.e. the Lateglacial and Holocene teeth. Based on these requirements, a series of research objectives have been devised for this chapter. These objectives are outlined in the next section.

8.2.3. Objectives of this chapter

In this chapter, the potential influences of environmental factors and diagenesis on the $\delta^{13}C$ values of the rodent teeth from Britain will be assessed via the following objectives:

1. Investigate how the $\delta^{13}C$ values of rodent teeth from Britain have changed during the Late Holocene.
2. Use published models of carbon isotope fractionation to estimate how the $\delta^{13}C$ values of C_3 plants have varied over the past 14,500 years.
3. Compare the estimated changes in the $\delta^{13}C$ values of C_3 plants with the shifts in the $\delta^{13}C$ values of the rodent teeth from Britain.
4. Correct the $\delta^{13}C$ values of the rodent teeth for temporal variations in atmospheric CO_2.
5. Evaluate the effect of precipitation changes on the $\delta^{13}C$ values of the rodent teeth.

Objective 1 has been addressed by undertaking isotopic analyses on rodent teeth from two Late Holocene archaeological sites: 1) Longstone Edge, Derbyshire (~4000 yr BP), and 2) Danebury, Hampshire (~ 2000 yr BP). These sites were chosen for several reasons. Firstly, both sites pre-date the recent shifts in atmospheric CO_2 (Figures 8.3b and 8.4). Furthermore, existing proxy records from northwest Europe indicate that mean temperatures and precipitation amounts at ~4000 and ~2000 yr BP were relatively comparable to the present day (Davis et al., 2003; Charman, 2010). Finally, due to their relatively recent age, the Late Holocene teeth are less likely to have experienced diagenetic alteration compared to the Pleistocene teeth. Therefore, any differences between the $\delta^{13}C$ values of the Late Holocene and modern teeth are likely to primarily result from the recent changes in $\delta^{13}C_a$ and pCO_2. This means that the data from the Late Holocene teeth can be used to examine and quantify the effect that the recent atmospheric shifts have had on $\delta^{13}C_{rt}$ values.

For Objective 2, $\delta^{13}C_p$ values were calculated for the past 14,500 years, because this is the period that encompasses the teeth from Gully Cave, Longstone Edge, Danebury, and the modern sites. The selected models account for temporal changes in the $\delta^{13}C$ value and partial pressure of atmospheric CO_2. Comparing the magnitudes of the modelled shifts in $\delta^{13}C_p$ values, with the shifts in the $\delta^{13}C$ values of the rodent teeth from Britain, therefore enables the responses of the $\delta^{13}C_{rt}$ values to atmospheric changes to be assessed (Objective 3). The shifts in the $\delta^{13}C_p$ values can then be subtracted from the shifts in the $\delta^{13}C_{rt}$ data (Objective 4), to enable the residual $\delta^{13}C_{rt}$ changes to be determined. These residual changes can be used to evaluate the contribution of precipitation to the temporal variations in the $\delta^{13}C$ values of the rodent teeth (Objective 5). The following section outlines the materials and methods that were used to address these objectives.

8.3. Materials and Methods

8.3.1. Late Holocene teeth

8.3.1.1. Longstone Edge, Derbyshire

Ten *Microtus agrestis* upper right first molars, ten *Arvicola terrestris* upper right first molars, and three *A. terrestris* mandibles with *in situ* teeth were provided by Historic England at Fort Cumberland, Portsmouth, for this research. All of the specimens originate from sample 5094.2 in sample context 1060, which corresponds to the layer of firm clayey silt at the base of the central cist grave within Barrow 1 at Longstone Edge (Last, 2014). Specimens were specifically chosen from this sample context for three reasons. Firstly, *Microtus* and *Arvicola* teeth are highly abundant within the cist grave deposits (Andrews & Fernandez-Jalvo, 2012). Secondly, the sediments of context 1060 are relatively well-consolidated, and occur at the base of the cist grave (Last, 2014). Therefore, these deposits, and the rodent teeth contained within them, are less likely to have experienced post-depositional disturbance compared to the overlying deposits. Finally, context 1060 is associated with two human skeletons that have been radiocarbon dated to between 4239 and 3927 calibrated years BP (cal yr BP). Consequently, the chronology of the cist grave deposits is relatively well established.

Despite this, bioturbation plus the recent fissuring of the Barrow 1 mound (Last, 2014) may have led to the mixing of the deposits within the cist grave, and the intrusion of younger material from the overlying mound deposits. To assess whether this has occurred, the three *A. terrestris* mandibles (Table 8.2) were submitted to the Oxford Radiocarbon Accelerator Unit for radiocarbon dating. The largest mandibles with *in situ* teeth were preferentially selected in order to: 1) ensure that sufficient bone collagen was available for radiocarbon dating, and 2) enable the isotope values of the *in situ* teeth to be compared with the isotope values of the *A. terrestris* upper first molars. Carbon isotope analyses were also undertaken on the bone collagen from the mandibles, enabling the $\delta^{13}C$ offset between the tooth bioapatite and bone collagen to be calculated.

Upper first molars (M^1) belonging to the species *Microtus agrestis* and *Arvicola terrestris* were also selected from Longstone Edge. These teeth were chosen because analyses have been undertaken on *M. agrestis* M^1 from the modern sites, and *Microtus* M^1 and *Arvicola* incisors from Gully Cave. The results of the modern study in Chapter 5 demonstrate that there are often significant and consistent offsets between the $\delta^{13}C$ values of different tooth types (first molars, second molars, third molars and incisors). Previous studies have also shown that in modern rodent communities, statistically significant differences occur between the mean $\delta^{13}C$ values of *M. agrestis* and *A. terrestris* teeth (Gehler et al., 2012). Therefore, when assessing the influences of environmental variables on temporal differences in the $\delta^{13}C$ values of rodent teeth, comparisons should be made between teeth of the same type and taxon. The *Microtus* and *Arvicola* M^1 from Longstone Edge were selected for this purpose.

Table 8.2: *Descriptions of the* Arvicola terrestris *mandibles from Longstone Edge that were selected for radiocarbon dating and isotopic analyses.*

Specimen code	**Element type**	***In situ* teeth**
LE-At-MA1	Right mandible	M_1, M_2 and incisor
LE-At-MA2	Left mandible	M_1, M_2 and incisor
LE-At-MA3	Right mandible	Incisor

8.3.1.2. Danebury, Hampshire

Ten *Microtus agrestis* upper left first molars from Danebury were provided by the Hampshire Cultural Trust for this study. Five teeth were selected from each of two pits: 1) Pit 923, and 2) Pit 955. These pits were chosen because they are two of only a small number of pits at the site from which relatively large numbers of *M. agrestis* individuals have been recovered (Coy, 1982). However, the chronologies for these pits are relatively poor. Both pits contain

few diagnostic or datable pottery sherds, and the few sherds that are identifiable do not occur in all sedimentary layers within the pits (Cunliffe, 1995). The five teeth from Pit 923 originate from sedimentary layer 6. Layer 3 within this pit has been tentatively assigned to ceramic phase 3 (2420-2310 yr BP), although is more likely to date to ceramic phase 7 (2200-2000 yr BP) (Cunliffe, 1995). Therefore, layer 6 in Pit 923 likely dates to the latter occupation phases of the Iron Age hillfort at Danebury (~2200-1900 yr BP). The five teeth from Pit 955 originate from layer 3, which has likewise been assigned to ceramic phase 7 (Cunliffe, 1995). Therefore, all of the teeth selected from Danebury likely date to between 2200 and 1900 yr BP.

8.3.2. Analytical methods

The oxygen and carbon isotope ratios of the rodent teeth from Longstone Edge and Danebury were analysed at the Bloomsbury Environmental Isotope Facility. The three *A. terrestris* mandibles were pre-treated according to the methods of Brock et al. (2010), graphitized, and dated by Accelerator Mass Spectrometry (Bronk Ramsey et al., 2004). Following purification for radiocarbon dating, the carbon ($\delta^{13}C$) and nitrogen ($\delta^{15}N$) isotope ratios of the bone collagen were also analysed.

8.3.3. Descriptive statistics

Basic descriptive statistics (mean, range etc.) were calculated for the $\delta^{18}O$ and $\delta^{13}C$ data from Longstone Edge and Danebury. T-tests were also used to assess whether the mean isotope values of the isolated and *in situ* teeth from Longstone Edge, and the teeth from the two pits at Danebury, are statistically different at 95% confidence. T-tests were chosen because the $\delta^{18}O$ and $\delta^{13}C$ data from both sites are normally distributed (Shapiro-Wilk tests, $p > 0.05$). All statistical tests were performed using PAST version 3.11 (Hammer et al., 2001).

8.3.4. Comparing the $\delta^{13}C$ values of the modern and Late Holocene teeth

To address Objective 1, the $\delta^{13}C$ values of the teeth from Longstone Edge and Danebury will be compared with the $\delta^{13}C$ values of the modern teeth. The comparisons will be restricted to the *Microtus agrestis* first molars, in order to eliminate any differences resulting from inter-species and inter-tooth isotopic offsets. The $\delta^{13}C$ values of C_3 plants and rodent teeth are also likely to differ between the study sites due to spatial variations in temperature and precipitation across Britain (see Section 3.2). Therefore, the measured $\delta^{13}C_{rt}$ values were adjusted for inter-site differences in latitude, altitude and mean annual precipitation, after the methods of Hare et al. (2018). The $\delta^{13}C$ values were adjusted to a latitude of 51.2°, an altitude of 100 m, and a MAP of 800 mm/yr. These values were chosen because they are similar to the geographical characteristics of Somerset at the present day (see Table 3.1). Adjustments were made to the conditions in Somerset in order to enable the $\delta^{13}C$ values of the modern and Late Holocene teeth to be compared with the $\delta^{13}C$ values of the teeth from Gully Cave in Somerset. The adjusted $\delta^{13}C$ values ($\delta^{13}C_{adj}$) were calculated using the following equations (Hare et al., 2018):

$$\delta^{13}C_{adj} = \delta^{13}C + \delta' \quad (8.1)$$

$$\delta' = \delta_{alt} + \delta_{MAP} + \delta_{lat} \quad (8.2)$$

where δ_{alt} is the adjustment for altitude (m), δ_{MAP} is the adjustment for Mean Annual Precipitation (mm/yr), and δ_{lat} is the adjustment for latitude (degrees). These adjustments were quantified using the equations below, which are adapted from Equation 1 in Kohn (2010):

$$\delta_{alt} = 0.00019 \times [100 - \text{altitude (m)}] \quad (8.3)$$

$$\delta_{MAP} = [-5.61 \times \log_{10} (800 + 300)] - [-5.61 \times \log_{10} (MAP + 300)] \quad (8.4)$$

$$\delta_{lat} = (-0.0124 \times 51.2) - (-0.0124 \times \text{latitude}) \quad (8.5).$$

The altitude, MAP, and latitude values for the modern and Late Holocene sites are shown in Table 3.1. Quantitative MAP data for Britain at ~4000 and ~2000 yr BP are not currently available. Therefore, the present-day MAP values at Longstone Edge and Danebury were used, based on the assumption that past climatic conditions at these sites were approximately comparable to today.

8.3.5. Modelling temporal changes in the $\delta^{13}C$ values of C_3 plants

The methods used for calculating temporal variations in the $\delta^{13}C$ values of C_3 plants have been adapted from the methods used in the study by Hare et al. (2018). This study examined how changes in $\delta^{13}C_a$, pCO_2 and MAP between the Last Glacial Maximum and Holocene influenced the $\delta^{13}C$ values of C_3 plants and faunal collagen from the Northern Hemisphere. Hare et al. (2018) used four different models to estimate the temporal changes in $\delta^{13}C_p$ values. The first model is that of Farquhar et al. (1982). As discussed in Section 2.2.2.1, this model describes carbon isotope fractionation during C_3 photosynthesis as a function of both the $\delta^{13}C$ value and partial pressure of atmospheric CO_2:

$$\delta^{13}C_p = \delta^{13}C_a - a - (b - a) \times C_i/C_a \quad (8.6).$$

In this model, the ratio of pCO_2 in the intercellular air spaces relative to the atmosphere (C_i/C_a) was assumed to be constant (Hare et al., 2018). The second (Voelker-2016a) and third (Voelker-2016g) models are adapted versions of Equation 8.6, whereby the C_i/C_a ratio is assumed to vary linearly with the pCO_2 of the atmosphere (C_a). These two models differ in that the C_i/C_a ratio is calculated specifically for angiosperms and gymnosperms, respectively (Voelker et al., 2016). The final model (SJ-2012) is a hyperbolic correlation between the $\delta^{13}C$ discrimination in C_3 plants ($\Delta^{13}C_p$) and pCO_2 in parts per million by volume (ppmv) (Schubert & Jahren, 2012):

$$\Delta^{13}C_p = \frac{28.26 \times 0.21 \times (pCO_2 + 25)}{28.26 + [0.21 \times (pCO_2 + 25)]} \quad (8.7).$$

This equation is based on the results of growth experiments undertaken on two angiosperm taxa (Schubert & Jahren, 2012). The $\delta^{13}C$ discrimination reflects the fractionation between the $\delta^{13}C$ of a plant and the $\delta^{13}C$ of atmospheric CO_2, and is defined by the following equation (Farquhar & Richards, 1984):

$$\Delta^{13}C_p = \frac{1000 \times (\delta^{13}C_a - \delta^{13}C_p)}{\delta^{13}C_p + 1000} \quad (8.8).$$

Re-arranging Equation 8.8 enables the calculation of plant $\delta^{13}C$ values:

$$\delta^{13}C_p = \frac{1000 \times (\delta^{13}C_a - \Delta^{13}C_p)}{\Delta^{13}C_p + 1000} \quad (8.9).$$

By using Equations 8.7 and 8.9 in combination, changes in $\delta^{13}C_p$ values due to variations in pCO_2 (Equation 8.7) and $\delta^{13}C_a$ (Equation 8.9) can therefore be estimated.

Since members of the genera *Microtus* and *Arvicola* mainly feed on angiosperms such as grasses and sedges (Table 4.1), the Voelker-2016a and SJ-2012 models were considered the most appropriate for estimating temporal shifts in the $\delta^{13}C$ values of C_3 plants for this chapter. The atmospheric CO_2 data for these models were derived from the published literature. The globally-averaged $\delta^{13}C_a$ data, illustrated in Figure 8.3b, originate from published compilations of recent flask measurements of atmospheric CO_2 (1978-2015 AD), plus measurements of trapped CO_2 within Antarctic ice cores (> 1978 AD) (Rubino et al., 2013; Eggleston et al., 2016a,b; Graven et al., 2017). The $\delta^{13}C_a$ values for 2015-2018 were estimated using an average annual rate of $\delta^{13}C$ depletion of 0.02‰ (Keeling et al., 2005). The atmospheric pCO_2 data were obtained from published Antarctic ice core datasets (Monnin

et al., 2004a,b; Rubino et al., 2013), shown in Figure 8.4. Repeat measurements for each year were averaged. The pCO_2 level for the present day was estimated at 408 ppm, based on recent atmospheric measurements (NOAA, 2018).

In the Voelker-2016a model, the value of *a* in Equation 8.6 is 4.4‰ (O'Leary, 1981; Farquhar et al., 1982). This constant represents the isotopic fractionation caused by the diffusion of CO_2 through air. Constant *b* represents the average isotopic fractionation during carbon fixation. This fractionation has been shown to vary between -27 and -30‰ (Wong et al., 1979; O'Leary, 1981; O'Leary, 1988). Nevertheless, Schubert & Jahren (2012) argue that the minimum likely value for this fractionation factor is 28.3‰. This value was consequently used in this chapter. The C_i/C_a ratio was calculated using the following equation derived for angiosperms (Voelker et al., 2016):

$$C_i/C_a = (0.00031 \times C_a) + 0.649 \quad (8.10)$$

where C_a is the pCO_2 of the atmosphere in ppmv.

The $\delta^{13}C_p$ values calculated using the Voelker-2016a and SJ-2012 models are assumed to broadly reflect the average $\delta^{13}C$ values of C_3 plants. Nevertheless, the $\delta^{13}C$ values of plants within modern C_3 ecosystems also vary across a range of around 15‰, with a 1σ standard deviation of 1.62‰ (Figure 8.2b) (Kohn, 2010). Therefore, uncertainties on the average $\delta^{13}C_p$ values were approximated by adding this standard deviation to the 1σ analytical errors on the $\delta^{13}C_a$ and pCO_2 measurement data. The $\delta^{13}C_a$ and pCO_2 datasets, and the $\delta^{13}C_p$ values calculated using the two models, are listed in Appendix F.

8.3.6. Comparing the $\delta^{13}C$ values of the rodent teeth with the modelled $\delta^{13}C$ values of C_3 plants

In order to compare the $\delta^{13}C$ values of the rodent tissues with the modelled $\delta^{13}C$ values of C_3 plants, the rodent tooth and collagen data were converted to dietary $\delta^{13}C$ values. An enrichment factor ($\varepsilon_{apatite\text{-}diet}$) of +11.5 ± 0.15‰, measured in modern prairie voles (*Microtus ochrogaster*) (Passey et al., 2005),

was used to calculate $\delta^{13}C_d$ values from the rodent tooth data. The bone collagen $\delta^{13}C$ values from Longstone Edge were also converted to $\delta^{13}C_d$ values using an enrichment factor ($\varepsilon_{collagen\text{-}diet}$) of 3.9 ± 0.6‰, measured in modern mice and rats fed on a pure C_3 diet (DeNiro & Epstein, 1978; Deniro & Epstein, 1981; Ambrose & Norr, 1993; Tieszen & Fagre, 1993; Jim et al., 2004). For each site, the uncertainties in the enrichment factors were added to and subtracted from the maximum and minimum $\delta^{13}C_d$ values, in order to determine the maximum range in the $\delta^{13}C$ of the diet.

In Section 8.5, the mean calculated $\delta^{13}C_d$ values for the teeth from the modern sites, Danebury, Longstone Edge and Gully Cave are compared with the modelled $\delta^{13}C_p$ values. The similarities between the $\delta^{13}C$ values of the diet and the modelled $\delta^{13}C$ values of C_3 plants are assessed. The magnitudes of the temporal variations in $\delta^{13}C_p$ and $\delta^{13}C_d$ values are also compared. Finally, the shifts in the $\delta^{13}C_p$ values are subtracted from the shifts in the dietary $\delta^{13}C$ values, to evaluate the residual changes that are not explainable by variations in atmospheric CO_2. These residual shifts are discussed in the context of changes in mean annual precipitation.

8.4. Results: Late Holocene teeth

8.4.1. Longstone Edge, Derbyshire

8.4.1.1. Radiocarbon dates and $\delta^{13}C$ of bone collagen

The radiocarbon dates and isotopic results for the bone collagen from the three *A. terrestris* mandibles are shown in Table 8.3. The C/N ratios for the mandibles (3.2) fall within the range of values that are thought to indicate good collagen preservation (2.9-3.6) (Deniro, 1985). The $\delta^{13}C$ values of the bone collagen consistently lie between -23 and -22‰, although the $\delta^{13}C$ value for the left mandible (MA2) is slightly depleted compared to the $\delta^{13}C$ values of the right mandibles (MA1 and MA3).

The radiocarbon dates also differ between the mandibles. The calibrated dates for MA1 and MA3 are similar at around 4000 cal yr BP. In contrast, the date for MA2 is ~1400 years younger, at between 2725 and 2489

cal yr BP. This suggests that the left mandible originated from younger deposits within the Barrow 1 mound.

Figure 8.5 compares the dates for the *A. terrestris* mandibles with the published dates for 1) the human skeletons from the cist grave, and 2) the food vessel cremation from the base of the barrow mound. This figure shows that MA1 and MA3 are of a similar age to the cist grave skeletons and food vessel. Due to their position within the cist grave deposits, these mandibles likely post-date the placement of the skeletons within the grave, and pre-date the construction of the overlying mound, which is thought to have begun following the deposition of the food vessel cremation. This interpretation is not inconsistent with the dating evidence (Figure 8.5). In contrast, MA2 post-dates the start of the mound construction by ~1250-1480 years. This suggests that this mandible is intrusive within the grave deposits. There is, therefore, a possibility that some of the selected *A. terrestris* and *M. agrestis* upper molars also post-date the construction of the mound. As a result, the isotope values of the teeth may vary depending on the periods during which the teeth formed.

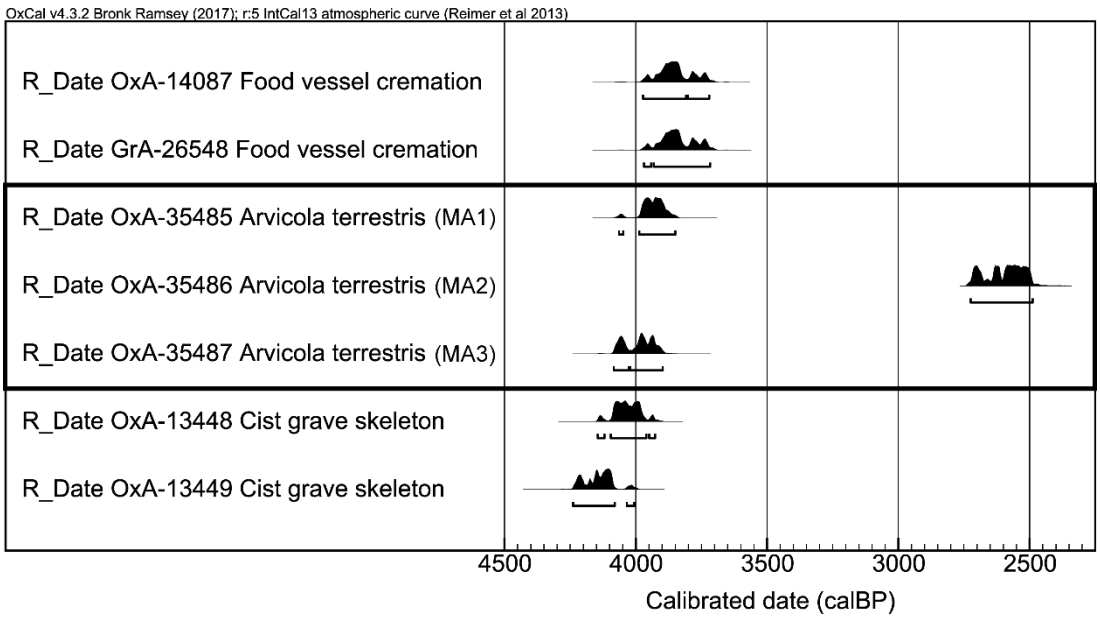

Figure 8.5: *Calibrated radiocarbon dates for the* Arvicola terrestris *mandibles (highlighted with a black box), the human skeletons from the cist grave, and food vessel cremation from the base of the cist grave at Longstone Edge. The dates for the human skeletons and food vessel are from Marshall et al. (2014).*

Table 8.3: *Radiocarbon dating and isotopic results for the bone collagen from the three* Arvicola terrestris *mandibles from Longstone Edge, Derbyshire. The calibrated dates are shown in years before AD 1950 (BP), and in years BC for comparison.*

Lab number	Sample code	Sample material	C/N ratio	$\delta^{13}C$ of collagen (‰ VPDB)	$\delta^{15}N$ (‰)	Radiocarbon age (yr BP) ± Error	Calibrated date range (95% confidence)		Posterior density estimate (95% probability)
							cal yr BC	cal yr BP	cal yr BP
OxA-35485	LE-At-MA1	*Arvicola terrestris* right mandible	3.2	-22.3 ± 0.2	3.5 ± 0.3	3622 ± 27	2115–1901	4064–3850	3987–3850 (92.5%) 4064–4048 (2.9%)
OxA-35486	LE-At-MA2	*Arvicola terrestris* left mandible	3.2	-22.8 ± 0.2	4.5 ± 0.3	2499 ± 25	776–540	2725–2489	-
OxA-35487	LE-At-MA3	*Arvicola terrestris* right mandible	3.2	-22.1 ± 0.2	2.7 ± 0.3	3658 ± 27	2135–1949	4084–3898	4022–3898 (64.7%) 4084–4027 (30.7%)

8.4.1.2. $\delta^{18}O$ of teeth

The $\delta^{18}O$ values of the teeth from Longstone Edge span a range of 4.4‰, from -8.8‰ to -4.4‰ (Figure 8.6). The *in situ* incisors from mandibles MA2 and MA3 have similar $\delta^{18}O$ values of around -5.7‰. The $\delta^{18}O$ values of the first and second molars from MA2 are also similar at around -6.5‰. In contrast, the mean $\delta^{18}O$ value of the teeth from MA1 (-4.47‰) is significantly enriched compared to the teeth from MA2 (-6.27‰) (T-test, $p < 0.05$).

The mean $\delta^{18}O$ value for all of the mandibular teeth (-5.42‰) is also significantly enriched compared to the mean $\delta^{18}O$ value of the ten *A. terrestris* upper first molars (-7.44‰) (T-test, $p < 0.01$). The $\delta^{18}O$ values of these molars vary between -8.8 and -6.5‰ (range = 2.2‰). The $\delta^{18}O$ values of the ten *Microtus agrestis* M^1 span a broader range of 3.2‰, between -7.6 and -4.4‰. The mean $\delta^{18}O$ value of the *Microtus* M^1 is -6.26‰, and is significantly enriched compared to the mean value of the *Arvicola* M^1 (T-test, $p < 0.01$).

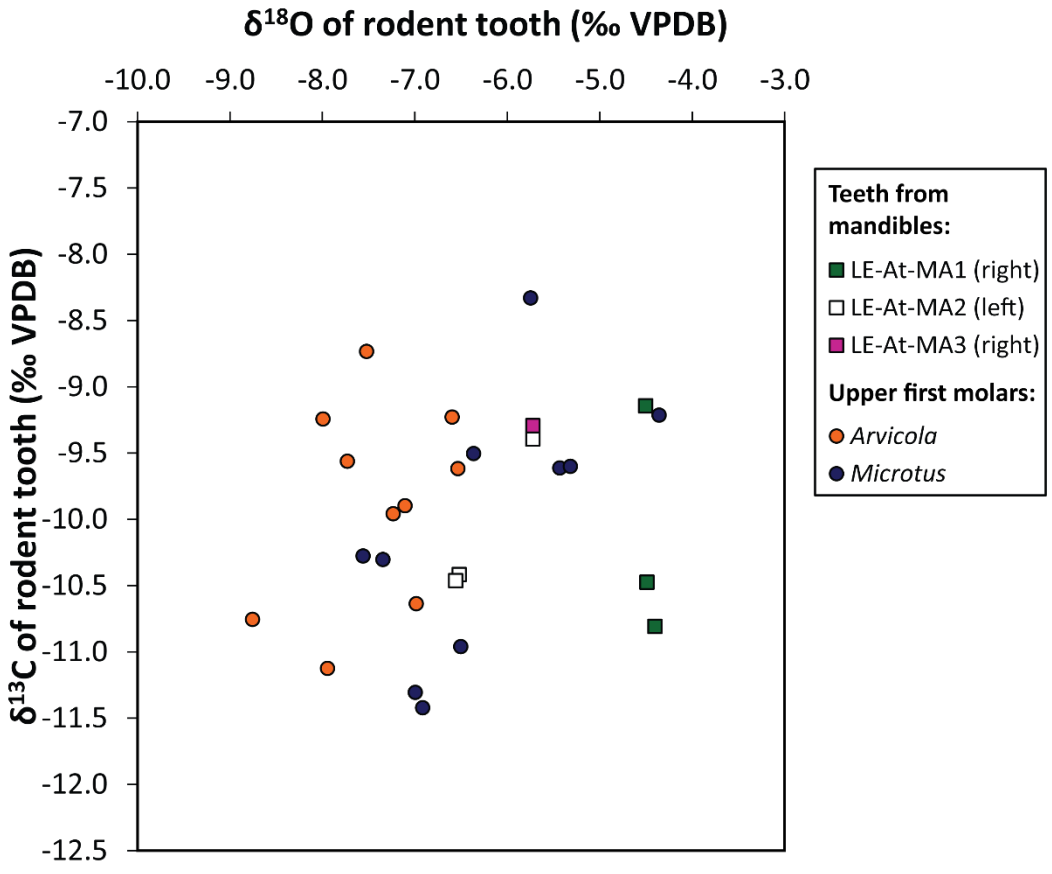

Figure 8.6: *Oxygen and carbon isotope results for the rodent teeth from Longstone Edge.*

8.4.1.3. $\delta^{13}C$ of teeth

The $\delta^{13}C$ values of the teeth from Longstone Edge vary from -11.4 to -8.3‰ (range = 3.1‰) (Figure 8.6). There is no statistically significant difference between the mean $\delta^{13}C$ values of the teeth from MA1 (-10.14‰) and MA2 (-10.09‰) (T-test, $p > 0.05$). Thus, despite the differences in the ages of these mandibles, their $\delta^{13}C_{rt}$ values are comparable. The $\delta^{13}C$ value of the incisor from MA3 is also similar to the $\delta^{13}C$ values of the incisors from MA1 and MA2. In both MA1 and MA2, the $\delta^{13}C$ value of the incisor is enriched compared to the first molar, and the $\delta^{13}C$ value of the first molar is enriched relative to the second molar. The mean $\delta^{13}C$ offsets between the tooth bioapatite and bone collagen from the three *A. terrestris* mandibles fall between 12 and 13‰ (Table 8.4).

The $\delta^{13}C$ values of the *A. terrestris* M^1 range from -11.1 to -8.7‰ (range = 2.4‰), with a mean value of -9.88‰. There is no statistically significant difference between the mean $\delta^{13}C$ of the *A. terrestris* M^1 and the mean $\delta^{13}C$ of the mandibular teeth (-9.95‰) (T-test, $p > 0.05$). The mean $\delta^{13}C$ of the *Arvicola* M^1 is also not statistically different from the mean $\delta^{13}C$ of the *Microtus* M^1 (T-test, $p > 0.05$). The $\delta^{13}C$ values of the *M. agrestis* M^1 vary between -11.4 and -8.3‰ (range = 3.1‰), with a mean value of -10.05‰.

Table 8.4: *Calculated offsets between the mean $\delta^{13}C$ value of the teeth and the $\delta^{13}C$ value of bone collagen ($\Delta^{13}C_{apatite\text{-}collagen}$) for each* Arvicola terrestris *mandible from Longstone Edge.*

Mandible	Mean $\delta^{13}C$ of tooth bioapatite (‰ VPDB)	$\delta^{13}C$ of bone collagen (‰)	$\Delta^{13}C_{apatite\text{-}collagen}$
LE-At-MA1	-10.14	-22.31	12.17
LE-At-MA2	-10.09	-22.78	12.69
LE-At-MA3	-9.30	-22.05	12.75

8.4.2. Danebury, Hampshire

8.4.2.1. $\delta^{18}O$ and $\delta^{13}C$ of teeth

The oxygen and carbon isotope results for the *M. agrestis* upper first molars from Danebury are shown in Figure 8.7. The $\delta^{18}O$ values of the teeth from Pit 923 vary between -4.7 and -3.8‰ (range = 0.8‰), whereas the teeth from Pit 955 vary between -5.9 and -4.1‰ (range = 1.8‰). The mean $\delta^{18}O_{rt}$ value for Pit 923 (-4.11‰) is enriched compared to the mean value for Pit 955 (-5.02‰), although this difference is not statistically significant at 95% confidence (T-test, $p = 0.07$).

In contrast, there is a statistically significant difference between the mean $\delta^{13}C$ values of the teeth from Pit 923 (-12.05‰) and Pit 955 (-13.48‰) (T-test, $p < 0.01$). The $\delta^{13}C_{rt}$ values for Pit 923 range from -12.4 to -11.2‰ (range = 1.2‰), whereas the $\delta^{13}C_{rt}$ values for Pit 955 range from -13.8 to -12.7‰ (range = 1.1‰).

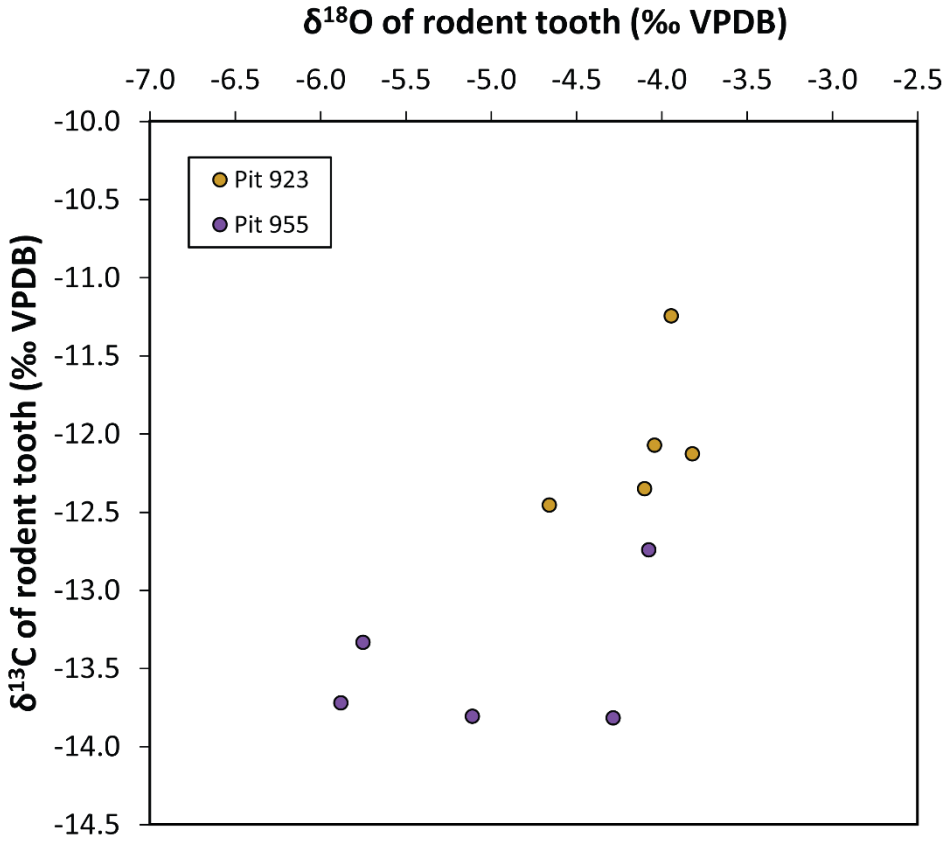

Figure 8.7: *Oxygen and carbon isotope results for the rodent teeth from Danebury.*

8.4.3. Comparisons between Longstone Edge and Danebury

The mean $\delta^{18}O$ value of the *M. agrestis* teeth from Longstone Edge is significantly depleted compared to the mean $\delta^{18}O$ values of the *M. agrestis* teeth from both Pits 923 and 955 from Danebury (T-tests, $p < 0.01$). In contrast, the mean $\delta^{13}C$ of the *M. agrestis* teeth from Longstone Edge is significantly enriched compared to the teeth from Danebury (T-test, $p < 0.01$).

8.4.4. Comparisons between the Late Holocene and modern teeth

8.4.4.1. $\delta^{18}O$ of teeth

The $\delta^{18}O$ values of the *Microtus agrestis* teeth from the Late Holocene and modern study sites are plotted in Figure 8.8. Only the modern data from Somerset, Surrey and East Yorkshire are shown, because Longstone Edge is located near to East Yorkshire, whereas Danebury is situated between Somerset and Surrey (Figure 3.1). The mean $\delta^{18}O$ value of the *M. agrestis* teeth from Longstone Edge is enriched compared to the modern teeth from East Yorkshire, but is similar to the modern mean $\delta^{18}O_{rt}$ for Somerset. In addition, the $\delta^{18}O$ values of the Longstone Edge teeth fall entirely within the range in $\delta^{18}O$ values of the Somerset teeth. In contrast, the mean $\delta^{18}O$ values of the teeth from Danebury lie at the upper end of the range in values of the modern teeth from Somerset (Figure 8.8).

8.4.4.2. $\delta^{13}C$ of teeth

The mean $\delta^{13}C$ values of the *Microtus agrestis* first molars, following adjustments for geographical variability, are shown in Figure 8.9. The adjustments were all relatively minor (within ± 0.4‰). Figure 8.9 demonstrates that the mean $\delta^{13}C_{rt}$ values follow a clear, negative polynomial trend from 4000 yr BP to the present day. The average rate of decline between ~2100 yr BP and the present day (0.0024‰/yr) is more than 1.5 times higher than the rate of decline between ~4000 and 2100 yr BP (0.0015‰/yr). In addition, there is no overlap between the $\delta^{13}C$ values of the modern and Late Holocene teeth. The total average depletion in $\delta^{13}C_{rt}$ over the past 4000 years is ~8‰.

However, this temporal trend is dependent upon the assumption that all of the *M. agrestis* teeth from Longstone Edge date to ~4000 yr BP. As shown in Figure 8.5, the *A. terrestris* mandibles from Longstone Edge fall within two time intervals: 1) ~3900-4100 yr BP, and 2) ~2500-2700 yr BP. Therefore, some of the *M. agrestis* and *A. terrestris* M^1 may differ in age. Despite this, the mean $\delta^{13}C$ values of the *A. terrestris* teeth from mandibles MA1 (~3950 yr BP) and MA2 (~2600 yr BP) are similar. This suggests that the $\delta^{13}C$ values of the *A. terrestris* teeth do not decline during the Late Holocene. Nevertheless, the teeth from MA1 and MA2 represent only two individuals. Within modern *A. terrestris* populations, large inter-individual differences in $\delta^{13}C_{rt}$ values are often observed (Gehler et al., 2012). Thus, the similarity in the mean $\delta^{13}C_{rt}$ values for the mandibles dating to 3950 and 2600 yr BP may be coincidental.

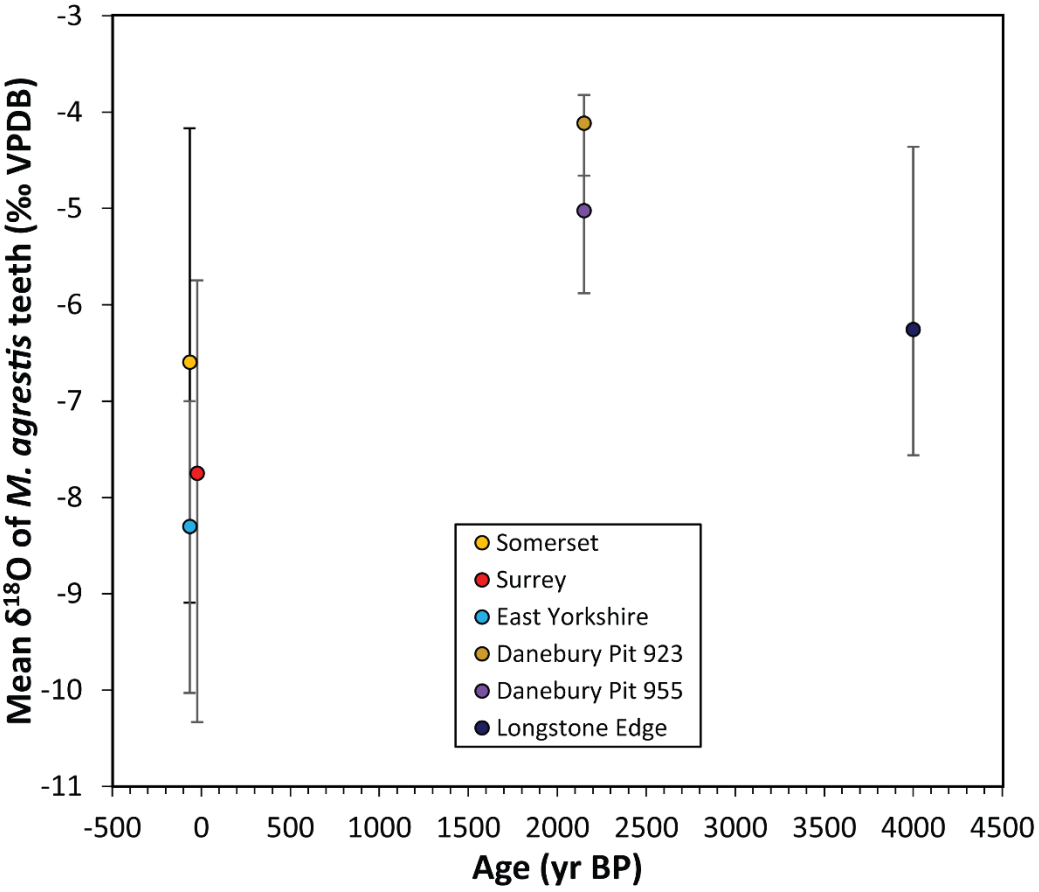

Figure 8.8: *Changes in the mean $\delta^{18}O$ values of the* Microtus agrestis *teeth from Britain over the past 4000 years. The errors bars represent the ranges in the $\delta^{18}O$ values of the teeth from each site.*

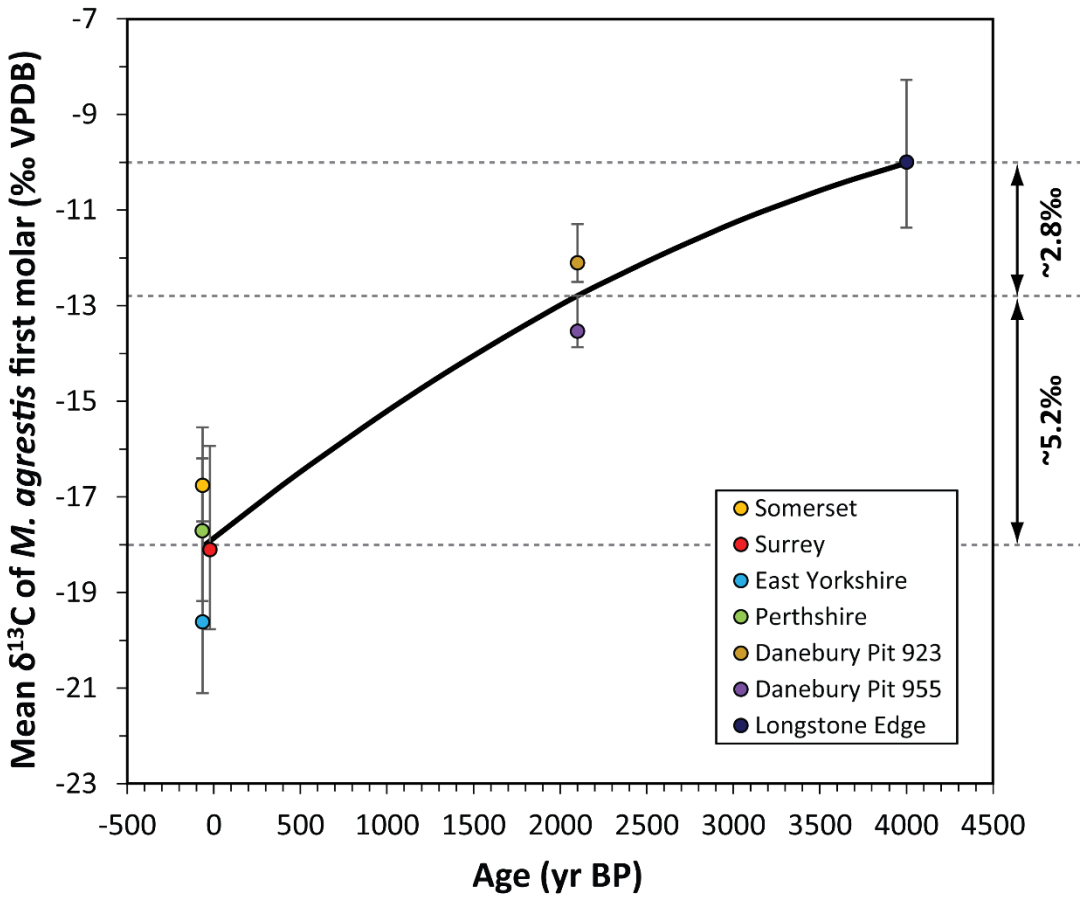

Figure 8.9: *Changes in the mean $\delta^{13}C$ values of the* Microtus agrestis *first molars from Britain over the past 4000 years. The error bars represent the ranges in the $\delta^{13}C$ values of the teeth from each site.*

8.4.5. Interpretations

8.4.5.1. $\delta^{18}O$ of teeth

The modern analogue study of Chapter 5 demonstrated that the mean $\delta^{18}O$ values of rodent teeth are related to the mean $\delta^{18}O$ of local meteoric water ($\delta^{18}O_{mw}$). At the present day, the $\delta^{18}O$ values of meteoric water sources near to Longstone Edge are similar to those in East Yorkshire (Figure 3.2). In contrast, the $\delta^{18}O$ values of the *M. agrestis* teeth from Longstone Edge suggest that mean $\delta^{18}O_{mw}$ values were enriched compared to East Yorkshire today. Since $\delta^{18}O_{mw}$ values in Britain are correlated with air temperature

(Darling & Talbot, 2003), the $\delta^{18}O_{rt}$ values for Longstone Edge might imply that temperatures at ~4000 yr BP were warmer than today.

The $\delta^{18}O$ values of the teeth from Danebury are likewise enriched compared to today. The $\delta^{18}O$ values of modern meteoric water sources near to Danebury are similar to $\delta^{18}O_{mw}$ values in Somerset (Figure 3.2). However, the $\delta^{18}O_{rt}$ data for Danebury lie above the mean $\delta^{18}O$ values of modern teeth from Somerset, suggesting that temperatures at Danebury were higher than present.

These interpretations are consistent with Late Holocene climate records from Britain. Pollen-based palaeotemperature reconstructions for Northwest Europe suggest that mean annual and mean summer temperatures at ~4000 and ~2000 yr BP were up to 1°C higher than today (Davis et al., 2003). Palaeo-precipitation records also suggest that the climate was relatively dry between ~2150 and 2000 yr BP (Charman, 2010). This reduction in precipitation may have increased the evaporative enrichment of meteoric water sources during this interval. This effect may have contributed to the enriched $\delta^{18}O$ values of the teeth from Danebury.

The results from Longstone Edge also show that the mean $\delta^{18}O$ value of the *M. agrestis* M^1 is significantly enriched compared to the mean $\delta^{18}O$ of the *A. terrestris* M^1. This difference between the $\delta^{18}O$ values of *Microtus* and *Arvicola* teeth has also been observed in modern analogue studies (Gehler et al., 2012), studies on Pleistocene teeth from fossil caves in France (Royer et al., 2014), and in the data collected from Gully Cave (Chapter 7). The data from Longstone Edge are therefore consistent with the expected $\delta^{18}O_{rt}$ differences between *Microtus* and *Arvicola.* These differences can be attributed to the ecological preferences of the taxa (see Sections 4.2.1.1 and 7.6.4.3).

On the other hand, the $\delta^{18}O$ values of the teeth from the *A. terrestris* mandibles are enriched compared to the $\delta^{18}O$ values of the *A. terrestris* M^1 (Figure 8.6). The results of the modern analogue study (Chapter 5) also showed that the $\delta^{18}O$ values of lower teeth are often slightly enriched compared to upper teeth. This difference may provide an explanation for the enriched $\delta^{18}O$ values of the mandibular teeth. Furthermore, the range in $\delta^{18}O$

values of *A. terrestris* teeth within modern populations is typically fairly broad (3.9‰) (Gehler et al., 2012). Thus the differences between the $\delta^{18}O$ values of the M^1 and mandibular teeth may also result from the natural intra-population variability in $\delta^{18}O_{rt}$ values.

8.4.5.2. $\delta^{13}C$ of tooth bioapatite and collagen

The ~5-8‰ differences between the $\delta^{13}C$ values of the modern and Late Holocene teeth (Figure 8.9) are consistent with the mean $\delta^{13}C$ offsets between the modern and Pleistocene rodent teeth from Britain (Figure 8.1, Table 8.1). This consistency in the $\delta^{13}C$ offsets across all study sites therefore suggests that the same factors have caused a depletion in the $\delta^{13}C$ values of the modern teeth relative to the fossil teeth. The data from the Late Holocene teeth also indicate that the shift from enriched to depleted $\delta^{13}C_{rt}$ values occurred within the past ~2000 years (Figure 8.9). The most plausible explanations for this shift are the recent changes in the $\delta^{13}C$ value and partial pressure of atmospheric CO_2 (Figures 8.3b and 8.4). Nevertheless, the atmospheric shifts began only ~200 years ago, whereas the $\delta^{13}C_{rt}$ data indicate a gradual decline since ~4000 yr BP (Figure 8.9). Despite this, the mean $\delta^{13}C$ values of the teeth are likely to vary within and between the sites due to variations in the plant taxa that were locally available for consumption by the rodents (see Table 2.1). The significant differences between the $\delta^{13}C$ values of the teeth from the two pits at Danebury (Figure 8.7) clearly demonstrate this spatial variability. Therefore, the apparent decline in $\delta^{13}C_{rt}$ values between 4000 yr BP (Longstone Edge) and 2000 yr BP (Danebury) may simply reflect the natural variability in the $\delta^{13}C$ values of C_3 plants within and between ecosystems.

The data from the Late Holocene teeth additionally demonstrate that the enriched $\delta^{13}C$ values of the fossil teeth are unlikely to result from diagenetic alteration. This is because the teeth from the Late Holocene sites are less likely to have experienced diagenesis compared to the Pleistocene teeth. Indeed, the C/N ratios for the *A. terrestris* mandibles suggest that the bone collagen from these specimens is well-preserved. Therefore, the Late Holocene bioapatite is also likely to have retained its original isotopic values.

Moreover, inter-site differences in 1) taphonomy, and 2) the length of time over which diagenesis could occur, would be expected to cause large differences in the magnitude of isotopic alteration between the pre-modern sites. However, for all study sites except Gully Cave, large variations in the mean $\delta^{13}C$ offset between the modern and fossil teeth are not observed (Figure 8.1; Table 8.1).

Despite this, the $\Delta^{13}C_{apatite\text{-}collagen}$ values calculated for the *A. terrestris* mandibles from Longstone Edge (+12-13‰) are more than twice the values measured in modern mice and rats fed on a C_3 diet (+6.0 ± 0.65‰) (Ambrose & Norr, 1993; Tieszen & Fagre, 1993; Jim et al., 2004), as well as modern gerbils (+6.5 ± 1.4‰) (Jeffrey, 2016). This may imply that the $\delta^{13}C$ values of the teeth from Longstone Edge have been diagenetically altered. Nevertheless, as yet, no studies have investigated the bioapatite-collagen $\delta^{13}C$ offset in arvicoline rodents. Therefore, it is possible that this offset differs in arvicoline rodents compared to mice, rats and gerbils. However, variations in $\Delta^{13}C_{apatite\text{-}collagen}$ values in large herbivorous mammals that have fed solely on C_3 plants are usually within ± 1‰ (e.g. Lee-Thorp et al., 1989; Clementz et al., 2009). Thus any inter-taxon differences in the bioapatite-collagen offset are likely to be relatively small.

An alternative explanation for the large $\Delta^{13}C_{apatite\text{-}collagen}$ values may be differences in the $\delta^{13}C$ values of the dietary macronutrients that are recorded within bioapatite and collagen. The $\delta^{13}C$ of bioapatite records the $\delta^{13}C$ value of the energy component of the diet (namely carbohydrates), whereas the $\delta^{13}C$ of collagen reflects the $\delta^{13}C$ of dietary protein (Krueger & Sullivan, 1984; Ambrose & Norr, 1993; Tieszen & Fagre, 1993; Jim et al., 2004). In experiments undertaken on laboratory rats fed on a diet consisting of protein from C_3 sources, but energy from isotopically-enriched C_3 or C_4 sources, the measured $\delta^{13}C$ offsets between bioapatite and collagen varied between 7.4 and 11.5‰ (Ambrose & Norr, 1993; Jim et al., 2004). The maximum offset in these experiments (11.5‰) is relatively similar to the offsets measured for the *A. terrestris* mandibles from Longstone Edge (12-13‰). Carbon isotope enrichment factors between bioapatite and the diet appear to be larger in voles than in mice and rats (Passey et al., 2005), and the data from the *A. terrestris* mandibles are consistent with this pattern. The $\Delta^{13}C_{apatite\text{-}collagen}$ values for these mandibles (Table 8.4) may therefore suggest that the *A. terrestris*

individuals from Longstone Edge consumed a mixed diet comprising C_3 or C_4 carbohydrates with enriched $\delta^{13}C$ values, and C_3 proteins with average $\delta^{13}C$ values. However, as aforementioned, records from northwest Europe indicate that C_3 plants have constituted nearly 100% of the vegetation in Britain during the Holocene (Collins & Jones, 1986; Rao et al., 2012). As a result, it is highly unlikely that rodents living in Britain during this period would have consumed a significant quantity of C_4 plants within their diet. Nevertheless, it is possible that the rodents from Longstone Edge consumed energy sources with $\delta^{13}C$ values near to the maximum of the recorded isotopic range for C_3 plants (Figure 8.2). These ideas are investigated further in Section 8.5.

8.4.6. Summary

The results from Longstone Edge and Danebury demonstrate that pre-modern rodent teeth from Britain have $\delta^{13}C$ values that are ~5-8‰ enriched compared to modern teeth. The shift from enriched to depleted $\delta^{13}C_{rt}$ values occurred within the past 2000 years. The influence of diagenesis on this temporal shift in $\delta^{13}C$ values is argued to be minimal, due to the consistency in the $\delta^{13}C$ offsets between modern and fossil teeth across all sites, and the preservation of the specimens from the archaeological sites. The temporal shift in $\delta^{13}C_{rt}$ is likely to primarily result from recent anthropogenic changes in atmospheric CO_2. However, the large $\delta^{13}C$ offsets between the tooth bioapatite and bone collagen from Longstone Edge suggest that changes in the rodents' diets may have also contributed to this temporal shift in $\delta^{13}C$ values. This dietary change likely involved a shift in the $\delta^{13}C$ values of the carbohydrates within the plants consumed by the rodents.

The $\delta^{18}O$ values of the teeth from Longstone Edge and Danebury are also enriched compared to present-day values. This enrichment is consistent with warmer temperatures in Britain during the Mid-Late Holocene, and possibly drier conditions at Danebury at ~2000 yr BP. Differences in the $\delta^{18}O$ values of the *Microtus* and *Arvicola* teeth are consistent with the ecological preferences of these taxa.

8.5. Results and Interpretations: Variations in the $\delta^{13}C$ values of rodent teeth over the past 14,500 years

8.5.1. Modelled $\delta^{13}C$ values of C_3 plants

The $\delta^{13}C$ values of C_3 plants, estimated using the Voelker-2016a and SJ-2012 models, are shown in Figure 8.10. The greatest change in $\delta^{13}C_p$ values over the past 14,500 years is the recent depletion resulting from the anthropogenic shifts in $\delta^{13}C_a$ and pCO_2 (Figures 8.3b and 8.4). Both models indicate that this depletion began ~1750 AD (~200 yr BP). The magnitude of the $\delta^{13}C_p$ depletion between 1750 and 2015 AD is around 2.9‰ in the Voelker-2016a model, and 3.8‰ in the SJ-2012 model.

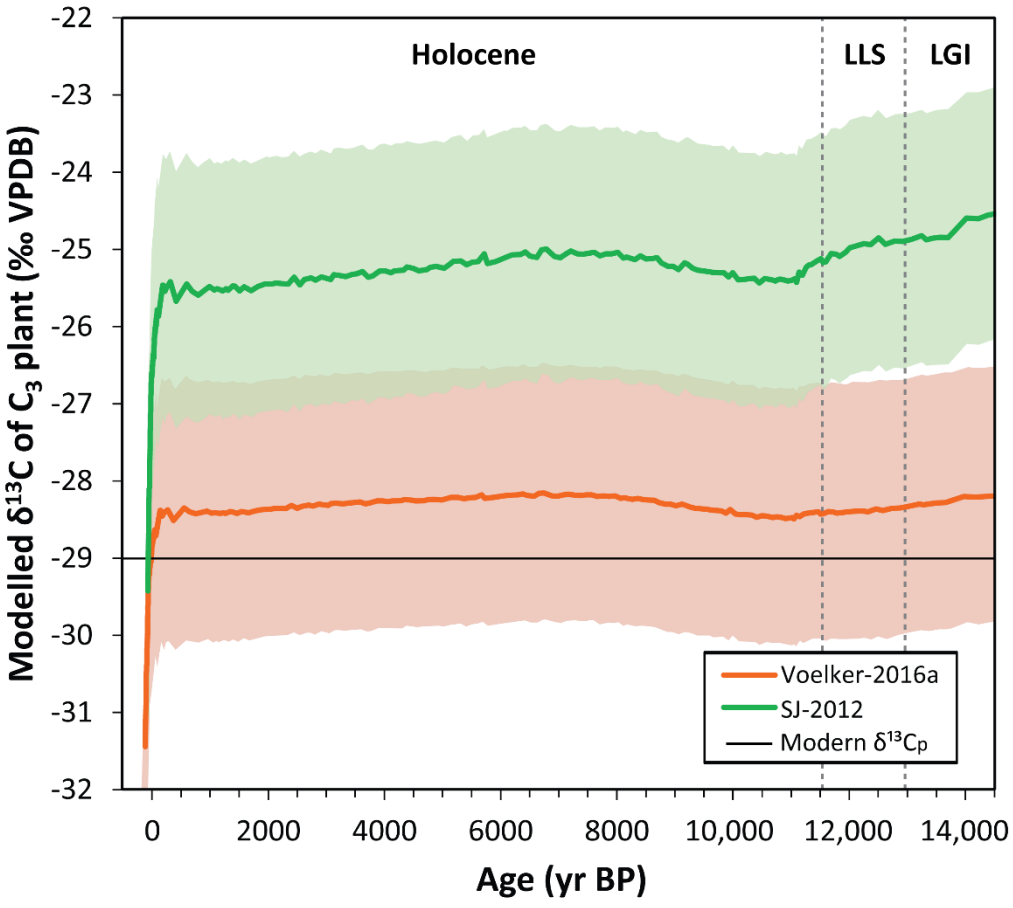

Figure 8.10: *Variations in the $\delta^{13}C$ values of C_3 plants over the past 14,500 years, estimated using the Voelker-2016a and SJ-2012 models. The modern global mean $\delta^{13}C$ value for C_3 plants (from Kohn, 2010) is shown for comparison. The climatic stages are also labelled (LLS = Loch Lomond Stadial, LGI = Lateglacial Interstadial).*

Apart from this recent decline, the $\delta^{13}C_p$ values estimated by the Voelker-2016a model are relatively stable over the past 14,500 years. The only notable changes are a 0.30‰ depletion between 14,500 yr BP in the Lateglacial Interstadial (LGI), and 11,100 yr BP in the Early Holocene (Figure 8.10). This is followed by a 0.33‰ increase until ~6,700 yr BP in the Middle Holocene. These shifts are more pronounced in the SJ-2012 record (Figure 8.10); the magnitude of the decline from the LGI to Early Holocene is 0.89‰, whereas the increase from the Early to Middle Holocene is 0.42‰. The relatively enriched $\delta^{13}C_p$ values during the LGI and LLS result from reduced pCO_2 levels (Figure 8.4), while the relatively depleted $\delta^{13}C_p$ values in the Early Holocene are due to the high pCO_2 and relatively depleted $\delta^{13}C_a$.

Figure 8.10 also shows that the absolute $\delta^{13}C_p$ values calculated using the two models differ by ~1-3‰. The measured global mean $\delta^{13}C$ value for C_3 plants, corrected to a $\delta^{13}C_a$ value of -8.0‰, is -28.5‰ (Kohn, 2010). The SJ-2012 model predicts a comparable mean $\delta^{13}C_p$ value (-28.4‰) for similar atmospheric conditions. In contrast, the Voelker-2016a model generates a mean $\delta^{13}C_p$ value that is 2.2‰ more depleted than the measured global average $\delta^{13}C_p$. This suggests that the SJ-2012 model provides more accurate estimates for the mean $\delta^{13}C$ values of C_3 plants. The offsets between the two models may be related to inaccuracies in the *a* and *b* constants chosen for the Voelker-2016a model, or uncertainties in the relationship between C_i/C_a and C_a (Hare et al., 2018). Indeed, the r^2 value for this relationship in angiosperms is relatively poor (0.11), due to the large degree of scatter in the data (Voelker et al., 2016). Therefore in the following discussions, comparisons will only be made with the $\delta^{13}C_p$ values generated using the SJ-2012 model.

8.5.2. Comparisons between modelled $\delta^{13}C$ values of C_3 plants and measured $\delta^{13}C$ values of rodent teeth and bone collagen

The mean $\delta^{13}C$ values of the diet ($\delta^{13}C_d$), calculated using the $\delta^{13}C$ values of the modern rodent first molars from Britain, are consistent with: 1) the mean and range in $\delta^{13}C$ values of C_3 plants predicted by the SJ-2012 model, and 2) the measured global average $\delta^{13}C$ value for C_3 plants (Figure 8.11).

Conversely, the $\delta^{13}C_d$ values for the pre-modern first molars are higher than the average modelled $\delta^{13}C_p$ values. The $\delta^{13}C_d$ values for Danebury overlap with the mean $\delta^{13}C_p$ value, whereas the $\delta^{13}C_d$ values for the *Microtus* teeth from Longstone Edge and Gully Cave are ~4‰ enriched compared to the mean $\delta^{13}C_p$. The $\delta^{13}C_d$ values for the *Arvicola* teeth from Gully Cave are further enriched, with a mean offset of ~6‰ from the $\delta^{13}C_p$ values.

The enriched $\delta^{13}C$ values of the *Arvicola* teeth from Gully Cave may be partly related to inter-tooth isotopic differences, in addition to the inter-taxon differences in dietary preferences or carbon isotope fractionation suggested in Section 7.6.4.2. The *Microtus* teeth from Gully Cave are all upper first molars, whereas the *Arvicola* teeth are upper incisors. The $\delta^{13}C$ results for the *A. terrestris* teeth from Longstone Edge (Figure 8.6) showed that the incisors from mandibles MA1 and MA2 were ~1.0-1.3‰ enriched compared to the first molars. This may partly explain why the $\delta^{13}C$ values of the *Arvicola* incisors from Gully Cave are ~1-3‰ enriched compared to the *Microtus* molars (Figure 8.11). Interestingly, in modern *M. agrestis* teeth from Britain (Chapter 5), and *A. terrestris* teeth from Germany (Gehler et al., 2012), the opposite pattern is seen, whereby the $\delta^{13}C$ values of the incisors are significantly and consistently depleted compared to the molars. These inter-tooth $\delta^{13}C$ differences have been attributed to seasonal variations in dietary preferences, combined with offsets between the periods of the year during which the teeth mineralized (see section 5.6.1.3). The differences in the patterns of inter-tooth $\delta^{13}C$ offsets between the modern and fossil rodents may therefore result from temporal variations in seasonal dietary preferences or the seasons of tooth mineralization.

While the $\delta^{13}C_d$ values calculated from the fossil tooth bioapatite are enriched compared to the modelled $\delta^{13}C$ values of C_3 plants, the $\delta^{13}C_d$ values calculated from the bone collagen are consistent, within uncertainties, with the $\delta^{13}C_p$ values estimated from SJ-2012 model (Figure 8.12). This is the case for both the *A. terrestris* mandibles from Longstone Edge, and an *A. terrestris* mandible from Gully Cave, which has been radiocarbon dated to the early part of the Lateglacial Interstadial (Schreve, 2012b). The offsets between the $\delta^{13}C_d$ values calculated from the bone collagen and tooth bioapatite are ~5‰.

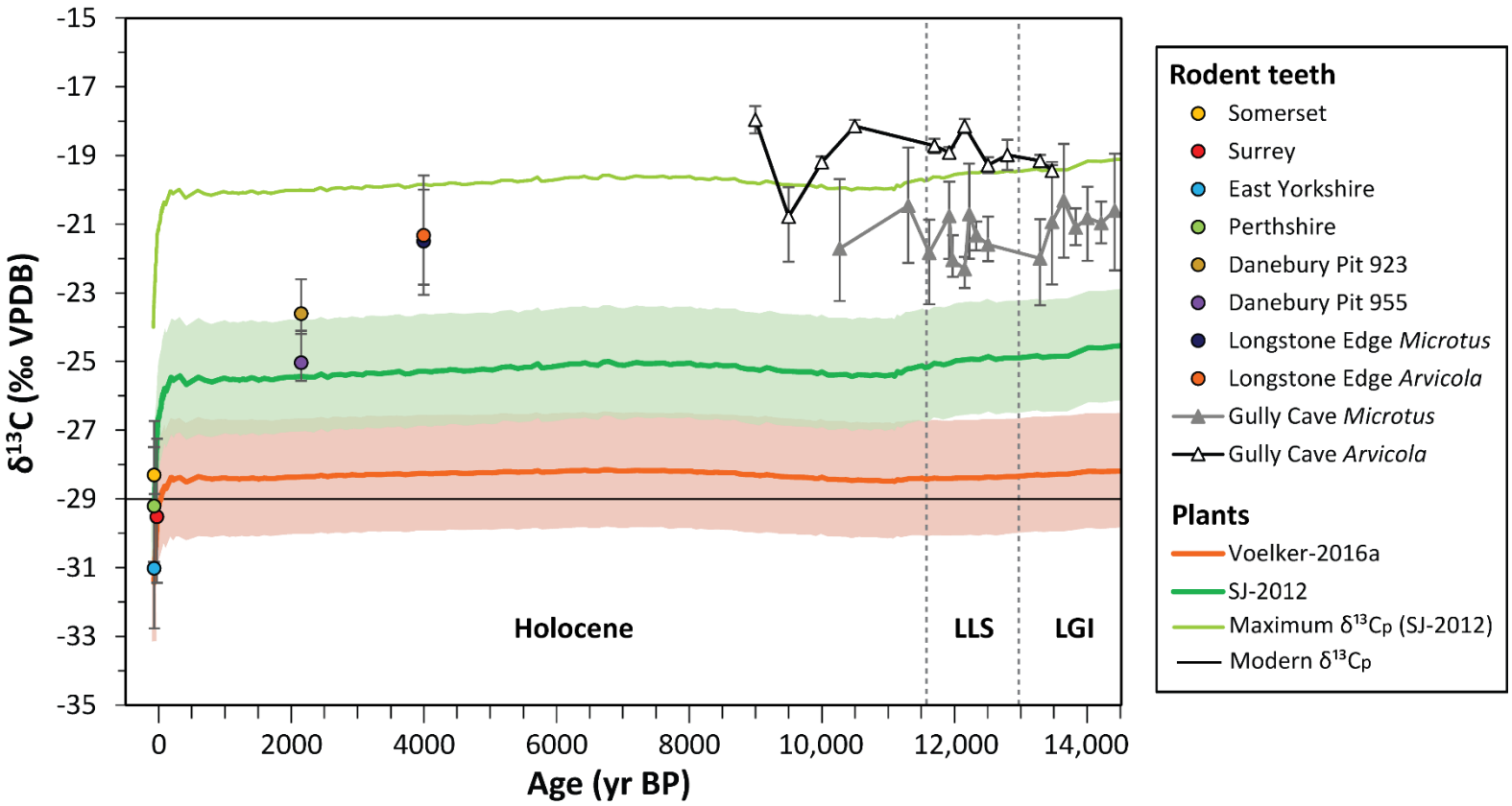

Figure 8.11: *Comparisons between the modelled $\delta^{13}C$ values of C_3 plants, and the dietary $\delta^{13}C$ values calculated from the $\delta^{13}C$ values of the modern and fossil rodent first molars from Britain, and fossil* Arvicola *incisors from Gully Cave. The modern $\delta^{13}C$ of C_3 plants (from Kohn, 2010), and the maximum $\delta^{13}C$ of C_3 plants calculated using the SJ-2012 model, are shown for comparison.*

8.5.3. Influences of environmental factors on temporal variations in the $\delta^{13}C$ values of rodent bioapatite and collagen

The SJ-2012 model accounts for the influences of variations in the $\delta^{13}C$ value and partial pressure of atmospheric CO_2 on the $\delta^{13}C$ values of C_3 plants (Equations 8.7-8.8). However, the $\delta^{13}C_d$ values for the fossil rodent teeth are ~4-6‰ enriched compared to the modelled $\delta^{13}C_p$ values (Figure 8.11). This indicates that atmospheric CO_2 changes are not sufficient to explain the temporal variations in the $\delta^{13}C$ values of rodent teeth from Britain.

Nevertheless, offsets of similar magnitudes are observed between the $\delta^{13}C_d$ values calculated from the fossil bioapatite and bone collagen (Figure 8.12). As aforementioned, bioapatite reflects the $\delta^{13}C$ of the energy source or whole diet, whereas collagen reflects the $\delta^{13}C$ of dietary protein (Ambrose & Norr, 1993). The $\delta^{13}C_d$ offsets between the bioapatite and collagen from Longstone Edge and Gully Cave therefore imply that between ~14,500 and 4000 yr BP, the $\delta^{13}C$ values of the energy and protein sources in the rodents' diets differed. In section 8.4.5.2, it was proposed that the rodents from the fossil sites may have derived energy from enriched C_3 or C_4 plant sources, while the bone collagen reflected protein from C_3 sources. This was based on the large $\delta^{13}C$ offsets (+12-13‰) between the *A. terrestris* bioapatite and collagen from Longstone Edge (Table 8.4). Interestingly, the $\Delta^{13}C_{apatite\text{-}collagen}$ value for the *A. terrestris* specimens from Gully Cave is 12.7‰, which is entirely consistent with the values calculated for Longstone Edge (Table 8.4). This supports the suggestion that the pre-modern bioapatite and collagen record differences in the $\delta^{13}C$ values of the dietary components.

Laboratory experiments show that the $\delta^{13}C$ enrichment between rodent bioapatite and the diet ($\varepsilon_{apatite\text{-}diet}$) is relatively consistent, regardless of the $\delta^{13}C$ composition of the whole diet (Ambrose & Norr, 1993; Jim et al., 2004). Therefore, the $\varepsilon_{apatite\text{-}diet}$ value of 11.5‰, measured in modern voles fed on a C_3 diet (Passey et al., 2005), should generate accurate $\delta^{13}C_d$ values for the fossil rodents (Figure 8.13). In contrast, the $\delta^{13}C$ enrichment between the collagen and the diet ($\varepsilon_{collagen\text{-}diet}$) varies depending on the $\delta^{13}C$ value of the whole diet (Ambrose & Norr, 1993; Jim et al., 2004). Laboratory rats fed on a diet comprising enriched C_3 or C_4 energy sources, and C_3 protein sources,

have $\varepsilon_{collagen\text{-}diet}$ values of between +1.84 and -2.33‰ (Ambrose & Norr, 1993; Jim et al., 2004). These $\varepsilon_{collagen\text{-}diet}$ values are between ~2.1 and 6.2‰ different from the mean $\varepsilon_{collagen\text{-}diet}$ value measured in rats fed on a pure C_3 diet (+3.9‰) (DeNiro & Epstein, 1978; Deniro & Epstein, 1981; Ambrose & Norr, 1993; Tieszen & Fagre, 1993; Jim et al., 2004). The magnitude of this difference in $\varepsilon_{collagen\text{-}diet}$ values is comparable to the magnitude of the offset between the $\delta^{13}C_d$ values for the fossil bioapatite and bone collagen from Britain (Figure 8.12). In addition, the enrichment factor between the $\delta^{13}C$ of the collagen and the $\delta^{13}C$ of the diet for Longstone Edge is -0.96‰ (Figure 8.13). This value is consistent with a diet composed of isotopically-enriched C_3 or C_4 plant sources. Figure 8.13 summarises these offsets between the $\delta^{13}C$ values of bioapatite, collagen and the diet for the *A. terrestris* individuals from Longstone Edge.

In order to assess whether the rodent tissues record a C_3 or C_4 diet, the maximum $\delta^{13}C$ values of C_3 plants were calculated for the past 14,500 years using the SJ-2012 model. In an atmosphere with a $\delta^{13}C$ value of -8‰, the maximum typical $\delta^{13}C$ value of C_3 plants is -23‰ (Kohn, 2010). The SJ-2012 model was used to correct this maximum value for temporal changes in $\delta^{13}C_p$ values resulting from variations in atmospheric CO_2. The calculated maximum $\delta^{13}C$ values for C_3 plants are shown in Figures 8.11 and 8.12. These figures demonstrate that the enriched dietary $\delta^{13}C$ values for the rodents from Longstone Edge and Gully Cave fall within the maximum range in $\delta^{13}C$ values for C_3 plants. The significant differences in $\delta^{13}C_{rt}$ values between Longstone Edge and Gully Cave, and the modern sites, can consequently be attributed to a shift in the $\delta^{13}C$ composition of the C_3 diet consumed by the rodents. The rodents from Longstone Edge and Gully Cave are consistent with a diet composed of C_3 energy sources with highly enriched $\delta^{13}C$ values, but C_3 protein sources with average $\delta^{13}C$ values. In contrast, the modern rodents consumed C_3 energy sources with average $\delta^{13}C$ values that are consistent with the modern global mean $\delta^{13}C_p$. The rodents from Danebury may represent an intermediary stage between these two extremes, whereby the rodents consumed C_3 plants with $\delta^{13}C$ values only slightly enriched compared to the local mean (Figure 8.11).

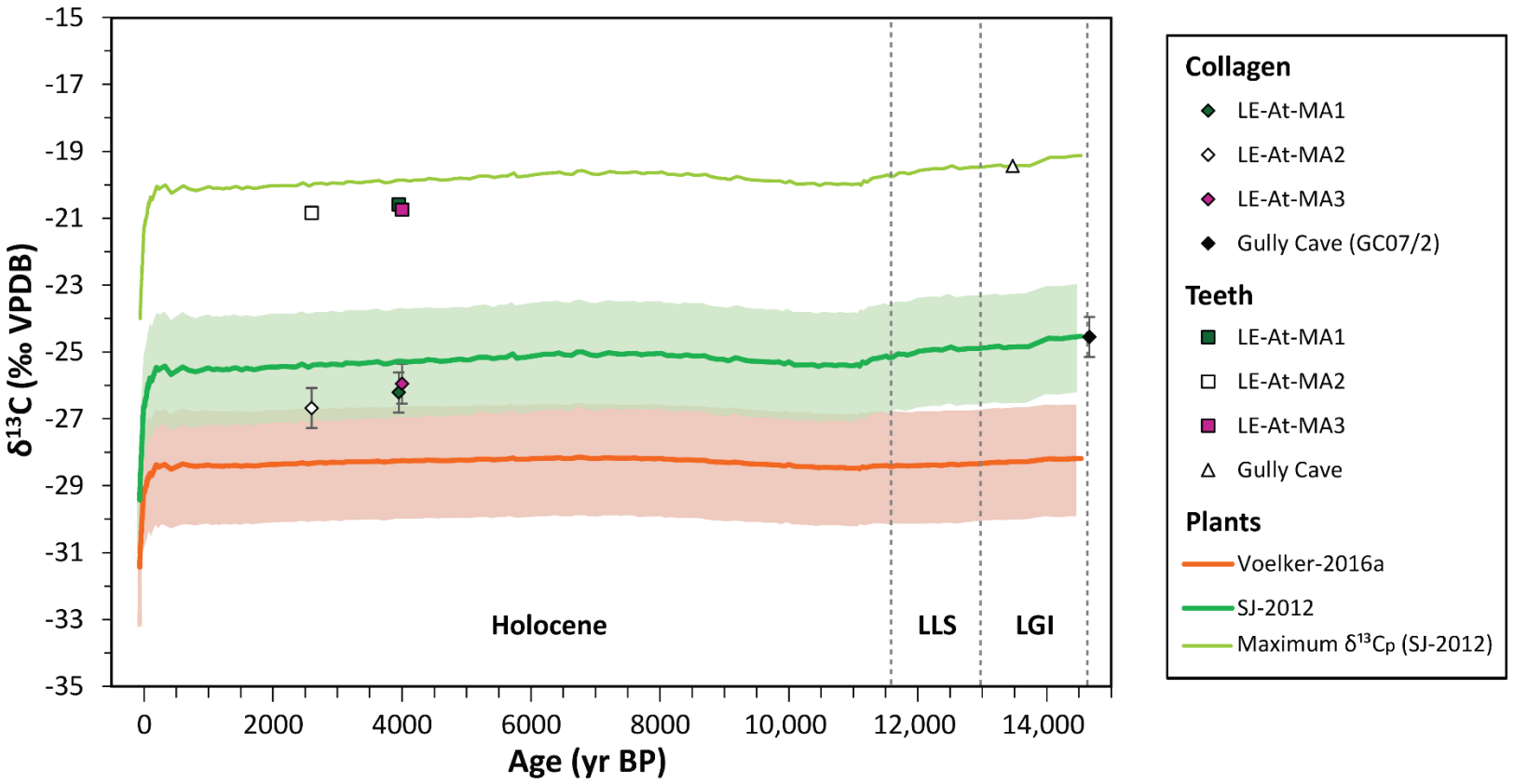

Figure 8.12: *Comparisons between the modelled $\delta^{13}C$ values of C_3 plants, and the dietary $\delta^{13}C$ values calculated from the $\delta^{13}C$ values of the* Arvicola terrestris *incisor bioapatite and bone collagen from Britain. The maximum $\delta^{13}C$ value of C_3 plants, calculated using the SJ-2012 model, is shown for comparison. The collagen $\delta^{13}C$ value for Gully Cave was obtained from Schreve (2012b).*

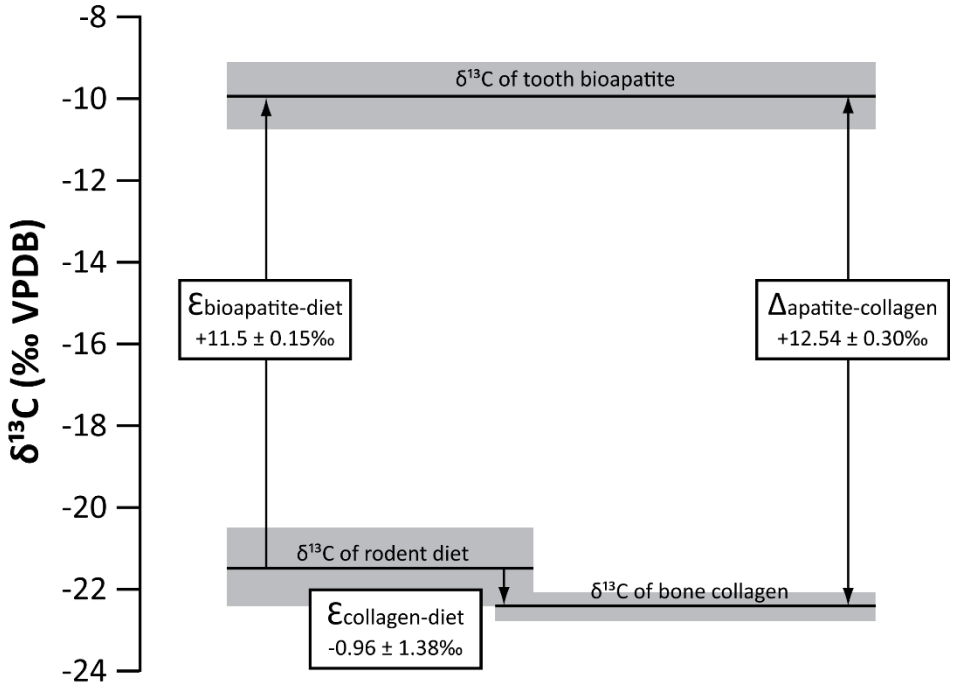

Figure 8.13: *Schematic diagram illustrating the mean offsets between the $\delta^{13}C$ values of the tooth bioapatite, bone collagen and rodent diet from Longstone Edge. The $\delta^{13}C$ of the rodent diet was calculated from the $\delta^{13}C$ of tooth bioapatite, using the published bioapatite-diet offset of 11.5 ± 0.15‰ (Passey et al., 2005). The grey shading represents the ranges in the $\delta^{13}C$ values of the bioapatite, collagen and diet.*

Even though the $\delta^{13}C$ values of the fossil bioapatite, bone collagen and C_3 plants are offset, the relative magnitudes of the temporal shifts in these values are similar. For example, the average differences in the $\delta^{13}C$ values of bone collagen between Gully Cave and Longstone Edge are larger than the average differences in the $\delta^{13}C$ of incisor bioapatite between these sites (Table 8.5). The bone collagen from Gully Cave dates to the onset of the LGI at ~14,600 yr BP, whereas the incisor dates to the mid-LGI at ~13,500 yr BP. The pCO_2 levels at the onset of the LGI are lower than in the mid-late LGI (Figure 8.4). Given that plant $\delta^{13}C$ values increase with decreasing pCO_2 (Schubert & Jahren, 2012), $\delta^{13}C_p$ values are expected to be higher during the early LGI than during middle LGI. This is indeed observed in the $\delta^{13}C_p$ record generated from the SJ-2012 model; $\delta^{13}C_p$ values are ~0.3‰ different between the early and middle LGI (Figure 8.10). Accordingly, the difference in $\delta^{13}C_p$

values between 14,600 and 4000 yr BP is ~0.3‰ larger than the difference in $\delta^{13}C_p$ values between 13,500 and 4000 yr BP (Table 8.5). This ~0.3‰ difference is also reflected in the bioapatite and collagen data (Table 8.5). This suggests that the variations in the $\delta^{13}C$ values of rodent tissues during the LGI were primarily driven by changes in pCO_2. Table 8.5 also demonstrates that the relative magnitudes of the temporal shifts in $\delta^{13}C$ values are consistent in the plant, bioapatite and collagen datasets. This evidence supports that argument that the fossil rodent tissues have not undergone significant diagenetic alteration.

Despite this, the absolute magnitudes of the temporal shifts in $\delta^{13}C$ values are larger in the bioapatite and collagen records than in the modelled $\delta^{13}C_p$ record (Table 8.5). The modelled $\delta^{13}C$ values of C_3 plants only reflect changes in $\delta^{13}C_a$ and pCO_2. Therefore, other environmental factors, in addition to $\delta^{13}C_a$ and pCO_2, must have contributed to the offset in the $\delta^{13}C$ values of bioapatite and collagen between the LGI and Late Holocene. By subtracting the temporal differences in $\delta^{13}C_p$ values from the temporal differences in the $\delta^{13}C$ values of the rodent bioapatite and collagen, the residual isotopic shifts can be calculated. The results of these calculations are shown in Table 8.6. The residual shifts in the $\delta^{13}C$ values of bioapatite and collagen are relatively consistent at ~0.78-0.86‰. The slightly higher shift in collagen $\delta^{13}C$ values between 14,600 and 2600 yr BP (Table 8.6) may result from the natural variability in the $\delta^{13}C$ values of rodent tissues within a population, plus analytical errors. These temporal $\delta^{13}C$ shifts likely result from climatic differences between the Lateglacial Interstadial and Late Holocene.

As mentioned in Section 8.2.2, the climate during the Lateglacial period was relatively arid (e.g. Kasse, 2002). The ~0.8‰ difference in the $\delta^{13}C$ values of the rodent tissues between the LGI and Late Holocene may therefore result from a shift from drier to wetter conditions. Equation 8.4 was used to estimate the magnitude of this change in mean annual precipitation. A shift of 0.78-0.86‰ corresponds to an increase in MAP of ~300 mm/yr, from ~500 mm/yr during the LGI to ~800 mm/yr in the Late Holocene. Model simulations for MAP changes in Britain between the Last Glacial Maximum (~21,000 yr BP) and the pre-industrial period (~200 yr BP) are of a similar magnitude, at between ~180 and 365 mm/yr (Braconnot et al., 2007; Ludwig et al., 2016).

Table 8.5: *Calculated mean differences in the $\delta^{13}C$ values of C_3 plants (from the SJ-2012 model),* Arvicola terrestris *bone collagen, and* Arvicola terrestris *incisor bioapatite between Gully Cave (GC) and Longstone Edge (LE). The data for Longstone Edge at ~4000 yr BP consist of the $\delta^{13}C$ values of the collagen and incisor bioapatite from mandibles MA1 and MA3. The data for Longstone Edge at ~2600 yr BP consist of the $\delta^{13}C$ values of the collagen and incisor bioapatite from mandible MA2. The uncertainties on the mean difference in the $\delta^{13}C$ of C_3 plants is based on the 1σ uncertainties on the atmospheric CO_2 measurements. The uncertainties on the mean $\delta^{13}C$ differences in the collagen and incisor bioapatite between Gully Cave and Longstone Edge represent 1σ standard deviations on the mean differences.*

Approximate ages of material, yr BP (Study Site)	**Mean difference in $\delta^{13}C$ of C_3 plants (‰)**	**Mean difference in $\delta^{13}C$ of bone collagen (‰)**	**Mean difference in $\delta^{13}C$ of incisor bioapatite (‰)**
14600 (GC) - 4000 (LE)	0.75 ± 0.04	1.53 ± 0.18	-
13500 (GC) - 4000 (LE)	0.43 ± 0.06	-	1.23 ± 0.11
14600 (GC) - 2600 (LE)	0.86 ± 0.03	2.13 ± 0.50	-
13500 (GC) - 2600 (LE)	0.55 ± 0.04	-	1.40 ± 0.05

Table 8.6: *Residual shifts in the $\delta^{13}C$ values of* A. terrestris *bone collagen and* A. terrestris *incisor bioapatite between Gully Cave (GC) and Longstone Edge (LE). These shifts were calculated by subtracting the mean differences in the $\delta^{13}C$ values of C_3 plants (Column 2 in Table 8.5) from the mean differences in the $\delta^{13}C$ values of collagen and incisor bioapatite (Columns 3 and 4 in Table 8.5).*

Approximate ages of material, yr BP (Study Site)	Residual difference in $\delta^{13}C$ of bone collagen (‰)	Residual difference in $\delta^{13}C$ of incisor bioapatite (‰)
14600 (GC) - 4000 (LE)	0.78 ± 0.22	-
13500 (GC) - 4000 (LE)	-	0.79 ± 0.16
14600 (GC) - 2600 (LE)	1.27 ± 0.42	-
13500 (GC) - 2600 (LE)	-	0.86 ± 0.15

8.6. Discussion

8.6.1. Temporal variations in the $\delta^{13}C$ values of rodent teeth from Britain

The $\delta^{13}C$ values of the rodent teeth from Britain have varied over the past 800 ka (Figure 8.14). The most significant change during this period is a ~5-8‰ decline in $\delta^{13}C_{rt}$ values between 4000 years ago and the present day (Figure 8.9). The recent anthropogenic shifts in the $\delta^{13}C$ value and partial pressure of atmospheric CO_2 explain approximately 4‰ of this change in $\delta^{13}C_{rt}$ values (Figure 8.10). The remaining 1-4‰ change has been attributed to a shift in the $\delta^{13}C$ composition of the rodents' diet. This shift is from a diet with a mean $\delta^{13}C$ value towards the maximum value for typical C_3 plants, to a diet consistent with the average $\delta^{13}C$ value of C_3 plants. As shown in Figure 8.14, the $\delta^{13}C$ values of the teeth from all pre-modern sites overlap. This suggests that arvicoline rodents in Britain consumed an isotopically-enriched

C_3 diet throughout the Middle-Late Pleistocene and Holocene, until at least ~2000 yr BP.

Although the influence of diagenesis on the temporal differences in tooth $\delta^{13}C$ values cannot be entirely ruled out, it can be argued that most teeth have experienced negligible alteration, based on several lines of evidence. Firstly, relatively young (~2000-4000 yr BP) and well-preserved teeth have enriched $\delta^{13}C$ values compared to the modern teeth. In addition, the magnitude of isotopic enrichment is relatively consistent across all pre-modern study sites (Figure 8.14), regardless of the depositional and geological environment of the site, and the age of the fossil teeth. Furthermore, the mean differences between the $\delta^{13}C$ values of tooth bioapatite from Gully Cave and Longstone Edge (Figure 8.12) are comparable to the differences between the $\delta^{13}C$ of bone collagen from these sites. The C/N ratios indicate that the bone collagen is well-preserved (Table 8.3). It is therefore considered unlikely that the temporal shifts in the $\delta^{13}C$ of bioapatite and collagen would be similar if the bioapatite had undergone significant alteration.

The relative changes in the $\delta^{13}C$ of bioapatite and collagen between Gully Cave and Longstone Edge are also consistent with the expected shifts in the $\delta^{13}C$ values of C_3 plants between the Lateglacial and Late Holocene periods (Figure 8.12). The temporal shifts in $\delta^{13}C_p$ values can be attributed to changes in $\delta^{13}C_a$, pCO_2, and mean annual precipitation. The stratigraphic changes in the $\delta^{13}C$ values of the rodent teeth from Westbury Cave likewise parallel fluctuations in atmospheric CO_2 and climate (see Section 7.5.4.2). This suggests that the $\delta^{13}C$ values of the fossil rodent teeth accurately record the responses of local C_3 plants to variations in environmental factors.

Finally, the $\delta^{18}O$ values of the fossil rodent teeth are consistent with the climatic conditions that prevailed during the periods in which the teeth formed (Section 8.4.5.1, Chapters 6-7). If the fossil teeth had been diagenetically altered due to, for example, the incorporation of detrital carbonate, both the $\delta^{18}O$ and $\delta^{13}C$ values of the dental carbonate would be expected to be altered. However, there is no convincing evidence that this has occurred at any of the pre-modern sites. Therefore, the temporal variations in the $\delta^{13}C$ values of the rodent teeth from Britain are likely to primarily result from variations in the environmental signals.

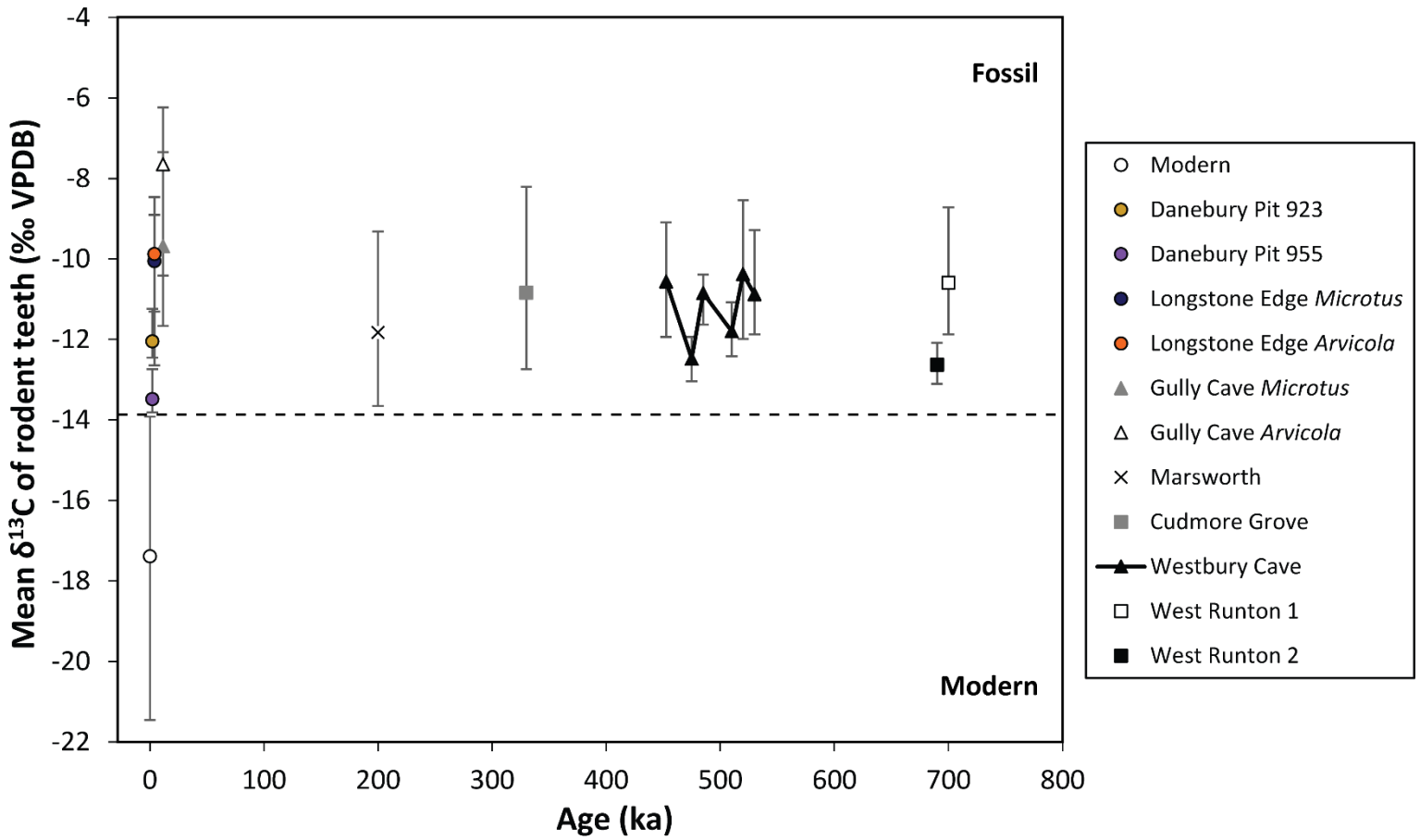

Figure 8.14: *The means and ranges in the carbon isotope values of all rodent teeth analysed in this thesis. The dashed line marks the division between the $\delta^{13}C$ values of the modern and pre-modern (fossil) rodent teeth.*

8.6.2. Temporal variations in the $\delta^{13}C$ values of Quaternary mammalian tissues from Europe

The study undertaken by Hare et al. (2018) is one of the few to have investigated temporal patterns in the $\delta^{13}C$ values of mammalian tissues from Europe. This study used the Voelker-2016a and SJ-2012 models to estimate changes in plant $\delta^{13}C$ values since the Last Glacial Maximum. The modelled $\delta^{13}C_p$ changes were compared with published collagen data from large herbivorous mammals. Hare et al. (2018) found that the Voelker-2016a model provided the closest match for the temporal $\delta^{13}C$ shifts in the faunal record, while the SJ-2012 model overestimated these shifts. Hare et al. (2018) therefore suggested that the SJ-2012 model should not be used to infer changes in the $\delta^{13}C$ values of angiosperms or faunal tissues. Nevertheless, in the present research, the SJ-2012 model was found to provide the most accurate estimates for changes in the $\delta^{13}C$ values of rodent tissues from Britain (Figures 8.11 and 8.12). This implies that the rodent tissues record larger magnitude shifts in $\delta^{13}C_p$ values compared to large mammal tissues.

Hare et al. (2018) also found that changes in MAP in Eurasia between the Last Glacial Maximum and Holocene led to an average shift in the $\delta^{13}C$ of faunal collagen of -0.4 ± 0.88‰. This mean shift is smaller than the residual $\delta^{13}C$ differences calculated from the bioapatite and collagen data from Britain (Table 8.6). This likewise suggests that rodent teeth are more sensitive to variations in plant $\delta^{13}C$ values. This sensitivity has been recognized in previous studies (Hynek et al., 2012; Arppe et al., 2015), and results from the fact that environmental signals recorded in rodent teeth are time-averaged over a period of only a few weeks (Kohn, 2004). As a result, rodent teeth are able to record small temporal and spatial variations in $\delta^{13}C_p$ values. Furthermore, the faunal collagen data used by Hare et al. (2018) are derived from multiple mammalian taxa. Due to inter-taxon differences in dietary preferences and $\varepsilon_{collagen\text{-}diet}$ values, the $\delta^{13}C$ values of collagen from different mammals may vary significantly. This variability is reflected in the large uncertainty (0.88‰) in the estimated mean $\delta^{13}C$ shift resulting from changes in MAP. Therefore, when examining temporal shifts in the $\delta^{13}C$ values of mammalian tissues, analyses should ideally be restricted to a single taxon.

In studies that have investigated changes in the $\delta^{13}C$ values of mammalian collagen from a single taxon (e.g. horse and deer), declines of ~2‰ are observed between the Lateglacial period and the Late Holocene, from values of around -20‰ to -22‰ (Richards & Hedges, 2003; Stevens & Hedges, 2004). Both the magnitude of the $\delta^{13}C$ decline and the absolute $\delta^{13}C$ values of the large mammal collagen are consistent with the rodent collagen data from Britain (Tables 8.3 and 8.5). This demonstrates that the $\delta^{13}C$ values of tissues from different mammalian taxa in Europe are responding to the same environmental factors. As aforementioned, these shifts between the Lateglacial and Late Holocene can be attributed to changes in atmospheric CO_2 and MAP.

8.6.3. Previous research on the $\delta^{13}C$ values of Quaternary rodent teeth

Only one previous study has investigated variations in the $\delta^{13}C$ of rodent dental carbonate during the Late Pleistocene and Holocene. This study found that the $\delta^{13}C$ values of gerbil teeth from North Africa are, on average, approximately 4-7‰ more enriched at ~15,000 yr BP than at the present day (Jeffrey, 2016). These offsets between the modern and fossil teeth are consistent with the offsets observed in the $\delta^{13}C_{rt}$ data from Britain (Figure 8.14; Table 8.1). In addition, the dietary $\delta^{13}C$ values for the fossil gerbil teeth lie towards the maximum $\delta^{13}C$ values for C_3 plants (Jeffrey, 2016). This pattern is also observed in the rodent data from Britain (Figure 8.11). Temporal variations in the $\delta^{13}C$ values of rodent teeth over the past 15,000 years are therefore similar across a geographically widespread area, from Britain to North Africa. These similarities strongly suggest that the $\delta^{13}C$ values of rodent teeth from these regions are responding to the same environmental factors. Jeffrey (2016) primarily attributes the enriched $\delta^{13}C$ values of the fossil teeth to: 1) a higher $\delta^{13}C$ of atmospheric CO_2, and 2) a minor contribution of C_4 plants to the gerbils' diets. The data from Britain likewise suggest that changes in atmospheric CO_2 and diet are the primary factors responsible for the $\delta^{13}C$ offsets between the modern and fossil rodent teeth (Figures 8.11-8.13).

8.6.4. $\delta^{13}C$ offsets between bioapatite and collagen

Most studies on the $\delta^{13}C$ values of Quaternary mammalian tissues have focussed on bone or tooth collagen. Nevertheless, a few studies have analysed both bioapatite and collagen from the same specimen, enabling the $\delta^{13}C$ offset between bioapatite and collagen ($\Delta^{13}C_{apatite\text{-}collagen}$) to be calculated. For example, analyses of large herbivore teeth from the MIS 3 deposits at Kent's Cavern in southwest Britain yielded $\Delta^{13}C_{apatite\text{-}collagen}$ values of between 9 and 11.3‰ (Bocherens et al., 1995). Large herbivore teeth from a MIS 2 cave site in Italy likewise generated $\Delta^{13}C_{apatite\text{-}collagen}$ values of ~9-10‰ (Iacumin et al., 1997). These $\delta^{13}C$ offsets between fossil bioapatite and collagen are larger than the offsets measured in modern large herbivores (~7-8‰) (Sullivan & Krueger, 1981; Lee-Thorp et al., 1989). The $\Delta^{13}C_{apatite\text{-}collagen}$ values measured in the fossil rodent teeth from Britain are also larger than the offsets in modern rodents (Figure 8.13). This consistent pattern across different herbivore taxa therefore supports the suggestion that the $\delta^{13}C$ values of dietary carbohydrates and proteins were different in the past compared to the present day.

8.7. Conclusions

The $\delta^{13}C$ values of rodent teeth from Britain have declined significantly over the past ~2000 years, due to anthropogenic changes in the $\delta^{13}C$ value and partial pressure of atmospheric CO_2. A decrease in the $\delta^{13}C$ value of the rodents' diet is also suggested to have contributed to this decline. Variations in the $\delta^{13}C$ values of rodent bioapatite and collagen between the Lateglacial period and Holocene primarily result from shifts in atmospheric CO_2 and mean annual precipitation. Similar temporal changes are seen in the $\delta^{13}C$ values of bioapatite and collagen from large herbivorous mammals. This suggests that the $\delta^{13}C$ values of rodent tissues from Britain accurately record variations in the environmental factors that influence the $\delta^{13}C$ values of C_3 plants.

The following chapter summarises the key findings of this thesis. The advantages and limitations of the various applications of stable isotopes in rodent dental carbonate for reconstructing Quaternary climate variability are discussed. Suggestions for future research on this topic are also provided.

Stable isotopes in small mammal dental carbonate: investigating their applications for reconstructing Quaternary climate variability

Elizabeth Peneycad

Royal Holloway, University of London

(Volume 2)

Submitted for the degree of Doctor of Philosophy

September 2018

Table of Contents

9. Evaluating the applications of stable isotopes in rodent dental carbonate for reconstructing Quaternary climate variability

9.1. Introduction

This chapter highlights the key findings of this thesis in order to evaluate the advantages and limitations of using stable isotopes in rodent teeth for reconstructing Quaternary climate variability in Britain and further afield. The chapter begins by discussing the various causes of variability in the $\delta^{18}O$ and $\delta^{13}C$ values of rodent teeth. These causes dictate the ways in which the $\delta^{18}O_{rt}$ and $\delta^{13}C_{rt}$ data can be used in palaeoenvironmental reconstructions. Suggestions for further research are provided in light of this review. The wider significance of the findings for the utilization of stable isotopes in rodent bioapatite to answer palaeoenvironmental questions is also discussed.

9.2. Causes of variability in the $\delta^{18}O$ and $\delta^{13}C$ of rodent bioapatite

The first part of this research (Chapter 5) aimed to improve our understanding of the variability in the $\delta^{18}O$ and $\delta^{13}C$ values of rodent bioapatite within and between populations. This aim was addressed by undertaking a modern analogue study on *Microtus agrestis* teeth from barn owl pellets collected at four sites across Britain. The $\delta^{18}O$ and $\delta^{13}C$ values of the teeth were considered to reflect the $\delta^{18}O$ of local meteoric water and the $\delta^{13}C$ of the diet, respectively. Two potential sources of isotope variability within rodent populations were investigated: 1) differences between the mineralization periods of molars and incisors, and 2) variations in the meteoric water and

vegetation sources consumed by different individuals in a population. The data were also compared with published studies in order to identify differences in the patterns of variability between different rodent taxa. In addition, the results of the studies on Quaternary rodent teeth from Britain (Chapters 6-8) have revealed consistencies and differences in the patterns of $\delta^{18}O$ and $\delta^{13}C$ variability between rodent teeth and rodent taxa over time. These patterns will be summarised and discussed in the following section.

The modern analogue study was also undertaken in order to investigate the relationship between the $\delta^{18}O$ of rodent bioapatite and the $\delta^{18}O$ of meteoric water in mid-latitude regions. The objectives of this investigation were to: 1) assess the validity of existing calibrations relating the $\delta^{18}O$ of rodent bioapatite to the $\delta^{18}O$ of local water, and 2) develop a new calibration for rodent dental carbonate that can be applied to the reconstruction of past $\delta^{18}O_{mw}$ values. The application of these calibrations to the $\delta^{18}O$ data from the interglacial sites in Britain (Chapter 6) provided further insight into their validity for reconstructing palaeoclimatic conditions. The key findings and implications of this research are summarised below.

9.2.1. Inter-tooth and intra-population variability

The results of the modern study demonstrate that, in general, differences between the $\delta^{18}O$ values of arvicoline molars and incisors are: 1) relatively small (≤ 1.5‰), 2) not statistically significant, and 3) not systematic within and between individuals within a population. Therefore, differences in the periods of tooth mineralization usually have no appreciable impact on the mean $\delta^{18}O$ values of continuously-growing molars and incisors. These results confirm previous work on dental phosphate from various rodent taxa across Europe (Royer et al., 2013a).

On occasion, however, inter-tooth $\delta^{18}O$ differences are significant (2-4‰) and consistent across a whole rodent population. These differences are attributed to changes in the $\delta^{18}O$ of local meteoric water during the months in which the molars and incisors mineralized. Systematic isotopic offsets such as these have the potential to impact the interpretation of $\delta^{18}O$ data obtained

from fossil teeth of a single type. This is because the mean $\delta^{18}O$ values of the molars or incisors may not provide an accurate representation of the mean $\delta^{18}O$ of meteoric water. Nevertheless, significant $\delta^{18}O$ offsets between molars and incisors from the same taxon are unlikely to be important in fossil rodent assemblages. This is due to the fact that rodent teeth are sampled differently in modern and fossil environments. The teeth from the modern owl pellets represent short intervals of time (a few weeks or months). Consequently, any variations in $\delta^{18}O_{mw}$ values during these intervals will be expressed as systematic offsets between the $\delta^{18}O$ values of the sampled molars and incisors. In contrast, rodent remains within sedimentary deposits often accumulate over hundreds of years. This means that fossil assemblages are likely to comprise a mixture of molars and incisors that mineralized during different months of different years. As a result, inter-tooth $\delta^{18}O$ differences resulting from monthly variations in $\delta^{18}O_{mw}$ will be masked. This means that the average $\delta^{18}O$ values of fossil arvicoline molars and incisors can both provide accurate values for the average $\delta^{18}O$ of local meteoric water.

In distinct contrast, the $\delta^{13}C$ values of arvicoline molars and incisors are significantly (1-4‰) and systematically offset in both modern and fossil populations from Northwest Europe. In modern *M. agrestis* populations from Britain, and an *A. terrestris* population from northwest Germany (Gehler et al., 2012), the $\delta^{13}C$ values of the incisors are significantly and, in most cases, consistently depleted compared to the $\delta^{13}C$ values of the molars. Conversely, in the fossil rodent populations from Longstone Edge and Gully Cave in Britain, the $\delta^{13}C$ values of the incisors are significantly and consistently enriched compared to the molars. These results show that the $\delta^{13}C$ value of a vole tooth is dependent on the tooth type. These inter-tooth $\delta^{13}C$ offsets are suggested to result from seasonal variations in the rodents' diets, combined with the differences between the mineralization periods of molars and incisors. Intra-population ranges in $\delta^{13}C_{rt}$ values are also significant (~2-5‰). Variations in diet therefore have an important influence on the $\delta^{13}C$ values of rodent teeth. This means that in order to estimate the average $\delta^{13}C$ of the diet, analyses need to be undertaken on both molars and incisors.

The variability in $\delta^{18}O_{rt}$ values between individuals is also significant, and can be explained by spatial and temporal variations in the $\delta^{18}O$ values of

local drinking water sources consumed by rodents. The intra-population variability in the $\delta^{18}O$ values of modern *M. agrestis* teeth is relatively consistent at ~2-3‰. The standard deviations on the mean $\delta^{18}O_{rt}$ values for the *M. agrestis* populations are also relatively narrow (< 1‰). Therefore, provided that sufficient numbers of rodent teeth are analysed, the mean $\delta^{18}O$ value of meteoric water can be estimated from the mean $\delta^{18}O$ of rodent bioapatite to within ± 0.5‰.

9.2.2. Inter-species differences

The data from the modern sites (Chapter 5), Gully Cave (Chapter 7), and Longstone Edge (Chapter 8) show that the patterns of variability in the isotope values of rodent teeth also differ between taxa. In modern and fossil environments, the mean $\delta^{18}O$ values of *Microtus* teeth are typically enriched compared to the mean $\delta^{18}O$ values of *Arvicola* teeth from the same site (Gehler et al., 2012; Royer et al., 2013a; Royer et al., 2014). There is, therefore, a clear and systematic inter-taxon offset in the $\delta^{18}O$ of meteoric water recorded within *Microtus* and *Arvicola* teeth. This offset has been attributed to differences in the ecological preferences of the rodent taxa. Members of the genus *Microtus* generally inhabit open grassland environments, where isotopically-enriched waters derived from plants and small water bodies are likely to contribute significantly to the total ingested water. Conversely, *A. terrestris* generally lives near to flowing streams, which are likely to have average $\delta^{18}O$ values similar to the mean annual $\delta^{18}O_{mw}$. The consistent offset observed between the $\delta^{18}O$ values of *Microtus* and *Arvicola* teeth therefore suggests that species ecology plays a key role in the ways in which the $\delta^{18}O$ values of rodent teeth record the $\delta^{18}O$ of local meteoric water. This has implications for the development and utilization of modern calibrations between $\delta^{18}O_{rt}$ and $\delta^{18}O_{mw}$ (see following section).

Furthermore, inter-tooth differences in $\delta^{18}O$ and $\delta^{13}C$ values are frequently greater in *Microtus* than in *Arvicola*. This is due to the shorter mineralization periods and resultant lesser time-averaging of the environmental signals recorded within *Microtus* teeth (Royer et al., 2013a).

The $\delta^{18}O$ values of *Microtus* teeth are therefore potentially useful for reconstructing the seasonal range in $\delta^{18}O_{mw}$ values (Royer et al., 2013a). Indeed, the increased ranges in the $\delta^{18}O$ values of the rodent teeth from Westbury Cave and Gully Cave are suggested to result from a more continental climate. Nevertheless, the increased variability in the $\delta^{18}O$ values of *Microtus* teeth may reduce the precision with which mean $\delta^{18}O_{mw}$ values can be estimated from these teeth. This issue is clearly evident in the results from Gully Cave (Figure 7.14). Therefore, in order to generate precise reconstructions of past $\delta^{18}O_{mw}$ values from *Microtus* teeth, large $\delta^{18}O_{rt}$ datasets are required.

9.2.3. Relationship between the $\delta^{18}O$ of rodent bioapatite and $\delta^{18}O$ of meteoric water

Although $\delta^{18}O_{rt}$ values within modern populations are variable, a strong spatial relationship exists between the mean $\delta^{18}O_{rt}$ of a population and the mean $\delta^{18}O$ of surface meteoric water. For the three modern sites in England (Somerset, Surrey and East Yorkshire), the mean $\delta^{18}O$ values of the rodent teeth parallel the spatial pattern in the mean $\delta^{18}O$ of meteoric water across Britain. This is due to the fact that rodents obtain their drinking water from local surface water sources. However, the data from Perthshire deviate from the relationship between the mean $\delta^{18}O_{rt}$ and mean $\delta^{18}O_{mw}$ in England. This is likely due to the influence of isotopically-depleted spring snowmelt on the $\delta^{18}O$ values of the water sources that were sampled from this area, plus a summer bias in the mineralization of the sampled rodent teeth.

While the mean $\delta^{18}O$ values of the rodent teeth also parallel the modelled $\delta^{18}O$ values of precipitation ($\delta^{18}O_{pt}$), the relationship between $\delta^{18}O_{rt}$ and $\delta^{18}O_{pt}$ differs from the relationship between $\delta^{18}O_{rt}$ and $\delta^{18}O_{mw}$. This difference is suggested to result from two factors. Firstly, the modelled $\delta^{18}O$ values of precipitation, and especially the $\delta^{18}O_{pt}$ value for Perthshire, are inaccurate and imprecise due to: 1) the poor spatial resolution of precipitation measurements in Britain, upon which the modelled $\delta^{18}O_{pt}$ values are based, and 2) the lack of consideration for rainout effects in the $\delta^{18}O_{pt}$ model.

Secondly, the mean $\delta^{18}O$ values of surface water sources are typically enriched compared to the mean $\delta^{18}O$ of precipitation, and the magnitude of this enrichment is likely to vary spatially. As a result, the slope of the spatial relationship between $\delta^{18}O_{rt}$ and $\delta^{18}O_{mw}$ will differ from the spatial relationship between $\delta^{18}O_{rt}$ and $\delta^{18}O_{pt}$.

Despite this, the slope of the regression between the $\delta^{18}O$ of *M. agrestis* dental carbonate and the $\delta^{18}O$ of surface meteoric water in England (1.36 ± 0.11) is consistent, within uncertainties, with the slopes of published regressions between the $\delta^{18}O$ of vole phosphate and the $\delta^{18}O$ of precipitation in Northwest Europe (1.14 ± 0.18) (Longinelli et al., 2003; Royer et al., 2013a). In addition, the differences between the y-intercept coefficients for the calibrations based on carbonate and phosphate in rodent bioapatite (7.9-11.2‰) are consistent with the offsets between the $\delta^{18}O$ values of carbonate and phosphate measured in modern rodents (8.5-11.4‰). This indicates that the relationship between the $\delta^{18}O$ of rodent bioapatite and the $\delta^{18}O$ of local water is relatively consistent for mid-latitude regions.

The higher slope coefficient for the regression based on *M. agrestis* tooth carbonate is suggested to relate to differences in the water data used to develop the regressions (meteoric water vs. precipitation), plus possible inter-species differences in the ways in which $\delta^{18}O_{mw}$ is recorded within rodent bioapatite. As aforementioned, consistent inter-species $\delta^{18}O_{rt}$ offsets have been observed between *Microtus* and *Arvicola*. It is therefore highly likely that the relationship between $\delta^{18}O_{rt}$ and $\delta^{18}O_{mw}$ may differ between other rodent taxa (e.g. Velivetskaya et al., 2014). Since *Microtus* is likely to consume a proportion of isotopically-enriched water sources, the mean $\delta^{18}O$ of local meteoric water may not provide an accurate value for the mean $\delta^{18}O$ of the drinking water ($\delta^{18}O_{dw}$) in this taxon. As a consequence, the slope and y-intercept coefficients of the regression between $\delta^{18}O_{rt}$ and $\delta^{18}O_{dw}$ in *Microtus* may differ slightly from the coefficients of the modern regression developed in Chapter 5 (Equation 5.8). Despite this, Longinelli et al. (2003) found that the $\delta^{18}O$ values of *Microtus* and *Arvicola* bioapatite from Europe have comparable relationships with the $\delta^{18}O$ of precipitation. Therefore, differences between *Microtus* and *Arvicola* in the relationship between $\delta^{18}O_{rt}$ and $\delta^{18}O_{dw}$ are likely

to be 1) fairly minor, and 2) encompassed by the uncertainties in the fit of the regression line described by Equation 5.8.

This suggestion is supported by the $\delta^{18}O_{mw}$ reconstructions generated for the three Middle Pleistocene interglacial localities in Britain (Chapter 6). Past $\delta^{18}O_{mw}$ values were estimated by substituting $\delta^{18}O$ data from *Mimomys savini, Arvicola cantiana,* and *Microtus* sp. teeth into Equation 5.8. The $\delta^{18}O_{mw}$ values for all three sites are consistent with the palaeoclimate evidence from coeval proxies. In contrast, the Longinelli et al. (2003) and Royer et al. (2013a) equations underestimated the likely mean $\delta^{18}O$ of meteoric water at Cudmore Grove. This is due to the fact that these equations are based upon $\delta^{18}O$ data for precipitation rather than surface meteoric water. This shows that modern calibrations between $\delta^{18}O_{rt}$ and $\delta^{18}O_{pt}$ are unsuitable for the reconstruction of past $\delta^{18}O_{mw}$ values. The Navarro et al. (2004) equation, which was modified by Ruddy (2005) to relate the mean $\delta^{18}O_{rt}$ to the mean $\delta^{18}O$ of summer precipitation, produced $\delta^{18}O_{pt}$ values consistent with the mean $\delta^{18}O$ of meteoric water. However, the mean $\delta^{18}O$ of summer precipitation has not necessarily been comparable to the mean $\delta^{18}O_{mw}$ throughout the Quaternary period. Therefore, the modified Navarro et al. (2004) equation is also not suitable for reconstructing the past $\delta^{18}O$ of meteoric water. The implications of these findings are discussed further in the next section.

9.2.4. Wider implications

9.2.4.1. Sampling rodent teeth for isotopic analysis

Due to the variability in the $\delta^{18}O$ and $\delta^{13}C$ values of rodent teeth within a population, ≥ 5 fossil teeth should be sampled from each sedimentary unit for isotopic analysis (Royer et al., 2013a). This is to ensure that the mean $\delta^{18}O_{rt}$ and $\delta^{13}C_{rt}$ values provide accurate and precise representations of the average palaeoenvironmental conditions during the period in which the sedimentary unit was deposited. The results for Cudmore Grove, which are based on dental carbonate data from only 4 teeth, show that reliable $\delta^{18}O_{mw}$ reconstructions can be generated from analyses of small numbers of teeth. Nevertheless, the uncertainties on the calculated mean $\delta^{18}O_{mw}$ for this site are relatively large.

Additionally, $\delta^{18}O_{mw}$ reconstructions based on limited data are less likely to be accurate, as $\delta^{18}O_{rt}$ variability has a greater influence on the mean $\delta^{18}O_{mw}$ value. As a consequence, mean $\delta^{18}O_{mw}$ values calculated using data from < 5 rodent teeth per sedimentary unit should be interpreted with caution. For example, in the study by Navarro et al. (2004), ≤ 4 teeth were sampled per sedimentary level through the La Baume de Gigny cave sequence in France. Although the fluctuations in $\delta^{18}O_{rt}$ values through the sequence may reflect abrupt climatic changes, these fluctuations could also reflect the natural intra-population variability in the $\delta^{18}O$ values of the rodent teeth within each sedimentary layer. Consequently, the validity of the climatic interpretations made by Navarro et al. (2004) is debatable.

The modern study also indicates that $\delta^{18}O_{mw}$ reconstructions can be generated from the $\delta^{18}O$ values of both arvicoline molars and incisors. Nevertheless, in order to minimize the variability resulting from inter-tooth $\delta^{18}O$ differences, analyses should ideally be restricted to a single tooth type. On the other hand, when sampling arvicoline teeth for carbon isotope analyses, data from both the molars and incisors may be beneficial. This is discussed further in section 9.2.4.3.

Analyses of rodent teeth for the purpose of reconstructing temporal changes in $\delta^{18}O_{mw}$ values should also be restricted to a single genus. This is because the ecological preferences of rodents have a key influence on the food and drinking water sources that they consume, and the resultant mean $\delta^{18}O_{mw}$ recorded within their teeth. Inter-species differences in the durations of tooth mineralization may also result in variations in $\delta^{18}O_{rt}$ values between taxa. Nevertheless, these inter-species differences may present opportunities for the reconstruction of specific environmental parameters during the Quaternary period. These opportunities are discussed in section 9.2.4.3.

9.2.4.2. Regressions relating the $\delta^{18}O$ of rodent bioapatite to the $\delta^{18}O$ of local water

Intra-population and inter-taxon variations in the $\delta^{18}O$ values of rodent teeth have significant implications for the development and utilization of modern

calibrations between $\delta^{18}O_{rt}$ and $\delta^{18}O_{mw}$. The results of the modern analogue study indicate that the mean $\delta^{18}O_{rt}$ of a population is correlated with the mean $\delta^{18}O$ of meteoric water. As mentioned, in order to obtain an accurate and precise mean $\delta^{18}O_{rt}$ value for a specific site, ≥ 5 teeth must be sampled. Therefore, calibrations that are largely based upon analyses of only 1-2 teeth per site are likely to be imprecise (i.e. Navarro et al., 2004; Royer et al., 2013a).

Furthermore, in all published studies on rodent bioapatite from Europe, the mean $\delta^{18}O$ of bioapatite has been assumed to correlate with the mean $\delta^{18}O$ of local water in the same way across all rodent taxa (Longinelli et al., 2003; Navarro et al., 2004; Royer et al., 2013a). Nevertheless, due to ecological differences, the mean $\delta^{18}O$ of local water is unlikely to provide an accurate value for the mean $\delta^{18}O$ values of the drinking water sources consumed by every taxon within a rodent community. These ecological differences are acknowledged by Navarro et al. (2004) and Royer et al. (2013a), yet their calibrations are based upon data from multiple (8-10) rodent species. Any inter-taxon differences in the relationship between $\delta^{18}O_{rt}$ and $\delta^{18}O_{dw}$ may have reduced the accuracy and precision of these calibrations. In addition, these calibrations may not be reliable for reconstructing $\delta^{18}O_{dw}$ values for individual taxa. Both of these calibrations are also based on data from pooled samples of teeth. Due to inter-tooth and inter-individual $\delta^{18}O$ variability, the average $\delta^{18}O_{rt}$ of a pooled sample may not necessarily provide an accurate value for the mean $\delta^{18}O_{rt}$ of a population. Consequently, due to the issues with the methods used by Navarro et al. (2004) and Royer et al. (2013a) in the development of their calibrations, the validity of these calibrations may be called into question.

Moreover, the calibrations of Longinelli et al. (2003) and Royer et al. (2013a) are based upon modelled mean annual $\delta^{18}O$ values of precipitation. As aforementioned, modelled $\delta^{18}O_{pt}$ values are sometimes unreliable. In addition, rodents consume surface water sources, which due to the influence of evaporation, are typically enriched compared to the mean $\delta^{18}O$ of precipitation. As a result, calibrations between $\delta^{18}O_{rt}$ and $\delta^{18}O_{pt}$ underestimate the mean $\delta^{18}O$ of rodent drinking water. This is clearly evident in the results for Cudmore Grove. Despite this, the Longinelli et al. (2003) and Royer et al. (2013a) calibrations both provide acceptable values for the likely mean $\delta^{18}O_{pt}$

at this site. However, due to the aforementioned issues regarding the sampling methods used by Royer et al. (2013a), the Longinelli et al. (2003) calibration is suggested here to be the most valid. This is because this calibration was developed using multiple individually-sampled rodent specimens from a limited number of taxa (*Microtus*, *Arvicola* and *Apodemus*). Therefore, in studies aiming to reconstruct the mean $\delta^{18}O$ of precipitation from the $\delta^{18}O$ of arvicoline phosphate, the Longinelli et al. (2003) equation should be used. Conversely, for applications requiring the reconstruction of the past $\delta^{18}O$ of rodent drinking water (e.g. the coupled isotope approach), a calibration based on $\delta^{18}O_{mw}$ data, such as Equation 5.8, should be used.

9.2.4.3. Applications of $\delta^{18}O$ and $\delta^{13}C$ in rodent bioapatite for palaeoenvironmental reconstructions

The modern relationship between the mean $\delta^{18}O$ of rodent bioapatite and mean $\delta^{18}O$ of meteoric water indicates that the $\delta^{18}O$ values of fossil rodent bioapatite can potentially be used to reconstruct past $\delta^{18}O_{mw}$ compositions. Additionally, inter-species and intra-population variations in $\delta^{18}O_{rt}$ values can potentially be utilized to understand $\delta^{18}O_{mw}$ variations within past environments. For example, in taxa in which evaporatively-enriched water sources notably contribute to the total water intake (e.g. selected species of *Microtus*), $\delta^{18}O_{rt}$ values may provide an indication of relative humidity. Moreover, in rodents with relatively short mineralization periods, $\delta^{18}O_{rt}$ values may provide a record of short-term $\delta^{18}O_{mw}$ variability. These applications are discussed further in Sections 9.3 and 9.4.

The consistent inter-tooth $\delta^{13}C$ offsets observed in the modern and fossil voles also have significant implications for the applications of the $\delta^{13}C$ values of rodent bioapatite for reconstructing dietary changes. Firstly, systematic differences between the $\delta^{13}C$ values of fossil molars and incisors offer an opportunity for examining changes in the seasonality of the diet, or the seasonality of tooth mineralization. For example, the inter-tooth $\delta^{13}C$ patterns in the modern voles were suggested to relate to the diets during the seasons in which the teeth mineralized. The enriched $\delta^{13}C$ values of the molars

correspond to a winter-spring diet dominated by grasses, whereas the depleted incisor values reflect a diverse spring-summer diet. The opposing inter-tooth patterns in the $\delta^{13}C$ data from Longstone Edge and Gully Cave may suggest that the fossil molars mineralized during summer-autumn, whereas the incisors mineralized during autumn-winter. Alternatively, the diets consumed by the rodents during each season may have differed in the past. This shows that analyses of both molars and incisors can provide valuable information on seasonal dietary changes. However, this potential application could be limited by the difficulties in identifying rodent incisors to species or genus level. Differences in diets between species may contribute to differences between the $\delta^{13}C$ values of molars and incisors within fossil assemblages. Therefore, analyses of rodent molars and incisors ideally need to be restricted to a single taxon.

Secondly, in studies aiming to investigate variations in rodent diets or local vegetation over geological time, the season of tooth mineralization must be taken into consideration. Indeed, previous studies have primarily restricted analyses to single tooth types (first molars or incisors) in order to minimize the influence of inter-tooth isotopic variation on results (Hynek et al., 2012; Kimura et al., 2013; Arppe et al., 2015). Nevertheless, the results from the present research demonstrate that temporal shifts in the season of tooth mineralization or the seasonal composition of the diet can result in shifts in $\delta^{13}C_{rt}$ values that are independent of environmental fluctuations in vegetation or climate. Thus, even if analyses are restricted to a single tooth type, potential shifts in rodent ecology should be considered in the interpretation of the results. Moreover, where possible, analyses should be undertaken on both molars and incisors in order to eliminate seasonal dietary shifts as a contributor to temporal shifts in $\delta^{13}C_{rt}$ values.

9.2.5. Further work

The results of the modern study clearly demonstrate that further research is greatly needed on the relationship between the $\delta^{18}O$ of rodent bioapatite and the $\delta^{18}O$ of local water. In particular, additional data are needed to investigate

how this relationship differs between rodent taxa. This would require analyses to be undertaken on ≥ 5 teeth per taxon and per site across a range in $\delta^{18}O$ values of meteoric water. Since *Arvicola* and *Microtus* teeth are especially abundant in Quaternary fossil assemblages in Europe, additional analyses of modern teeth from these taxa would be highly beneficial for developing calibrations for palaeoenvironmental research. Further analyses on *M. agrestis* dental carbonate and corresponding $\delta^{18}O$ values of surface waters would also aid in assessing the reliability of the calibration generated in this thesis. The contributions of isotopically-enriched plant water sources to the $\delta^{18}O$ values of *Microtus* teeth also need to be assessed.

In addition, a better understanding is needed regarding the ways in which $\delta^{13}C_{rt}$ values vary in response to changing diets. Carbon isotope analyses of the key vegetation sources that modern rodents likely consume, plus corresponding analyses of rodent teeth, may help to address this issue.

9.3. $\delta^{18}O$ of rodent dental carbonate as a palaeoclimate proxy

In this thesis, the $\delta^{18}O$ values of fossil rodent teeth have been used in two different applications for reconstructing palaeoclimatic conditions in Britain: 1) coupling the mean $\delta^{18}O$ of fossil rodent teeth with the mean $\delta^{18}O$ of coeval mollusc shells to quantify mean summer temperatures during interglacial stages (Chapter 6), and 2) using the $\delta^{18}O$ values of rodent teeth from stratified cave sequences to reconstruct millennial-scale climatic fluctuations (Chapter 7). The key outcomes of these applications, and the implications for further uses of these methods in palaeoenvironmental research, are discussed in this section.

9.3.1. Coupled isotope approach

The results of Chapter 6 demonstrate that the coupled isotope approach can be successfully used to generate reliable mean summer palaeotemperatures for Quaternary interglacial stages. For both West Runton and Cudmore Grove, the coupled isotope approach produced mean summer temperatures that are

consistent, within uncertainties, with palaeotemperature estimates reconstructed using the palaeoecological proxies from these sites. On the other hand, the isotope-based temperature estimates for Marsworth are slightly lower than indicated by the palaeoecological proxies. This discrepancy is attributed to differences in the $\delta^{18}O$ values of meteoric water recorded by the rodent teeth and mollusc shells. *Galba truncatula* generally lives in small water bodies, but is also found outside of water in wet muddy patches (Ellis, 1926). This mollusc therefore lives in environments that are susceptible to evaporation, and as a result, the $\delta^{18}O$ values of the shells from Marsworth are significantly enriched. It was therefore concluded that only mollusc taxa that live permanently submerged within water should be utilized for the coupled isotope approach.

The results also emphasize another key requirement for the application of the coupled isotope approach: the fossil rodent teeth and mollusc shells must be coeval. Fossil remains from sedimentary layers that have accumulated rapidly and in a low-energy depositional environment are therefore the most suitable for use in this approach. This requirement means that palaeotemperature reconstructions generated from the coupled $\delta^{18}O$ values of rodent teeth and aquatic mollusc shells are likely to be the most reliable in low-energy fluvial contexts.

Despite this, the coupled isotope approach offers an additional tool for generating quantitative palaeotemperature estimates for interglacial stages. Multi-proxy palaeotemperature reconstructions for terrestrial areas are important for understanding the variability in interglacial climates during the Quaternary period (e.g. Candy et al., 2016). For example, quantitative temperature data have proved valuable for investigating the expression of the Mid-Brunhes Event (MBE) in terrestrial records (Candy et al., 2010; Blain et al., 2012; Candy & McClymont, 2013). The MBE refers to a transition that occurred between MIS 13 and MIS 11, from relatively cooler interglacials, to interglacials that were characterised by enhanced warmth (Jansen et al., 1986; Hodell et al., 2003; Tzedakis et al., 2009). However, proxy records from the North Atlantic region provide no evidence for this shift in the intensity of interglacial warmth (Candy & McClymont, 2013). This suggests that the expression of the MBE is spatially variable. The utilization of the coupled

isotope approach for reconstructing interglacial temperatures can, therefore, potentially provide additional palaeoclimate data to explore these spatial patterns in the MBE in greater detail.

9.3.2. $\delta^{18}O$ of rodent teeth from caves

The results from Westbury Cave and Gully Cave show that the $\delta^{18}O$ values of rodent teeth from stratified cave sequences can provide useful and reliable records of palaeoclimate variability. At both sites, the stratigraphic patterns in the $\delta^{18}O$ values of the rodent teeth replicate the known climatic fluctuations that occurred during the periods in which the cave sequences accumulated. The $\delta^{18}O_{rt}$ data from Westbury Cave record two temperate peaks separated by a cold interval. These results are consistent with the ecological interpretations of the rodent assemblages from Westbury Cave. Moreover, the peaks and troughs in the $\delta^{18}O_{rt}$ data can be correlated with the interglacial sub-stages of MIS 13. The relative magnitudes of the $\delta^{18}O_{rt}$ peaks, whereby the second peak is higher than the first, are consistent with proxy records that suggest MIS 13a was warmer than MIS 13c (Figure 7.7).

Similarly, the $\delta^{18}O$ values of the *Microtus* and *Arvicola* teeth from Gully Cave parallel the millennial-scale climatic fluctuations during the Lateglacial-Holocene period (Figure 7.15). The Gully Cave data also replicate the distinctive regional patterns in climate during the Younger Dryas and early Holocene intervals. The bipartite climatic structure of the Younger Dryas is clearly observed in the mean $\delta^{18}O$ values of the rodent teeth dating to the Loch Lomond Stadial in Britain. Furthermore, the $\delta^{18}O_{rt}$ values during the Holocene are relatively depleted compared to values during the Lateglacial Interstadial. This pattern is notably consistent with lake records from Britain, and is thought to result from a shift in the seasonality of precipitation during the early Holocene (Candy et al., 2015). Therefore, both the hemispheric and regional environmental patterns are accurately reproduced by the $\delta^{18}O_{rt}$ data from Gully Cave.

However, at both cave sites, the $\delta^{18}O$ values of the *Microtus* teeth that correspond to the stadial and glacial stages are consistently more enriched

than expected for intervals characterised by low mean air temperatures. This pattern is suggested to result from: 1) a summer bias in rodent predation during the coldest phases of stadials and glacials, combined with 2) the evaporative enrichment of drinking water sources under arid glacial conditions. The first of these factors relates to the influence of snow cover in limiting the frequency of predation during the winter months. As a result, fossil rodent assemblages from cold stages are likely to be dominated by individuals predated during the warmest months of the year. Consequently, the mean $\delta^{18}O_{rt}$ reflects enriched $\delta^{18}O_{mw}$ values during summer.

Aridity can also cause an enrichment in the $\delta^{18}O$ of surface water. This aridity is reflected in the $\delta^{18}O_{mw}$ values reconstructed using the *Microtus* teeth from Gully Cave, which are highly enriched compared to modern meteoric water sources in southern Britain. These results therefore support the suggestion that *Microtus* consumes water sources that are sensitive to evaporation. The influence of evaporation on *Microtus* $\delta^{18}O_{rt}$ values is likely to be particularly significant during arid glacial and stadial stages. Indeed, anomalously enriched $\delta^{18}O_{rt}$ values are likewise seen in modern rodents from cold, mountainous areas. For example, rodents from the Pyrenean Mountains have $\delta^{18}O_{rt}$ values that a more enriched than predicted by the depleted $\delta^{18}O$ values of local precipitation (Royer et al., 2013a). This indicates that factors other than temperature can have an important influence on the mean $\delta^{18}O$ values of rodent teeth during cold stages. Interpretations of $\delta^{18}O_{rt}$ data from glacial and stadial stages should therefore consider the potential influences of changing temperature, humidity, and predation on isotopic values.

In contrast, however, the $\delta^{18}O$ values of the *Arvicola* teeth from Gully Cave are consistent with a climate cooler than present throughout the Lateglacial period. This shows that the $\delta^{18}O$ values of the water sources consumed by *Arvicola* are not significantly influenced by evaporative enrichment. Consequently, the absolute $\delta^{18}O$ values of *Arvicola* teeth can provide an accurate reflection of the mean $\delta^{18}O$ of precipitation during cold stages.

Despite the limitations with using the $\delta^{18}O$ values of *Microtus* teeth as a palaeoclimate proxy during cold stages, the results from Westbury Cave and Gully Cave show that coherent records of temporal climatic fluctuations can

be generated from the mean $\delta^{18}O$ values of *Microtus* teeth from cave sequences. This application therefore has the potential to provide essential new climate records for cave sites in Europe. Moreover, $\delta^{18}O_{rt}$ data from caves can be potentially used to examine the structure of millennial-scale climatic shifts in terrestrial areas. For example, the data from Gully Cave show a bipartite climatic structure during the Loch Lomond Stadial. Previously, this structure has primarily been studied using marine cores from the North Atlantic (Jennings et al., 2006), and lake records from continental Europe (Bakke et al., 2009). However, the preservation of the mid-Younger Dryas transition in the data from Gully Cave demonstrates that short-term climatic shifts can potentially be examined using the $\delta^{18}O$ values of rodent teeth from other cave sequences in Europe. Nonetheless, the use of this proxy requires an understanding of the ecological, taphonomic and chronological contexts of the fossil rodent assemblages. As demonstrated by the data from Gully Cave, inter-species differences in rodent ecology and in the processes involved in the accumulation of rodent remains can affect the absolute $\delta^{18}O$ values of samples of fossil rodent teeth. Consequently, studies intending to use the $\delta^{18}O$ values of rodent teeth from caves for palaeoclimate reconstructions should, where possible: 1) focus on rodent taxa that can reliably record the mean $\delta^{18}O$ of precipitation (e.g. *Arvicola*), and 2) investigate the taphonomy of the rodent remains in order to understand the processes by which the fossil assemblages accumulated.

9.3.3. Further work

The results from the cave sites show that while *Microtus* teeth can provide useful records for examining the structure of millennial-scale climatic fluctuations, *Arvicola* teeth offer great potential as proxies for the absolute $\delta^{18}O$ values of precipitation during glacial stages. Further analyses of *Arvicola* teeth from cave deposits dating to the Lateglacial period would be beneficial for examining whether this suggestion is valid for various sites across Northwest Europe. The potential use of the $\delta^{18}O$ of *Microtus* teeth as a proxy for relatively humidity during cold stages also requires further exploration.

9.4. Reconstructing the $\delta^{18}O$ of meteoric water for Quaternary climate stages

In mid-latitude regions, the $\delta^{18}O$ of precipitation is linearly correlated with mean annual air temperature (Dansgaard, 1964; Rozanski et al., 1993). This modern relationship is often utilized to quantify past temperatures using $\delta^{18}O_{mw}$ values reconstructed from mammalian teeth (Arppe & Karhu, 2006; Tütken et al., 2007; Bernard et al., 2009). These reconstructions rely on the assumption that the spatial relationship between $\delta^{18}O_{pt}$ and temperature was the same in the past as the present day (Fricke & O'Neil, 1999). However, this assumption is not necessarily valid. For instance, temporal changes in atmospheric circulation patterns may affect the sources and transport pathways of moisture to mid-latitude regions, which can influence the resultant $\delta^{18}O$ of precipitation (Fricke & O'Neil, 1999). Consequently, determining the spatial and temporal variations in the $\delta^{18}O$ of precipitation is essential for assessing whether the assumption of a constant $\delta^{18}O_{pt}$-temperature relationship is valid. This is also important for testing and improving simulations of global $\delta^{18}O_{pt}$ patterns, generated using isotope-based General Circulation Models. Proxy reconstructions of the past $\delta^{18}O$ values of meteoric water have proven essential for this purpose (Jouzel et al., 2000; Jasechko et al., 2015). The mean $\delta^{18}O$ values of rodent teeth, which are a proxy for the mean $\delta^{18}O$ of meteoric water, therefore have the potential to provide an important contribution to our understanding of $\delta^{18}O_{pt}$ variability.

The review in Section 9.3 illustrates that the $\delta^{18}O$ values of rodent teeth from interglacial stages reliably record the mean $\delta^{18}O$ of meteoric water fractionated under mean air temperatures. Therefore, for interglacial stages, mean $\delta^{18}O_{rt}$ is a predictable proxy for $\delta^{18}O_{pt}$ and temperature. Conversely, for glacial and stadial stages, the $\delta^{18}O$ values of *Microtus* teeth are relatively enriched due to a seasonal bias in predation plus aridity. Consequently, the $\delta^{18}O$ values of *Microtus* teeth from cold stages often reflect changes that are independent of air temperature. On the other hand, the $\delta^{18}O$ values of *Arvicola* teeth can potentially provide a reliable proxy for the mean $\delta^{18}O$ of precipitation and mean air temperatures during interstadial and stadial stages. Therefore, in future studies aiming to reconstruct reliable $\delta^{18}O$ values of precipitation,

analyses should focus on: 1) *Microtus* or *Arvicola* teeth from interglacial stages, and 2) *Arvicola* teeth from interstadial and stadial stages.

In addition to generating $\delta^{18}O_{mw}$ values for reconstructing palaeotemperatures, the $\delta^{18}O$ values of Quaternary rodent teeth can also provide valuable information on changes in humidity and surface hydrology. For example, the enriched $\delta^{18}O$ values of the *Microtus* teeth during the Lateglacial period at Gully Cave provide an indication of relatively humidity. Moreover, the $\delta^{18}O$ values of the rodent teeth from the different sections at West Runton record an increase in the $\delta^{18}O$ of the water body over time, which cannot be explained by changes in temperature. These shifts in $\delta^{18}O_{mw}$ relate to the gradual infilling and evaporation of the water body. This shows that $\delta^{18}O_{rt}$ values can be used to understand local changes in hydrology, as well as regional changes in humidity resulting from climatic variations.

9.5. Palaeoenvironmental variability recorded in the $\delta^{13}C$ values of rodent teeth

In Chapter 8, the $\delta^{13}C$ values of rodent teeth from Britain were demonstrated to have undergone a significant (5-8‰) shift within the past 2000 years. This shift is suggested to result from the recent anthropogenic changes in the $\delta^{13}C$ value and partial pressure of atmospheric CO_2, plus a change in the compositions of the rodents' diets. Decreases in the $\delta^{13}C$ values of rodent bone collagen and rodent teeth between the Lateglacial Interstadial and the Late Holocene are consistent with the magnitudes of $\delta^{13}C$ changes resulting from an increase in pCO_2 and mean annual precipitation. This shows that the $\delta^{13}C$ values of rodent tissues can provide key information on temporal changes in environmental parameters.

Despite this, the results of this thesis have also highlighted that several unanswered questions remain with regards to the relationships between the $\delta^{13}C$ values of Quaternary rodent teeth and rodent diets. The $\delta^{13}C$ values of pre-modern rodent teeth from both Britain and North Africa suggest that past rodents consumed highly enriched C_3 diets. Conversely, the $\delta^{13}C$ values of pre-modern rodent collagen are consistent with an average C_3 diet. As a result,

$\delta^{13}C$ offsets between bioapatite and collagen are much larger than expected for rodents consuming a typical C_3 diet. This was tentatively suggested to result from the consumption of C_3 energy sources with enriched $\delta^{13}C$ values, and protein sources with average $\delta^{13}C$ values. The possible mechanisms responsible for this offset between the $\delta^{13}C$ values of the energy and protein sources in the diet are currently unclear. Moreover, the data suggest that the shift in the diet must have occurred within the past 2000 years. This implies that the cause of the recent decline in the $\delta^{13}C$ of the diet may be related to anthropogenic impacts on the $\delta^{13}C$ values of the dietary sources.

In order to test these ideas, further research is critically needed. To assess the timing and causes of the recent decline in $\delta^{13}C_{rt}$ values, analyses need to be undertaken on teeth that pre-date the recent anthropogenic changes in atmospheric CO_2, but are younger than 2000 years old. Teeth that date to the 17^{th}-18^{th} century would be ideal for this purpose, as this is around the time of the onset of the atmospheric CO_2 changes. Collagen $\delta^{13}C$ data are also needed from modern rodents in Northwest Europe, in order to assess whether the differences between the $\delta^{13}C$ values of modern and fossil rodent bioapatite are replicated in the $\delta^{13}C$ values of bone collagen. Finally, carbon isotope data are needed from modern and fossil rodent tissues in other areas of Europe, in order to establish whether the temporal $\delta^{13}C$ shifts observed in Britain and North Africa are consistent across different regions of the world. This is essential for: 1) understanding how recent anthropogenic changes in the isotopic baseline have influenced the $\delta^{13}C$ values of rodent tissues, and 2) making accurate palaeoenvironmental interpretations of the $\delta^{13}C$ values of fossil rodent bioapatite.

9.6. Summary

The results of this thesis have demonstrated that the $\delta^{18}O$ and $\delta^{13}C$ values of rodent dental carbonate can be reliably and valuably utilized in a range of applications for the reconstruction of Quaternary climate variability. The $\delta^{18}O$ values of rodent teeth can be applied to the reconstruction of the $\delta^{18}O$ of meteoric water and summer temperatures during interglacial stages. These

reconstructions can potentially be used to: 1) address questions about the spatial variability in the climatic expression of interglacial stages in terrestrial areas, and 2) understand temporal and spatial variations in the $\delta^{18}O$ of precipitation. The $\delta^{18}O$ values of rodent teeth from caves can also provide reliable records of millennial-scale climatic fluctuations during interglacial and glacial stages. These records can potentially provide information on the structure of abrupt climatic shifts in terrestrial areas. On the other hand, the $\delta^{13}C$ values of rodent teeth offer a potential proxy for changes in atmospheric CO_2 and precipitation. However, further work is needed in order to: 1) understand how the relationship between $\delta^{18}O_{rt}$ and $\delta^{18}O_{mw}$ varies due to differences in the ecological preferences of rodent taxa, 2) develop modern calibrations for this isotopic relationship using robust sampling methods, 3) examine the effect of seasonal dietary shifts on the $\delta^{13}C$ values of rodent teeth, and 4) investigate the causes and geographical consistency of the offset between the $\delta^{13}C$ values of modern and pre-modern rodent bioapatite.

10. Conclusions

The overall goal of this research was to investigate the applications of the stable isotope values of rodent dental carbonate for reconstructing Quaternary climate variability. This goal was explored via five primary aims. The key findings of the research, in relation to these aims, are summarised below.

Aim 1:

- The mean $\delta^{18}O$ of rodent dental carbonate is strongly correlated with the mean $\delta^{18}O$ of meteoric water in mid-latitude regions. This correlation is comparable to published regressions for the relationship between the $\delta^{18}O$ of phosphate in rodent bioapatite and the $\delta^{18}O$ of precipitation in Europe. The $\delta^{18}O$ of rodent dental carbonate can therefore be used as a proxy for the $\delta^{18}O$ of meteoric water.
- However, the relationship between the $\delta^{18}O$ of rodent bioapatite and the $\delta^{18}O$ of local water varies depending on the water isotope data that are used. This relationship may also vary between rodent taxa. Further work is needed in order to develop robust, species-specific calibrations between the $\delta^{18}O$ values of rodent teeth and meteoric water.

Aim 2:

- There are no significant differences between the $\delta^{18}O$ values of molars and incisors from arvicoline rodents. Both tooth types can therefore be used to reconstruct the past $\delta^{18}O$ of meteoric water.
- The $\delta^{13}C$ values of arvicoline molars and incisors are systematically offset by around 1-4‰. These offsets result from seasonal variations in the $\delta^{13}C$ value of the diet, combined with differences in the periods during which molars and incisors mineralize.
- The $\delta^{18}O$ and $\delta^{13}C$ values of rodent teeth vary by ~2-5‰ between different individuals within a rodent population. This variability is caused by inter-individual differences in the $\delta^{18}O$ values of the meteoric water sources and the $\delta^{13}C$ values of the diets consumed by rodents.

- The $\delta^{18}O$ values of tooth bioapatite are typically more enriched and more variable in *Microtus* than in *Arvicola*. This is due to differences between the ecological preferences and the durations of tooth mineralization in these taxa.
- Due to this variability in the $\delta^{18}O$ and $\delta^{13}C$ values of rodent teeth, ≥ 5 teeth of the same taxon must be analysed from each sedimentary unit for use in palaeoenvironmental reconstructions.
- Further work is needed in order to establish how seasonal variations in the diet are recorded in the $\delta^{13}C$ values of rodent molars and incisors.

Aim 3:

- Coupling the $\delta^{18}O$ of rodent dental carbonate with the $\delta^{18}O$ of aquatic mollusc shell aragonite provides reliable palaeotemperature estimates for interglacial stages. Moreover, the $\delta^{18}O$ values of rodent teeth from interglacial stages provide a reliable proxy for the mean $\delta^{18}O$ of meteoric water.
- The coupled isotope approach therefore offers an additional tool for generating quantitative palaeotemperature data. This tool can potentially be used to used investigate interglacial variability during the Quaternary period.
- However, this approach is best applied to fluvial sites at which the sediments accumulated rapidly and under low energy conditions.

Aim 4:

- The $\delta^{18}O$ values of rodent teeth from stratified cave sequences can provide reliable records of short-term palaeoclimatic fluctuations.
- The $\delta^{18}O$ values of *Microtus* and *Arvicola* teeth reliably reproduce the structure of millennial-scale climatic shifts during interglacial and glacial stages. The $\delta^{18}O$ values of rodent teeth from caves therefore provide a means for examining the patterns of abrupt climatic variations in terrestrial areas.
- Nevertheless, during glacial and stadial intervals, the $\delta^{18}O$ values of *Microtus* teeth are enriched due to 1) the influence of aridity on the $\delta^{18}O$ values of the drinking and food water sources consumed by this taxon,

and 2) a summer bias in the predation of rodents. Therefore, the absolute $\delta^{18}O$ values of *Microtus* teeth cannot provide accurate records for the $\delta^{18}O$ of precipitation during cold stages.

- On the other hand, the $\delta^{18}O$ values of *Arvicola* teeth can be used to accurately reconstruct the mean $\delta^{18}O$ of precipitation during both warm and cold stages.

Aim 5:

- Differences between the $\delta^{13}C$ values of modern and fossil rodent teeth can be largely explained by the recent anthropogenic shifts in the $\delta^{13}C$ value and partial pressure of atmospheric CO_2.
- Diagenesis is argued to have had a minimal influence on the decline in the $\delta^{13}C$ values of rodent teeth within the past 2000 years. This is supported by the consistency of the $\delta^{13}C$ differences between modern and fossil teeth across multiple sites and time periods.
- Residual $\delta^{13}C$ offsets between modern and fossil teeth may result from shifts in the compositions of rodent diets. However, further analyses of recent rodent teeth from Europe are needed to assess the timing, magnitude and causes of recent temporal shifts in the $\delta^{13}C$ values of rodent teeth.
- Variations in $\delta^{13}C_{rt}$ values between glacial and interglacial stages are consistent with temporal changes in atmospheric CO_2 and the amount of precipitation.
- Therefore, the $\delta^{13}C$ of rodent dental carbonate is a potentially useful proxy for reconstructing palaeoenvironmental variability during the Quaternary period.

11. Bibliography

Adams, N.F. (2017) Early Pleistocene palaeontology of Westbury Cave, Somerset. *The Palaeontological Association Newsletter*, 94, pp.79–84.

Ahn, J., Wahlen, M., Deck, B.L., Brook, E.J., Mayewski, P.A., Taylor, K.C. & White, J.W.C. (2004) A record of atmospheric CO_2 during the last 40,000 years from the Siple Dome, Antarctica ice core. *Journal of Geophysical Research D: Atmospheres*, 109, D13305.

Al-Aasm, I.S. & Veizer, J. (1986a) Diagenetic stabilization of aragonite and low-Mg calcite, I. Trace elements in Rudists. *Journal of Sedimentary Research*, 56 (1), pp.138–152.

Al-Aasm, I.S. & Veizer, J. (1986b) Diagenetic stabilization of aragonite and low-Mg calcite, II. Stable isotopes in Rudists. *Journal of Sedimentary Research*, 56 (6), pp.763–770.

Alibhai, S.K. & Gipps, J.H.W. (1991) Field vole, Microtus agrestis. In: G. B. Corbet & S. Harris eds. *The Handbook of British Mammals*. Oxford, Blackwell, pp.203–208.

Ambrose, S.H. & Norr, L. (1993) Experimental evidence for the relationship of the carbon isotope ratios of whole diet and dietary protein to those of bone collagen and carbonate. In: J. B. Lambert & G. Grupe eds. *Prehistoric Human Bone: Archaeology at the Molecular Level*. Berlin, Germany, Springer-Verlag, pp.1–37.

Amori, G. (1999) Chionomys nivalis. In: A. J. Mitchel-Jones, G. Amori, W. Bogdanowicz, B. Kryštufek, P. J. H. Reijnders, F. Spitzenberger, M. Stubbe, J. B. M. Thissen, V. Vohralík, & J. Zima eds. *The Atlas of European Mammals*. London, Academic Press.

Anderson, T.F. & Arthur, M.A. (1983) Stable Isotopes of oxygen and carbon and their application to sedimentologic and paleoenviromental problems. In: T. F. Anderson, I. R. Kaplan, J. Veizer, & L. S. Land eds. *Stable Isotopes in Sedimentary Geochemistry, Society of Economic Palaeontologists and Mineralogists, Short Course, Vol. 10*. pp.1–151.

Andrews, J.E. (2006) Palaeoclimatic records from stable isotopes in riverine tufas: Synthesis and review. *Earth-Science Reviews*, 75 (1–4), pp.85–104.

Andrews, J.E., Riding, R. & Dennis, P.F. (1993) Stable isotopic compositions of Recent freshwater cyanobacterial carbonates from the British Isles: local and regional environmental controls. *Sedimentology*, 40 (2), pp.303–314.

Andrews, J.E., Riding, R. & Dennis, P.F. (1997) The stable isotope record of environmental and climatic signals in modern terrestrial microbial carbonates from Europe. *Palaeogeography, Palaeoclimatology, Palaeoecology*, 129 (1), pp.171–189.

Andrews, P. (1990) *Owls, Caves and Fossils*. Chicago, University of Chicago Press.

Andrews, P., Cook, J.A., Currant, A.P. & Stringer, C.B. (1999) *Westbury Cave. The Natural History Museum Excavations 1976-1984.* Univeristy of Bristol, Western Archaeological and Specialist Press.

Andrews, P. & Fernandez-Jalvo, Y. (2012) Bronze Age barrows at Longstone Edge: Taphonomy and site formation. *Quaternary International*, 275, pp.43–54.

Apolinarska, K. & Pelechaty, M. (2017) Inter- and intra-specific variability in $\delta^{13}C$ and $\delta^{18}O$ values of freshwater gastropod shells from Lake Lednica, western Poland. *Acta Geologica Polonica*, 67 (3), pp.441–458.

Arens, N.C., Jahren, A.H. & Amnundson, R. (2000) Can C_3 plants faithfully record the carbon isotopic composition of atmospheric carbon dioxide? *Paleobiology*, 26 (261), pp.137–164.

Arppe, L., Kaakinen, A., Passey, B.H., Zhang, Z. & Fortelius, M. (2015) Small mammal tooth enamel carbon isotope record of C_4 grasses in late Neogene China. *Global and Planetary Change*, 133, pp.288–297.

Arppe, L.M. & Karhu, J.A. (2006) Implications for the Late Pleistocene climate in Finland and adjacent areas from the isotopic composition of mammoth skeletal remains. *Palaeogeography, Palaeoclimatology, Palaeoecology*, 231 (3–4), pp.322–330.

Atkinson, T.C., Briffa, K.R. & Coope, G.R. (1987) Seasonal temperatures in Britain during the past 22,000 years, reconstructed using beetle remains. *Nature*, 325 (6105), pp.587–592.

Aucour, A.-M., Sheppard, S.M.F. & Savoye, R. (2003) $\delta^{13}C$ of fluvial mollusk shells (Rhone River): a proxy for dissolved inorganic carbon. *Limnology*

and Oceanography, 48 (6), pp.2186–2193.

Ayliffe, L.K., Chivas, A.R. & Leakey, M.G. (1994) The retention of primary oxygen isotope compositions of fossil elephant skeletal phosphate. *Geochimica et Cosmochimica Acta*, 58 (23), pp.5291–5298.

Ayliffe, L.K., Lister, A.M. & Chivas, A.R. (1992) The preservation of glacial-interglacial climatic signatures in the oxygen isotopes of elephant skeletal phosphate. *Palaeogeography, Palaeoclimatology, Palaeoecology*, 99 (3–4), pp.179–191.

Bada, J.L., Wang, X.S. & Hamilton, H. (1999) Preservation of key biomolecules in the fossil record: Current knowledge and future challenges. *Philosophical Transactions of the Royal Society B: Biological Sciences*, 354 (1379), pp.77–87.

Badeck, F.W., Tcherkez, G., Nogués, S., Piel, C. & Ghashghaie, J. (2005) Post-photosynthetic fractionation of stable carbon isotopes between plant organs - A widespread phenomenon. *Rapid Communications in Mass Spectrometry*, 19 (11), pp.1381–1391.

Bakke, J., Lie, O., Heegaard, E., Dokken, T., Haug, G.H., Birks, H.H., Dulski, P. & Nilsen, T. (2009) Rapid oceanic and atmospheric changes during the Younger Dryas cold period. *Nature Geoscience*, 2 (3), pp.202–205.

Barbour, M.M. (2007) Stable oxygen isotope composition of plant tissue: A review. *Functional Plant Biology*, 34 (2), pp.83–94.

Barham, M., Blyth, A.J., Wallwork, M.D., Joachimski, M.M., Martin, L., Evans, N.J., Laming, B. & McDonald, B.J. (2017) Digesting the data - Effects of predator ingestion on the oxygen isotopic signature of micro-mammal teeth. *Quaternary Science Reviews*, 176, pp.71–84.

Batasaikhan, N., Tsytsulina, K., Formozov, N. & Sheftel, B. (2016) Microtus gregalis. The IUCN List of Threatened Species 2016: e.T13431A115112748. [Accessed: 2 June 2018]

Bauska, T.K., Baggenstos, D., Brook, E.J., Mix, A.C., Marcott, S.A., Petrenko, V. V, Schaefer, H., Severinghaus, J.P. & Lee, J.E. (2016) Carbon isotopes characterize rapid changes in atmospheric carbon dioxide during the last deglaciation. *Proceedings of the National Academy of Sciences of the United States of America*, 113 (13), pp.3465–3470.

Bauska, T.K., Joos, F., Mix, A.C., Roth, R., Ahn, J. & Brook, E.J. (2015) Links between atmospheric carbon dioxide, the land carbon reservoir and climate over the past millennium. *Nature Geoscience*, 8 (5), pp.383–387.

Bearcock, J.M. & Smedley, P.L. (2010) Baseline groundwater chemistry: the Palaeogene of the Thames Basin. *British Geological Survey Groundwater Programme Report, OR/10/057*.

Bender, M.M. (1971) Variations in the $^{13}C/^{12}C$ ratios of plants in relation to the pathway of photosynthetic carbon dioxide fixation. *Phytochemistry*, 10 (6), pp.1239–1244.

Bernard, A., Daux, V., Lécuyer, C., Brugal, J.-P., Genty, D., Wainer, K., Gardien, V., Fourel, F. & Jaubert, J. (2009) Pleistocene seasonal temperature variations recorded in the $\delta^{18}O$ of Bison priscus teeth. *Earth and Planetary Science Letters*, 283 (1–4), pp.133–143.

Berninger, F., Sonninen, E., Aalto, T. & Lloyd, J. (2000) Modeling ^{13}C discrimination in tree rings. *Global Biogeochemical Cycles*, 14 (1), pp.213–223.

Beswick, P. (2014) Prehistoric pottery. In: Last, J., The excavation of two round barrows on Longstone Edge, Derbyshire. In: *Derbyshire Archaeological Journal, 134*. pp.117–125.

Birks, H.H. & Birks, H.J.B. (2014) To what extent did changes in July temperature influence Lateglacial vegetation patterns in NW Europe? *Quaternary Science Reviews*, 106, pp.262–277.

Birks, S.J. & Edwards, T.W.D. (2009) Atmospheric circulation controls on precipitation isotope-climate relations in western Canada. *Tellus, Series B: Chemical and Physical Meteorology*, 61 (3), pp.566–576.

Bischoff, J.L. & Fyfe, W.S. (1968) Catalysis, inhibition, and the calcite-aragonite problem. Part 1: The aragonite-calcite transformation. *American Journal of Science*, 266, pp.65–79.

Bishop, M.J. (1974) A preliminary report on the middle Pleistocene mammal bearing deposits of Westbury-Sub-Mendip, Somerset. *Proceedings of the University of Bristol Spelaeological Society*, 13 (3), pp.301–318.

Bishop, M.J. (1975) Earliest record of man's presence in Britain. *Nature*, 253 (5487), pp.95–97.

Blain, H.-A., Cuenca-Bescos, G., Lozano-Fernandez, I., Lopez-Garcia, J.M., Olle, A., Rosell, J. & Rodriguez, J. (2012) Investigating the Mid-Brunhes Event in the Spanish terrestrial sequence. *Geology*, 40 (11), pp.1051–1054.

Blaise, E. & Balasse, M. (2011) Seasonality and season of birth of modern and late Neolithic sheep from south-eastern France using tooth enamel $\delta^{18}O$ analysis. *Journal of Archaeological Science*, 38 (11), pp.3085–3093.

Blake, R.E., O'Neil, J.R. & Garcia, G.A. (1997) Oxygen isotope systematics of biologically mediated reactions of phosphate: I. Microbial degradation of organophosphorus compounds. *Geochimica et Cosmochimica Acta*, 61 (20), pp.4411–4422.

Bocherens, H., Fogel, M.L., Tuross, N. & Zeder, M. (1995) Trophic structure and climatic information from isotopic signatures in Pleistocene cave fauna of Southern England. *Journal of Archaeological Science*, 22 (2), pp.327–340.

Böhme, G. (2000) Fossile Amphibien und Reptilien im Quartär Thüringens. *Veröffentlichungen Naturkundemuseum Erfurt*, 19, pp.79–97.

Böhme, G. (1996) Zur historischen Entwicklung der Herpetofaunen Mitteleuropas im Eiszeitalter (Quartär). In: R. Günther ed. *Die Amphibien und Reptilien Deutschlands*. Stuttgart, Gustav Fischer Verlag, pp.30–39.

Böhme, M. (2010) Ectothermic vertebrates, climate and environment of the West Runton Freshwater Bed (early Middle Pleistocene, Cromerian). *Quaternary International*, 228 (1–2), pp.63–71.

Böhme, M., Ilg, A., Ossig, A. & Kuchenhoff, H. (2006) New method to estimate paleoprecipitation using fossil amphibians and reptiles and the middle and late Miocene precipitation gradients in Europe. *Geology*, 34 (6), pp.425–428.

Bonafini, M., Pellegrini, M., Ditchfield, P. & Pollard, A.M. (2013) Investigation of the 'canopy effect' in the isotope ecology of temperate woodlands. *Journal of Archaeological Science*, 40 (11), pp.3926–3935.

Bond, G., Broecker, W., Johnsen, S., McManus, J., Labeyrie, L., Jouzel, J. & Bonani, G. (1993) Correlations between climate records from North Atlantic sediments and Greenland ice. *Nature*, 365 (6442), pp.143–147.

Bowen, G.J. (2017) The Online Isotopes in Precipitation Calculator, Version 3.1. Available from: <http://waterisotopes.org.> [Accessed 7 February 2018].

Bowen, G.J. (2018) Gridded maps of the isotopic composition of meteoric waters. Available from: <http://www.waterisotopes.org.> [Accessed 7 February 2018].

Bowen, G.J. & Revenaugh, J. (2003) Interpolating the isotopic composition of modern meteoric precipitation. *Water Resources Research*, 39 (10), 1299.

Bowen, G.J. & Wilkinson, B. (2002) Spatial distribution of $\delta^{18}O$ in meteoric precipitation. *Geology*, 30 (4), pp.315–318.

Boyce, C.C.K. (1991) Water Vole, Arvicola terrestris. In: G. B. Corbet & S. Harris eds. *The Handbook of British Mammals*. Oxford, Blackwell, pp.212–218.

Braconnot, P., Otto-Bliesner, B., Harrison, S., Joussaume, S., Peterchmitt, J.Y., Abe-Ouchi, A., Crucifix, M., Driesschaert, E., Fichefet, T., Hewitt, C.D., Kageyama, M., Kitoh, A., Laîné, A., Loutre, M.F., Marti, O., Merkel, U., Ramstein, G., Valdes, P., Weber, S.L., Yu, Y. & Zhao, Y. (2007) Results of PMIP2 coupled simulations of the Mid-Holocene and last glacial maximum - Part 1: Experiments and large-scale features. *Climate of the Past*, 3 (2), pp.261–277.

Brady, A.L., White, C.D., Longstaffe, F.J. & Southam, G. (2008) Investigating intra-bone isotopic variations in bioapatite using IR-laser ablation and micromilling: Implications for identifying diagenesis? *Palaeogeography, Palaeoclimatology, Palaeoecology*, 266 (3–4), pp.190–199.

Bridgland, D.R. (1994) *Quaternary of the Thames*. Dordrecht, Springer.

Bridgland, D.R. (1988) The Pleistocene fluvial stratigraphy and palaeogeography of Essex. *Proceedings of the Geologists' Association*, 99 (4), pp.291–314.

Bridgland, D.R., Harding, P., Allen, P., Candy, I., Cherry, C., George, W., Horne, D.J., Keen, D.H., Penkman, K.E.H., Preece, R.C., Rhodes, E.J., Scaife, R., Schreve, D.C., Schwenninger, J.-L., Slipper, I., Ward, G.R., White, M.J., White, T.S. & Whittaker, J.E. (2013) An enhanced record of MIS 9 environments, geochronology and geoarchaeology: data from construction of the High Speed 1 (London–Channel Tunnel) rail-link and

other recent investigations at Purfleet, Essex, UK. *Proceedings of the Geologists' Association*, 124 (3), pp.417–476.

Brock, F., Higham, T., Ditchfield, P. & Ramsey, C.B. (2010) Current pretreatment methods for AMS radiocarbon dating at the Oxford Radiocarbon Accelerator Unit (ORAU). *Radiocarbon*, 52 (1), pp.103–112.

Bronk Ramsey, C. (2009) Bayesian Analysis of Radiocarbon Dates. *Radiocarbon*, 51 (1), pp.337–360.

Bronk Ramsey, C., Higham, T. & Leach, P. (2004) Towards high-precision AMS: progress and limitations. *Radiocarbon*, 46 (1), pp.17–24.

Brooks, J.R., Flanagan, L.B., Buchmann, N. & Ehleringer, J.R. (1997) Carbon isotope composition of boreal plants: Functional grouping of life forms. *Oecologia*, 110 (3), pp.301–311.

Brooks, S.J., Matthews, I.P., Birks, H.H. & Birks, H.J.B. (2012) High resolution Lateglacial and early-Holocene summer air temperature records from Scotland inferred from chironomid assemblages. *Quaternary Science Reviews*, 41, pp.67–82.

Brown, L. (1995) Pottery production. In: B. Cunliffe ed. *Danebury: An Iron Age Hillfort in Hampshire. Volume 6: A hillfort community in perspective*. York, Council for British Archaeology, CBA Research Report no. 102, pp.53–65.

Brown, T., Bradley, C., Grapes, T. & Boomer, I. (2011) Hydrological assessment of Star Carr and the Hertford catchment, Yorkshire, UK. *Journal of Wetland Archaeology*, 11 (1), pp.36–55.

Browne, S. (1995) The small mammals. In: B. Cunliffe ed. *Danebury: An Iron Age Hillfort in Hampshire. Volume 6: A hillfort community in perspective*. York, Council for British Archaeology, CBA Research Report no. 102, pp.234–238.

Bryant, D.J. & Froelich, P.N. (1995) A model of oxygen isotope fractionation in body water of large mammals. *Geochimica et Cosmochimica Acta*, 59 (21), pp.4523–4537.

Bryant, J.D., Koch, P.L., Froelich, P.N., Showers, W.J. & Genna, B.J. (1996) Oxygen isotope partitioning between phosphate and carbonate in mammalian apatite. *Geochimica et Cosmochimica Acta*, 60 (24),

pp.5145–5148.

Buchardt, B. & Weiner, S. (1981) Diagenesis of aragonite from Upper Cretaceous ammonites: a geochemical case-study. *Sedimentology*, 28 (3), pp.423–438.

Bugler, M.J., Grimes, S.T., Leng, M.J., Rundle, S.D., Price, G.D., Hooker, J.J. & Collinson, M.E. (2009) Experimental determination of a Viviparus contectus thermometry equation. *Rapid Communications in Mass Spectrometry*, 23 (18), pp.2939–2951.

Bump, J.K., Fox-Dobbs, K., Bada, J.L., Koch, P.L., Peterson, R.O. & Vucetich, J.A. (2007) Stable isotopes, ecological integration and environmental change: wolves record atmospheric carbon isotope trend better than tree rings. *Proceedings of the Royal Society of London B: Biological Sciences*, 274 (1624), pp.2471–2480.

Butet, A. & Delettre, Y.R. (2011) Diet differentiation between European arvicoline and murine rodents. *Acta Theriologica*, 56 (4), pp.297–304.

Calandra, I., Labonne, G., Mathieu, O., Henttonen, H., Lévêque, J., Milloux, M.J., Renvoisé, É., Montuire, S. & Navarro, N. (2015) Isotopic partitioning by small mammals in the subnivium. *Ecology and Evolution*, 5 (18), pp.4132–4140.

Candy, I. & Alonso-Garcia, M. (2018) A 1 Ma sea surface temperature record from the North Atlantic and its implications for the early human occupation of Britain. *Quaternary Research*. https://doi.org/10.1017/qua.2018.62

Candy, I., Coope, G.R., Lee, J.R., Parfitt, S.A., Preece, R.C., Rose, J. & Schreve, D.C. (2010) Pronounced warmth during early Middle Pleistocene interglacials: Investigating the Mid-Brunhes Event in the British terrestrial sequence. *Earth-Science Reviews*, 103 (3–4), pp.183–196.

Candy, I., Farry, A., Darvill, C.M., Palmer, A., Blockley, S.P.E., Matthews, I.P., MacLeod, A., Deeprose, L., Farley, N., Kearney, R., Conneller, C., Taylor, B. & Milner, N. (2015) The evolution of Palaeolake Flixton and the environmental context of Star Carr: An oxygen and carbon isotopic record of environmental change for the early Holocene. *Proceedings of the Geologists' Association*, 126 (1), pp.60–71.

Candy, I. & McClymont, E.L. (2013) Interglacial intensity in the North Atlantic

over the last 800 000 years: investigating the complexity of the mid-Brunhes Event. *Journal of Quaternary Science*, 28 (4), pp.343–348.

Candy, I., Preece, R.C., White, T.S. & Sherriff, J. (2014) The $\delta^{18}O$ value of non-marine mollusc shells from Middle and Late Pleistocene terrace deposits of the River Thames. In: D. R. Bridgland, P. Allen, & T. S. White eds. *The Quaternary of the Lower Thames & Eastern Essex*. London, Quaternary Research Association, pp.27–31.

Candy, I. & Schreve, D. (2007) Land–sea correlation of Middle Pleistocene temperate sub-stages using high-precision uranium-series dating of tufa deposits from southern England. *Quaternary Science Reviews*, 26 (9–10), pp.1223–1235.

Candy, I., Schreve, D.C., Sherriff, J. & Tye, G.J. (2014) Marine Isotope Stage 11: Palaeoclimates, palaeoenvironments and its role as an analogue for the current interglacial. *Earth-Science Reviews*, 128, pp.18–51.

Candy, I., Schreve, D. & White, T.S. (2015) MIS 13-12 in Britain and the North Atlantic: Understanding the palaeoclimatic context of the earliest Acheulean. *Journal of Quaternary Science*, 30 (7), pp.593–609.

Candy, I., White, T.S. & Elias, S. (2016) How warm was Britain during the Last Interglacial? A critical review of Ipswichian (MIS 5e) palaeotemperature reconstructions. *Journal of Quaternary Science*, 31 (8), pp.857–868.

Casey, M.M. & Post, D.M. (2011) The problem of isotopic baseline: Reconstructing the diet and trophic position of fossil animals. *Earth-Science Reviews*, 106 (1), pp.131–148.

Cerling, T.E. & Harris, J.M. (1999) Carbon isotope fractionation between diet and bioapatite in ungulate mammals and implications for ecological and paleoecological studies. *Oecologia*, 120 (3), pp.347–363.

Cerling, T.E. & Quade, J. (1993) Stable carbon and oxygen isotopes in soil carbonates. In: P. Swart, J. A. McKenzie, K. C. Lohmann, & S. Savin eds. *Climate Change in Continental Isotope Records*. Geophysical Monographs 78, American Geophysical Union, pp.217–231.

Cerling, T.E., Solomon, D.K., Quade, J. & Bowman, J.R. (1991) On the isotopic composition of carbon in soil carbon dioxide. *Geochimica et Cosmochimica Acta*, 55 (11), pp.3403–3405.

Cernusak, L.A., Tcherkez, G., Keitel, C., Cornwell, W.K., Santiago, L.S., Knohl, A., Barbour, M.M., Williams, D.G., Reich, P.B., Ellsworth, D.S., Dawson, T.E., Griffiths, H.G., Farquhar, G.D. & Wright, I.J. (2009) Why are non-photosynthetic tissues generally ^{13}C enriched compared with leaves in C_3 plants? Review and synthesis of current hypotheses. *Functional Plant Biology*, 36 (3), pp.199–213.

Charman, D.J. (2010) Centennial climate variability in the British Isles during the mid-late Holocene. *Quaternary Science Reviews*, 29 (13–14), pp.1539–1554.

Chenery, C.A., Pashley, V., Lamb, A.L., Sloane, H.J. & Evans, J.A. (2012) The oxygen isotope relationship between the phosphate and structural carbonate fractions of human bioapatite. *Rapid Communications in Mass Spectrometry*, 26 (3), pp.309–319.

Chritz, K.L., Dyke, G.J., Zazzo, A., Lister, A.M., Monaghan, N.T. & Sigwart, J.D. (2009) Palaeobiology of an extinct Ice Age mammal: Stable isotope and cementum analysis of giant deer teeth. *Palaeogeography, Palaeoclimatology, Palaeoecology*, 282 (1–4), pp.133–144.

Clark, I.D. & Fritz, P. (1997) *Environmental Isotopes in Hydrogeology*. Boca Raton, USA, Lewis Publishers.

Clark, J.G.D. (1954) *Excavations at Star Carr: an early Mesolithic site at Seamer near Scarborough, Yorkshire*. Cambridge, Cambridge University Press.

Clementz, M.T., Fox-Dobbs, K., Wheatley, P. V., Koch, P.L. & Doak, D.F. (2009) Revisiting old bones: Coupled carbon isotope analysis of bioapatite and collagen as an ecological and palaeoecological tool. *Geological Journal*, 44 (5), pp.605–620.

Collins, J.D. (2012) Assessing mussel shell diagenesis in the modern vadose zone at Lyon's Bluff (22OK520), Northeast Mississippi. *Journal of Archaeological Science*, 39 (12), pp.3694–3705.

Collins, R.P. & Jones, M.B. (1986) The influence of climatic factors on the distribution of C_4 species in Europe. *Vegetatio*, 64 (2–3), pp.121–129.

Coope, G.R. (2000) Coleoptera from Beeston and West Runton, Norfolk. In: S. G. Lewis, C. A. Whiteman, & R. C. Preece eds. *The Quaternary of Norfolk and Suffolk Field Guide*. London, Quaternary Research Association, pp.73–75.

Coope, G.R. (2010a) Coleoptera from the Cromerian Type Site at West Runton, Norfolk, England. *Quaternary International*, 228 (1–2), pp.46–52.

Coope, G.R. (2010b) Coleopteran faunas as indicators of interglacial climates in central and southern England. *Quaternary Science Reviews*, 29 (13–14), pp.1507–1514.

Coplen, T.B., Kendall, C. & Hopple, J. (1983) Comparison of stable isotope reference samples. *Nature*, 302 (5905), pp.236–238.

Corbet, G. & Harris, S. (1991) *The Handbook of British Mammals*. Oxford, Blackwell.

Coy, J. (1982) *Small mammals and amphibians from Danebury, Hampshire*. Department of the Environment, Faunal Remains Project, University of Southampton.

Craig, H. (1961) Isotopic Variations in Meteoric Waters. *Science*, 133 (3465), pp.1702–1703.

Craig, H. (1965) The measurement of oxygen isotope palaeotemperatures. In: E. Tongiorgi ed. *Stable Isotopes in Oceanographic Studies and Palaeotemperatures*. Pisa, Consiglio Nazionale Della Richerche. Laboratorio de Geologia Nucleare, pp.161–182.

Crowley, B.E. & Wheatley, P. V. (2014) To bleach or not to bleach? Comparing treatment methods for isolating biogenic carbonate. *Chemical Geology*, 381, pp.234–242.

Cunliffe, B. (1984a) *Danebury, an Iron Age Hillfort in Hampshire. Volume 1. The Excavations, 1969-1978: the site*. Research Report 52a, Council for British Archaeology, London.

Cunliffe, B. (1971) Danebury, Hampshire: First Interim Report on the Excavation, 1969-70. *The Antiquaries Journal*, 51 (2), pp.240–252.

Cunliffe, B. (1976) Danebury, Hampshire: Second Interim Report on the Excavations 1971-5. *The Antiquaries Journal*, 56 (2), pp.198–216.

Cunliffe, B. (1984b) *Danebury: an Iron Age Hillfort in Hampshire. Volume 2. The Excavations , 1969-1978 : the finds*. Research Report 52b, Council for British Archaeology, London.

Cunliffe, B. (1995) *Danebury: An Iron Age Hillfort in Hampshire. Volume 6: A hillfort community in perspective*. CBA Research Report no. 102, Council for British Archaeology, York.

Cunliffe, B. & Poole, C. (1991a) *Danebury: an Iron Age Hillfort in Hampshire. Volume 4. The Excavations 1979-88: the site*. Research Report 73a, Council for British Archaeology, London.

Cunliffe, B. & Poole, C. (1991b) *Danebury: an Iron Age Hillfort in Hampshire. Volume 5. The Excavations, 1979-88: the finds*. Research Report 73b, Council for British Archaeology, London.

Currant, A.P. (1986) The Lateglacial mammal fauna of Gough's Cave, Cheddar, Somerset. *Proceedings of the University of Bristol Spelaeological Society*, 17 (3), pp.286–304.

Currant, A. & Jacobi, R. (2001) A formal mammalian biostratigraphy for the Late Pleistocene of Britain. *Quaternary Science Reviews*, 20 (16), pp.1707–1716.

D'Angela, D. & Longinelli, A. (1990) Oxygen isotopes in living mammal's bone phosphate: Further results. *Chemical Geology: Isotope Geoscience section*, 86 (1), pp.75–82.

Dansgaard, W. (1964) Stable isotopes in precipitation. *Tellus*, 16 (4), pp.436–468.

Dansgaard, W., Johnsen, S.J., Clausen, H.B., Dahl-Jensen, D., Gundestrup, N.S., Hammer, C.U., Hvidberg, C.S., Steffensen, J.P., Sveinbjörnsdottir, A.E., Jouzel, J. & Bond, G. (1993) Evidence for general instability of past climate from a 250-kyr ice-core record. *Nature*, 364 (6434), pp.218–220.

Darling, W.. (2004) Hydrological factors in the interpretation of stable isotopic proxy data present and past: a European perspective. *Quaternary Science Reviews*, 23 (7–8), pp.743–770.

Darling, W., Bath, A. & Talbot, J. (2003) The O and H stable isotope composition of freshwaters in the British Isles. 2, surface waters and groundwater. *Hydrology and Earth System Sciences*, 7 (2), pp.183–195.

Darling, W. & Talbot, J. (2003) The O and H stable isotope composition of freshwaters in the British Isles. 1. Rainfall. *Hydrology and Earth System Sciences*, 7 (2), pp.163–182.

Darling, W.G. & Bath, A.H. (1988) A stable isotope study of recharge

processes in the English Chalk. *Journal of Hydrology*, 101 (1–4), pp.31–46.

Darling, W.G. & Bowes, M.J. (2016) A long-term study of stable isotopes as tracers of processes governing water flow and quality in a lowland river basin: The upper Thames, UK. *Hydrological Processes*, 30, pp.2178–2195.

Davies, S.M. (1999) Stable isotopic investigation of modern and fossil freshwater molluscs. Unpublished PhD Thesis, Royal Holloway, University of London.

Davies, S.M., Rose, J., Branch, N.P. & Candy, I. (2000) West Runton (TG188 432 & TG 185 432). Pre-glacial Freshwater Muds and Coastal Sands and Gravels. In: S. G. Lewis, C. A. Whiteman, & R. C. Preece eds. *The Quaternary of Norfolk and Suffolk Field Guide*. London, Quaternary Research Association, pp.61–65.

Davies, T.T. & Hooper, P.R. (1963) The determination of the calcite: aragonite ratio in mollusc shells by X-ray diffraction. *Mineralogical Magazine*, 33 (262), pp.608–612.

Davis, B.A.S., Brewer, S., Stevenson, A.C. & Guiot, J. (2003) The temperature of Europe during the Holocene reconstructed from pollen data. *Quaternary Science Reviews*, 22 (15–17), pp.1701–1716.

Dawson, T.E. & Ehleringer, J.R. (1991) Streamside trees that do not use stream water. *Nature*, 350 (6316), pp.335–337.

De Deckker, P. (1979) The Middle Pleistocene ostracod fauna of the West Runton Freshwater Bed, Norfolk. *Palaeontology*, 22, pp.293–316.

Deines, P., Langmuir, D. & Harmon, R. (1974) Stable carbon isotope ratios and the existence of a gas phase in the evolution of carbonate ground waters. *Geochimica et Cosmochimica Acta*, 38 (7), pp.1147–1164.

Deniro, M.J. (1985) Postmortem preservation and alteration of in vivo bone collagen isotope ratios in relation to palaeodietary reconstruction. *Nature*, 317 (6040), pp.806–809.

DeNiro, M.J. & Epstein, S. (1978) Influence of diet on the distribution of carbon isotopes in animals. *Geochimica et Cosmochimica Acta*, 42 (5), pp.495–506.

DeNiro, M.J. & Epstein, S. (1981) Influence of diet on the distribution of

nitrogen isotopes in animals. *Geochimica et Cosmochimica Acta*, 45 (3), pp.341–351.

Denton, G.H., Alley, R.B., Comer, G.C. & Broecker, W.S. (2005) The role of seasonality in abrupt climate change. *Quaternary Science Reviews*, 24 (10–11), pp.1159–1182.

Diefendorf, A.F., Mueller, K.E., Wing, S.L., Koch, P.L. & Freeman, K.H. (2010) Global patterns in leaf ^{13}C discrimination and implications for studies of past and future climate. *Proceedings of the National Academy of Sciences*, 107 (13), pp.5738–5743.

Dongmann, G., Nürnberg, H.W., Förstel, H. & Wagener, K. (1974) On the enrichment of $H_2{}^{18}O$ in the leaves of transpiring plants. *Radiation and Environmental Biophysics*, 11 (1), pp.41–52.

Douka, K., Hedges, R.M. & Higham, T.G. (2010) Improved AMS ^{14}C dating of shell carbonates using high-precision X-Ray Diffraction and a novel density separation protocol (CarDS). *Radiocarbon*, 52 (2), pp.735–751.

Driessens, F.C.M. & Verbeeck, R.M.H. (1990) *Biominerals*. Florida, USA, CRC Press.

Drucker, D., Bocherens, H., Bridault, A. & Billiou, D. (2003) Carbon and nitrogen isotopic composition of red deer (Cervus elaphus) collagen as a tool for tracking palaeoenvironmental change during the Late-Glacial and Early Holocene in the northern Jura (France). *Palaeogeography, Palaeoclimatology, Palaeoecology*, 195 (3–4), pp.375–388.

Drucker, D.G., Bridault, A., Hobson, K.A., Szuma, E. & Bocherens, H. (2008) Can carbon-13 in large herbivores reflect the canopy effect in temperate and boreal ecosystems? Evidence from modern and ancient ungulates. *Palaeogeography, Palaeoclimatology, Palaeoecology*, 266 (1), pp.69–82.

Duchesne, D., Gauthier, G. & Berteaux, D. (2011) Habitat selection, reproduction and predation of wintering lemmings in the Arctic. *Oecologia*, 167 (4), pp.967–980.

Eggleston, S., Schmitt, J., Bereiter, B., Schneider, R. & Fischer, H. (2016a) Evolution of the stable carbon isotope composition of atmospheric CO_2 over the last glacial cycle. *Paleoceanography and Palaeoclimatology*, 31 (3), pp.434–452.

Eggleston, S., Schmitt, J., Bereiter, B., Schneider, R. & Fischer, H. (2016b) Antarctic ice core 155,000 year CO_2 and gas stable isotope data [Internet]. Available from: <https://www.ncdc.noaa.gov/paleo/study/19942> [Accessed 26 June 2018].

Ehleringer, J.R. & Cerling, T.E. (2002) C_3 and C_4 Photosynthesis. In: H. A. Mooney & J. G. Canadell eds. *Volume 2, The Earth System: biological and ecological dimensions of global environmental change, Encyclopedia of Global Environmental Change*. Chicester, Wiley & Sons, pp.186–190.

Ehleringer, J.R. & Cerling, T.E. (2001) Photosynthetic pathways and climate. In: E.-D. Schulze, M. Heimann, S. P. Harrison, E. A. Holland, J. Lloyd, I. C. Prentice, & D. Schimel eds. *Global Biogeochemical Cycles in the Climate System*. San Diego, California, Academic Press, pp.267–277.

Ehleringer, J.R., Cerling, T.E. & Helliker, B.R. (1997) C_4 photosynthesis, atmospheric CO_2 , and climate. *Oecologia*, 112 (3), pp.285–299.

Ehleringer, J.R. & Cooper, T.A. (1988) Correlations between carbon isotope ratio and microhabitat in desert plants. *Oecologia*, 76 (4), pp.562–566.

Ehleringer, J.R., Field, C.B., Lin, Z. & Kuo, C. (1986) Leaf carbon isotope and mineral composition in subtropical plants along an irradiance cline. *Oecologia*, 70 (4), pp.520–526.

Elliott, J.C., Holcomb, D.W. & Young, R.A. (1985) Infrared determination of the degree of substitution of hydroxyl by carbonate ions in human dental enamel. *Calcified Tissue International*, 37 (4), pp.372–375.

Ellis, A.E. (1926) *British Snails: A Guide to Non-Marine Gastropoda of Great Britain and Ireland, Pliocene to Recent*. Oxford, Oxford University Press.

Elsig, J., Schmitt, J., Leuenberger, D., Schneider, R., Eyer, M., Leuenberger, M., Joos, F., Fischer, H. & Stocker, T.F. (2009) Stable isotope constraints on Holocene carbon cycle changes from an Antarctic ice core. *Nature*, 461 (7263), pp.507–510.

Emrich, K., Ehhalt, D.H. & Vogel, J.C. (1970) Carbon isotope fractionation during the precipitation of calcium carbonate. *Earth and Planetary Science Letters*, 8 (5), pp.363–371.

Epstein, S., Thompson, P. & Yapp, C.J. (1977) Oxygen and hydrogen

isotopic ratios in plant cellulose. *Science*, 198 (4323), pp.1209–1215.

Fabre, M., Lécuyer, C., Brugal, J.-P., Amiot, R., Fourel, F. & Martineau, F. (2011) Late Pleistocene climatic change in the French Jura (Gigny) recorded in the $\delta^{18}O$ of phosphate from ungulate tooth enamel. *Quaternary Research*, 75 (3), pp.605–613.

Farquhar, G., O'Leary, M. & Berry, J. (1982) On the relationship between carbon isotope discrimination and the intercellular carbon dioxide concentration in leaves. *Australian Journal of Plant Physiology*, 9 (2), pp.121-137.

Farquhar, G.D. & Richards, R. (1984) Isotopic composition of plant carbon correlates with water-use efficiency of wheat genotypes. *Australian Journal of Plant Physiology*, 11 (6), pp.539–552.

Feng, X., Faiia, A.M. & Posmentier, E.S. (2009) Seasonality of isotopes in precipitation: A global perspective. *Journal of Geophysical Research*, 114, D08116.

Fernández-García, M., López-García, J.M. & Lorenzo, C. (2016) Palaeoecological implications of rodents as proxies for the Late Pleistocene-Holocene environmental and climatic changes in northeastern Iberia. *Comptes Rendus - Palevol*, 15 (6), pp.707–719.

Ferns, P.N. (1976) Diet of a Microtus Agrestis population in south west Britain. *Oikos*, 27 (3), pp.506–511.

Field, M.H. (1993) Plant macrofossils from the Lower Channel sediments at Marsworth, Buckinghamshire, UK. *New Phytologist*, 123 (1), pp.195–201.

Field, M.H. & Peglar, S.M. (2010) A palaeobotanical investigation of the sediments from the West Runton Mammoth site. *Quaternary International*, 228 (1–2), pp.38–45.

Field, R.D. (2010) Observed and modeled controls on precipitation $\delta^{18}O$ over Europe: From local temperature to the Northern Annular Mode. *Journal of Geophysical Research Atmospheres*, 115, D12101.

Flanagan, L.B., Comstock, J.P. & Ehleringer, J.R. (1991) Comparison of modeled and observed environmental influences on the stable oxygen and hydrogen isotope composition of leaf water in Phaseolus vulgaris L. *Plant physiology*, 96 (2), pp.588–596.

Fox, D.L. & Fisher, D.C. (2001) Stable isotope ecology of a Late Miocene population of Gomphotherium productus (Mammalia, Proboscidea) from Port of Entry Pit, Oklahoma, USA. *Palaios*, 16 (3), pp.279–293.

Francey, R.J., Allison, C.E., Etheridge, D.M., Trudinger, C.M., Enting, I.G., Leuenberger, M., Langenfelds, R.L., Michel, E. & Steele, L.P. (1999) A 1000-year high precision record of $\delta^{13}C$ in atmospheric CO_2. *Tellus Series B*, 51 (2), pp.170–193.

Fraser, R.A., Grün, R., Privat, K. & Gagan, M.K. (2008) Stable-isotope microprofiling of wombat tooth enamel records seasonal changes in vegetation and environmental conditions in eastern Australia. *Palaeogeography, Palaeoclimatology, Palaeoecology*, 269 (1–2), pp.66–77.

Fretter, V. & Graham, A. (1978) The prosobranch molluscs of Britain and Denmark. Part 3 - Neritacea, Viviparacea, Valvatacea, terrestrial and freshwater Littorinacea and Rissoacea. *Journal of Molluscan Studies, Supplement*, 5, pp.101–152.

Fricke, H. & O'Neil, J. (1999) The correlation between $^{18}O/^{16}O$ ratios of meteoric water and surface temperature: its use in investigating terrestrial climate change over. *Earth and Planetary Science Letters*, 170, pp.181–196.

Fricke, H.C. & Wing, S.L. (2004) Oxygen isotope and paleobotanical estimates of temperature and $\delta^{18}O$-latitude gradients over North America during the Early Eocene. *American Journal of Science*, 304 (7), pp.612–635.

Friedli, H., Lötscher, H., Oeschger, H., Siegenthaler, U. & Stauffer, B. (1986) Ice core record of the $^{13}C/^{12}C$ ratio of atmospheric CO_2 in the past two centuries. *Nature*, 324 (6094), pp.237–238.

Fritz, P. & Poplawski, S. (1974) ^{18}O and ^{13}C in the shells of freshwater molluscs and their environments. *Earth and Planetary Science Letters*, 24 (1), pp.91–98.

García-Alix, A. (2015) A multiproxy approach for the reconstruction of ancient continental environments. The case of the Mio-Pliocene deposits of the Granada Basin (Southern Iberian Peninsula). *Global and Planetary Change*, 131, pp.1–10.

García-Alix, A., Delgado Huertas, A., Martín Suárez, E. & Freudenthal, M.

(2013) Environmental conditions vs. landscape. Assessment of the factors that influence small mammal fauna distribution in Southern Iberia during the latest Messinian by mean of stable isotopes. *Palaeogeography, Palaeoclimatology, Palaeoecology*, 386, pp.492–500.

Garvie-Lok, S.J., Varney, T.L. & Katzenberg, M.A. (2004) Preparation of bone carbonate for stable isotope analysis: the effects of treatment time and acid concentration. *Journal of Archaeological Science*, 31 (6), pp.763–776.

Gąsiorowski, M., Hercman, H. & Socha, P. (2014) Isotopic analysis (C, N) and species composition of rodent assemblage as a tool for reconstruction of climate and environment evolution during Late Quaternary: A case study from Biśnik Cave (Częstochowa Upland, Poland). *Quaternary International*, 339–340, pp.139–147.

Gat, J.R. (1996) Oxygen and hydrogen isotopes in the hydrological cycle. *Annual Review of Earth and Planetary Sciences*, 24, pp.225–262.

Gazis, C. & Feng, X. (2004) A stable isotope study of soil water: Evidence for mixing and preferential flow paths. *Geoderma*, 119 (1–2), pp.97–111.

Gehler, A., Tütken, T. & Pack, A. (2012) Oxygen and carbon isotope variations in a modern rodent community - implications for palaeoenvironmental reconstructions. *PloS one*, 7 (11), e49531.

Genoni, L., Iacumin, P., Nikolaev, V., Gribchenko, Y. & Longinelli, A. (1998) Oxygen isotope measurements of mammoth and reindeer skeletal remains: an archive of Late Pleistocene environmental conditions in Eurasian Arctic. *Earth and Planetary Science Letters*, 160 (3–4), pp.587–592.

Gibbard, P.L., Boreham, S., Andrews, J.E. & Maher, B.A. (2010) Sedimentation, geochemistry and palaeomagnetism of the West Runton Freshwater Bed, Norfolk, England. *Quaternary International*, 228 (1–2), pp.8–20.

Gorman, M.L. (1991) Orkney and Guernsey voles, Microtus arvalis. In: G. B. Corbet & S. Harris eds. *The Handbook of British Mammals*. Oxford, Blackwell, pp.208–211.

Grassineau, N. V. (2006) High-precision EA-IRMS analysis of S and C isotopes in geological materials. *Applied Geochemistry*, 21 (5), pp.756–765.

Graven, H., Allison, C.E., Etheridge, D.M., Hammer, S., Keeling, R.F., Levin, I., Meijer, H.A.J., Rubino, M., Tans, P.P., Trudinger, C.M., Vaughn, B.H. & White, J.W.C. (2017) Compiled records of carbon isotopes in atmospheric CO_2 for historical simulations in CMIP6. *Geoscientific Model Development*, 10 (12), pp.4405–4417.

Green, C.P., Coope, G.R., Currant, A.P., Holyoak, D.T., Ivanovich, M., Jones, R.L., Keen, D.H., McGregor, D.F.M. & Robinson, J.E. (1984) Evidence of two temperate episodes in late Pleistocene deposits at Marsworth, UK. *Nature*, 309 (5971), pp.778–781.

Grimes, S.T., Collinson, M.E., Hooker, J.J. & Mattey, D.P. (2008) Is small beautiful? A review of the advantages and limitations of using small mammal teeth and the direct laser fluorination analysis technique in the isotope reconstruction of past continental climate change. *Palaeogeography, Palaeoclimatology, Palaeoecology*, 266 (1–2), pp.39–50.

Grimes, S.T., Hooker, J.J., Collinson, M.E. & Mattey, D.P. (2005) Summer temperatures of late Eocene to early Oligocene freshwaters. *Geology*, 33, pp.189–192.

Grimes, S.T., Mattey, D.P., Collinson, M.E. & Hooker, J.J. (2004) Using mammal tooth phosphate with freshwater carbonate and phosphate palaeoproxies to obtain mean paleotemperatures. *Quaternary Science Reviews*, 23, pp.967–976.

Grimes, S.T., Mattey, D.P., Hooker, J.J. & Collinson, M.E. (2003) Paleogene paleoclimate reconstruction using oxygen isotopes from land and freshwater organisms: the use of multiple paleoproxies. *Geochimica et Cosmochimica Acta*, 67 (21), pp.4033–4047.

Hammer, Ø., Harper, D.A.T. & Ryan, P.D. (2001) Paleontological statistics software package for education and data analysis. *Palaeontologia Electronica*, 4 (1), pp.9–18.

Hansson, L. (1971) Small rodent food, feeding and population dynamics: a comparison between granivorous and herbivorous species in Scandinavia. *Oikos*, 22 (2), pp.183–198.

Hare, P.E. (1980) Organic geochemistry of bone and its relation to the survival of bone in the natural environment. In: A. K. Behrensmeyer & A. P. Hill eds. *Fossils in the Making*. Chicago, University of Chicago Press,

pp.208–222.

Hare, V.J., Loftus, E., Jeffrey, A. & Ramsey, C.B. (2018) Atmospheric CO_2 effect on stable carbon isotope composition of terrestrial fossil archives. *Nature Communications*, 9 (1), 252.

Hays, P.D. & Grossman, E.L. (1991) Oxygen isotopes in meteoric calcite cements as indicators of continental paleoclimate. *Geology*, 19 (5), pp.441–444.

Heaton, T.H.E. (1999) Spatial, species, and temporal variations in the $^{13}C/^{12}C$ ratios of C_3 plants: Implications for palaeodiet studies. *Journal of Archaeological Science*, 26 (6), pp.637–649.

Heppleston, P.B. (1972) Life history and population fluctuations of *Lymnaea truncatula* (Mull), the snail vector of fascioliasis. *Journal of Applied Ecology*, 9 (1), pp.235–248.

Héran, M.-A., Lécuyer, C. & Legendre, S. (2010) Cenozoic long-term terrestrial climatic evolution in Germany tracked by $\delta^{18}O$ of rodent tooth phosphate. *Palaeogeography, Palaeoclimatology, Palaeoecology*, 285 (3–4), pp.331–342.

Hernández Fernández, M., Álvarez Sierra, M.Á. & Peláez-Campomanes, P. (2007) Bioclimatic analysis of rodent palaeofaunas reveals severe climatic changes in Southwestern Europe during the Plio-Pleistocene. *Palaeogeography, Palaeoclimatology, Palaeoecology*, 251 (3–4), pp.500–526.

Higgins, P. & MacFadden, B.J. (2009) Seasonal and geographic climate variabilities during the Last Glacial Maximum in North America: Applying isotopic analysis and macrophysical climate models. *Palaeogeography, Palaeoclimatology, Palaeoecology*, 283 (1), pp.15–27.

Hillson, S. (2005) *Teeth*. 2nd Edition. Cambridge, UK, Cambridge University Press.

Hobbie, E.A. & Werner, R.A. (2004) Intramolecular, compound-specific, and bulk carbon isotope patterns in C_3 and C_4 plants: A review and synthesis. *New Phytologist*, 161 (2), pp.371–385.

Hodell, D.A., Kanfoush, S.L., Venz, K.A., Charles, C.D. & Sierro, F.J. (2003) The mid-brunhes transition in ODP sites 1089 and 1090 (Subantarctic South Atlantic). In: *Geophysical Monograph Series*. American

Geophysical Union (AGU), pp.113–129.

Holman, J.A. (1993) Pleistocene Herpetofauna of Westbury-Sub-Mendip Cave, England. *Cranium*, 10 (2), pp.87–96.

Holman, J.A., Stuart, A.J. & Clayden, J.D. (1990) A middle pleistocene herpetofauna from Cudmore Grove, Essex, England, and its paleogeographic and paleoclimatic implications. *Journal of Vertebrate Paleontology*, 10 (1), pp.86–94.

Hopley, P.J., Latham, A.G. & Marshall, J.D. (2006) Palaeoenvironments and palaeodiets of mid-Pliocene micromammals from Makapansgat Limeworks, South Africa: A stable isotope and dental microwear approach. *Palaeogeography, Palaeoclimatology, Palaeoecology*, 233 (3), pp.235–251.

Horne, D.J. (2007) A Mutual Temperature Range method for Quaternary palaeoclimatic analysis using European nonmarine Ostracoda. *Quaternary Science Reviews*, 26 (9–10), pp.1398–1415.

Horne, D.J., Curry, B.B. & Mesquita-Joanes, F. (2012) Mutual Climatic Range Methods for Quaternary Ostracods. *Developments in Quaternary Science*, 17, pp.65–84.

Horton, T.W., Defliese, W.F., Tripati, A.K. & Oze, C. (2016) Evaporation induced ^{18}O and ^{13}C enrichment in lake systems: A global perspective on hydrologic balance effects. *Quaternary Science Reviews*, 131, pp.365–379.

Hubick, K., Farquhar, G. & Shorter, R. (1986) Correlation between water-use efficiency and carbon isotope discrimination in diverse peanut (Arachis) germplasm. *Australian Journal of Plant Physiology*, 13 (6), pp.803–816.

Hudson, J.D. (1977) Stable isotopes and limestone lithification. *Journal of the Geological Society*, 133 (6), pp.637–660.

Hynek, S.A., Passey, B.H., Prado, J.L., Brown, F.H., Cerling, T.E. & Quade, J. (2012) Small mammal carbon isotope ecology across the Miocene-Pliocene boundary, northwestern Argentina. *Earth and Planetary Science Letters*, 321–322, pp.177–188.

Iacumin, P., Bocherens, H., Delgado Huertas, A., Mariotti, A. & Longinelli, A. (1997) A stable isotope study of fossil mammal remains from the Paglicci cave, Southern Italy. N and C as palaeoenvironmental

indicators. *Earth and Planetary Science Letters*, 148 (1–2), pp.349–357.

Iacumin, P., Bocherens, H., Mariotti, A. & Longinelli, A. (1996) Oxygen isotope analyses of co-existing carbonate and phosphate in biogenic apatite: a way to monitor diagenetic alteration of bone phosphate? *Earth and Planetary Science Letters*, 142 (1–2), pp.1–6.

Iacumin, P., Di Matteo, A., Nikolaev, V. & Kuznetsova, T.V. (2010) Climate information from C, N and O stable isotope analyses of mammoth bones from northern Siberia. *Quaternary International*, 212 (2), pp.206–212.

Iacumin, P., Nikolaev, V., Genoni, L., Ramigni, M., Ryskov, Y.G. & Longinelli, A. (2004a) Stable isotope analyses of mammal skeletal remains of Holocene age from European Russia: A way to trace dietary and environmental changes. *Geobios*, 37 (1), pp.37–47.

Iacumin, P., Nikolaev, V., Ramigni, M. & Longinelli, A. (2004b) Oxygen isotope analyses of mammal bone remains from Holocene sites in European Russia: palaeoclimatic implications. *Global and Planetary Change*, 40 (1–2), pp.169–176.

IAEA/WMO (2018) Global Network of Isotopes in Precipitation. The GNIP database. Available from: <https://nucleus.iaea.org/wiser.> [Accessed 28 April 2018].

Isarin, R.F.B., Renssen, H. & Vandenberghe, J. (1998) The impact of the North Atlantic Ocean on the Younger Dryas climate in northwestern and central Europe. *Journal of Quaternary Science*, 13 (5), pp.447–453.

Jacob, H. & Sonntag, C. (1991) An 8-year record of the seasonal variation of ^{2}H and ^{18}O in atmospheric water vapour and precipitation at Heidelberg, Germany. *Tellus B*, 43 (3), pp.291–300.

Jacobi, R. (2004) The Late Upper Palaeolithic lithic collection from Gough's Cave, Cheddar, Somerset and human use of the cave. *Proceedings of the Prehistoric Society*, 70, pp.1–92.

Jacobi, R.M. & Higham, T.F.G. (2009) The early Lateglacial re-colonization of Britain: new radiocarbon evidence from Gough's Cave, southwest England. *Quaternary Science Reviews*, 28 (19–20), pp.1895–1913.

Jahren, A.H., Arens, N.C. & Harbeson, S.A. (2008) Prediction of atmospheric $\delta^{13}CO_2$ using fossil plant tissues. *Reviews of Geophysics*, 46 (1), RG1002.

Jansen, J.H.F., Kuijpers, A. & Troelstra, S.R. (1986) A Mid-Brunhes climatic event: long-term changes in global atmosphere and ocean circulation. *Science*, 232 (4750), pp.619–622.

Jasechko, S., Lechler, A., Pausata, F.S.R., Fawcett, P.J., Gleeson, T., Cendon, D.I., Galewsky, J., LeGrande, A.N., Risi, C., Sharp, Z.D., Welker, J.M., Werner, M. & Yoshimura, K. (2015) Late-glacial to late-Holocene shifts in global precipitation $\delta^{18}O$. *Climate of the Past*, 11 (10), pp.1375–1393.

Jeffrey, A. (2016) Exploring palaeoaridity using stable oxygen and carbon isotopes in small mammal teeth: a case study from two Late Pleistocene archaeological cave sites in Morocco, North Africa. PhD thesis, St Cross College, University of Oxford.

Jeffrey, A., Denys, C., Stoetzel, E. & Lee-Thorp, J.A. (2015) Influences on the stable oxygen and carbon isotopes in gerbillid rodent teeth in semi-arid and arid environments: Implications for past climate and environmental reconstruction. *Earth and Planetary Science Letters*, 428, pp.84–96.

Jeffrey, A., Stoetzel, E., Parfitt, S., Barton, N., Nespoulet, R., El Hajraoui, M.A., Bouzouggar, A., Denys, C. & Lee-Thorp, J.A. (2016) Oxygen and carbon isotopes in Gerbillinae (gerbil) teeth provide palaeoaridity records in two Late Pleistocene Moroccan sites. *Quaternary International*, 404, pp.175.

Jenkins, G.J., Perry, M.C. & Prior, M.J. (2009) *The climate of the United Kingdom and recent trends*. Exeter, Hadley Centre, Met Office.

Jenkyns, H.C., Gale, A.S. & Corfield, R.M. (1994) Carbon- and oxygen-isotope stratigraphy of the English Chalk and Italian Scaglia and its palaeoclimatic significance. *Geological Magazine*, 131 (1), pp.1–34.

Jennings, A.E., Hald, M., Smith, M. & Andrews, J.T. (2006) Freshwater forcing from the Greenland Ice Sheet during the Younger Dryas: Evidence from southeastern Greenland shelf cores. *Quaternary Science Reviews*, 25 (3-4), pp.282–298.

Jim, S., Ambrose, S.H. & Evershed, R.P. (2004) Stable carbon isotopic evidence for differences in the dietary origin of bone cholesterol, collagen and apatite: implications for their use in palaeodietary reconstruction. *Geochimica et Cosmochimica Acta*, 68 (1), pp.61–72.

Jones, A.M., O'Connell, T.C., Young, E.D., Scott, K., Buckingham, C.M., Iacumin, P. & Brasier, M.D. (2001) Biogeochemical data from well preserved 200 ka collagen and skeletal remains. *Earth and Planetary Science Letters*, 193 (1–2), pp.143–149.

Jones, M.D., Leng, M.J., Eastwood, W.J., Keen, D.H. & Turney, C.S.M. (2002) Interpreting stable-isotope records from freshwater snail-shell carbonate: A Holocene case study from Lake Gölhisar, Turkey. *Holocene*, 12 (5), pp.629–634.

Jouzel, J., Hoffmann, G., Koster, R.D. & Masson, V. (2000) Water isotopes in precipitation: Data/model comparison for present-day and past climates. *Quaternary Science Reviews*, 19 (1-5), pp.363–379.

Jouzel, J., Masson-Delmotte, V., Cattani, O., Dreyfus, G., Falourd, S., Hoffmann, G., Minster, B., Nouet, J., Barnola, J.M., Chappellaz, J., Fischer, H., Gallet, J.C., Johnsen, S., Leuenberger, M., Loulergue, L., Luethi, D., Oerter, H., Parrenin, F., Raisbeck, G., Raynaud, D., Schilt, A., Schwander, J., Selmo, E., Souchez, R., Spahni, R., Stauffer, B., Steffensen, J.P., Stenni, B., Stocker, T.F., Tison, J.L., Werner, M. & Wolff, E.W. (2007) Orbital and millennial antarctic climate variability over the past 800,000 years. *Science*, 317 (5839), pp.793–796.

Juby, C. (2004) The palaeoenvironments of the pre-glacial deposits at West Runton. BSc Dissertation, Royal Holloway, University of London.

Kahlke, R.D., García, N., Kostopoulos, D.S., Lacombat, F., Lister, A.M., Mazza, P.P.A., Spassov, N. & Titov, V. V. (2011) Western Palaearctic palaeoenvironmental conditions during the Early and early Middle Pleistocene inferred from large mammal communities, and implications for hominin dispersal in Europe. *Quaternary Science Reviews*, 30 (11–12), pp.1368–1395.

Kasse, C. (2002) Sandy aeolian deposits and environments and their relation to climate during the Last Glacial Maximum and Lateglacial in northwest and central Europe. *Progress in Physical Geography*, 26 (4), pp.507–532.

Keeling, C.D., Piper, S.C., Bacastow, R.B., Wahlen, M., Whorf, T.P., Heimann, M. & Meijer, H.A. (2005) Atmospheric CO_2 and $^{13}CO_2$ Exchange with the Terrestrial Biosphere and Oceans from 1978 to 2000: Observations and Carbon Cycle Implications. In: *A History of Atmospheric CO2 and Its Effects on Plants, Animals, and Ecosystems*.

New York, Springer-Verlag, pp.83–113.

Keen, D.H. (2001) Towards a late middle Pleistocene non-marine molluscan biostratigraphy for the British Isles. *Quaternary Science Reviews*, 20 (16-17), pp.1657–1665.

Kerney, M.P. (1999) *Atlas of the land and freshwater molluscs of Britain and Ireland*. Great Horkesley, Essex, Harley Books.

Kim, S. & O'Neil, J. (1997) Equilibrium and nonequilibrium oxygen isotope effects in synthetic carbonates. *Geochimica et Cosmochimica Acta*, 61 (16), pp.3461–3475.

Kimura, Y., Jacobs, L.L., Cerling, T.E., Uno, K.T., Ferguson, K.M., Flynn, L.J. & Patnaik, R. (2013) Fossil mice and rats show isotopic evidence of niche partitioning and change in dental ecomorphology related to dietary shift in Late Miocene of Pakistan. *PLoS ONE*, 8, e69308.

Kirsanow, K. & Tuross, N. (2011) Oxygen and hydrogen isotopes in rodent tissues: Impact of diet, water and ontogeny. *Palaeogeography, Palaeoclimatology, Palaeoecology*, 310 (1–2), pp.9–16.

Klevezal, G.A., Pucek, M. & Sukhovskaja, L.I. (1990) Incisor growth in voles. *Acta Therologica*, 35 (3–4), pp.331–344.

Koch, P., Tuross, N. & Fogel, M. (1997) The effects of sample treatment and diagenesis on the isotopic integrity of carbonate in biogenic hydroxylapatite. *Journal of Archaeological Science*, 24, pp.417–429.

von Koenigswald, W. & Golenishev, F.N. (1979) A method for determining growth rates in continuously growing molars. *Journal of Mammalogy*, 60 (2), pp.397–400.

von Koenigswald, W. & van Kolfschoten, T. (1996) The Mimomys-Arvicola boundary and the enamel thickness quotient (SDQ) of Arvicola as stratigraphic markers in the Middle Pleistocene. In: C. Turner ed. *The early Middle Pleistocene in Europe: Proceedings of the SEQS Cromer Symposium, Norwich, UK, 3-7 September 1990*. Rotterdam, Balkema, pp.211–226.

Kohn, M., Schoeninger, M. & Valley, J. (1996) Herbivore tooth oxygen isotope compositions: effects of diet and physiology. *Geochimica et Cosmochimica Acta*, 60 (20), pp.3889–3896.

Kohn, M.J. (2010) Carbon isotope compositions of terrestrial C_3 plants as

indicators of (paleo)ecology and (paleo)climate. *Proceedings of the National Academy of Sciences*, 107 (46), pp.19691–19695.

Kohn, M.J. (2016) Carbon isotope discrimination in C_3 land plants is independent of natural variations in pCO_2. *Geochemical Perspectives Letters*, 2, pp.35–43.

Kohn, M.J. (2004) Comment: Tooth enamel mineralization in ungulates: implications for recovering a primary isotopic time-series, by B. H. Passey and T. E. Cerling (2002). *Geochimica et Cosmochimica Acta*, 68 (2), pp.403–405.

Kohn, M.J. & Cerling, T.E. (2002) Stable Isotope Compositions of Biological Apatite. In: M. J. Kohn, J. Rakovan, & J. M. Hughes eds. *Phosphates: Geochemical, Geobiological, and Materials Importance*. Washington D.C., Mineralogical Society of America, pp.455–488.

Kohn, M.J., Schoeninger, M.J. & Barker, W.W. (1999) Altered states: effects of diagenesis on fossil tooth chemistry. *Geochimica et Cosmochimica Acta*, 63 (18), pp.2737–2747.

Kohn, M.J. & Welker, J.M. (2005) On the temperature correlation of $\delta^{18}O$ in modern precipitation. *Earth and Planetary Science Letters*, 231 (1–2), pp.87–96.

Kontoyannis, C.G. & Vagenas, N.V. (2000) Calcium carbonate phase analysis using XRD and FT-Raman spectroscopy. *The Analyst*, 125 (2), pp.251–255.

Körner, C., Farquhar, G.D. & Roksandic, Z. (1988) A global survey of carbon isotope discrimination in plants from high altitude. *Oecologia*, 74 (4), pp.623–632.

Körner, C., Farquhar, G.D. & Wong, S.C. (1991) Carbon isotope discrimination by plants follows latitudinal and altitudinal trends. *Oecologia*, 88 (1), pp.30–40.

Korslund, L. & Steen, H. (2006) Small rodent winter survival: Snow conditions limit access to food resources. *Journal of Animal Ecology*, 75 (1), pp.156–166.

Koster, R.D., de Valpine, D.P. & Jouzel, J. (1993) Continental water recycling and $H_2{}^{18}O$ concentrations. *Geophysical Research Letters*, 20 (20), pp.2215–2218.

Kovács, J., Moravcová, M., Újvári, G. & Pintér, A.G. (2012) Reconstructing the paleoenvironment of East Central Europe in the Late Pleistocene using the oxygen and carbon isotopic signal of tooth in large mammal remains. *Quaternary International*, 276–277, pp.145–154.

Krishnamurthy, R. V. & Epstein, S. (1990) Glacial-interglacial excursion in the concentration of atmospheric CO_2: effect in the $^{13}C/^{12}C$ ratio in wood cellulose. *Tellus B*, 42 (5), pp.423–434.

Krueger, H.W. (1991) Exchange of carbon with biological apatite. *Journal of Archaeological Science*, 18 (3), pp.355–361.

Krueger, H.W. & Sullivan, C.H. (1984) Models for Carbon Isotope Fractionation Between Diet and Bone. In: *Stable Isotopes in Nutrition. American Chemical Society Symposium Series 258.* Washington D.C., American Chemical Society, pp.205–220.

Kryštufek, B. (1999) Microtus subterraneus. In: A. J. Mitchel-Jones, G. Amori, W. Bogdanowicz, B. Kryštufek, P. J. H. Reijnders, F. Spitzenberger, M. Stubbe, J. B. M. Thissen, V. Vohralík, & J. Zima eds. *The Atlas of European Mammals*. London, Academic Press, pp.250–251.

Lafuente, B., Downs, R.T., Yang, H. & Stone, N. (2015) The power of databases: the RRUFF project. In: T. Armbruster & R. M. Danisi eds. *Highlights in Mineralogical Crystallography*. Berlin, Germany, de Gruyter.

Lane, C.S., Brauer, A., Blockley, S.P.E. & Dulski, P. (2013) Volcanic ash reveals time-transgressive abrupt climate change during the Younger Dryas. *Geology*, 41 (12), pp.1251–1254.

Lang, B., Brooks, S.J., Bedford, A., Jones, R.T., Birks, H.J.B. & Marshall, J.D. (2010) Regional consistency in Lateglacial chironomid-inferred temperatures from five sites in north-west England. *Quaternary Science Reviews*, 29 (13–14), pp.1528–1538.

Lang, N. & Wolff, E.W. (2011) Interglacial and glacial variability from the last 800 ka in marine, ice and terrestrial archives. *Climate of the Past*, 7 (2), pp.361–380.

Last, J. (2014) The excavation of two round barrows on Longstone Edge, Derbyshire. *Derbyshire Archaeological Journal*, 134, pp.81–174.

Laudon, H., Hemond, H.F., Krouse, R. & Bishop, K.H. (2002) Oxygen 18 fractionation during snowmelt: Implications for spring flood hydrograph separation. *Water Resources Research*, 38 (11), 1258.

Lawler, H.A. (1987) Sampling for isotopic responses in surface waters. *Earth Surface Processes and Landforms*, 12 (5), pp.551–559.

Lawrence, J.R. & White, J.W.C. (1991) The elusive climate signal in the isotopic composition of precipitation. In: H. P. Taylor, J. R. O'Neil, & I. R. Kaplan eds. *Stable Isotope Geochemistry: A Tribute to Samuel Epstein*. The Geochemical Society, Special Publication, pp.169–185.

Lécuyer, C., Balter, V., Martineau, F., Fourel, F., Bernard, A., Amiot, R., Gardien, V., Otero, O., Legendre, S., Panczer, G., Simon, L. & Martini, R. (2010) Oxygen isotope fractionation between apatite-bound carbonate and water determined from controlled experiments with synthetic apatites precipitated at 10–37°C. *Geochimica et Cosmochimica Acta*, 74 (7), pp.2072–2081.

Lecuyer, C., Grandjean, P. & Sheppard, S.M.F. (1999) Oxygen isotope exchange between dissolved phosphate and water at temperatures ≤ 135°C: Inorganic versus biological fractionations. *Geochimica et Cosmochimica Acta*, 63 (6), pp.855–862.

Lee-Thorp, J.A. (1989) Stable carbon isotopes in deep time: the diets of fossil fauna and hominids. PhD thesis, University of Cape Town.

Lee-Thorp, J.A., Sealy, J.C. & van der Merwe, N.J. (1989) Stable carbon isotope ratio differences between bone collagen and bone apatite, and their relationship to diet. *Journal of Archaeological Science*, 16 (6), pp.585–599.

Lee-Thorp, J. & van der Merwe, N.J. (1987) Carbon isotope analysis of fossil bone apatite. *South African Journal of Science*, 83 (11), pp.712–715.

Lee-Thorp, J.A. & van der Merwe, N.J. (1991) Aspects of the chemistry of modern and fossil biological apatites. *Journal of Archaeological Science*, 18 (3), pp.343–354.

Lee-Thorp, J. & Sponheimer, M. (2003) Three case studies used to reassess the reliability of fossil bone and enamel isotope signals for paleodietary studies. *Journal of Anthropological Archaeology*, 22 (3), pp.208–216.

Leng, M.J. & Marshall, J.D. (2004) Palaeoclimate interpretation of stable

isotope data from lake sediment archives. *Quaternary Science Reviews*, 23 (7–8), pp.811–831.

Leroy, S.A.G., Arpe, K. & Mikolajewicz, U. (2011) Vegetation context and climatic limits of the Early Pleistocene hominin dispersal in Europe. *Quaternary Science Reviews*, 30 (11–12), pp.1448–1463.

Leuenberger, M., Siegenthaler, U. & Langway, C.C. (1992) Carbon isotope composition of atmospheric CO_2 during the last ice age from an Antarctic ice core. *Nature*, 357 (6378), pp.488–490.

Li, H.C. & Ku, T.L. (1997) $\delta^{13}C$-$\delta^{18}O$ covariance as a paleohydrological indicator for closed-basin lakes. *Palaeogeography, Palaeoclimatology, Palaeoecology*, 133 (1–2), pp.69–80.

Lindars, E.S., Grimes, S.T., Mattey, D.P., Collinson, M.E., Hooker, J.J. & Jones, T.P. (2001) Phosphate $\delta^{18}O$ determination of modern rodent teeth by direct laser fluorination: an appraisal of methodology and potential application to palaeoclimate reconstruction. *Geochimica et Cosmochimica Acta*, 65 (15), pp.2535–2548.

Linz, E. & Müller, G. (1981) Isotopen-geochemische Untersuchungen an Mollusken-Schalen verschiedener Seen Mitteleuropas. *Tschermaks Mineralogische und Petrographische Mitteilungen*, 29 (1), pp.55–65.

Lisiecki, L.E. & Raymo, M.E. (2005) A Pliocene-Pleistocene stack of 57 globally distributed benthic $\delta^{18}O$ records. *Paleoceanography*, 20, PA1003.

Lisiecki, L.E. & Raymo, M.E. (2009) Diachronous benthic $\delta^{18}O$ responses during late Pleistocene terminations. *Paleoceanography*, 24 (3), PA3210.

Lister, A.M. & Stuart, A.J. (2008) The impact of climate change on large mammal distribution and extinction: Evidence from the last glacial/interglacial transition. *Comptes Rendus - Geoscience*, 340 (9–10), pp.615–620.

Lister, A.M. & Stuart, A.J. (2010) The West Runton mammoth (Mammuthus trogontherii) and its evolutionary significance. *Quaternary International*, 228 (1–2), pp.180–209.

Loader, N.J., Robertson, I. & McCarroll, D. (2003) Comparison of stable carbon isotope ratios in the whole wood, cellulose and lignin of oak tree-

rings. *Palaeogeography, Palaeoclimatology, Palaeoecology*, 196 (3–4), pp.395–407.

Lock, G. & Brown, L. (1995) Animal bone erosion, pottery abrasion and the reliability of pit phasing. In: B. Cunliffe ed. *Danebury: An Iron Age Hillfort in Hampshire. Volume 6: A hillfort community in perspective*. York, Council for British Archaeology, CBA Research Report no. 102, pp.126–128.

Loftus, E., Rogers, K. & Lee-Thorp, J. (2015) A simple method to establish calcite: Aragonite ratios in archaeological mollusc shells. *Journal of Quaternary Science*, 30 (8), pp.731–735.

Long, E.S., Sweitzer, R.A., Diefenbach, D.R. & Ben-David, M. (2005) Controlling for anthropogenically induced atmospheric variation in stable carbon isotope studies. *Oecologia*, 146 (1), pp.148–156.

Longinelli, A. (1984) Oxygen isotopes in mammal bone phosphate: a new tool for paleohydrological and paleoclimatological research? *Geochimica et Cosmochimica Acta*, 48 (2), pp.385–390.

Longinelli, A., Iacumin, P., Davanzo, S. & Nikolaev, V. (2003) Modern reindeer and mice: revised phosphate–water isotope equations. *Earth and Planetary Science Letters*, 214 (3–4), pp.491–498.

Longinelli, A. & Peretti Padalino, A. (1980) Oxygen isotopic composition of water from mammal blood: first results. *European Journal of Mass Spectrometry in Biochemical, Medicine and Environmental Research*, 1 (3), pp.135–139.

López-García, J.M., dalla Valle, C., Cremaschi, M. & Peresani, M. (2015a) Reconstruction of the Neanderthal and Modern Human landscape and climate from the Fumane cave sequence (Verona, Italy) using small-mammal assemblages. *Quaternary Science Reviews*, 128, pp.1–13.

López-García, J.M., Soler, N., Maroto, J., Soler, J., Alcalde, G., Galobart, À., Bennàsar, M. & Burjachs, F. (2015b) Palaeoenvironmental and palaeoclimatic reconstruction of the Latest Pleistocene of L'Arbreda Cave (Serinyà, Girona, northeastern Iberia) inferred from the small-mammal (insectivore and rodent) assemblages. *Palaeogeography, Palaeoclimatology, Palaeoecology*, 435, pp.244–253.

Lourantou, A., Lavrič, J. V., Köhler, P., Barnola, J.-M., Paillard, D., Michel, E., Raynaud, D. & Chappellaz, J. (2010) Constraint of the CO_2 rise by

new atmospheric carbon isotopic measurements during the last deglaciation. *Global Biogeochemical Cycles*, 24 (2), p.GB2015.

Lovegrove, B.G. (2003) The influence of climate on the basal metabolic rate of small mammals: a slow-fast metabolic continuum. *Journal of comparative physiology. B, Biochemical, systemic, and environmental physiology*, 173 (2), pp.87–112.

Ludwig, P., Schaffernicht, E.J., Shao, Y. & Pinto, J.G. (2016) Regional atmospheric circulation over Europe during the last Glacial maximum and its links to precipitation. *Journal of Geophysical Research*, 121 (5), pp.2130–2145.

Luz, B. & Kolodny, Y. (1985) Oxygen isotope variations in phosphate of biogenic apatites, IV. Mammal teeth and bones. *Earth and Planetary Science Letters*, 75 (1), pp.29–36.

Luz, B., Kolodny, Y. & Horowitz, M. (1984) Fractionation of oxygen isotopes between mammalian bone-phosphate and environmental drinking water. *Geochimica et Cosmochimica Acta*, 48 (8), pp.1689–1693.

MacDonald, D. & Barrett, P. (1993) *Collins Field Guide: Mammals of Britain & Europe*. London, Harper Collins.

Marino, B.D. & McElroy, M.B. (1991) Isotopic composition of atmospheric CO_2 inferred from carbon in C_4 plant cellulose. *Nature*, 349 (6305), pp.127–131.

Marino, B.D., McElroy, M.B., Salawitch, R.J. & Spaulding, W.G. (1992) Glacial-to-interglacial variations in the carbon isotopic composition of atmospheric CO_2. *Nature*, 357 (6378), pp.461–466.

Markova, A.K. & Puzachenko, A.Y. (2016) The European small mammal faunas related to the first half of the Middle Pleistocene. *Quaternary International*, 420, pp.378–390.

Marshall, J., Jones, R. & Crowley, S. (2002) A high resolution late-glacial isotopic record from Hawes Water, northwest England: Climatic oscillations: Calibration and comparison of palaeotemperature proxies. *Palaeogeography, Palaeoclimatology, Palaeoecology*, 185, pp.25–40.

Marshall, J.D., Lang, B., Crowley, S.F., Weedon, G.P., van Calsteren, P., Fisher, E.H., Holme, R., Holmes, J.A., Jones, R.T., Bedford, A., Brooks, S.J., Bloemendal, J., Kiriakoulakis, K. & Ball, J.D. (2007) Terrestrial

impact of abrupt changes in the North Atlantic thermohaline circulation: Early Holocene, UK. *Geology*, 35 (7), pp.639–642.

Marshall, P., Last, J., Bronk Ramsey, C. & van der Plicht, H. (2014) Radiocarbon dating. In: Last, J., The excavation of two round barrows on Longstone Edge, Derbyshire. *Derbyshire Archaeological Journal,* 134, pp.105–112.

Martin, C., Bentaleb, I., Kaandorp, R., Iacumin, P. & Chatri, K. (2008) Intra-tooth study of modern rhinoceros enamel $\delta^{18}O$: Is the difference between phosphate and carbonate $\delta^{18}O$ a sound diagenetic test? *Palaeogeography, Palaeoclimatology, Palaeoecology*, 266 (3–4), pp.183–189.

Masson-Delmotte, V., Dreyfus, G., Braconnot, P., Johnsen, S., Jouzel, J., Kageyama, M., Landais, A., Loutre, M.F., Nouet, J., Parrenin, F., Raynaud, D., Stenni, B. & Tuenter, E. (2006) Past temperatures reconstructions from deep ice cores: relevance for future climate changes. *Climate of the Past*, 2 (4), pp.145–165.

Maul, L.C., Heinrich, W.D., Parfitt, S.A. & Paunescu, A.C. (2007) Comment on the correlation between magnetostratigraphy and the evolution of Microtus (Arvicolidae, Rodentia, Mammalia) during the Early and early Middle Pleistocene. *CFS Courier Forschungsinstitut Senckenberg*, (259), pp.243–263.

Maul, L.C. & Parfitt, S.A. (2010) Micromammals from the 1995 Mammoth Excavation at West Runton, Norfolk, UK: Morphometric data, biostratigraphy and taxonomic reappraisal. *Quaternary International*, 228 (1–2), pp.91–115.

Mayhew, D.F. (1977) Avian predators as accumulators of fossil mammal material. *Boreas*, 6 (1), pp.25–31.

McConnaughey, T.A. & Gillikin, D.P. (2008) Carbon isotopes in mollusk shell carbonates. *Geo-Marine Letters*, 28 (5–6), pp.287–299.

McCormac, F.G., Baillie, M.G.L., Pilcher, J.R., Brown, D.M. & Hoper, S.T. (1994) $\delta^{13}C$ Measurements from the Irish Oak Chronology. *Radiocarbon*, 36 (1), pp.27–35.

McManus, J.F., Oppo, D.W. & Cullen, J.L. (1999) A 0.5-Million-year record of millennial-scale climate variability in the North Atlantic. *Science*, 283 (5404), pp.971–975.

McMillan, N.F. (1968) *British shells*. London, Frederick Warne & Co.

Medina, E. & Minchin, P. (1980) Stratification of $\delta^{13}C$ values of leaves in Amazonian rain forests. *Oecologia*, 45 (3), pp.377–378.

van der Merwe, N. (1982) Carbon Isotopes, Photosynthesis, and Archaeology. *American Scientist*, 70 (6), pp.596–606.

van der Merwe, N.J. & Medina, E. (1991) The canopy effect, carbon isotope ratios and foodwebs in amazonia. *Journal of Archaeological Science*, 18 (3), pp.249–259.

Met Office (2018) UK climate. Available from: <https://www.metoffice.gov.uk/public/weather/climate> [Accessed 23 June 2018].

Mikkola, H. (1983) *Owls of Europe*. Carlton, T. & A.D. Poyser.

Monnin, E., Steig, E.J., Siegenthaler, U., Kawamura, K., Schwander, J., Stauffer, B., Stocker, T.F., Morse, D.L., Barnola, J.-M., Bellier, B., Raynaud, D. & Fischer, H. (2004a) Evidence for substantial accumulation rate variability in Antarctica during the Holocene, through synchronization of CO_2 in the Taylor Dome, Dome C and DML ice cores. *Earth and Planetary Science Letters*, 224 (1–2), pp.45–54.

Monnin, E., Steig, E.J., Siegenthaler, U., Kawamura, K., Schwander, J., Stauffer, B., Stocker, T.F., Morse, D.L., Barnola, J.-M., Bellier, B., Raynaud, D. & Fischer, H. (2004b) EPICA Dome C Ice Core High Resolution Holocene and Transition CO_2 data. [Internet]. Available from: <https://www.ncdc.noaa.gov/paleo/study/2479> [Accessed 26 June 2018].

Mook, W.G. & Vogel, J.C. (1968) Isotopic equilibrium between shells and their environment. *Science*, 159 (3817), pp.874–875.

Morecroft, M.D. & Woodward, F.I. (1990) Experimental investigations on the environmental determination of $\delta^{13}C$ at different altitudes. *Journal of Experimental Botany*, 41 (231), pp.1303–1308.

Moros, M., Emeis, K., Risebrobakken, B., Snowball, I., Kuijpers, A., McManus, J. & Jansen, E. (2004) Sea surface temperatures and ice rafting in the Holocene North Atlantic: Climate influences on northern Europe and Greenland. *Quaternary Science Reviews*, 23 (20–22 Special issue), pp.2113–2126.

Murton, J.B., Baker, A., Bowen, D.Q., Caseldine, C.J., Coope, G.R., Currant, A.P., Evans, J.G., Field, M.H., Green, C.P., Hatton, J., Ito, M., Jones, R.L., Keen, D.H., Kerney, M.P., McEwan, R., McGregor, D.F.M., Parish, D., Robinson, J.E., Schreve, D.C. & Smart, P.L. (2001) A late Middle Pleistocene temperate-periglacial-temperate sequence (Oxygen Isotope Stages 7-5e) near Marsworth, Buckinghamshire, UK. *Quaternary Science Reviews*, 20 (18), pp.1787–1825.

Murton, J.B., Bowen, D.Q., Candy, I., Catt, J.A., Currant, A., Evans, J.G., Frogley, M.R., Green, C.P., Keen, D.H., Kerney, M.P., Parish, D., Penkman, K., Schreve, D.C., Taylor, S., Toms, P.S., Worsley, P. & York, L.L. (2015) Middle and Late Pleistocene environmental history of the Marsworth area, south-central England. *Proceedings of the Geologists' Association*, 126 (1), pp.18-49.

Navarro, N., Lécuyer, C., Montuire, S., Langlois, C. & Martineau, F. (2004) Oxygen isotope compositions of phosphate from arvicoline teeth and Quaternary climatic changes, Gigny, French Jura. *Quaternary Research*, 62 (2), pp.172–182.

Nelson, B.K., Deniro, M.J., Schoeninger, M.J., De Paolo, D.J. & Hare, P.. (1986) Effects of diagenesis on strontium, carbon, nitrogen and oxygen concentration and isotopic composition of bone. *Geochimica et Cosmochimica Acta*, 50 (9), pp.1941–1949.

Nesje, A., Dahl, S.O. & Bakke, J. (2004) Were abrupt Lateglacial and early-Holocene climatic changes in northwest Europe linked to freshwater outbursts to the North Atlantic and Arctic Oceans? *Holocene*, 14 (2), pp.299–310.

Newesely, H. (1989) Fossil bone apatite. *Applied Geochemistry*, 4 (3), pp.233–245.

NOAA (2018) Recent Global CO_2 Trend. Available from: <https://www.esrl.noaa.gov/gmd/ccgg/trends/global.html> [Accessed 25 August 2018].

Norrdahl, K. & Korpimaki, E. (2002) Seasonal changes in the numerical responses of predators to cyclic vole populations. *Ecography*, 25 (4), pp.428–438.

O'Leary, M.H. (1981) Carbon isotope fractionation in plants. *Phytochemistry*, 20 (4), pp.553–567.

O'Leary, M. (1988) Carbon isotopes in photosynthesis. *Bioscience*, 38 (5), pp.328–336.

Park, R. & Epstein, S. (1960) Carbon isotope fractionation during photosynthesis. *Geochimica et Cosmochimica Acta*, 21 (1–2), pp.110–126.

Passey, B.H. & Cerling, T. (2006) In situ stable isotope analysis ($\delta^{13}C$, $\delta^{18}O$) of very small teeth using laser ablation GC/IRMS. *Chemical Geology*, 235 (3–4), pp.238–249.

Passey, B.H., Robinson, T.F., Ayliffe, L.K., Cerling, T.E., Sponheimer, M., Dearing, M.D., Roeder, B.L. & Ehleringer, J.R. (2005) Carbon isotope fractionation between diet, breath CO_2, and bioapatite in different mammals. *Journal of Archaeological Science*, 32 (10), pp.1459–1470.

Pearson, C.L., Ważny, T., Kuniholm, P.I., Botić, K., Durman, A. & Seufer, K. (2014) Potential for a New Multimillennial Tree-Ring Chronology from Subfossil Balkan River Oaks. *Radiocarbon*, 56 (4), pp.S51–S59.

Peel, M.C., Finlayson, B.L. & McMahon, T.A. (2007) Updated world map of the Köppen-Geiger climate classification. *Hydrology and Earth System Sciences*, 11 (5), pp.1633–1644.

Pellegrini, M., Lee-Thorp, J. a. & Donahue, R.E. (2011) Exploring the variation of the $\delta^{18}Op$ and $\delta^{18}Oc$ relationship in enamel increments. *Palaeogeography, Palaeoclimatology, Palaeoecology*, 310 (1–2), pp.71–83.

Pellegrini, M., Pouncett, J., Jay, M., Pearson, M.P. & Richards, M.P. (2016) Tooth enamel oxygen "isoscapes" show a high degree of human mobility in prehistoric Britain. *Scientific Reports*, 6, 34986.

Pellegrini, M. & Snoeck, C. (2016) Comparing bioapatite carbonate pre-treatments for isotopic measurements: Part 2 — Impact on carbon and oxygen isotope compositions. *Chemical Geology*, 420, pp.88–96.

Peneycad, E. (2013) Oxygen stable isotopes in water vole teeth: their importance as a palaeoclimatic proxy for Pleistocene Britain. BSc Dissertation, Royal Holloway University of London.

Penkman, K.E.H., Preece, R.C., Bridgland, D.R., Keen, D.H., Meijer, T., Parfitt, S.A., White, T.S. & Collins, M.J. (2013) An aminostratigraphy for the British Quaternary based on Bithynia opercula. *Quaternary science*

reviews, 61, pp.111–134.

Penkman, K.E.H., Preece, R.C., Keen, D.H. & Collins, M.J. (2010) Amino acid geochronology of the type Cromerian of West Runton, Norfolk, UK. *Quaternary international*, 228 (1–2), pp.25–37.

Penkman, K.E.H., Preece, R.C., Keen, D.H., Maddy, D., Schreve, D.C. & Collins, M.J. (2007) Testing the aminostratigraphy of fluvial archives: the evidence from intra-crystalline proteins within freshwater shells. *Quaternary Science Reviews*, 26 (22–24), pp.2958–2969.

Petit, J.R., Jouzel, J., Raynaud, D., Barkov, N.I., Barnola, J.M., Basile, I., Bender, M., Chappellaz, J., Davis, M., Delaygue, G., Delmotte, M., Kotiyakov, V.M., Legrand, M., Lipenkov, V.Y., Lorius, C., Pépin, L., Ritz, C., Saltzman, E. & Stievenard, M. (1999) Climate and atmospheric history of the past 420,000 years from the Vostok ice core, Antarctica. *Nature*, 399 (6735), pp.429–436.

Podlesak, D.W., Torregrossa, A.-M., Ehleringer, J.R., Dearing, M.D., Passey, B.H. & Cerling, T.E. (2008) Turnover of oxygen and hydrogen isotopes in the body water, CO_2, hair, and enamel of a small mammal. *Geochimica et Cosmochimica Acta*, 72 (1), pp.19–35.

Polley, H.W., Johnson, H.B., Marino, B.D. & Mayeux, H.S. (1993) Increase in C_3 plant water-use efficiency and biomass over glacial to present CO_2 concentrations. *Nature*, 361 (6407), pp.61–64.

Preece, R.. (2001) Molluscan evidence for differentiation of interglacials within the ‘Cromerian Complex’. *Quaternary Science Reviews*, 20 (16–17), pp.1643–1656.

Preece, R.C. (2010) The molluscan fauna of the Cromerian type site at West Runton, Norfolk. *Quaternary International*, 228 (1–2), pp.53–62.

Preece, R.C. & Parfitt, S.A. (2000) The Cromer Forest-bed Formation: new thoughts on an old problem. In: S. G. Lewis, C. A. Whiteman, & R. C. Preece eds. *The Quaternary of Norfolk and Suffolk Field Guide*. London, Quaternary Research Association, pp.29–34.

Preece, R.C. & Parfitt, S.A. (2008) The Cromer Forest-bed Formation: some recent developments relating to early human occupation and lowland glaciation. In: I. Candy, J. R. Lee, & A. M. Harrison eds. *The Quaternary of Northern East Anglia Field Guide*. Quaternary Research Association, pp.60–83.

Preece, R.C. & Parfitt, S.A. (2012) The Early and early Middle Pleistocene context of human occupation and lowland glaciation in Britain and northern Europe. *Quaternary International*, 271, pp.6–28.

Pryor, A.J.E., Stevens, R.E., O'Connell, T.C. & Lister, J.R. (2014) Quantification and propagation of errors when converting vertebrate biomineral oxygen isotope data to temperature for palaeoclimate reconstruction. *Palaeogeography, Palaeoclimatology, Palaeoecology*, 412, pp.99–107.

Pushkina, D., Bocherens, H. & Ziegler, R. (2014) Unexpected palaeoecological features of the Middle and Late Pleistocene large herbivores in southwestern Germany revealed by stable isotopic abundances in tooth enamel. *Quaternary International*, 339–340, pp.164–178.

Quade, J., Cerling, T.E., Barry, J.C., Morgan, M.E., Pilbeam, D.R., Chivas, A.R., Lee-Thorp, J.A. & van der Merwe, N.J. (1992) A 16-Ma record of paleodiet using carbon and oxygen isotopes in fossil teeth from Pakistan. *Chemical Geology*, 94 (3), pp.183–192.

Rao, Z., Guo, W., Cao, J., Shi, F., Jiang, H. & Li, C. (2017) Relationship between the stable carbon isotopic composition of modern plants and surface soils and climate: A global review. *Earth-Science Reviews*, 165, pp.110–119.

Rao, Z.G., Chen, F.H., Zhang, X., Xu, Y.B., Xue, Q. & Zhang, P.Y. (2012) Spatial and temporal variations of C_3/C_4 relative abundance in global terrestrial ecosystem since the Last Glacial and its possible driving mechanisms. *Chinese Science Bulletin*, 57 (31), pp.4024–4035.

Rasmussen, S.O., Andersen, K.K., Svensson, A.M., Steffensen, J.P., Vinther, B.M., Clausen, H.B., Siggaard-Andersen, M.L., Johnsen, S.J., Larsen, L.B., Dahl-Jensen, D., Bigler, M., Röthlisberger, R., Fischer, H., Goto-Azuma, K., Hansson, M.E. & Ruth, U. (2006) A new Greenland ice core chronology for the last glacial termination. *Journal of Geophysical Research: Atmospheres*, 111, D06102.

Reid, C. (1882) *The geology of the country around Cromer*. Memoirs of the Geological Survey, England and Wales.

Reid, C. (1890) *The Pliocene deposits of Britain*. Memoirs of the Geological Survey, England and Wales.

Reimer, P.J., Bard, E., Bayliss, A., Beck, J.W., Blackwell, P.G., Ramsey, C.B., Buck, C.E., Cheng, H., Edwards, R.L., Friedrich, M., Grootes, P.M., Guilderson, T.P., Haflidason, H., Hajdas, I., Hatté, C., Heaton, T.J., Hoffmann, D.L., Hogg, A.G., Hughen, K.A., Kaiser, K.F., Kromer, B., Manning, S.W., Niu, M., Reimer, R.W., Richards, D.A., Scott, E.M., Southon, J.R., Staff, R.A., Turney, C.S.M. & van der Plicht, J. (2013) IntCal13 and Marine13 Radiocarbon Age Calibration Curves 0–50,000 Years cal BP. *Radiocarbon*, 55 (4), pp.1869–1887.

Reynard, L.M., Meltzer, D.J., Emslie, S.D. & Tuross, N. (2015) Stable isotopes in yellow-bellied marmot (Marmota flaviventris) fossils reveal environmental stability in the late Quaternary of the Colorado Rocky Mountains. *Quaternary Research*, 83 (2), pp.345–354.

Richards, M.P. & Hedges, R.E.M. (2003) Variations in bone collagen $\delta^{13}C$ and $\delta^{15}N$ values of fauna from Northwest Europe over the last 40,000 years. *Palaeogeography, Palaeoclimatology, Palaeoecology*, 193 (2), pp.261–267.

Rink, W.J., Schwarcz, H.P., Stuart, A.J., Lister, A.M., Marseglia, E. & Brennan, B.J. (1996) ESR dating of the type Cromerian freshwater bed at West Runton, U.K. *Quaternary Science Reviews*, 15 (7), pp.727–738.

Roberts, M.B. & Parfitt, S.A. (1999) *Boxgrove: A Middle Pleistocene hominid site at Eartham Quarry, Boxgrove, West Sussex*. London, English Heritage.

Robertson, I., Switsur, V.R., Carter, A.H.C., Barker, A.C., Waterhouse, J.S., Briffa, K.R. & Jones, P.D. (1997) Signal strength and climate relationships in $^{13}C/^{12}C$ ratios of tree ring cellulose from oak in east England. *Journal of Geophysical Research: Atmospheres*, 102 (D16), pp.19507–19516.

Roe, H.M., Coope, G.R., Devoy, R.J.N., Harrison, C.J.O., Penkman, K.E.H., Preece, R.C. & Schreve, D.C. (2009) Differentiation of MIS 9 and MIS 11 in the continental record: vegetational, faunal, aminostratigraphic and sea-level evidence from coastal sites in Essex, UK. *Quaternary Science Reviews*, 28, pp.2342–2373.

Rogers, K.L. & Wang, Y. (2002) Stable isotopes in pocket gopher teeth as evidence of a Late Matuyama climate shift in the Southern Rocky Mountains. *Quaternary Research*, 57 (2), pp.200–207.

Romanek, C.S., Grossman, E.L. & Morse, J.W. (1992) Carbon isotopic fractionation in synthetic aragonite and calcite: Effects of temperature and precipitation rate. *Geochimica et Cosmochimica Acta*, 56 (1), pp.419–430.

Rose, J., Juby, C., Bullen, M., Davies, S., Branch, N., Gammage, Z., Candy, I. & Palmer, A. (2008) The stratigraphy, sedimentology, palaeoenvironments and duration of the early Middle Pleistocene sediments at West Runton, north Norfolk. In: I. Candy, J. R. Lee, & A. M. Harrison eds. *The Quaternary of Northern East Anglia Field Guide*. Quaternary Research Association, pp.157–181.

Royer, A., Lécuyer, C., Montuire, S., Amiot, R., Legendre, S., Cuenca-Bescós, G., Jeannet, M. & Martineau, F. (2013a) What does the oxygen isotope composition of rodent teeth record? *Earth and Planetary Science Letters*, 361, pp.258–271.

Royer, A., Lécuyer, C., Montuire, S., Escarguel, G., Fourel, F., Mann, A. & Maureille, B. (2013b) Late Pleistocene (MIS 3-4) climate inferred from micromammal communities and $\delta^{18}O$ of rodents from Les Pradelles, France. *Quaternary Research*, 80, pp.113–124.

Royer, A., Lécuyer, C., Montuire, S., Primault, J., Fourel, F. & Jeannet, M. (2014) Summer air temperature, reconstructions from the last glacial stage based on rodents from the site Taillis-des-Coteaux (Vienne), Western France. *Quaternary Research*, 82 (2), pp.420–429.

Royer, A., Montuire, S., Legendre, S., Discamps, E., Jeannet, M. & Lécuyer, C. (2016) Investigating the Influence of Climate Changes on Rodent Communities at a Regional-Scale (MIS 1-3, Southwestern France) *PLOS ONE*, 11 (1), e0145600.

Rozanski, K., Araguas-Araguas, L. & Gonfiantini, R. (1992) Relation between long-term trends of Oxygen-18 isotope composition of precipitation and climate. *Science*, 258 (5084), pp.981–985.

Rozanski, K., Araguás-Araguás, L. & Gonfiantini, R. (1993) Isotopic patterns in modern global precipitation. In: P. Swart, J. A. McKenzie, K. C. Lohmann, & S. Savin eds. *Climate Change in Continental Isotope Records*. Geophysical Mongraph. American Geophysical Union, pp.1–36.

Rozanski, K., Sonntag, C. & Münnich, K.O. (1982) Factors controlling stable

isotope composition of European precipitation. *Tellus*, 34 (2), pp.142–150.

Rubino, M., Etheridge, D.M., Trudinger, C.M., Allison, C.E., Battle, M.O., Langenfelds, R.L., Steele, L.P., Curran, M., Bender, M., White, J.W.C., Jenk, T.M., Blunier, T. & Francey, R.J. (2013) A revised 1000 year atmospheric $\delta^{13}C$-CO_2 record from Law Dome and South Pole, Antarctica. *Journal of Geophysical Research: Atmospheres*, 118 (15), pp.8482–8499.

Ruddy, M. (2005) Oxygen stable isotope analysis of water vole (Arvicola) incisor tooth enamel: a proxy record of terrestrial climate from MIS 9 Britain. *Unpublished MSc Thesis, Royal Holloway, University of London*.

Sage, R.F. & Monson, R.K. (1999) *C_4 Plant Biology*. London, Academic Press Limited.

Sánchez, B., Prado, J.L. & Alberdi, M.T. (2004) Feeding ecology, dispersal, and extinction of South American Pleistocene gomphotheres (Gomphotheriidae, Proboscidea). *Paleobiology*, 30 (1), pp.146–161.

Salamolard, M., Butet, A., Leroux, A. & Bretagnolle, V. (2000) Responses of an avian predator to variations in prey density at a temperate latitude. *Ecology*, 81 (9), pp.2428–2441.

Saurer, M., Siegwolf, R.T.W. & Schweingruber, F.H. (2004) Carbon isotope discrimination indicates improving water-use efficiency of trees in northern Eurasia over the last 100 years. *Global Change Biology*, 10 (12), pp.2109–2120.

Schleser, G.H. & Jayasekera, R. (1985) $\delta^{13}C$-variations of leaves in forests as an indication of reassimilated CO_2 from the soil. *Oecologia*, 65 (4), pp.536–542.

Schoeninger, M.J. & DeNiro, M.J. (1982) Carbon isotope ratios of apatite from fossil bone cannot be used to reconstruct diets of animals. *Nature*, 297 (5867), pp.577–578.

Schrag, D.P., Adkins, J.F., McIntyre, K., Alexander, J.L., Hodell, D.A., Charles, C.D. & McManus, J.F. (2002) The oxygen isotopic composition of seawater during the Last Glacial Maximum. *Quaternary Science Reviews*, 21 (1–3), pp.331–342.

Schreve, D. (2006) *Interim Report on Excavations at Gully Cave, Ebbor*

Gorge, Somerset.

Schreve, D. (2007) *Second Interim Report on Excavations at Gully Cave, Ebbor Gorge, Somerset*.

Schreve, D. (2010) *Third Interim Report on Excavations at Gully Cave, Ebbor Gorge, Somerset*.

Schreve, D. (2011) *Fourth Interim Report on Excavations at Gully Cave, Ebbor Gorge, Somerset*.

Schreve, D. (2012a) *Fifth Interim Report on Excavations at Gully Cave, Ebbor Gorge, Somerset*.

Schreve, D. (2012b) *Sixth Interim Report on Excavations at Gully Cave, Ebbor Gorge, Somerset*.

Schreve, D. (2014) *Eighth Interim Report on Excavations at Gully Cave, Ebbor Gorge, Somerset*.

Schreve, D. (2015) *Ninth Interim Report on Excavations at Gully Cave, Ebbor Gorge, Somerset*.

Schreve, D. (2016) *Tenth Interim Report on Excavations at Gully Cave, Ebbor Gorge, Somerset*.

Schreve, D.C. (2001) Differentiation of the British late Middle Pleistocene interglacials: The evidence from mammalian biostratigraphy. *Quaternary Science Reviews*, 20, pp.1693–1705.

Schreve, D.C., Bridgland, D.R., Allen, P., Blackford, J.J., Gleed-Owen, C.P., Griffiths, H.I., Keen, D.H. & White, M.J. (2002) Sedimentology, palaeontology and archaeology of late Middle Pleistocene River Thames terrace deposits at Purfleet, Essex, UK. *Quaternary Science Reviews*, 21 (12–13), pp.1423–1464.

Schreve, D.C., Currant, A.P. & Stringer, C.B. (1999) Correlation of the Westbury deposits. In: P. Andrews, J. A. Cook, A. P. Currant, & C. B. Stringer eds. *Westbury Cave. The Natural History Museum Excavations 1976-1984.* Univeristy of Bristol, Western Archaeological and Specialist Press, pp.275–284.

Schubert, B.A. & Jahren, A.H. (2012) The effect of atmospheric CO_2 concentration on carbon isotope fractionation in C_3 land plants. *Geochimica et Cosmochimica Acta*, 96, pp.29–43.

Schubert, B.A. & Jahren, A.H. (2015) Global increase in plant carbon isotope fractionation following the last glacial maximum caused by increase in atmospheric pCO_2. *Geology*, 43 (5), pp.435–438.

Sepulcre, S., Durand, N. & Bard, E. (2009) Mineralogical determination of reef and periplatform carbonates: Calibration and implications for paleoceanography and radiochronology. *Global and Planetary Change*, 66 (1–2), pp.1–9.

Sesé, C. & Villa, P. (2008) Micromammals (rodents and insectivores) from the early Late Pleistocene cave site of Bois Roche (Charente, France): Systematics and paleoclimatology. *Geobios*, 41 (3), pp.399–414.

Shahack-Gross, R., Tchernov, E. & Luz, B. (1999) Oxygen isotopic composition of mammalian skeletal phosphate from the Natufian Period, Hayonim Cave, Israel: Diagenesis and paleoclimate. *Geoarchaeology*, 14 (1), pp.1–13.

Sharma, S., Joachimski, M.M., Tobschall, H.J., Singh, I.B., Tewari, D.P. & Tewari, R. (2004) Oxygen isotopes of bovid teeth as archives of paleoclimatic variations in archaeological deposits of the Ganga plain, India. *Quaternary Research*, 62 (1), pp.19–28.

Sharp, Z.D., Atudorei, V. & Furrer, H. (2000) The effect of diagenesis on oxygen isotope ratios of biogenic phosphates. *American Journal of Science*, 300 (3), pp.222–237.

Shenbrot, G.I. & Krasnov, B.R. (2005) *An atlas of the geographic distribution of the Arvicoline rodents of the world (Rodentia: Muridae, Arvicolinae)*. Pensoft Publishers, Sofia.

Sherlock, R.L. (1922) The geology of the country around Aylesbury and Hemel Hemstead. In: *Memoirs of the Geological Survey of England and Wales, Sheet 238*. London.

Sherriff, J. (2016) The palaeoenvironmental context of hominin occupation in Britain during Marine Oxygen Isotope Stage 11. PhD thesis, Royal Holloway University of London.

Siegenthaler, U., Stocker, T.F., Monnin, E., Lüthi, D., Schwander, J., Stauffer, B., Raynaud, D., Barnola, J.M., Fischer, H., Masson-Delmotte, V. & Jouzel, J. (2005) Atmospheric science: Stable carbon cycle-climate relationship during the late pleistocene. *Science*, 310 (5752), pp.1313–1317.

Sinka, K.J. (1993) Developing the Mutual Climatic Range method of palaeoclimatic reconstruction. PhD thesis, University of East Anglia.

Smedley, M.P., Dawson, T.E., Comstock, J.P., Donovan, L.A., Sherill, D.E., Cook, C.S. & Ehleringer, J.R. (1991) Seasonal carbon isotope discrimination in a grassland community. *Oecologia*, 85 (3), pp.314–320.

Smith, B.N. & Epstein, S. (1971) Two categories of $^{13}C/^{12}C$ ratios for higher plants. *Plant Physiology*, 47 (3), pp.380–384.

Smith, B.N., Herath, H.M.W. & Chase, J.B. (1973) Effect of growth temperature on carbon isotopic ratios in barley, pea and rape. *Changes*, 14 (1), pp.177–182.

Smith, B.N., Oliver, J. & Millan, C.M.C. (1976) Influence of carbon source, oxygen concentration, light intensity, and temperature on $^{13}C/^{12}C$ ratios in plant tissues. *Botanical Gazette*, 137 (2), pp.99–104.

Smith, G. & Wilson, R.A. (1980) Seasonal variations in the microclimate of Lymnaea truncatula habitats. *Journal of Applied Ecology*, 17, pp.329–342.

Smith, H.J., Fischer, H., Wahlen, M., Mastroianni, D. & Deck, B. (1999) Dual modes of the carbon cycle since the Last Glacial Maximum. *Nature*, 400 (6741), pp.248–250.

Snoeck, C. & Pellegrini, M. (2015) Comparing bioapatite carbonate pre-treatments for isotopic measurements: Part 1—Impact on structure and chemical composition. *Chemical Geology*, 417, pp.394–403.

Sonju Clasen, A.B. & Ruyter, I.E. (1997) Quantitative determination of Type A and Type B carbonate in human deciduous and permanent enamel by means of Fourier Transform Infrared Spectrometry. *Advances in Dental Research*, 11, pp.523–527.

Soulsby, C., Malcolm, R., Helliwell, R., Ferrier, R.C. & Jenkins, A. (2000) Isotope hydrology of the Allt a' Mharcaidh catchment, Cairngorms, Scotland: implications for hydrological pathways and residence times. *Hydrological Processes*, 14 (4), pp.747–762.

Sparks, B.W. (1964) Non-marine mollusca and Quaternary ecology. *The Journal of Animal Ecology*, 33, pp.87–98.

Sparks, B.W. (1980) Land and freshwater mollusca of the West Runton Freshwater Bed. In: R. G. West ed. *The pre-glacial Pleistocene of the*

Norfolk and Suffolk coasts. Cambridge, Cambridge University Press, pp.25–27.

Speed, M., Tetzlaff, D., Hrachowitz, M. & Soulsby, C. (2011) Evolution of the spatial and temporal characteristics of the isotope hydrology of a montane river basin. *Hydrological Sciences Journal*, 56 (3), pp.426–442.

Sponheimer, M. & Lee-Thorp, J.A. (1999) Alteration of enamel carbonate environments during fossilization. *Journal of Archaeological Science*, 26 (2), pp.143–150.

Sternberg, L.D.S.L.O.R. (1989) A model to estimate carbon dioxide recycling in forests using $^{13}C/^{12}C$ ratios and concentrations of ambient carbon dioxide. *Agricultural and Forest Meteorology*, 48 (1–2), pp.163–173.

Stevens, R.E. & Hedges, R.E. (2004) Carbon and nitrogen stable isotope analysis of northwest European horse bone and tooth collagen, 40,000 BP–present: Palaeoclimatic interpretations. *Quaternary Science Reviews*, 23 (7–8), pp.977–991.

Stewart, G., Turnbull, M., Schmidt, S. & Erskine, P. (1995) ^{13}C natural abundance in plant communities along a rainfall gradient: a biological integrator of water availability. *Australian Journal of Plant Physiology*, 22 (1), pp.51-55.

Stewart, J.R. (2010) The bird remains from the West Runton Freshwater Bed, Norfolk, England. *Quaternary International*, 228 (1–2), pp.72–90.

Still, C.J., Berry, J.A., Collatz, G.J. & DeFries, R.S. (2003) Global distribution of C_3 and C_4 vegetation: Carbon cycle implications. *Global Biogeochemical Cycles*, 17 (1), 1006.

Strachan, R. & Jefferies, D.J. (1993) *The water vole Arvicola terrestris in Britain 1989-1990: its distribution and changing status*. London, Vincent Wildlife Trust.

Stringer, C.B., Andrews, P. & Currant, A.P. (1996) Palaeoclimatic significance of mammalian faunas from Westbury Cave, Somerset, England. In: C. Turner ed. *The early Middle Pleistocene in Europe: Proceedings of the SEQS Cromer Symposium, Norwich, UK, 3-7 September 1990*. Rotterdam, Balkema, pp.135–143.

Stuart, A.J. (1974) Pleistocene history of the British vertebrate fauna. *Biological Reviews*, 49 (2), pp.225–266.

Stuart, A.J. (1992) The Pleistocene Vertebrate Faunas of West Runton, Norfolk, England. *Cranium*, 9 (2), pp.77–84.

Stuart, A.J. (2000) The West Runton Freshwater Bed. In: S. G. Lewis, C. A. Whiteman, & R. C. Preece eds. *The Quaternary of Norfolk and Suffolk Field Guide*. London, Quaternary Research Association, pp.67–72.

Stuart, A.J. & Lister, A.M. (2010) Introduction: The West Runton Freshwater Bed and the West Runton Mammoth. *Quaternary International*, 228 (1–2), pp.1–7.

Stuart, A.J. & Lister, A.M. (2001) The mammalian faunas of Pakefield/Kessingland and Corton, Suffolk, UK: evidence for a new temperate episode in the British early Middle Pleistocene. *Quaternary Science Reviews*, 20 (16–17), pp.1677–1692.

Stuiver, M. (1970) Oxygen and carbon isotope ratios of fresh-water carbonates as climatic indicators. *Journal of Geophysical Research*, 75 (27), pp.5247–5257.

Stuiver, M., Burk, R.L. & Quay, P.D. (1984) $^{13}C/^{12}C$ ratios in tree rings and the transfer of biospheric carbon to the atmosphere. *Journal of Geophysical Research*, 89 (D7), 11731.

Sullivan, C.H. & Krueger, H.W. (1981) Carbon isotope analysis of separate chemical phases in modern and fossil bone. *Nature*, 292 (5821), pp.333–335.

Sutcliffe, A.J. & Kowalski, K. (1976) *Pleistocene rodents of the British Isles*. Bulletin of the British Museum (Natural History) Geology, Vol. 27, No. 2, London.

Talbot, M.R. (1990) A review of the palaeohydrological interpretation of carbon and oxygen isotopic ratios in primary lacustrine carbonates. *Chemical Geology: Isotope Geoscience Section*, 80 (4), pp.261–279.

Tast, J. (1966) The Root Vole, Microtus oeconomus (Pallas), as an inhabitant of seasonally flooded land. *Annales zoologici fennici*, 3 (1), pp.127–171.

Taylor, I. (1994) *Barn owls: predator-prey relationships and conservation*. Cambridge, UK, Cambridge University Press.

Teeri, J.A. & Stowe, L.G. (1976) Climatic patterns and the distribution of C_4 grasses in North America. *Oecologia*, 23 (1), pp.1–12.

Tieszen, L.L. (1991) Natural variations in the carbon isotope values of plants: Implications for archaeology, ecology, and paleoecology. *Journal of Archaeological Science*, 18 (3), pp.227–248.

Tieszen, L.L., Boutton, T.W., Tesdahl, K.G. & Slade, N.A. (1983) Fractionation and turnover of stable carbon isotopes in animal tissues: Implications for $\delta^{13}C$ analysis of diet. *Oecologia*, 57 (1–2), pp.32–37.

Tieszen, L.L. & Fagre, T. (1993) Effect of diet quality and composition on the isotopic composition of respiratory CO_2, bone collagen, bioapatite, and soft tissues. In: J. B. Lambert & G. Grupe eds. *Prehistoric Human Bone: Archaeology at the Molecular Level*. Berlin, Germany, Springer-Verlag, pp.121–156.

Toft, N.L., Anderson, J.E. & Nowak, R.S. (1989) Water use efficiency and carbon isotope composition of plants in a cold desert environment. *Oecologia*, 80 (1), pp.11–18.

Troughton, J.H. (1972) Carbon isotope fractionation by plants. In: T. A. Rafter & T. L. Grant-Taylor eds. *Proceedings of the Eighth Radiocarbon Dating Conference*. Wellington, Royal Society of New Zealand, pp.E39–E57.

Troughton, J.H. & Card, K.A. (1975) Temperature effects on the carbon-isotope ratio of C_3, C_4 and Crassulacean-acid-metabolism (CAM) plants. *Planta*, 123 (2), pp.185–190.

Tütken, T., Furrer, H. & Walter Vennemann, T. (2007) Stable isotope compositions of mammoth teeth from Niederweningen, Switzerland: Implications for the Late Pleistocene climate, environment, and diet. *Quaternary International*, 164–165, pp.139–150.

Tütken, T., Vennemann, T.W., Janz, H. & Heizmann, E.P.J. (2006) Palaeoenvironment and palaeoclimate of the Middle Miocene lake in the Steinheim basin, SW Germany: A reconstruction from C, O, and Sr isotopes of fossil remains. *Palaeogeography, Palaeoclimatology, Palaeoecology*, 241 (3–4), pp.457–491.

Tütken, T., Vennemann, T.W. & Pfretzschner, H.-U. (2008) Early diagenesis of bone and tooth apatite in fluvial and marine settings: Constraints from combined oxygen isotope, nitrogen and REE analysis. *Palaeogeography, Palaeoclimatology, Palaeoecology*, 266 (3–4), pp.254–268.

Tzedakis, P.C., Raynaud, D., McManus, J.F., Berger, A., Brovkin, V. & Kiefer, T. (2009) Interglacial diversity. *Nature Geoscience*, 2 (11), pp.751–755.

Velivetskaya, T.A., Smirnov, N.G., Kiyashko, S.I., Ignat'ev, A. V., Olenev, G. V. & Evdokimov, N.G. (2014) Effects of environmental factors and species identity on oxygen and carbon isotope composition of teeth in recent small mammals of the Urals. *Russian Journal of Ecology*, 45 (2), pp.136–142.

Vinther, B.M., Clausen, H.B., Johnsen, S.J., Rasmussen, S.O., Andersen, K.K., Buchardt, S.L., Dahl-Jensen, D., Seierstad, I.K., Siggaard-Andersen, M.L., Steffensen, J.P., Svensson, A., Olsen, J. & Heinemeier, J. (2006) A synchronized dating of three Greenland ice cores throughout the Holocene. *Journal of Geophysical Research: Atmospheres*, 111 (13), D13102.

Voelker, S.L., Brooks, J.R., Meinzer, F.C., Anderson, R., Bader, M.K.-F., Battipaglia, G., Becklin, K.M., Beerling, D., Bert, D., Betancourt, J.L., Dawson, T.E., Domec, J.C., Guyette, R.P., Körner, C., Leavitt, S.W., Linder, S., Marshall, J.D., Mildner, M., Ogée, J., Panyushkina, I., Plumpton, H.J., Pregitzer, K.S., Saurer, M., Smith, A.R., Siegwolf, R.T.W., Stambaugh, M.C., Talhelm, A.F., Tardif, J.C., Van de Water, P.K., Ward, J.K. & Wingate, L. (2016) A dynamic leaf gas-exchange strategy is conserved in woody plants under changing ambient CO_2: Evidence from carbon isotope discrimination in paleo and CO_2 enrichment studies. *Global Change Biology*, 22 (2), pp.889–902.

Vogel, J.C. (1982) Koolstofisotoopsamestelling van plantproteiene. *Suid-Afikaanse Tydskrif vir Natuurwetenskap en Tegnologie*, 1 (1), pp.7–8.

Vogel, J.C. (1978) Recycling of carbon in a forest environment. *Oecologia Plantarum*, 13, pp.89–94.

Vogel, J.C., Fuls, A., Visser, E. & Becker, B. (1993) Pretoria calibration curve for short-lived samples, 1930-3350 BC. *Radiocarbon*, 35 (1), pp.73–85.

Waghorne, R., Hancock, J.D.R. & Candy, I. (2012) Environmental controls on the $\delta^{18}O$ composition of freshwater calcite and aragonite in a temperate, lowland river system: significance for palaeoclimatic studies. *Proceedings of the Geologists' Association*, 123 (4), pp.576–583.

Walker, M.J.C. (1995) Climatic changes in Europe during the last

glacial/interglacial transition. *Quaternary International*, 28, pp.63–76.

Walker, M.J.C., Coope, G.R., Sheldrick, C., Turney, C.S.M., Lowe, J.J., Blockley, S.P.E. & Harkness, D.D. (2003) Devensian Lateglacial environmental changes in Britain: A multi-proxy environmental record from Llanilid, South Wales, UK. *Quaternary Science Reviews*, 22 (5–7), pp.475–520.

Wang, Y. & Cerling, T.E. (1994) A model of fossil tooth and bone diagenesis: implications for paleodiet reconstruction from stable isotopes. *Palaeogeography, Palaeoclimatology, Palaeoecology*, 107 (3–4), pp.281–289.

Van de Water, P.K., Leavitt, S.W. & Betancourt, J.L. (1994) Trends in Stomatal Density and $^{13}C/^{12}C$ Ratios of Pinus flexilis Needles During Last Glacial-Interglacial Cycle. *Science*, 264 (5156), pp.239–243.

Weber, J.-M., Aubry, S., Ferrari, N., Fischer, C., Feller, N.L., Meia, J.-S. & Meyer, S. (2002) Population changes of different predators during a water vole cycle in a central European mountainous habitat. *Ecography*, 25 (1), pp.95–101.

Wershaw, R.L., Friedman, I., Heller, S.J. & Frank, P.A. (1966) Hydrogen isotopic fractionation of water passing through trees. In: G. D. Hobson & S. G.C. eds. *Advances in Organic Geochemistry*. Oxford, Pergamon Press, pp.55–67.

West, R.G. (1980) *The pre-glacial Pleistocene of the Norfolk and Suffolk coasts*. Cambridge, Cambridge University Press.

White, R., Dennis, P. & Atkinson, T. (1999) Experimental calibration and field investigation of the oxygen isotopic fractionation between biogenic aragonite and water. *Rapid communications in mass spectrometry : RCM*, 13 (13), pp.1242–1247.

Williams, R.A.D. & Elliott, J.C. (1989) *Basic and Applied Dental Biochemistry*. Edinburgh, Dental Series, Churchill Livingstone.

Wong, W.W., Benedict, C.R. & Kohel, R.J. (1979) Enzymic fractionation of the stable carbon isotopes of carbon dioxide by ribulose-1,5-bisphopshate carboxylase. *Plant Physiology*, 63 (5), pp.852–856.

Yapp, C.J. & Epstein, S. (1977) Climatic implications of D/H ratios of meteoric water over North America (9500–22,000 B.P.) as inferred from

ancient wood cellulose CH hydrogen. *Earth and Planetary Science Letters*, 34 (3), pp.333–350.

Yin, Q.Z. & Berger, A. (2010) Insolation and CO_2 contribution to the interglacial climate before and after the Mid-Brunhes Event. *Nature Geoscience*, 3 (4), pp.243–246.

Yin, Q. & Berger, A. (2015) Interglacial analogues of the Holocene and its natural near future. *Quaternary Science Reviews*, 120, pp.28–46.

Yoder, C.J. & Bartelink, E.J. (2010) Effects of different sample preparation methods on stable carbon and oxygen isotope values of bone apatite: A comparison of two treatment protocols. *Archaeometry*, 52 (1), pp.115–130.

Young, G.H.F., Bale, R.J., Loader, N.J., Mccarroll, D., Nayling, N. & Vousden, N. (2012) Central England temperature since AD 1850: The potential of stable carbon isotopes in british oak trees to reconstruct past summer temperatures. *Journal of Quaternary Science*, 27 (6), pp.606–614.

Young, M.R. (1975) The life cycles of six species of freshwater molluscs in the Worcester-Birmingham canal. *Journal of Molluscan Studies*, 41 (6), pp.533–548.

Zazzo, A., Lécuyer, C. & Mariotti, A. (2004a) Experimentally-controlled carbon and oxygen isotope exchange between bioapatites and water under inorganic and microbially-mediated conditions. *Geochimica et Cosmochimica Acta*, 68 (1), pp.1–12.

Zazzo, A., Lécuyer, C., Sheppard, S.M.F., Grandjean, P. & Mariotti, A. (2004b) Diagenesis and the reconstruction of paleoenvironments: A method to restore original $\delta^{18}O$ values of carbonate and phosphate from fossil tooth enamel. *Geochimica et Cosmochimica Acta*, 68 (10), pp.2245–2258.

Zimmerman, J.K. & Ehleringer, J.R. (1990) Carbon isotope ratios are correlated with irradiance levels in the Panamanian orchid Catasetum viridiflavum. *Oecologia*, 83 (2), pp.247–249.

Zimmerman, U., Ehhalt, D. & Muennich, K.O. (1967) Soil-water movement and evapotranspiration: changes in the isotopic composition of the water. In: *Symposium on Isotopes in Hydrology, 14-18 November 1966*. Vienna, International Atomic Energy Agency (IAEA), pp.567–584.

Appendix A: Carbon isotope fractionation data from the literature

The following tables list the carbon isotope data that were obtained from the published literature in order to calculate $\delta^{13}C$ enrichment factors between bioapatite and the diet, and collagen and the diet, in modern rodents. Enrichment factors were calculated using the following equations from Passey et al., (2005):

$$\alpha_{tissue\text{-}diet} = \frac{1000 + \delta_{tissue}}{1000 + \delta_{diet}} \quad (A1)$$

$$\varepsilon_{tissue\text{-}diet} = (\alpha_{tissue\text{-}diet} - 1) \times 1000 \quad (A2)$$

where α is the fractionation factor, and ε is the enrichment factor.

Table A.1: *Carbon isotope data for modern rodent bioapatite and corresponding diets. Enrichment factors were calculated for each individual. Averages and standard deviations on the enrichment factors, shown in bold, were calculated for mice and rat bones, vole* (Microtus ochrogaster) *teeth and woodrat* (Neotoma cinerea) *teeth. References: 1) DeNiro and Epstein (1978), 2) Ambrose and Norr (1993), 3) Tieszen and Fagre (1993), 4), Jim et al. (2004), 5) Passey et al. (2005), 6) Podlesak et al. (2008).*

Taxon	$\delta^{13}C$ of diet (‰)	$\delta^{13}C$ of bioapatite (‰ VPDB)	$\varepsilon_{apatite\text{-}diet}$ (‰)	Reference
Lab mouse	-22.3	-12.6	9.92	1
	-22.3	-12.6	9.92	
	-22.3	-12.5	10.02	
	-19.3	-9.8	9.69	
	-19.3	-9.8	9.69	
	-19.3	-9.8	9.69	
Lab rat	-25.2	-15.7	9.75	2
	-24.3	-13.4	11.17	
	-12.1	-2.9	9.31	
	-17.1	-7.7	9.56	
	-22.5	-13.5	9.21	
	-14.6	-5.2	9.54	
	-14.7	-5.6	9.24	

Lab mouse	-25.6	-16.8	9.03	3
	-22.1	-16.3	5.93	
	-17.4	-6.9	10.69	
	-24.6	-15.2	9.64	
	-23.2	-14.3	9.11	
	-19.9	-8.8	11.33	
	-23.0	-14.2	9.01	
	-11.5	-3.1	8.50	
Lab rat	-24.9	-14.0	11.18	4
	-23.9	-15.0	9.12	
	-14.7	-5.9	8.93	
	-14.7	-5.8	9.03	
	-12.2	-3.0	9.31	
	-12.2	-3.2	9.11	
	-12.2	-3.2	9.11	
	-22.3	-13.2	9.31	
	-22.3	-12.7	9.82	
Mean			**9.50**	
Standard deviation			**0.96**	
Microtus ochrogaster	-26.1	-14.8	11.6	5
	-26.1	-15.0	11.4	
	-26.1	-14.8	11.6	
	-26.1	-15.1	11.3	
Mean			**11.47**	
Standard deviation			**0.15**	
Neotoma cinerea	-25.9	-15.2	11.0	6
	-25.9	-15.2	11.0	
	-25.9	-15.4	10.8	
	-25.9	-15.1	11.1	
	-25.9	-15.2	11.0	
	-25.9	-15.2	11.0	
	-25.9	-15.2	11.0	
	-25.9	-15.2	11.0	
Mean			**10.97**	
Standard deviation			**0.09**	

Table A.2: *Carbon isotope data for modern mouse and rat bone collagen and corresponding C_3 diets. Averages and standard deviations on the enrichment factors are shown in bold. References: 1) DeNiro and Epstein (1978), 2) Deniro and Epstein (1981), 3) Ambrose and Norr (1993), 4) Tieszen and Fagre (1993), 5) Jim et al. (2004).*

Taxon	$\delta^{13}C$ of diet (‰)	$\delta^{13}C$ of collagen (‰ VPDB)	$\varepsilon_{collagen\text{-}diet}$ (‰)	Reference
Lab mouse	-22.3	-18.6	3.78	1
	-19.3	-16.5	2.86	
	-22.3	-17.9	4.50	

Lab mouse	-19.3	-15.5	3.87	2
	-18.3	-14.8	3.57	
Lab rat	-25.2	-21.4	3.90	3
Lab mouse	-25.6	-21.9	3.80	4
Lab rat	-24.9	-20.0	5.03	5
	-23.9	-19.8	4.20	
Mean			**3.94**	
Standard deviation			**0.60**	

Table A.3: *Calculated carbon isotope offsets between bioapatite and collagen ($\Delta^{13}C_{apatite\text{-}collagen}$) for modern mice and rats fed on a pure C_3 diet. Averages and standard deviations on the enrichment factors are shown in bold. References: 1) DeNiro and Epstein (1978), 2) Ambrose and Norr (1993), 3) Tieszen and Fagre (1993), 4) Jim et al. (2004).*

Taxon	**$\delta^{13}C$ of collagen (‰ VPDB)**	**$\delta^{13}C$ of bioapatite (‰ VPDB)**	**$\Delta_{apatite\text{-}collagen}$ (‰)**	**Reference**
Lab mouse	-18.6	-12.6	6.1	1
	-18.6	-12.6	6.1	
	-18.6	-12.5	6.2	
	-16.5	-9.8	6.8	
	-16.5	-9.8	6.8	
	-16.5	-9.8	6.8	
Lab rat	-21.4	-15.7	5.8	2
Lab mouse	-21.9	-16.8	5.2	3
Lab rat	-20.0	-14.0	6.1	4
	-19.8	-15.0	4.9	
Mean			**6.1**	
Standard deviation			**0.65**	

Table A.4: *Carbon isotope data for modern rat bone collagen and a diet consisting of enriched C_3 and C_4 energy sources and C_3 protein sources. Averages and standard deviations on the enrichment factors are shown in bold. References: 1) Ambrose and Norr (1993), 2) Jim et al. (2004).*

Taxon	$\delta^{13}C$ of diet (‰)	$\delta^{13}C$ of collagen (‰ VPDB)	$\varepsilon_{collagen\text{-}diet}$ (‰)	Reference
Lab rat	-12.1	-13.8	-1.72	1
	-22.5	-20.7	1.84	
	-14.6	-16.0	-1.42	
	-14.7	-16.9	-2.23	
	-14.7	-17.0	-2.33	2
	-14.7	-16.8	-2.13	
Mean			**-1.33**	
Standard deviation			**1.59**	

Table A.5: *Calculated carbon isotope offsets between collagen and bioapatite ($\Delta^{13}C_{apatite\text{-}collagen}$) for rats fed on a diet of enriched C_3 or C_4 energy sources and C_3 protein sources. Averages and standard deviations on the enrichment factors are shown in bold. References: 1) Ambrose and Norr (1993), 2) Jim et al. (2004).*

Taxon	$\delta^{13}C$ of collagen (‰ VPDB)	$\delta^{13}C$ of bioapatite (‰ VPDB)	$\Delta_{apatite\text{-}collagen}$ (‰)	Reference
Lab rat	-13.8	-2.9	11.05	1
	-20.7	-13.5	7.35	
	-16.0	-5.2	10.98	
	-16.9	-5.6	11.49	
	-17.0	-5.9	11.29	2
	-16.8	-5.8	11.19	
Mean			**-10.56**	
Standard deviation			**1.58**	

Appendix B: Isotope measurement techniques and analytical precision

This Appendix provides additional detail on the methods used in the analyses of the carbonate standards and samples in: 1) the Stable Isotope Laboratory in the Department of Earth Sciences, Royal Holloway University of London (RHUL), and 2) the Bloomsbury Environmental Isotope Facility, University College London (BEIF). The instruments, measurement techniques and data reduction procedures that were used by each laboratory to determine the $\delta^{18}O$ and $\delta^{13}C$ values of the carbonates (relative to VPDB) are outlined here. Further information is also provided on the internal and external precision of the isotopic measurements of the carbonate standards during the periods of analysis at each laboratory. Finally, estimates for the precision on isotopic measurements of rodent bioapatite are supplied, based upon replicate analyses of individual samples.

B.1. Isotopic analyses at RHUL

The Stable Isotope Laboratory at RHUL uses a GV Instruments Multiflow preparation system teamed with an IsoPrime isotope ratio mass spectrometer to measure the isotope compositions of carbonates. During each analytical run, analyses are undertaken on 18 samples with unknown isotopic compositions, 2 international carbonate standards with known isotopic compositions (NBS-19, a limestone, and LSVEC, a lithium carbonate), and 2-3 replicates of an internal calcite standard (RHBNC). Carbon dioxide gas is liberated from the carbonates through a reaction with 100% orthophosphoric acid at 90°C. A syringe is used to add ~0.25 ml of acid to each vial containing a standard or sample. The acid is added to the vials in the first 12 positions in the run approximately 90 minutes before the acid is added to the final 11 vials. This is done to ensure that the duration of the reaction with the acid is similar for the standards/samples within the first and second halves of the analytical run (the analysis of 12 standards/samples takes ~90 minutes). The carbonates are left to react with the acid for a total of ~3 hours. The CO_2 gas produced from each standard or sample is transferred to the mass spectrometer via

continuous helium flow. Isotopic measurements are made by comparing the mean isotope ratios of two aliquots of CO_2 gas produced from the standard/sample, with the isotope ratios of a reference gas held within a tank.

The isotope ratios of the samples are calibrated using the relationships between the measured and known isotope values of the carbonate standards. Approximately 300-400 µg of NBS-19 and RHBNC, and approximately 200-300 µg of LSVEC, is weighed for each analysis of a standard. NBS-19 and LSVEC have internationally accepted $\delta^{18}O$ and $\delta^{13}C$ values on the VPDB scale, which encompass the full range of possible isotopic values of the samples. Two-point linear regressions can therefore be generated, relating the known and measured $\delta^{18}O$ and $\delta^{13}C$ ratios of these standards (Figure B.1). The measured $\delta^{18}O$ and $\delta^{13}C$ values of the samples are then substituted into the equations for these regressions, to produce calibrated isotope values for the samples.

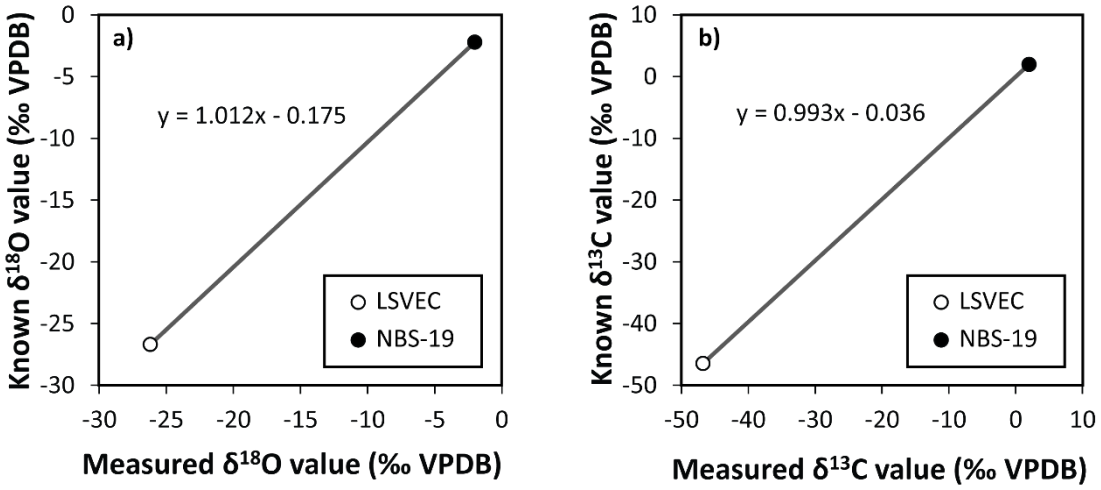

Figure B.1: *Example graphs illustrating the methods used at RHUL to calibrate the oxygen (a) and carbon (b) isotope values of the samples. The measured oxygen and carbon isotope values of the samples are substituted for 'x' in the equations for the regression lines in a) and b). These equations vary between analytical runs, due to variations in the measured isotope values of the standards (LSVEC and NBS-19).*

The internal precision for each measurement of NBS-19, LSVEC or RHBNC (i.e. the 1σ standard deviation on the measured isotope ratios of the two gas aliquots produced during each analysis of a standard) is typically within ± 0.10‰ for $\delta^{18}O$ and ± 0.05‰ for $\delta^{13}C$. This level of precision is compliant with internationally accepted guidelines. The internal precision for each measurement of a sample is likewise usually better than ± 0.10‰ for both $\delta^{18}O$ and $\delta^{13}C$. Occasionally, however, the precision is between 0.1 and 0.2‰, and for a few samples, is poorer than 0.2‰ (see Table B.3). The poorer precision on the measured isotope values of certain samples is generally due to the small quantity of sample analysed. For some samples, however, a lower precision may also result from internal variability in the isotopic composition of the tooth (see section B.3 for further discussion of this).

The internal standard (RHBNC) is analysed at the beginning, middle and end of each run in order to determine the internal precision for the run and the external precision across multiple runs. RHBNC has a known $\delta^{13}C$ value of +3.25‰ (Grassineau, 2006), while the $\delta^{18}O$ value of this standard varies between approximately -10.7 and -10.4‰ (Figure B.2a). During the analysis period for this thesis, the measured $\delta^{13}C$ values for RHBNC fell within 0.08‰ of the known value (Figure B.2b). For individual runs, the 1σ standard deviation precision on the measured isotope values of RHBNC was generally within ± 0.10‰ for $\delta^{18}O$, and ± 0.05‰ for $\delta^{13}C$ (Table B.1). The 1σ external precision on the RHBNC measurements was ± 0.08‰ for $\delta^{18}O$, and ± 0.04‰ for $\delta^{13}C$. This external precision is consistent with the typical precision on measurements of RHBNC at RHUL (within ± 0.10‰ for $\delta^{18}O$ and within ± 0.05‰ for $\delta^{13}C$).

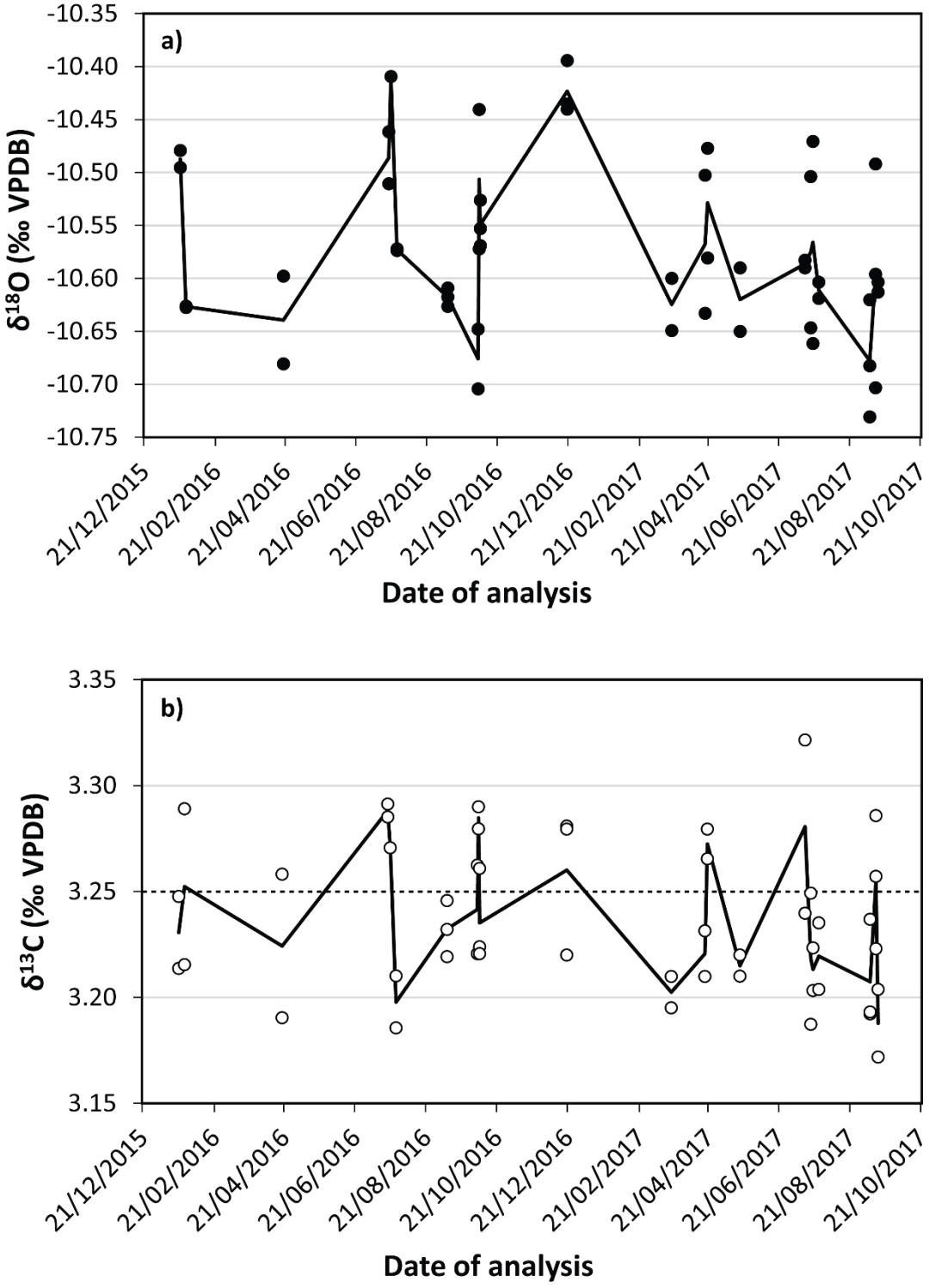

Figure B.2: *Variations in the measured oxygen (a) and carbon (b) isotope values of RHBNC at RHUL during the period of analysis for this thesis. The solid black lines indicate changes in the mean measured isotope values of RHBNC between each run during the analysis period. The dotted black line in b) marks the known carbon isotope value of RHBNC.*

Table B.1: *Isotope results for the analyses of the RHBNC standard at RHUL. The average measured values are the mean isotope values for the two or three analyses of the standard in each run. The accepted $\delta^{13}C$ value for RHBNC is +3.25‰. The difference from the accepted value was calculated by subtracting the measured value from the accepted value. The 1σ standard deviations indicate the internal precision on the $\delta^{18}O$ and $\delta^{13}C$ values for each run.*

Date of analysis	Number of analyses	$\delta^{18}O$ (‰ VPDB)		$\delta^{13}C$ (‰ VPDB)		
		Average measured value	1σ standard deviation	Average measured value	Difference from accepted value	1σ standard deviation
21/01/2016	2	-10.49	0.01	3.23	0.02	0.02
26/01/2016	2	-10.63	0.00	3.25	0.00	0.05
19/04/2016	2	-10.64	0.06	3.22	0.03	0.05
19/07/2016	2	-10.49	0.03	3.29	-0.04	0.00
21/07/2016	1	-10.41	-	3.27	-0.02	-
26/07/2016	2	-10.57	0.00	3.20	0.05	0.02
08/09/2016	3	-10.62	0.01	3.23	0.02	0.01
04/10/2016	2	-10.68	0.04	3.24	0.01	0.03
05/10/2016	2	-10.51	0.09	3.28	-0.03	0.01
06/10/2016	3	-10.55	0.02	3.24	0.01	0.02
20/12/2016	3	-10.42	0.03	3.26	-0.01	0.03
20/03/2017	2	-10.62	0.03	3.20	0.05	0.01
18/04/2017	2	-10.57	0.09	3.22	0.03	0.02
20/04/2017	2	-10.53	0.07	3.27	-0.02	0.01
18/05/2017	2	-10.62	0.04	3.22	0.04	0.01
13/07/2017	2	-10.59	0.01	3.28	-0.03	0.06
18/07/2017	2	-10.58	0.10	3.22	0.03	0.04
20/07/2017	2	-10.57	0.13	3.21	0.04	0.01
25/07/2017	2	-10.61	0.01	3.22	0.03	0.02
07/09/2017	3	-10.68	0.06	3.21	0.04	0.03
12/09/2017	3	-10.60	0.11	3.26	-0.01	0.02
14/09/2017	2	-10.61	0.01	3.19	0.06	0.02

B.2. Isotopic analyses at BEIF

The Bloomsbury Environmental Isotope Facility uses similar preparation procedures to RHUL. A Thermo Finnigan GasBench II is paired with a ThermoFisher Delta Plus XP mass spectrometer in order to measure the isotope compositions of carbonates. Carbon dioxide is produced from the carbonates through a reaction with 100% orthophosphoric acid, heated at 45°C. A syringe is used to add the acid to all standards and samples according to the order of their analysis. The GasBench uses continuous helium flow to transfer the CO_2 gas from the standard/sample to the mass spectrometer. Isotope measurements are made by comparing the mean isotope ratios of five aliquots of CO_2 gas generated from the sample, with the isotope ratios of a reference gas held within a tank. The 1σ standard deviations on the measured isotope ratios of the five gas aliquots for each standard or sample are typically within ± 0.05‰.

The internal standard, BDH, is analysed at every fourth position in an analytical run. For each analysis, a near-constant weight of BDH (130 ± 5 µg) is used, in order to eliminate the influence of sample size on the measured isotopic ratios of the standard. BDH has known oxygen and carbon isotope ratios, which are assumed to remain constant throughout the run. The differences between the known and measured isotopic ratios of BDH are used to calculate the isotopic composition of the CO_2 reference gas for each BDH analysis. However, due to instrument drift, the apparent isotopic composition of the reference gas varies during a run. The analysis of the BDH standard at every fourth position enables the impact of instrument drift on the measurement of isotopic ratios to be monitored, and corrections for this drift to be applied. The CO_2 gas liberated from each sample is compared with the interpolated isotopic composition of the reference gas in order to produce isotopic ratios for each sample in terms of their deviation from BDH.

At every eighth position within a run, an additional BDH standard is analysed to assess the effect of sample size on the measured isotopic ratios. These secondary BDH standards are weighed into differently sized aliquots, ranging between 80 and 180 µg. Regressions are then generated for each analytical run, which relate the gas peak intensity to the measured oxygen or

carbon isotope ratio of the BDH standard. These regressions are used to correct the oxygen and carbon isotope ratios of the unknown samples in the run. The isotope ratios of the samples are then converted to the VPDB scale using the known $\delta^{18}O$ and $\delta^{13}C$ values of BDH.

Within every run, 2-3 replicate analyses of the international carbonate standard, NBS-19, are also undertaken. NBS-19 is treated as an unknown sample, and thus measured isotopic ratios are calibrated to the BDH standard. The calibrated isotope values for NBS-19 can consequently be compared with the internationally accepted $\delta^{18}O$ and $\delta^{13}C$ values for this standard, to assess their accuracy. The analyses of NBS-19 additionally enable the internal precision of each run and the external precision across multiple runs to be calculated.

The NBS-19 data generated during this research are displayed in Figure B.3, and summarised in Table B.2. During the first two analytical runs, the measured $\delta^{18}O$ values of NSB-19 are 0.2-0.4‰ lower than the accepted value for this standard (Figure B.3a). These offsets are greater than the typical uncertainties on oxygen isotope measurements of carbonates (± 0.1‰). Corrections were therefore applied to the $\delta^{18}O$ values of the samples in these runs, according to the average difference between the measured and accepted $\delta^{18}O$ of NBS-19 (Table B.2). In contrast, the mean measured $\delta^{18}O$ values for NBS-19 during the final two runs are consistent with the accepted value, and thus no corrections were applied to the sample data generated from these runs.

The internal precision (1σ standard deviation) on the $\delta^{18}O$ values of NBS-19 was relatively poor for the runs undertaken during May 2018 (Table B.2). An issue was identified with the flushing of the sample gas to the mass spectrometer during these runs. This issue is likely responsible for the poor accuracy and precision of the results. In order to check the reliability of the measured $\delta^{18}O$ values, 26 bioapatite samples were re-analysed in July 2018. Differences in the isotope results between the two analyses are ≤ 1‰ for $\delta^{18}O$ and ≤ 0.6‰ for $\delta^{13}C$. These differences are discussed further in section B.3.

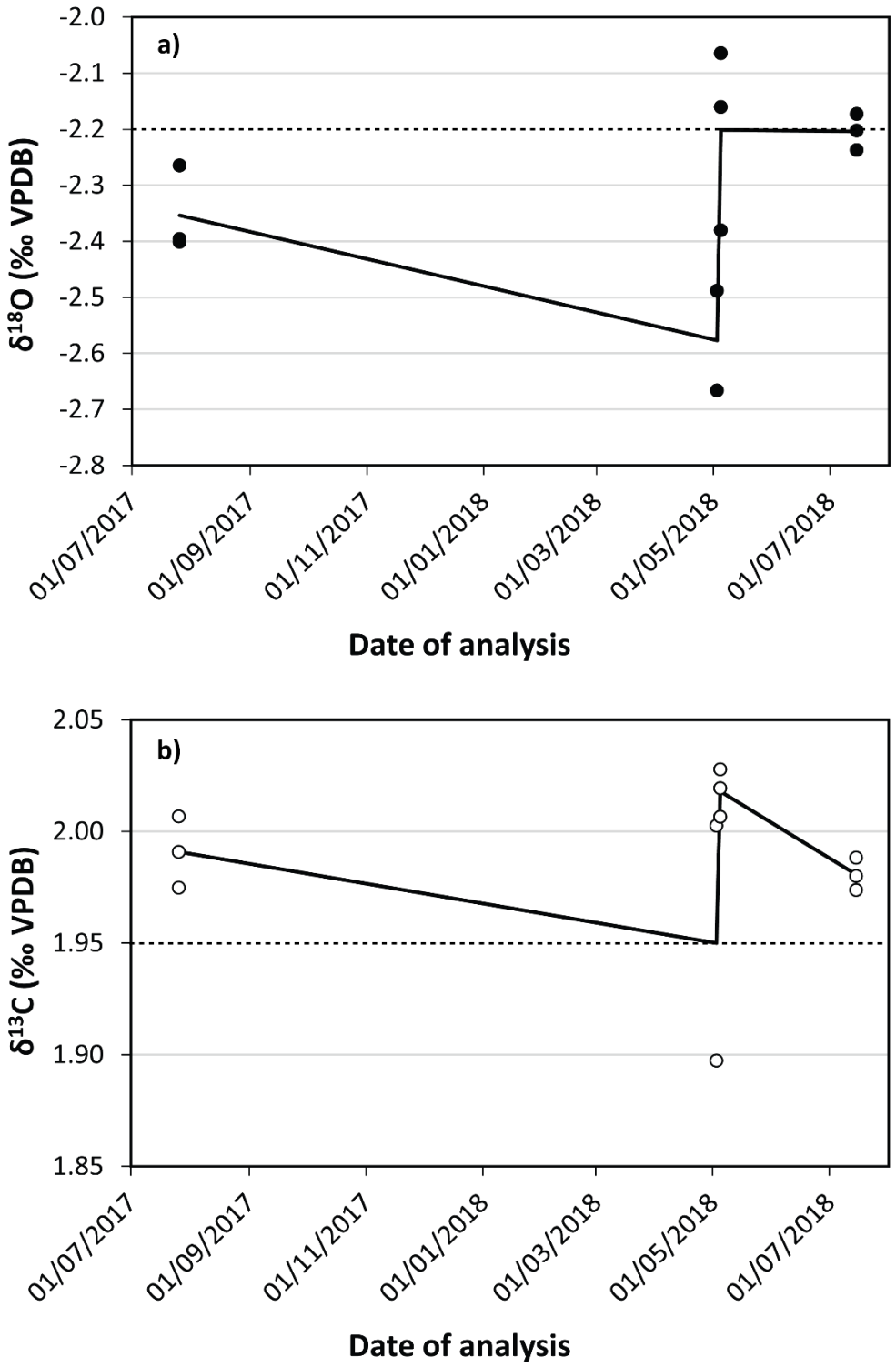

Figure B.3: *Variations in the measured oxygen (a) and carbon (b) isotope values of NBS-19 at BEIF during the period of analysis for this thesis. The solid black lines indicate changes in the mean measured isotope values of NBS-19 between each run during the analysis period. The dotted black lines mark the accepted oxygen and carbon isotope values of NBS-19.*

The measured $\delta^{13}C$ values of NBS-19 are within ± 0.08‰ of the accepted value (Figure B.3b), and the internal precision (1σ) is better than ± 0.05‰ for all analytical runs (Table B.2). Again, the precision on the measured $\delta^{13}C$ values of NBS-19 is the poorest for the analyses undertaken in May 2018 (Figure B.3b), due to the reasons outlined above.

The external precision (1σ) on the measured $\delta^{18}O$ values of NBS-19 is ± 0.17‰. Excluding the results from May 2018, the external precision for $\delta^{18}O$ is ± 0.10‰. The external precision on the measured $\delta^{13}C$ values of NBS-19 is ± 0.03‰. These levels of precision fall within internationally accepted guidelines.

Table B.2: *Isotope results for the analyses of the NBS-19 standard at BEIF. The average measured values are the mean isotope values for the two or three analyses of the standard in each run, calibrated to BDH. The accepted $\delta^{18}O$ and $\delta^{13}C$ values for NBS-19 are -2.20‰ and +1.95‰, respectively. The difference from the accepted value was calculated by subtracting the measured value from the accepted value. The 1σ standard deviations indicate the internal precision on the $\delta^{18}O$ and $\delta^{13}C$ values for each run.*

Date of analysis	Number of analyses	$\delta^{18}O$ (‰ VPDB)			$\delta^{13}C$ (‰ VPDB)		
		Average measured value	Difference from accepted value	1σ standard deviation	Average measured value	Difference from accepted value	1σ standard deviation
26/07/2017	3	-2.35	0.15	0.08	1.99	-0.04	0.02
03/05/2018	2	-2.58	0.38	0.17	1.95	0.00	0.05
05/05/2018	3	-2.20	0.00	0.16	2.02	-0.07	0.01
15/07/2018	3	-2.20	0.00	0.03	1.98	-0.03	0.01

B.3. Precision on the isotopic measurements of tooth bioapatite

The data from RHUL and BEIF show that the internal and external precision on multiple analyses of the carbonate standards is typically better than ± 0.10‰ for $\delta^{18}O$ and ± 0.05‰ for $\delta^{13}C$. These estimates of precision are based upon replicate analyses of identical aliquots of pure carbonates, whereas the analyses for this thesis were undertaken on unknown samples of carbonate in tooth bioapatite. Due to day-to-day variations in the average isotopic values of the water and dietary sources consumed by mammals, the $\delta^{18}O$ and $\delta^{13}C$ values of bioapatite carbonate vary across a tooth, parallel to the direction of growth (e.g. Passey & Cerling, 2006). Intra-tooth variations in the isotopic composition of bioapatite may result in variability in the measured isotopic ratios of multiple aliquots of the same tooth sample. This would, in turn, result in a poorer precision on isotopic measurements of bioapatite carbonate, when compared with measurements undertaken on pure carbonates.

Duplicate analyses, with each analysis in a different run, were undertaken on several of the tooth samples that were selected for this research. The $\delta^{18}O$ and $\delta^{13}C$ data for these duplicate analyses are presented in Tables B.3 and B.4, respectively. These data are used here to provide an estimate for the typical 1σ standard deviation precision on individual isotopic measurements of bioapatite carbonate.

Differences in measured isotope values between replicate analyses of rodent bioapatite carbonate are generally within ± 1‰ for $\delta^{18}O$ and ± 0.5‰ for $\delta^{13}C$ at both RHUL and BEIF (Tables B.3 and B.4). However, for some of the upper teeth from Cobham, differences in the measured $\delta^{18}O$ values between replicate analyses are larger, at ~2.5‰ (Table B.3). The 1σ standard deviation uncertainties on the isotopic measurements of the gas peaks for these samples are also relatively broad (~0.2‰). The measured $\delta^{18}O$ values of RHBNC during the runs in which the upper teeth from Cobham were analysed (19/04/2016 and 20/03/2017) are similar, and the internal precision for each of these runs falls within acceptable limits (see Figure B.2a and Table B.1). Therefore, the large $\delta^{18}O$ differences between replicate analyses of these teeth cannot be attributed to a poor accuracy or precision in the measurement

of isotopic ratios. These differences may alternatively result from a relatively large intra-tooth variability in isotopic compositions. This may have been combined with the incomplete crushing of the teeth during sample preparation, which would have led to poorly homogenised bulk tooth samples.

To estimate the precision on $\delta^{18}O$ and $\delta^{13}C$ values for an individual measurement of bioapatite carbonate, the method of replicates was used. Each sample measurement (X_{meas}) is assumed to reflect the true value of the sample (X_{true}) plus a random component or uncertainty (e_i) with a normal distribution and a mean of zero. This can be expressed by the following equation:

$$X_{meas} = X_{true} + e_i \quad \text{(B.1).}$$

The difference in values between two replicate measurements of the same sample [$X_{meas}(1)$ and $X_{meas}(2)$] can be used to estimate the uncertainty component of an individual measurement, because:

$$X_{meas}(1) - X_{meas}(2) = e_i(1) - e_i(2) \quad \text{(B.2).}$$

Two replicate measurements were undertaken on a series of samples of bioapatite carbonate, and the moduli of the differences between the isotope values obtained during the first and second analyses were calculated (see Tables B.3 and B.4 for differences in $\delta^{18}O$ and $\delta^{13}C$ values between replicate analyses). The variance (var) of the differences between the two replicate measurements is equal to the sum of the variances for each individual measurement. Since $e_i(1)$ and $e_i(2)$ are normally distributed variables, their variances are the same. Therefore, it can be stated that:

$$\text{var}\,[|e_i(1) - e_i(2)|] = \text{var}\,[e_i(1)] + \text{var}\,[e_i(2)] = 2\,\text{var}[e_i] \quad \text{(B.3).}$$

Given that variance equals the square of standard deviation, the 1σ standard deviation (s.d.) on the differences between the two replicate measurements can be expressed as follows:

$$\text{s.d.}\,[\,|e_i(1) - e_i(2)|\,] = \sqrt{2} \times \text{s.d.}[e_i] \qquad \text{(B.4)}$$

where s.d.[e_i] is the 1σ standard deviation precision on an individual isotopic measurement. Equation B.4 was used to estimate the precision on individual $\delta^{18}O$ and $\delta^{13}C$ measurements of rodent bioapatite carbonate. Since RHUL and BEIF use different data reduction procedures, the precision was calculated using the data from each lab individually. The 1σ precision on an individual analysis of bioapatite carbonate at RHUL is ± 0.50‰ for $\delta^{18}O$ and ± 0.18‰ for $\delta^{13}C$. If the samples with anomalously large differences in $\delta^{18}O$ values between replicate analyses are excluded (highlighted in bold in Table B.3), the precision on $\delta^{18}O$ is ± 0.26‰. The 1σ precision on an individual measurement of bioapatite carbonate at BEIF is ± 0.20‰ for $\delta^{18}O$ and ± 0.12‰ for $\delta^{13}C$.

Table B.3: *Oxygen isotope results (‰ VPDB) for the replicate analyses of the samples of rodent tooth bioapatite. The 1σ uncertainty for each sample represents the 1σ standard deviation on the isotopic measurements of the multiple CO_2 gas peaks. The 1σ uncertainty on the mean value for each sample is the standard error of the mean. Numbers that are underlined highlight analyses for which the precision is relatively poor (approximately ± 0.2‰). Numbers shown in bold highlight anomalously large differences between A1 and A2. Specimen codes: WR = West Runton, Norfolk; WH = West Horrington, Somerset; CO = Cobham, Surrey; MA = Marsworth, Buckinghamshire; GC = Gully Cave, Somerset; RM1 = lower right first molar; RI = lower right incisor; UR = upper right tooth; UL = upper left tooth.*

Specimen code	Analysis 1 (A1)		Analysis 2 (A2)		Difference in value between A1 and A2 (A1-A2)	Mean value of A1 and A2	1σ uncertainty on mean value
	Value	1σ uncertainty	Value	1σ uncertainty			
RHUL analyses							
WR-MS1	-5.7	0.05	-5.7	0.02	0.1	-5.7	0.03
WR-I	-5.4	0.03	-6.5	0.08	0.7	-7.1	0.37
WR-MS2	-6.7	0.08	-7.4	0.03	1.1	-6.0	0.53
WH-1-RM1	-8.4	0.01	-9.2	0.02	0.8	-8.8	0.41
WH-2-RM1	-7.9	0.07	-8.6	0.11	0.8	-8.3	0.38
WH-3-RM1	-6.6	0.10	-7.7	0.04	1.1	-7.2	0.54
WH-4-RM1	-7.7	0.04	-8.8	0.03	1.1	-8.2	0.55
WH-6-RM1	-8.6	0.05	-9.6	0.22	1.0	-9.1	0.51
WH-7-RM1	-7.7	0.06	-7.7	0.09	0.0	-7.7	0.02
WH-8-RM1	-8.4	0.02	-9.1	0.06	0.7	-8.8	0.36
WH-1-RI	-7.1	0.16	-7.5	0.04	0.5	-7.3	0.23
WH-2-RI	-6.7	0.03	-6.9	0.03	0.2	-6.8	0.10
WH-3-RI	-5.2	0.12	-4.9	0.10	-0.3	-5.0	0.15
WH-4-RI	-6.3	0.02	-6.7	0.02	0.5	-6.5	0.23

WH-6-RI	-7.4	0.05	-7.8	0.05	0.4	-7.6	0.20
WH-7-RI	-5.7	0.08	-5.0	0.06	-0.7	-5.4	0.36
WH-8-RI	-7.0	0.18	-7.0	0.03	0.0	-7.0	0.02
WH-9-RI	-6.8	0.05	-6.6	0.08	-0.2	-6.7	0.10
CO-7-RM1	-9.4	0.12	-8.8	0.03	-0.6	-9.1	0.30
CO-1-RI	-8.7	0.15	-8.3	0.02	-0.4	-8.5	0.21
CO-2-RI	-7.4	0.07	-7.5	0.03	0.1	-7.5	0.06
CO-3-RI	-7.6	0.10	-7.8	0.07	0.2	-7.7	0.11
CO-5-RI	-5.6	0.04	-6.2	0.05	0.7	-5.9	0.33
CO-6-RI	-5.6	0.08	-5.9	0.06	0.4	-5.7	0.19
CO-7-RI	-7.7	0.07	-7.3	0.07	-0.4	-7.5	0.19
CO-8-RI	-7.6	0.01	-8.3	0.03	0.7	-7.9	0.37
CO-9-RI	-7.2	0.14	-8.5	0.08	1.3	-7.9	0.65
CO-9-URM1	-7.6	0.04	-10.4	0.09	**2.7**	-9.0	1.37
CO-9-URM2	-10.7	0.07	-11.4	0.17	0.7	-11.0	0.37
CO-9-URI	-7.6	0.21	-10.2	0.03	**2.5**	-8.9	1.26
CO-9-ULM1	-7.7	0.22	-10.2	0.10	**2.4**	-9.0	1.22
CO-9-ULM2	-10.2	0.06	-11.1	0.22	1.0	-10.7	0.48
CO-9-ULI	-8.3	0.18	-10.9	0.03	**2.5**	-9.6	1.27
MA-3-J9-T1	-3.6	0.08	-3.8	0.01	0.2	-3.7	0.10
MA-3-J10-T2	-7.5	0.01	-7.9	0.16	0.4	-7.7	0.19
MA-3-J16-T2	-7.6	0.05	-7.9	0.05	0.3	-7.8	0.17
MA-2-L10-T4	-5.9	0.07	-6.3	0.01	0.4	-6.1	0.22
MA-2-L11-T1	-6.5	0.00	-7.8	0.01	1.3	-7.1	0.63
BEIF analyses							
GC-1-3	-6.6	0.03	-6.9	0.10	0.2	-6.8	0.12
GC-3-2	-4.0	0.10	-4.4	0.10	0.5	-4.2	0.24
GC-3-3	-2.9	0.10	-3.8	0.10	1.0	-3.4	0.48
GC-3-4	-0.6	0.10	-1.6	0.10	1.0	-1.1	0.51
GC-4-1	-2.3	0.10	-2.2	0.10	-0.1	-2.2	0.05

GC-4-2	-2.1	0.10	-2.2	0.10	0.1	-2.1	0.04
GC-4-4	-2.2	0.10	-2.3	0.10	0.1	-2.3	0.04
GC-4-5	-3.2	0.10	-3.6	0.10	0.4	-3.4	0.22
GC-5-1	-3.7	0.14	-4.0	0.10	0.3	-3.8	0.17
GC-5-2	-4.1	0.10	-4.3	0.10	0.2	-4.2	0.09
GC-5-3	-1.0	0.10	-1.4	0.10	0.4	-1.2	0.19
GC-5-5	-6.2	0.10	-5.9	0.10	-0.3	-6.0	0.16
GC-6-1	-4.3	0.10	-4.5	0.10	0.2	-4.4	0.11
GC-6-4	-7.2	0.10	-7.2	0.10	0.0	-7.2	0.02
GC-6-5	-6.4	0.10	-6.9	0.10	0.4	-6.6	0.22
GC-7-1	-6.8	0.10	-6.7	0.10	-0.1	-6.8	0.04
GC-7-2	-5.1	0.10	-5.7	0.10	0.6	-5.4	0.30
GC-7-3	-7.6	0.10	-7.7	0.10	0.0	-7.6	0.01
GC-7-4	-8.5	0.10	-8.3	0.10	-0.2	-8.4	0.11
GC-5-2	-4.1	0.10	-4.3	0.10	0.2	-4.2	0.09
GC-5-3	-1.0	0.10	-1.4	0.10	0.4	-1.2	0.19
GC-5-5	-6.2	0.10	-5.9	0.10	-0.3	-6.0	0.16
GC-6-1	-4.3	0.10	-4.5	0.10	0.2	-4.4	0.11
GC-6-4	-7.2	0.10	-7.2	0.10	0.0	-7.2	0.02
GC-6-5	-6.4	0.10	-6.9	0.10	0.4	-6.6	0.22
GC-7-1	-6.8	0.10	-6.7	0.10	-0.1	-6.8	0.04
GC-7-2	-5.1	0.10	-5.7	0.10	0.6	-5.4	0.30
GC-7-3	-7.6	0.10	-7.7	0.10	0.0	-7.6	0.01
GC-7-4	-8.5	0.10	-8.3	0.10	-0.2	-8.4	0.11
GC-8-4	-3.7	0.14	-4.3	0.10	0.7	-4.0	0.33
GC-9-3	-6.6	0.14	-6.8	0.10	0.2	-6.7	0.09
GC-10-4	-2.4	0.14	-3.2	0.10	0.8	-2.8	0.38
GC-12-2	-2.4	0.14	-3.0	0.10	0.5	-2.7	0.26
GC-13-1	0.5	0.14	0.1	0.10	0.4	0.3	0.21
GC-14-4	-0.6	0.14	-0.9	0.10	0.2	-0.8	0.12
GC-15-4	-1.8	0.14	-2.6	0.10	0.8	-2.2	0.40

Table B.4: *Carbon isotope results (‰ VPDB) for the replicate analyses of the samples of rodent tooth bioapatite. The 1σ uncertainty for each sample represents the 1σ standard deviation on the isotopic measurements of the multiple CO_2 gas peaks. The 1σ uncertainty on the mean value for each sample is the standard error of the mean. Specimen codes: WR = West Runton, Norfolk; WH = West Horrington, Somerset; CO = Cobham, Surrey; MA = Marsworth, Buckinghamshire; GC = Gully Cave, Somerset; RM1 = lower right first molar; RI = lower right incisor; UR = upper right tooth; UL = upper left tooth.*

Specimen code	Analysis 1 (A1)		Analysis 2 (A2)		Difference in value between A1 and A2 (A1-A2)	Mean value of A1 and A2	1σ uncertainty on mean value
	Value	1σ uncertainty	Value	1σ uncertainty			
RHUL analyses							
WR-MS1	-13.1	0.00	-13.3	0.10	0.2	-13.2	0.08
WR-I	-12.7	0.00	-12.4	0.10	-0.3	-12.5	0.16
WR-MS2	-12.1	0.00	-11.8	0.00	-0.2	-12.0	0.12
WH-1-RM1	-15.7	0.05	-15.4	0.04	-0.3	-15.6	0.17
WH-2-RM1	-16.8	0.03	-16.6	0.24	-0.2	-16.7	0.11
WH-3-RM1	-16.2	0.03	-16.4	0.03	0.2	-16.3	0.08
WH-4-RM1	-17.6	0.01	-17.4	0.01	-0.2	-17.5	0.11
WH-6-RM1	-17.7	0.07	-17.7	0.09	0.0	-17.7	0.01
WH-7-RM1	-17.1	0.07	-16.8	0.02	-0.2	-16.9	0.11
WH-8-RM1	-17.4	0.04	-17.5	0.14	0.1	-17.4	0.05
WH-1-RI	-16.4	0.01	-16.1	0.02	-0.3	-16.2	0.16
WH-2-RI	-17.8	0.01	-17.9	0.01	0.1	-17.8	0.05
WH-3-RI	-17.1	0.02	-17.4	0.04	0.2	-17.3	0.11
WH-4-RI	-17.9	0.00	-18.1	0.01	0.2	-18.0	0.09
WH-6-RI	-18.4	0.07	-18.6	0.05	0.2	-18.5	0.10
WH-7-RI	-17.6	0.04	-17.3	0.00	-0.2	-17.4	0.12

WH-8-RI	-18.0	0.09	-18.0	0.01	0.0	-18.0	0.01
WH-9-RI	-17.4	0.03	-16.6	0.02	-0.7	-17.0	0.37
CO-7-RM1	-18.9	0.06	-18.5	0.01	-0.4	-18.7	0.19
CO-1-RI	-18.7	0.01	-20.0	0.02	1.2	-19.4	0.61
CO-2-RI	-16.7	0.04	-16.7	0.09	0.0	-16.7	0.02
CO-3-RI	-16.7	0.04	-16.6	0.07	-0.1	-16.7	0.06
CO-5-RI	-17.2	0.04	-17.0	0.01	-0.2	-17.1	0.10
CO-6-RI	-14.8	0.01	-15.1	0.02	0.2	-15.0	0.11
CO-7-RI	-19.5	0.05	-19.4	0.02	-0.1	-19.4	0.03
CO-8-RI	-17.4	0.01	-17.4	0.01	0.0	-17.4	0.02
CO-9-RI	-19.0	0.08	-19.0	0.04	0.0	-19.0	0.02
CO-9-URM1	-18.5	0.06	-18.7	0.06	0.2	-18.6	0.08
CO-9-URM2	-18.4	0.02	-18.4	0.07	0.0	-18.4	0.02
CO-9-URI	-18.9	0.08	-18.9	0.02	0.1	-18.9	0.03
CO-9-ULM1	-18.1	0.06	-18.5	0.02	0.4	-18.3	0.19
CO-9-ULM2	-18.2	0.06	-18.2	0.20	-0.1	-18.2	0.03
CO-9-ULI	-19.0	0.11	-19.2	0.02	0.2	-19.1	0.08
MA-3-J9-T1	-12.0	0.03	-11.5	0.04	-0.5	-11.8	0.25
MA-3-J10-T2	-11.5	0.02	-10.9	0.10	-0.6	-11.2	0.31
MA-3-J16-T2	-9.8	0.01	-8.8	0.06	-1.0	-9.3	0.50
MA-2-L10-T4	-12.2	0.03	-12.1	0.03	-0.2	-12.2	0.08
MA-2-L11-T1	-10.0	0.03	-9.7	0.02	-0.3	-9.9	0.14
BEIF analyses							
GC-1-3	-11.2	0.02	-11.9	0.03	0.6	-11.6	0.32
GC-3-2	-10.4	0.02	-10.6	0.03	0.2	-10.5	0.09
GC-3-3	-9.7	0.02	-10.2	0.03	0.5	-9.9	0.24
GC-3-4	-9.4	0.02	-9.6	0.03	0.2	-9.5	0.10
GC-4-1	-8.4	0.02	-8.5	0.03	0.1	-8.4	0.05
GC-4-2	-8.4	0.02	-8.8	0.03	0.4	-8.6	0.19
GC-4-4	-8.9	0.02	-9.1	0.03	0.2	-9.0	0.09

GC-4-5	-9.7	0.02	-10.3	0.03	0.6	-10.0	0.28
GC-5-1	-7.8	0.04	-8.0	0.03	0.2	-7.9	0.09
GC-5-2	-10.1	0.02	-10.5	0.03	0.4	-10.3	0.20
GC-5-3	-8.2	0.02	-8.7	0.03	0.5	-8.4	0.25
GC-5-5	-10.0	0.02	-10.1	0.03	0.1	-10.1	0.06
GC-6-1	-10.5	0.02	-11.0	0.03	0.5	-10.8	0.27
GC-6-4	-11.0	0.02	-10.8	0.03	-0.2	-10.9	0.11
GC-6-5	-9.8	0.02	-10.2	0.03	0.4	-10.0	0.18
GC-7-1	-10.6	0.02	-10.8	0.03	0.2	-10.7	0.10
GC-7-2	-10.7	0.02	-10.8	0.03	0.2	-10.7	0.08
GC-7-3	-10.4	0.02	-10.8	0.03	0.4	-10.6	0.19
GC-7-4	-10.6	0.02	-11.0	0.03	0.4	-10.8	0.22
GC-5-2	-10.1	0.02	-10.5	0.03	0.4	-10.3	0.20
GC-5-3	-8.2	0.02	-8.7	0.03	0.5	-8.4	0.25
GC-5-5	-10.0	0.02	-10.1	0.03	0.1	-10.1	0.06
GC-6-1	-10.5	0.02	-11.0	0.03	0.5	-10.8	0.27
GC-6-4	-11.0	0.02	-10.8	0.03	-0.2	-10.9	0.11
GC-6-5	-9.8	0.02	-10.2	0.03	0.4	-10.0	0.18
GC-7-1	-10.6	0.02	-10.8	0.03	0.2	-10.7	0.10
GC-7-2	-10.7	0.02	-10.8	0.03	0.2	-10.7	0.08
GC-7-3	-10.4	0.02	-10.8	0.03	0.4	-10.6	0.19
GC-7-4	-10.6	0.02	-11.0	0.03	0.4	-10.8	0.22
GC-8-4	-9.8	0.04	-9.8	0.03	0.0	-9.8	0.02
GC-9-3	-10.4	0.04	-10.2	0.03	-0.2	-10.3	0.08
GC-10-4	-9.5	0.04	-9.6	0.03	0.0	-9.5	0.02
GC-12-2	-9.3	0.04	-9.8	0.03	0.4	-9.5	0.21
GC-13-1	-9.3	0.04	-9.4	0.03	0.1	-9.4	0.05
GC-14-4	-9.6	0.04	-9.4	0.03	-0.2	-9.5	0.09
GC-15-4	-9.9	0.04	-9.6	0.03	-0.3	-9.8	0.17

Appendix C: Isotope data for modern analogue study (Chapter 5)

The following tables list the oxygen and carbon isotope data obtained from the modern *Microtus agrestis* teeth from West Horrington in Somerset, Cobham in Surrey, Beeford in East Yorkshire, and Perth in Perthshire. The oxygen and hydrogen isotope data from the meteoric water sources in Somerset and Perthshire are also listed.

Table C.1: *Final oxygen and carbon isotope data for the* Microtus agrestis *teeth from the lower right mandibles, with 1σ standard deviation uncertainties. Site numbers: 1) West Horrington, Somerset, 2) Cobham, Surrey, 3) Beeford, East Yorkshire, 4a) Perth Site A, Perthshire, 4b) Perth Site B, Perthshire. Tooth types: I = incisor, M_1 = first molar, M_2 = second molar, M_3 = third molar.*

Site	Individual number	Tooth type	$\delta^{18}O$ (‰)			$\delta^{13}C$ (‰)	
			VPDB	VSMOW	1σ uncertainty	VPDB	1σ uncertainty
1	1	I	-7.3	23.4	0.23	-16.2	0.16
1	1	M_1	-8.8	21.8	0.41	-15.6	0.17
1	1	M_2	-6.5	24.2	0.09	-15.3	0.10
1	1	M_3	-6.8	23.9	0.07	-14.7	0.07
1	2	I	-6.8	23.9	0.10	-17.8	0.05
1	2	M_1	-8.3	22.4	0.38	-16.7	0.11
1	2	M_2	-5.6	25.1	0.02	-16.2	0.05
1	2	M_3	-6.6	24.1	0.09	-15.5	0.07
1	3	I	-5.0	25.7	0.15	-17.3	0.11
1	3	M_1	-7.2	23.5	0.54	-16.3	0.08
1	3	M_2	-4.2	26.6	0.06	-15.6	0.05
1	3	M_3	-4.8	26.0	0.01	-15.2	0.06
1	4	I	-6.5	24.2	0.23	-18.0	0.09
1	4	M_1	-8.2	22.4	0.55	-17.5	0.11
1	4	M_2	-5.8	24.9	0.07	-17.0	0.08
1	4	M_3	-5.7	25.0	0.10	-16.2	0.04
1	5	I	-5.9	24.8	0.05	-17.6	0.10
1	5	M_1	-7.3	23.3	0.06	-17.1	0.06
1	5	M_2	-6.0	24.7	0.08	-16.6	0.07
1	5	M_3	Not analysed due to insufficient material				

1	6	I	-7.6	23.1	0.20	-18.5	0.06
1	6	M_1	-9.1	21.5	0.51	-17.7	0.01
1	6	M_2	-6.0	24.7	0.09	-17.0	0.03
1	6	M_3	-6.7	24.1	0.08	-16.5	0.05
1	7	I	-5.4	25.4	0.36	-17.4	0.12
1	7	M_1	-7.7	23.0	0.02	-16.9	0.11
1	7	M_2	-4.2	26.5	0.10	-16.6	0.02
1	7	M_3	-4.7	26.0	0.08	-16.3	0.01
1	8	I	-7.0	23.7	0.02	-18.0	0.05
1	8	M_1	-8.8	21.9	0.36	-17.4	0.05
1	8	M_2	-6.0	24.7	0.08	-16.8	0.03
1	8	M_3	-6.5	24.2	0.06	-16.7	0.06
1	9	I	-6.7	24.0	0.10	-17.0	0.03
1	9	M_1	-8.0	22.7	0.01	-17.2	0.01
1	9	M_2	-6.6	24.1	0.11	-16.0	0.04
1	9	M_3	Results unreliable due to small sample size				
2	1	I	-8.5	22.1	0.21	-19.4	0.61
2	1	M_1	-7.5	23.2	0.09	-19.4	0.03
2	1	M_2	-7.6	23.0	0.00	-19.1	0.01
2	1	M_3	-8.0	22.7	0.03	-18.9	0.03
2	2	I	-7.5	23.2	0.06	-16.7	0.02
2	2	M_1	-7.9	22.8	0.06	-16.0	0.02
2	2	M_2	-7.8	22.8	0.07	-15.9	0.04
2	2	M_3	-7.8	22.8	0.12	-15.3	0.07
2	3	I	-7.7	23.0	0.11	-16.7	0.06
2	3	M_1	-7.3	23.4	0.08	-16.3	0.03
2	3	M_2	-7.6	23.1	0.17	-15.5	0.13
2	3	M_3	-7.8	22.9	0.02	-15.7	0.15
2	4	I	-7.7	23.0	0.06	-17.8	0.06
2	4	M_1	-10.3	20.3	0.10	-17.5	0.00
2	4	M_2	-7.8	22.9	0.00	-16.5	0.03
2	4	M_3	-8.0	22.7	0.11	-14.6	0.09
2	5	I	-5.9	24.8	0.33	-17.1	0.10
2	5	M_1	Tooth not available for analysis				
2	5	M_2	-6.4	24.3	0.09	-17.1	0.06
2	5	M_3	-6.4	24.3	0.01	-16.6	0.00
2	6	I	-5.7	25.0	0.19	-15.0	0.11
2	6	M_1	-5.8	24.9	0.00	-15.6	0.04
2	6	M_2	-8.1	22.6	0.02	-14.5	0.05
2	6	M_3	-8.9	21.7	0.15	-14.5	0.00
2	7	I	-7.5	23.2	0.19	-19.4	0.03
2	7	M_1	-9.1	21.5	0.30	-18.7	0.19
2	7	M_2	-9.2	21.4	0.10	-17.6	0.06
2	7	M_3	-9.8	20.9	0.02	-17.1	0.10
2	8	I	-7.9	22.7	0.37	-17.4	0.02
2	8	M_1	-7.3	23.4	0.03	-17.0	0.02

2	8	M_2	-7.5	23.2	0.05	-16.6	0.02
2	8	M_3	-7.4	23.3	0.20	-16.0	0.07
2	9	I	-7.9	22.8	0.65	-19.0	0.02
2	9	M_1	-7.9	22.8	0.05	-18.7	0.05
2	9	M_2	-7.7	22.9	0.05	-18.4	0.02
2	9	M_3	-8.1	22.6	0.16	-17.7	0.07
3	1	I	-8.5	22.2	0.15	-21.5	0.03
3	1	M_1	-9.2	21.4	0.08	-20.4	0.02
3	1	M_2	-8.5	22.2	0.09	-19.2	0.07
3	1	M_3	-7.0	23.7	0.06	-17.5	0.09
3	2	I	-8.4	22.3	0.02	-20.4	0.02
3	2	M_1	-10.0	20.6	0.04	-20.1	0.03
3	2	M_2	-8.1	22.5	0.06	-19.5	0.04
3	2	M_3	-8.1	22.5	0.03	-18.5	0.06
3	3	I	-7.6	23.1	0.08	-18.6	0.05
3	3	M_1	-7.7	22.9	0.05	-18.9	0.06
3	3	M_2	-7.6	23.1	0.03	-18.9	0.04
3	3	M_3	-7.7	22.9	0.08	-17.3	0.09
3	4	I	-7.6	23.1	0.03	-18.4	0.01
3	4	M_1	-7.3	23.3	0.01	-17.7	0.05
3	4	M_2	-7.0	23.7	0.09	-16.8	0.04
3	4	M_3	-7.8	22.9	0.02	-15.5	0.02
3	5	I	-10.0	20.6	0.09	-20.8	0.01
3	5	M_1	-8.4	22.3	0.03	-17.1	0.01
3	5	M_2	-9.1	21.6	0.01	-19.1	0.01
3	5	M_3	-9.6	21.0	0.07	-18.1	0.09
3	6	I	-8.2	22.4	0.07	-18.6	0.02
3	6	M_1	-8.1	22.6	0.01	-17.7	0.00
3	6	M_2	-7.6	23.1	0.06	-17.2	0.10
3	6	M_3	-8.3	22.4	0.03	-16.9	0.03
3	7	I	-8.9	21.8	0.01	-18.5	0.07
3	7	M_1	-8.8	21.8	0.05	-17.9	0.04
3	7	M_2	-9.1	21.6	0.11	-17.6	0.03
3	7	M_3	-9.5	21.1	0.07	-16.2	0.11
3	8	I	-8.3	22.4	0.00	-21.0	0.01
3	8	M_1	-7.6	23.1	0.02	-20.7	0.02
3	8	M_2	-8.2	22.4	0.03	-20.3	0.06
3	8	M_3	-8.4	22.3	0.04	-20.1	0.03
3	9	I	-8.4	22.2	0.01	-20.1	0.01
3	9	M_1	-8.2	22.4	0.02	-19.2	0.01
3	9	M_2	-8.7	21.9	0.10	-18.6	0.03
3	9	M_3	-7.5	23.2	0.05	-17.7	0.00
4a	1	I	-6.7	24.0	0.05	-17.1	0.02
4a	1	M_1	-7.3	23.4	0.09	-16.9	0.01
4a	1	M_2	-7.3	23.4	0.13	-16.3	0.06
4a	1	M_3	-7.2	23.5	0.11	-15.4	0.11

4a	2	I	-6.2	24.5	0.04	-16.9	0.00
4a	2	M_1	-7.0	23.7	0.04	-16.8	0.04
4a	2	M_2	-6.8	23.9	0.00	-16.2	0.02
4a	2	M_3	-6.9	23.8	0.13	-15.4	0.12
4a	3	I	-7.0	23.7	0.09	-18.6	0.04
4a	3	M_1	-7.3	23.4	0.01	-17.7	0.02
4a	3	M_2	-7.7	23.0	0.09	-17.7	0.00
4a	3	M_3	-7.0	23.7	0.07	-16.7	0.09
4a	4	I	-6.6	24.2	0.07	-18.4	0.02
4a	4	M_1	-7.3	23.4	0.05	-19.1	0.00
4a	4	M_2	-6.6	24.1	0.07	-18.2	0.09
4a	4	M_3	-6.7	24.0	0.07	-17.9	0.01
4a	5	I	-7.9	22.8	0.05	-18.6	0.05
4a	5	M_1	-8.2	22.5	0.01	-18.3	0.03
4a	5	M_2	-7.8	22.9	0.01	-16.3	0.01
4a	5	M_3	-8.8	21.8	0.23	-16.3	0.06
4b	6	I	-7.2	23.5	0.13	-17.6	0.01
4b	6	M_1	-7.9	22.7	0.02	-16.1	0.07
4b	6	M_2	-7.8	22.9	0.05	-16.4	0.02
4b	6	M_3	-7.4	23.2	0.05	-15.6	0.01
4b	7	I	-6.9	23.8	0.04	-18.0	0.00
4b	7	M_1	-7.6	23.1	0.01	-16.1	0.03
4b	7	M_2	-7.6	23.1	0.07	-16.7	0.03
4b	7	M_3	-7.2	23.5	0.09	-13.9	0.03
4b	8	I	-6.8	23.9	0.03	-18.6	0.00
4b	8	M_1	-7.6	23.1	0.07	-18.4	0.05
4b	8	M_2	-7.8	22.9	0.02	-17.9	0.00
4b	8	M_3	-7.3	23.4	0.09	-16.8	0.01
4b	9	I	-5.6	25.1	0.01	-18.5	0.04
4b	9	M_1	-5.4	25.4	0.06	-18.7	0.01
4b	9	M_2	-7.3	23.4	0.07	-17.6	0.10
4b	9	M_3	-7.9	22.8	0.10	-15.8	0.02
4b	10	I	-6.8	23.9	0.04	-17.8	0.02
4b	10	M_1	-7.9	22.8	0.00	-17.9	0.01
4b	10	M_2	-7.3	23.4	0.01	-16.8	0.01
4b	10	M_3	-7.2	23.5	0.16	-15.2	0.10

Table C.2 (overleaf): *Final oxygen and carbon isotope data for the lower left and upper* Microtus agrestis *teeth from the modern sites. Site numbers: 1) West Horrington, Somerset, 2) Cobham, Surrey, 3) Beeford, East Yorkshire, Tooth types: I = incisor, M_1 = first molar, M_2 = second molar, M_3 = third molar.*

Site	Individual number	Tooth type	Side	$\delta^{18}O$ (‰ VPDB)		$\delta^{13}C$ (‰ VPDB)	
				Value	1σ uncertainty	Value	1σ uncertainty
1	3	I	Lower left	-6.9	0.02	-17.8	0.03
1	3	M_1	Lower left	-6.9	0.09	-16.5	0.01
1	3	M_2	Lower left	-6.4	0.09	-15.8	0.01
1	3	M_3	Lower left	Not analysed - insufficient material			
1	3	I	Upper right	-6.5	0.04	-17.2	0.09
1	3	M_1	Upper right	-7.3	0.09	-16.5	0.03
1	3	M_2	Upper right	-6.8	0.06	-13.9	0.06
1	3	M_3	Upper right	-6.3	0.13	-14.5	0.01
1	3	I	Upper left	-7.9	0.09	-17.5	0.02
1	3	M_1	Upper left	-7.1	0.07	-16.4	0.04
1	3	M_2	Upper left	-7.9	0.09	-16.0	0.01
1	3	M_3	Upper left	-7.0	0.06	-15.9	0.05
2	9	I	Lower left	-8.2	0.10	-19.3	0.02
2	9	M_1	Lower left	-8.2	0.01	-18.7	0.03
2	9	M_2	Lower left	-10.0	0.11	-18.2	0.08
2	9	M_3	Lower left	-10.2	0.11	-17.4	0.05
2	9	I	Upper right	-7.6	0.04	-18.9	0.08
2	9	M_1	Upper right	-7.6	0.21	-18.5	0.06
2	9	M_2	Upper right	-11.0	0.37	-18.4	0.02
2	9	M_3	Upper right	-9.7	0.13	-17.9	0.00
2	9	I	Upper left	-8.3	0.18	-19.0	0.11
2	9	M_1	Upper left	-7.7	0.22	-18.1	0.06
2	9	M_2	Upper left	-10.7	0.48	-18.2	0.03
2	9	M_3	Upper left	-10.3	0.04	-18.2	0.09
3	1	I	Lower left	-8.1	0.04	-21.1	0.01
3	1	M_1	Lower left	-9.0	0.03	-20.6	0.00
3	1	M_2	Lower left	-9.4	0.10	-19.8	0.04
3	1	M_3	Lower left	-10.4	0.14	-19.9	0.03
3	1	I	Upper right	-9.9	0.11	-21.4	0.00
3	1	M_1	Upper right	-8.8	0.08	-18.8	0.05
3	1	M_2	Upper right	-9.4	0.11	-20.2	0.01
3	1	M_3	Upper right	-10.4	0.02	-19.9	0.06
3	1	I	Upper left	-10.2	0.05	-21.3	0.01
3	1	M_1	Upper left	-9.7	0.08	-20.6	0.01
3	1	M_2	Upper left	-11.2	0.02	-19.8	0.04
3	1	M_3	Upper left	-10.3	0.08	-18.8	0.06

Table C.3: *Matrix for the differences between the $\delta^{18}O$ values (‰ VPDB) of the teeth from Individual 3 from West Horrington, Somerset. The differences were calculated by subtracting the $\delta^{18}O$ value of the tooth in the column of the table, from the $\delta^{18}O$ value of the tooth in the row of the table. R = right side tooth, L = left side tooth, i = lower incisor, m_1 = lower first molar, m_2 = lower second molar, m_3 = lower third molar, I = upper incisor, M^1 = upper first molar, M^2 = upper second molar, M^3 upper third molar.*

	Rm_1	**RM^1**	**Lm_1**	**LM^1**	**Rm_2**	**RM^2**	**Lm_2**	**LM^2**	**Rm_3**	**RM^3**	**LM^3**	**Ri**	**RI**	**Li**
RM^1	0.1													
Lm_1	-0.3	-0.4												
LM^1	0.0	-0.2	0.2											
Rm_2	-3.0	-3.2	-2.7	-3.0										
RM^2	-0.3	-0.5	-0.1	-0.3	2.7									
Lm_2	-0.8	-0.9	-0.5	-0.7	2.3	-0.4								
LM^2	0.7	0.6	1.0	0.8	3.7	1.1	1.5							
Rm_3	-2.4	-2.5	-2.1	-2.3	0.6	-2.0	-1.6	-3.1						
RM^3	-0.9	-1.1	-0.6	-0.9	2.1	-0.6	-0.2	-1.6	1.5					
LM^3	-0.1	-0.3	0.1	-0.1	2.9	0.2	0.6	-0.9	2.2	0.8				
Ri	-2.2	-2.3	-1.9	-2.1	0.8	-1.8	-1.4	-2.9	0.2	-1.3	-2.0			
RI	-0.7	-0.9	-0.4	-0.7	2.3	-0.4	0.0	-1.4	1.7	0.2	-0.6	1.5		
Li	-0.3	-0.5	0.0	-0.3	2.7	0.0	0.4	-1.0	2.1	0.6	-0.2	1.9	0.4	
LI	0.7	0.6	1.0	0.8	3.7	1.1	1.5	0.0	3.1	1.6	0.9	2.9	1.4	1.0

Table C.4: *Matrix for the differences between the $\delta^{13}C$ values (‰ VPDB) of the teeth from Individual 3 from West Horrington, Somerset. The differences were calculated by subtracting the $\delta^{13}C$ value of the tooth in the column of the table, from the $\delta^{13}C$ value of the tooth in the row of the table. R = right side tooth, L = left side tooth, i = lower incisor, m_1 = lower first molar, m_2 = lower second molar, m_3 = lower third molar, I = upper incisor, M^1 = upper first molar, M^2 = upper second molar, M^3 upper third molar.*

	Rm_1	**RM^1**	**Lm_1**	**LM^1**	**Rm_2**	**RM^2**	**Lm_2**	**LM^2**	**Rm_3**	**RM^3**	**LM^3**	**Ri**	**RI**	**Li**
RM^1	0.2													
Lm_1	0.2	0.0												
LM^1	0.1	-0.1	-0.1											
Rm_2	-0.6	-0.8	-0.8	-0.8										
RM^2	-2.3	-2.5	-2.5	-2.5	-1.7									
Lm_2	-0.5	-0.6	-0.7	-0.6	0.2	1.9								
LM^2	-0.3	-0.4	-0.5	-0.4	0.4	2.1	0.2							
Rm_3	-1.0	-1.2	-1.2	-1.2	-0.4	1.3	-0.6	-0.8						
RM^3	-1.8	-2.0	-2.0	-2.0	-1.2	0.5	-1.4	-1.6	-0.8					
LM^3	-0.4	-0.6	-0.6	-0.5	0.2	1.9	0.0	-0.2	0.6	1.4				
Ri	1.0	0.8	0.8	0.8	1.6	3.3	1.4	1.2	2.0	2.8	1.4			
RI	0.9	0.7	0.7	0.8	1.6	3.3	1.4	1.2	1.9	2.7	1.3	-0.1		
Li	1.5	1.3	1.3	1.4	2.1	3.9	2.0	1.8	2.5	3.3	1.9	0.5	0.6	
LI	1.2	1.0	1.0	1.1	1.9	3.6	1.7	1.5	2.2	3.0	1.6	0.2	0.3	-0.3

Table C.5: *Matrix for the differences between the $\delta^{18}O$ values (‰ VPDB) of the teeth from Individual 9 from Cobham, Surrey. The differences were calculated by subtracting the $\delta^{18}O$ value of the tooth in the column of the table, from the $\delta^{18}O$ value of the tooth in the row of the table. R = right side tooth, L = left side tooth, i = lower incisor, m_1 = lower first molar, m_2 = lower second molar, m_3 = lower third molar, I = upper incisor, M^1 = upper first molar, M^2 = upper second molar, M^3 upper third molar.*

	Rm_1	**RM^1**	**Lm_1**	**LM^1**	**Rm_2**	**RM^2**	**Lm_2**	**LM^2**	**Rm_3**	**RM^3**	**Lm_3**	**LM^3**	**Ri**	**RI**	**Li**
RM^1	-0.3														
Lm_1	0.3	0.6													
LM^1	-0.2	0.1	-0.5												
Rm_2	-0.2	0.1	-0.5	0.0											
RM^2	2.7	3.0	2.4	2.9	2.9										
Lm_2	2.1	2.4	1.8	2.2	2.2	-0.7									
LM^2	2.3	2.6	2.0	2.4	2.4	-0.5	0.2								
Rm_3	0.2	0.4	-0.2	0.3	0.3	-2.6	-1.9	-2.1							
RM^3	1.7	2.0	1.4	1.9	1.9	-1.0	-0.3	-0.5	1.6						
Lm_3	2.3	2.6	2.0	2.4	2.4	-0.5	0.2	0.0	2.1	0.5					
LM^3	2.4	2.7	2.1	2.6	2.6	-0.3	0.4	0.2	2.3	0.7	0.2				
Ri	0.0	0.3	-0.3	0.1	0.1	-2.8	-2.1	-2.3	-0.2	-1.8	-2.3	-2.5			
RI	-0.3	0.0	-0.6	-0.1	-0.1	-3.0	-2.3	-2.5	-0.4	-2.0	-2.5	-2.7	-0.2		
Li	0.3	0.6	0.0	0.5	0.5	-2.4	-1.7	-1.9	0.2	-1.4	-1.9	-2.1	0.4	0.6	
LI	0.4	0.7	0.1	0.6	0.6	-2.3	-1.6	-1.8	0.3	-1.3	-1.8	-2.0	0.5	0.7	0.1

Table C.6: *Matrix for the differences between the $\delta^{13}C$ values (‰ VPDB) of the teeth from Individual 9 from Cobham, Surrey. The differences were calculated by subtracting the $\delta^{13}C$ value of the tooth in the column of the table, from the $\delta^{13}C$ value of the tooth in the row of the table. R = right side tooth, L = left side tooth, i = lower incisor, m_1 = lower first molar, m_2 = lower second molar, m_3 = lower third molar, I = upper incisor, M^1 = upper first molar, M^2 = upper second molar, M^3 upper third molar.*

	Rm_1	**RM^1**	**Lm_1**	**LM^1**	**Rm_2**	**RM^2**	**Lm_2**	**LM^2**	**Rm_3**	**RM^3**	**Lm_3**	**LM^3**	**Ri**	**RI**	**Li**
RM^1	-0.2														
Lm_1	0.0	0.2													
LM^1	-0.6	-0.4	-0.6												
Rm_2	-0.3	-0.1	-0.3	0.3											
RM^2	-0.3	-0.1	-0.3	0.3	0.0										
Lm_2	-0.6	-0.4	-0.5	0.1	-0.3	-0.3									
LM^2	-0.5	-0.3	-0.5	0.1	-0.2	-0.2	0.0								
Rm_3	-1.1	-0.9	-1.0	-0.4	-0.8	-0.7	-0.5	-0.5							
RM^3	-0.9	-0.7	-0.8	-0.3	-0.6	-0.6	-0.3	-0.3	0.2						
Lm_3	-1.3	-1.1	-1.3	-0.7	-1.0	-1.0	-0.8	-0.8	-0.3	-0.4					
LM^3	-0.5	-0.3	-0.5	0.1	-0.2	-0.2	0.0	0.0	0.5	0.3	0.8				
Ri	0.3	0.4	0.3	0.9	0.5	0.6	0.8	0.8	1.3	1.1	1.6	0.8			
RI	0.1	0.3	0.2	0.8	0.4	0.4	0.7	0.7	1.2	1.0	1.4	0.7	-0.1		
Li	0.5	0.7	0.6	1.2	0.8	0.9	1.1	1.1	1.6	1.4	1.9	1.1	0.3	0.4	
LI	0.3	0.5	0.3	0.9	0.6	0.6	0.8	0.8	1.3	1.1	1.6	0.8	0.0	0.1	-0.3

Table C.7: *Matrix for the differences between the $\delta^{18}O$ values (‰ VPDB) of the teeth from Individual 1 from Beeford, East Yorkshire. The differences were calculated by subtracting the $\delta^{18}O$ value of the tooth in the column of the table, from the $\delta^{18}O$ value of the tooth in the row of the table. R = right side tooth, L = left side tooth, i = lower incisor, m_1 = lower first molar, m_2 = lower second molar, m_3 = lower third molar, I = upper incisor, M^1 = upper first molar, M^2 = upper second molar, M^3 upper third molar.*

	Rm_1	**RM^1**	**Lm_1**	**LM^1**	**Rm_2**	**RM^2**	**Lm_2**	**LM^2**	**Rm_3**	**RM^3**	**Lm_3**	**LM^3**	**Ri**	**RI**	**Li**
RM^1	-0.4														
Lm_1	-0.2	0.3													
LM^1	0.5	0.9	0.7												
Rm_2	-0.7	-0.3	-0.6	-1.3											
RM^2	0.2	0.7	0.4	-0.3	1.0										
Lm_2	0.2	0.6	0.3	-0.3	0.9	-0.1									
LM^2	2.0	2.4	2.2	1.5	2.7	1.8	1.8								
Rm_3	-2.2	-1.8	-2.0	-2.7	-1.5	-2.4	-2.4	-4.2							
RM^3	1.2	1.6	1.3	0.7	1.9	0.9	1.0	-0.8	3.4						
Lm_3	1.1	1.6	1.3	0.6	1.9	0.9	1.0	-0.9	3.4	0.0					
LM^3	1.1	1.5	1.3	0.6	1.8	0.9	0.9	-0.9	3.3	-0.1	-0.1				
Ri	-0.7	-0.3	-0.5	-1.2	0.0	-0.9	-0.9	-2.7	1.5	-1.9	-1.9	-1.8			
RI	0.6	1.1	0.8	0.1	1.4	0.4	0.5	-1.3	2.9	-0.5	-0.5	-0.4	1.4		
Li	-1.1	-0.7	-1.0	-1.6	-0.4	-1.4	-1.3	-3.1	1.1	-2.3	-2.3	-2.2	-0.4	-1.8	
LI	1.0	1.5	1.2	0.5	1.8	0.8	0.8	-1.0	3.2	-0.1	-0.1	-0.1	1.7	0.4	2.1

Table C.8: *Matrix for the differences between the $\delta^{13}C$ values (‰ VPDB) of the teeth from Individual 1 from Beeford, East Yorkshire. The differences were calculated by subtracting the $\delta^{13}C$ value of the tooth in the column of the table, from the $\delta^{13}C$ value of the tooth in the row of the table. R = right side tooth, L = left side tooth, i = lower incisor, m_1 = lower first molar, m_2 = lower second molar, m_3 = lower third molar, I = upper incisor, M^1 = upper first molar, M^2 = upper second molar, M^3 upper third molar.*

	Rm_1	**RM^1**	**Lm_1**	**LM^1**	**Rm_2**	**RM^2**	**Lm_2**	**LM^2**	**Rm_3**	**RM^3**	**Lm_3**	**LM^3**	**Ri**	**RI**	**Li**
RM^1	-1.6														
Lm_1	0.2	1.8													
LM^1	0.2	1.8	0.0												
Rm_2	-1.2	0.5	-1.4	-1.4											
RM^2	-0.2	1.4	-0.4	-0.4	0.9										
Lm_2	-0.6	1.0	-0.8	-0.8	0.5	-0.4									
LM^2	-0.6	1.1	-0.8	-0.8	0.6	-0.3	0.0								
Rm_3	-2.9	-1.3	-3.1	-3.1	-1.7	-2.6	-2.3	-2.3							
RM^3	-0.6	1.1	-0.8	-0.8	0.6	-0.3	0.1	0.0	2.3						
Lm_3	-0.5	1.1	-0.7	-0.7	0.6	-0.3	0.1	0.0	2.3	0.0					
LM^3	-1.6	0.0	-1.9	-1.9	-0.5	-1.4	-1.0	-1.1	1.2	-1.1	-1.1				
Ri	1.1	2.7	0.8	0.8	2.2	1.3	1.7	1.6	3.9	1.6	1.6	2.7			
RI	1.0	2.6	0.8	0.8	2.1	1.2	1.6	1.6	3.9	1.5	1.5	2.6	-0.1		
Li	0.7	2.3	0.5	0.5	1.8	0.9	1.3	1.2	3.6	1.2	1.2	2.3	-0.4	-0.3	
LI	0.9	2.5	0.6	0.6	2.0	1.1	1.5	1.4	3.7	1.4	1.4	2.5	-0.2	-0.1	0.2

Table C.9: *Oxygen and hydrogen isotope data for the water samples from Somerset and Perthshire.*

Site	**Water body**	**$\delta^{18}O$ (‰ VSMOW)**	**δD (‰ VSMOW)**
Somerset	River Sheppey (Keward Brook), Wells Market Cross fountain	-6.3	-39.0
Somerset	River Sheppey, Mill Lane, Coxley	-5.8	-36.8
Somerset	River Axe, Wookey	-6.4	-39.3
Somerset	River Brue, Westhay	-5.5	-35.7
Perthshire	Ordie Burn, on National Cycle Route 77	-8.0	-51.5
Perthshire	Shochie Burn, near Moneydie	-7.9	-51.4
Perthshire	Coldrochie Burn, south of Moneydie	-7.9	-51.5
Perthshire	Stream near Cotterton	-8.1	-53.3

Appendix D: Data for West Runton, Cudmore Grove and Marsworth (Chapter 6)

The following tables list the sample information and oxygen and carbon isotope data from the fossil rodent teeth from West Runton, Cudmore Grove and Marsworth, plus the oxygen and carbon isotope data from the fossil shells from Marsworth. The assemblage and taphonomic information for the small mammal and mollusc remains from Marsworth are also included here.

D.1. West Runton, Norfolk

Table D.1.1: *Descriptions of the rodent teeth from West Runton that were selected for isotopic analysis.*

Height above base of WRFB (cm)	Sample section	Specimen code	Species	Element type	Side	General descriptions
40-45	WR7	WR-MS1	*Mimomys savini*	Lower M1	Left	- Rootles molar with a *Mimomys* fold that is broken at the external tip - Minor corrosion of enamel due to digestion
40-45	WR7	WR-I	Not identifiable	Upper incisor	Right?	- Fragment consisting of the cusp end of an incisor - Inner surface of dentine pitted
50-55	WR6	WR-MS2	*Mimomys cf. savini*	Upper M2	Right	- Rooted molar - Well-preserved - No evidence of digestion - Dentine missing at occlusal surface

Table D.1.2: *Isotope data for the* Mimomys savini *incisors from West Runton (from Peneycad, 2013).*

Specimen code	$\delta^{18}O$ of tooth carbonate (‰ VPDB)		$\delta^{13}C$ of tooth carbonate (‰ VPDB)	
	Value	1σ uncertainty	Value	1σ uncertainty
WR-1	-7.9	0.10	-11.5	0.04
WR-2	-7.8	0.12	-8.7	0.01
WR-3	-7.7	0.03	-8.9	0.06
WR-4	-7.7	0.05	-8.7	0.04
WR-5	-8.4	0.07	-11.3	0.05
WR-6	-7.3	0.04	-11.9	0.06
WR-7	-7.7	0.04	-11.8	0.03
WR-8	-7.5	0.12	-10.9	0.05
WR-9	-7.9	0.03	-11.6	0.07

Table D.1.3: *Final isotope data for the three teeth from West Runton (Table D.1.1) that were investigated in this thesis.*

Specimen code	$\delta^{18}O$ of tooth carbonate (‰ VPDB)		$\delta^{13}C$ of tooth carbonate (‰ VPDB)	
	Value	1σ uncertainty	Value	1σ uncertainty
WR-MS1	-5.7	0.03	-13.2	0.08
WR-I	-6.0	0.53	-12.5	0.16
WR-MS2	-7.1	0.37	-12.0	0.12

Table D.1.4: *Oxygen isotope values of meteoric water, calculated using the $\delta^{18}O$ values of rodent tooth carbonate from West Runton.*

Specimen code	$\delta^{18}O$ of meteoric water (‰ VSMOW)	1σ uncertainty (‰)
WR-1	-6.95	0.20
WR-2	-6.89	0.22
WR-3	-6.83	0.12
WR-4	-6.84	0.15
WR-5	-7.32	0.18
WR-6	-6.53	0.13
WR-7	-6.79	0.14
WR-8	-6.64	0.22
WR-9	-6.97	0.13

WR-MS1	-5.28	0.23
WR-I	-6.34	0.21
WR-MS2	-5.49	0.25

D.2. Cudmore Grove, Essex

Table D.2.1: *Details of the* Arvicola cantiana *upper incisors from Unit 3 at Cudmore Grove that were analysed for this thesis.*

Specimen code	Description
CG-1	3 fragments of enamel ~4-5 mm in length
CG-4	Complete left upper incisor
CG-5	4 fragments of enamel, 2 of which are large (5-8 mm long)
CG-14	Near-complete right upper incisor; part of the apex is broken

Table D.2.2: *Oxygen and carbon isotope data for the* Arvicola cantiana *upper incisors from Cudmore Grove.*

Specimen code	$\delta^{18}O$ of tooth carbonate (‰ VPDB)		$\delta^{13}C$ of tooth carbonate (‰ VPDB)	
	Value	1σ uncertainty	Value	1σ uncertainty
CG-1	-5.0	0.09	-9.7	0.01
CG-4	-6.4	0.00	-12.7	0.03
CG-5	-5.1	0.02	-12.7	0.00
CG-14	-4.7	0.07	-8.2	0.01

Table D.2.3: *Oxygen isotope values of meteoric water, calculated using the $\delta^{18}O$ values of the* A. cantiana *incisor carbonate from Cudmore Grove.*

Specimen code	$\delta^{18}O$ of meteoric water (‰ VSMOW)	1σ uncertainty (‰)
CG-1	-4.72	0.26
CG-4	-5.84	0.12
CG-5	-4.85	0.20
CG-14	-4.52	0.27

Table D.2.4: *Oxygen isotope values of* A. cantiana *incisor phosphate from Cudmore Grove, and the $\delta^{18}O$ values of local water calculated from these values using various modern calibration equations. The phosphate data are from Ruddy (2005).*

Specimen code	$\delta^{18}O$ of incisor phosphate (‰ VSMOW)	$\delta^{18}O$ of local water (‰ VSMOW)		
		Navarro et al. (2004), modified by Ruddy (2005)	Longinelli et al. (2003)	Royer et al. (2013a)
CG-1	15.97	-5.01	-6.23	-7.35
CG-2	16.23	-4.69	-6.00	-7.12
CG-3	15.08	-6.13	-7.01	-8.13
CG-5	17.28	-3.38	-5.08	-6.20
CG-6	15.32	-5.83	-6.80	-7.92
CG-7	17.21	-3.46	-5.14	-6.26
CG-8	14.71	-6.59	-7.33	-8.46
CG-9	15.41	-5.71	-6.72	-7.84
CG-10	16.33	-4.56	-5.91	-7.04
CG-12	15.01	-6.21	-7.07	-8.19
CG-13	17.02	-3.70	-5.31	-6.43
CG-15	14.95	-6.29	-7.12	-8.25

D.3. Marsworth, Buckinghamshire

This section provides background information on the sediment samples from Level 3 (gravelly calcareous sands) and Level 2 (organic muds) at Marsworth, which were analysed in this research. Descriptions of the small mammal and molluscan assemblages recovered from the sediment samples are included, and taphonomic observations are summarised and discussed. The second half of this section lists the oxygen and carbon isotope data from the sampled rodent teeth and shells.

D.3.1. Sediment samples

Table D.3.1: *Summary of the sediment samples obtained from the Buckinghamshire County Museum Resource Centre.*

Stratigraphic Unit	Grid square	Date of collection
Level 3	J9	31/10/82
Level 3	J10	23/01/83
Level 3	J15	31/10/82
Level 3	J16	31/10/82
Level 2	J10	17/12/82
Level 2	J12	06/05/83
Level 2	K9	24/07/81
Level 2	K9	29/07/81
Level 2	K10	31/07/81
Level 2	K13	12/04/82
Level 2	K15	30/06/82
Level 2	L10	22/05/81
Level 2	L11	29/05/81
Level 2	L13	-

D.3.2. Small mammal remains from Level 3

A total of 305 bone fragments, 17 molar fragments, and 10 incisor fragments were found in the four sediment samples from Level 3. The mammalian remains from this level show a high degree of breakage; more than 95% of the bones and 100% of the teeth are incomplete. Moreover, approximately 25-50% of the bones and 25-50% of the teeth show evidence for the rounding of broken edges and protruding elements. Incisor fragments show a greater degree of rounding than molar fragments. Approximately 25-50% of limb bone fragments have one or more longitudinal cracks along the shaft. Several of these fragments are additionally pitted and flaked across the whole outer surface. A small proportion of teeth also have this cracked and pitted appearance.

In contrast, evidence for localised surface corrosion on the bones and teeth, indicative of digestion by a predator, is infrequent. Only one or two molars show possible minor digestion of the enamel at the occlusal surface, indicated by the pitting and slight rounding of the salient angles.

The anterior cap is preserved on 4 lower M_1 specimens and has the characteristic morphology of the species *Microtus oeconomus*. Most of the incisors are small, and thus are also likely to originate from a species within the genus *Microtus*. Two fragments of the posterior section of a mandible, with both the M_1 and M_2 *in situ*, were also found within sample J15. The dilambdodont morphology of the molars, with dark staining on the tips of the cusps, is characteristics of the family Soricidae. Based on the size and morphology of the mandible, and in particular the morphology of the ascending ramus fragment, the jaw has been assigned to the species *Sorex araneus*. This is a first time this species has been recorded in the Marsworth deposits. At the present day, this species is widely distributed across Europe, and lives in a range of habitats from thick grassland to bushy scrub (MacDonald and Barrett, 1993). Therefore, its presence at Marsworth is not inconsistent with the other palaeoenvironmental proxy evidence from the site (Murton et al., 2001).

D.3.3. Molluscan remains from Level 3

A total of 66 shell fragments were identified in the samples from Level 3. Most gastropods were preserved as fragments consisting of 1-3 whorls at the apex or centre of the shell. The majority of the shells are very small (< 2 mm) and thus the assemblage is likely dominated by the remains of juvenile individuals. Some shells also show signs of surface wear (flaking and pitting). The most common taxa are *Trochulus* cf. *hispidus* and *Cepaea*. Land taxa represent 87% of the assemblage from Level 3, while the remains of aquatic taxa are comparatively scarce, constituting only 13% of the assemblage. *Galba truncatula* is the most abundant aquatic mollusc taxon.

D.3.4. Mammalian remains from Level 2

A total of around 850 bone fragments were recovered from the ten sediment samples from Level 2. Small mammal teeth are less abundant than in Level 3, with only 12 molar fragments and 10 incisor fragments discovered in seven

out of the ten samples that were investigated. The bones and teeth are highly fragmented; 90-95% of the specimens from Level 2 are incomplete. In addition, the broken edges on approximately 25% of bones and 25% of the teeth are slightly or moderately rounded, and ~5-10% of the bones are cracked, pitted or flaked.

The frequency of low-moderate digestion on the teeth from Level 2 is much higher than for the Level 3 specimens. Slight surface etching of the enamel and rounding of the salient angles at the occlusal surface of molars can be seen on approximately 10-15% of the specimens, and 5-10% of the molars show moderate rounding of the salient angles with some penetration of the enamel.

The fragmentary nature of the fossil material precluded the taxonomic identification of the majority of the small mammal teeth, though again the anterior cap was preserved on 4 first lower molars. Based on the morphology of this cap, these teeth have been identified to the species *Microtus oeconomus*.

D.3.5. Molluscan remains from Level 2

Molluscan remains are more abundant in Level 2 compared to Level 3, with 12 taxa identified from a total of 350 shell fragments. Again, most fragments consist of only the apical or central whorls of the shell. However, the completeness of the shells is generally greater compared to Level 3, and surface pitting or flaking is less frequent. Remains of aquatic taxa comprise 11% of the molluscan assemblage, while land taxa dominate at a frequency of 89%. *Trochulus hispidus* is by far the most highly represented species in the assemblage, constituting 40% of all identified shell remains from Level 2. *Galba truncatula* is the most common aquatic species.

D.3.6. Interpretations of the mammalian assemblages

The dominance of *Microtus* sp. remains in the small mammal assemblage from Level 3, and in particular the presence of *M. oeconomus*, is consistent with the

published results from the Lower Channel sediments at Marsworth (Murton et al., 2001). Conversely, despite recovering ~700 mammalian specimens from Level 2, rodent remains have not been previously recorded from these sediments (Murton et al., 2001). Several fragments of *Microtus* sp. teeth, including four *M. oeconomus* molars, were discovered in the Level 2 sediments investigated in this research. These discoveries demonstrate that microtine rodents, and especially *M. oeconomus*, persisted within the landscape throughout the deposition of Levels 3 and 2. This suggests that environmental conditions remained relatively stable during the accumulation of the Lower Channel sediments.

The taphonomic observations suggest that the mammalian remains from Levels 3 and 2 have been affected by various taphonomic agents. This is not unexpected given that the material has been transported from the surrounding landscape and deposited within a stream channel. Evidence for digestion indicates that some of the rodent teeth originate from the deposition of pellets by a predator. The difference in the degree of digestion between Levels 3 and 2 suggests that the remains in these sediments were accumulated by different predators. The light digestion on a small number of teeth from Level 3 is consistent with a Category 1 predator, such as the barn owl, while the relatively higher frequency and degree of digestion of the Level 2 teeth is suggestive of a Category 1-2 predator, such as the short-eared owl. However, it should be noted that these interpretations are based upon a small assemblage of teeth, and thus differences in the frequencies of digestion may be due to sample bias. Furthermore, it is likely that the skeletal material has been derived from various sources (i.e. natural deaths and predation), thus altering the frequencies of taphonomic modifications from a natural predator assemblage.

The high level of breakage and fragmentation of the mammalian remains, however, is uncharacteristic of an assemblage accumulated solely by a Category 1 or 2 predator (Andrews, 1990). Category 1-2 predators cause the breakage of < 5% of the teeth within an assemblage (Andrews, 1990). Therefore, other processes must be responsible for this breakage. Some of the teeth are slightly rounded, indicating that attrition occurred during transport. The frequency of rounding is greater in the samples from Level 3.

The Level 3 sediments consist of coarse gravelly sands, which were transported and deposited under high-energy conditions. This high-energy transport would have most likely resulted in the attrition and breakage of the small mammal material.

Some of the rodent remains from Level 3 are also cracked, pitted and flaked. These surface features are typically associated with weathering (Andrews, 1990), suggesting that some of the remains may have been exposed on the land surface for several years before being transported into the Lower Channel. This weathering may have also weakened the teeth, rendering them more susceptible to breakage.

In contrast, the Level 2 sediments are much finer grained, and were deposited under lower energy conditions. Nevertheless, the frequency of tooth breakage is still ~25%, and there is no evidence for weathering. Therefore, in addition to fluvial transport, other processes such as the trampling of the material by large mammals visiting the stream to drink, may have also contributed to the breakage of the teeth.

In summary, the rodent teeth were transported from the local landscape and deposited within the stream channel. The rodent teeth likely originate from owl pellets plus individuals that died naturally. The evidence for weathering indicates that some of the teeth and shells were exposed on the land surface before being washed into the stream. The high degree of breakage and slight rounding also suggests that the remains may have been transported a reasonable distance before deposition. Nevertheless, the palaeoecological evidence from Levels 3 and 2 suggests that the stream was predominantly slow-flowing (Murton et al., 2001). Therefore, the rodent remains may have been mainly transported into the channel during flood events. Consequently, the fossil teeth and shells likely record environmental conditions local to Marsworth, and potentially span a relatively short period of time.

D.3.7. Interpretations of the mollusc assemblages

There are no notable differences in the taxonomic composition of the molluscan assemblages from Levels 3 and 2. Moreover, the relative proportions of aquatic and land taxa from the two Levels are very similar,

indicating that no significant changes in environmental conditions occurred during the interval in which these sediments were deposited. These interpretations are in agreement with the current understanding of the palaeoenvironmental conditions represented by Lower Channel deposits at Marsworth (Murton et al., 2001).

The majority of the molluscan taxa identified in the analysed samples have been reported in previous studies on the deposits at Marsworth (Green et al., 1984; Murton et al., 2001, 2015). However, *Merdigera obscura* and *Pomatias elegans* are newly recognised taxa for this site. Nevertheless, the shells attributed to these species are relatively poorly preserved, and thus it is possible that these specimens have been misidentified; *Cochlicopa* sp. and *Carychium* sp. are similar in overall morphology to *Merdigera obscura*, and have been identified in previous molluscan analyses undertaken on the Lower Channel sediments from Marsworth (Murton et al., 2001, 2015). The shell identified to *P. elegans* is particularly abraded and thus the taxonomic identification of this specimen is not entirely certain.

Despite this, the presence of these species at Marsworth is not inconsistent with the existing palaeoenvironmental evidence from the site. Both species are typically found in areas underlain by calcareous bedrock (Ellis, 1926; McMillan, 1968). The geology surrounding Marsworth is predominantly Cretaceous Chalk, and thus soils in this area are likely to be rich in calcium carbonate. In addition, both *M. obscura* and *P. elegans* live in woodland, shrubland and dry bank habitats (Ellis, 1926; McMillan, 1968). While evidence for the occurrence of woodland near Marsworth is limited, small patches of trees and dry open grassland areas likely existed in the local area (Murton et al., 2001). Therefore, it is possible that small numbers of shells of these species, as discovered in the Level 3 and 2 deposits, could have been transported to and deposited within the Lower Channel from the surrounding landscape.

D.3.8. Rodent teeth and mollusc shells selected for analysis

Table D.3.2: *Rodent teeth from Marsworth that were selected for isotopic analysis.*

Specimen code	Stratigraphic level	Grid square	Size fraction (mm)	Taxon	Element type	Side
MA-3-J9-T1	3	J9	1-2	Not identifiable	Upper incisor	Right
MA-3-J10-T1	3	J10	> 2	*Microtus* sp.	Lower M_1	Right
MA-3-J10-T2	3	J10	1-2	Not identifiable	Lower incisor	Right
MA-3-J10-T3	3	J10	1-2	Not identifiable	Lower incisor fragment	?
MA-3-J10-T6	3	J10	1-2	*Microtus oeconomus*	Lower M_1 fragment	Right
MA-3-J10-T7	3	J10	1-2	*Microtus oeconomus*	Lower M_1 fragment	Left
MA-3-J10-T8	3	J10	1-2	*Microtus* sp.	Lower M_1 fragment	Left
MA-3-J10-T9	3	J10	1-2	*Microtus* sp.	Lower M_1 fragment	Right
MA-3-J10-T10	3	J10	1-2	*Microtus* sp.	Upper M^1 fragment	Left
MA-3-J15-T1	3	J15	1-2	Not identifiable	Lower incisor fragment	?
MA-3-J16-T1	3	J16	1-2	Not identifiable	Upper incisor fragment	Right
MA-3-J16-T2	3	J16	1-2	Not identifiable	Lower incisor fragment	?
MA-2-K15-T2	2	K15	1-2	*Microtus* sp.	Lower M_2 fragment	Left
MA-2-K15-T3	2	K15	1-2	*Microtus* sp.	Lower M_3	Left
MA-2-K15-T4	2	K15	1-2	*Microtus* sp.	Molar fragment	?
MA-2-K15-T6	2	K15	1-2	*Microtus oeconomus*	Lower M_1 fragment	Right
MA-2-L10-T2	2	L10	1-2	*Microtus* sp.	Lower M_2	Left
MA-2-L10-T3	2	L10	1-2	*Microtus* sp.	Upper M^3 fragment	Left?
MA-2-L10-T4	2	L10	1-2	Not identifiable	Upper incisor	Left?
MA-2-L11-T1	2	L11	1-2	Not identifiable	Upper incisor	Right

Table D.3.3: Galba truncatula *mollusc shells from Marsworth that were selected for isotopic analysis.*

Specimen code	Stratigraphic level	Grid square
MA-3-G1	3	J10
MA-3-G2	3	J10
MA-2-G1	2	J10
MA-2-G2	2	J10
MA-2-G3	2	K9
MA-2-G4	2	K10
MA-2-G5	2	K10
MA-2-G6	2	K10
MA-2-G7	2	K13
MA-2-G8	2	K13
MA-2-G9	2	K15
MA-2-G10	2	K15
MA-2-G11	2	L10
MA-2-G12	2	L10
MA-2-G13	2	L11
MA-2-G14	2	L11
MA-2-G15	2	J12
MA-2-G16	2	K9
MA-2-G17	2	L13
MA-2-G18	2	L13

D.3.9. Isotope data

Table D.3.4: *Final oxygen and carbon isotope results for the fossil rodent teeth from Marsworth.*

Specimen code	$\delta^{18}O$ of tooth carbonate (‰ VPDB)		$\delta^{13}C$ of tooth carbonate (‰ VPDB)	
	Value	1σ uncertainty	Value	1σ uncertainty
MA-3-J9-T1	-3.7	0.10	-11.8	0.25
MA-3-J10-T1	-7.5	0.14	-11.8	0.06
MA-3-J10-T2	-7.7	0.19	-11.2	0.31
MA-3-J10-T3	-5.7	0.03	-9.9	0.03
MA-3-J10-T6	-7.8	0.09	-12.7	0.06
MA-3-J10-T7	-5.9	0.09	-13.7	0.01
MA-3-J10-T8	-7.4	0.05	-11.8	0.05
MA-3-J10-T9	-8.0	0.15	-12.1	0.02
MA-3-J10-T10	-6.3	0.14	-13.5	0.10
MA-3-J15-T1	-7.8	0.01	-12.0	0.00

MA-3-J16-T1	-6.3	0.00	-11.4	0.00
MA-3-J16-T2	-7.8	0.17	-9.3	0.50
MA-2-K15-T2	-7.6	0.04	-12.2	0.07
MA-2-K15-T3	-7.7	0.02	-12.1	0.01
MA-2-K15-T4	-9.2	0.06	-12.9	0.07
MA-2-K15-T6	-6.9	0.04	-12.2	0.04
MA-2-L10-T2	-7.9	0.03	-10.3	0.01
MA-2-L10-T3	-7.4	0.14	-13.3	0.08
MA-2-L10-T4	-6.1	0.22	-12.2	0.08
MA-2-L11-T1	-6.5	0.00	-10.0	0.03

Table D.3.5: *Oxygen and carbon isotope results for the mollusc shells from Marsworth.*

Specimen code	**$\delta^{18}O$ of shell aragonite (‰ VPDB)**		**$\delta^{13}C$ of shell aragonite (‰ VPDB)**	
	Value	**1σ uncertainty**	**Value**	**1σ uncertainty**
MA-3-G1	-4.2	0.08	-8.6	0.04
MA-3-G2	-4.7	0.03	-12.0	0.06
MA-2-G1	-0.6	0.07	-8.1	0.00
MA-2-G3	-4.8	0.11	-12.1	0.00
MA-2-G4	-2.2	0.10	-9.4	0.03
MA-2-G5	-4.8	0.04	-11.2	0.04
MA-2-G7	-2.0	0.11	-9.8	0.01
MA-2-G8	-1.1	0.09	-10.0	0.02
MA-2-G9	-2.7	0.04	-9.4	0.00
MA-2-G11	-1.8	0.00	-9.5	0.00
MA-2-G12	-4.8	0.09	-10.6	0.04
MA-2-G13	-4.2	0.07	-10.7	0.02
MA-2-G15	-4.4	0.10	-10.9	0.02
MA-2-G16	-3.2	0.06	-8.5	0.02
MA-2-G17	-0.9	0.07	-9.6	0.01
MA-2-G18	-2.1	0.03	-9.5	0.04

Table D.3.6: *Oxygen isotope values of meteoric water, calculated using the $\delta^{18}O$ values of the rodent teeth from Marsworth.*

Specimen code	**$\delta^{18}O$ of meteoric water (‰ VSMOW)**	**1σ uncertainty (‰)**
MA-3-J9-T1	-3.77	0.35
MA-3-J10-T1	-6.69	0.20

MA-3-J10-T2	-6.80	0.24
MA-3-J10-T3	-5.31	0.18
MA-3-J10-T6	-6.90	0.16
MA-3-J10-T7	-5.42	0.22
MA-3-J10-T8	-6.57	0.14
MA-3-J10-T9	-7.03	0.21
MA-3-J10-T10	-5.75	0.23
MA-3-J15-T1	-6.90	0.10
MA-3-J16-T1	-5.77	0.13
MA-3-J16-T2	-6.87	0.13
MA-2-L10-T2	-7.85	0.12
MA-2-L10-T4	-6.10	0.30
MA-2-L11-T1	-6.49	0.12
MA-2-K15-T2	-7.58	0.12
MA-2-K15-T3	-7.75	0.11
MA-2-K15-T4	-9.23	0.19
MA-2-K15-T6	-6.93	0.13

Appendix E: Isotope data for Westbury Cave and Gully Cave (Chapter 7)

The following tables list the sample information and isotope data for the rodent teeth from Westbury Cave and Gully Cave.

E.1. Westbury Cave

Table E.1.1: *Summary of the* Microtus *sp(p). upper first molars from Westbury Cave that were selected for isotopic analysis. Rows marked with a dash indicate not applicable. R = right, L = left.*

Stratigraphic Unit	Unit description	Year of collection	Additional comments	Specimen code	Element side
8	Bone gravel	1980	- Sample from the W3 extension	WSM-8-1	R
				WSM-8-2	L
				WSM-8-3	L
				WSM-8-4	R
				WSM-8-5	R
11	Pink Breccia	1978	- Sample group A - Specimens from sample no. 48 - Sample collected from near the top of the unit at the western end of section W2	WSM-11a-1	L
				WSM-11a-2	R
				WSM-11a-3	L
				WSM-11a-4	L
				WSM-11a-5	L
				WSM-11a-6	R
				WSM-11a-7	R
				WSM-11a-8	L
				WSM-11a-9	R
				WSM-11a-10	L
			- Sample group B - Specimens from sample no. 94, a bulk sample of unknown origin within the unit - Sample from section W2	WSM-11b-1	L
				WSM-11b-2	R
				WSM-11b-3	L
				WSM-11b-4	R
				WSM-11b-5	L
12	Dark Brown Breccia	1978	- Specimens from sample no. 72 in Unit 12/2 - Sample collected from the W2 section	WSM-12-1	R
				WSM-12-2	R
				WSM-12-3	L
				WSM-12-4	R

	(or Red Cervid Breccia)			WSM-12-5	L
				WSM-12-6	R
				WSM-12-7	L
				WSM-12-8	R
				WSM-12-9	R
				WSM-12-10	R
13	Lower part of Brown Silt	1979	- Specimens from sample no. 219 in Unit 13/1 - Sample collected from the western end of the unit at section W2/9	WSM-13-1	R
				WSM-13-2	L
				WSM-13-3	L
				WSM-13-4	L
				WSM-13-5	R
				WSM-13-6	R
				WSM-13-7	L
				WSM-13-8	L
				WSM-13-9	L
				WSM-13-10	R
14	Green silty rodent breccia	1978	- Specimens from sample no. 8, collected from Unit 14/1 at the section W9	WSM-14-1	R
				WSM-14-2	R
				WSM-14-3	L
				WSM-14-4	R
				WSM-14-5	R
				WSM-14-6	L
				WSM-14-7	R
				WSM-14-8	R
				WSM-14-9	L
				WSM-14-10	R
	Grey-green layer	1979	- Specimens from bulk sample no. 2 - Sample collected from Unit 14/2 at section W2	WSM-14/2-1	R
				WSM-14/2-2	R
				WSM-14/2-3	R
				WSM-14/2-4	L
				WSM-14/2-5	L
15/3	Light red-brown layer	1979	- Specimens from sample no. 21 - Sample collected from section W2	WSM-15/3-1	R
				WSM-15/3-2	R
				WSM-15/3-3	R
				WSM-15/3-4	R
15/2	Mole layer	1979	- Specimens from sample no. 97 - Sample collected from section W2/9	WSM-15/2-1	R
				WSM-15/2-2	L
				WSM-15/2-3	R
				WSM-15/2-4	L
				WSM-15/2-5	R
				WSM-15/2-6	L
				WSM-15/2-7	L
				WSM-15/2-8	L
15/5	Brown weathered horizon	1979	- Specimens from sample no. 12	WSM-15/5-1	R
				WSM-15/5-2	L
				WSM-15/5-3	L

			- Sample collected from section W2	WSM-15/5-4	L
				WSM-15/5-5	R
				WSM-15/5-6	R
15/8	Rodent Earth (or Rodent Bed II)	1977	- Specimens from sample no. 43 - Sample collected from section W2	WSM-15/8-1	L
				WSM-15/8-2	R
				WSM-15/8-3	R
				WSM-15/8-4	R
				WSM-15/8-5	L
				WSM-15/8-6	R
				WSM-15/8-7	R
				WSM-15/8-8	R
				WSM-15/8-9	L
				WSM-15/8-10	R
				WSM-15/8-11	R
				WSM-15/8-12	L
18	Grey silty breccia	1980	- Specimens from sample no. 318, collected from Unit 18/6 in section W5	WSM-18/6-1	L
				WSM-18/6-2	R
				WSM-18/6-3	L
	Brown breccia with pink silty matrix	1980	- Sample group A - Specimens from sample no. 134 in section W10 - Sample probably from Unit 18/4	WSM-18a-1	R
				WSM-18a-2	L
				WSM-18a-3	L
	Cobble bed with pink matrix	1980	- Sample group B - Specimens from sample no. 130 - Sample probably from Unit 18/4	WSM-18b-1	R
				WSM-18b-2	L
				WSM-18b-3	R
19/14	Rodent Breccia (or Rodent Bed III)	1977	- Sample group A - Specimens from sample no. 165**,** collected from section W5	WSM-19/14a-1	R
				WSM-19/14a-2	R
				WSM-19/14a-3	L
				WSM-19/14a-4	L
				WSM-19/14a-5	L
		1977	- Sample group B - Specimens from sample no. 176, collected from section W5	WSM-19/14b-1	L
				WSM-19/14b-2	R
				WSM-19/14b-3	L
				WSM-19/14b-4	L
				WSM-19/14b-5	R
19/15	Lower Yellow Silty Breccia	1980	- Sample group A - Specimens from sample no. 44, collected from section W5	WSM-19/15a-1	R
				WSM-19/15a-2	R
				WSM-19/15a-3	L
	Lower Yellow Breccia	1980	- Sample group B - Specimens from sample no. 312, collected from section W5	WSM-19/15b-1	L
				WSM-19/15b-2	L
				WSM-19/15b-3	L

Table E.1.2: *Oxygen and carbon isotope results for the* Microtus *sp(p). upper first molars from Westbury Cave. RHUL = sample analysed in the Department of Earth Sciences, Royal Holloway University of London; BEIF = sample analysed at Bloomsbury Environmental Isotope Facility. Results that are highlighted in red are outliers, or are considered unreliable due to the small size of the sample.*

Specimen number	Lab	$\delta^{18}O$ (‰ VPDB)		$\delta^{13}C$ (‰ VPDB)	
		Value	1σ uncertainty	Value	1σ uncertainty
WSM-8-1	RHUL	-8.3	0.06	-10.6	0.08
WSM-8-2	RHUL	-3.9	0.14	-10.4	0.11
WSM-8-3	RHUL	-7.0	0.01	-10.5	0.03
WSM-8-4	RHUL	-7.9	0.09	-11.2	0.08
WSM-8-5	RHUL	-7.8	0.10	-11.2	0.10
WSM-11a-1	RHUL	-6.9	0.10	-9.3	0.03
WSM-11a-2	RHUL	-6.5	0.12	-10.6	0.02
WSM-11a-3	RHUL	-8.8	0.09	-10.3	0.04
WSM-11a-4	RHUL	-8.7	0.09	-10.3	0.10
WSM-11a-5	RHUL	-10.6	0.11	-12.0	0.08
WSM-11a-6	RHUL	-7.3	0.04	-10.6	0.06
WSM-11a-7	RHUL	-7.3	0.10	-10.5	0.02
WSM-11a-8	RHUL	-7.7	0.04	-11.4	0.08
WSM-11a-9	RHUL	-7.4	0.10	-11.4	0.01
WSM-11a-10	RHUL	-6.0	0.12	-10.4	0.02
WSM-11b-1	RHUL	-7.1	0.05	-11.6	0.04
WSM-11b-2	RHUL	-7.2	0.09	-11.9	0.04
WSM-11b-3	RHUL	-7.1	0.00	-11.8	0.01
WSM-11b-4	RHUL	-7.1	0.02	-10.7	0.00
WSM-11b-5	RHUL	-8.6	0.09	-11.5	0.01
WSM-12-1	RHUL	-9.0	0.04	-11.6	0.01
WSM-12-2	RHUL	-6.4	0.05	-9.7	0.02
WSM-12-3	RHUL	-5.5	0.07	-10.9	0.04
WSM-12-4	RHUL	-8.5	0.13	-12.0	0.07
WSM-12-5	RHUL	-6.5	0.03	-10.6	0.05
WSM-12-6	Sample lost during analysis				
WSM-12-7	Sample lost during analysis				
WSM-12-8	RHUL	-8.2	0.10	-8.5	0.01
WSM-12-9	RHUL	-6.5	0.09	-10.4	0.02
WSM-12-10	Sample lost during analysis				
WSM-13-1	RHUL	-7.0	0.10	-10.6	0.01
WSM-13-2	RHUL	-6.2	0.02	-10.5	0.02
WSM-13-3	RHUL	-6.1	0.05	-9.6	0.02
WSM-13-4	RHUL	-5.8	0.00	-10.5	0.07
WSM-13-5	RHUL	-8.1	0.03	-10.9	0.02

WSM-13-6	RHUL	-7.2	0.04	-9.7	0.00
WSM-13-7	RHUL	-6.7	0.02	-10.3	0.02
WSM-13-8	RHUL	-6.9	0.10	-10.2	0.07
WSM-13-9	RHUL	-7.6	0.07	-10.3	0.07
WSM-13-10	RHUL	-6.4	0.05	-10.1	0.02
WSM-14-1	RHUL	-7.7	0.08	-11.8	0.03
WSM-14-2	RHUL	-8.4	0.06	-11.3	0.06
WSM-14-3	RHUL	-7.9	0.03	-11.1	0.00
WSM-14-4	RHUL	-7.9	0.11	-11.5	0.05
WSM-14-5	RHUL	-8.7	0.04	-12.3	0.10
WSM-14-6	RHUL	-9.0	0.03	-11.3	0.05
WSM-14-7	RHUL	-8.7	0.00	-12.2	0.04
WSM-14-8	RHUL	-7.6	0.04	-11.8	0.03
WSM-14-9	RHUL	-7.8	0.02	-11.9	0.03
WSM-14-10	RHUL	-7.5	0.09	-12.1	0.02
WSM-14/2-1	RHUL	-11.2	0.11	-13.9	0.04
WSM-14/2-2	RHUL	-7.7	0.10	-12.4	0.04
WSM-14/2-3	RHUL	-9.0	0.12	-11.8	0.08
WSM-14/2-4	RHUL	-7.7	0.02	-11.5	0.01
WSM-14/2-5	RHUL	-6.9	0.05	-11.5	0.06
WSM-15/3-1	RHUL	-6.3	0.05	-11.7	0.05
WSM-15/3-2	RHUL	-7.7	0.03	-12.1	0.01
WSM-15/3-3	RHUL	-8.0	0.03	-12.4	0.08
WSM-15/3-4	RHUL	-8.7	0.07	-11.8	0.01
WSM-15/2-1	RHUL	-4.8	0.04	-10.7	0.00
WSM-15/2-2	RHUL	-3.0	0.02	-10.6	0.02
WSM-15/2-3	BEIF	-4.6	0.10	-10.6	0.03
WSM-15/2-4	BEIF	-5.2	0.10	-11.6	0.03
WSM-15/2-5	BEIF	-4.4	0.10	-10.5	0.03
WSM-15/2-6	BEIF	-4.8	0.10	-11.0	0.03
WSM-15/2-7	BEIF	-3.8	0.10	-10.5	0.03
WSM-15/2-8	Sample lost during analysis				
WSM-15/5-1	BEIF	-6.5	0.10	-11.5	0.03
WSM-15/5-2	BEIF	-6.6	0.10	-11.5	0.03
WSM-15/5-3	BEIF	-5.3	0.10	-10.7	0.03
WSM-15/5-4	BEIF	-5.5	0.10	-10.4	0.03
WSM-15/5-5	Sample lost during analysis				
WSM-15/5-6	BEIF	-4.6	0.10	-10.5	0.03
WSM-15/8-1	BEIF	-6.5	0.10	-12.2	0.03
WSM-15/8-2	BEIF	-2.2	0.10	-12.0	0.03
WSM-15/8-3	Not analysed – insufficient material				
WSM-15/8-4	BEIF	-7.7	0.10	-12.5	0.03
WSM-15/8-5	Not analysed – insufficient material				
WSM-15/8-6	BEIF	-5.3	0.10	-12.7	0.03
WSM-15/8-7	RHUL	-13.0	0.19	-13.0	0.19
WSM-15/8-8	RHUL	-12.2	0.11	-14.4	0.11

WSM-15/8-9	RHUL	-8.2	0.16	-12.3	0.06
WSM-15/8-10	RHUL	-6.8	0.09	-13.0	0.06
WSM-15/8-11	RHUL	-5.8	0.12	-11.9	0.07
WSM-15/8-12	RHUL	-9.1	0.14	-12.6	0.08
WSM-18/6-1	RHUL	-6.0	0.03	-10.0	0.06
WSM-18/6-2	RHUL	-6.9	0.05	-10.9	0.02
WSM-18/6-3	RHUL	-5.4	0.02	-10.1	0.00
WSM-18a-1	RHUL	-8.3	0.12	-10.3	0.02
WSM-18a-2	RHUL	-6.1	0.03	-10.0	0.05
WSM-18a-3	RHUL	-5.9	0.08	-9.8	0.08
WSM-18b-1	RHUL	-4.2	0.11	-9.1	0.07
WSM-18b-2	RHUL	-6.4	0.10	-10.6	0.02
WSM-18b-3	RHUL	-5.2	0.09	-9.5	0.04
WSM-19/14a-1	RHUL	-6.4	0.00	-11.3	0.05
WSM-19/14a-2	RHUL	-6.0	0.02	-9.8	0.05
WSM-19/14a-3	RHUL	-4.9	0.01	-10.7	0.05
WSM-19/14a-4	RHUL	-6.9	0.01	-10.7	0.02
WSM-19/14a-5	RHUL	-7.5	0.10	-11.8	0.05
WSM-19/14b-1	RHUL	-7.6	0.00	-10.2	0.06
WSM-19/14b-2	RHUL	-8.7	0.02	-11.8	0.01
WSM-19/14b-3	RHUL	-7.5	0.05	-10.9	0.00
WSM-19/14b-4	RHUL	-7.2	0.01	-11.9	0.05
WSM-19/14b-5	RHUL	-4.5	0.04	-10.3	0.05
WSM-19/15a-1	RHUL	-5.5	0.05	-9.6	0.02
WSM-19/15a-2	RHUL	-10.4	0.27	-9.8	0.15
WSM-19/15a-3	RHUL	-6.6	0.05	-10.6	0.02
WSM-19/15b-1	RHUL	-7.4	0.09	-11.5	0.05
WSM-19/15b-2	RHUL	-5.5	0.03	-10.9	0.03
WSM-19/15b-3	RHUL	-6.6	0.02	-11.0	0.03

Table E.1.3: *Mean oxygen isotope values of meteoric water, calculated using the $\delta^{18}O$ values of the* Microtus *sp(p). teeth from Westbury Cave.*

Stratigraphic Unit	$\delta^{18}O$ of meteoric water (‰ VSMOW)	1σ standard deviation uncertainty
8	-6.85	0.50
11	-6.59	0.68
12	-6.46	1.05
13	-6.12	0.63
14	-7.08	0.53
15/3	-6.80	0.83
15/2	-4.27	0.78
15/5	-5.27	0.78
15/8	-6.32	1.10
18	-5.56	0.98
19	-5.96	0.95

E.2. Gully Cave

Table E.2.1: *Oxygen and carbon isotope data for the* Arvicola terrestris *incisors from Gully Cave (from Peneycad, 2013). The samples are listed in order of age (youngest to oldest).*

Specimen number	Grid square	Depth relative to datum (cm)	$\delta^{18}O$ (‰ VPDB)		$\delta^{13}C$ (‰ VPDB)	
			Value	1σ uncertainty	Value	1σ uncertainty
GC-7a	G3	-40 to -50	-8.8	0.03	-6.2	0.03
GC-7b			-8.5	0.11	-6.7	0.03
GC-8	G3	-50 to -60	-9.5	0.02	-10.4	0.03
GC-1a	G0	+30 to +20	-7.7	0.07	-8.8	0.03
GC-1b			-8.7	0.02	-8.6	0.01
GC-2	F0	+20 to +10	-7.9	0.03	-7.7	0.02
GC-9	G3	-70 to -100	-10.2	0.09	-6.6	0.03
GC-5	G2	-40	-8.7	0.02	-7.2	0.06
GC-12	G3	-120 to -130	-13.3	0.02	-7.4	0.01
GC-3	G0	-20 to -30	-10.2	0.00	-6.7	0.06
GC-4	F2	-33 to -50	-9.3	0.00	-7.8	0.08
GC-6a	G0	-40 to -60	-8.4	0.05	-7.7	0.05
GC-6b			-11.7	0.04	-7.2	0.04
GC-10	E2	-115 to -125	-8.3	0.00	-7.7	0.02
GC-11	F2	-120 to -130	-8.0	0.02	-7.9	0.01

Table E.2.2: *Oxygen isotope values of meteoric water, calculated from the $\delta^{18}O$ values of the* Arvicola terrestris *incisors from Gully Cave.*

Climatic interval		Specimen numbers	Mean $\delta^{18}O$ of meteoric water (‰ VSMOW)	1σ standard deviation uncertainty (‰)
Holocene		1a, 1b, 2, 5, 7a, 7b, 8, 9	-7.61	0.71
Loch Lomond Stadial	Late	3, 4, 12	-9.30	1.83
	Early	6a, 6b	-8.60	1.97
Lateglacial Interstadial		10, 11	-7.13	0.24

Table E.2.3: *Summary of the* Microtus *sp(p). upper molars from Gully Cave that were selected for isotopic analysis. The samples are listed in order of age (youngest to oldest).*

Specimen number	Grid square	Depth relative to datum (cm)	Element side
GCEG-1-1	G4	-60 to -100	L
GCEG-1-2			R
GCEG-1-3			L
GCEG-1-4			R
GCEG-1-5			L
GCEG-2-1	G4	-140 to -150	L
GCEG-2-2			R
GCEG-2-3			R
GCEG-2-4			L
GCEG-2-5			R
GCEG-3-1	G3	-110 to -120	R
GCEG-3-2			L
GCEG-3-3			R
GCEG-3-4			R
GCEG-3-5			R
GCEG-4-1	G3	-120 to -130	R
GCEG-4-2			L
GCEG-4-3			L
GCEG-4-4			L
GCEG-4-5			L
GCEG-6-1	F0	-10 to -20	L
GCEG-6-3			L

GCEG-6-4			L
GCEG-6-5			L
GCEG-7-1	F0	-20 to -30	L
GCEG-7-2			L
GCEG-7-3			L
GCEG-7-4			L
GCEG-7-5			L
GCEG-5-1	G3	-130 to -140	R
GCEG-5-2			L
GCEG-5-3			L
GCEG-5-4			L
GCEG-5-5			L
GCEG-8-1	F0	-30 to -40	L
GCEG-8-2			L
GCEG-8-3			L
GCEG-8-4			L
GCEG-8-5			L
GCEG-9-1	F0	-40 to -50	L
GCEG-9-2			R
GCEG-9-3			R
GCEG-9-4			L
GCEG-9-5			L
GCEG-10-1	F0	-50 to -60	L
GCEG-10-2			L
GCEG-10-3			R
GCEG-10-4			R
GCEG-10-5			L
GCEG-11-1	F0	-60 to -70	R
GCEG-11-2			R
GCEG-11-3			L
GCEG-11-4			L
GCEG-11-5			L
GCEG-12-1	F0	-70 to -80	R
GCEG-12-2			L
GCEG-12-3			L
GCEG-12-4			R
GCEG-12-5			R
GCEG-13-1	F0	-80 to -90	L
GCEG-13-2			R
GCEG-13-3			L
GCEG-13-4			L
GCEG-13-5			L
GCEG-14-1	F2	-140 to -150	L
GCEG-14-2			L
GCEG-14-3			R
GCEG-14-4			R

GCEG-14-5			L
GCEG-15-1	F2	-150 to -160	L
GCEG-15-2			R
GCEG-15-3			R
GCEG-15-4			R
GCEG-15-5			R
GCEG-16-1	D3	-175 to -215	L
GCEG-16-2			R
GCEG-16-3			L
GCEG-16-4			L
GCEG-16-5			L

Table E.2.4: *Oxygen and carbon isotope results for the* Microtus *sp(p). upper molars from Gully Cave.*

Specimen number	$\delta^{18}O$ (‰ VPDB)		$\delta^{13}C$ (‰ VPDB)	
	Value	1σ uncertainty	Value	1σ uncertainty
GCEG-1-1	-3.7	0.03	-10.7	0.02
GCEG-1-2	-2.0	0.03	-8.4	0.02
GCEG-1-3	-6.8	0.12	-11.6	0.32
GCEG-1-4	Not analysed – insufficient material			
GCEG-1-5	-4.9	0.03	-10.3	0.02
GCEG-2-1	-0.1	0.03	-9.2	0.02
GCEG-2-2	-3.9	0.03	-8.3	0.02
GCEG-2-3	-5.3	0.03	-10.5	0.02
GCEG-2-4	-3.0	0.10	-7.4	0.02
GCEG-2-5	-3.2	0.14	-9.4	0.04
GCEG-3-1	-3.9	0.10	-10.1	0.02
GCEG-3-2	-4.2	0.24	-10.5	0.09
GCEG-3-3	-3.4	0.48	-9.9	0.24
GCEG-3-4	-1.1	0.51	-9.5	0.10
GCEG-3-5	-6.3	0.14	-11.6	0.04
GCEG-4-1	-2.2	0.05	-8.4	0.05
GCEG-4-2	-2.1	0.04	-8.6	0.19
GCEG-4-3	-6.1	0.14	-10.3	0.04
GCEG-4-4	-2.3	0.04	-9.0	0.09
GCEG-4-5	-3.4	0.22	-10.0	0.28
GCEG-6-1	-4.4	0.11	-10.8	0.27
GCEG-6-3	Not analysed – insufficient material			
GCEG-6-4	-7.2	0.02	-10.9	0.11
GCEG-6-5	-6.6	0.22	-10.0	0.18
GCEG-7-1	-6.8	0.04	-10.7	0.10

GCEG-7-2	-5.4	0.30	-10.7	0.08
GCEG-7-3	-7.6	0.01	-10.6	0.19
GCEG-7-4	-8.4	0.11	-10.8	0.22
GCEG-7-5	-7.83	0.14	-11.17	0.04
GCEG-5-1	-3.8	0.17	-7.9	0.09
GCEG-5-2	-4.2	0.09	-10.3	0.20
GCEG-5-3	-1.2	0.19	-8.4	0.25
GCEG-5-4	-6.3	0.10	-9.3	0.02
GCEG-5-5	-6.0	0.16	-10.1	0.06
GCEG-8-1	-6.0	0.14	-9.9	0.04
GCEG-8-2	-3.5	0.14	-10.1	0.04
GCEG-8-3	-7.7	0.14	-9.6	0.04
GCEG-8-4	-4.0	0.33	-9.8	0.02
GCEG-8-5	-3.1	0.14	-9.7	0.04
GCEG-9-1	-6.7	0.14	-9.5	0.04
GCEG-9-2	-4.5	0.14	-10.4	0.04
GCEG-9-3	-6.7	0.09	-10.3	0.08
GCEG-9-4	-2.6	0.14	-10.2	0.04
GCEG-9-5	-5.7	0.14	-10.1	0.04
GCEG-10-1	-4.7	0.14	-11.7	0.04
GCEG-10-2	-2.5	0.14	-9.7	0.04
GCEG-10-3	-5.2	0.14	-10.7	0.04
GCEG-10-4	-2.8	0.38	-9.5	0.02
GCEG-10-5	-5.2	0.14	-10.9	0.04
GCEG-11-1	-6.2	0.14	-11.1	0.04
GCEG-11-2	-6.7	0.14	-9.7	0.04
GCEG-11-3	-2.9	0.14	-9.9	0.04
GCEG-11-4	-6.1	0.14	-7.9	0.04
GCEG-11-5	-5.8	0.14	-8.6	0.04
GCEG-12-1	-4.9	0.14	-7.4	0.04
GCEG-12-2	-2.7	0.26	-9.5	0.21
GCEG-12-3	-5.6	0.14	-10.3	0.04
GCEG-12-4	-5.1	0.14	-7.3	0.04
GCEG-12-5	-6.6	0.14	-9.4	0.04
GCEG-13-1	0.3	0.21	-9.4	0.05
GCEG-13-2	-6.0	0.14	-9.9	0.04
GCEG-13-3	Not analysed – insufficient material			
GCEG-13-4	-4.1	0.14	-9.2	0.04
GCEG-13-5	-1.4	0.14	-9.9	0.04
GCEG-14-1	-2.1	0.14	-8.9	0.04
GCEG-14-2	1.3	0.14	-8.6	0.04
GCEG-14-3	0.2	0.14	-9.2	0.04
GCEG-14-4	-0.8	0.12	-9.5	0.09
GCEG-14-5	-2.1	0.14	-10.4	0.04
GCEG-15-1	0.9	0.14	-9.0	0.04
GCEG-15-2	-2.7	0.14	-9.9	0.04

GCEG-15-3	-1.7	0.14	-9.2	0.04
GCEG-15-4	-2.2	0.40	-9.8	0.17
GCEG-15-5	-2.2	0.14	-9.5	0.04
GCEG-16-1	-0.3	0.14	-8.6	0.04
GCEG-16-2	-3.1	0.14	-10.7	0.04
GCEG-16-3	-1.8	0.14	-9.2	0.04
GCEG-16-4	-5.9	0.14	-7.6	0.04
GCEG-16-5	-4.8	0.14	-9.4	0.04

Table E.2.5: *Average oxygen isotope values of meteoric water, calculated from the* $\delta^{18}O$ *values of the* Microtus *sp(p). teeth from Gully Cave.*

Mean calibrated date (cal yr BP)	**Dating error (yr)**	**Sample group numbers**	**$\delta^{18}O$ of meteoric water (‰ VSMOW)**	**1σ standard deviation uncertainty (‰)**
10270	153	1	-4.26	1.75
11307	99	2	-3.29	1.63
11771	150	3-4	-3.60	1.55
12065	179	6-7	-6.12	1.23
12223	188	5	-4.23	1.76
12420	178	8-9	-4.78	1.59
13294	127	10	-4.05	1.18
13561	179	11-12	-4.95	1.34
13829	179	13	-3.08	2.31
14110	206	14-15	-1.80	1.37
14419	310	16	-3.35	1.90

Appendix F: Isotope data for Longstone Edge and Danebury and modelled $\delta^{13}C$ values of C_3 plants (Chapter 8)

The following tables list the oxygen and carbon isotope data for Longstone Edge and Danebury, the modelled $\delta^{13}C$ values of C_3 plants for the past 14,500 years, and the calculated $\delta^{13}C$ values of rodent diet for all study sites.

F.1. Data for Longstone Edge and Danebury

Table F.1.1. *Specimen information and isotope data for the upper first molars and mandibular teeth from Longstone Edge. M^1 = upper first molar, M_1 = lower first molar, M_2 = lower second molar, M_3 = lower third molar, I = lower incisor.*

Specimen code	Species	Tooth type	$\delta^{18}O$ (‰ VPDB)		$\delta^{13}C$ (‰ VPDB)	
			Value	1σ uncertainty	Value	1σ uncertainty
LE-Ma-1	*Microtus agrestis*	Right M^1	-6.4	0.10	-9.5	0.04
LE-Ma-2			-7.6	0.10	-10.3	0.04
LE-Ma-3			-7.3	0.10	-10.3	0.04
LE-Ma-4			-6.5	0.10	-11.0	0.04
LE-Ma-5			-7.0	0.10	-11.3	0.04
LE-Ma-6			-6.9	0.10	-11.4	0.04
LE-Ma-7			-5.8	0.10	-8.3	0.04
LE-Ma-8			-5.4	0.10	-9.6	0.04
LE-Ma-9			-5.3	0.10	-9.6	0.04
LE-Ma-10			-4.4	0.10	-9.2	0.04
LE-At-1	*Arvicola terrestris*	Right M^1	-6.6	0.10	-9.2	0.04
LE-At-2			-7.1	0.10	-9.9	0.04
LE-At-3			-7.2	0.10	-10.0	0.04
LE-At-4			-7.5	0.10	-8.7	0.04
LE-At-5			-8.8	0.10	-10.8	0.04
LE-At-6			-8.0	0.10	-9.2	0.04
LE-At-7			-7.9	0.10	-11.1	0.04
LE-At-8			-6.5	0.10	-9.6	0.04
LE-At-9			-7.7	0.10	-9.6	0.04
LE-At-10			-7.0	0.10	-10.6	0.04
LE-At-MA1-RM1	*Arvicola terrestris*	Right M_1	-4.5	0.10	-10.5	0.04
LE-At-MA1-RM2		Right M_2	-4.4	0.10	-10.8	0.04
LE-At-MA1-RI		Right I	-4.5	0.10	-9.1	0.04

LE-At-MA2-LM1		Left M_1	-6.5	0.10	-10.4	0.04
LE-At-MA2-LM2		Left M_2	-6.6	0.10	-10.5	0.04
LE-At-MA2-LI		Left I	-5.7	0.10	-9.4	0.04
LE-At-MA3-RI		Right I	-5.7	0.10	-9.3	0.04

Table F.1.2. *Specimen information and isotope data for the upper left first molars from Danebury.*

Specimen number	**Pit number**	**$\delta^{18}O$ (‰ VPDB)**		**$\delta^{13}C$ (‰ VPDB)**	
		Value	**1σ error**	**Value**	**1σ error**
DA-923-1	923	-3.9	0.10	-11.2	0.04
DA-923-2		-4.7	0.10	-12.5	0.04
DA-923-3		-4.0	0.10	-12.1	0.04
DA-923-4		-3.8	0.10	-12.1	0.04
DA-923-5		-4.1	0.10	-12.3	0.04
DA-955-1	955	-5.9	0.10	-13.7	0.04
DA-955-2		-5.8	0.10	-13.3	0.04
DA-955-3		-5.1	0.10	-13.8	0.04
DA-955-4		-4.1	0.10	-12.7	0.04
DA-955-5		-4.3	0.10	-13.8	0.04

F.2. Carbon isotope adjustments for geographical variability

Table F.2.1: *Calculated adjustment factors for the tooth $\delta^{13}C$ data from the modern and Late Holocene study sites, and Gully Cave. The adjustments are for a latitude of 51.2°, altitude of 100 m above sea level and mean annual precipitation of 800 mm/yr. Lat. = latitude, Alt. = altitude, MAP = mean annual precipitation.*

Study site	**Modern geographical characteristics of site**			**Adjustments (‰)**			**Total adjustment (‰)**
	Lat.	Alt.	MAP	Lat.	Alt.	MAP	
West Horrington	51.22	159	814	0.000	-0.011	0.031	0.02
Cobham	51.32	22	657	0.001	0.015	-0.339	-0.32
Beeford	53.98	9	621	0.034	0.017	-0.432	-0.38
Perth A	56.43	33	722	0.065	0.013	-0.179	-0.10
Perth B	56.47	103	722	0.065	-0.001	-0.179	-0.11
Danebury	51.14	126	779	-0.001	-0.005	-0.047	-0.05
Longstone Edge	53.30	349	835	0.026	-0.047	0.076	0.05
Gully Cave	51.23	134	900	0.000	-0.006	0.212	0.21

F.3. Modelled $\delta^{13}C$ values of C_3 plants

Table F.3.1: *Carbon isotope values of C_3 plants for the past 14,500 years, estimated using the SJ-2012 and Voelker-2016a models. The data for the $\delta^{13}C$ value of atmospheric CO_2 ($\delta^{13}C_a$) and partial pressure of atmospheric CO_2 (pCO_2), which were used to calculate the $\delta^{13}C$ values of C_3 plants, are also shown. The pCO_2 data originate from: NOAA (2018) (for -65 to -68 yr BP), Rubino et al. (2013) (for -51 to 1796 yr BP), and Monnin et al. (2004) (for 1830 to 14532 yr BP). The $\delta^{13}C_a$ data originate from: Graven et al. (2017) (for -65 to 100 yr BP), Rubino et al. (2013) (for 100 to 1796 yr BP), and Eggleston et al. (2016) (for 1830 to 14532 yr BP).*

Age (yr BP)	pCO_2 (ppm)		$\delta^{13}C_a$ (‰)		$\delta^{13}C$ of C_3 plants (‰): SJ-2012			$\delta^{13}C$ of C_3 plants (‰): Voelker-2016a	
	Value	Error	Value	Error	Average value	Error	Maximum value	Average value	Error
-68	408	0.10	-8.50	0.02	-29.43	1.62	-24.03	-31.43	1.64
-66	402.81	0.10	-8.46	0.02	-29.33	1.64	-23.93	-31.36	1.64
-65	399.41	0.10	-8.44	0.02	-29.27	1.64	-23.87	-31.31	1.64
-51	368.02	0.05	-8.07	0.02	-28.52	1.64	-23.12	-30.71	1.64
-48	361.78	0.37	-8.03	0.02	-28.40	1.63	-23.00	-30.62	1.64
-46	359.65	0.09	-7.95	0.02	-28.29	1.64	-22.89	-30.53	1.64
-44	357.11	0.26	-7.88	0.02	-28.19	1.64	-22.79	-30.44	1.64
-43	353.95	0.03	-7.85	0.02	-28.12	1.64	-22.72	-30.38	1.64
-42	353.72	0.33	-7.85	0.04	-28.11	1.65	-22.71	-30.38	1.66
-41	352.22	0.10	-7.86	0.02	-28.10	1.64	-22.70	-30.38	1.64
-40	350.81	0.28	-7.86	0.02	-28.08	1.64	-22.68	-30.37	1.64
-39	349.63	0.15	-7.84	0.03	-28.05	1.65	-22.65	-30.34	1.65
-38	347.60	0.40	-7.80	0.02	-27.98	1.63	-22.58	-30.29	1.64
-37	344.86	0.03	-7.75	0.02	-27.89	1.64	-22.49	-30.22	1.64
-36	343.46	0.03	-7.72	0.02	-27.84	1.64	-22.44	-30.18	1.64

-35	342.05	0.50	-7.71	0.02	-27.81	1.63	-22.41	-30.16	1.64
-33	340.71	0.22	-7.68	0.04	-27.76	1.66	-22.36	-30.12	1.66
-29	334.85	0.65	-7.56	0.02	-27.56	1.63	-22.16	-29.95	1.64
-27	333.96	0.63	-7.54	0.02	-27.53	1.63	-22.13	-29.93	1.64
-26	332.37	0.04	-7.49	0.02	-27.46	1.64	-22.06	-29.86	1.64
-24	331.55	0.63	-7.40	0.02	-27.36	1.63	-21.96	-29.77	1.64
-22	329.38	0.63	-7.35	0.02	-27.27	1.63	-21.87	-29.70	1.64
-21	325.43	1.34	-7.33	0.03	-27.19	1.63	-21.79	-29.65	1.66
-20	324.56	0.63	-7.32	0.02	-27.17	1.63	-21.77	-29.64	1.64
-19	323.79	0.63	-7.31	0.02	-27.15	1.63	-21.75	-29.62	1.64
-17	321.33	1.16	-7.29	0.02	-27.09	1.62	-21.69	-29.58	1.65
-16	320.98	1.74	-7.26	0.02	-27.06	1.61	-21.66	-29.55	1.65
-15	319.54	0.95	-7.23	0.02	-27.00	1.62	-21.60	-29.51	1.65
-14	319.12	0.94	-7.19	0.02	-26.96	1.62	-21.56	-29.47	1.65
-13	318.43	0.63	-7.15	0.02	-26.91	1.63	-21.51	-29.42	1.64
-12	317.75	0.63	-7.11	0.02	-26.86	1.63	-21.46	-29.38	1.64
-11	318.21	1.72	-7.08	0.02	-26.84	1.61	-21.44	-29.35	1.65
-10	313.09	1.81	-7.06	0.02	-26.73	1.61	-21.33	-29.29	1.65
-9	314.16	1.81	-7.04	0.02	-26.73	1.61	-21.33	-29.28	1.65
-8	315.34	1.72	-7.02	0.02	-26.73	1.61	-21.33	-29.27	1.65
-7	315.64	1.16	-7.01	0.03	-26.73	1.63	-21.33	-29.26	1.66
-6	315.34	0.64	-7.00	0.02	-26.71	1.63	-21.31	-29.25	1.64
-5	314.71	2.21	-7.00	0.02	-26.70	1.60	-21.30	-29.24	1.66
-4	312.60	0.63	-6.99	0.02	-26.66	1.63	-21.26	-29.22	1.64
-2	312.18	0.41	-6.98	0.02	-26.64	1.63	-21.24	-29.20	1.64
0	312.83	0.64	-6.98	0.02	-26.65	1.63	-21.25	-29.21	1.64
1	309.69	0.41	-6.98	0.02	-26.60	1.63	-21.20	-29.19	1.64
2	311.57	2.21	-6.98	0.02	-26.63	1.60	-21.23	-29.20	1.66
3	312.03	0.63	-6.98	0.02	-26.64	1.63	-21.24	-29.20	1.64
4	312.26	2.21	-6.98	0.02	-26.64	1.60	-21.24	-29.20	1.66
5	310.94	3.12	-6.98	0.02	-26.62	1.59	-21.22	-29.19	1.66

6	312.36	2.21	-6.97	0.02	-26.63	1.60	-21.23	-29.20	1.66
8	312.37	2.21	-6.96	0.02	-26.62	1.60	-21.22	-29.19	1.66
9	309.77	2.21	-6.96	0.02	-26.58	1.60	-21.18	-29.17	1.66
10	310.38	0.64	-6.95	0.02	-26.58	1.63	-21.18	-29.16	1.64
11	310.83	0.63	-6.94	0.02	-26.58	1.63	-21.18	-29.15	1.64
12	311.74	0.64	-6.93	0.03	-26.58	1.64	-21.18	-29.15	1.65
13	307.41	1.16	-6.93	0.02	-26.51	1.62	-21.11	-29.12	1.65
14	308.65	3.18	-6.93	0.02	-26.53	1.59	-21.13	-29.13	1.66
15	306.32	1.16	-6.92	0.02	-26.48	1.62	-21.08	-29.10	1.65
16	307.71	0.63	-6.91	0.02	-26.50	1.63	-21.10	-29.10	1.64
17	307.11	1.16	-6.90	0.02	-26.48	1.62	-21.08	-29.09	1.65
18	308.26	0.63	-6.89	0.02	-26.49	1.63	-21.09	-29.08	1.64
19	305.74	1.74	-6.89	0.02	-26.45	1.61	-21.05	-29.07	1.65
21	305.47	0.05	-6.87	0.03	-26.42	1.65	-21.02	-29.04	1.65
22	307.24	0.64	-6.86	0.02	-26.44	1.63	-21.04	-29.05	1.64
25	304.88	0.63	-6.86	0.02	-26.40	1.63	-21.00	-29.03	1.64
27	305.60	3.18	-6.86	0.02	-26.41	1.59	-21.01	-29.04	1.66
30	301.88	1.16	-6.87	0.02	-26.36	1.62	-20.96	-29.02	1.65
31	304.61	2.21	-6.87	0.02	-26.41	1.60	-21.01	-29.04	1.66
32	303.85	0.67	-6.87	0.02	-26.39	1.63	-20.99	-29.03	1.64
34	301.92	0.63	-6.87	0.02	-26.36	1.63	-20.96	-29.02	1.64
36	300.70	2.21	-6.86	0.02	-26.33	1.60	-20.93	-29.00	1.66
37	301.30	0.63	-6.85	0.02	-26.33	1.63	-20.93	-28.99	1.64
39	298.36	1.72	-6.84	0.02	-26.27	1.61	-20.87	-28.96	1.65
40	297.87	1.16	-6.83	0.02	-26.25	1.62	-20.85	-28.95	1.65
41	301.50	2.21	-6.82	0.02	-26.31	1.60	-20.91	-28.96	1.66
44	298.48	0.64	-6.79	0.02	-26.22	1.63	-20.82	-28.91	1.64
45	299.02	0.63	-6.78	0.02	-26.22	1.63	-20.82	-28.91	1.64
46	295.99	0.94	-6.76	0.02	-26.15	1.62	-20.75	-28.86	1.65
48	295.61	2.01	-6.75	0.02	-26.13	1.60	-20.73	-28.85	1.65
50	294.22	1.16	-6.73	0.02	-26.09	1.62	-20.69	-28.82	1.65

51	296.16	2.21	-6.73	0.02	-26.12	1.60	-20.72	-28.84	1.66
56	293.49	0.94	-6.72	0.02	-26.07	1.62	-20.67	-28.81	1.65
57	295.09	0.64	-6.72	0.02	-26.10	1.63	-20.70	-28.82	1.64
58	295.17	0.63	-6.72	0.02	-26.10	1.63	-20.70	-28.82	1.64
60	290.92	1.16	-6.71	0.02	-26.01	1.62	-20.61	-28.78	1.65
61	292.34	0.94	-6.71	0.02	-26.04	1.62	-20.64	-28.79	1.65
63	294.34	0.63	-6.71	0.02	-26.07	1.63	-20.67	-28.80	1.64
64	288.12	2.01	-6.70	0.02	-25.95	1.60	-20.55	-28.75	1.65
66	289.49	0.62	-6.70	0.02	-25.98	1.63	-20.58	-28.76	1.64
67	292.46	0.95	-6.69	0.02	-26.02	1.62	-20.62	-28.77	1.65
70	287.77	1.16	-6.69	0.02	-25.94	1.62	-20.54	-28.73	1.65
73	289.33	0.63	-6.68	0.02	-25.95	1.63	-20.55	-28.73	1.64
76	291.56	2.21	-6.67	0.02	-25.98	1.60	-20.58	-28.74	1.66
77	286.66	1.34	-6.67	0.02	-25.90	1.62	-20.50	-28.70	1.65
80	287.16	1.16	-6.67	0.02	-25.91	1.62	-20.51	-28.71	1.65
82	289.02	1.72	-6.66	0.02	-25.93	1.61	-20.53	-28.71	1.65
83	285.05	1.34	-6.66	0.02	-25.86	1.62	-20.46	-28.68	1.65
86	286.65	1.16	-6.65	0.02	-25.88	1.62	-20.48	-28.68	1.65
87	285.35	0.94	-6.65	0.02	-25.85	1.62	-20.45	-28.68	1.65
88	287.17	0.63	-6.64	0.02	-25.88	1.63	-20.48	-28.68	1.64
91	286.63	0.41	-6.63	0.02	-25.86	1.63	-20.46	-28.66	1.64
93	283.16	1.16	-6.62	0.02	-25.78	1.62	-20.38	-28.63	1.65
95	285.57	0.63	-6.62	0.02	-25.83	1.63	-20.43	-28.65	1.64
96	288.05	2.21	-6.62	0.02	-25.87	1.60	-20.47	-28.67	1.66
99	287.13	0.63	-6.61	0.02	-25.85	1.63	-20.45	-28.65	1.64
100	284.00	1.16	-6.61	0.04	-25.79	1.64	-20.39	-28.63	1.67
105	283.18	1.16	-6.62	0.13	-25.78	1.73	-20.38	-28.63	1.76
106	283.53	1.16	-6.69	0.01	-25.86	1.61	-20.46	-28.70	1.64
107	281.58	1.16	-6.69	0.02	-25.82	1.62	-20.42	-28.69	1.65
117	284.45	0.94	-6.68	0.09	-25.87	1.69	-20.47	-28.70	1.72
187	277.16	0.63	-6.41	0.09	-25.46	1.70	-20.06	-28.37	1.71

198	277.23	0.63	-6.41	0.09	-25.47	1.70	-20.07	-28.38	1.71
227	277.64	0.94	-6.48	0.12	-25.54	1.72	-20.14	-28.45	1.75
256	277.36	0.63	-6.44	0.06	-25.50	1.67	-20.10	-28.41	1.68
321	273.78	0.41	-6.43	0.09	-25.42	1.70	-20.02	-28.37	1.71
420	283.95	0.64	-6.49	0.06	-25.67	1.67	-20.27	-28.50	1.68
601	278.36	0.41	-6.37	0.09	-25.45	1.70	-20.05	-28.34	1.71
699	282.41	0.63	-6.39	0.07	-25.54	1.68	-20.14	-28.39	1.69
804	284.51	1.27	-6.40	0.06	-25.59	1.66	-20.19	-28.42	1.69
901	280.97	0.63	-6.41	0.06	-25.54	1.67	-20.14	-28.40	1.68
992	277.41	0.41	-6.42	0.05	-25.48	1.66	-20.08	-28.39	1.67
1075	279.42	1.41	-6.43	0.05	-25.53	1.64	-20.13	-28.41	1.68
1128	278.62	1.41	-6.43	0.05	-25.51	1.64	-20.11	-28.41	1.68
1188	279.29	2.21	-6.43	0.05	-25.52	1.63	-20.12	-28.41	1.69
1220	279.99	0.41	-6.43	0.05	-25.54	1.66	-20.14	-28.42	1.67
1281	278.45	0.41	-6.43	0.05	-25.51	1.66	-20.11	-28.40	1.67
1313	279.59	0.41	-6.43	0.05	-25.53	1.66	-20.13	-28.41	1.67
1398	276.56	0.41	-6.43	0.05	-25.47	1.66	-20.07	-28.39	1.67
1432	276.79	0.94	-6.43	0.05	-25.48	1.65	-20.08	-28.39	1.68
1513	280.00	0.41	-6.43	0.05	-25.54	1.66	-20.14	-28.42	1.67
1593	277.80	0.41	-6.42	0.04	-25.49	1.65	-20.09	-28.39	1.66
1709	280.25	0.62	-6.42	0.04	-25.53	1.65	-20.13	-28.41	1.66
1830	278.0	1.20	-6.41	0.04	-25.48	1.64	-20.08	-28.38	1.67
1948	276.9	0.70	-6.40	0.04	-25.45	1.65	-20.05	-28.36	1.67
2069	276.7	0.80	-6.40	0.04	-25.45	1.64	-20.05	-28.36	1.67
2150	276.7	0.80	-6.39	0.04	-25.44	1.64	-20.04	-28.35	1.67
2228	277.6	1.30	-6.38	0.04	-25.44	1.63	-20.04	-28.35	1.67
2352	277.9	0.50	-6.38	0.04	-25.45	1.65	-20.05	-28.35	1.66
2453	273.9	1.10	-6.37	0.04	-25.36	1.64	-19.96	-28.31	1.67
2550	278.9	0.60	-6.37	0.04	-25.46	1.65	-20.06	-28.35	1.66
2625	275.3	1.60	-6.37	0.04	-25.39	1.63	-19.99	-28.32	1.67
2743	274.7	1.20	-6.36	0.04	-25.37	1.64	-19.97	-28.31	1.67

2820	276.3	0.90	-6.36	0.04	-25.40	1.64	-20.00	-28.32	1.67
2918	274.6	0.80	-6.35	0.04	-25.36	1.64	-19.96	-28.30	1.67
3078	276.3	1.50	-6.35	0.04	-25.39	1.63	-19.99	-28.31	1.67
3138	273.1	1.10	-6.35	0.04	-25.33	1.64	-19.93	-28.28	1.67
3219	274.0	0.30	-6.34	0.04	-25.33	1.65	-19.93	-28.28	1.66
3337	275.0	0.60	-6.34	0.04	-25.35	1.65	-19.95	-28.29	1.66
3454	273.4	1.30	-6.34	0.04	-25.32	1.63	-19.92	-28.28	1.67
3531	273.0	0.80	-6.34	0.04	-25.32	1.64	-19.92	-28.27	1.67
3628	271.5	1.00	-6.34	0.04	-25.29	1.64	-19.89	-28.26	1.67
3724	275.4	0.50	-6.34	0.04	-25.36	1.65	-19.96	-28.29	1.66
3802	274.9	1.30	-6.33	0.04	-25.34	1.63	-19.94	-28.28	1.67
3921	271.7	1.00	-6.33	0.04	-25.28	1.64	-19.88	-28.25	1.67
4019	271.6	0.70	-6.33	0.04	-25.28	1.65	-19.88	-28.25	1.67
4117	272.8	0.80	-6.33	0.04	-25.30	1.64	-19.90	-28.26	1.67
4176	271.5	0.90	-6.33	0.04	-25.28	1.64	-19.88	-28.25	1.67
4335	271.1	0.80	-6.33	0.04	-25.27	1.64	-19.87	-28.25	1.67
4395	269.1	0.60	-6.33	0.03	-25.23	1.64	-19.83	-28.23	1.65
4496	269.8	1.00	-6.33	0.03	-25.24	1.63	-19.84	-28.24	1.66
4596	271.5	0.80	-6.33	0.03	-25.28	1.63	-19.88	-28.25	1.66
4737	270.7	0.50	-6.33	0.03	-25.26	1.64	-19.86	-28.25	1.65
4797	269.3	1.00	-6.33	0.03	-25.23	1.63	-19.83	-28.24	1.66
4895	268.6	1.10	-6.33	0.03	-25.22	1.63	-19.82	-28.23	1.66
5033	269.8	1.20	-6.33	0.03	-25.24	1.63	-19.84	-28.24	1.66
5114	267.6	0.60	-6.33	0.03	-25.20	1.64	-19.80	-28.22	1.65
5196	265.3	1.70	-6.33	0.03	-25.15	1.62	-19.75	-28.21	1.66
5318	265.2	0.80	-6.33	0.03	-25.15	1.63	-19.75	-28.21	1.66
5419	267.6	2.00	-6.33	0.03	-25.20	1.61	-19.80	-28.22	1.66
5521	265.9	0.90	-6.33	0.03	-25.17	1.63	-19.77	-28.21	1.66
5621	265.5	0.80	-6.33	0.03	-25.16	1.63	-19.76	-28.21	1.66
5721	260.7	1.60	-6.33	0.03	-25.06	1.62	-19.66	-28.17	1.66
5780	266.7	0.90	-6.33	0.03	-25.18	1.63	-19.78	-28.22	1.66

5921	265.5	0.80	-6.33	0.04	-25.16	1.64	-19.76	-28.21	1.67
6064	263.2	0.60	-6.33	0.04	-25.11	1.65	-19.71	-28.19	1.66
6102	262.7	0.90	-6.33	0.03	-25.10	1.63	-19.70	-28.19	1.66
6205	261.2	0.70	-6.33	0.03	-25.07	1.64	-19.67	-28.18	1.66
6349	261.1	0.40	-6.33	0.03	-25.07	1.64	-19.67	-28.18	1.65
6430	259.4	0.60	-6.33	0.03	-25.03	1.64	-19.63	-28.16	1.65
6514	262.1	0.90	-6.33	0.03	-25.09	1.63	-19.69	-28.18	1.66
6631	262.9	0.50	-6.33	0.03	-25.10	1.64	-19.70	-28.19	1.65
6713	258.1	1.40	-6.33	0.03	-25.01	1.62	-19.61	-28.15	1.66
6792	257.6	0.90	-6.33	0.03	-25.00	1.63	-19.60	-28.15	1.66
6930	262.3	0.90	-6.33	0.03	-25.09	1.63	-19.69	-28.18	1.66
7031	263.0	0.70	-6.33	0.03	-25.11	1.64	-19.71	-28.19	1.66
7132	260.7	0.60	-6.33	0.03	-25.06	1.64	-19.66	-28.17	1.65
7211	258.4	0.80	-6.34	0.03	-25.02	1.63	-19.62	-28.17	1.66
7328	260.1	0.60	-6.34	0.03	-25.06	1.64	-19.66	-28.18	1.65
7424	260.4	0.40	-6.34	0.03	-25.06	1.64	-19.66	-28.18	1.65
7521	259.7	0.90	-6.34	0.03	-25.05	1.63	-19.65	-28.18	1.66
7617	259.2	0.70	-6.34	0.03	-25.04	1.63	-19.64	-28.17	1.66
7714	260.8	1.40	-6.35	0.03	-25.08	1.62	-19.68	-28.19	1.66
7813	259.6	0.50	-6.35	0.03	-25.06	1.64	-19.66	-28.18	1.65
7915	259.3	0.90	-6.36	0.03	-25.06	1.63	-19.66	-28.19	1.66
8017	258.3	1.20	-6.36	0.03	-25.04	1.62	-19.64	-28.18	1.66
8118	261.3	0.90	-6.37	0.03	-25.11	1.63	-19.71	-28.22	1.66
8174	260.7	0.40	-6.37	0.03	-25.10	1.64	-19.70	-28.21	1.65
8315	261.8	1.00	-6.38	0.03	-25.13	1.63	-19.73	-28.23	1.66
8412	259.0	1.10	-6.39	0.03	-25.08	1.63	-19.68	-28.22	1.66
8508	260.9	0.70	-6.39	0.03	-25.12	1.64	-19.72	-28.23	1.66
8599	260.4	0.60	-6.40	0.03	-25.12	1.64	-19.72	-28.24	1.65
8697	259.3	1.00	-6.41	0.03	-25.11	1.63	-19.71	-28.24	1.66
8772	262.0	0.80	-6.42	0.03	-25.17	1.63	-19.77	-28.27	1.66
8883	263.7	1.20	-6.43	0.04	-25.22	1.63	-19.82	-28.29	1.67

8974	263.8	0.80	-6.43	0.04	-25.22	1.64	-19.82	-28.30	1.67
9067	265.2	0.90	-6.44	0.04	-25.26	1.64	-19.86	-28.32	1.67
9171	260.6	1.70	-6.45	0.04	-25.18	1.62	-19.78	-28.29	1.67
9224	260.9	0.60	-6.46	0.04	-25.19	1.65	-19.79	-28.30	1.66
9310	263.0	0.40	-6.47	0.04	-25.24	1.65	-19.84	-28.33	1.66
9399	263.8	1.20	-6.48	0.04	-25.27	1.63	-19.87	-28.35	1.67
9604	264.4	0.40	-6.49	0.03	-25.29	1.64	-19.89	-28.36	1.65
9657	264.2	0.90	-6.50	0.03	-25.30	1.63	-19.90	-28.37	1.66
9776	264.0	0.30	-6.51	0.03	-25.30	1.64	-19.90	-28.38	1.65
9846	263.4	0.10	-6.52	0.03	-25.30	1.65	-19.90	-28.38	1.65
9931	265.7	0.50	-6.53	0.03	-25.36	1.64	-19.96	-28.41	1.65
10001	264.9	0.40	-6.49	0.03	-25.30	1.64	-19.90	-28.36	1.65
10093	267.5	0.40	-6.53	0.03	-25.39	1.64	-19.99	-28.42	1.65
10192	266.9	0.60	-6.54	0.03	-25.39	1.64	-19.99	-28.43	1.65
10263	266.0	1.10	-6.55	0.03	-25.38	1.63	-19.98	-28.43	1.66
10370	265.1	1.60	-6.56	0.03	-25.38	1.62	-19.97	-28.44	1.66
10458	267.6	0.70	-6.57	0.03	-25.43	1.64	-20.03	-28.46	1.66
10550	264.8	0.60	-6.57	0.03	-25.38	1.64	-19.98	-28.44	1.65
10640	264.8	0.40	-6.58	0.03	-25.39	1.64	-19.99	-28.45	1.65
10712	265.0	0.80	-6.59	0.03	-25.40	1.63	-20.00	-28.46	1.66
10732	265.3	0.40	-6.59	0.03	-25.41	1.64	-20.01	-28.47	1.65
10785	264.4	1.50	-6.59	0.03	-25.39	1.62	-19.99	-28.46	1.66
10822	264.1	0.70	-6.59	0.03	-25.38	1.64	-19.98	-28.46	1.66
10896	264.2	1.10	-6.60	0.03	-25.40	1.63	-20.00	-28.47	1.66
10952	264.5	0.40	-6.61	0.03	-25.41	1.64	-20.01	-28.48	1.65
11008	264.0	0.50	-6.61	0.03	-25.40	1.64	-20.00	-28.48	1.65
11066	263.0	1.30	-6.61	0.03	-25.38	1.62	-19.98	-28.47	1.66
11099	265.2	0.80	-6.61	0.03	-25.43	1.63	-20.03	-28.49	1.66
11144	258.8	0.70	-6.61	0.03	-25.30	1.63	-19.90	-28.44	1.66
11195	260.8	0.50	-6.61	0.03	-25.34	1.64	-19.94	-28.45	1.65
11263	255.4	0.30	-6.62	0.04	-25.23	1.65	-19.83	-28.42	1.66

11310	253.9	0.60	-6.62	0.03	-25.20	1.64	-19.80	-28.41	1.65
11349	253.8	0.80	-6.62	0.03	-25.20	1.63	-19.80	-28.41	1.66
11468	250.7	1.10	-6.63	0.03	-25.14	1.63	-19.74	-28.40	1.66
11515	249.7	0.40	-6.63	0.03	-25.12	1.64	-19.72	-28.39	1.65
11554	251.1	0.30	-6.65	0.03	-25.17	1.64	-19.77	-28.42	1.65
11602	250.7	0.90	-6.65	0.03	-25.16	1.63	-19.76	-28.42	1.66
11695	245.3	1.10	-6.66	0.03	-25.05	1.63	-19.65	-28.39	1.66
11784	245.3	0.60	-6.67	0.03	-25.06	1.64	-19.66	-28.40	1.65
11838	246.6	0.50	-6.67	0.03	-25.09	1.64	-19.69	-28.41	1.65
11941	243.2	0.40	-6.69	0.03	-25.04	1.64	-19.64	-28.40	1.65
12017	240.3	0.30	-6.70	0.04	-24.98	1.65	-19.58	-28.39	1.66
12258	237.5	0.50	-6.71	0.04	-24.93	1.65	-19.53	-28.38	1.66
12372	237.6	0.60	-6.72	0.04	-24.94	1.65	-19.54	-28.39	1.66
12511	234.2	0.30	-6.71	0.04	-24.85	1.65	-19.45	-28.36	1.66
12625	238.3	1.10	-6.70	0.04	-24.94	1.63	-19.54	-28.38	1.67
12789	237.3	0.50	-6.68	0.03	-24.89	1.64	-19.49	-28.35	1.65
12927	237.9	0.20	-6.67	0.03	-24.90	1.64	-19.50	-28.34	1.65
13068	237.6	0.60	-6.65	0.03	-24.87	1.64	-19.47	-28.32	1.65
13252	236.4	0.90	-6.63	0.03	-24.82	1.63	-19.42	-28.29	1.66
13332	239.2	0.50	-6.62	0.03	-24.88	1.64	-19.48	-28.30	1.65
13440	238.6	0.60	-6.61	0.04	-24.85	1.65	-19.45	-28.29	1.66
13574	238.6	0.30	-6.60	0.04	-24.84	1.65	-19.44	-28.28	1.66
13711	239.1	0.40	-6.59	0.04	-24.85	1.65	-19.45	-28.27	1.66
14022	228.5	0.60	-6.59	0.03	-24.60	1.63	-19.20	-28.19	1.65
14230	228.4	0.70	-6.60	0.03	-24.60	1.63	-19.20	-28.20	1.66
14387	226.1	0.60	-6.61	0.03	-24.56	1.63	-19.16	-28.20	1.65
14532	225.2	0.50	-6.61	0.03	-24.54	1.64	-19.14	-28.19	1.65

F.4. Calculated $\delta^{13}C$ values of rodent diet

Table F.4.1: *Carbon isotope values of rodent diet, calculated using the adjusted $\delta^{13}C$ values of the modern and fossil first molars from Britain, and the adjusted $\delta^{13}C$ values of the fossil incisors from Longstone Edge and Gully Cave (see Table F.2.1 for the adjustments). The dietary $\delta^{13}C$ values were calculated using a bioapatite-diet $\delta^{13}C$ enrichment factor of 11.5 ± 0.15‰ (Passey et al., 2005). The data in this table are plotted in Figures 8.11 and 8.12. WH = West Horrington, Somerset, CO = Cobham, Surrey, EY = East Yorkshire, PE = Perthshire, DA = Danebury, LE = Longstone Edge, GCEG = Gully Cave:* Microtus *upper first molars, GC = Gully Cave:* Arvicola *incisors*.

Age (yr BP)	Specimen number	$\delta^{13}C$ of tooth (‰ VPDB)	$\delta^{13}C$ of diet (‰ VPDB)		
			Average	Maximum	Minimum
-65	WH-1-RMI	-15.5	-27.0	-26.7	-27.4
	WH-2-RMI	-16.7	-28.2	-27.9	-28.5
	WH-3-RMI	-16.3	-27.8	-27.5	-28.0
	WH-4-RMI	-17.5	-29.0	-28.8	-29.3
	WH-5-RMI	-17.1	-28.6	-28.4	-28.8
	WH-6-RMI	-17.7	-29.2	-29.0	-29.4
	WH-7-RMI	-16.9	-28.4	-28.2	-28.7
	WH-8-RMI	-17.4	-28.9	-28.7	-29.1
	WH-9-RMI	-17.2	-28.7	-28.5	-28.8
	WH-3-LM1	-16.5	-27.9	-27.8	-28.1
	WH-3-URM1	-16.4	-27.9	-27.8	-28.1
	WH-3-ULM1	-16.4	-27.9	-27.7	-28.1
-23	CO-1-RM1	-19.8	-31.3	-31.1	-31.4
	CO-2-RM1	-16.3	-27.8	-27.7	-28.0
	CO-3-RM1	-16.6	-28.1	-27.9	-28.3
	CO-4-RM1	-17.8	-29.3	-29.1	-29.4
	CO-6-RM1	-15.9	-27.4	-27.2	-27.6
	CO-7-RM1	-19.0	-30.5	-30.2	-30.9
	CO-8-RM1	-17.4	-28.9	-28.7	-29.0
	CO-9-RM1	-19.1	-30.6	-30.3	-30.8
	CO-9-LM1	-19.0	-30.5	-30.3	-30.7
	CO-9-URM1	-18.9	-30.4	-30.1	-30.6
	CO-9-ULM1	-18.4	-29.9	-29.7	-30.1
-65	EY-1-RM1	-20.8	-32.3	-32.1	-32.5
	EY-2-RM1	-20.5	-32.0	-31.8	-32.1
	EY-3-RM1	-19.2	-30.7	-30.5	-30.9
	EY-4-RM1	-18.1	-29.6	-29.4	-29.8
	EY-5-RM1	-17.5	-29.0	-28.9	-29.2
	EY-6-RM1	-18.1	-29.6	-29.5	-29.8

	EY-7-RM1	-18.2	-29.7	-29.6	-29.9
	EY-8-RM1	-21.1	-32.6	-32.4	-32.8
	EY-9-RM1	-19.5	-31.0	-30.9	-31.2
	EY-1-LM1	-21.0	-32.5	-32.4	-32.7
	EY-1-URM1	-19.2	-30.7	-30.5	-30.9
	EY-1-ULM1	-21.0	-32.5	-32.3	-32.7
-66	PE-1-RM1	-17.0	-28.5	-28.4	-28.7
	PE-2-RM1	-16.9	-28.4	-28.2	-28.6
	PE-3-RM1	-17.8	-29.3	-29.2	-29.5
	PE-4-RM1	-19.2	-30.7	-30.5	-30.8
	PE-5-RM1	-16.2	-27.7	-27.5	-27.9
	PE-6-RM1	-16.2	-27.7	-27.5	-27.9
	PE-7-RM1	-16.2	-30.0	-29.8	-30.2
	PE-8-RM1	-18.5	-30.3	-30.2	-30.5
	PE-9-RM1	-18.8	-29.9	-29.7	-30.0
	PE-10-RM1	-18.0	-29.5	-29.4	-29.7
2100	DA-923-1	-11.3	-22.8	-22.6	-23.0
	DA-923-2	-12.5	-24.0	-23.8	-24.2
	DA-923-3	-12.1	-23.6	-23.4	-23.8
	DA-923-4	-12.2	-23.7	-23.5	-23.9
	DA-923-5	-12.4	-23.9	-23.7	-24.1
	DA-955-1	-13.8	-25.3	-25.1	-25.5
	DA-955-2	-13.4	-24.9	-24.7	-25.1
	DA-955-3	-13.9	-25.4	-25.2	-25.5
	DA-955-4	-12.8	-24.3	-24.1	-24.5
	DA-955-5	-13.9	-25.4	-25.2	-25.6
4000	LE-Ma1	-9.5	-21.0	-20.8	-21.1
	LE-Ma2	-10.2	-21.7	-21.5	-21.9
	LE-Ma3	-10.2	-21.7	-21.6	-21.9
	LE-Ma4	-10.9	-22.4	-22.2	-22.6
	LE-Ma5	-11.3	-22.8	-22.6	-22.9
	LE-Ma6	-11.4	-22.9	-22.7	-23.1
	LE-Ma7	-8.3	-19.8	-19.6	-20.0
	LE-Ma8	-9.6	-21.1	-20.9	-21.2
	LE-Ma9	-9.5	-21.0	-20.9	-21.2
	LE-Ma10	-9.2	-20.7	-20.5	-20.9
	LE-At1	-9.2	-20.7	-20.5	-20.9
	LE-At2	-9.8	-21.3	-21.2	-21.5
	LE-At3	-9.9	-21.4	-21.2	-21.6
	LE-At4	-8.7	-20.2	-20.0	-20.4
	LE-At5	-10.7	-22.2	-22.0	-22.4
	LE-At6	-9.2	-20.7	-20.5	-20.9
	LE-At7	-11.1	-22.6	-22.4	-22.8
	LE-At8	-9.6	-21.1	-20.9	-21.3
	LE-At9	-9.5	-21.0	-20.8	-21.2
	LE-At10	-10.6	-22.1	-21.9	-22.3

3950	LE-At-MA1-RM1	-10.4	-21.9	-21.8	-22.1
	LE-At-MA1-RI	-9.1	-20.6	-20.4	-20.7
2600	LE-At-MA2-LM1	-10.4	-21.9	-21.7	-22.0
	LE-At-MA2-LI	-9.3	-20.8	-20.7	-21.0
4000	LE-At-MA3-RI	-9.2	-20.7	-20.6	-20.9
10270	GCEG-1-1	-10.7	-22.2	-22.0	-22.3
	GCEG-1-2	-8.4	-19.9	-19.7	-20.0
	GCEG-1-3	-11.6	-23.1	-22.9	-23.2
	GCEG-1-5	-10.3	-21.8	-21.6	-21.9
11307	GCEG-2-1	-9.2	-20.7	-20.5	-20.8
	GCEG-2-2	-8.3	-19.8	-19.6	-20.0
	GCEG-2-3	-10.5	-22.0	-21.8	-22.1
	GCEG-2-4	-7.4	-18.9	-18.8	-19.1
	GCEG-2-5	-9.4	-20.9	-20.7	-21.1
11621	GCEG-3-1	-10.1	-21.6	-21.4	-21.7
	GCEG-3-2	-10.5	-22.0	-21.8	-22.2
	GCEG-3-3	-9.9	-21.4	-21.3	-21.6
	GCEG-3-4	-9.5	-21.0	-20.9	-21.2
	GCEG-3-5	-11.6	-23.1	-23.0	-23.3
11922	GCEG-4-1	-8.4	-19.9	-19.8	-20.1
	GCEG-4-2	-8.6	-20.1	-19.9	-20.3
	GCEG-4-3	-10.3	-21.8	-21.6	-22.0
	GCEG-4-4	-9.0	-20.5	-20.3	-20.7
	GCEG-4-5	-10.0	-21.5	-21.3	-21.7
11976	GCEG-6-1	-10.8	-22.3	-22.1	-22.4
	GCEG-6-4	-10.9	-22.4	-22.2	-22.5
	GCEG-6-5	-10.0	-21.5	-21.3	-21.7
12154	GCEG-7-1	-10.7	-22.2	-22.0	-22.3
	GCEG-7-2	-10.7	-22.2	-22.1	-22.4
	GCEG-7-3	-10.6	-22.1	-21.9	-22.3
	GCEG-7-4	-10.8	-22.3	-22.2	-22.5
	GCEG-7-5	-11.2	-22.7	-22.5	-22.9
12223	GCEG-5-1	-7.9	-19.4	-19.2	-19.6
	GCEG-5-2	-10.3	-21.8	-21.7	-22.0
	GCEG-5-3	-8.4	-19.9	-19.8	-20.1
	GCEG-5-4	-9.3	-20.8	-20.6	-21.0
	GCEG-5-5	-10.1	-21.6	-21.4	-21.7
12331	GCEG-8-1	-9.9	-21.4	-21.2	-21.6
	GCEG-8-2	-10.1	-21.6	-21.4	-21.8
	GCEG-8-3	-9.6	-21.1	-20.9	-21.3
	GCEG-8-4	-9.8	-21.3	-21.1	-21.5
	GCEG-8-5	-9.7	-21.2	-21.0	-21.4
12509	GCEG-9-1	-9.5	-21.0	-20.8	-21.2
	GCEG-9-2	-10.4	-21.9	-21.7	-22.1

	GCEG-9-3	-10.3	-21.8	-21.6	-22.0
	GCEG-9-4	-10.2	-21.7	-21.5	-21.9
	GCEG-9-5	-10.1	-21.6	-21.4	-21.8
13294	GCEG-10-1	-11.7	-23.2	-23.0	-23.4
	GCEG-10-2	-9.7	-21.2	-21.0	-21.4
	GCEG-10-3	-10.7	-22.2	-22.0	-22.4
	GCEG-10-4	-9.5	-21.0	-20.9	-21.2
	GCEG-10-5	-10.9	-22.4	-22.2	-22.5
13472	GCEG-11-1	-11.1	-22.6	-22.4	-22.8
	GCEG-11-2	-9.7	-21.2	-21.1	-21.4
	GCEG-11-3	-9.9	-21.4	-21.2	-21.6
	GCEG-11-4	-7.9	-19.4	-19.2	-19.6
	GCEG-11-5	-8.6	-20.1	-19.9	-20.3
13651	GCEG-12-1	-7.4	-18.9	-18.7	-19.1
	GCEG-12-2	-9.5	-21.0	-20.9	-21.2
	GCEG-12-3	-10.3	-21.8	-21.6	-22.0
	GCEG-12-4	-7.3	-18.8	-18.7	-19.0
	GCEG-12-5	-9.4	-20.9	-20.7	-21.1
13829	GCEG-13-1	-9.4	-20.9	-20.7	-21.1
	GCEG-13-2	-9.9	-21.4	-21.2	-21.6
	GCEG-13-4	-9.2	-20.7	-20.5	-20.9
	GCEG-13-5	-9.9	-21.4	-21.2	-21.5
14008	GCEG-14-1	-8.9	-20.4	-20.2	-20.6
	GCEG-14-2	-8.6	-20.1	-19.9	-20.3
	GCEG-14-3	-9.2	-20.7	-20.5	-20.9
	GCEG-14-4	-9.5	-21.0	-20.8	-21.2
	GCEG-14-5	-10.4	-21.9	-21.7	-22.1
14213	GCEG-15-1	-9.0	-20.5	-20.3	-20.7
	GCEG-15-2	-9.9	-21.4	-21.2	-21.6
	GCEG-15-3	-9.2	-20.7	-20.5	-20.9
	GCEG-15-4	-9.8	-21.3	-21.1	-21.5
	GCEG-15-5	-9.5	-21.0	-20.8	-21.2
14419	GCEG-16-1	-8.6	-20.1	-19.9	-20.3
	GCEG-16-2	-10.7	-22.2	-22.0	-22.3
	GCEG-16-3	-9.2	-20.7	-20.5	-20.8
	GCEG-16-4	-7.6	-19.1	-18.9	-19.3
	GCEG-16-5	-9.4	-20.9	-20.7	-21.1
9000 (estimate)	GC-7A	-6.2	-17.7	-17.6	-17.9
9000 (estimate)	GC-7B	-6.7	-18.2	-18.0	-18.4
9500 (estimate)	GC-8	-10.4	-21.9	-21.7	-22.1
9500 (estimate)	GC-1A	-8.8	-20.3	-20.2	-20.5

9500 (estimate)	GC-1B	-8.6	-20.1	-19.9	-20.2
10000 (estimate)	GC-2	-7.7	-19.2	-19.0	-19.4
10500	GC-9	-6.6	-18.1	-18.0	-18.3
11700 (estimate)	GC-5	-7.2	-18.7	-18.5	-18.9
11922	GC-12	-7.4	-18.9	-18.8	-19.1
12154	GC-3	-6.6	-18.1	-17.9	-18.4
12509	GC-4	-7.8	-19.3	-19.0	-19.5
12800 (estimate)	GC-6A	-7.7	-19.2	-19.0	-19.4
12800 (estimate)	GC-6B	-7.2	-18.7	-18.6	-18.9
13294	GC-10	-7.7	-19.2	-19.0	-19.3
13472 (estimate)	GC-11	-7.9	-19.4	-19.3	-19.6